SPECTROCHIMICA ACTA

Founder Editor

A. GATTERER S.J. +

Editors

U.S.A.

V. A. FASSEL *Ames, Iowa*

F. A. MILLER *Pittsburgh*

UNITED KINGDOM

H. W. THOMPSON *Oxford*

EDITORIAL ADVISORY BOARD

B. Bak, *Copenhagen*
N. S. Bayliss, *Perth, W. Aust.*
L. J. Bellamy, *Waltham Abbey*
Wallace R. Brode, *Washington, D.C.*
C. G. Cannon, *Pontypool*
C. G. Carlsson, *Stockholm*
B. L. Crawford, *Minneapolis*
G. Duyckaerts, *Liège*
C. Feldman, *Oak Ridge*
H. Friedman, *Washington*
W. Gordy, *Durham, N.C.*
D. Hadzi, *Ljubljana*
D. F. Hornig, *Princeton, N.J.*
R. N. Jones, *Ottawa*
H. Kaiser, *Dortmund*
M. Kasha, *Tallahassee*
J. A. A. Ketelaar, *Amsterdam*
J. Lecomte, *Paris*
E. Loeuille, *Paris*
R. C. Lord, *Cambridge, Mass.*
S. L. Mandelstam, *Moscow*
A. Mangini, *Bologna*
J. R. McNally, *Oak Ridge*
R. Mecke, *Freiburg*
A. C. Menzies, *London*
S. Mizushima, *Tokyo*
R. L. Mitchell, *Aberdeen*
G. Porter, *Sheffield*
W. C. Price, *London*
R. E. Richards, *Oxford*
H. Schüler, *Hechingen-Hohenzollern*
B. F. Scribner, *Washington D.C.*
N. Sheppard, *Cambridge*
H. Shull, *Bloomington, Indiana*
D. M. Smith, *Wembley*
E. H. S. van Someren, *Broxbourne*
H. Stammreich, *São Paulo*
B. Vodar, *Bellevue, S. et O.*
A. Walsh, *Melbourne*
H. L. Welsh, *Toronto*
M. Kent Wilson, *Medford, Mass.*
N. Wright, *Midland (Mich.)*

VOLUME XII

1958

PERGAMON PRESS

NEW YORK · LONDON · PARIS · LOS ANGELES

VOL. 12 1958

Spectrochim. Acta

SPECTROCHIMICA ACTA

CONTENTS OF VOLUME XII

No. 1

E. Bright Wilson, Jr: Determination of the order of atoms in a linear molecule . . . 1
L. E. Owen and D. C. Manning: Mechanized arc-spark stand for emission spectrography . . 4
J. M. Martin, Jr., R. W. B. Johnston and M. J. O'Neal: Infrared absorption of solid state *n*-paraffins—relationship to crystalline type 12
F. González-Sánchez: Infra-red spectra of the benzene carboxylic acids 17
L. B. Archibald and A. D. E. Pullin: Solvent effects in infra-red spectra of compounds containing the carbonyl group 34
H. R. Linton and E. R. Nixon: Infrared spectrum and force constants of silyl-d_3 iodide . . 41
A. Stojiljković and D. H. Whiffen: The vibration frequencies of the symmetrical *p*-dihalogenobenzenes 47
A. Stojiljković and D. H. Whiffen: The vibration frequencies of unsymmetrical *p*-dihalogenobenzenes 57
C. Riminton, S. F. Mason and O. Kennard: Porphin 65
R. A. Ford and Miss F. Parry: Electronic and vibrational states of carbonyl compounds—I. Electronic states of camphorquinone 78
N. S. Ham and A. Walsh: Microwave-powdered Raman sources 88
Research Notes
G. C. Pimentel: The promise and problems of the matrix isolation method for spectroscopic studies 94
E. F. Runge and F. R. Bryan: Excitation of atomic emission lines of nitrogen in steel by means of a high-energy, single-discharge source 96
L. E. Owen: Automatic film washer-rinser-dryer 99
Reports of Meetings 101
Notices of Meetings 105
Papers to be published in future issues 107
Erratum 108

Nos. 2/3

D. W. Grant, D. E. Glanville and G. L. Strachan: A simple arrangement for the measurement of absorption spectra of aqueous systems at elevated temperatures 109
Robert C. Hirt: Ultraviolet absorption vapour spectra of pyrazine and chloropyrazine . . 114
R. C. Hirt and R. G. Schmitt: Ultraviolet absorption spectra of derivatives of symmetric triazine—II. Oxo-triazines and their acyclic analogs 127
J. Burdon and D. H. Whiffen: Infrared spectra of fluoro-cyclo olefins 139
T. T. Crow and R. T. Lagemann: Infrared spectrum of sulfuryl bromofluoride 143
R. C. Lord, D. W. Mayo, H. E. Opitz and J. S. Peake: The preparation and vibrational spectra of disilylacetylene 147
Brian Stevens: A relationship between some bond properties of diatomic molecules and the ionization potentials of their constituent atoms 154
D. Hadzi and M. Pintar: The OH in-plane deformation and the C—O stretching frequencies in monomeric carboxylic acids and their association shifts 162
M. Mack and N. Spielberg: Statistical factor in X-ray intensity measurements 169
L. M. Sutcliffe: Rydberg term tables 179
R. Norman Jones and Armand Nadeau: Cavity type micro-cells for infrared spectrometry . 183
E. G. McRae: Solvent effects on merocyanine spectra 192
J. K. Hurwitz: Spectrographic analysis of segregates with a dynamic micro-volume technique—II. Experimental verification of theory 211
D. F. Smith: Infrared spectra analysis for hydrogen fluoride 224
D. M. Anderson, L. J. Bellamy and R. L. Williams: The infrared spectra of some gem dihydroxy compounds and their deuterated derivatives 233
Ichiro Nakagawa, San-Ichiro Mizushima, A. J. Saraceno, T. J. Lane and J. V. Quagliano: Infrared absorption spectra of inorganic co-ordination complexes—XVI. Normal vibrations of sulfamic acid, $H_3N^+SO_3^-$ 239
Leo H. Spinar and John L. Margrave: Absorption spectra of gaseous alkali metal hydroxides at high temperatures 244
George R. Bird, A. Danti and R. C. Lord: Pure rotational absorption of NO_2 in the 50–200 micron region 247
Masamichi Tsuboi, Takaharu Onishi, Ichiro Nakagawa, Takehiko Shimanouchi and San-Ichiro Mizushima: Assignments of the vibrational frequencies of glycine 253

VOL. 12 1958

Contents

D. P. Stevenson and H. M. McConnell: Ultraviolet criteria for monoaromaticity . 262

Research Notes:
Giulio Milazzo: Spectrum tables used for wavelength identification in the Schuman region 275
Dale A. Clark and Anton P. Boer: A method of mounting micro samples for infrared spectrometry 276
S. Meyer and O. G. Koch: Ein Elektrodenheizblock zur Lösungsspektralanalyse . . . 278
Hans Feilchenfeld: The stretching frequency as a function of the interatomic distance in straight hydrogen bonds 280

Book Reviews:
L. J. Bellamy: "Einführung in die Ultrarot Spektroskopie" by W. Brügel 284
W. C. Price: "Fundamentals of Optics" by Francis A. Jenkins and Harvey E. White . . 284
M. Margoshes: "Flame Photometry" by F. Burriel-Martí and J. Ramírez-Nuñoz . . 285
Papers to be published in future issues 286
Publisher's Notice 288

No. 4

M. C. De Wilde-Delvaux et Ph. Teyssié: Etude spectrographique infra-rouge de quelques β-dicétones 289
A. Yamaguchi, I. Ichishima and S. Mizushima: Polarization of the reflected infrared radiation from an echelette grating 294
G. Porter and Emma Strachan: The electronic spectra of benzyl 299
Chantal Garrigou-Lagrange, Jeanne-Marie Lebas et Marie-Louise Josien: Etude comparée des spectres de vibration des dérivés paradisubstitués du benzène—I. Region 670–1600 cm^{-1} 305
F. A. Miller and R. B. Hannan, Jr.: The ultraviolet absorption spectrum of dicyanoacetylene 321
R. N. Kniseley, V. A. Fassel, B. B. Quinney, C. Tremmel, W. A. Gordon, and W. J. Hayles: Quantitative spectrographic analysis of the rare earth elements—IX. Determination of rare earth impurities commonly associated with purified samarium, gadolinium, terbium and yttrium 332
D. F. Hornig, H. F. White and F. P. Reding: The infrared spectra of crystalline H_2O, D_2O and HDO 338
R. Andrisano and G. Paffalardo: Absorption spectra in the near ultraviolet of some α- and β-monosubstituted derivatives of thiophene 350
B. Bak and D. Christensen: Infrared absorption spectra of deuterated vinyl fluorides . . 355

Report of Meeting:
9th Annual Pittsburg Conference on Analytical Chemistry and Applied Spectroscopy . . 370

Research Notes:
R. Mecke and K. Noack: Untersuchungen über die Beeinflussung der Frequenz und Intensität der $\nu_{C=O-}$ und $\nu_{C=C-}$ Banden im I.R.-Spektrum ungesättigter Ketone durch Konjugation und sterische Hinderung 391
C. T. J. Alkemade and M. H. Voorhuis: On the problem of calcium depression by phosphorus in flame photometry 394
R. A. Ford: Spin-forbidden transitions in the electronic spectrum of acetaldehyde . . 394
P. T. Gilbert Jr.: Determination of indium by flame photometry 397
G. Mitchell: Correction de l'intensité des raies Raman pour l'absorption du milieu diffusant 400
H. Stammreich, D. Bassi and O. Sala: Raman spectrum and force constants of the chromate ion 403

Book Review:
"Atomic Energy Levels. Vol. III" by Charlotte E. Moore (reviewed by Ernest van Someren) 406
Papers to be published in future issues 407
Errata 408

VOL.
12
1958

SUBJECT INDEX TO VOLUME XII

Absorption spectra (visible, ultra-violet) of
- acetaldehyde 394
- aromatic hydrocarbons 262
- benzyl 299
- camphorquinone 78
- dicyanoacetylene 321
- merocyanines 192
- oxotriazines 127
- perchloric acid solutions 112
- porphin 65
- thiophenes, α and β substituted 350

Acetaldehyde, ultraviolet spectrum of 394
Alkali hydroxides, infrared spectra 244

Benzene carboxylic acids, infrared spectra 17
Benzyl, electronic spectrum of 299
Bond properties of diatomic molecules and ionization potentials of atoms . . 154
Book Reviews:
- 'Einführung in die Ultrarotspektroskopie' by W. Brügel 284
- 'Fundamentals of Optics' by F. A. Jenkins and H. E. White 284
- 'Flame Photometry' by F. Burriel-Martí and J. Ramírez-Muñoz . . . 285
- 'Atomic Energy Levels' by C. E. Moore 406

Camphorquinone, absorption spectrum of 78
Carbon monoxide, emission in vacuum ultraviolet 275
Carboxylic acids and deutero derivatives, infrared spectra 162
Chloropyrazine, ultraviolet spectrum of 114
Chromate ion, Raman spectrum and force constants 403

Dicyanoacetylene, ultraviolet absorption of 321
Dihalogenobenzenes (*p*-symm.) infrared spectra 47
Dihalogenobenzenes (*p*-unsymm.) infrared spectra 57
Diketones, infrared spectra of 289
Disilyl acetylene, vibrational spectrum 147
Disubstituted benzenes, infrared spectra 305

Emission spectrographic analysis:
- depression of calcium by phosphorus 394
- determination of oxygen in metals 108
- high energy single discharge source 96
- mechanized arc-spark 4
- rare-earth elements 332
- segregates, with dynamic micro-volume technique 211

Emission spectrum of camphorquinone 78
Etiocholane-3:17-dione, infrared spectrum 186

Flame photometry, for determination of indium 397
Fluoro-*cyclo*-olefines, infrared spectra 139

Force constants and molecular structure:
determination of order of atoms in linear molecule 1
silyl-d_3-iodide 41

Glycine, infrared spectrum and vibration frequencies 253

H_2O, D_2O, HDO, (crystalline), infrared spectra 338
Hydrogen bonding:
in diketones 289
relation between vibration frequency and interatomic distance 280
Hydrogen fluoride, analysis by infrared spectrum 224

Indium, determination by flame photometry 397
Infrared spectra of:
alkali metal hydroxide vapours 244
benzene carboxylic acids 17
carboxylic acids and deutero derivatives 162
compounds containing the carbonyl group (solvent effects) 34
deuterated vinyl fluorides 355
dihalogeno-benzenes (*p*-symm.) 47
dihalogeno-benzenes (*p*-unsymm.) 57
diketones 289
disilyl acetylene 147
disubstituted benzenes (para) 305
etiocholane-3:17-dione 186
fluoro-*cyclo*-olefines 139
gem-dihydroxy compounds and deutro derivatives 233
glycine 253
hydrogen fluoride, for analysis 224
H_2O, D_2O, HDO 338
nitrogen dioxide 247
paraffins (n), in relation to crystalline type 12
porphin 65
silyl-d_3-iodide 41
sulfamic acid 239
sulfuryl bromofluoride 143
unsaturated Ketones 391
Instrumentation:
Absorption spectra of solutions at elevated temperatures 109
Automatic film washer-rinser-drier 99
Cavity-type microcell for infrared spectroscopy 183
Electrode mounting device for spectral analysis of solutions 278
High-energy single-discharge source for emission lines of nitrogen . . . 96
Mechanized arc-spark for emission spectroscopy 4
Microsample mount for infrared measurements 276
Microwave-powered Raman source 88
Polarization with echelette grating 294
Ionization potential of atoms 154

Keto-enol equilibrium in diketones 892

Matrix isolation method for spectroscopic studies 94
Meetings, reports of:
I.U.P.A.C. Molecular Spectroscopy Commission 101
4th Symposium on Spectroscopy, Japan 102

VOL.
12
1958

Meetings, reports of (*continued*)
Symposium on Spectroscopy, India 103
6th Symposium, South-eastern Seminar, Florida 104
9th Pittsburg Conference 1958 370

Monoaromaticity, ultraviolet criteria for 262

Nitrogen dioxide, rotational spectrum 247

Oxotriazines, ultraviolet absorption of 127
Oxygen in metals, spectrographic determination of (erratum) 108

Paraffins, infrared spectra of 12
Porphin, absorption spectra of 65
Pyrazine, ultraviolet spectrum of 114

Raman spectra:
chromate ion 403
dihalogenobenzenes (para) 47
intensity corrections with solutions 400
Rare earths, emission spectra analysis 332
Rydberg term tables 179

Schumann region, standard wavelengths for 275
Silyl-d_3-iodide, infrared spectrum of 41
Solvent effects on:
carbonyl group vibration bands 34
keto-enol equilibria 289
merocyanine spectra 192
Sulfamic acid, infrared spectrum 239
Sulfuryl bromofluoride, infrared spectrum 143

Thiophenes, substituted, ultraviolet spectra 350

Unsaturated ketones, effect of conjugation and steric hindrance upon infrared spectrum 391

Vibrational frequencies of:
carbonyl group 162
deuterated vinyl fluorides 355
dihalogenobenzenes (*p*-symm.) 47
dihalogenobenzenes (*p*-unsymm.) 57
gem dihydroxy compounds 233
glycine 253
Vinyl fluorides (deuterated), infrared spectra 355

X-ray intensity measurements 169

AUTHOR INDEX TO VOLUME XII

(B.R. indicates a Book Review)

Alkemade C. T. J. 394
Anderson D. M. 233
Andrisano R. 350
Archibald L. B. 34
Bak B. 355
Bassi D. 403
Bellamy L. J. 233, 284 (B.R.)
Bird G. R. 247
Boer A. P. 276
Bryan F. R. 96
Burdon J. 139
Christensen D. 355
Clark D. A. 276
Crow T. T. 143
Danti A. 247
Fassel V. A. 332
Feilchenfeld H. 280
Ford R. A. 78, 394
Garrigou-Lagrange C. 305
Gilbert P. T., Jr. 397
Glanville D. E. 109
González-Sánchez F. 17
Gordon W. A. 332
Grant D. W. 109
Hadži D. 162
Ham N. S. 88
Hannan R. B., Jr. 321
Hayles W. J. 332
Hirt R. C. 114, 127
Hornig D. F. 338
Hurwitz J. K. 211
Ichishima I. 294
Johnston R. W. B. 12
Jones R. N. 183
Josien M.-L. 305
Kennard O. 65
Kniseley R. N. 332
Koch O. G. 278
Lagemann R. T. 143
Lane T. J. 239
Lebas J.-M. 305
Linton H. R. 41
Lord R. C. 147, 247
Mack M. 169
McConnell H. M. 262
McRae E. G. 192
Manning D. C. 4
Margoshes M. 285 (B.R.)
Margrave J. L. 244
Martin J. M., Jr. 12
Mason S. F. 65
Mayo D. W. 147
Mecke R. 391
Meyer S. 278
Michel G. 400
Milazzo G. 275
Miller F. A. 321
Mizushima S.-I. 239, 253, 294
Nadeau A. 183
Nakagawa I. 239, 253
Nixon E. R. 41
Noack K. 391
O'Neal M. J. 12
Onishi T. 253
Opitz H. E. 147
Owen L. E. 4, 99
Pappalardo G. 350
Parry F. 78
Peake J. S. 147
Pimentel G. C. 94
Pintar M. 162
Porter G. 299
Price W. C. 284 (B.R.)
Pullin A. D. E. 34
Quagliano J. V. 239
Quinney B. B. 332
Reding F. P. 338
Rimington C. 65
Runge E. F. 96
Sala O. 403
Saraceno A. J. 239
Schmitt R. G. 127
Shimanouchi T. 253
Smith D. F. 224
Spielberg N. 169
Spinar L. H. 244
Stammreich H. 403
Stevens B. 154
Stevenson D. P. 262
Stojiljković A. 47, 57
Strachan E. 299
Strachan G. L. 109
Sutcliffe L. M. 179
Teyssié Ph. 289
Tremmel C. 332
Tsuboi M. 253
van Someren E. H. S. 406 (B.R.)
Voorhuis M. H. 394
Walsh A. 88
Whiffen D. H. 47, 57, 139
White H. F. 338
Williams R. L. 233
Wilde-Delvaux M. C. de 289
Wilson E. Bright, Jr. 1
Yamaguchi A. 294

VOL. 12 1958

Spectrochimica Acta, 1958, Vol. 12, pp. 1 to 3. Pergamon Press Ltd., London

Determination of the order of atoms in a linear molecule

E. Bright Wilson, Jr.
Mallinckrodt Chemical Laboratory, Harvard University, Cambridge, Massachusetts, U.S.A.

(*Received* 14 *November* 1957)

Abstract—The force constants determined from the infra-red or Raman spectra of a sufficient number of isotopic species can decide between alternative arrangement of atoms in a linear molecule. A convenient method of calculation of force constants is given which uses as co-ordinates all the interatomic distances whether bonded or not. A diagonal force-constant matrix in these co-ordinates has the correct number of independent elements. Large values indicate bonded distances; small ones non-bonded distances. Advantage is taken of the fact that the G matrix is of the same form whether the co-ordinates used are dependent or not.

Introduction

Infra-red spectroscopy has several times [1,2] been used to determine the order of the atoms in linear molecules. By comparing the values of the force constants obtained from analysis on the basis of alternative models, a choice can sometimes be made.

The purpose of this paper is to point out a convenient way of carrying out the calculations involved in such problems.

Method

The basic idea is to use a co-ordinate system for setting up the secular equation for the stretching frequencies, which is independent of the order of the atoms. Such a system is the set of changes in all interatomic distances, whether bonded or non-bonded. For example, in linear XYZ (or ZXY, YZX), one would use the co-ordinates Δr_{xy}, Δr_{yz} and Δr_{zy}, where r_{xy} is the distance from X to Y. There are $\frac{1}{2}n(n-1)$ such co-ordinates, if n is the number of atoms. Only $n-1$ of these are independent, but all will be used nevertheless.

The potential energy is taken to be diagonal, i.e. in the example

$$2V = f_{xy}(\Delta r_{xy})^2 + f_{yz}(\Delta r_{yz})^2 + f_{zx}(\Delta r_{zx})^2 \qquad (1)$$

and therefore has $\frac{1}{2}n(n-1)$ force constants. These are linear combinations of the $\frac{1}{2}n(n-1)$ force constants (including interaction constants) in terms of an independent set of co-ordinates. The force constants introduced above are independent, even though the co-ordinates are not.

The secular equation will be obtained by the use of the G matrix [3]. This can be written down by the usual rules whether the co-ordinates employed are independent or not. In the present instance a diagonal element, say $G_{xy,\,xy}$, is the sum of the reciprocal masses of the two atoms, i.e. $(1/m_x) + (1/m_y)$. A non-diagonal element will vanish unless the two co-ordinates share one atom, in which case $G_{xy,\,yz} = \pm(1/m_y)$. The minus sign appears when the shared atom is between the other two atoms.

The secular equation can be written in expanded form conveniently, since the force-constant matrix F is diagonal. It is

$$\sum_{s=0}^{n} (-1)^s \lambda^{n-s} \Sigma G^{(s)} F^{(s)} = 0 \tag{2}$$

where $G^{(s)}$, $F^{(s)}$ are s-rowed diagonal minors of G and F and the inner sum is over all such s-rowed diagonal minors [4].

The F and G matrices are independent of the order of the atoms except for the signs in G. Interchange of order of a pair of atoms will not change the value of any diagonal minor of G, so the secular equation is independent of the order of the atoms.

From experimental observations on the stretching vibrations of a sufficient number of isotopic forms of the molecule, the $\frac{1}{2}n(n-1)$ force constants are determined. Those associated with bonded distances will ordinarily be larger than those associated with non-bonded distances, thus yielding the information necessary to determine the order of the atoms.

Example. The sum of roots of the secular equation in HCN is

$$\Sigma\lambda = (\mu_C + \mu_H)f_{CH} + (\mu_C + \mu_N)f_{CN} + (\mu_N + \mu_H)f_{NH} \tag{3}$$

in which $\mu_x = 1/m_x$. Data is available [5] for $H^{12}C^{14}N$, $D^{12}C^{14}N$ and $D^{13}C^{14}N$ so that there are three equations for the three unknowns. From these one obtains

$$\Delta\mu_H(f_{CH} + f_{NH}) = \Delta\Sigma\lambda \tag{4}$$

$$\Delta'\mu_C(f_{CH} + f_{CN}) = \Delta'\Sigma\lambda \tag{5}$$

if Δ represents the change HCN to DCN and Δ' that from $D^{12}CN$ to $D^{13}CN$. Numerically,

$$f_{CH} + f_{NH} = 5{\cdot}6 \times 10^5 \text{ dyn/cm.}$$

$$f_{CH} + f_{CN} = 25{\cdot}5 \times 10^5$$

From these and equation (3) one obtains

$$f_{CH} \simeq 6{\cdot}1 \times 10^5$$

$$f_{NH} \simeq -0{\cdot}5 \times 10^5$$

Consequently H is bonded to C and C to N, as expected.

If the molecule is known to have a centre of symmetry, symmetry co-ordinates may be used. For example, with $Ag(CN)_2^-$, the evidence [2] shows that there is a centre of symmetry. The infra-red active modes are antisymmetric. As co-ordinates one could use

$$\begin{aligned}
(\tfrac{1}{2})^{\frac{1}{2}}(\Delta r_{AgC_1} - \Delta r_{AgC_2}) &= R_{AgC} \\
(\tfrac{1}{2})^{\frac{1}{2}}(\Delta r_{AgN_1} - \Delta r_{AgN_2}) &= R_{AgN} \\
(\tfrac{1}{2})^{\frac{1}{2}}(\Delta r_{C_1N_1} - \Delta r_{C_2N_2}) &= R_{CN}
\end{aligned} \tag{6}$$

VOL. 12 1958

In terms of these the G matrix is easily found, and consequently the antisymmetric factor of the secular equation. The sum of the roots for this is

$$\lambda_3 + \lambda_4 = (2\mu_{Ag} + \mu_C)F_{AgC} + (2\mu_{Ag} + \mu_N)F_{AgN} + (\mu_C + \mu_N)F_{CN}$$

in which the F's are the diagonal force constants in terms of the symmetry coordinates. If Δ represents the change due to substituting the carbon isotope and Δ' the change due to the nitrogen isotope, one has

$$\Delta(\lambda_3 + \lambda_4) = \Delta\mu_C(F_{AgC} + F_{CN})$$

$$\Delta'(\lambda_3 + \lambda_4) = \Delta\mu_N(F_{AgN} + F_{CN})$$

In published work [2] on $Ag(CN)_2^-$ both frequencies were given for the normal compound but only the high frequency for the isotopic species. However, the product rule [6] (which is also independent of the order of the atoms) can be used to determine the low frequency and thus give the sum of the roots. The result is

$$F_{AgC} + F_{CN} = 18{\cdot}3 \times 10^5 \text{ dyn/cm.}$$

$$F_{AgN} + F_{CN} = 16{\cdot}7 \times 10^5 \text{ dyn/cm.}$$

which shows that $F_{AgC} > F_{AgN}$ and therefore supports the structure with Ag–C bonds. However, because of the relative weakness of the Ag–C bonds, the evidence is not as conclusive as would be desirable. The whole argument as given neglects anharmonicity.

If the expressions involving the sum of the roots do not suffice because of lack of data, the other invariants can be employed to assist in the determination of the force constants. However, these will require the solution of quadratic or higher equations and can lead to multiple solutions. It can happen that one solution supports one structure while another solution supports a different order of the atoms. In such a case the bending frequencies may be decisive or more isotopic data may be required.

References

[1] Lanseth A. and Moller C. K. *Acta Chem. Scand.* 1950 **4** 937.

[2] Jones L. H. *J. Chem. Phys.* 1957 **26** 1578; 1957 **27** 468, 665.

[3] Wilson E. B., Decius J. C. and Cross P. C. *Molecular Vibrations* p. 61. McGraw-Hill, New York 1955.

[4] Wilson E. B., Decius J. C. and Cross P. C. *Molecular Vibrations* p. 68. McGraw-Hill, New York 1955.

[5] Richardson W. S. *J. Chem. Phys.* 1951 **19** 1213.

[6] Redlich O. *Z. Phys. Chem.* B 1935 **28** 371; Teller quoted by Angus *et al.* *J. Chem. Soc.* 1936 971, or see [3] p. 183.

Spectrochimica Acta, 1958, Vol. 12, pp. 4 to 11. Pergamon Press Ltd., London

Mechanized arc-spark stand for emission spectrography*

L. E. Owen and D. C. Manning†
Technical Division, Goodyear Atomic Corporation, Portsmouth, Ohio, U.S.A.

(*Received* 16 *May* 1957)

Abstract—A motor-driven arc-spark stand for emission spectrography is described. The associated control circuit provides push-button or semiautomatic positioning of the electrode carrying arms, including auto-monitoring of the arc gap. Push-button or automatic opening and closing of the electrode holding jaws is also available. The mechanical design is based upon the stand developed at Iowa State College.

Introduction

Our constant efforts to relieve analysts of routine mechanical operations wherever possible, have led to the development or modification of several basic components of laboratory instrumentation. A system providing semiautomatic arc-gap control was recently described [1]. To utilize this system efficiently and to provide further mechanization of operation, a new excitation stand has been designed and built using the geometrical proportions of the stand developed at Iowa State College [2]. The advantages of the basic design are versatility, accessibility, and ease of cleaning. In the redesigned version, manually operated knobs and linkages formerly in the base of the stand are eliminated. The stand is light, weighing only 22 lb. Electric motors are provided to drive the electrode arms up and down, and to open and close the jaws.

VOL. 12 1958

Features

Manually operated push-button or toggle-switch preselection with automatic follow-up make possible the following controlled actions:

(1) The vertical positions of the electrode carrying arms can be changed any time by push-button control.
(2) Burning electrodes can be automatically repositioned to maintain the proper arc gap. This feature is provided at a predetermined time after the start of excitation. The rapidity of this movement is less than that of Action (1) as explained under "Dual-Speed Arm Drive."
(3) Either or both of the electrode arms can retreat automatically from their gapped position to a limit position at the end of an excitation period.
(4) The jaws of the electrode arms can be opened at any time by push-button control.
(5) Both electrodes can be released automatically from their holding jaws at the end of an excitation period.

Design and construction

Commercially adapted models of the Iowa State College stand were built for use

* This work was performed under contract AT-(33-2)-1 with the United States Atomic Energy Commission.
† Present address: National Spectrographic Laboratories Inc., Cleveland, Ohio.

with the spectrographs operated in the Goodyear Atomic Corporation Laboratories. Unfortunately, the mechanical compromise necessitated by decreased optical bench height reduced operating ease and the clearances in the stand. It was necessary to remove all operating components from the space between the optical bench and the floor of the stand chamber to provide the desired range of movement for the bottom electrode arm.

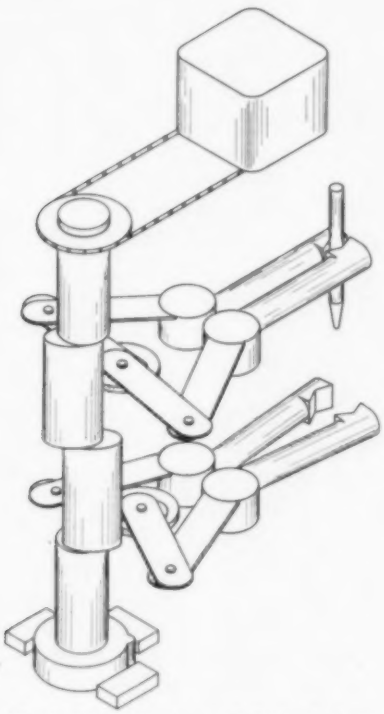

Fig. 1. Cam operator and electrode jaws.

Motors to raise and lower the electrode arms are mounted on the vertical shafts of the electrode arm screws. A gain in constructional simplicity results from the direct coupling of these motors. The cam-driving motor for opening and closing the jaws is mounted well forward on the stand. This keeps the center of gravity of the stand between the ways of the optical bench. A roller link drive connects the motor shaft to the cam (Fig. 1).

The stand is designed for the lower electrode to be at ground potential. This situation is advantageous when using auxiliary electrical equipment in connection with the excitation (e.g. motor to drive rotating electrode), since such a device does not have to be insulated electrically from the discharge. The stand may be used, however, with a source requiring two power leads by adding another input connection directly below the one shown in Fig. 2. A safety switch and magnetic door latch are incorporated in the design. A 110 V outlet is provided within the excitation chamber to power the accessory equipment. This outlet is capped when not in use.

Elaborate mechanisms as used in commercial stands for shifting the electrodes laterally, either for alignment or during excitation, are not provided. Since the optical path of a spectrograph is predetermined and fixed, alignment of the electrode axis is designed and fabricated to the accuracy required. Arc wandering, for which some operators attempt to compensate by constantly shifting the light source, can be dealt with optically. The back and side toward the spectrograph are easily removed for cleaning, or for introduction of unusual samples (Fig. 3).

The removable exhaust stack is located so that vapors travel away from the direction of useful light propagation, in order to minimize self-absorption. Connections to the back of the stand are avoided to reduce optical-bench torque. Operation of the internal mechanism is observed through the transparent plastic rear panel.

The stand is clamped to the optical bench by a continuous bar under the front edge and a screw at the rear. The moment of the stand is such that no force acts on the screw contact. The screw also prevents undesired movement of the stand along the optical bench.

A system permitting the pre-excitation alignment of the electrodes is provided. An integral-lens, miniature lamp projects a shadow image of the electrodes onto a translucent area of the cover glass for the Polaroid viewing port. Although this simple projection system is inoperative after excitation begins, further gap monitoring is a function of the automatic monitoring system.

An initial model of the redesigned stand provided individual jaw opening action, and a two-part, single-axis cam which was rotated by solenoids located at the top and bottom of the cam. Either or both of the electrode holding jaws could be opened at any time. The open period of their cycle was adjustable for a tenth of a second to infinity. This design was not adopted since the results obtained did not justify the complex electrical circuitry required for the large differential between starting and holding torque. The present motor-driven, single-cam design [3], which has a simple and reliable control circuit for the motor, relinquishes only the ability to open the jaws simultaneously.

VOL. 12 1958

Operation

Manual control of arm position

Fig. 4 shows a circuit diagram for the stand. Motor M_1 raises and lowers the top electrode arm under push-button control. Switch S_{11} when actuated energizes relay R_8 whose contact R_{8B} reverses position, releasing the d.c. brake on motor M_1 and causing it to drive in the proper direction to raise the arm. Switch S_6 when actuated energizes relay R_5 whose contact R_{5B} reverses position releasing the d.c. brake on M_1 and causing it to drive in the direction which lowers the arm. Motor M_2 drives the bottom electrode arm and is similarly controlled for raising by S_7 with R_7 and for lowering by S_{12} with R_9.

Automatic monitoring

Auto-monitoring is based upon automation of the functions of switches S_6 and S_7 which control the driving of the electrode arms toward the optic axis. The electrodes are driven towards the axis until an image of their incandescent tips

L.
2
58

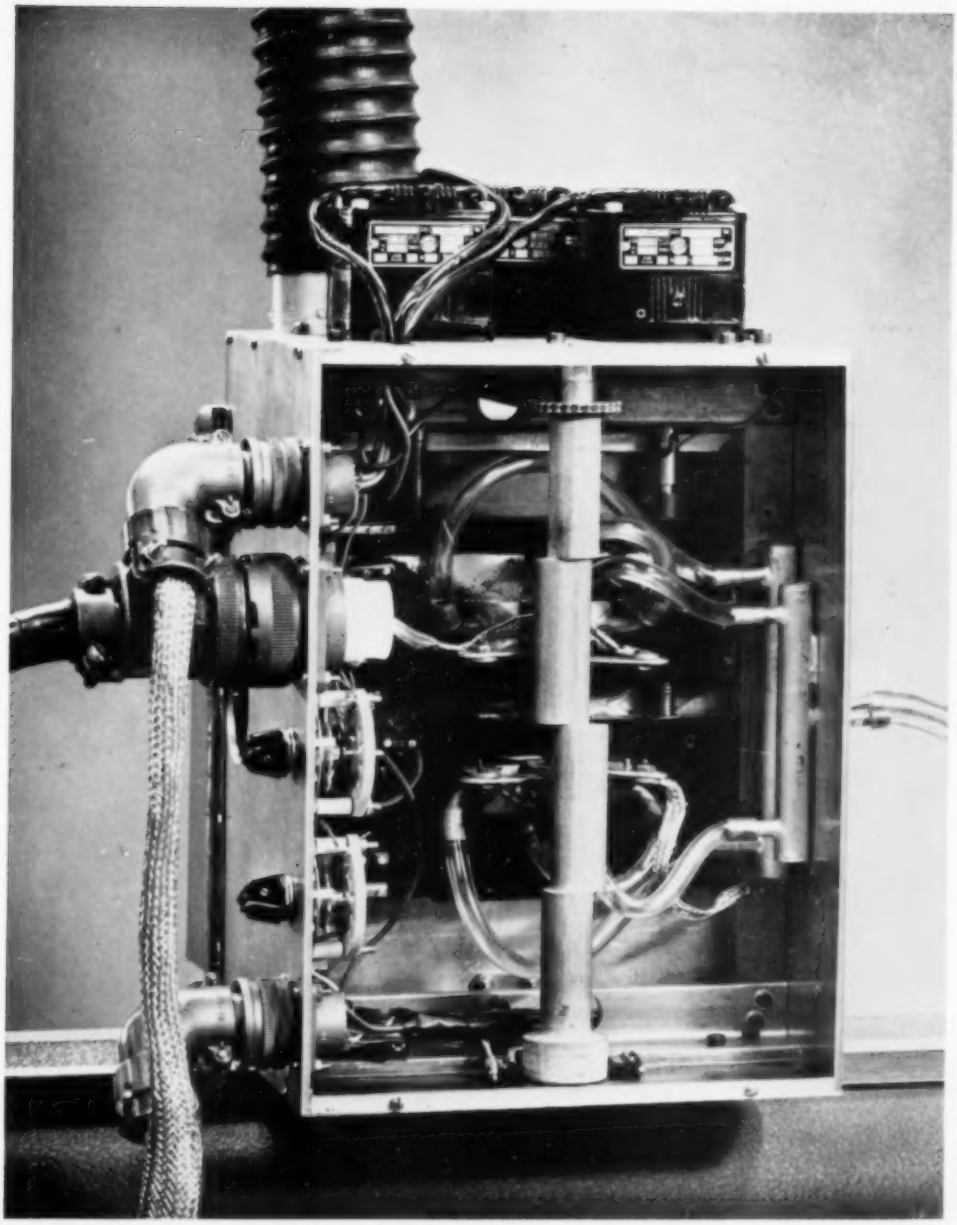

Fig. 2. Rear view of mechanized stand.

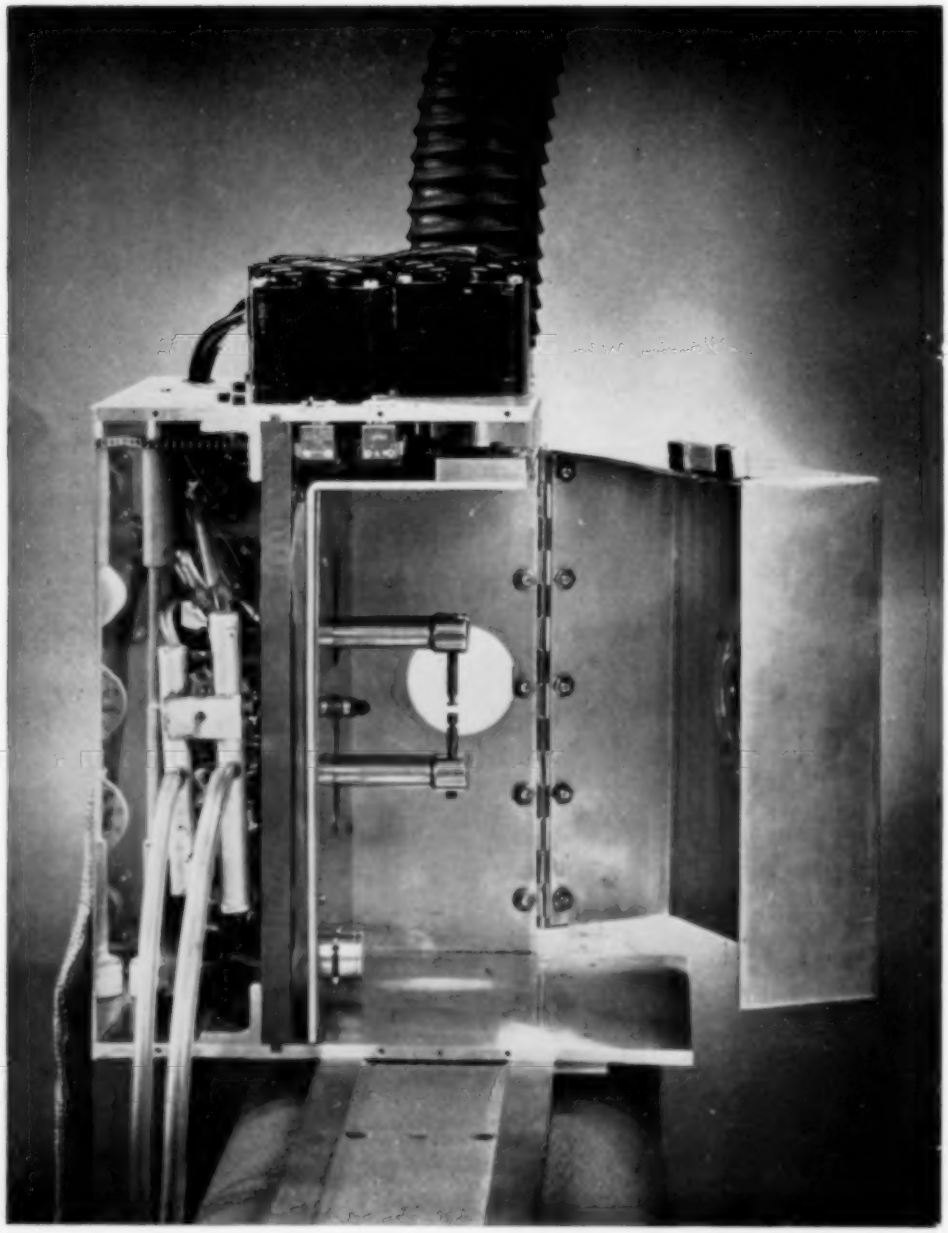

Fig. 3. Side view of mechanized stand.

VOL.
12
1958

falls upon the phototransistors. A cylindrical lens with its axis horizontal produces the image of the excitation gap without horizontal detail. Such an image eliminates the need for precise registration of the electrode tips with respect to the phototransistors.

Automatic control with this monitoring scheme is not possible until the electrode tips are incandescent. Premature attempts at control are prevented by time delay relay R_2 which receives a signal from the power source during the period of excitation. This signal is fed through switches S_1 and S_2 which must be closed when the gap is to be automatically monitored. At a predetermined time after R_2 is energized, contacts R_{2A} and R_{2B} close permitting contacts R_{3A} and R_{4A} to operate relays R_5 and R_7 which control the driving of the upper and lower electrode arms toward the optic axis.

Considering only the upper arm, contact R_{3A} while closed causes the upper electrode arm to be lowered by energizing R_5. As the glowing electrode tip descends, its image rises to present a band of infrared radiation to the phototransistor PT_1. When the photosensitive area of the transistor is filled with radiation, its conduction increases and it actuates relay R_3. Contact R_{3A} then opens and M_1 stops. As the electrode vaporizes, its image moves and R_3 is de-energized, closing R_{3A} which restarts M_1 lowering the upper electrode until the phototransistor again is satisfied. Transistor PT_2 with relay R_4 similarly controls the lower electrode arm.

Switches S_3, S_4, and S_5 limit the movement of the arms toward the optic axis. Switch S_4 limits the lowest position of the top arm while S_5 limits the highest position of the bottom arm. Since these limiting positions have an overlap area, S_3 is incorporated to prevent the arms from jamming together.

Automatic back-off

A signal pulse from the source unit, upon termination of an exposure, momentarily operates relay R_1. The circuit to R_8 is completed when R_{1A} closes, if toggle switch S_{10} is positioned (closed) for automatic back-off of the upper arm. R_8 also starts M_1 and, in closing its contact R_{8A}, locks the relay to the power line. Therefore, M_1 raises the upper electrode arm until limit switch S_8 opens. This cuts off R_8 and the motor stops. Toggle switch S_{10} also has a momentary position obtained manually, by which it can initiate the drive-away of the upper arm independent of the operation of R_{1A}. The back-off of the lower arm is similarly controlled by the circuit section involving R_{1B}, R_9, S_{13}, and S_9.

A new limit switch circuit provides preset, adjustable limiting positions for this feature. The limits are set to suit the electrode dimensions of a particular technique or to suit the operator's preference. S_8 and S_9 represent, respectively, the limit switches for the highest permitted position of the top electrode arm and the lowest permitted position of the bottom electrode arm. Switches S_8 and S_9 are, however, not as simple as they are diagrammed. Each switch is a combination of a rotary selector switch and a special shorting finger device (Fig. 5) which is selectively actuated by the position of the electrode holding arm slide. The circuit is successively completed, as represented by S_8, when the roller affixed to the place carrying the electrode arm travels across the separate fingers of the shorting device. The rotary selector switch can open the circuit to any individual finger.

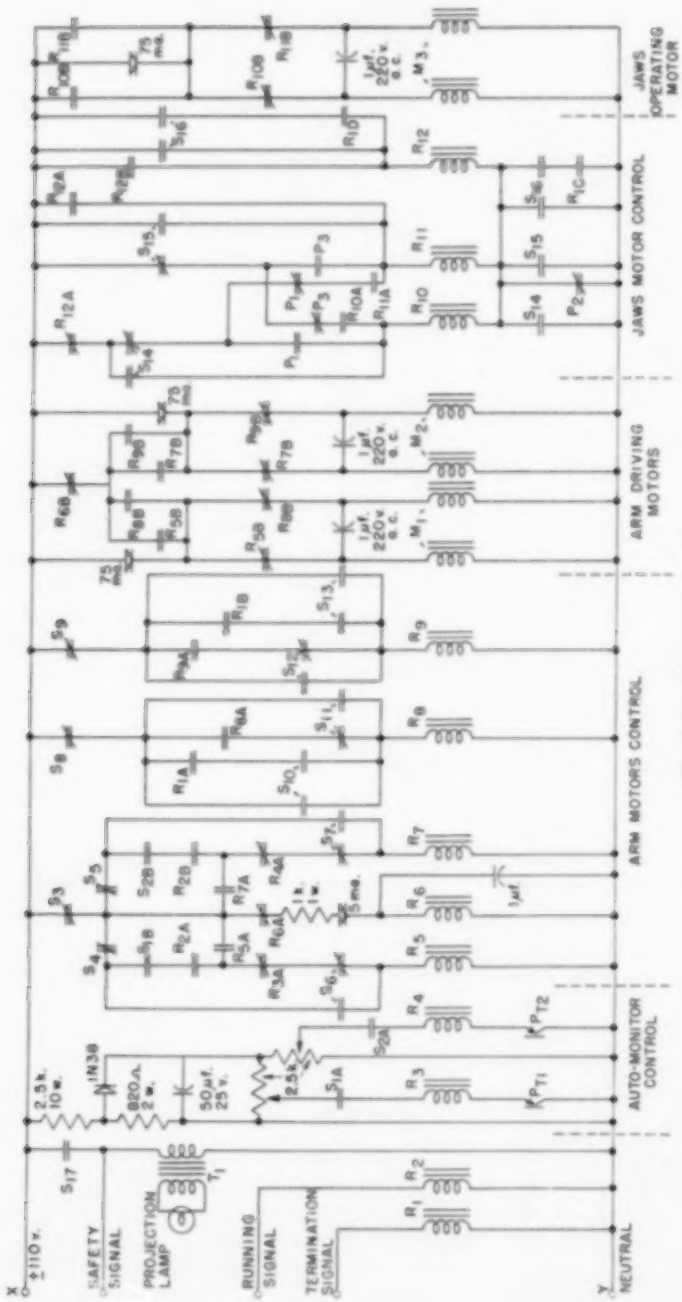

Fig. 4. Stand control circuit.

VOL. 12 1958

Components

Switch	*Function*	*Specification*
S_1	Set-up auto-monitoring of top electrode	DPST toggle
S_2	Set-up auto-monitoring of bottom electrode	DPST toggle
S_3	Limit approach of electrode arms to one another	SPSTNC, pin actuated
S_4	Limit lowest position of top electrode arm	SPSTNC, pin actuated
S_5	Limit highest position of bottom electrode arm	SPSTNC, pin actuated
S_6	Cause top electrode to descend	SPDT, push button
S_7	Cause bottom electrode to raise	SPDT, push button
S_8	Limit highest position of top electrode arm	SPSTNC, pin actuated
S_9	Limit lowest position of bottom electrode arm	SPSTNC, pin actuated
S_{10}	Set-up or start drive of top arm to high limit	SPDTCO, toggle
S_{11}	Cause top electrode to raise	SPDT, push button
S_{12}	Cause bottom electrode to descend	SPDT, push button
S_{13}	Set-up or start drive of bottom arm to low limit	SPDTCO, toggle
S_{14}	Cause top electrode holding jaws to cycle through open position	DPDT, push button
S_{15}	Cause bottom electrode holding jaws to cycle through open position	DPDT, push button
S_{16}	Set-up or cause both electrode holding jaws to cycle through open position	DPDTCO, toggle
S_{17}	Safety switch for stand door	SPSTNO, pin actuated
P_1	Signal opening of bottom jaw	SPDT, pin actuated
P_2	Register "home" position of jaw opening cam	SPSTNO, pin actuated
P_3	Signal opening of top jaw	SPDT, pin actuated
Relay		
R_1	Transfer excitation termination signal	4 PSTNO, 110 V a.c.
R_2	Transfer excitation signal after time delay	DPSTNO, 110 V a.c.
R_3	Transfer electrode position signal for top electrode	SPSTNC, high sensitivity
R_4	Transfer electrode position signal for bottom electrode	Close differential, 8 kΩ, 0·5 mA.
R_5	Control lowering of top electrode arm	DPDT, 110 V a.c.
R_6	Provide dual-speed feature	DPSTNC, 6·5 kΩ, 2 mA.
R_7	Control raising of bottom electrode arm	DPDT, 110 V a.c.
R_8	Control raising of top electrode arm	DPDT, 110 V a.c.
R_9	Control lowering of bottom electrode arm	DPDT, 110 V a.c.
R_{10}	Control opening of top electrode holding jaws	DPDT, 110 V a.c.
R_{11}	Control opening of bottom electrode holding jaws	DPDT, 110 V a.c.
R_{12}	Control successive opening of both electrode holding jaws	DPDT, 110 V a.c.
Motor		
M_1	Drive top electrode arm	1/1500 h.p. integral gear speed reducer 2 winding, capacitor run
M_2	Drive bottom electrode arm	
M_3	Drive jaw operating cam	
Phototransistor		
PT_1	React to radiation	Germanium NPN junction
PT_2	React to radiation	Germanium NPN junction

Key: DP.....Double Pole SP.....Single Pole DT.....Two Way ST.....One Way CO.....Centre Off NC.....Normally Closed NO.....Normally Open

When this is done, the circuit of S_8 is effectively opened as the roller advances to the particular finger involved. The limiting position to which the arm can be raised is therefore dependent upon the setting of the selector switch. The six separate fingers, and positions, are about 6 mm apart.

Dual-speed arm drive

A special feature of the new stand is the dual-speed drive of the electrode arms. It is desirable, particularly for *automatic back-off*, that the vertical movement of the electrode carrying arms be quite rapid. Manual push-button control of the

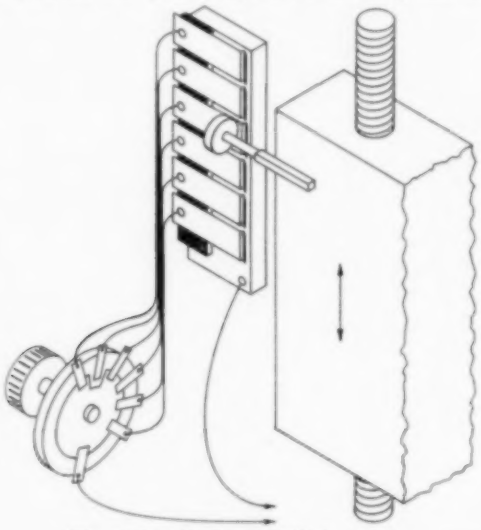

Fig. 5. Detail of special limit switch.

movement of the arms toward the optical axis is also practical with rapid drives. For the automatic repositioning of electrodes as they burn away, however, the speed of the drive should be slower than for the other two situations.

To satisfy all of these conditions, a drive motor fast enough to give rapid motion of the arms is used. Special circuitry then provides for slower operation during auto-monitoring.

The operation of relay R_5 or R_7 through R_{5A} or R_{7A}, energizes the network composed of contact R_{6A}, the 1 kΩ resistor, the 5 mA rectifier, the 1 μF capacitor and relay R_6. The components are arranged to cause R_6 to oscillate. Therefore, contact R_{6B} is not constantly closed but is open for a percentage of time which is determined by the component values in the oscillating network. The fact that R_{6B} is closed only part of the time results in a slower output speed for M_1 without a loss in torque. Relay R_6 is isolated except when auto-monitoring of one or both electrodes is desired. The slow speed can be over-ridden at any time to lower the top electrode, by operation of push-button switch S_6.

Jaw opening

The jaws of the top electrode arm are controlled by push-button switch S_{14};

VOL. 12 1958

when this switch is operated, it energizes relay R_{10} which removes the d.c. brake and applies power to the motor M_3 which drives a cam. This cam has sections which operate the jaw mechanisms (Fig. 1 and 2). It also has a switch section actuating switches P_1, P_2, and P_3. Normally closed P_2 is open in the "home" position of the cam. As M_3 drives in the direction required to open the top jaw the contacts of P_2 are closed. As R_{10A} closes upon initial excitation of R_{10}, R_{10} stays locked to the line although S_{14} is actuated only momentarily. Motor M_3 drives the cam until the top jaws are completely open. At this point switch P_3 is actuated by the switch section of the cam.

The normally closed side of P_3 opens to release relay R_{10}. Simultaneously the open side of P_3 closes to energize relay R_{11}. The contacts of R_{11} serve to keep it energized and to drive M_3 in the direction reversing the cam, and closing the top jaws. When the jaws are closed, the cam is in its home position and P_2 opens releasing R_{11} and stopping the motor. The opening of the bottom jaws is controlled by S_{15} in a manner analogous to the operation of the top jaws by S_{14}.

Automatic electrode dumping

Provision is made for successive opening of both electrode holding jaws for the purpose of dumping used electrodes, which fall into a steel tray. Switch S_{16}, with a center-off position, has a momentary position (1) which can initiate the dumping action and a set-up position (2) for carrying out the action upon termination of an excitation period.

Relay R_{12} will be energized when S_{16} is in the set-up position (2) and R_{1C} and R_{1D} closes after termination of excitation. This isolates R_{10} and brings in R_{11} which starts the cam-driving motor M_3. The closure of P_2 as the cam leaves its home position keeps R_{11} and R_{12} operating. The cam revolves a full revolution, successively opening the lower and upper arm jaws. P_1 and P_3 do not interrupt the cycle because they are removed from control by R_{12B}. Upon completion of a full revolution the cam is at its home position, opening P_2 and releasing R_{12} and R_{11}. Switch S_{16} thrown to its momentary position can initiate the same action at any time.

Skilled operators also use this action for loading electrodes. After used electrodes have been dumped and the jaws cleaned the operator again actuates the "dump" switch. As the upper and lower jaws successively open, the upper and lower electrodes are loaded into position for the next exposure.

Summary

The completely mechanized arc-spark stand described in this article increases the efficiency of spectrographic operators by reducing operational effort and complexity. The associated control circuit which permits elaborate function from simple prime movers is reliable and long-lived. The feature of semiautomatic arc-gap monitoring improves the reproducibility of excitations.

References

[1] Owen L. E. *J. Appl. Spectr.* 1956 **10** 203.

[2] Weber J., Heidel R. H., Kehres P. W., Cook H. D. and Fassel V. A. *Spectrochim. Acta* 1953 **5** 345.

[3] Borts D., Weber J. and Fassel V. A. Unpublished work on single-cam actuation.

Spectrochimica Acta, 1958, Vol. 12, pp. 12 to 16. Pergamon Press Ltd., London

Infrared absorption of solid state *n*-paraffins—relationship to crystalline type

J. M. Martin, Jr., R. W. B. Johnston and M. J. O'Neal
Shell Oil Company, Houston Research Laboratory, P.O. Box 2527, Houston, Texas, U.S.A.

(*Received* 9 *May* 1957)

Abstract—A number of pure *n*-paraffins (C_{17}–C_{36}) have been studied in the 650–800 cm^{-1} infrared region. Differences were obtained between paraffins of odd and even carbon numbers at temperatures below that of the solid phase transitions. Spectra of the odd carbon number *n*-paraffins below C_{26}, and both odd and even carbon number *n*-paraffins above C_{26} are characterized by a splitting of the 721 cm^{-1} band into a 718–728 cm^{-1} doublet. The even carbon number *n*-paraffins below C_{26} are characterized by a single absorption band at 715 cm^{-1}. The observations are related to other published information concerning crystal structures and infrared absorptions of paraffins and long hydrocarbon chain polymers.

Introduction

The infrared absorption doublet occurring near 725 cm^{-1} in the spectra of polyethylene and other polymers containing long hydrocarbon chains has been studied extensively [1–5]. A similar doublet occurring in the spectra of commercial paraffin waxes at room temperature has been studied by the authors, the results of which will be published elsewhere [6]. In the course of an investigation of commercial waxes, the authors had occasion to examine several pure normal paraffins. The results of these studies supplement information obtained from more extensive studies [2–5, 7] of the basic crystal structures involved.

Experimental

Early studies were carried out on a Beckman IR-2 spectrophotometer. These data were supplemented by additional studies carried out on a Perkin–Elmer Model 21 double beam instrument. Limited use was also made of X-ray diffraction techniques.

Spectra of both melts and solids were obtained in a specially designed high-temperature cell described elsewhere [6]. The design was such that spectra could be obtained at any desired temperature. The temperature was measured with an iron–constantan thermocouple connected to an *L* and *N* portable potentiometer. The thermocouple was placed in direct contact with the sample. The samples were introduced as melts into the preheated cell from a heated hypodermic syringe. In some instances it was desirable to obtain spectra below the instrument temperature. This was accomplished by blowing dry nitrogen vapors through a coil (immersed in a liquid nitrogen bath) and into the sample cell compartment of the infrared spectrophotometer.

Results

Several pure normal paraffins, including some of both the odd and even carbon number paraffins, were examined in the 650–800 cm^{-1} region. When examined

VOL. 12 1958

as liquids, or in the crystalline form occurring between the melting and transition temperature, all of the samples exhibited the characteristic single absorption band at 721 cm^{-1}. When the temperature of the sample was decreased below the temperature at which the solid phase transition occurred, differences in the infrared spectra were observed.

The spectra of the odd carbon number normal paraffins below C_{26} and all of the normal paraffins above C_{26} that were examined (C_{17}, C_{21}, C_{27}, C_{28}, C_{30}, C_{36}) were characterized by a splitting of the 721 cm^{-1} band into a 718–728 cm^{-1} doublet.

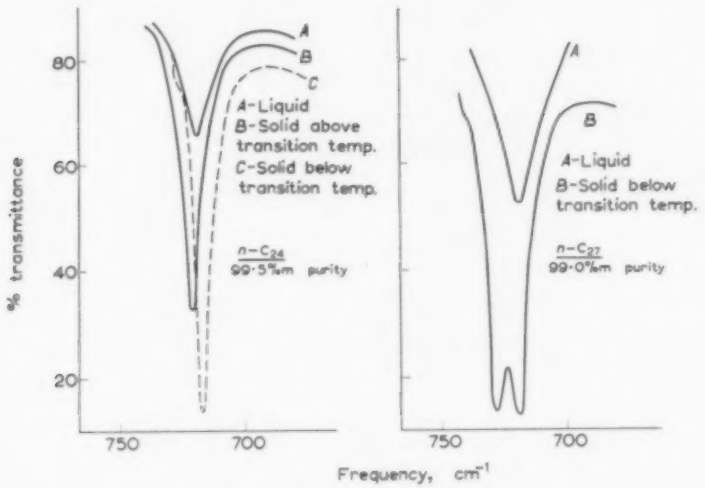

Fig. 1. Effect of temperature on infrared absorption of *n*-paraffins.

The even carbon number normal paraffins below C_{26}, (C_{16}, C_{22}, C_{24}) were characterized by a single absorption band in this region; however, the band is shifted from 721 cm^{-1} to 715 cm^{-1}.

These differences are exemplified by the spectra of C_{24} and C_{27} normal paraffins shown in Fig. 1. The actual temperatures were not recorded in these runs. However, the spectra of the low-temperature crystalline forms were obtained well below the transition temperatures.

Discussion

The differences observed in the spectra of the normal paraffins are attributed to differences in crystal structure. Such differences are known to occur in infrared spectra as a result of polymorphic crystalline phase transitions [1, 2, 4, 8]. The normal paraffins have also been reported to crystallize into several different crystalline configurations [9, 10]. X-ray data showed that the absorption doublet at 718–728 cm^{-1} appears in the spectra of commercial paraffin waxes with the formation of an orthorhombic crystallite. On the other hand, a sample of a C_{30} normal paraffin, which was identified as a monoclinic crystallite by X-ray analysis, was also characterized by an identical absorption doublet at 718 and 728 cm^{-1}.

These results are in agreement with the findings of Krimm *et al.* [3] who concluded that the polarization characteristics of the doublet for these crystalline types were the same.

Mazee [11] has reported the crystal structure of the C_{24} normal paraffin to be triclinic in the low-temperature stable form. More recently Smith [12] has reported a similar structure for C_{20} and C_{22} normal paraffins. Thus, the occurrence of a single infrared absorption band at 715 cm^{-1} is believed to result from the more densely packed triclinic crystalline configuration. Chapman [13] has reached similar conclusions in his study of the polymorphism of glycerides.

These results appear to be in agreement with Stein and Sutherland's conclusions [4] that the splitting of the absorption band at 721 cm^{-1} results from interaction between methylene groups as changes in the unit cell dimensions cause adjacent molecules to be brought closer together. If the splitting of the 721 cm^{-1} band can be explained by such interaction in the cases of orthorhombic and monoclinic crystallites, then it does not seem unreasonable to expect an enhancement of such effects in the more densely packed triclinic structure. Such increased interaction may explain the shift of the low-frequency component to 715 cm^{-1}, as well as the complete disappearance of the high-frequency component.

It is interesting to compare the results obtained in this study, with regard to the actual frequencies, to those predicted from theoretical considerations. It has been predicted from theory [7] that both components of the doublet should be at a higher frequency than the vibrational mode of the isolated molecule. Our observations indicate that the frequencies of the doublet actually bracket the frequency of the single band observed in the melt. These observations are in agreement with those of Krimm *et al.* [3].

VOL. 12 1958

It has been pointed out by Templin [14], by Schaerer *et al.* [15] and by Smith [12] that the addition of a few per cent of neighbouring homologs as impurities will convert triclinic and monoclinic forms into an orthorhombic crystalline type. An infrared study of the effect of contaminants on the crystal structure of pure normal paraffins has been carried out, the results of which support these conclusions. However, from the infrared data alone it would be presumptuous to conclude what the resulting crystal structure might be.

C_{22} and C_{24} normal paraffins were blended to obtain mixtures for testing the effects of mixing. Use of these two even carbon number normal paraffins is of special interest since each shows the single 715 cm^{-1} absorption band below the transition temperature. Presented in Fig. 2 are spectra of blends to illustrate the effects of adding varying amounts of C_{22} and C_{24} normal paraffin. The addition of only 4 per cent wt. of C_{22} results in the occurrence of the high-frequency component though it is of much lower intensity than the low-frequency band. The increase in intensity of the high-frequency component with increasing concentration of C_{22} is also observed. The two bands reached equal intensity at 15 per cent wt. of C_{22} with a further increase to 50 per cent wt. producing no additional change.

Of considerable interest also is the fact that the position of the low-frequency component migrates from 715 cm^{-1} as the concentration of C_{22} is increased. This effect can best be seen in Fig. 3 where the degree of band splitting is observed to be dependent upon both concentration and chain length of the minor component.

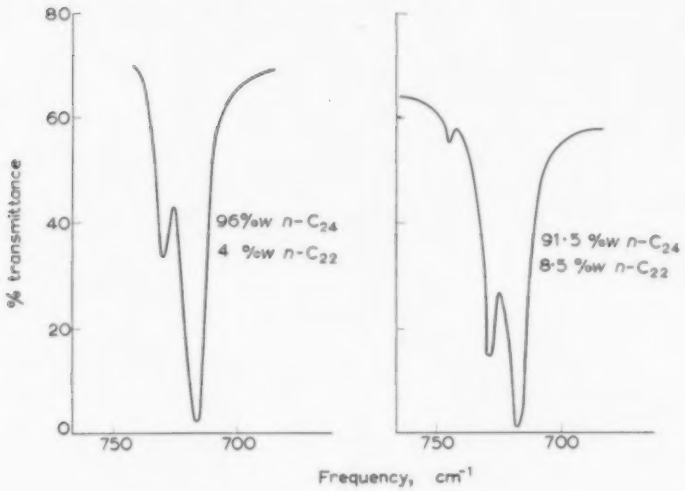

Fig. 2. Infrared spectra of *n*-paraffin mixtures.

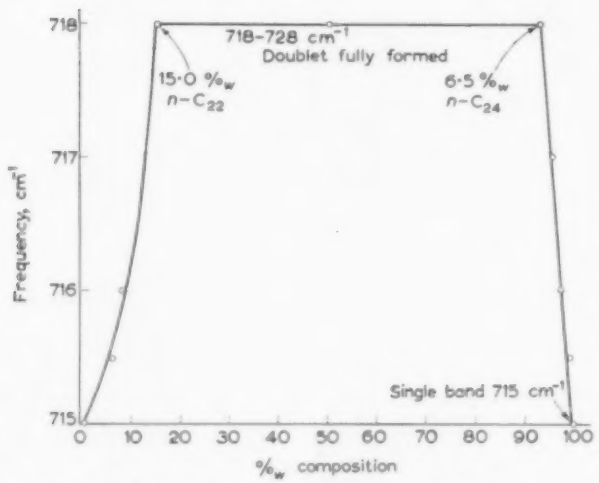

Fig. 3. Effect of mixing on infrared absorption of *n*-paraffins.

Similar observations of the effect of concentration on degree of band splitting have also been reported by Krimm *et al.* [3].

The effect of chain length was further emphasized by blending <5 per cent of C_{27} in C_{24}. The fully formed doublet was observed with both components exhibiting equal intensity at 718 and 728 cm^{-1}. These results obtained from increasing chain length may indicate a folding of the longer chain ends into the interstices of the crystal lattice in such a way as to prevent close packing of the unit cell. Smith [16] offers a similar explanation for results obtained from X-ray studies.

Acknowledgements—The authors wish to acknowledge the help of the Shell Development Company for the pure normal paraffins obtained from the Emeryville Research Laboratory. Acknowledgement is also made for X-ray diffraction data obtained at the Shell Oil Company, Wood River Research Laboratory.

References

[1] Chapman D. *Nature, Lond.* 1955 **176** 216.
[2] Elliott A., Ambrose E. J. and Temple R. B. *J. Chem. Phys.* 1948 **16** 877.
[3] Krimm S., Liang C. Y. and Sutherland G. B. B. M. *J. Chem. Phys.* 1956 **25** 549.
[4] Stein R. S. and Sutherland G. B. B. M. *J. Chem. Phys.* 1954 **22** 1993.
[5] Tobin M. C. and Carrano M. J. *J. Chem. Phys.* 1956 **25** 1044.
[6] Martin J. M., Johnston R. W. B., Cannon H. J. and O'Neal M. J. To be published.
[7] Stein R. S. *J. Chem. Phys.* 1955 **23** 734.
[8] Kendall D. N. *Analyt. Chem.* 1953 **25** 382.
[9] Gray C. G. *J. Inst. Petrol.* 1943 **29** 226.
[10] Koolvoort J. *J. Inst. Petrol.* 1938 **24** 338.
[11] Mazee W. M. *Rec. Trav. Chim. Pays-Bas* 1948 **67** 197.
[12] Smith A. E. *J. Chem. Phys.* 1953 **21** 2229.
[13] Chapman D. *J. Chem. Soc.* 1957 **III** 2715.
[14] Templin P. R. *Industr. Engng Chem. (Industr.)* 1956 **48** 155.
[15] Schaerer A. A., Busso C. J., Smith A. E. and Skinner L. B. *J. Amer. Chem. Soc.* 1955 **77** 2017.
[16] Smith A. E. Private communication.

VOL. 12 1958

Spectrochimica Acta, 1958, Vol. 12, pp. 17 to 33. Pergamon Press Ltd., London

Infra-red spectra of the benzene carboxylic acids*

FELIPE GONZÁLEZ-SÁNCHEZ
Instituto Nacional del Combustible, Sección de Zaragoza, Zaragoza, Spain

(*Received* 10 *September* 1957)

Abstract—The infra-red absorption spectra of the 12 benzene carboxylic acids and their 4 hydrates have been measured between 2–15 μ as mulls in Nujol. The spectra have been analysed and the principal bands related to particular molecular groupings. The completeness of this series of spectra makes it interesting to study some correlations between molecular structure and infra-red spectra, in particular (a) COOH bands and (b) vibrations associated with the benzene system as a function of the type of substitution. The spectra of the 12 anhydrous acids do not exhibit any free O—H absorption, indicating that there exists in the acids a high inter- and intra-molecular association. The spectra of the hydrates show these compounds to have hydrogen bonds between the C=O groups and the water of hydration. Examination of the spectra shows that dimeric COOH gives rise to 5 bands between 2 and 15 μ (5000–665 cm^{-1}). The COOH band near 900 cm^{-1} disappears in the hydrates. This seems to confirm that association in the latter takes place through the water molecules and, also, that it appears advisable to assign this absorption to the out-of-plane O—H deformation vibration in the dimeric ring. This series of acids constitutes an example where existing correlations for the determination of the type of benzene substitution do not apply in full. The electrophylic COOH group is regarded as responsible for the deviations. The spectra are highly specific and make possible a ready characterization of any acid. This should prove useful in any analytical work involving these acids, particularly the higher members.

Introduction

IN view of the scientific and present, as well as potential, commercial importance of the benzene carboxylic acids it was thought of interest to undertake a systematic study [1] to determine for both acids and their methyl esters properties hitherto unknown or not well defined, which in addition to increasing our knowledge of these compounds, could be used in the future for their better characterization. Data on these compounds is so meagre that apart from melting points practically no other important, analytical or physical properties are known for the acids and esters higher than the difunctional ones. Furthermore, characterization of the acids by their melting points is unreliable because the latter are not definite [1], except that of benzoic acid. Thus, as it was found in the course of an investigation of the acid mixtures obtained by oxidation of coal [2], analyses of these compounds, individually or in mixtures, require, to make it both accurate and rapid, a knowledge of properties which still is not available. In a recent paper [1] the preparation in a high state of purity of the 9 benzene carboxylic acids giving solid, neutral methyl esters as well as of these esters was described, and melting points for the esters were given. The purpose of the present paper, second in said study, is to report the infra-red spectra of the 12 benzene carboxylic acids and their

* Taken in part from a portion of a thesis submitted in partial fulfilment of the requirements for the Dr.Sc. degree at the University of Zaragoza, July 1955. Presented at the XIV International Congress of Pure and Applied Chemistry (Organic Chemistry), Zurich, 21–27 July, 1955.

4 hydrates, measured on high purity samples from 2 to 16 μ, as Nujol mulls.

A specific spectrum has been obtained for each of the benzene carboxylic acids. This will permit a ready characterization of any of the compounds which at present is very difficult to accomplish, especially on a micro scale. Inasmuch as these spectra form one of the few, if not the first, complete series which have appeared on infra-red spectra of the twelve possible substituted benzene derivatives with a single substituent other than an alkyl radical, they are also of value to study different correlations between infra-red spectra and molecular structure. Although earlier work on infra-red spectra of carboxylic acids of all types is relatively abundant [3], little is to be found in it on the benzene carboxylic acids as a whole. While more or less complete spectra of benzoic and *o*- and *p*-phthalic acids have been discussed in some publications [4–6], the author does not know of any published infra-red spectra of benzene carboxylic acids higher than the dibasic ones, apart from the inclusion of mellitic acid in a collection of spectra [7].

Experimental

All spectra were automatically recorded from 2 to 16 μ as Nujol mulls, with the Baird Model A infra-red spectrophotometer of the Mellon Institute, Pittsburgh, U.S.A., equipped with a rock salt prism. The positions of some bands were fixed more accurately by measuring some regions of the spectra with the D-209 Hilger spectrophotometer of the Instituto de Optica Daza Valdes, Madrid, operated as a single beam instrument and calibrated with ammonia, benzene, water and CO_2 bands and polystyrene films. The author is indebted to Dr. A. HIDALGO for the latter measurements. Wavelengths in the 1725–660 cm^{-1} (5·8–15·15 μ) range are believed to be accurate to about $\pm 0{\cdot}02$ μ, although for broad or weak bands the error of judging the centre may exceed this. Bands in the region above 1800 cm^{-1} are possibly less accurate.

The compounds used were high purity samples. Characteristics and method of preparation of *iso*phthalic (1–3), terephthalic (1–4), hemimellitic (1–2–3), trimesic (1–3–5), prehnitic (1–2–3–4), mellophanic (1–2–3–5), pyromellitic (1–2–4–5) penta- and mellitic (hexa) acids were described elsewhere [1]. *o*-Phthalic acid was prepared by aqueous hydrolysis of Baker's reagent grade phthalic anhydride (Found: C, 57·72; H, 3·74. $C_8H_6O_4$ requires C, 57·83; H, 3·64 per cent). Trimellitic acid was purified by repeated heatings followed by vacuum distillation of the resulting anhydride [8] and then by repeated crystallization from diluted hydrochloric acid. In total, six successive sublimations and six successive crystallizations were made (Found: C, 51·51; H, 2·88. $C_9H_6O_6$ requires C, 51·44; H, 2·88 per cent). On the basis of methods used and experimental results, it is believed that the prepared samples of the last 2 acids are at least, like the former 9 [1], 99·5 per cent pure. The benzoic acid was a Bureau of Standards certified product, 99·9 per cent pure. The 4 hydrates were obtained from the corresponding pure acids.

Results and discussion

The spectra of the 12 acids and the 4 hydrates are shown in Figs. 1, 2 and 3 as plots of percentage transmittance against wavelength and wave number.

VOL. 12 1958

The positions of the bands, their intensity and suggested tentative assignments are summarized in Table 1. The intensity and shape symbols have the usual meanings, with those likely to cause confusion distinguished as follows: *s* = strong; *sh* = shoulder and *sp* = sharp. The following abbreviations have been used for designating the benzene system vibration frequencies: νC—H (C—H

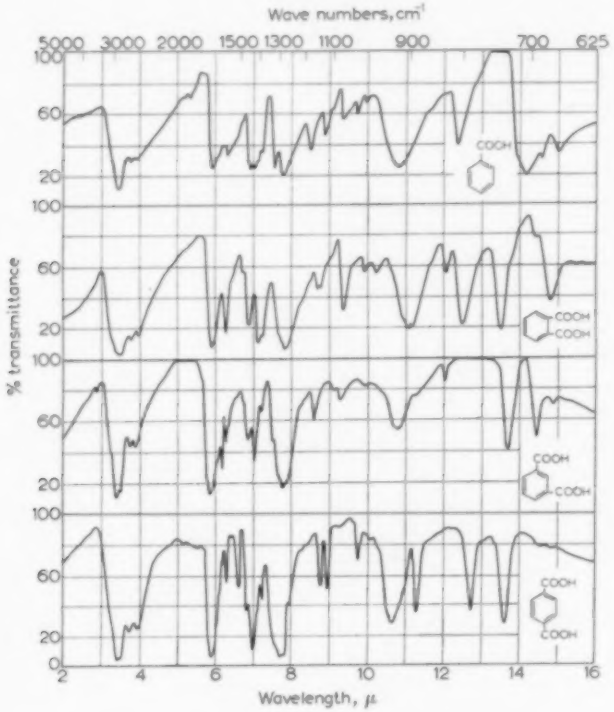

Fig. 1.

stretchings); νC—C (C—C stretchings); βC—H (in-plane C—H deformations); γC—H (out-of-plane C—H deformations); ring (ring breathings); ϕC—C (out-of-plane ring deformations). νO—H (O—H stretchings); νC=O (C=O stretchings) COOH (COOH vibrations); N (Nujol) and *a* (associated) are used for other assignments.

The infra-red patterns show as whole a great deal of fine structure in the range 1700–650 cm^{-1}. In contrast with the relative lack of definition observed for spectra of long-chain fatty acids [9–13], the differences among the spectra of the benzene carboxylic acids, whether isomers or not, anhydrous or hydrates, are marked. This is due mainly to bands associated with the particular type of benzene substitution. It can be concluded that the spectra are specific and will afford a means for the characterization of the acids.

It should be noted that in the molecules of the benzene carboxylic acids there

are present only a benzene nucleus, more or less substituted, and carboxyl groups. This gives some sort of simplicity to the complexity of the compounds, which taken together with the completeness of this series of spectra, makes it interesting

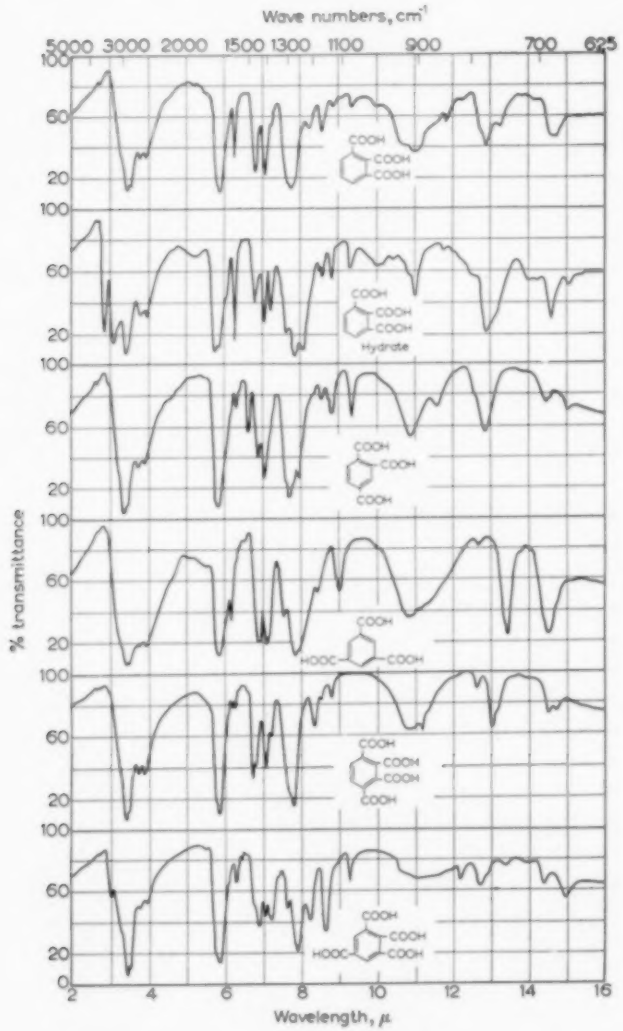

Fig. 2.

to study certain general features associated with structural diagnosis problems; in particular (a) bands due to the COOH group and (b) vibrations associated with the specific type of substitution. With this view in mind an attempt has been made to relate most of the principal bands to particular molecular groupings, as summarized in Table 1 and discussed below under appropriate headings. The

VOL. 12 1958

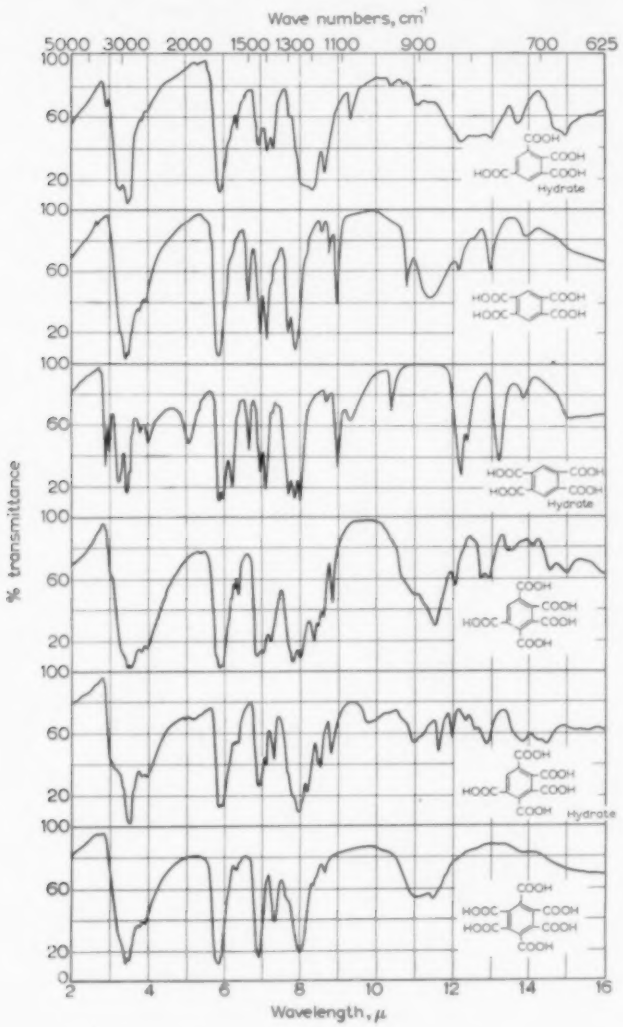

Fig. 3.

assignments made are based on a comparative study of these spectra and data drawn from generalization charts [3, 14–17, 18*], pertinent references therein, literature cited as well as from the author's unpublished spectra of the methyl esters of these acids [19]. Although most of the assignments are believed to be reliable, part of them must be taken as extremely tentative in view of well known difficulties in interpreting the spectra of complex compounds in the region below 1300 cm^{-1}.

* This paper, summarizing and discussing in detail present knowledge on characteristic vibration frequences of substituted benzenes, only became known to the author after completion of the assignments presented, but in view of its thoroughness it has also been considered in the discussion. The abbreviations used by the above authors for the benzene system vibrations have been adopted in the present communication.

Table 1. Infra-red spectra of the 12 benzene carboxylic acids and their 4 hydrates

Mono		1–2		1–3	
cm^{-1}	Assignment	cm^{-1}	Assignment	cm^{-1}	Assignment
2640* *vw*	νO—H *a*	3030† *sh*		2640 *w*	νO—H *a*
2530* *vw*	νO—H *a*	2640 *w*	νO—H *a*	2530 *w*	νO—H *a*
1876 *w*		2530 *w*	νO—H *a*	1689 *vs*	νC=O *a*
1686 *s*	νC=O	1689 *vs*	νC=O *a*	1610 *m, sp*	νC—C
1602 *vw*	νC—C	1592 *s, sp*	νC—C	1585 *m, dp*	νC—C
1582 *w*	νC—C	1492 *w*	νC—C	1502 *vw*	νC—C
1493 *vw*	νC—C	1458 *sh*	*N*	1455 *m*	νC—C *N*
1458 *sh*	*N*	1456 *s*	νC—C	1414 *s, sp*	COOH
1449 *s, sp*	νC—C	1403 *vs*	COOH	1377 *w, sp*	*N*
1420 *s, sp*	COOH	1377 *w, sh*	*N*	1326 *vw, sh*	νC—C
1377 *w*	*N*	1309 *sh*	νC—C	1279 *s*	COOH
1321 *s, sp*	νC—C	1287 *sh*		1205 *sh*	
1287 *vs*	COOH	1282 *vs*	COOH	1161 *m, sp*	βC—H
1212 *sh*		1267 *sh*		1093 *w*	βC—H
1176 *m, sp*	βC—H	1212 *sh*		1073 *m*	βC—H
1127 *m, sp*	βC—H?	1152 *m*	βC—H	1002 *w*	ring
1100 *vw*		1143 *w*	βC—H	928 *s, br*	COOH *a*
1068 *m*	βC—H	1071 *s, sp*	βC—H	885 *w*	γC—H
1050 *sh*		1008 *m*	ring	832 *w*	
1028 *m*	βC—H	978 *m*	γC—H	729 *s*	φC—C
1002 *w*	ring	903 *vs, br*	COOH *a*	689 *s*	
930 *s, br*	COOH *a*	855 *sh*	γC—H?	672 *w*	
858 *vw, sh*		831 *m, sp*			
808 *m*	γC—H	799 *s*			
705 *vs*	φC—C	741 *s*	γC—H		
685 *w*		693 *w*	φC—C		
667 *m, br*		675 *s*			
		645 *vw, br*			

* A mean value is given for these two bands in all acids: 2640 ± 30 cm^{-1} and 2530 ± 30 cm^{-1}.
† This absorption (νO—H *a* + νC—H) is not included in the remaining compounds, although it occurs in all acids as a shoulder at about this position.

COOH *Vibrations*

O—H *stretching vibrations*

Anhydrous acids. None of these compounds shows any indication of free O—H absorption. In the case of benzoic acid and even in that of other non-vicinal substituted acids this is easily understood through the known formation of dimer rings by intermolecular hydrogen bonding association [20–23]. In the case of other higher acids, especially those highly substituted with vicinal groups, it is somewhat difficult to visualize, on steric grounds, a polymerization of such a degree and way as to involve *direct* intermolecular bonding of all the O—H of the molecules, except maybe in some highly symmetrical acids, such as the 1–3–5. This suggests that, in all, the acids are strongly inter- and intra-molecularly

VOL. 12 1958

Table 1 (*continued*)

1–4		1–2–3		1–2–3 Hydrate	
cm^{-1}	Assignment	cm^{-1}	Assignment	cm^{-1}	Assignment
2640 *w*	νOH *a*	2640 *w*	νO—H *a*	3497 *s, sp*	νO—H
2530 *w*	νOH *a*	2530 *w*	νO—H *a*	3436 *sh*	νO—H
1686 *vs*	νC=O *a*	1704 *vs*	νC=O *a*	3226 *s*	νH_2O *a*
1613 *vw, sh*	νC—C	1592 *s, sp*	νC—C	2640 *w*	νO—H *a*
1585 *m, sp*	νC—C	1468 *s*	νC—C	2530 *w*	νO—H *a*
1510 *m, sp*	νC—C	1458 *sh*	*N*	1887 *w, br*	H_2O?
1458 *m, sp*	νC—C *N*	1410 *s, sp*	COOH	1730 *vs*	νC=O
1425 *vs, sp*	COOH	1377 *vw*	*N*	1701 *vs*	νC=O *a*
1377 *w*	*N*	1282 *vs, br*	COOH	1592 *vs, sp*	νC—C
1320 *sh*	νC—C	1210 *w*		1468 *s, sp*	νC—C *N*
1286 *vs*	COOH	1161 *m, sp*	βC—H	1412 *s, sp*	COOH
1253 *sh*		1127 *w*		1377 *s, sp*	*N*
1205 *sh*		1070 *w, sp*	βC—H	1304 *s*	νC—C?
1182 *vw*	βC—H	998 *w*	ring	1269 *vs*	COOH
1135 *m, sp*		922 *s, br*	COOH *a*	1238 *vs*	COOH?
1112 *m, sp*	βC—H	905 *s*	γC—H	1172 *vw*	
1081 *vw*		843 *w*		1163 *m, sp*	βC—H
1021 *m, sp*	βC—H	817 *vw*	γC—H	1130 *m, sp*	
1002 *vw*	ring	784 *w, sh*		1071 *m, sp*	βC—H
990 *vw*	γC—H?	775 *s*	γC—H	996 *w*	ring
935 *s, br*	COOH *a*	755 *m, sh*		982 *w*	
882 *s, sp*	γC—H	725 *w*	ϕC—C	958 *vw*	γC—H
783 *s, sp*		705 *w*		904 *m*	γC—H
735 *s*		683 *m*		847 *w*	
732 *s*	ϕC—C	675 *m*		810 *m, sh*	γC—H
667 *vw*				775 *s*	γC—H
				756 *sh*	
				714 *w*	ϕC—C
				702 *w*	
				683 *m*	
				660 *w*	

bonded and highly dimerized or polymerized and that possibly, as a consequence, there exists in the crystal lattice a special state of forces conferring to all O—H and (C=O) an even bonding character.

On the other hand, all the acids present a broad absorption band which commencing at about 3350 cm^{-1} (3 μ) merges into those of Nujol oil at 2900 cm^{-1} (3·45 μ) and extends to lower frequencies clearly showing a subgroup of weak bands between 2700 and 2500 cm^{-1} (3·7–4 μ). The strongly-bonded hydroxyl is responsible for this broad band. Considering that all these acids and the 4 hydrates exhibit submaxima between 2700 and 2500 cm^{-1} (Table 2), it can be concluded, in agreement with other authors' findings, that the associated O—H . . . O band of the bonded carboxylic acids has a main absorption at about 3000 cm^{-1} (3·3 μ)

Table 1 (*continued*)

1–2–4		1–3–5		1–2–3–4	
cm^{-1}	Assignment	cm^{-1}	Assignment	cm^{-1}	Assignment
2640 *w*	νO—H *a*	2640 *vw*	νO—H *a*	2640 *w*	νO—H *a*
2530 *w*	νO—H *a*	2530 *vw*	νO—H *a*	2530 *w*	νO—H *a*
1698 *vs*	νC=O *a*	1704 *vs*	νC=O *a*	1704 *vs*	νC=O *a*
1582 *w, sp*	νC=C	1608 *m, sp*	νC=C	1600 *vw, sp*	νC—C
1499 *s, sp*	νC—C	1580 *vw, sh*	νC—C	1585 *w, sp*	νC—C
1458 *sh*	*N*	1454 *s, sp*	νC—C *N*	1475 *s, sp*	νC—C
1439 *s, sp*	νC—C	1404 *s, sp*	COOH	1458 *w*	*N*
1408 *s, sp*	COOH	1377 *sh*	*N*	1404 *s, sp*	COOH
1377 *sh*	*N*	1323 *m*	νC—C	1377 *w*	*N*
1286 *vs*	COOH	1274 *vs, br*	COOH	1310 *sh*	νC—C?
1252 *m, sp*		1253 *s*		1276 *vs*	COOH
1200 *sh*		1179 *w*	βC—H	1195 *m, sp*	
1163 *w*	βC—H	1107 *m*		1170 *w*	βC—H
1140 *vw*		997 *sh*	ring	1131 *w, sp*	
1127 *m*	βC—H	922 *s, br*	COOH *a*	922 *m, br*	COOH *a*
1071 *m, sp*	βC—H	880 *s, sh*	γC—H?	893 *m, sp*	γC—H?
980 *vw*	ring	787 *w*		879 *w, sh*	
922 *s, br*	COOH *a*	743 *s*		792 *w*	
862 *m, br*	γC—H?	688 *s*	φC—C	767 *m*	γC—H?
796 *sh*				760 *sh*	
777 *s*	γC—H			689 *m*	φC—C?
689 *w*	φC—C			680 *w*	
660 *m*					

and another secondary one in the interval 2700–2500 cm^{-1}. It has been pointed out by FLETT [4] that the latter branch is one of the most characteristic of the carboxyl group and can be used for its detection, even in spectra run as oil pastes. This is confirmed here. However, since this subgroup of weak bands seems to be associated with the strongly-bonded hydroxyl, whether or not this is of carboxylic nature [3], some care should be exercised in using this band to detect carboxyl groups without taking into account other characteristic regions. The low dispersion of the NaCl prism and the interference of Nujol in the O—H stretching region have rendered it impossible to observe all the bands in this region and even to give exact frequency values to the few encountered. In order to obtain more information on these points a study was undertaken to investigate the acids in the said region under the high resolution of the LiF prism and as KBr pellets. This investigation, together with the re-examination of the NaCl region and the measurement of the KBr one, both by the KBr technique, forms the subject of another paper [24].

Hydrates. As discussed in a previous paper [1], only 4 benzene carboxylic acids give hydrates. The 1–2–3, 1–2–3–5 and 1–2–4–5-acids give dihydrates and the penta-acid a pentahydrate. As this infra-red work shows the only hydrates

VOL. 12 1958

Table 1 (*continued*)

1–2–3–5		1–2–3–5 Hydrate		1–2–4–5	
cm^{-1}	Assignment	cm^{-1}	Assignment	cm^{-1}	Assignment
3300 *w*	νO—H	3448 *w*	νO—H	2640 *vw*	νO—H *a*
2640 *vw*	νO—H *a*	3115 *s*	νH_2O *a*	2530 *vw*	νO—H *a*
2530 *vw*	νO—H *a*	2640 *vw*	νO—H *a*	1704 *vs*	νC=O *a*
1701 *vs*	νC=O *a*	2530 *vw*	νO—H *a*	1576 *vw*	νC—C
1585 *m, sp*	νC—C	1875	H_2O?	1506 *m, sp*	νC—C
1475 *sh*	νC—C	1701 *vs*	νC=O *a*	1458 *sh*	*N*
1458 *sh*	*N*	1585 *m, sp*	νC—C	1442 *s, sp*	νC—C
1445 *s, sp*	νC—C	1475 *sh*	νC—C	1410 *vs, sp*	COOH
1416 *m, sp*	COOH	1451 *m*	νC—C *N*	1377 *sh*	*N*
1391 *m*	COOH?	1420 *vw*	COOH	1302 *s, sp*	νC—C?
1377 *m*	*N*	1406 *s, sp*	COOH	1273 *vs, sp*	COOH
1305 *m, sp*	νC—C?	1377 *m, sp*	*N*	1164 *vw, sp*	βC—H
1263 *s*	COOH	1299 *w*	νC—C?	1138 *w, sp*	
1209 *m*		1274 *sh*		1115 *s, sp*	βC—H
1156 *s, sp*	βC—H	1250 *vs, br*	COOH	925 *m, sp*	γC—H
1074 *m, sp*	βC—H	1208 *vs*		879 *m, br*	COOH *a*
943 *m*	γC—H	1157 *vs*	βC—H	819 *m*	γC—H?
909 *m, br*	COOH *a*	1073 *m*	βC—H	798 *vw*	
862 *m*		965 *w*	γC—H	767 *m*	ϕC—C?
820 *m*	γC—H?	935 *vw*		717 *w, br*	
785 *m*		870 *w, br*		668 *w*	
751 *w*		819 *m*	γC—H?		
715 *vw, br*		785 *m*			
693 *m*	ϕC—C?	769 *m*			
667 *m*		730 *m*			
		690 *m*	ϕC—C?		
		667 *m*			

which are fairly stable are those of hemimellitic (1–2–3) and pyromellitic (1–2–4–5) acids, particularly the latter. It is therefore recommended that these acids, except the pyromellitic one, be always examined in an anhydrous condition as already indicated in the previous paper [1]. In agreement with the above, it is easily seen that the spectra of the hydrates of mellophanic (1–2–3–5) and penta-acids are of ill-defined structure as compared with those of the other two stable hydrates. The most likely reason for this is that the samples used were actually a mixture of both anhydrous and hydrate forms. Because of this, only the spec tra of the stable hemimellitic and pyromellitic acid hydrates will be examined in detail.

The spectrum of hemimellitic (1–2–3) acid hydrate exhibits a sharp band at 3497 cm^{-1} (2·86 μ) with a shoulder at 3436 cm^{-1} (2·91 μ), and that of pyromellitic (1–2–4–5) acid hydrate a pair of sharp bands at 3484 (2·87 μ) and 3356 cm^{-1} (2·98 μ). They are assigned to stretching vibrations of free, or very weakly bonded,

Table 1 (*continued*)

1-2-4-5 Hydrate		Penta	
cm^{-1}	Assignment	cm^{-1}	Assignment
3484 *s, sp*	νO—H	3367 *sh*	νO—H
3356 *s, sp*	νO—H	2640 *vw*	νO—H *a*
3115 *s*	νH_2O *a*	2530 *vw*	νO—H *a*
2640 *vw*	νO—H *a*	1704 *vs*	νC=O
2530 *vw*	νO—H *a*	1600 *w, sp*	νC—C
1992 *m*	H_2O?	1575 *m, sh*	νC—C
1709 *vs*	νC=O	1458 *s*	*N*
1681 *vs*	νC=O *a*	1436 *s, sp*	νC—C
1613 *s, sp*	H_2O?	1391 *m*	COOH
1576 *sh*	νC—C	1307 *sh*	νC—C?
1506 *m, sp*	νC—C	1285 *vs*	COOH
1458 *sh*	*N*	1251 *s*	
1442 *s, sp*	νC—C	1203 *m, sp*	
1410 *s, sp*	COOH	1188 *w*	
1377 *vw*	*N*	1163 *m, sp*	βC—H
1351 *vw*		1139 *m, sp*	
1302 *vs, sp*	νC—C?	940 *m, sh*	γC—H?
1276 *vs, sp*	COOH	915 *m, br*	COOH *a*
1248 *vs, sp*	COOH?	869 *s*	
1152 *w*	βC—H	834 *m, sp*	
1115 *s, sp*	βC—H	787 *m*	
1073 *w*		773 *m*	
961 *m, sp*	γC—H	744 *w, br*	
819 *s, sp*	γC—H?	708 *w*	
806 *w*		687 *m*	
755 *s*	ϕC—C?	667 *m*	
720 *w*			

hydroxyl of the carboxylic groups. Another sharp, strong band occurs in these hydrates at 3226 cm^{-1} (3·10 μ) and 3115 cm^{-1} (3·21 μ) respectively, which is assigned to bonded water molecules. These assignments are based on the assumption that, in these hydrates, the acid molecules instead of being directly associated are presumably linked intermolecularly through water molecules. A somewhat similar phenomenon has been discussed by GROVE [25] in connection with the gladiolic acid hemihydrate. This assumption receives considerable support from the following characteristic features appearing in the hydrates spectra but not in those of the anhydrous acids: (a) The occurrence of the two pairs of bands under discussion at about 3570–3350 cm^{-1} (2·8–3·0 μ) and 3225–3115 cm^{-1} (3·1–3·2 μ); (b) the resolution of the C=O stretching near 1700 cm^{-1} (5·9 μ) in two well-defined bands; (c) one of the carbonyl stretching frequencies near 1700 cm^{-1} of the pyromellitic hydrate is lower than the corresponding frequency of the anhydrous compounds, indicating that there exists a stronger bonding,

VOL. 12 1958

Table 1 (*continued*)

Penta hydrate		Hexa	
cm^{-1}	Assignment	cm^{-1}	Assignment
3367 *sh*	νO—H	2640 *w*	νO—H *a*
3226 *vw*	νH_2O *a*	2530 *w*	νO—H *a*
2640 *w*	νO—H *a*	1706 *vs*	νC=O
2530 *w*	νO—H *a*	1590 *vw*	νC—C
1715 *vs*	νC=O	1572 *w, sp*	νC—C
1686 *vs*	νC=O *a*	1454 *vs*	*N*
1600 *w, sp*	νC—C	1433 *vs, sh*	νC—C
1575 *w, sp*	νC—C	1377 *sh*	*N*
1458 *s*	*N*	1358 *m, sp*	COOH
1453 *s*	νC—C	1305 *sh*	νC—C?
1414 *m, sp*	COOH	1250 *vs*	COOH
1377 *m, sp*	*N*	1198 *vw, sh*	
1309 *vw, sh*	νC—C?	1149 *w*	
1285 *s, sh*		967 *vw, sh*	
1251 *vs*	COOH	909 *m, br*	COOH *a*
1221 *m*		865 *m*	
1188 *w, sh*		846 *sh*	
1172 *m, sp*	βC—H	725 *w*	
1139 *m, sp*		680 *w*	
1015 *m, br*?			
940 *sh*	γC—H?		
860 *m, sp*			
835 *m, sp*			
810 *vw*			
790 *w*			
773 *m*			
724 *m, br*			
708 *m*			
688 *m*			

probably between the C=O and the water molecules, whereas the other is higher, pointing to a free or weakly bonded C=O; (d) the COOH band near 1250 cm^{-1} (8 μ) appears unfolded and (e) the disappearance, especially in pyromellitic and hemimellitic acids hydrates, of the broad dimer band near 900 cm^{-1}.

It is remarkable that in both hydrates, not only the free O—H bands, but also the C=O ones as well as those at about 1250 cm^{-1}, appear to be split in two. All these facts suggest, in accordance with the above discussion, that in these hydrates there exist two types of COOH, one strongly associated, probably to the water molecules, and another free or only weakly bonded, possibly, if so, internally.

C=O *stretching vibrations*

A strong carbonyl absorption band occurs in all the spectra of the anhydrous acids near 1700 cm^{-1} (5·9 μ), as shown in Table 2. Within the precision of the

measurements, the frequency of this band in the different acids is as follows: benzoic, *o*-phthalic, *iso*phthalic and terephthalic acids, 1689 $\pm$ 6 cm^{-1} (5·92 $\pm$ 0·02 μ); tri-, tetra-, penta- and hexa-acids, 1701 $\pm$ 6 cm^{-1} (5·88 $\pm$ 0·02 μ). The C=O frequency of benzoic and the 3 phthalic acids falls therefore in the normal range for simple associated aryl acids [3, 26]. In contrast to this, a clear shift of about 10 cm^{-1} to higher frequencies is observed in C=O stretching bands of the remaining eight tri-, tetra-, penta- and hexa-acids. It follows, therefore, that the presence in the benzene nucleus of more than two carboxyl groups results in an

Table 2. Characteristic frequencies of the COOH group in the benzene carboxylic acids

Acid	Between 2500 and 2700 cm^{-1}	Near 1700 cm^{-1}	Near 1400 cm^{-1}	Near 1250 cm^{-1}	Near 900 cm^{-1}
Mono	Two weak bands at 2640 $\pm$ 30 cm^{-1} and 2530 $\pm$ 30 cm^{-1}	1686	1420	1287	930
1–2		1689	1403	1282	903
1–3		1689	1414	1279	928
1–4		1686	1425	1286	935
1–2–3		1704	1410	1282	922
1–2–3 hydrate		1730	1412	1269	—
		1701		(1238?)	
1–2–4		1698	1408	1286	922
1–3–5		1704	1404	1274	922
1–2–3–4		1704	1404	1276	924
1–2–3–5		1701	1416	1263	909
1–2–3–5 hydrate		1701	1406	1250	—
1–2–4–5		1704	1410	1273	879
1–2–4–5 hydrate		1709	1410	1276	—
		1681		(1248?)	
Penta		1704	1391	1285	915
				(1251?)	
Penta hydrate		1715	1414	1251	—
		1686			
Hexa		1706	1358	1250	909

increase in the C=O frequencies similar, although less strong, to that observed in aryl acids having powerful electron-attracting substituents, such as NO_2 [4, 27]. It should be noted that in the two groups of 3 isomers, tri- and tetra-, the member having the lowest frequency is always the asymmetrical one (1–2–4, 1–2–3–5), i.e. that having an isolated carboxyl group in a meta position to the others. Of the 12 acids, the hexa- appears to give the highest frequency. The hydrate spectra show two well resolved carbonyl bands (Table 2). The possible origin of this has been discussed under O—H vibrations.

Other carboxy vibrations

In addition to the above COOH vibrations at 3000–2500 and 1700 cm^{-1}, three major bands at 1400, 1250 and 900 cm^{-1} (7·1, 8 and 11 μ) have also been reported by several investigators as due to the associated carboxyl group [4, 5,

VOL. 12 1958

21–23, 28]. In the present work it has been possible to ascribe, in all the acids and hydrates, appropriate bands to the 1400 and 1250 cm^{-1} vibrations and, also, in all the anhydrous compounds to the 900 cm^{-1} absorption, as shown in Table 2. The 3 bands are, moreover, strong or at least of medium intensity and in most cases the strongest ones in the region 1500–650 cm^{-1}. This provides strong confirmation that the dimeric COOH group gives rise to the above 3 absorptions in the 1500–650 cm^{-1} range, although in certain cases not all may appear to be distinct due to interaction and overlapping with bands arising from other groupings in the molecules, typical examples of which are, for instance, the methylene and methyl groups vibrating near 1400 cm^{-1}. The fact that the band near 1250 cm^{-1} is usually of great strength and often, as in these acids, the strongest one in the 1500-650 cm^{-1} range, makes this absorption more characteristic than those at 1400 and 900 cm^{-1}, which in some acids have been found missing or of uncertain identification [4, 5]. Unfortunately many classes of compounds having the C—O group absorb in this region.

There is marked disagreement concerning assignment of the bands near 1400 and 1250 cm^{-1} in carboxylic acids, as discussed in detail in some publications [5, 29]. Hadži and Sheppard [5] have found out that these bands often correspond to closely coupled OH deformation and C—O stretching vibrations. Present work does not permit us to make any clear-cut assignment in the acids studied and accordingly the bands are considered simply as due to COOH. It should be mentioned, however, that the neutral methyl esters of the acids under discussion all show [19] strong absorption near 1250 cm^{-1}, thus making it probable that this band in the acids receives a significant contribution from the νC—O mode. The 900 cm^{-1} band has been assigned to the out-of-plane deformation mode of O—H in the dimer ring [5]. If this assignment is correct the vibration must be sensitive to any change in the nature of the hydrogen bonding of the acid O—H. On passing from the spectra of anhydrous acids to those of corresponding hydrates, whose hydrogen bonding involves the water molecules and is therefore different from that in the anhydrous compounds, the 900 cm^{-1} band disappears completely. This strongly confirms the soundness of the above assignment which is also proposed here for the anhydrous acids studied. Reminiscences of the band are observed in the spectra of two hydrates (1–2–3–5 and penta), but this is due, as explained under O—H vibrations, to the anhydrous–hydrate mixed character of the samples used.

Bands associated with O=C—O skeletal vibrations in carboxylic acids have been found by some authors [5, 29, 30] in the range 700–575 cm^{-1} (14·3–17·4 μ). In the present acids this region corresponds also to that where in- and out-of-plane ring deformations as well as substituent sensitive vibrations may occur, thus making it difficult to choose appropriate frequencies for those absorptions. It appears, however, that some of the weak or medium bands shown by the spectra below 700 cm^{-1}, in particular those below 680 cm^{-1}, might possibly involve skeletal COOH absorptions.

Benzene System Vibrations

C—H *stretching vibrations*

These are fused with the strong O—H stretching and Nujol bands near 3000 cm^{-1} (3·3 μ).

C—C *stretching vibrations*

Bands due to stretching vibrations of the C—C of benzene ring in the 1625–1470 cm^{-1} (6·15–6·8 μ) region appear at the expected positions near 1600, 1580 and 1500 cm^{-1} (6·25, 6·33 and 6·67 μ) [3, 6, 14–18]. It is noticeable that wide variations in intensities and position occur as well as the disappearance of some of these bands in the different compounds. This is undoubtedly related to the type of substitution and to electronic and conjugation effects of the COOH group. The 1500 cm^{-1} band appears distinct in most of the compounds. In those where it is missing, a possible shift to lower frequencies and a low intensity may have resulted in overlap by the Nujol or the νC—C bands near 1450 cm^{-1}. The 1600 cm^{-1} band cannot be found in the majority of the acids, although this can be partly traced because of its usual weakness, to masking, by the strong C=O band. In the acids where the 1600 cm^{-1} band is absent, a shoulder appears to occur rather consistently at about the expected position on the C=O band. The 1580 cm^{-1} band occurs systematically, with variable strength, in all compounds. In some acids, such as the vicinal 1–2–3, the band rises clearly in frequency over the mean value. The above confirms that the 1580 cm^{-1} band is enhanced in intensity in aromatic compounds having unsaturated substituents, such as carbonyl, where conjugation with the ring is possible [3, 6].

A medium or strong band occurs in practically all acids at 1450 $\pm$ 20 cm^{-1} (6·8 $\pm$ 0·9 μ) and it is assigned to a νC—C vibration. Because of overlapping with the 1458 cm^{-1} (6·86 μ) Nujol band it has been difficult in some instances to give exact frequency values to this band. A medium band occurs in some of the compounds near 1320 cm^{-1} (7·58 μ) and it is tentatively assigned to a νC—C vibration [31, 32]. In other compounds the absorption, if it exists, is masked off by the strong and complex COOH band at 1250 cm^{-1}. It will be seen from the spectra that the latter absorption shows in most cases a shoulder, sometimes resolved, at about 1320–1300 cm^{-1}, which might be related to the band mentioned.

Other benzene system vibrations

These vibrations, appearing below 1250 cm^{-1}, comprise in- and out-of-plane C—H deformations, ring breathings, in- and out-of-plane ring deformations and substituent sensitive vibrations. Any complete assignment of appropriate frequencies to these vibrations in all compounds is practically impossible with the data in hand, the more so since this series of acids constitutes a clear example where existing correlations for the determination of the type of substitution [3, 14–17] do not apply in full for any of the compounds. Not even the detailed study of individual vibrational frequencies of RANDLE and WHIFFEN [18] applies totally, even after taking into account that some of the possible out-of-plane C—H deformations are obscured by the broad and complex absorption of the COOH group near 900 cm^{-1}. In view of the above the tentative assignments made have been limited to those deduced mainly by analogies among the acids and by comparison with the spectra of their neutral methyl esters [19]. The references just mentioned have also been used as a supplementary guide. The nature of the compounds was also of some help. They possess only a benzene

VOL. 12 1958

nucleus and COOH groups. Once all principal vibrations of the latter were assigned it appeared that the remaining important bands were likely to be associated with the benzene system and, in particular in the 1200–750 cm^{-1} range, with C—H deformations. In accord with this is the fact that in the spectrum of mellitic acid, which has no hydrogens remaining on the ring, most of the fine structure shown by the other acids, under same conditions, is washed out in the region noted. At the same time, however, this spectrum also shows that even after disappearance of all hydrogens on the ring there still remain in the said range some weak or medium bands which cannot belong to C—H deformations.

The assignments are shown in Table 1. The most uncertain ones are followed by a ? sign. Although the assignments are to be considered as tentative, it is believed that a significant number of them are certain and that, in any case, the majority of the frequencies chosen are fundamental vibrations. This is expected to be particularly true for the mono-, di- and tri-compounds for which the assignments agree on general lines, but not without exceptions, with recent findings [18].

The COOH group effects strongly the out-of-plane C—H deformations in the region below 1000 cm^{-1}, shifting them in some cases to frequencies higher than those where they normally appear in compounds having inert or electron-donating substituents. It appears [33] that these alterations are caused by the electrophilic character of the COOH group which on conjugation tends to deplete the aromatic nucleus of π electrons raising the values of the C—H deformation frequencies. These shifts have also been observed in some nitro-compounds [3] and in some substituted benzoic acids [4]. Such shifts are observed clearly in the mono- and para-acids, as reported also by other authors [33]. It will be noted that the C—H deformation vibration appearing normally [3, 14–18] in the mono-compounds near 750 cm^{-1} and in the para-compounds near 820 cm^{-1} is shifted in benzoic and terephthalic acids to 808 and 882 cm^{-1} respectively. Interpretation of this region is complicated still further by the fact that mellitic acid, with no hydrogens remaining on the ring, gives also a medium band at 865 cm^{-1}. This raises the doubt if the medium or strong absorption which occurs near this position in most of the tri-, tetra- and penta-acids can be exclusively taken, at least in these compounds, as an out-of-plane C—H deformation mode. On account of the above, a band near the said position has been left without assignment in the 1–2–3–5 and penta-acids, although this is not intended to mean that it may not be due to a C—H deformation or receive a significant contribution from this vibration mode. On picking out the out-of-plane ring deformation frequencies it was found that although many of the acids give bands near 690 and 675 cm^{-1}, the latter disappear in some of the corresponding methyl esters. This suggests the possibility, but does not establish, that such absorptions might be related to substituent sensitive vibrations of other types of band. As alternative assignments to those in Table 1 for the ϕC—C vibration, the following are suggested for the acids which follow: benzoic, 685 cm^{-1}; phthalic, 675 cm^{-1}; *iso*phthalic, 675 cm^{-1}; 1–2–3, 705 or 683 cm^{-1}; 1–3–5, 743 cm^{-1}; 1–2–3–4, 760 cm^{-1}.

In the region 1275–1000 cm^{-1} a weak or medium weak band appears in some acids, including the hexa- one, between 1080 and 1150 cm^{-1} which does not seem

to belong to a C—H deformation. A weak band, sometimes resolved but usually appearing as a shoulder, is shown by the majority of the acids near 1200 cm^{-1}. It seems possible that the above two bands, in particular the latter, might involve some substituent sensitive vibration or combination band rather constant in position.

Acknowledgements—This paper is based partly on work performed by the author during 1951–1953 as a "Guest Fellow" at the Coal Research Laboratory, Carnegie Institute of Technology, Pittsburgh, Penn., U.S.A., on a Scholarship of the Instituto Nacional del Combustible of the Patronato Juan de la Cierva de Investigacion Tecnica of Spain. The author has pleasure in expressing his appreciation and gratitude to Dr. H. H. LOWRY, Director of the Coal Research Laboratory, and Dr. H. C. HOWARD, Assistant Director of the same Laboratory, for facilities provided and for their continued interest and helpful advice during the experimental work. Thanks are also due to Dr. V. GÓMEZ ARANDA, Director of the Instituto Nacional de Combustible at Zaragoza, for valuable suggestions. The ultimate microanalyses were performed by Huffman Microanalytical Laboratories, Wheatridge Co., U.S.A.

References

[1] GONZÁLEZ-SÁNCHEZ F. *Tetrahedron* 1957 **1** 231.
[2] GONZÁLEZ-SÁNCHEZ F. *Combustibles (Zaragoza)* 1955 **15** 273, 361.
[3] BELLAMY L. J. *The Infra-red Spectra of Complex Molecules*. Methuen, London 1954.
[4] FLETT M. ST. C. *J. Chem. Soc.* 1951 962.
[5] HADŽI D. and SHEPPARD N. *Proc. Roy. Soc.* A 1953 **216** 247.
[6] RANDALL H. M., FOWLER R. C., FUSON N. and DANGL J. R. *Infrared Determination of Organic Structures*. Van Nostrand, New York 1949.
[7] CANNON C. G. and SUTHERLAND G. B. B. M. *Spectrochim. Acta* 1951 **4** 373.
[8] ROY A. N. and HOWARD H. C. *J. Amer. Chem. Soc.* 1952 **74** 3239.
[9] SHREVE O. D., HEETHER M. R., KNIGHT H. B. and SWERN D. *Analyt. Chem.* 1950 **22** 1498.
[10] O'CONNOR R. T., FIELD E. T. and SINGLETON W. S. *J. Amer. Oil Chem. Soc.* 1951 **28** 154.
[11] FREEMAN N. K. *J. Amer. Chem. Soc.* 1952 **74** 2523.
[12] SINCLAIR R. G., MCKAY A. F. and JONES R. N. *J. Amer. Chem. Soc.* 1952 **74** 2570.
[13] SINCLAIR R. G., MCKAY A. F., MYERS G. S. and JONES R. N. *J. Amer. Chem. Soc.* 1952 **74** 2578.
[14] THOMPSON H. W. *J. Chem. Soc.* 1948 328.
[15] BARNES R. B., GORE R. C., STAFFORD R. W. and WILLIAMS V. Z. *Analyt. Chem.* 1948 **20** 402; BARNES R. B., GORE R. C., LIDDEL U. and WILLIAMS V. Z. *Infrared Spectroscopy*. Reinhold, New York 1944.
[16] COLTHUP N. B. *J. Opt. Soc. Amer.* 1950 **40** 397.
[17] MCMURRY H. L. and THORNTON V. *Analyt. Chem.* 1952 **24** 318.
[18] RANDLE R. R. and WHIFFEN D. H. *Molecular Spectroscopy*. The Institute of Petroleum, London 1955.
[19] GONZÁLEZ-SÁNCHEZ F. To be published shortly.
[20] GILLETE R. H. and DANIELS F. *J. Amer. Chem. Soc.* 1936 **58** 1139; GILLETE R. H. *J. Amer. Chem. Soc.* 1936 **58** 1143.
[21] BONNER L. G. and HOFSTADTER R. *J. Chem. Phys.* 1938 **6** 531; HERMAN R. C. and HOFSTADTER R. *J. Amer. Chem. Soc.* 1938 **6** 534.
[22] DAVIES M. M. and SUTHERLAND G. B. B. M. *J. Chem. Phys.* 1938 **6** 755.
[23] BUSWELL A. M., RODEBUSH W. H. and ROY M. F. *J. Amer. Chem. Soc.* 1938 **60** 2239.
[24] HIDALGO A. and GONZÁLEZ-SÁNCHEZ F. Paper presented at the International Meeting of European Molecular Spectroscopists, Freiburg i. Br. (Germany), 9–13 July 1957.
[25] GROVE J. F. *J. Chem. Soc.* 1952 3345.
[26] GROVE J. F. and WILLIS H. A. *J. Chem. Soc.* 1951 877.

VOL. 12 1958

[27] Flett M. St. C. *Trans. Faraday Soc.* 1948 **44** 767.
[28] Lecomte J. *Traité de Chimie Organique* (Edited by Grignard and Baum) Vol. II. Masson et Cie., Paris 1936.
[29] Fuson N., Josien L., Jones E. A. and Lawson J. R. *J. Chem. Phys.* 1952 **20** 1627.
[30] Thomas O. *Disc. Faraday Soc.* 1950 **9** 339.
[31] Mair R. D. and Hornig D. F. *J. Chem. Phys.* 1949 **17** 1236.
[32] Miller F. A. *J. Chem. Phys.* 1956 **24** 996.
[33] Kross R. D., Fassel V. A. and Margosches M. *J. Amer. Chem. Soc.* 1956 **78** 1332.

L.
2
58

Spectrochimica Acta, 1958, Vol. 12, pp. 34 to 40. Pergamon Press Ltd., London

Solvent effects in infra-red spectra of compounds containing the carbonyl group

L. B. ARCHIBALD* and A. D. E. PULLIN
The Chemistry Department, Queen's University, Belfast, N. Ireland

(*Received* 11 *November* 1957)

Abstract—The solvent dependence of the frequencies and integrated absorption intensities of the carbonyl stretching vibration of several ketones and nitrogen disubstituted amides has been examined. Near-linear relations have been found to exist between the frequencies of pairs of similar solutes in a variety of solvents, and similar relations appear to hold for intensities. There is also some evidence that it may be useful, in solutions where specific solvent–solute interaction is small, to investigate solvent effects with a view to establishing whether it is possible to arrange solvents in a single order of increasing depression of the solute frequencies valid for a wide variety of solutes. For the carbonyl compounds considered, approximately linear increases of integrated absorption intensities with decrease of the carbonyl stretching frequency have been found. The shapes and half-intensity widths of the bands are considered briefly.

A DETAILED examination of solvent effects on the frequency, half-width and integrated intensity of the carbonyl stretching band of acetaldehyde, acetone and di-*iso*propyl ketone has been made by BAYLISS, COLE and LITTLE [1]. It seemed of interest to us to make similar measurements on other carbonyl compounds and in particular to extend the range to compounds containing a more polar carbonyl group. Benzophenone (I), *NN* diethylacetamide (II), and *NN* diphenylacetamide (III) were chosen. Nitrogen di-substituted amides were chosen to avoid N–H hydrogen bonding effects. Spectra were obtained of solutions of I and II in ten solvents and, because of solubility limitations, of III in seven solvents. Eight of the ten solvents were the same as those used by BAYLISS *et al.* [1].

Experimental

II and III were obtained from HOPKINS and WILLIAMS. The boiling point (II, 186°) and melting point (III, 102·5°) showed that they were sufficiently pure to be used without further purification. I was recrystallized from alcohol to a constant melting point of 47·5°. Analar solvents were used where possible. Other solvents were purified by standard methods. The chloroform used was washed six times with an equal volume of water, dried over $CaCl_2$ and distilled before use. Solutions were made up by weighing suitable quantities of solute into 10 ml volumetric flasks and making up to the mark with solvent. All spectra were obtained with a Perkin–Elmer model 21 spectrophotometer, with NaCl prism. The thickness of the absorption cell was 0·096 mm. Spectra were recorded in each case from 1760 to 1560 cm^{-1} at 2 mm/cm^{-1}. A calibration spectrum for the region of the band maximum was obtained afresh each time immediately after obtaining the spectrum with a given solvent. Significant errors, from inexact

* Now at the Linen Industry Research Association, Lambeg, Lisburn, Co. Antrim.

VOL. 12 1958

positioning or non-uniformity of the recording paper, were avoided by tracing reference lines on the recording chart by momentarily closing the beam before and after each solution and calibration spectrum. The frequencies quoted for band maxima should be correct to better than 1·0 cm^{-1}. Half-widths and integrated absorption intensities were determined by the procedure given by RAMSAY [2]. Spectra at three concentrations were obtained for each combination of compound and solvent. The corrections to obtain the true values of the half-intensity band width $\Delta\nu_{\frac{1}{2}}'$ were obtained from Table 2 of Ramsay's paper, and the mean of the three values for the three concentrations taken. Band areas were measured over a range of ± 60 cm^{-1} from the band maximum, using Simpson's rule, taking intercepts every 2 cm^{-1}. RAMSAY's "Method II." an extension of method of WILSON and WELLS, was then used to obtain the true integrated absorption intensities A. Wing corrections were taken from Table 5 of RAMSAY's paper.

Results

The results are summarized in Table 1.

Integrated absorption intensities A are defined by:

$$A = \frac{1}{Cl}\int \log_e\left(\frac{I_0}{I}\right)_\nu d\nu$$

where c is the solute concentration in g moles/litre
l is the cell thickness in cm and ν are cm^{-1}.

The figures for acetone are from Bayliss's paper: his intensities figures have here been converted into $\log_e$ units. Integrated absorption intensity values in Table 1 may be compared with values previously reported by BARROW [3]. His values of $A \times 10^{-4}$ were: acetone in chloroform and in carbon tetrachloride, 1·9 and 1·55; benzophenone in chloroform and in carbon tetrachloride, 2·4 and 2·2; diethylacetamide in chloroform, 5·7. These values agree with ours to within 6 per cent. Recently, THOMPSON, NEEDHAM and JAMESON [4] have measured some integrated absorption intensities, using a more rigorous extrapolation procedure than that used by us. Their value ($A \times 10^{-4}$) for benzophenone in chloroform is 2·17. As indicated in the discussion, the values of $\Delta\nu_{1/2}$ have at best only semi-quantitative significance.

Discussion

From even casual inspection of the spectra obtained, it was evident that the band shapes departed considerably from the ideal shape usually assumed. Considerable asymmetry of band shape was often present, especially in the spectra of II. In the case of II this asymmetry was greatest for the solutions in the non-polar solvents *n*-hexane, *cyclo*-hexane and carbon tetrachloride, and could be partly accounted for by assuming there to be an underlying weak band 7–10 cm^{-1} on the low-frequency side of the maximum of the main band, while in acetonitrile and chloroform solutions the asymmetry was much reduced. In carbon disulphide solution the band was approximately symmetrical about the band maximum, but was noticeably narrower at optical densities above half the maximum optical density than would be expected on the basis of a Lorentz-type curve calculated

from the half-intensity band width. The spectrum of I in 1:2-dichloroethane showed a poorly defined shoulder on the low-frequency side close to the band maximum. The asymmetry of the bands of II may be caused by dipole–dipole association of the diethylacetamide molecules. The greater asymmetry of the band in less polar solvents is in accord with this hypothesis. Cannon [5] has suggested that dipole–dipole association is important in solutions of N-mono-substituted amides.

Table 1

Solvent	Acetone			Benzophenone (I)		
		$\Delta\nu_{1/2}$	$A \times 10^{-4}$		$\Delta\nu_{1/2}$	$A \times 10^{-4}$
Chloroform	1711·5	13	2·01	1661	17	2·41
1:2-Dichloroethane	—	—	—	1662	13	2·18
Acetonitrile	—	—	—	1663	12·5	2·22
Benzene	1717	10·5	1·60	1665	10	2·06
Carbon disulphide	1717·5	12	1·37	1666	9·5	2·09
Carbon tetrachloride	1719	11·5	1·60	1668	9·5	2·09
Tetrachloro-ethylene	1720	10·5	1·60	1669	8·0	1·99
Diethyl ether	1721	11	1·41	1671	8·1	1·89
*cyclo*hexane	1723	13	1·28	1674	8·5	1·74
n-Hexane	1723·5	15	1·28	1674	8·5	1·71
	NN diethylacetamide (II)			NN diphenylacetamide (III)		
Chloroform	1630	22·5	5·41	1664	25	4·46
1:2-Dichloroethane	1641	20	5·04	1674	19	4·19
Acetonitrile	1641	17	4·62	1675	16	4·08
Benzene	1653	18·5	4·35	1684	11	3·59
Carbon disulphide	1653	18	4·43	1684	12	3·74
Carbon tetrachloride	1654	23	4·81	1684	16·5	3·93
Tetrachloro-ethylene	1658	21·5	4·64	—	—	—
Diethyl ether	1662	17	3·95	1688	12	3·45
*cyclo*Hexane	1668	13·5	4·20	—	—	—
n-Hexane	1668	13·5	4·13	—	—	—

The theory of frequency shifts and intensity changes of infra-red bands with change of dielectric constant has been discussed by a number of authors. (For a recent summary see reference 6.) As a discussion of the theory of these effects is being prepared for publication by one of us (A. D. E. P.) this aspect will only be touched on here. An alternative approach is to consider the following questions:

(a) Can solvents be placed in an order of increasing effect on the spectra of the solute molecule irrespective of the solute: i.e. can one establish a solvent order, independent of the nature of the solute?

(b) Are there any internal relations between the frequency shifts, half-intensity band widths and integrated intensities for one solute in a variety of solvents?

(a) *Solvent order*. For solutions of all six carbonyl compounds considered by Bayliss *et al.* and by us, the frequency of the carbonyl stretching mode is highest

VOL. 12 1958

in *n*-hexane. The other solvents can be placed in a single series for all six compounds with respect to the extent to which they lower the carbonyl frequency, with one small exception. This is acetaldehyde in ether for which the frequency given by BAYLISS *et al.* has to be raised by 0·5 cm^{-1} to keep a common solvent order. This solvent order for the eight solvents is as given in Table 1 for acetone.

A single solvent order is also found for the solutions of the three compounds in our study when the additional solvents not used by BAYLISS *et al.* (1 : 2 dichloroethane and acetonitrile) are included. If the solvent order for the three solutes and twelve solvents used by BAYLISS *et al.* is considered, the frequency of acetaldehyde in ether has to be raised by 0·5 cm^{-1} as before, and also the frequency of acetaldehyde in chloroform lowered by 1 cm^{-1} to maintain a unique solvent order.

The solvent order for the six non-polar solvents valid for all six solutes differs from that predicted by the Kirkwood–Bauer relation [6, 1] which predicts the order *n*-hexane, *cyclo*hexane, carbon tetrachloride, benzene, tetrachloroethylene and carbon disulphide, if the refractive indices or dielectric constants quoted by BAYLISS are used, and also differs from that predicted by the Kirkwood–Bauer relation if refractive indices for 6 μ are used throughout*. If the frequencies for acetone, di-*iso*propyl ketone, acetaldehyde, I and II in solution in these non-polar solvents are plotted against the solvent refractive index function $(n^2 - 1)/(2n^2 + 1)$ as in Fig. 3 of BAYLISS's paper [1], it is found that for each solute, the points for carbon disulphide, tetrachloroethylene and *n*-hexane lie very close to a straight line, while the point for *cyclo*hexane is always above the line (i.e. the observed frequency is "too high") and the points for carbon tetrachloride and benzene lie below the line (i.e. the observed frequencies are "too low"), the point for benzene deviating from the line more than that for carbon tetrachloride. The very close similarity of the disposition of the plots for the six solutes indicates the correctness of the data which should provide a test for any theory of solvent effect on infra-red spectra.

It should be noted that in general the possibility of arranging solvents in a solvent order will be affected by the accuracy to which the frequencies are determined. Thus a more accurate determination of the frequencies of III in benzene, carbon disulphide and carbon tetrachloride might necessitate a solvent order for this solute different from that for the other solutes.

It would be of interest to know how far the same solvent order holds for other types of solute. WHIFFEN [10] has studied the variation with solvent of the frequency and integrated absorption intensity of the C—Cl stretching vibration of chloroform at ~760 cm^{-1}. Of the solvents used, five were the same as those employed by BAYLISS *et al.* (assuming for our purpose solutions in *n*-hexane and *n*-heptane to be equivalent). The same solvent order for the extent of frequency lowering is found in both cases, i.e. *n*-hexane (or *n*-heptane), *cyclo*hexane, carbon disulphide, benzene and dioxane. Again this order is different from that predicted by the

* There do not appear to have been any determinations of the refractive index of *n*-hexane or *cyclo*hexane in the infra-red, so that extrapolation from visible *n* values is necessary. Other values are: C_6H_6, 1·42 [7]; CCl_4, 1·435 [8]; C_2Cl_4, 1·48 [9]; all at 6μ; CS_2, 1·44 at 1670 cm^{-1} [8], 1·48 at 1720 cm^{-1} by extrapolation using a simple dispersion formula from data given in the reference.

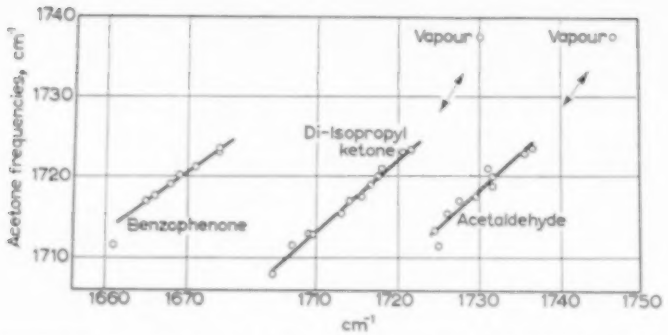

Fig. 1. Plots showing the relations between the solvent-dependent values of the carbonyl frequencies of acetaldehyde, di*iso*propylketone, I (abscissae) and of acetone (ordinates). Values for acetaldehyde, di*iso*propylketone and acetone from Bayliss *et al.*

Kirkwood–Bauer theory. Measurement of the frequency of the NH stretching mode of pyrrole in a variety of solvents are reported in a paper by Josien and Fuson [11]. Although the same solvent order for the extent of frequency lowering is found for the five solvents (*n*-hexane or *n*-heptane, *cyclo*hexane, carbon disulphide, benzene and acetone) in common between this work on pyrrole and that on chloroform, it is clear that specific solute–solvent interactions are of great importance in determining the frequency lowering of hydrogenic vibrations in solution [11, 12] so that it is more useful to consider regularities within this class [13] separately.

Besides the correlation of solvent order, a near-linear relation is found between the frequencies of acetone, acetaldehyde, di*iso*propyl ketone and I in the different solvents, and between the frequencies of II and III (Figs. 1 and 2). There is a considerable scatter in the plot of the frequencies of II and of III against those of acetone, though, as mentioned above, the same solvent order is maintained.

It is interesting to consider whether similar relations exist between the intensities. Examination of Table 1 shows that though there is a general similarity of solvent behaviour with respect to intensity, there are a number of individual variations. In Fig. 3, illustrative plots are given for intensities for pairs of solutes.

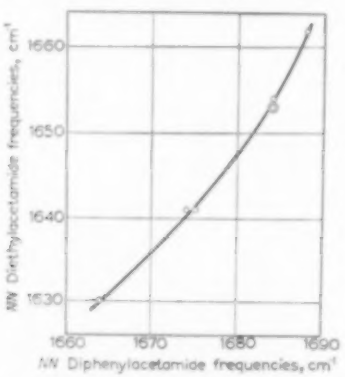

Fig. 2. Plot showing the relation between the solvent-dependent value of the carbonyl frequencies of III (abscissae) and II (ordinates).

VOL. 12 1958

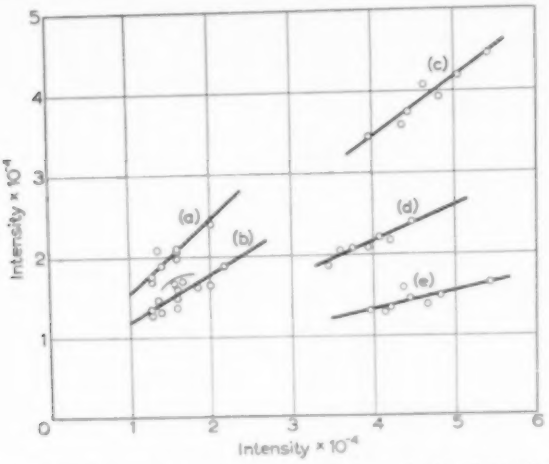

Fig. 3. Plots showing the relations between the solvent-dependent values of the integrated absorption intensity of one solute ($A \times 10^{-4}$ values) and the corresponding values for a second solute. The solute pairs (abscissae given first) are: (a) acetone, benzophenone; (b) acetone, di*iso*propylketone (c) NN diethylacetamide, NN diphenylacetamide; (d) NN diphenylacetamide, benzophenone (e) NN diethylacetamide, di*iso*propylketone. Values for acetone and di*iso*propylketone from Bayliss *et al.*

It will be observed that the change of intensity with solvent is roughly proportional to the intensity, that is the fractional change of integrated absorption intensity changes similarly for changes of solvent among these six compounds.

(b) *Internal relations.* Fig. 4 shows the results of plotting the integrated absorption intensity values against the frequencies for the carbonyl band of individual solutes in the various solvents. It is seen that the slopes of the lines are quite

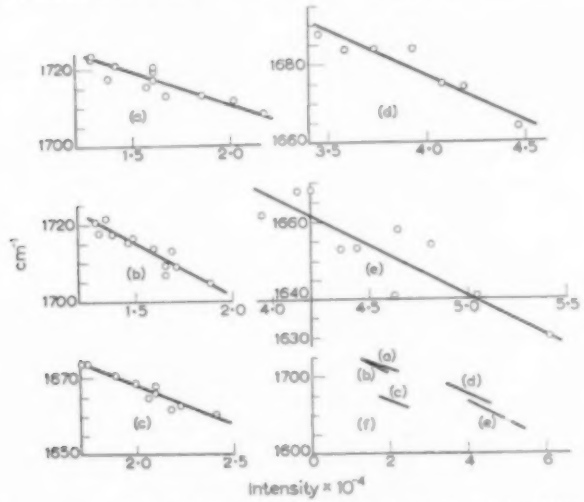

Fig. 4. Plots of frequency (ordinates) against integrated absorption intensities (abscissae, $A \times 10^{-4}$) for (a) acetone, (b) di*iso*propylketone, (c) benzophenone, (d) NN diphenylacetamide, (e) NN diethylacetamide, (f) relation of separate plots to each other. Values for acetone and di*iso*propylketone from Bayliss *et al.*

similar but that the points for each solute lie on separate ν–A lines. There do not seem to be any obvious regularities in the half-intensity band widths, though the bands are usually broader in chloroform solution than in most of the other solvents and the bands in ether solution fairly narrow.

References

[1] Bayliss N. S., Cole A. R. H. and Little L. H. *Aust. J. Chem.* 1955 **8** 26.
[2] Ramsay D. A. *J. Amer. Chem. Soc.* 1952 **74** 72.
[3] Barrow G. M. *J. Chem. Phys.* 1953 **21** 2008.
[4] Thompson H. W., Needham R. W. and Jameson D. *Spectrochim. Acta* 1957 **6** 208.
[5] Cannon C. G. *Mikrochim. Acta* 1955 **2/3** 555.
[6] Jones R. N. and Sandorfy C. *Technique of Organic Chemistry* Vol. IX: *Chemical Applications of Spectroscopy* p. 299. Interscience, New York 1956.
[7] Vincent-Geisse J. and Lecomte, J. *C. R. Acad. Sci., Paris* 1957 **244** 577.
[8] Pfund A. H. *J. Opt. Soc. Amer.* 1935 **25** 351.
[9] Landolt–Bornstein Physikalische-Chemische Tabellen, II, p. 967 Julius Springer, Berlin 1923.
[10] Whiffen D. H. *Trans. Faraday Soc.* 1953 **49** 878.
[11] Josien M. L. and Fuson N. *J. Chem. Phys.* 1954 **22** 1169, 1264.
[12] Jones L. H. and Badger R. M. *J. Amer. Chem. Soc.* 1951 **73** 3132.
[13] Gordy W. *J. Chem. Phys.* 1941 **9** 204.

VOL.
12
1958

Spectrochimica Acta, 1958, Vol. 12, pp. 41 to 46. Pergamon Press Ltd., London

Infrared spectrum and force constants of silyl-d_3 iodide

H. R. Linton and E. R. Nixon
Department of Chemistry, University of Pennsylvania, Philadelphia, Pennsylvania, U.S.A.

(*Received* 15 *September* 1957)

Abstract—The infrared spectrum of gaseous SiD_3I has been examined in the region from 4000 to 300 cm^{-1} and all six of the fundamentals observed and assigned. The hitherto unobserved ν_3 fundamental of SiH_3I is also reported. The Coriolis zeta constants and vibrational force constants for SiD_3I are discussed.

Introduction

The infrared spectrum of silyl iodide from 2 to 20 μ under rather high resolution has been reported by Dixon and Sheppard [1]. Their values for five of the six fundamental frequencies and for the Coriolis coupling constants ζ of the type E fundamentals are listed in Table 1. The frequency of the remaining fundamental,

Table 1. Fundamental frequencies and zeta constants of silyl iodide

Description		SiH_3I*		SiD_3I	
		Freq. (cm^{-1})	ζ	Freq. (cm^{-1})	ζ
Sym Si–H stretch	$\nu_1(a_1)$	2191·8		1575	
Sym. SiH_3 deform.	$\nu_2(a_1)$	903		664	
Si–I stretch	$\nu_3(a_1)$	362†		351·5	
Anti. Si–H stretch	$\nu_4(e)$	2205·6	0.015	1607	0.145
Anti. SiH_3 deform.	$\nu_5(e)$	941	−0·196		−0·197
SiH_3 rock	$\nu_6(e)$	592·4	0·199	435	0·085

* Reference [1].
† This research.

the Si–I stretching mode ν_3, was estimated as 355 cm^{-1} from the combination band $\nu_3 + \nu_6$ at 947·4 cm^{-1}. From the mean separation of the P and R maxima in three parallel bands, the Q line structures of the three perpendicular fundamentals and an assumed Si–H distance of 1·48 Å, these authors calculated the following parameters: H–Si–H angle, 109° 54′ ± 25′ and Si–I distance, 2·435 ± 0·001 Å.

During the course of study of a series of silyl compounds, we prepared samples of both SiH_3I and SiD_3I and took the opportunity to investigate the spectrum of the deuterated iodide as well as to locate the ν_3 frequency in SiH_3I.

Experimental

Our silyl iodide was prepared by reacting silane with hydrogen iodide over an aluminum iodide catalyst according to the procedure described in the literature [2]. The product was subjected to repeated vacuum fractional distillations through a series of cold traps; at −43°, −63°, −96° and −190°C. The bulk of the silyl

iodide collected in the −96° trap and a small quantity of SiH_2I_2 in the −43° trap, while the unreacted SiH_4 and HI passed through into the −190° trap and virtually nothing was trapped at −63°.

In the case of SiD_3I, the SiD_4 was prepared from $SiCl_4$ and $LiAlD_4$ (Metal Hydrides, Inc.) and the DI from D_2O (Stuart Oxygen Co., 99·6 per cent pure) and a mixture of red phosphorus and iodine. Our final sample of SiD_3I had a vapor pressure of 12·35 cm at 0°C. (SiH_3I has a vapor pressure 12·39 cm [2].) It is evident from the infrared spectrum discussed below that our sample did contain a

Table 2. Infrared spectrum of SiD_3I

Frequency (cm^{-1})	Rel. int.	Assign.	Frequency (cm^{-1})	Rel. int.	Assign.
342·7P			793·5P		
351·5	s	$\nu_3(a_1)$	801·5	s	$SiHD_2I$
357·5R			807R		
435	w	$\nu_6(e)$	(860)	w	$2\nu_6(A_1 + E)$
493·5P			1168·5P		
501	w	Impurity	1178	vw	Impurity
507R			1183R		
659·3P			1353	vw	$2\nu_5(A_1 + E)$
664	vs	$\nu_2(a_1)$			
670·5R			1568·5P		
			1575	s	$\nu_1(a_1)$
660			1581R		
to	w	$\nu_5(e)$			
690			1607	s	$\nu_4(e)$

s = strong, w = weak.

small percentage of $SiHD_2I$. Moreover, silyl iodide reacts readily with moisture to yield disilyl ether and hydrogen iodide, and despite our precautions to prevent any hydrolysis, the spectra at our highest gas pressures (12–13 cm) did show very weak absorption close to 1100 cm^{-1}, corresponding to the very intense band reported for $(SiD_3)_2O$ [3].

The gas cells, 10 cm in length, were of glass with either KBr or CsBr windows and the spectra were recorded on a Perkin–Elmer single-beam, double-pass spectrometer with LiF, NaCl, KBr and CsBr prisms. The absorption bands found in the range from 4000 to 300 cm^{-1}, aside from the aforementioned weak ether band at 1100 cm^{-1} and a very weak band at 2205 cm^{-1} due to $SiHD_2I$, are plotted in Fig. 1 and are listed in Table 2.

Discussion of spectra

First, as may be seen in Fig. 1, the Si–I stretching frequency ν_3 in SiH_3I actually lies at 362 cm^{-1}. The Q branch of this relatively intense parallel band is undetectably weak and the P–R separation is 11·0 cm^{-1}.

VOL. 12 1958

The assignments of the fundamentals in SiD_3I offer no difficulty. With the three parallel A_1 vibrations, the Si–D stretch ν_1 is the strong band at 1575 cm^{-1}, the SiD_3 deformation ν_2 is the very intense band at 664 cm^{-1} and the Si–I stretch ν_3 is assigned as the strong 351·5 cm^{-1} band. The perpendicular Si–D stretch ν_4 overlaps ν_1, but its center is obviously close to 1607 cm^{-1}. The SiD_3 deformation ν_5 is obscured by the much more intense ν_2, but at our highest gas pressures the Q

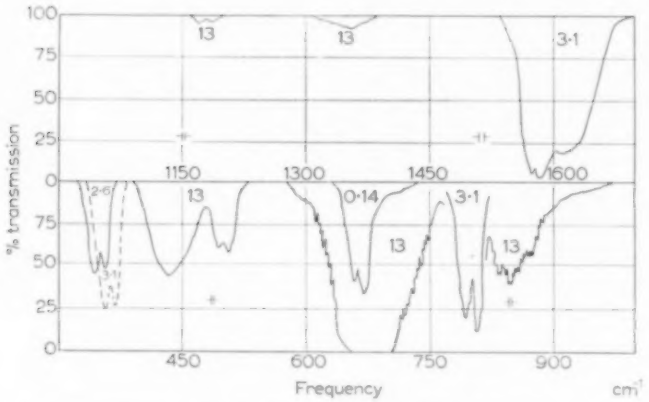

Fig. 1. Infrared spectrum of SiD_3I. Spectral slit widths and gas pressures in cm (in 10 cm cell) are indicated. Low-frequency band of SiH_3I shown in dashed line.

lines of ν_5 are observable at both edges of the band and the band center must lie somewhere between 660 and 690 cm^{-1}. The final E vibration, the SiD_3 rocking mode ν_6, falls at 435 cm^{-1}.

If one assumes the same geometry as that given for SiH_3I [1], then the rotational constants for SiD_3I turn out to be: $A = 1{\cdot}424$ and $B = 0{\cdot}09486$ cm^{-1}. According to the approximate formulas of GERHARD and DENNISON [4], one should expect a spacing of 13·7 cm^{-1} between the P and R maxima in the parallel bands. The spacings actually observed in the three A_1 fundamentals are 11·5, 11·2 and 14·8 cm^{-1}, with an average value of 12·5 cm^{-1}.

The characteristic symmetric top intensity alternation of the Q lines, "strong, weak, weak, strong, . . .", is readily apparent in both edges of the ν_5 band. The average spacing of the 18Q lines measured is 3·22 cm^{-1} and with the approximation that the rotational constants of the molecule are independent of the vibrational state, the equation for this spacing

$$\Delta\nu_i = 2[A(1 - \zeta_i) - B]$$

yields $\zeta_5 = -0{\cdot}197$.

The weak band at about 860 cm^{-1} is assigned as $2\nu_6$. Unlike $2\nu_6$ in SiH_3I, the parallel component of this band is not especially predominant. While the intensity pattern of the Q lines of the E component is irregular, the Q lines are rather evenly spaced and the average spacing 3·14 cm^{-1} of some 20 lines gives $\zeta_{2\nu_6} = -0{\cdot}171$. The relation $\zeta_{2\nu_6} = -2\zeta_6$ [5] allows us to calculate ζ_6 as 0·085, which in turn gives a Q line spacing $\Delta\nu_6$ of 2·42 cm^{-1}. Since this is beyond the limit of our

resolution in this region, it explains the absence of any fine structure in the ν_6 band.

From the sum of the zeta constants [5]

$$\zeta_4 + \zeta_5 + \zeta_6 = B/2A = 0{\cdot}0333$$

one obtains $\zeta_4 = 0{\cdot}145$ and $\Delta\nu_4 = 2{\cdot}25\ \text{cm}^{-1}$, again explaining the lack of fine structure in ν_4. In comparing our ζ values with those of Dixon and Sheppard [1], it should be kept in mind that we have not taken into account the dependence of A and B upon the vibrational state.

In addition to a very weak band at 1353 cm^{-1} which we assign as $2\nu_5$, there remain to be discussed in the spectrum of SiD_3I a strong parallel band at 801·5 cm^{-1}, a weak parallel band at 501 cm^{-1} and finally a very weak parallel band at

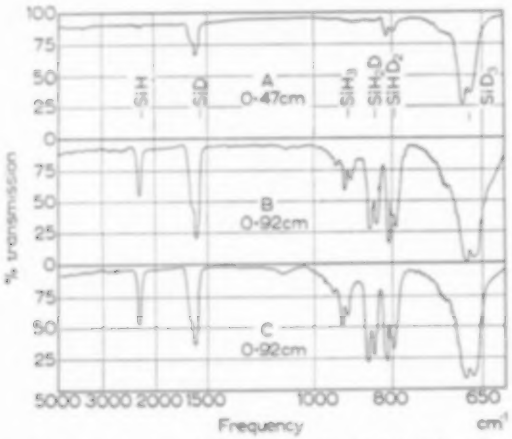

Fig. 2. Infrared spectra: *A*, sample of SiD_3I; B, silyl iodide from reaction of *A* with SiH_2I_2; C, silyl iodide from reaction of *B* with SiH_2I_2. Gas pressures in 10 cm cell shown.

1178 cm^{-1}. The 801·5 cm^{-1} band cannot be assigned in any reasonable manner to SiD_3I, but it does fall at just about the expected frequency for the deformation of an $SiHD_2$ group. That this is the correct interpretation was shown in the following way. Approximately equal weights of our SiD_3I sample and of SiH_2I_2 were condensed into a flask containing some aluminum iodide. After 15 hr at 75° the material was removed and fractionated. The infrared spectrum of the monoiodide fraction, shown in Fig. 2B, exhibited the bands at 801·5 and 2205 cm^{-1} with greatly enhanced intensity. The latter band is clearly due to the Si–H stretching frequency and the new bands that appear at 840·5 and 903 cm^{-1} are the deformations of SiH_2D and SiH_3. Further hydrogen–deuterium exchange was accomplished by permitting this monoiodide fraction to stand another 15 hr at 75° with a fresh batch of SiH_2I_2. The spectrum of the monoiodide from this second treatment, shown in Fig. 2C, proves the increased concentrations of the more completely hydrogenated iodides.

The very weak band at 1178 cm^{-1} cannot be the difference band $\nu_4 - \nu_6$, even though its calculated position (1172 cm^{-1}) is close, since one should then find

VOL. 12 1958

the more intense combination $\nu_4 + \nu_6$ at about 2042 cm^{-1}, but there is no trace of absorption in this region. There being no apparent way to assign either the 1178 or 501 cm^{-1} band to SiD_3I, we must assume that these weak bands belong to some unknown impurity.

Force constants

For silyl iodide we have assumed a potential energy function containing nine force constants.

$$\begin{aligned}
2V = {} & f_d[(\Delta d_1)^2 + (\Delta d_2)^2 + (\Delta d_3)^2] + f_D(\Delta D)^2 \\
& + f_\alpha[(\Delta\alpha_{12})^2 + (\Delta\alpha_{23})^2 + (\Delta\alpha_{31})^2] \\
& + f_\beta[(\Delta\beta_1)^2 + (\Delta\beta_2)^2 + (\Delta\beta_3)^2] \\
& + 2f_{dd}[(\Delta d_1)(\Delta d_2) + (\Delta d_1)(\Delta d_3) + (\Delta d_2)(\Delta d_3)] \\
& + 2f_{\alpha\alpha}[(\Delta\alpha_{12})(\Delta\alpha_{23}) + (\Delta\alpha_{12})(\Delta\alpha_{31}) + (\Delta\alpha_{23})(\Delta\alpha_{31})] \\
& + 2f_{\beta\beta}[(\Delta\beta_1)(\Delta\beta_2) + (\Delta\beta_1)(\Delta\beta_3) + (\Delta\beta_2)(\Delta\beta_3)] \\
& + 2f_{\alpha\beta}[(\Delta\alpha_{12})(\Delta\beta_1 + \Delta\beta_2) + (\Delta\alpha_{23})(\Delta\beta_2 + \Delta\beta_3) + (\Delta\alpha_{31})(\Delta\beta_1 + \Delta\beta_3)] \\
& + 2f'_{\alpha\beta}[(\Delta\alpha_{12})(\Delta\beta_3) + (\Delta\alpha_{23})(\Delta\beta_1) + (\Delta\alpha_{31})(\Delta\beta_2)]
\end{aligned}$$

Table 3. Force constants and frequencies of SiD_3I

Force constants (dyne/cm)		Obs. freq.	Calc. freq.
f_d	$2{\cdot}7746 \times 10^5$	1575	1560·7
f_{dd}	$0{\cdot}0207 \times 10^5$	664	678·6
f_D	$1{\cdot}9514 \times 10^5$	351·5	341·7
$f_\alpha - f_{\alpha\alpha}$	$0{\cdot}2001 \times 10^{-11}$	1607	1596·7
$f_\beta - f_{\beta\beta}$	$1{\cdot}0380 \times 10^{-11}$	(675)	674·1
$3/2(f_{\alpha\alpha} + f_{\beta\beta}) - 3f_{\alpha\beta}$	$-0{\cdot}1415 \times 10^{-11}$	435	433·8

in which d_i refers to the ith Si–H bond, D to the Si–I bond, α_{ij} to the H_i–Si–H_j angle and β_i to the H_i–Si–I angle. For purposes of force-constant calculations, we have taken the equilibrium values as $d = 1{\cdot}48$ Å, $D = 2{\cdot}45$ Å and both α and β as tetrahedral angles. Making the further assumption that $f_{\alpha\beta} = f'_{\alpha\beta}$, we then used the six fundamental frequencies of SiH_3I to evaluate by the familiar WILSON matrix method [6] the six combinations of force constants given in Table 3. This set of constants was then employed to calculate the fundamentals of SiD_3I, also given in Table 3.

The observed and calculated values agree fairly well. The largest discrepancy amounts to 2·8 per cent and the mean error is 1·3 per cent. Our constants f_d and f_{dd} compare favorably with the values 2·72 and 0·09 given for the corresponding force constants in the silanes [7]. The normal co-ordinate for the ν_3 mode consists very largely of the Si–I stretch and consequently it is not surprising that our value for f_D agrees well with the $1{\cdot}93 \times 10^5$ computed for the SiH_3–I stretch in the diatomic approximation.

Acknowledgements—One of us (H. R. L.) acknowledges with gratitude the support accorded him under a Fellowship from the Allied Chemical & Dye Corporation.

References

[1] Dixon R. N. and Sheppard N. *J. Chem. Phys.* 1955 **23** 215; *Trans. Faraday Soc.* 1957 **53** 282.
[2] Emeleus H. J., Maddock A. G. and Reid C. *J. Chem. Soc.* 1941 353.
[3] Lord R. C., Robinson D. W. and Schumb W. C. *J. Amer. Chem. Soc.* 1956 **78** 1327.
[4] Gerhard S. L. and Dennison D. M. *Phys. Rev.* 1933 **43** 197.
[5] Johnston M. and Dennison D. M. *Phys. Rev.* 1935 **48** 868.
[6] Wilson E. B. Jr. *J. Chem. Phys.* 1939 **7** 1047; 1941 **9** 76.
[7] Meal J. H. and Wilson M. K. *J. Chem. Phys.* 1956 **24** 385.

VOL.
12
1958

Spectrochimica Acta, 1958, Vol. 12, pp. 47 to 56. Pergamon Press Ltd., London

The vibration frequencies of the symmetrical *p*-dihalogenobenzenes

A. Stojiljković* and D. H. Whiffen
The Chemistry Department, The University, Birmingham 15, England

(*Received* 6 *November* 1957)

Abstract—The infra-red spectra of *p*-dichlorobenzene, *p*-dibromobenzene, and *p*-diiodobenzene have been measured in solution and in potassium chloride disks, and Raman spectra of the last two compounds examined in solution. The results, together with earlier Raman measurements, lead to an assignment of the majority of the 30 fundamental frequencies. In the light of these assignments, some adjustments are made in the assignments of *p*-difluorobenzene.

1. Introduction

There has been much interest in the correlation of infra-red vibrations frequencies of aromatic compounds [1–4] with the electronic properties of the substituents, especially the Hammett sigma function. There is need for a complete assignment for the simpler compounds, so that the changes of frequency can be more closely related to changes of mass and force constant, and so a deeper insight obtained into the empirical relationships. Following the earlier assignment of the monohalogenobenzenes [5], the present contribution relates to the symmetrical *p*-disubstituted benzenes. *p*-Difluorobenzene has been thoroughly studied by Ferguson, Hudson, Nielsen and Smith [6], while the infra-red spectra of the other dihalogen compounds have been partially measured by Lecomte [7] and by Parodi [8]. The Raman spectra have been measured by several workers, notably Kohlrausch [9, 10] and Paulsen [11].

2. Experimental

The infra-red measurements were made on a single-beam Grubb–Parsons spectrometer. The solid measurements refer to potassium chloride disks and the solution measurements to carbon tetrachloride and tetrachlorethylene solutions from 3300 to 1300 cm^{-1} and carbon disulphide solutions from 1300 to 400 cm^{-1}, using sodium chloride and potassium bromide prisms. Path lengths up to 1 mm and solutions up to 25 g/100 cm^3 were employed. Extinction coefficients were approximately measured, but in view of the possible errors and the time required to obtain accurate values, the results are only given in approximate form. In the tables, bands with extinction coefficients greater than 300 are marked *vvs*; between 100 and 300, *vs;* between 30 and 100, *s;* between 10 and 30, *m;* from 1 to 3, *vw*; and below 1, *vvw*. The Raman spectra of *p*-dibromo and *p*-diiodobenzene were measured in chloroform and carbon disulphide solutions respectively, using a Hilger larger aperture Raman spectrograph with photographic detection and dispersion of 16 Å/mm. The polarization properties were obtained from exposures with polaroid cylinders round the sample tube, two exposures being taken with the incident light polarized parallel and perpendicular to the tube axis. The results together with the assignment are given in Tables 1, 2 and 3.

* On leave from Faculty of Science, Belgrade University.

Table 1. Infra-red and Raman spectra of *p*-dichlorobenzene

Infra-red		Raman [9, 11 12] melt	Interpretation
Solution	Solid		
		299 (8) *dp*	b_{2g} fundamental
		330 (12) *p*	a_g fundamental
		351 (3) *dp*	b_{3g} fundamental
		384 (0)	
484 *s*	484	480 (0)	b_{3u} fundamental
546 *s*	546		b_{1u} fundamental
558 *w*	558		
		598 (0)	$2 \times 299 = 598$; $2 \times a_g = a_g$
		628 (8) *dp*	b_{3g} fundamental
		747 (12) *p*	a_g fundamental
783 *w*	785		$299 + 484 = 783$; $b_{2g} \times b_{3u} = b_{1u}$
		811 ($\frac{1}{2}$) *dp*	b_{1g} fundamental
816 *vvs*	816		b_{3u} fundamental
934 *vw*			b_{2g} fundamental
951 *vvw*	951		a_u fundamental
1013 *vvs*	1013		b_{1u} fundamental
		1069	$330 + 747 = 1077$; $a_g \times a_g = a_g$
1087 *vvs*	1085		b_{1u} fundamental
		1087 (8) *p*	$2 \times 546 = 1092$; $2 \times b_{1u} = a_g$
		1106 (12) *p*	a_g fundamental
1104 *m*	1109		b_{2u} fundamental
1112 *m*	1123		$299 + 816 = 1115$; $b_{3g} \times b_{3u} = b_{1u}$
1140 *vvw*	1148		$330 + 816 = 1146$; $a_g \times b_{3u} = b_{3u}$
		1169 (5) *p*	a_g fundamental
1168 *w*	1175		$484 + 689 = 1173$; $b_{3u} \times b_{2g} = b_{1u}$
1219 *vw*	1219		$405 + 811 = 1216$; $a_u \times b_{1g} = b_{1u}$
		1233 ($\frac{1}{2}$)	$299 + 934 = 1233$; $b_{2g} \times b_{2g} = a_g$
		1248 *dp*	
1260 *w*	1260		b_{2u} fundamental
1285 *vvw*	1282		$546 + 747 = 1293$; $b_{1u} \times a_g = b_{1u}$
		1291 (3)	b_{3g} fundamental
1295 *vvw*	1294		$484 + 811 = 1295$; $b_{3u} \times b_{1g} = b_{2u}$
		1378 (1) *dp*	$2 \times 689 = 1378$; $2 \times b_{2g} = a_g$
1393 *s*	1393		b_{2u} fundamental
1416 *m*	1416		$484 + 934 = 1418$; $b_{3u} \times b_{2g} = b_{1u}$
1442 *vvw*			$330 + 1104 = 1434$; $a_g \times b_{2u} = b_{2u}$
1475 *vvs*	1473		b_{1u} fundamental
		1485 *dp*	$2 \times 747 = 1494$; $2 \times a_g = a_g$
1504 *w*			$689 + 816 = 1505$; $b_{2g} \times b_{3u} = b_{1u}$
1570 *vvw*		1573 (12) *dp*	a_g and b_{3g} fundamentals
		1632 ($\frac{1}{2}$)	$2 \times 816 = 1632$; $2 \times b_{3u} = a_g$
1630 *w*	1629		$811 + 816 = 1627$; $b_{1g} \times b_{3u} = b_{2u}$
1750 *vw*			$816 + 934 = 1750$; $b_{3u} \times b_{2g} = b_{1u}$
1760 *vw*			$811 + 951 = 1762$; $b_{1g} \times a_u = b_{1u}$
1821 *vvw*			$351 + 1475 = 1826$; $b_{3g} \times b_{1u} = b_{2u}$
1878 *m*	1881		$934 + 951 = 1885$; $b_{2g} \times a_u = b_{2u}$
1936 *vvw*			$934 + 1009 = 1934$; $b_{2g} \times b_{1u} = b_{3u}$
		3072 (1) *p*	a_g and b_{3g} fundamentals
3095 *w*			b_{2u} fundamental

{ = Fermi resonance.

VOL. 12 1958

Table 2. Infra-red and Raman spectra of *p*-dibromobenzene

Infra-red		Raman		Interpretation
Solution	Solid	Solution	Melt [9, 10]	
			165 (3)	
		218 *p*	214 (12)	a_g fundamental
		—	271 (7)	b_{2g} fundamental
			307 (1)	b_{3g} fundamental
429 *s*	427 *s*			b_{1u} fundamental
473 *s*	472 *s*			b_{3u} fundamental
		623 *dp*	625 (4)	b_{3g} fundamental
710 *vvw*		708 *p*	709 (10)	a_g fundamental
741 *vw*				$271 + 473 = 744$; $b_{2g} \times b_{3u} = b_{1u}$
807 *vvs*	807			b_{3u} fundamental
935 *w*				b_{2g} fundamental
950 *w*	953			a_u fundamental
997 *m*	995			
1003 *vvs*	1003			b_{1u} fundamental
1049 *vw*				$429 + 623 = 1052$; $b_{1u} \times b_{3g} = b_{2u}$
		1067 *p*	1064 (12)	a_g fundamental
1066 *vs*	1064			b_{1u} fundamental
1078 *s*	1085			$271 + 807 = 1078$; $b_{2g} \times b_{3u} = b_{1u}$
1100 *s*	1105			b_{2u} fundamental
1135 *w*	1134			$429 + 708 = 1137$; $b_{1u} \times a_g = b_{1u}$
1167 *vw*				$473 + 685 = 1158$; $b_{3u} \times b_{2g} = b_{1u}$
		1170 *p*	1170 (5)	a_g fundamental
1212 *w*	1214			$400 + 815 = 1215$; $a_u \times b_{1g} = b_{1u}$
1251 *w*	1252			b_{2u} fundamental
1280 *vw*				$218 + 1066 = 1284$; $a_g \times b_{1u} = b_{1u}$
			1289 ($\frac{1}{2}$)	b_{3g} fundamental
1294 *vw*				$473 + 815 = 1288$; $b_{3u} \times b_{2g} = b_{1u}$
			1368 (1)	$2 \times 685 = 1370$; $2 \times b_{2g} = a_g$
1381 *s*	1378			b_{2u} fundamental
1406 *w*				$473 + 935 = 1408$; $b_{3u} \times b_{2g} = b_{1u}$
1418 *w*	1420			$307 + 1100 = 1408$; $b_{3g} \times b_{2u} = b_{1u}$
1468 *vs*	1469			b_{1u} fundamental
1498 *m*				$429 + 1067 = 1496$; $b_{1u} \times a_g = b_{1u}$
1565 *vvw*		1570 *dp*	1565 (8)	a_g and b_{3g} fundamentals
			1618 (0)	$2 \times 807 = 1614$; $2 \times b_{3u} = a_g$
1619 *w*	1615			$807 + 815 = 1622$; $b_{3u} \times b_{1g} = b_{2u}$
1740 *vvw*	1746			$807 + 935 = 1742$; $b_{3u} \times b_{2g} = b_{1u}$
1765 *w*	1767			$815 + 950 = 1765$; $b_{1g} \times a_u = b_{1u}$
1880 *w*	1879			$935 + 950 = 1885$; $b_{2g} \times a_u = b_{2u}$
1932 *vvw*				$935 + 1003 = 1938$; $b_{2g} \times b_{1u} = b_{3u}$
		3068	3063 (4)	a_g and b_{3g} fundamentals
3080 *w*				b_{2u} fundamental

— = obscured by solvent

Table 3. Infra-red and Raman spectra of *p*-diiodobenzene

Infra-red		Raman		Interpretation
Solution	Solid	Solution	Solid (11)	
		157 *w*		a_g fundamental
		241 *vw*		b_{2g} fundamental
464 *s*	468			b_{3u} fundamental
			511 (0)	$2 \times 255 = 510$; $2 \times b_{3g} = a_g$
			592 (0)	
			624 (2)	b_{3g} fundamental
		680	686 (8)	a_g fundamental
709 *w*	722			$241 + 464 = 705$; $b_{2g} \times b_{3u} = b_{1u}$
			723 (0)	$2 \times 365 = 730$; $2 \times b_{2u} = a_g$
799 *vvs*	799			b_{2u} fundamental
			837 (0)	
936 *w*			926 ($\frac{1}{2}$)	b_{2g} fundamental
951 *w*				a_u fundamental
972 *m*	975			$365 + 624 = 989$; $b_{1u} \times b_{3g} = b_{2u}$
993 *vvs*	993			b_{1u} fundamental
		1044	1045 (8)	a_g fundamental
1047 *w*				$241 + 799 = 1040$; $b_{2g} \times b_{3u} = b_{1u}$
1065 *vs*	1067			b_{1u} fundamental
1100 *m*	1102			b_{2u} fundamental
1147 *vw*				$464 + 685 = 1149$; $b_{3u} \times b_{2g} = b_{1u}$
1175 *vw*		1175	1179 (5)	a_g fundamental
		1185		$241 + 936 = 1177$; $b_{2g} \times b_{2g} = a_g$
1212 *w*				$395 + 816 = 1211$; $a_u \times b_{1g} = b_{1u}$
1242 *m*	1246			b_{2u} fundamental
1264 *w*	1264			$157 + 1100 = 1257$; $a_g \times b_{2u} = b_{2u}$
1282 *vw*				$464 + 816 = 1280$; $b_{3u} \times b_{1g} = b_{2u}$
			1292 ($\frac{1}{2}$)	b_{3g} fundamental
			1366 ($\frac{1}{2}$)	$2 \times 685 = 1370$; $2 \times b_{2g} = a_g$
1374 *vs*	1369			b_{2u} fundamental
1394 *w*	1400			$464 + 936 = 1400$; $b_{3u} \times b_{2g} = b_{1u}$
1415 *w*				$365 + 1044 = 1411$; $b_{1u} \times a_g = b_{1u}$
		1450	1439 ($\frac{1}{2}$)	$365 + 1065 = 1430$; $b_{1u} \times b_{1u} = a_g$
1463 *vs*	1455			b_{1u} fundamental
1484 *w*				$685 + 799 = 1484$; $b_{2g} \times b_{3u} = b_{1u}$
1539 *vvw*				
1554 *vvw*		1552	1545 (6)	a_g and b_{3g} fundamentals
1615 *w*	1619			$799 + 816 = 1615$; $b_{3u} \times b_{1g} = b_{2u}$
1642 *vw*				$685 + 951 = 1636$; $b_{2g} \times a_u = b_{2u}$
1718 *vw*				$255 + 1463 = 1718$; $b_{3g} \times b_{1u} = b_{2u}$
1730 *vvw*				$799 + 936 = 1735$; $b_{3u} \times b_{2g} = b_{1u}$
1770 *w*	1770			$816 + 951 = 1766$; $b_{1g} \times a_u = b_{1u}$
1881 *w*	1880			$936 + 951 = 1887$; $b_{2g} \times a_u = b_{2u}$
		3056	3050	a_g and b_{3g} fundamentals
3050 *w*				b_{2u} fundamental

VOL. 12 1958

3. Discussion

The symmetry of these molecules is V_h and the 30 normal vibrations belong to the classes as indicated by $6a_g + 1b_{1g} + 3b_{2g} + 5b_{3g} + 2a_u + 5b_{1u} + 5b_{2u} + 3b_{3u}$, where the x-axis is taken perpendicular to the ring and the z-axis passes through the halogens, as recommended by the Joint Commission for Spectroscopy [13]. As a guide to the motions involved, the very approximate diagrams of the normal vibrations are given in Fig. 1. It must be emphasized that mixing of these

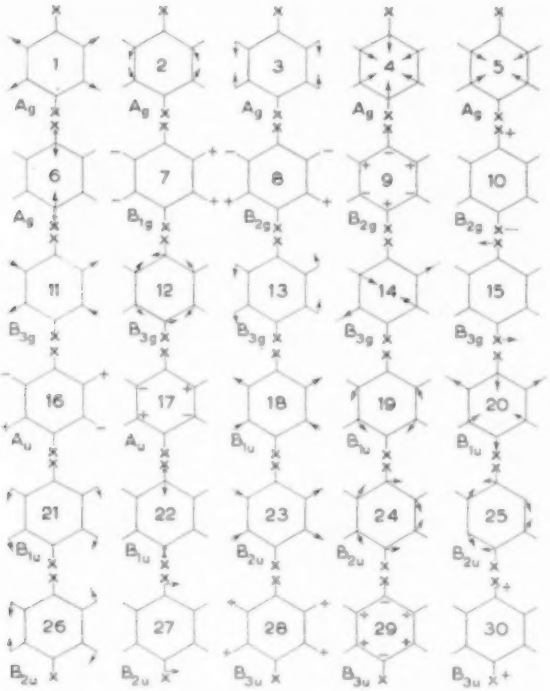

Fig. 1.

modes, which are based on the natural symmetry co-ordinates, may be very considerable and may differ in amount between the different molecules considered. All the g-classes are Raman-active and the u-classes infra-red-active, except a_u which is forbidden in both spectra, at least in the gas phase. Partial assignments are given by the earlier workers [7–11].

C—H stretch (*ν* C—H *nos* 1, 11, 18 *and* 23). The four C—H stretching frequencies are all expected to lie just over 3000 cm^{-1}, but a precise assignment is difficult, since they tend to mask each other and to interact with summation levels of the C—C stretch [2]. The strongest Raman line is likely to be due to the a_g frequency and the strongest infra-red band to the b_{2u} frequency, since in a crude approximation the b_{2u} bands should be three times as strong as the b_{1u}, because the C—H bonds make an angle of only 30° with the y-axis but 60° with the z.

C—C *stretch* (ν C—C *nos* 2, 12, 19 *and* 24). The two highest carbon stretches near 1580 cm^{-1} should appear in the Raman spectra, but in each case only one frequency is observed and this has been assigned to both the a_g and b_{3g} classes, it being presumed that the two lines overlie each other. The infra-red bands at *c.* 1460 and *c.* 1380 cm^{-1} are in each case clearly the b_{1u} and b_{2u} fundamentals. These both derive from a degenerate benzene frequency at 1485 cm^{-1}, but the b_{1u} frequency is raised by interaction with the lower C—*X* stretch, which is in contrast to a slight reduction by interaction with the C—H stretch in the parent benzene. The b_{2u} frequency is lowered, since it contains admixture of the C—*X* in-plane deformation which is naturally lowered on introduction of the heavier masses.

Ring frequencies (*ring nos* 4, 20 *and* 25). Three frequencies in Fig. 1 have been somewhat arbitrarily labelled ring frequencies. The b_{2u} frequency is predominantly a C—C stretch and is the counterpart of the disputed benzene frequency whose assignment at 1310 cm^{-1} has been established by MAIR and HORNIG [14].

The values selected near 1260 cm^{-1} are the infra-red bands which are least satisfactorily assigned as summation bands, but the bands are all weak and some doubt must remain about these assignments. The a_g ring frequencies are easily identified by strong polarized Raman lines and the b_{1u} frequencies depend on the substituent mass, since some C—*X* stretching motion is involved.

C—H *in-plane deformation* (β C—H *nos* 3, 13, 21 *and* 26). The four C—H in-plane deformation frequencies are characterized by the strong a_g Raman lines near 1170 cm^{-1}, the weaker b_{2g} lines near 1290 cm^{-1} together with the strong b_{1u} infra-red bands near 1000 cm^{-1} and weaker b_{2u} bands near 1100 cm^{-1}. For the dichloro-compound there are two possible bands for the latter, 1104 and 1112 cm^{-1} in solution but there is an alternative explanation for the second frequency, as given in Table 1.

Ring-deformation (α C—C—C *nos* 5 *and* 14). There are two vibrations related to the degenerate ring deformation of benzene at 606 cm^{-1}. One in the a_g class interacts considerably with the C—X stretching mode and gives rise to strong polarized Raman lines near 700 cm^{-1}, while the other is almost unchanged in form and frequency and the b_{2g} Raman lines all appear very near 625 cm^{-1}.

C—X *stretch* (ν C—X *nos* 6 *and* 22). As explained above, the C—X stretch modes interact considerably with the ring vibrations, and though the lowest a_g and b_{1u} modes have been designated C—X stretch, this is more a matter of formal book-keeping than a true description of the normal modes. The a_g polarized Raman lines below 400 cm^{-1} are easily assigned. The b_{1u} frequencies are more troublesome. STEWART [15] has argued for a value near 818 cm^{-1} in solid *p*-dichlorobenzene, but there are grounds given by KRUSE [16], who also measured the solid, for rejecting this assignment. Certainly the frequency should be below the value 737 cm^{-1} found [6] in *p*-difluorobenzene for the corresponding band. The values of infra-red bands found at 546 cm^{-1} in *p*-dichlorobenzene and 427 cm^{-1} in *p*-dibromobenzene are available for the b_{1u} class and if these are correct the *p*-diiodobenzene frequency will be below 400 cm^{-1}, the limit of measurement. There is one guide to its value, in that the band corresponding to its summation frequency with the 1044 cm^{-1} ring frequency is expected to appear with moderate

VOL. 12 1958

strength in the infra-red spectrum, since its analogue appears with the other compounds. If this is the band at 1415 cm^{-1} in *p*-diiodobenzene, the missing fundamental would be 371 cm^{-1}; a few other summation bands appear to involve this frequency and a value of 365 cm^{-1} best fits all the observations.

In-plane C—X *deformation* (β C—X *nos* 15 *and* 27). The medium Raman lines at 351 and 307 cm^{-1} appear to be the b_{3g} fundamentals of the dichloro- and the dibromo-compounds, but the corresponding line is not observed with the diiodobenzene. A value of 255 cm^{-1} would enable the Raman line at 511 cm^{-1} to be explained as 2×255. The b_{3u} frequencies are almost certainly below 400 cm^{-1} and not therefore capable of observation with a potassium bromide prism.

Out-of-plane C—H *deformation*. (γ C—H *nos* 7, 8, 16 *and* 28). The out-of-plane C—H deformations in the range 700 to 1000 cm^{-1} are not easily found directly from the spectra except for the extremely strong b_{3u} umbrella frequency. The remaining frequencies are infra-red inactive, though not infrequently appearing weakly in the infra-red in violation of the selection rules, but the summation bands from 1600 to 2000 cm^{-1} can prove useful [17, 18] in this part of the assignment. Partly on this basis the a_u frequencies have been given values near 950 cm^{-1}, the b_{2g} near 935 cm^{-1} and the b_{1g} near 810 cm^{-1}.

Out-of-plane skeleton deformation (ϕ C—C, *nos* 9, 17 *and* 29). The a_u skeleton mode does not involve movement of the substituents and its value should be close to that in benzene, namely 404 cm^{-1}, and slight evidence for this can be obtained from the summation bands. The b_{3u} mode deriving from the same degenerate benzene mode is raised slightly in frequency and made strongly infra-red active by admixture of the C—*X* out-of-plane deformation so that the frequencies are easily observed near 470 cm^{-1}. The third mode has been calculated [19] to be near 720 cm^{-1}, but this may be too high, and the summation bands appear to require values nearer 685 cm^{-1} for this b_{2g} frequency.

Out-of-plane C—X *deformation* (γ C—X *nos* 10 *and* 30). The b_{2g} frequencies which are primarily C—X deformation can be obtained from the Raman spectra, the requisite lines lying below 300 cm^{-1}. The infra-red active b_{3u} frequencies are expected to be lower still and would not be observable with a potassium bromide prism.

4. Spectral comparisons and assignment of *p*-fluorobenzene

The fundamental frequencies are gathered together in Table 4. If the bond distances and force constants were the same for all the halogens, each dichlorobenzene frequency would lie higher than the corresponding dibromobenzene frequency, which in turn would be higher than in diiodobenzene. This expectation is well fulfilled by the frequencies chosen, with the slight exception of the third a_g frequency. This may be a result of experimental error and solvent effects or it may be a reflection of the larger non-bonded van der Waals interaction between the bulky iodine atoms and the adjacent hydrogen atoms. This being established, it is important to see that the spectrum of difluorobenzene [6] conforms to the same pattern. Although most of the previously assigned fundamentals [6] fulfil this criterion, some changes suggest themselves.

In the a_g class it is clear that if the heavier halogen compounds are correctly assigned it is not permissible to assign both the strong polarized Raman lines at

Table 4. Correlation of fundamental vibration frequencies of symmetrical *p*-dihalogenobenzenes

			F, F	Cl, Cl	Br, Br	I, I
a_g	1	ν C—H	3084	3072	3068	3056
	2	ν C—C	1617	1573	1570	1552
	3	β C—H	1245	1169	1170	1175
	4	ring	1142	1106	1067	1044
	5	α C—C—C	858	747	708	680
	6	ν C—X	451	330	218	157
b_{1g}	7	γ C—H	800	811	(815)	(816)
b_{2g}	8	γ C—H	928	934	935	936
	9	ϕ C—C	692	(689)	(685)	(685)
	10	γ C—X	375	299	271	241
b_{3g}	11	ν C—H	3084	3072	3068	3056
	12	ν C—C	1617	1573	1570	1552
	13	β C—H	1285	1291	1289	1292
	14	α C—C—C	635	628	623	624
	15	β C—X	(427)	351	307	(255)
a_u	16	γ C—H	943	951	950	951
	17	ϕ C—C	?	(405)	(400)	(395)
b_{1u}	18	ν C—H	*c.* 3050	*c.* 3050	*c.* 3050	*c.* 3050
	19	ν C—C	1511	1475	1468	1463
	20	ring	1212	1087	1066	1065
	21	β C—H	1012	1013	1003	993
	22	ν C—X	737	546	429	(365?)
b_{2u}	23	ν C—H	3080	3095	3080	3050
	24	ν C—C	1437	1393	1381	1374
	25	ring	1285	1260	1251	1242
	26	β C—H	1085	1104	1100	1100
	27	β C—X	350	?	?	?
b_{3u}	28	γ C—H	833	816	807	799
	29	ϕ C—C	509	484	473	464
	30	γ C—X	186?	?	?	?

( ) frequency inferred from summation bands.

840 and 858·5 cm^{-1} to separate fundamentals; they are more plausibly assigned to the fundamental and the overtone of the lowest b_{3g} frequency at $854 = 2 \times 427$, which will also be due to an a_g level and therefore capable of Fermi interaction with the fundamental. Table 4 suggests that the missing fundamental must be sought a little above 1106 cm^{-1}; the Raman line at 1142 cm^{-1} has a depolarization ratio of 0·66 and is more satisfactorily assigned as an a_g than a b_{3g} frequency. To compensate for this change another b_{3g} frequency is required, and this is likely to

VOL. 12 1958

be near 1600 cm^{-1} by analogy with most benzene derivatives. The Raman line at 1617 cm^{-1} must therefore be assigned as an unresolved doublet, with components in both the a_g and b_{3g} classes. There is also some doubt about the lowest b_{3g} frequency. The Raman line originally assigned to this frequency at 507 cm^{-1} is given as *vvw* and has an alternative explanation as the b_{3u} fundamental appearing in violation of the selection rules. A value nearer 427 cm^{-1} seems preferable on three grounds: (a) it is nearer the position to be expected by extrapolation from the dibromo-(307 cm^{-1}) and the dichloro-benzene (351 cm^{-1}) frequencies; (b) its overtone provides an explanation for the Fermi resonance interaction of the 858 cm^{-1} a_g fundamental; (c) it agrees with the C—F in-plane bending frequencies [20] of *p*-fluorochloro-(420 cm^{-1}), fluorobromo-(416 cm^{-1}) and fluoroiodo-benzene (411 cm^{-1}). Comparison with the other compounds also requires the highest b_{2g} frequency to be raised above 887 cm^{-1}, and the value 928 cm^{-1}, which is required by the summation band assignment [17, 18], is suggested: a very weak infra-red band appears here in the liquid but not the vapour spectrum.

In the infra-red active classes the first difficulty concerns the third b_{2u} frequency which should be above the dichlorobenzene value of 1260 cm^{-1} and, by comparison with the other compounds, appear but weakly in the spectrum. The weak band at 1285 cm^{-1} in the liquid could be this frequency, but it remains to assign the strong absorptions at 1183 and 1212 cm^{-1}. The vapour spectrum of this region is confused, but the main intensity must be derived from the b_{1u} fundamental and there are three other b_{1u} levels in this neighbourhood, namely $451 + 737 = 1188\ a_g \times b_{1u} = b_{1u}$; $509 + 692 = 1201\ b_{3u} \times b_{2g} = b_{1u}$; $375 + 833 = 1208\ b_{2g} \times b_{3u} = b_{1u}$, all of which may borrow intensity from the fundamental and confuse the spectrum. The remaining fundamentals can remain unchanged from the earlier assignment, though special doubt must remain for the proper exact value of the lower a_u fundamental.

Acknowledgements—We wish to thank the British Rayon Research Association for the loan of the Raman spectrometer, and the Royal Society for a grant towards the purchase of the infra-red spectrometer. A. S. wishes to thank the British Council for the award of a scholarship.

References

[1] Bellamy L. J. *J. Chem. Soc.* 1955 2818, 4221.
[2] Lebas J. M. and Josien M. L. *Bull. Soc. Chim. Fr.* 1956 53, 57, 62.
[3] Kross R. D., Fassel V. A. and Margoshes M. J. *J. Amer. Chem. Soc.* 1956 **78** 1332.
[4] Kross R. D. and Fassel V. A. *J. Amer. Chem. Soc.* 1955 **77** 5858.
[5] Whiffen D. H. *J. Chem. Soc.* 1956, 1350.
[6] Ferguson E. E., Hudson R. L., Nielsen J. R. and Smith D. C. *J. Chem. Phys.* 1953 **21** 1457.
[7] Lecomte J. *J. Phys. Radium* 1937 **8** 489; 1938 **9** 3.
[8] Parodi M. *C. R. Acad. Sci., Paris* 1936 **202** 302.
[9] Herz E., Kohlrausch K. W. F. and Vogel R. *Mh. Chem.* 1946 **76** 200.
[10] Kohlrausch K. W. F. and Ypsilanti G. P. *Mh. Chem.* 1935 **66** 285.
[11] Paulsen O. *Mh. Chem.* 1939 **72** 244.
[12] Narain H. and Saksena B. D. *Indian J. Phys.* 1951 **25** 79.
[13] *J. Chem. Phys.* 1955 **23** 1997.
[14] Mair R. D. and Hornig D. F. *J. Chem. Phys.* 1949 **17** 1236.
[15] Stewart J. E. *J. Chem. Phys.* 1955 **23** 986.

[16] Kruse K. M. H. *J. Chem. Phys.* 1956 **25** 591.
[17] Whiffen D. H. *Spectrochim. Acta* 1955 **7** 253.
[18] Kakiuti Y. *J. Chem. Phys.* 1956 **25** 777.
[19] Whiffen D. H. *Molecular Spectroscopy* (Edited by G. Sell) p. 127. The Institute of Petroleum, London 1955.
[20] Narasimham N. H., El-Sabban M. Z. and Nielsen J. R. *J. Chem. Phys.* 1956 **24** 420.

VOL.
12
1958

Spectrochimica Acta, 1958, Vol. 12, pp. 57 to 64. Pergamon Press Ltd., London

The vibration frequencies of unsymmetrical *p*-dihalogenobenzenes

A. Stojiljković* and D. H. Whiffen
The Chemistry Department, The University, Birmingham 15, England

(*Received* 6 *November* 1957)

Abstract—The infra-red and Raman spectra of *p*-bromochlorobenzene, *p*-chloroiodobenzene, and *p*-bromoiodobenzene are presented and largely assigned by analogy with each other and with the remaining *p*-dihalogenobenzenes.

1. Introduction

In the previous paper [1], the vibration frequencies of the symmetrical *p*-dihalogenobenzenes were discussed, and this work has been extended to *p*-chlorobromobenzene, *p*-chloroidobenzene, and *p*-bromoiodobenzene. The unsymmetrical *p*-fluorohalogenobenzenes have already been studied by Narisimham, el-Sabban and Nielsen [2]. The experimental details are essentially the same as in the previous paper [1] and the results are given in Tables 1, 2, and 3.

2. Assignment

These molecules are of C_{2v} symmetry, and with the two-fold axis the z-axis and with the x-axis perpendicular to the ring, the 30 fundamental frequencies fall into the classes indicated by $11a_1 + 3a_2 + 6b_1 + 10b_2$. All the frequencies are permitted in the Raman spectrum and all but the a_2 in the infra-red. The selection rules are not therefore of great use in assigning the frequencies, but much help can be obtained by comparison between related molecules. The force constants and geometry of the molecules are scarcely affected by change of halogen and consequently the main features of comparison between isotopic molecules can be applied to these compounds, as if the halogens were different isotopes of the same element. Thus the frequencies of *p*-bromoiodobenzene should be slightly higher than the corresponding frequencies of *p*-diiodobenzene but slightly lower than those of *p*-dibromobenzene and of *p*-chloroiodobenzene. Consequently, instead of the usual detailed discussion of the assignment, the justification for the values chosen lies largely in Tables, 4, 5, and 6, in which these comparisons are shown. One or two changes of assignment have been made in the assignment of the fluorohalogenobenzenes [2]. For the sake of these tables, the symmetrical molecules have been treated as if they had only C_{2v} symmetry.

Besides the inequalities referred to above, any row of each table should show a smooth progression of frequency. Also, there should be a smooth progression of transition moment for both the infra-red and Raman spectra, since the mode of any frequency can be obtained by a small perturbation of either of its neighbours, and this is unlikely to provide large irregular intensity changes.

One example of the usefulness of this argument lies in the assignment of the two strong infra-red bands of *p*-bromochlorobenzene at 480 and 496 cm^{-1}. These

* On leave from Faculty of Science, Belgrade University.

Table 1. Infra-red and Raman spectra of *p*-bromochlorobenzene

Infra-red		Raman [3, 4]	Interpretation
Solution	Solid	Melt	
		261 (12)	a_1 fundamental
		284 (5)	b_1 fundamental
		333 (2)	b_2 fundamental
480 *s*	478		b_1 fundamental
496 *s*	493		a_1 fundamental
		624 (5)	b_2 fundamental
686 *vvw*			b_1 fundamental
730 *vvw*		730 (10)	a_1 fundamental
763 *vw*	768		$284 + 480 = 764$; $b_1 \times b_1 = a_1$
812 *vvs*	812		b_1 fundamental
		813	a_2 fundamental
935 *vw*			b_1 fundamental
951 *vvw*	952		a_2 fundamental
1009 *vvs*	1008		a_1 fundamental
1068 *vs*	1066	1071 (8)	a_1 fundamental
1087 *vs*	1086	1090 (12)	a_1 fundamental
1100 *s*	1104		b_2 fundamental
1166 *w*		1171 (5)	a_1 fundamental
1216 *w*			$403 + 812 = 1215$; $a_2 \times b_1 = b_2$
1258 *w*	1254		b_2 fundamental
1280 *vw*	1280		
1290 *vw*		1297 ($\frac{1}{2}$)	b_2 fundamental
		1370 (0)	$2 \times 686 = 1372$; $2 \times b_1 = a_1$
1390 *s*	1387		b_2 fundamental
1415 *m*	1410		$480 + 935 = 1415$; $b_1 \times b_1 = a_1$
1440 *w*	1434		$333 + 1100 = 1433$; $b_2 \times b_2 = a_1$
1471 *vs*	1469		a_1 fundamental
1506 *w*			$686 + 812 = 1498$; $b_1 \times b_1 = a_1$
		1557 (5)	b_2 fundamental
1570 *w*		1570 (5)	a_1 fundamental
1627 *w*			$812 + 813 = 1625$; $b_1 \times a_2 = b_2$
1765 *vw*			$813 + 951 = 1764$; $a_2 \times a_2 = a_1$
1812 *vvw*			$333 + 1471 = 1804$; $b_2 \times a_1 = b_2$
1880 *w*			$935 + 951 = 1886$; $b_1 \times a_2 = b_2$
1936 *vvw*			$935 + 1009 = 1944$; $b_1 \times a_1 = b_1$
3060 *w*			a_1 and b_2 fundamentals
		3066 (2)	a_1 and b_2 fundamentals

VOL. 12 1958

Table 2. Infra-red and Raman spectra of *p*-chloroiodobenzene

Infra-red		Raman		Interpretation
Solution	Solid	Solution	Melt [5]	
			169 (3)	b_2 fundamental
		223*p*	221 (10)	a_1 fundamental
			274 (2)	b_1 fundamental
			324 (0)	b_2 fundamental
476 *vs*	476			a_1 and b_1 fundamentals
		624	623 (3)	b_2 fundamental
721 *vw*		722*p*	720 (8)	a_1 fundamental
746 *vw*				$274 + 476 = 750$; $b_1 \times b_1 = a_1$
809 *vvs*	809			b_1 fundamental
936 *vvw*	936			b_1 fundamental
951 *vvw*	953			a_2 fundamental
1005 *vvs*	1004			a_1 fundamental
1054 *s*	1054	1056*p*	1052 (2)	a_1 fundamental
1090 *vvs*	1090	1091*p*	1086 (7)	a_1 fundamental
1100 *m*	1104			b_2 fundamental
1165 *w*				$476 + 690 = 1166$; $b_1 \times b_1 = a_1$
1172 *w*		1176	1172 (3)	a_1 fundamental
1196 *w*				$476 + 722 = 1198$; $a_1 \times a_1 = a_1$
1215 *w*	1215			$400 + 815 = 1215$; $a_2 \times a_2 = a_1$
1251 *w*	1252			b_2 fundamental
1289 *w*	1287		1287	b_2 fundamental
			1370	$2 \times 690 = 1380$; $2 \times b_1 = a_1$
1381 *s*	1380			b_2 fundamental
1411 *w*				$476 + 936 = 1412$; $b_1 \times b_1 = a_1$
1470 *vvs*	1467			a_1 fundamental
1506 *w*				$690 + 809 = 1499$; $b_1 \times b_1 = a_1$
1531 *vw*				$476 + 1054 = 1530$; $a_1 \times a_1 = a_1$
		1560		b_2 fundamental
1567 *w*		1575	1564 (5)	a_1 fundamental
1624 *w*				$809 + 815 = 1624$; $b_1 \times a_2 = b_2$
1740 *vvw*				$809 + 936 = 1745$; $b_1 \times b_1 = a_1$
1768 *vw*	1765			$815 + 951 = 1766$; $a_2 \times a_2 = a_1$
1806 *vvw*				$223 + 1575 = 1798$; $a_1 \times a_1 = a_1$
1880 *w*	1881			$936 + 951 = 1887$; $b_1 \times a_2 = b_2$
1936 *vvw*				$936 + 1005 = 1941$; $b_1 \times a_1 = b_1$
3060 *w*				a_1 and b_2 fundamentals
		3066*p*	3052 (3)	a_1 and b_2 fundamentals

Table 3. Infra-red and Raman spectra of *p*-bromoiodobenzene

Infra-red		Raman		Interpretation
Solution	Solid	Solution	Melt [6]	
		186 *p*	182 (6)	a_1 fundamental
			255 (2)	b_1 fundamental
			291 (0)	b_2 fundamental
470 *s*	469			b_1 fundamental
		623 *dp*	616 (1)	b_2 fundamental
697 *vvw*		698 *p*	691 (4)	a_1 fundamental
725 *vvw*	729			$255 + 470 = 725$; $b_1 \times b_1 = a_1$
737 *vvw*	737			
803 *vvs*	803			b_1 fundamental
936 *vw*				b_1 fundamental
954 *w*	952			a_2 fundamental
1000 *vvs*	1000			a_1 fundamental
1052 *m*	1050	1052 *p*	1045 (4)	a_1 fundamental
1069 *vvs*	1067	1068 *p*	1059 (2)	a_1 fundamental
1100 *s*	1097			b_2 fundamental
1154 *vw*				$470 + 685 = 1155$; $b_1 \times b_1 = a_1$
1171 *w*		1176 *p*	1170 (2)	a_1 fundamental
1213 *w*	1213			$400 + 813 = 1213$; $a_2 \times a_2 = a_1$
1248 *w*	1248			b_2 fundamental
1283 *vw*	1283			$\{470 + 813 = 1283$; $b_1 \times a_2 = b_2$
1296 *vvw*				$\{b_2$ fundamental
			1350 (1)	$2 \times 685 = 1370$; $2 \times b_1 = a_1$
1374 *vs*	1373			b_2 fundamental
1401 *m*	1398			$470 + 936 = 1406$; $b_1 \times b_1 = a_1$
1448 *s*	1445			$\{396? + 1052 = 1448$; $a_1 \times a_1 = a_1$
1467 *vs*	1467			$\{a_1$ fundamental
1486 *w*	1486			$685 + 803 = 1488$; $b_1 \times b_1 = a_1$
1517 *w*	1517			$470 + 1052 = 1522$; $b_1 \times a_1 = b_1$
1553 *vvw*		1561 *dp*	1555 (3)	a_1 and b_2 fundamentals
1621 *w*	1619			$803 + 813 = 1616$; $b_1 \times a_2 = b_2$
1652 *vvw*	1649			$470 + 1176 = 1646$; $b_1 \times a_1 = b_1$
1735 *vw*	1735			$803 + 936 = 1739$; $b_1 \times b_1 = a_1$
1769 *w*	1765			$813 + 954 = 1767$; $a_2 \times a_2 = a_1$
1882 *w*	1878			$936 + 954 = 1890$; $b_1 \times a_2 = b_2$
1932 *vvw*				$936 + 1000 = 1936$; $b_1 \times a_1 = a_1$
		3062		a_1 and b_2 fundamentals
3075 *w*				a_1 and b_2 fundamentals

{ = Fermi resonance

VOL. 12 1958

Table 4. Correlation of fundamental vibration frequencies of *p*-halogenochlorobenzenes

	F, Cl	Cl, Cl	Br, Cl	I, Cl
a_1	3078	3072	3066	3066
		ca. 3050	3060	3060
	1596	1573	1570	1575
	1489	1475	1471	1470
	1232	1169	1166	1176
	1154	1106	1087	1091
	1090	1087	1068	1054
	1015	1013	1009	1005
	839	747	730	722
	680	546	496	476
	376	330	261	223
a_2	949	951	951	951
	(804)	(811)	813	(815)
		(405)	(403)	(400)
b_1	936	934	935	936
	827	816	812	809
	(691)	(689)	686	(690)
	499	484	480	476
	336	299	284	274
	?	?	?	?
b_2	3101	3095	3066	3066
	3078	3072	3060	3060
	1596	1573	1557	1560
	1403	1393	1390	1381
	1289	1291	1290	1289
	1266	1260	1258	1251
	1126	1104	1100	1100
	630	628	624	624
	420	351	333	324
	267	?	?	?

Table 5. Correlation of fundamental vibration frequencies of *p*-halogenobromobenzenes

	F, Br	Cl, Br	Br, Br	I, Br
a_1	3077	3066	3068	3075
	3076	3060	3050	3062
	1586	1570	1570	1561
	1485	1471	1468	1467
	1228	1166	1170	1176
	1155	1087	1067	1068
	1066	1068	1066	1052
	1013	1009	1003	1000
	810	730	708	698
	596	496	429	(396?)
	290	261	218	186
a_2	945	951	950	954
	(894)	813	(815)	(813)
		(403)	(400)	(400)
b_1	931	935	935	936
	824	812	807	803
	689	686	(685)	(685)
	497	480	473	470
	323	284	271	255
	?	?	?	?
b_2	3115	3066	3080	3075
	3077	3060	3068	3062
	1586	1557	1570	1561
	1400	1390	1381	1374
	1289	1290	1289	1296
	1273	1258	1251	1248
	1090	1100	1100	1100
	627	624	623	623
	416	333	307	291
	224	?	?	?

VOL. 12 1958

are clearly the penultimate a_1 frequency and the fourth b_1 frequency, but the problem lies in deciding which is which. Reference to *p*-bromofluorobenzene [2] shows the b_1 frequency to lie below 497 cm^{-1} and reference to *p*-dibromobenzene

Table 6. Correlation of fundamental vibration frequencies of *p*-halogenoiodobenzenes

	F, I	Cl, I	Br, I	I, I
a_1		3066	3075	3056
		3060	3062	3050
	1591	1575	1561	1552
	1484	1470	1467	1463
	1228	1176	1176	1175
	1159	1091	1068	1065
	1050	1054	1052	1044
	1011	1005	1000	993
	806	722	698	680
	575	476	(396?)	(365?)
	244	223	186	157
a_2	949	951	954	951
	(800)	(815)	(813)	(816)
		(400)	(400)	(395)
b_1	931	936	936	936
	821	809	803	799
	688	(690)	(685)	(685)
	497	476	470	464
	309	274	255	241
	?	?	?	?
b_2	3069	3066	3075	3056
		3060	3062	3050
	1579	1560	1561	1552
	1393	1381	1374	1374
	1290	1289	1296	1292
	1260	1251	1248	1242
	1087	1100	1100	1100
	626	624	623	624
	411	324	291	(255?)
	196	?	?	?

[1] shows that it lies above 472 cm^{-1}, and the requirement that it lies evenly between these two frequencies indicates 480 cm^{-1} to be the b_1 *p*-bromochloro frequency. Correspondingly, the a_1 frequency is required to lie evenly between 596 and 427 cm^{-1}, and on this ground also the 496 cm^{-1} is slightly preferable for this class. For *p*-chloroiodobenzene Table 7 shows that the infra-red band at 476 cm^{-1} must be assigned to the b_1 class, but there is no second band for the a_1 frequency. In view of the fall of only 21 cm^{-1} in the a_1 frequency between the corresponding a_1 bands of *p*-bromofluorobenzene at 596 cm^{-1} and *p*-fluoroiodobenzene at 575 cm^{-1}, it seems unlikely that the *p*-chloroiodobenzene frequency is over

90 cm^{-1} below the *p*-bromochlorobenzene frequency at 496 cm^{-1} and so escaped detection; the more plausible alternative is that this frequency too lies at 476 cm^{-1} and that the a_1 and b_1 frequencies are not resolved.

Not only do the fundamental frequencies show a regular pattern, but also the

Table 7. Summation band of third and fourth b_1 frequencies and corresponding bands

Substituents	Observed	Summation
Cl, Cl	783	484 + 299 = 783
Cl, Br	763	480 + 284 = 764
Cl, I	746	476 + 274 = 750
Br, Br	741	473 + 271 = 744
Br, I	725	470 + 255 = 725
I, I	709	464 + 241 = 705

summation bands. For instance, the summation band of the fourth and fifth b_1 frequencies appears regularly in the infra-red spectra between 700 and 800 cm^{-1}, and this applies also to the corresponding summation band of the symmetrical disubstituted compounds. This regularity prevents these bands being assigned to the third b_1 frequency, expected to be about 700 cm^{-1}, since the corresponding frequency would be inactive in the symmetrical compounds. Table 7 shows the agreement for this summation-band assignment. There are other examples of the appearance of related summation bands, including that of the third and fourth b_1 frequencies near 1150 cm^{-1} and of the second and third near 1500 cm^{-1}. There is also a summation correlation in the Raman spectra near 1370 cm^{-1}, where each of the six compounds has a weak line which is assigned to the overtone of the third b_1 frequency near 685 cm^{-1}: this assignment is related to that [7] of the medium Raman line at 1406 cm^{-1} in benzene itself to the overtone of the b_{2g} frequency of 703 cm^{-1}, which is an out-of-plane deformation mode corresponding closely in form to the 685 cm^{-1} mode of the *para* substituted compounds.

Acknowledgements—We wish to thank the British Research Association for the loan of the Raman spectrometer, and the Royal Society for a grant towards the purchase of the infra-red spectrometer. A. S. wishes to thank the British Council for the award of a scholarship.

References

[1] STOJILJKOVIĆ A. and WHIFFEN D. H. *Spectrochim. Acta* 1958 **11** 47.
[2] NARASIMHAM N. A., EL-SABBAN M. Z. and NIELSEN J. R. *J. Chem. Phys.* 1956 **24** 420.
[3] PAULSEN O. *Mh. Chem.* 1939 **72** 244.
[4] HERZ E., KOHLRAUSCH K. W. F. and VOGEL R. *Mh. Chem.* 1946 **76** 200.
[5] KOHLRAUSCH K. W. F. and PONGRATZ A. *Mh. Chem.* 1934 **65** 199.
[6] KOHLRAUSCH K. W. F. and YPSILANTI G. P. *Mh. Chem.* 1935 **66** 285.
[7] HERZFELD N., INGOLD C. K. and POOLE H. G. *J. Chem. Soc.* 1946 316.

VOL. 12 1958

Spectrochimica Acta, 1958, Vol. 12, pp. 65 to 77. Pergamon Press Ltd., London

Porphin

C. Rimington,* S. F. Mason† and O. Kennard‡

(*Received* 24 *August* 1957)

Abstract—Pure porphin, synthesized by a new method, has been examined spectrophotometrically in the infra-red and visible regions. Crystallographic and X-ray diffraction data were recorded for single crystals. An explanation based on spectral theory is offered to account for the spectral characteristics. Some by-products formed during its synthesis have also been examined spectroscopically and it is inferred that they have contaminated many of the previous specimens of porphin and have thus introduced irrelevancies into the spectral absorption attributed to that substance.

Particular interest attaches to porphin, not only because it is the simplest member of the series to which the naturally-occurring porphyrins, haem and chlorophyll belong, but also because its absorption spectrum in the visible region appears to be an exception to the rules propounded by Stern and Wenderlein [1] relating spectral type to chemical structure in this series. Thus, whereas other porphyrins with alkyl substituents in the β-positions of the pyrrole rings have an aetio-type spectrum (Band IV > III > II > I), porphin in neutral solvent is reported by Stern and Wenderlein [2] and Stern, Wenderlein and Molvig [3] to have a phyllo-type spectrum (Band IV > II > III > I) which is displayed by porphyrins, such as phylloporphyrin, having some substituent group attached to a methene carbon atom. Porphin was synthesized in minute yield by Fischer and Gleim [4] and Rothemund [5]. It is probable that neither method yielded a pure product, since reported spectral measurements show considerable discrepancies. More recently, Eisner and Linstead [6] have described a synthesis of chlorin, from which porphin could be obtained secondarily in better yield [7]. Krol [8], working in this Department, has accomplished a direct synthesis of porphin in yields exceeding 5 per cent by a mechanism depending upon a free radical reaction. This material has now been subjected to rigorous criteria of purity, and spectral studies have been made upon it in the ultra-violet, visible and infra-red regions; powder and single-crystal X-ray examinations were also carried out. Some of the by-products of certain synthetic reactions designed to produce porphin and employed by Krol have been investigated. Some of these have absorption bands, indicating that they contaminated several of the porphin preparations studied by earlier workers, since these particular bands are absent from the spectrum of pure porphin.

Methods

The several reactions leading to porphin have been described by Krol [8]. Separation of the products and their purification is described below.

* Department of Chemical Pathology, University College Hospital Medical School, London W.C.1.
† Washington Singer Laboratories, University of Exeter.
‡ National Institute for Medical Research, Mill Hill, London N.W.7.

Chromatography. Al_2O_3 was "Aluminium oxide for chromatographic analysis" (Savory & Moore, Ltd.). MgO heavy magnesium oxide (British Drug Houses, Ltd.) was standardized to Grade III, according to Brockmann and Schodder [9].

Counter-current distribution. A 25 glass-tube Craig apparatus was used.

Solvents. These were carefully purified by standard methods.

Spectra. These were measured in a Unicam SP-500 photoelectric spectrophotometer or in a Cary recording spectrometer, and for the infra-red region a Perkin–Elmer instrument, model 12C, was used with LiF, NaCl and KBr prisms, and with the sample pressed into a disc with KBr.

X-ray diffraction. This was recorded using a standard Unicam 3 cm camera and Weissenberg apparatus.

Results

Purification of porphin

The benzene-soluble material synthesized from 2-hydroxymethyl pyrrole according to Krol [8] was passed through a column of Al_2O_3 which retained much brown material. It was then dissolved in benzene and chromatographed upon a column of MgO packed in benzene. Using an eluting mixture of benzene/chloroform/methanol (85/10/5), the porphin was obtained free from a narrow band with blue fluorescence which preceded it and a yellow-green band with red fluorescence which followed it slowly. The porphin solution at this stage exhibited no band at 635 mμ (see later).

Solvent was removed *in vacuo* and the material dissolved by warming in benzene and rechromatographed upon MgO, from which it was eluted by benzene as a single band and behaved as a homogeneous substance in the Craig machine. From the hot concentrated solvent it separated in large red, square tablets with shining lustre. For analysis it was dried *in vacuo* at 60°. (Found: C, 77·45; H, 4·67; N, 18·3. Calc. for $C_{20}H_{14}N_4$: C, 77·48; H, 4·52; N, 18·1 per cent).

An alternative method of purification was to subject the material from the Al_2O_3 column (see above) to counter-current distribution between ether and 0·45 N HCl. The blue fluorescent material remained in the first tubes, whilst another impurity passed rapidly on. After two such treatments the porphin was pure.

Spectral absorption of porphin

Absorption data in the visible region for porphin dissolved in benzene is presented in Table 1, together with some values from the literature. The spectral absorption measured by the Unicam spectrophotometer is plotted in Fig. 1, but the Cary tracings resolved the "shoulders" and revealed numerous smaller peaks. In order to show that none of the main bands was due to transition from thermally excited vibrational states, tracings were also made in ethanol at −80° and −180° but were essentially similar to those obtained at room temperature. At the lower temperature, however, the spectrum is considerably sharpened and, in particular, the Soret band is resolved. The visible absorption clearly arises from at least two electronic transitions, each with its own vibrational fine structure. The data obtained at −180° is presented in Table 2 and Fig. 2.

VOL. 12 1958

Table 1. Light absorption data for porphin

Present authors (benzene)*				Eisner and Linstead [6, 7] (benzene)		Stern, Wenderlein and Molvig [3] (benzene)		Albers and Knorr [19] (pyridine–ether)		Rothemund [5] (pyridine–ether)		Fischer and Gleim [4] (pyridine–ether)	
λ_{max}		$\varepsilon \times 10^{-3}$		λ_{max}	$\varepsilon \times 10^{-3}$	λ_{max}	$\varepsilon \times 10^{-3}$	λ_{max}	$\varepsilon \times 10^{-3}$	λ_{max}	Relative intensity	λ_{max}	Relative intensity
								683	1·50				
								671	1·57				
						634	0·16	630	0·67	632·3	1		
616·5	*617·3*	0·86	*0·87*	616	0·89	615	0·80	612	0·85	617·8	5	616·8	4
	(607)		*0·54*							605·4	1	606·5	3
	(590)		*1·04*							590·6	2	590·9	2
	(583)		*1·81*					585	0·78				
569	*571*	4·17	*4·11*	568·5	4·40					571·6	6	572·1	6
563·5	*564*	4·98	*4·98*	563	5·20	562	4·74	565	2·73	561·9	7	564·4	7
	(555)		*2·72*					559	3·20	552·7	3		
	(541)		*1·03*										
519·5	*520·8*	2·64	*2·80*	520	3·00	519	2·55	515	2·55	522·4	4	518·2	5
489·5	*490·3*	15·75	*14·9*	489·5	16·00	489	14·80	485	9·83	489·9	8	486·7	8
	(483)		*11·5*										
	(472)		*2·80*									460·0	1
	(464·5)		*2·02*										
396·5		264·0		395	261·0			390	168·0				

* Normal type: Unicam SP 500.
Italic type: Carey recording spectrometer. In parentheses: shoulders or inflexions.
All wavelengths in mμ.

In 5 per cent HCl porphin exhibits one well-defined band in the visible region (max. 537 mμ; $\varepsilon = 10{\cdot}9 \times 10^3$) and an intense Soret band (max. 393 mμ; $\varepsilon = 354{\cdot}4 \times 10^3$; Pruckner and Stern [10] give λ_{max} 392 mμ and $\varepsilon = 358 \times 10^3$ for their porphin in dioxan).

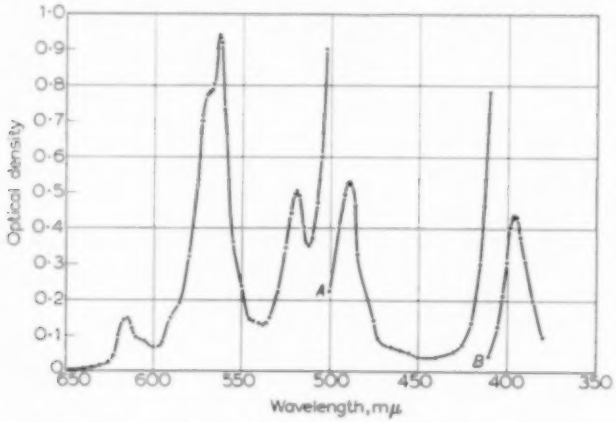

Fig. 1. Spectral absorption of porphin (Unicam SP 500; solvent benzene. At *A* solution diluted 1 in 5; at *B* further dilution of 1 in 20).

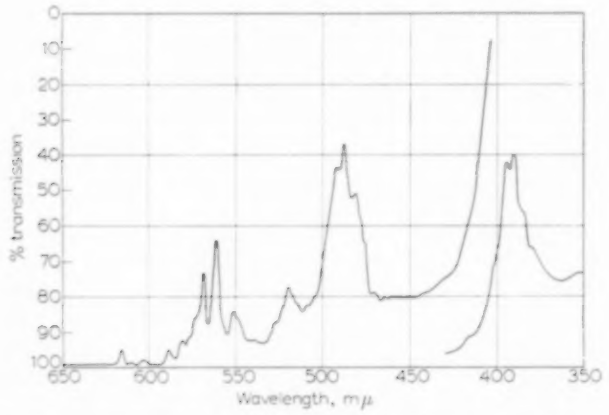

Fig. 2. Spectral absorption of porphin in ethanol at $-180°$ (Cary recording spectrometer). For Soret region, ten-fold dilution.

The infra-red absorption of porphin is recorded in Table 3 and Fig. 3.

The absorption spectrum of solid porphin was studied on crystals mounted on microscope slides. Plane-polarized light was used and the absorption spectra were observed through a microspectroscope replacing the eyepiece of a polarizing microscope. Direct comparison was made with the spectrum of a solution of porphin in benzene, using a comparison prism in the spectroscope eyepiece.

The crystals were too thin to be studied in orientations other than with the light travelling perpendicular to the plane of the platelets (the *c* crystallographic plane). In this orientation the crystals were strongly pleochroic and the absorption

VOL. 12 1958

spectrum showed a considerable strengthening of the absorption band at about 615·5 mμ (Fig. 4), when compared with the spectrum of the solution. All other bands were considerably weakened. The intensity and position of the prominent band varied in the two extinction positions. With the electric vector vibrating parallel to the *b* crystallographic axis, the band extended to almost 630 mμ and was stronger than in the other extinction position. In some crystals the band was almost completely absent in the latter position.

Crystallography

Optics. Porphin forms tabular, square, metallic-red monoclinic crystals showing diagonal extinction. Pleochroism is marked. With the electric vector vibrating in the plane of the platelets the colour changes from dark orange in one

Table 2. The visible and ultra-violet spectrum of porphin in ethanol solid glass at $-180°$

Maxima (mμ)	$\varepsilon \times 10^{-3}$	Maxima (mμ)	$\varepsilon \times 10^{-3}$
613·4	0·87	507·0	5·54
608·1	0·46	498·0	9·40
602·0	0·57	491·8	13·7
587·6	1·35	490·2	13·7
578·5	2·01	487·5	16·3
576·2	2·18	482·5	12·4
572·0	3·03	480·9	12·8
567·8	5·12	478·4	11·1
560·6	7·26	476·1	0·96
550·5	3·95	471·0	0·76
547·6	3·56	469·0	0·76
525·0	4·32	401·5	110
519·0	6·06	394·3	264
517·0	5·14	390·6	282
514·0	5·34	385·7	185

extinction position to light orange in the other. The direction of strong absorption is parallel to the *b* crystallographic axis.

X-ray data. Unit cell dimensions were determined from rotation photographs about the three crystallographic axes and from a Weissenberg photograph, with an accuracy of ± 1 per cent. Filtered Cu radiation $\lambda = 1{\cdot}5418$ Å was used. The density D was determined by centrifugation in a continuous gradient density column. The crystals are monoclinic with cell dimensions of: $a = 12{\cdot}35$ Å; $b = 12{\cdot}35$ Å; $c = 10{\cdot}30$ Å; $\beta = 102°$. There are four molecules in the unit cell; $D_{\text{meas.}} = 1{\cdot}336$ g/ml; $D_{\text{calcd.}} = 1{\cdot}339$ g/ml. Molecular weight calculated from formula = 310; molecular weight calculated from X-ray data = 308. Absent spectra: $h0l$ present with h even orders only, $0k0 : 040$ only observed. The probable space-group is $P2_1/a$ but Pa and $P2/a$ are also possible. With four molecules in the unit cell, there are no restrictions on the position or symmetry of the prototype molecule, unlike in the phthalocyanine series, where the symmetry

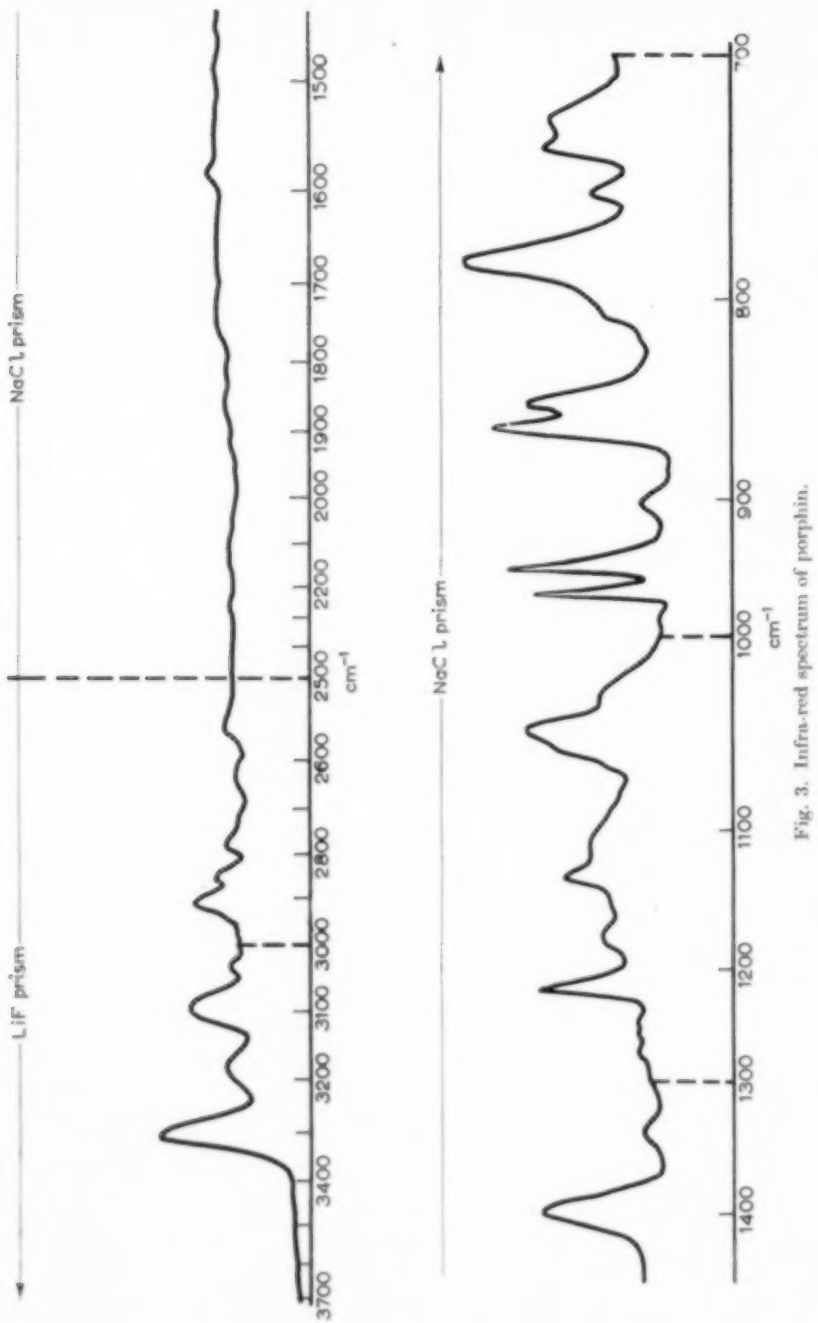

Fig. 3. Infra-red spectrum of porphin.

VOL. 12 1958

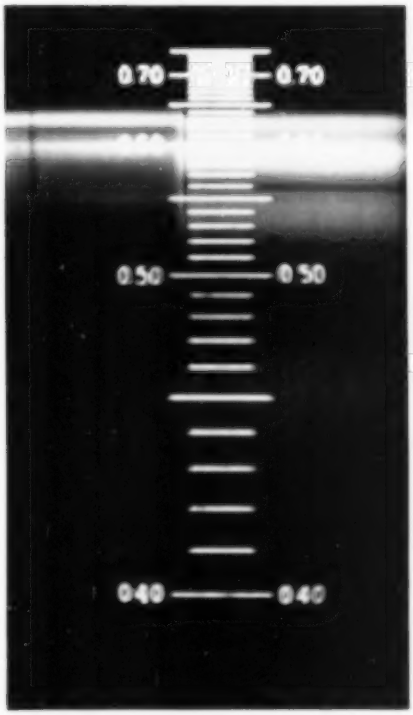

Fig. 4. Comparison of the absorption spectrum of a solution of porphin in benzene (right), viewed by ordinary light, and a crystal of porphin (left), viewed by plane polarized light with the electric vector vibrating parallel to the *b* crystallographic axis.

VOL.
12
1958

centre of the molecule was found to coincide with the symmetry centre of the unit cell, thus fixing the position of the molecule [11]. This circumstance renders more difficult the full structural analysis of crystalline porphin, which has not yet been undertaken.

Examination of by-products arising with porphin during different methods of synthesis

The reaction which provided the greatest number of by-products was that between 2-dimethylaminomethyl pyrrole, methyl iodide and magnesium in ether at room temperature [8, reaction 2] allowed to proceed for 20 hr. After

Table 3. Infra-red spectrum of porphin in a potassium bromide disc

Band position (cm^{-1})	Intensity	Band position (cm^{-1})	Intensity	Band position (cm^{-1})	Intensity
LiF prism		NaCl prism		NaCl prism	
3305	*ms*	2115	*w*	995	*w*
3181	*w*	2100	*w*	970	*s*
3102	*m*	1589	*w*	951	*s*
3036	*w*	1406	*m*	901	*m*
2997	*vw*	1352	*w*	853	*s*
2954	*w*	1281	*w*	841	*s*
2921	*ms*	1262	*w*	809	*w*
2851	*m*	1252	*w*	792	*w*
2782	*m*	1224	*s*	771	*s*
2742	*w*	1184	*m*	749	*m*
2669	*w*	1158	*w*	728	*s*
2654	*w*	1137	*m*	719	*s*
2597	*w*	1116	*w*	KBr prism	
2563	*w*	1057	*m*	690	*s*
2494	*w*	1048	*s*	638	*m*
2422	*w*	1033	*w*	618	*m*

s = strong.
ms = moderately strong.
m = moderate.
w = weak.
vw = very weak.

addition of acetic acid and water, the ether phase was removed and filtered through "supercel" to remove suspended dark material and shaken repeatedly with 5 per cent HCl. This extract was made alkaline by NaOH and left overnight at 0°. The precipitated pigment was collected on a filter and extracted by $CHCl_3$ (Soxhlet). The dark insoluble residue was rejected, the solution evaporated to dryness and the combined pigments dissolved by warming with benzene.

This solution was filtered through a column of MgO grade III and the chromatogram developed, with the result shown in Table 4.

Band 1. The spectral absorption of this pigment is shown in Fig. 5 and is characterized by a marked band at 635 mμ (order of intensity IV > I > II > III). The Soret band in 5 per cent HCl was sharp and intense with λ_{max} = 398 mμ.

Band 2. The red solution displayed no band at 635 mμ, the absorption spectrum much resembling that of porphin. Maxima 617, 564, 522 and 493 mμ with order of

Table 4. Chromatographic separation of pigments on MgO grade III

Developing mixture	Band no.	Appearance	Description of pigment
Benzene	1	Red, narrow	Overlapping, brown-red prisms from benzene
Benzene/chloroform (95/5)	2	Red	
Benzene/chloroform (90/10)	3	Red, very faint	
Benzene/chloroform/methanol (89/10/1)	4	Last traces of 3	
Benzene/chloroform/methanol (88·5/10/1·5)	5	Green	Overlapping, diamond-shaped brown-green plates from benzene
Benzene/chloroform/methanol (85/10/5)	6	Purple red.	Main band of porphin. Square tablets from benzene

VOL. 12 1958

intensity IV > II > III > I. In 5 per cent HCl the colour was mauve, there being one prominent band at 544 mμ and a much smaller one at *c.* 580 mμ; the Soret band was sharp and intense with λ_{max} 398 mμ.

Bands 3 *and* 4. Insufficient material for examination.

Band 5. Rechromatographed on MgO (benzene/chloroform/methanol, 85/10/5), a well defined green band was obtained preceded by a small amount of brownish-pink pigment; some dark material remained at the top of the column. The eluate was diluted four-fold with benzene for spectrophotometry. This pigment had a characteristically chlorin-like spectrum (Fig. 6) with maxima at 630, 602·5, 582, 534, 489 and 481 mμ (ratios of intensities, 1·0, 0·6, 0·83, 0·33, 0·260, 0·222). The pigment passed from the solvent into 20 per cent HCl, affording a blue solution in which the acid chlorin-type spectrum was observed (Fig. 7) with a pronounced maximum at 620 mμ; the sharp Soret band had λ_{max} 399–400 mμ.

Band 6. The crystalline pigment obtained from this fraction proved to be pure porphin.

When the same reaction between pyrrole-Mannich base magnesium and methyliodide in ether was terminated after 1·5 hr, the only pigments definitely identified were porphin and the chlorin. Warming the initial mixture for 2 hr and then leaving it at room temperature overnight resulted in a mixture of pigments which were separated in the following way. To the reaction mixture was added some acetic acid and then 0·1 N HCl to decompose the Grignard reagent. The acid layer and further washings with 0·1 N HCl removed a greenish-brown pigment

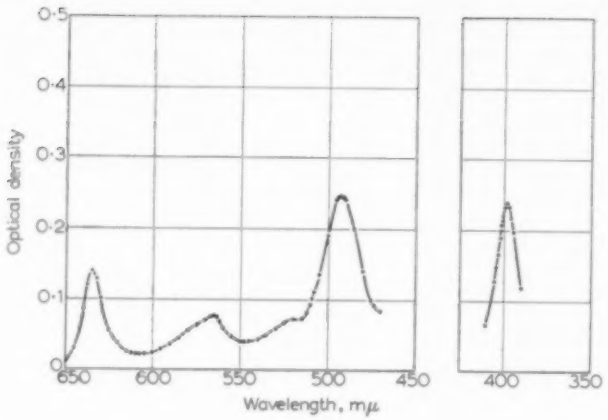

Fig. 5. Spectral absorption of the red pigment, band 1. From 650–470 mμ solvent benzene; for Soret region, solvent 5 per cent HCl.

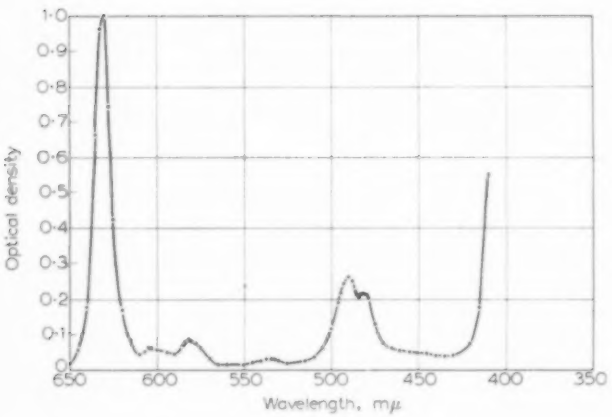

Fig. 6. Spectral absorption of the green pigment, band 5 (chlorin); solvent benzene.

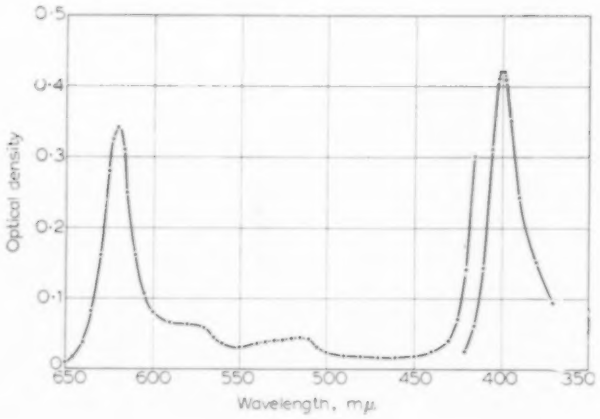

Fig. 7. Spectral absorption of the green pigment, band 5 (chlorin); solvent 20 per cent HCl. For Soret region, solution diluted 1 in 5.

which was purified by returning to ether, back to 0·1 N HCl and finally to benzene. During this process some amorphous dark material was removed, leaving a brownish solution with intense red fluorescence and a spectrum with bands at 632·5, 570, 535 and 494 mμ (order of intensity IV > I > II > III). In 5 per cent HCl it showed two rather broad maxima at 595 and 546 mμ and a rather broad Soret band at 398 mμ. This material would appear to have been that forming Band 1 (see above) but in an impure condition.

The ether solution remaining after extraction with 0·1 N HCl was shaken repeatedly with 5 per cent HCl, which left only impure chlorin in the ether phase Sodium acetate was added to the 5 per cent HCl extract and the pigments returned to ether, which was then dried ($MgSO_4$), removed by evaporation, and the residue dissolved in benzene and passed through a column of Al_2O_3 to remove dark, non-porphyrin material. Spectrophotometry of this solution revealed porphin contaminated by some of the pigment with absorption at 635 mμ. This preparation has been described in detail, since the spectral picture of the impure porphin solution resembled very closely that attributed to porphin by Stern and Wenderlein [2], Stern, Wenderlein and Molvig [3] and Rothemund [5] (see Table 1).

Reaction 3 of Krol [8], in which a suspension in ethanol of 2-dimethylaminomethyl pyrrole methiodide is added slowly to an excess of sodium ethoxide in boiling ethanol and the non-fluroescent mixture is then acidified and treated with excess of potassium persulphate, yielded only porphin, as did the addition of 2-hydroxymethyl pyrrole to a mixture of acetic acid and potassium persulphate at 60° (reaction 6).

VOL. 12 1958

Discussion

Older methods for synthesizing porphin, as for example, prolonged boiling of 2-pyrrolealdehyde with formic acid [4], have led to low yields of material of doubtful purity. A spectral absorption band at about 635 mμ has frequently been reported in such products and the spectrum as a whole has been of phyllo type. Eisner and Linstead's [6, 7] porphin prepared secondarily from chlorin, showed no band at 635 mμ. A convenient method for direct synthesis of porphin having been achieved in this laboratory [8], the physico-chemical characteristics of pure porphin have been determined and it has also been shown that, when using certain reactions, not only is chlorin formed as well as porphin but also smaller quantities of crystallizable by-products. One of these has a prominent absorption band at 634 mμ in benzene solution and has almost certainly contaminated the older preparations referred to since pure porphin exhibits no band at this wavelength.

The full X-ray structure analysis of crystalline porphin has not yet been undertaken. The unit-cell dimensions and some of the optical properties of the crystals have been determined and these suggest that the four molecules of porphin in the unit cell are all approximately parallel to the *b* crystallographic axis, with the molecular planes steeply inclined to the crystal axes. Reinforcement of light absorption would thus result parallel to the *b* axis.

The visible absorption spectrum of a solution of pure porphin is still of phyllo type (order of band intensities IV > II > III > I), which Stern and Wenderlein [1] considered characteristic of porphyrins having some substituent on a methene

carbon atom. The alkyl-substituted porphyrins such as aetioporphyrin, coproporphyrin, uroporphyrin, etc., have aetio-type spectra (order of band intensities IV > III > II > I) and the reason for the apparent departure from this rule in the case of porphin requires discussion. STERN and WENDERLEIN's [1] rules relating porphyrin structure and spectral absorption were purely empirical. Porphin with its cyclic system of conjugated double bonds offers an attractive opportunity for theoretical deductions, and calculations have been made, among others by KUHN [12], SIMPSON [13], LONGUET-HIGGINS, RECTOR and PLATT [14] and MATLOW [15], using either the free electron model or the linear combination of atomic orbitals–molecular orbital approximation. In a recent treatment PLATT [16] has given a semi-empirical interpretation, based on the L.C.A.O. and F.E.M. methods, of the spectra of a wide variety of porphyrin derivatives. Considering the parent molecule, porphin, in its dicationic or dianionic form where it has square symmetry (D_{4h}), it follows from the cyclic structure of the conjugated system that some orbitals, notably the lowest unfilled ones (g-orbitals in PLATT's nomenclature), are doubly degenerate. One of the g-orbitals has a nodal axis in the x-direction, the other in the y-direction, and the two axes being equivalent in the D_{4h} model of porphin, the two orbitals are of the same energy. The degeneracy may be understood, according to PLATT, to arise from the motion of an electron in a clockwise direction in one orbital and in an anticlockwise direction in the other. In porphin it is likely that the two highest filled levels (the f-orbitals), whilst not strictly degenerate, have nearly equal energies, so that they may be treated in the same way as the g-orbitals. An electron in an f-orbital may be considered to have an angular momentum of 4 units, and in a g-orbital a momentum of 5 units [16].

On exciting such an electron of angular momentum 4 to angular momentum 5 units, the two momenta may be either in the same or opposite directions. The whole molecule, which began in its ground state ^1A with zero angular momentum, may thus acquire momenta of either 1 or 9 units, clockwise or counter-clockwise. These two values of momentum will give two degenerate singlet states and two degenerate triplet states for the first excited configuration d^2e^2fg. These states may be called $^1B^0$, $^1Q^0$ and $^3B^0$, $^3Q^0$ where B and Q refer to 1 unit and 9 units of angular momentum respectively. Transitions from the ground state to the low Q states, involving large changes in angular momentum, will by expectation be comparatively weak, whereas transition to the higher B states will be strong and highly allowed. PLATT [16] thus identifies the visible bands of square (D_{4h}) porphin as the $e^2f^2\ ^1A$–$e^2fg\,^1Q^0$ transition, degenerate and almost forbidden, and the strong Soret band as the $e^2f^2\ ^1A$–$e^2fg\,^1B^0$ transition, degenerate and strongly allowed.

A further analysis of the bands in the visible region requires consideration of the positions of the two central hydrogen atoms. These are the only parts of the molecule which must violate the D_{4h} symmetry, but ERDMAN and CORWIN [17] have adduced good evidence that they are bound by normal covalent bonds to opposite N atoms.

The view is supported by a consideration of the molecular dimensions of phthalocyanine determined by ROBERTSON [11]. DONOHUE [18] pointed out that

in this molecule, hydrogen bonding between the adjacent nitrogen atoms would be most unlikely, since this would result in two unequal C—N—H bond angles, one 82° and the other 170°. Instead, the two hydrogen atoms would be expected to be attached to opposite nitrogen atoms and occupy positions in the centre of the molecule. By analogy, porphin would conform to D_{2h} symmetry.

Porphin in 5 per cent HCl shows only a single peak, clearly the A–Q transition, and an intense sharp Soret band, clearly the A–B transition of the truly symmetrical D_{4h} structure. The single ^1A–^1Q peak is probably a 0–1 vibrational band, which is normally the second peak in an acid porphyrin absorption spectrum, the 0–0 band being in the case of porphin a completely forbidden transition. The single acid Soret peak ^1A–^1B is probably the 0–0 band.

The complexities of the spectrum of porphin (free base) in benzene may now be attributed justifiably to the change from D_{4h} to D_{2h} symmetry, with removal of the degeneracy. Platt [16] remarks that the visible spectrum of D_{2h} porphin looks like a superposition of two of the D_4h spectra, about 800 Å apart, and therefore assigns bands I and II to the 0–0 and 0–1 vibrations of ^1A–$^1Q^0{}_x$ and bands III and IV to similar vibrations of ^1A–$^1Q^0{}_y$, where Q_x and Q_y are polarized in mutually perpendicular directions.

Our present data obtained on porphin in ethanol at −180° and using the Cary spectrometer resolve the visible absorption clearly into at least two electronic transitions, each with its own vibrational fine structure, the Soret band also being resolved (Table 2).

It may be concluded therefore that Stern and Wenderlein's [1, 2] empirical rule concerning aetio-type spectrum is in reality only a special case, in which substituents modify considerations of symmetry, of a more general physical relationship. Rather than being exceptional, porphin reveals the principles of this relationship on account of its relative chemical simplicity.

Infra-red spectrum

The porphin molecule may be assumed to be planar, and without the two central hydrogen atoms it has square symmetry, D_{4h} ($4/m\ mm$). If the two central hydrogen atoms are located on adjacent pyrrolic nitrogen atoms, the symmetry is reduced to C_{2v} (mm) (one two-fold axis through opposite meso-positions), but if they are located on opposite nitrogen atoms, or if they symmetrically hydrogen-bond a pair of nitrogen atoms each, the symmetry of the molecule is lowered only to D_{2h} (mmm) (three two-fold axes, two through the nitrogen atoms or through the meso-positions respectively).

Owing to their small mass relative to the mass of the porphin molecule as a whole, these hydrogen atoms may lead to no violation of the infra-red selection rules for the point group D_{4h} with respect to the ring vibrations of porphin, but their own motions, the N–H vibrations, should absorb radiation according to the selection rules of the point group to which the molecule belongs. For the C_{2v} group two N–H stretching vibration absorptions are allowed, but for the D_{2h} group only one. The spectrum of porphin shows only one band in the N–H stretching vibration region, that at 3305 cm^{-1}, and the infra-red evidence accordingly suggests that the porphin molecule has D_{2h} symmetry.

VOL. 12 1958

Summary

(1) The purity of porphin, synthesized by a new method, has been established.

(2) The spectral absorption of porphin has been measured in the infra-red region and in the visible region at room temperature and at −180°.

(3) Single crystals were examined crystallographically and X-ray diffraction data are presented.

(4) By-products formed during use of some of the new synthetic methods which have been employed have been separated by chromatography, crystallized and their spectral absorption has been studied. It is inferred that some of the spectral data to be found in the literature and attributed to porphin has been influenced by the presence of similar impurities.

(5) The present results have been considered from the standpoint of spectral theory and an explanation is offered of the absorption properties of porphin in neutral and in acid solvents.

(6) Crystals of porphin when viewed by plane polarized light afford a spectrum in which the intensity of the first band in the red (very weak in benzene solution) is greatly enhanced. The relation of this effect to the relative positions of the electric vector and the *b* crystallographic axis is recorded.

Acknowledgements—The authors thank Professor Sir Christopher Ingold for the use of the Cary spectrometer, and one of us (S. F. M.) the Australian National University for a Research Fellowship during the tenure of which part of the present work was carried out.

References

[1] Stern A. and Wenderlein H. *Z. Phys. Chem.* A 1936 **176** 81.
[2] Stern A. and Wenderlein H. *Z. Phys. Chem.* A 1936 **175** 405.
[3] Stern A., Wenderlein H. and Molvig A. *Z. Phys. Chem.* A 1936 **177** 40.
[4] Fischer H. and Gleim W. *Liebigs Ann.* 1936 **521** 157.
[5] Rothemund P. *J. Amer. Chem. Soc.* 1936 **58** 625.
[6] Eisner U. and Linstead R. P. *J. Chem. Soc.* 1955 3742.
[7] Eisner U. and Linstead R. P. *J. Chem. Soc.* 1955 3749.
[8] Krol S. *J. Org. Chem.* 1957 In press.
[9] Brockmann A. and Schodder H. *Ber. Dtsch. Chem. Ges.* 1941 **74** 73.
[10] Pruckner F. and Stern A. *Z. Phys. Chem.* A 1936 **177** 387.
[11] Robertson J. M. *J. Chem. Soc.* 1936 1195.
[12] Kuhn H. *J. Chem. Phys.* 1949 **17** 1198.
[13] Simpson W. T. *J. Chem. Phys.* 1949 **17** 1218.
[14] Longuet-Higgins H. G., Rector C. W. and Platt J. R. *J. Chem. Phys.* 1950 **181** 174.
[15] Matlow S. L. *J. Chem. Phys.* 1954 **23** 673.
[16] Platt J. R. *Radiation Biology* (Edited by A. Hollaender) Vol. 3, p. 71. McGraw-Hill, New York. 1956.
[17] Erdman J. G. and Corwin A. H. *J. Amer. Chem. Soc.* 1946 **68** 1885.
[18] Donohue J. *J. Phys. Chem.* 1952 **56** 502.
[19] Albers V. M. and Knorr H. V. *J. Chem. Phys.* 1936 **4** 22.

Spectrochimica Acta, 1958, Vol. 12, pp. 78 to 87. Pergamon Press Ltd., London

Electronic and vibrational states of carbonyl compounds—I

Electronic states of camphorquinone

R. A. FORD* and Miss F. PARRY†
Research Department, British Nylon Spinners Limited, Pontypool, England

(*Received* 26 *October* 1957)

Abstract—The absorption spectrum of camphorquinone has been recorded in a series of solvents at room temperature. The emission spectrum of crystalline camphorquinone has been recorded at 77°K and the lifetime of this emission in a rigid glass at 77°K has been observed to be $7{\cdot}1 \times 10^{-3}$ sec. The two main regions of absorption in the near ultra-violet and visible, Systems I and II, are assigned to the $^1A_1 \rightarrow {}^1B_1$ and $^1A_1 \rightarrow {}^1B_1$ transitions respectively. It is suggested that the very weak visible absorption, System III, is $^1A_1 \rightarrow {}^3B_1$ and the sharp yellow emission either $^3B_1 \rightarrow {}^1A_1$ or $^3A_2 \rightarrow {}^1A_1$. Solvent effects on Systems I and II are discussed in some detail since System I shows a small "red shift" in polar solvents although it is $n \rightarrow \pi$ in type. Modified rules for the effects of solvents on $n \rightarrow \pi$ transitions are suggested.

1. Introduction

OF LATE, considerable study has been made of the weak, long wavelength transitions in carbonyl compounds. In particular formaldehyde [1, 2, 3, 4], glyoxal [5] and biacetyl [6, 7, 8], have received detailed analyses. The main characteristics of these transitions, which involve the excitation of an electron from a 'lone pair' ($2p$) orbital localized on the oxygen atom to an extended, anti-bonding π MO., have been successfully accounted for by the simple LCAO. MO. theory developed by MULLIKEN and MCMURRY [9, 10], but it has not been found possible to extend this to include the related vibrational states [6, 11].

Camphorquinone [1] owes its yellow colour to a weak absorption system extending from 20,000–25,000 cm^{-1} which is similar in origin to the bands that cause glyoxal and biacetyl to be coloured. But since glyoxal and biacetyl are both normally in their planar *trans*-configurations [12], symmetry C_{2h}, whereas camphorquinone is locked into the planar *cis*-configuration by the rigid ring system (inter-carbonyl angle $\theta = 0$–$10°$ [13]) it was felt that a comparison of these spectra might reveal additional information about this class of α-diketones.

Since the intensity of electronic transitions in polyatomic molecules is controlled by the local symmetry, we shall consider the ground state of camphorquinone to be C_{2v}.

The infra-red and ultra-violet spectra of camphorquinone have been recorded previously by LEONARD and MADER [13] and by ALDER *et al.* [14], but we have been unable to find any previous analysis. In this investigation the absorption spectrum in a series of solvents at room temperature and the emission spectrum of the crystal at 77°K have been recorded. The lifetime of the emission at 77°K has been measured using a mechanical phosphoroscope.

* Present address, Mullard Research Laboratories, Salfords, Redhill, Surrey, England.
† On vacation study from Dept. of Physics, University of Birmingham.

VOL. 12 1958

2. Experimental

Camphorquinone, kindly prepared by Dr. A. G. PETO in these laboratories, was purified by recrystallization from petroleum ether followed by vacuum sublimation, and stored in the dark.

The emission spectrum of the crystal at 77°K was measured on a Bellingham and Stanley wavelength spectrometer using a glass prism. The dispersion was 1·4 Å/mm at 5000 Å, and 2·7 Å/mm at 6000 Å. The spectra were recorded photoelectrically with the sample only partially immersed in the liquid refrigerant to prevent interference from bubbles. A medium pressure mercury arc, chopped at 13 counts/sec, was used for excitation with a Wood's glass filter to select the 4047 Å and 3660 Å lines. This filter effectively removed the intense 4358 Å, 5461 Å and 5780 Å source lines. Internal calibration of the records was obtained by an electrical ticker system which was subsequently calibrated against a Zn–Cd–Mg arc. The period of scanning from 5000–6000 Å was 25 min.

Lifetime measurements, in a rigid glass at 77°K, were made with a mechanical phosphoroscope consisting of a pair of semi-circular sectors mounted 180° out of phase on a common shaft. The detector was a photon-multiplier which was coupled to a double beam C.R.O. for recording purposes. Calibration of these records was obtained by feeding a 50 counts/sec signal to the other C.R.O. trace. In this way lifetimes down to $\simeq 10^{-4}$ sec could be resolved using a synchronous motor to turn the phosphoroscope sectors at 50 rev/sec.

Absorption spectra were recorded at room temperature using a Unicam S.P. 500 with 10, 40, and 100 mm cells. Eastman–Kodak "Spectro" grade *n*-hexane and methanol were used without further purification for this work. Analar acetic acid was purified by fractional distillation using a 10 in. column packed with $\frac{1}{8}$ in. dia. glass helices. The 2,2,4-trimethyl pentane and methyl cyclohexane used for the rigid glass were also Eastman–Kodak "Spectro" grade, again used without further purification.

3. Results

Absorption spectrum

Solutions of camphorquinone in *n*-hexane show three regions of absorption; System I extending from 29,000–40,000 cm^{-1} and System II extending from 20,000–25,000 cm^{-1}, which are shown in Fig. 1, and System III, a very weak transition, extending from 17,000–19,000 cm^{-1} shown in Fig. 2. The similarity to the spectrum of biacetyl in *n*-hexane [14] is most striking.

System I. The most notable feature of this transition is the well resolved vibrational structure of seven bands. The two longest wavelength bands have been labelled α and β as they appear from their spacing to be separate from the five higher energy components which are labelled *a*, *b*, *c*, *d* and *e*. Details of the separations and a tentative partial analysis are given in Table 1.

This transition is very broad (half peak band width = 8000 cm^{-1}) and the intensity increases towards higher energies. The low intensity oscillator strength, $6{\cdot}38 \times 10^{-4}$, suggests that the transition is partially forbidden.

System II. This transition also shows some vibrational structure but the detail is insufficient for any analysis. It is much sharper than System I, its half-peak

band-width being 2500 cm^{-1} and shows no degradation to the red. However the similarity of its oscillator strength, $4{\cdot}2 \times 10^{-4}$, to that of System I suggests that both transitions are of the same type.

System III. This is a very weak transition only evident as a shoulder on the steep onset of the System II absorption. Since it is analogous in position to a weak singlet-triplet transition recently detected in solutions of biacetyl [8], the effect of perturbation by a "heavy atom" solvent [15, 16] was studied using ethyl iodide. Some evidence of the expected enhancement is shown Fig. 2.

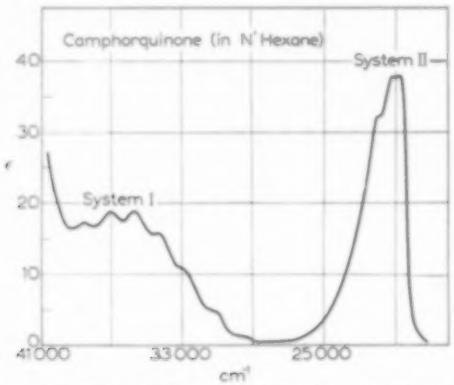

Fig. 1. Absorption spectrum of camphorquinone in *n*-hexane.

Table 1. System I of camphorquinone in *n*-hexane

Band	ν cm^{-1}	$\nu - 33{,}000$	Assignment
α	29,500	−3500	2(1750)
β	31,250	−1750	1750
a	33,000	0	$^1A_1 \rightarrow \mathrm{II}\ ^1B_1$
b	34,480	1480	
c	35,680	2680	
d	37,050	4050	
e	38,530	5530	

Solvent effects

Systems I and II have been studied in *n*-hexane, diethyl ether, methanol and acetic acid as shown in Figs. 3 and 4. On going to more polar solvents the vibrational structure of System I is retained although it becomes more diffuse, especially in acetic acid. In ether and methanol small red-shifts are observed accompanied by a small intensity increase. In 50 per cent acetic acid a clear intensity increase is observed, but the considerable change of band shape makes it difficult to be definite about the band shift. However it does appear that a small red-shift has occurred here also. Solvent effects on the corresponding transition of biacetyl do not seem to have been investigated [17].

VOL. 12 1958

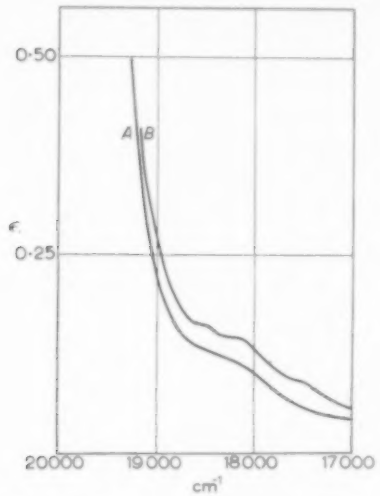

Fig. 2. Long wavelength absorption spectrum of camphorquinone in (a) *n*-hexane, (b) ethyl iodide.

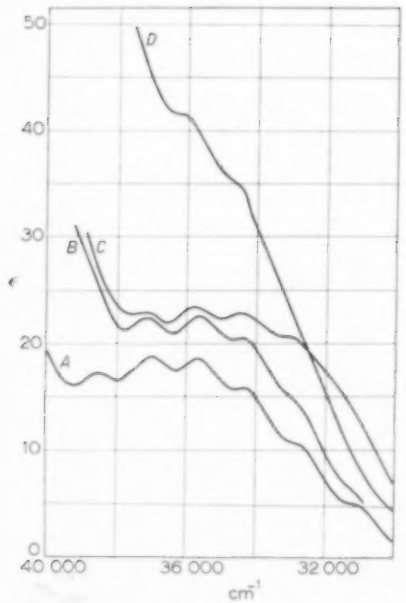

Fig. 3. System I of camphorquinone in different solvents; (a) *n*-hexane, (b) diethyl ether, (c) methanol, (d) 50 per cent acetic acid.

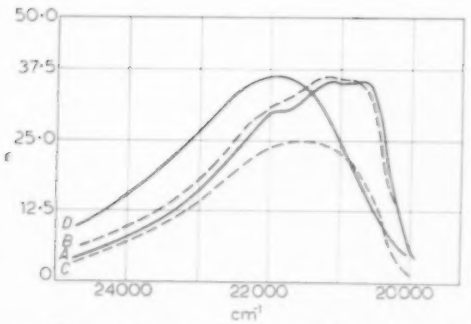

Fig. 4. System II of camphorquinone in different solvents; (a) *n*-hexane, (b) diethyl ether, (c) methanol, (d) 50 per cent acetic acid.

System II shows larger solvent effects than System I and what vibrational structure exists in *n*-hexane is completely lost in methanol and acetic acid. In these solvents the transition shows considerable blue-shifts the magnitudes of which are given in Table 2.

Table 2. Effects of solvents on System II of camphorquinone

Solvent	Band centre (cm^{-1})	Shift (cm^{-1})
n-hexane	21,100	0
diethyl ether	21,200	100
methanol	21,500	400
acetic acid	21,900	800

In ether and acetic acid there is little intensity change, but the intensity falls in methanol. Since the readings in methanol changed slowly with time, some of this reduction is certainly due to slow tautomeric [18] or chemical changes.

Emission spectrum

Crystals of camphorquinone at 77°K show a very sharp yellow emission extending from 16,500–18,000 cm^{-1} (half-peak band-width 600 cm^{-1}), which is shown in Fig. 5. There is some evidence of five small vibrational peaks showing separations

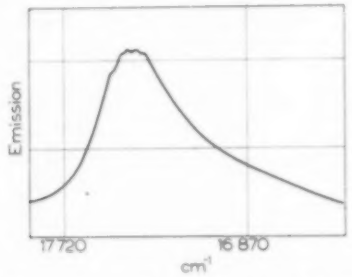

Fig. 5. Emission spectrum of crystalline camphorquinone at 77°K.

of 35–40 cm^{-1}, but as the details varied between specimens, this may be an artifact. No evidence of larger vibrational separations in this transition or of any other emission region was found.

The lifetime of the yellow emission measured in a rigid glass consisting of 8 parts methyl-*cyclo*hexane to 1 part 2,2,4-trimethyl pentane at 77°K was $7{\cdot}1 \times 10^{-3}$ sec. The lifetime of biacetyl measured at the same time for comparison was $5{\cdot}5 \times 10^{-3}$ sec. This is in reasonable agreement with McClure's [19] value of $2{\cdot}25 \times 10^{-3}$ sec obtained in E.P.A. at 77°K.

4. Discussion

Assignment of electronic transitions

The similarity between the absorption spectra of biacetyl and camphorquinone in *n*-hexane is such as to make a comparison between them profitable. Sidman

VOL. 12 1958

and McCLURE [6] have recently set down the one electron L.C.A.O. M.O.s and their derived electronic states for biacetyl. Details of the related orbitals for camphorquinone are given in Table 3.

The transitions to be expected from L.C.A.O. M.O. theory and the electronic states derived from them are given in Table 4.

Table 3. Electronic orbitals and symmetries for camphorquinone

L.C.A.O. M.O.s.† (one electron)	C_2z	$\sigma_v y$	C_{2v}	
$\pi_1\ (X_{O_1} + X_{C_1} + X_{C_2} + X_{O_2})$	−	+	B_1	T_x
$\pi_2\ (X_{O_1} + X_{C_1} - X_{C_2} - X_{O_2})$	+	−	A_2	
$n_1\ (Y_{O_1} + Y_{O_2})$	+	+	A_1	T_z
$n_2\ (Y_{O_1} - Y_{O_2})$	−	−	B_2	T_y
$\pi_3\ (X_{O_1} - X_{C_1} - X_{C_2} + X_{O_2})$	−	+	B_1	
$\pi_4\ (X_{O_1} - X_{C_1} + X_{C_2} - X_{O_2})$	+	−	A_2	

† X and Y represent atomic $2p$ wave functions which are symmetric about the X and Y molecular axes respectively.

The contour of System II of camphorquinone in n-hexane shows a remarkable similarity to the transition in biacetyl extending from 21,000–27,000 cm^{-1}. Both show three peaks; two closely spaced long wavelength components and a third at a larger separation to the blue. For sometime it was held that two electronic transitions were required to explain this region in biacetyl [20, 21], but SIDMAN and

Table 4. Electronic transitions and excited states of camphorquinone

Transitions	Orbital configuration	Electronic states
$n_1 \rightarrow \pi_3$	I	I^1B_1, I^3B_1
$n_1 \rightarrow \pi_4$	II	II^1A_2, II^3A_2
$n_2 \rightarrow \pi_3$	I	I^1A_2, I^3A_2
$n_2 \rightarrow \pi_4$	II	II^1B_1, II^3B_1
$\pi_2 \rightarrow \pi_3$	I	I^1B_2, I^3B_2
$\pi_2 \rightarrow \pi_4$	II	II^1A_1, II^3A_1

McCLURE [6] have shown with a better vibrational analysis that there is no evidence for more than one transition being involved. Accordingly we shall consider System II to be a single electronic transition. As with biacetyl, the transition shows considerable "blue shifts" on going into more polar solvents, the values of which were given in Table 2. Clearly it should be assigned to an $n \rightarrow \pi$ process of which the two lowest-energy singlet transitions are $n_1 \rightarrow \pi_3$ and $n_2 \rightarrow \pi_3$. In the absence of definite information on the origins of the absorption and emission transitions, a comparison of the intensity with biacetyl suggests that the transition is allowed by symmetry. In this case it is assigned $^1A_1 \rightarrow I\,^1B_1$. The low intensity is then due to the small overlap between the ground state and excited state wavefunctions.

The vibrational fine structure in System I is much more extensive than in System II, which suggests that the upper state of System I may be unstable. This agrees with the observation that solutions of camphorquinone undergo photochemical decomposition on illumination in this region. The bands labelled α and β appear at separations of 1750 cm^{-1} to the red of band a. These separations are almost exactly the size of the 1753 cm^{-1} ground state carbonyl stretching frequency of camphorquinone. Therefore the simplest explanation is that α and β are "hot" bands associated with the $1 \rightarrow 0$ and $2 \rightarrow 0$ transitions from a ground state in which this frequency is excited. In this case band a must be the 0–0 band. It is not however one of the most prominent bands, the intensity of the transition increasing towards higher energies. This indicates that the dimensions of the upper and lower states must differ considerably. The effect of solvents on System I is of particular interest since it shows a small "red shift" on going into more polar solvents. This is usually considered conclusive evidence that the transition cannot be $n \rightarrow \pi$ in type [22]. If this is so the most likely transition is $\pi_2 \rightarrow \pi_3$ which is an allowed transition to a I^1B_2 state. This should have a high intensity but the intensity of System I is low and very similar to that of System II, which is an $n \rightarrow \pi$ process. L.C.A.O. M.O. theory predicts two $n \rightarrow \pi$ transitions in this region $n_1 \rightarrow \pi_4$ and $n_2 \rightarrow \pi_4$ of which $n_2 \rightarrow \pi_4$ to an II^1B_1 upper state is allowed by symmetry. The intensity of this may be expected to be in the region of that observed, and Sidman and McClure [6] have assigned the corresponding absorption region in biacetyl extending from 31,000–42,000 cm^{-1} to the analogous $^1A_g \rightarrow II^1A_u$ transition. We believe this assignment to be correct and the red-shift of this transition in polar solvents to be an exception to the n—π blue-shift rule of McConnell. We shall discuss the reasons for this in a later section on solvent effects. Accordingly we assign System I in camphorquinone to an $^1A_1 \rightarrow II^1B_1$ transition. Clear cut evidence on this point could be obtained by using polarized light since the $\pi \rightarrow \pi$ process will be Y-polarized but the $n \rightarrow \pi$ process X-axis polarized.

We must now consider System III in relation to the yellow emission transition since the small enhancement of System III in ethyl iodide and the lifetime of $7{\cdot}1 \times 10^{-3}$ sec for the emission show that both are intercombination processes. Sidman and McClure [6] have found this region in biacetyl to be complex. They suggest that the weak visible absorption, which has recently been detected in solution by Forster [8], is $^1A_g \rightarrow I^3A_u$ whilst the strong green emission is $I^3B_g \rightarrow {}^1A_g$, radiationless conversion from the $I^3A_u \rightarrow I^3B_g$ states being of very high efficiency. Thus with the limited data available for camphorquinone it would be unwise to attempt anything but a tentative assignment. However, we can safely assume that we are dealing with $n \rightarrow \pi$ processes in which case the absorption transition is almost certainly the allowed $^1A_1 \rightarrow I^3B_1$ transition. The emission may be $I^3B_1 \rightarrow {}^1A_1$ or $I^3A_2 \rightarrow {}^1A_1$. It is worth noting that, as with biacetyl, the separation between the singlet and triplet states arising from the first excited $n \rightarrow \pi$ configuration is about 2500–3000 cm^{-1}, which is much greater than the value predicted by Reid [23] from overlap considerations. Also biacetyl and camphorquinone resemble each other in emitting mainly phosphorescence (triplet $\rightarrow$ singlet) whereas with glyoxal the predominant emission is fluorescence (singlet $\rightarrow$

VOL. 12 1958

singlet). This is probably due to the two CH_3 groups in biacetyl and the rigid ring system in camphorquinone lowering the frequency of, and therefore increasing, the population of excited torsional and bending states (of the intercarbonyl C—C bond) in their respective molecules. Since the slopes of the potential energy curves of the ground state and the first excited singlet or triplet states in these molecules, plotted as a function of twist about the C—C bond, are opposite in sign, [24] perturbations of this kind will decrease the overlap and paired character of the π-electrons thereby mixing a certain amount of triplet character into the ground state wavefunction [25].

Solvent effects

McConnell [22] has proposed the rule that "electronic transitions in molecules which have low intensities, because the ground and excited state charge distributions do not overlap strongly, are likely to give blue-shift bands." The combination of these intensity and solvent shift criteria has become standard practice for assigning $n \rightarrow \pi$ transitions. However with camphorquinone, System I shows a small red-shift in polar solvents although the transition is almost certainly $n \rightarrow \pi$ in type. We believe that the reason for this is solvent interaction modifying the π-electron resonance energy of the solute molecule.

If we consider the two carbonyl groups of camphorquinone separately their π M.O.s may be written:

Ground state: $\phi_1 = aX_{c_1} + bX_{o_1}$ $\quad$ $\phi_2 = aX_{c_2} + bX_{o_2}$

Excited state: $\phi_1^* = aX_{c_1} - bX_{o_1}$ $\quad$ $\phi_2^* = aX_{c_2} - bX_{o_2}$

Our reason for choosing this description is that changes in the π-electron resonance energy due to deviations from planarity are most likely to result from changes in the π-electron distribution over the intercarbonyl C—C bond, since the coupling here is weaker than in the C=O bonds. Then the splitting between the $I\,^1B_1$ and $II\,^1B_1$ states of the molecule will be the energy difference between the orbitals

$$\psi_{\pi_4} = (\phi_1^* + \phi_2^*) \quad \text{and} \quad \psi_{\pi_3} = (\phi_1^* - \phi_2^*)$$

Since (ϕ_1, ϕ_2) and (ϕ_1^*, ϕ_2^*) are pairs of degenerate orbitals

$$E_{\pi_4} - E_{\pi_3} = \left(E_1^* + \frac{\beta - E_1^* S}{1 + S}\right) - \left(E_1^* - \frac{\beta - E_1^* S}{1 - S}\right)$$

where $S = \int \phi_1^* \phi_2^* \, d\tau$ and β is the resonance integral. Because of the $(1 \pm S)$ term in these energy values, E_{π_4} should exceed E_1^* by a lesser amount than E_{π_3} lies below it. This is exactly what is found with camphorquinone, the splitting between Systems I and II being clearly asymmetric with respect to the 29,500 cm^{-1} transition in acetaldehyde.

The magnitude of this splitting will depend on the value of the overlap integral S, which will be reduced by any deviations from planarity since $S = a^\circ \cos\theta$, where θ is the intercarbonyl angle and a° is some function of θ. The effect of such reductions in splitting on the spectrum of camphorquinone will be to shift System I more slowly to the red than System II will shift to the blue as is in fact observed. This is shown diagrammatically in Fig. 6.

The possible ways in which solvent interaction could produce a perturbation of this type are either by mass coupling through interaction at the oxygen atoms which would flatten the potential curve for twist around the intercarbonyl C—C bond of the ground state thereby increasing the population of excited torsional states at room temperature, or by steric hindrance between solvent molecules

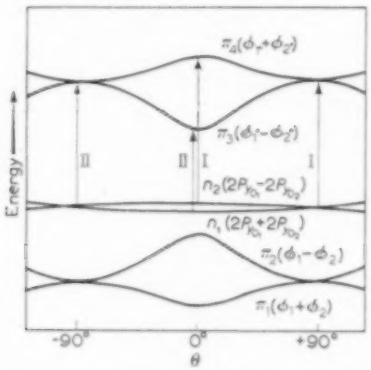

Fig. 6. Electronic orbital energies of camphorquinone as a function of twist around the intercarbonyl C—C bond.

interacting with the adjacent carbonyl groups. More work is required before a clear decision between these can be made. However from the difference between camphorquinone and glyoxal, where both the analogous transitions show blue shifts in polar solvents [22], it appears that steric hindrance may be the cause. This will assume importance only for the *cis* configuration.

The observed shifts of $n \rightarrow \pi$ transitions on going into polar solvents are of course the summation of a series of effects. In most cases the blue-shift due to the stabilization of the n-electrons in the ground state is the predominant effect. However, where solvent interaction can modify the π electron resonance energy of the solute, exceptions to this may occur. We may summarize the effects to be expected in this case as follows.

Transitions	π-Resonance energy increasing	π-Resonance energy decreasing
(a) Excitation to π-orbital with antinode in the region of the overlap change.	red-shift	blue-shift
(b) Excitation to π-orbital with node in the region of the overlap change.	blue-shift	red-shift

VOL. 12 1958

Acknowledgement—The authors wish to thank British Nylon Spinners Limited for permission to publish this work.

References

[1] Brand J. C. D. *J. Chem. Soc.* 1956 858.
[2] Brand J. C. D. and Reed R. I. *J. Chem. Soc.* 1957 2386.
[3] Walsh A. D. *J. Chem. Soc.* 1953 2306.
[4] Reid C. and Cohen A. D. *J. Chem. Phys.* 1956 **24** 85.
[5] Brand J. C. D. *Trans. Faraday Soc.* 1954 **50** 431.
[6] Sidman J. W. and McClure D. S. *J. Amer. Chem. Soc.* 1955 **77** 6461, 6471.
[7] Miyazawa T. *J. Chem. Soc. Japan* 1953 **74** 743.
[8] Forster L. S. *J. Chem. Phys.* 1957 **26** 1761.
[9] McMurry H. L. and Mulliken R. S. *Proc. Nat. Acad. Sci., Wash.* 1940 **26** 312.
[10] McMurry H. L. *J. Chem. Phys.* 1941 **9** 231, 241.
[11] Cannon C. G. and Ford R. A. European Molecular Spectroscopy Conference, Freiburg-im-Breisgau, July 1957.
[12] LuValle J. E. and Schomaker V. *J. Amer. Chem. Soc.* 1939 **61** 3520.
[13] Leonard N. J. and Mader P. M. *J. Amer. Chem. Soc.* 1950 **72** 5388.
[14] Alder K. *et al.* *Liebigs Ann.* 1955 **593** 23.
[15] Kasha M. *J. Chem. Phys.* 1952 **20** 71.
[16] Platt J. R. *J. Opt. Soc. Amer.* 1953 **43** 252.
[17] Holman R., Lundberg W. and Burr G. *J. Amer. Chem. Soc.* 1945 **67** 1669.
[18] Modiano J. and Pariaud J. C. *Bull. Soc. Chim. Fr.* 1952 **19** 642.
[19] McClure D. S. *J. Chem. Phys.* 1949 **17** 905.
[20] Lewis G. N. and Kasha M. *J. Amer. Chem. Soc.* 1945 **67** 994.
[21] Forster L. S. *J. Amer. Chem. Soc.* 1955 **77** 1417.
[22] McConnell H. *J. Chem. Phys.* 1952 **20** 700.
[23] Reid C. *J. Chem. Phys.* 1953 **21** 1906.
[24] Mulliken R. S. and Roothaan C. C. J. *Chem. Rev.* 1947 **41** 219.
[25] McConnell H. *J. Chem. Phys.* 1952 **20** 1043.

Spectrochimica Acta, 1958, Vol. 12, pp. 88 to 95. Pergamon Press Ltd., London

Microwave-powered Raman sources

NORMAN S. HAM and A. WALSH
Chemical Physics Section, Division of Industrial Chemistry, Commonwealth Scientific and Industrial Research Organization, Melbourne, Australia

(*Received* 22 *September* 1957)

Abstract—A description is given of a Raman source consisting of an annular, electrodeless lamp powered by microwaves (2450 Mc). The construction of helium, mercury and sodium lamps is described and their performance illustrated by Raman spectra excited by He 5876 Å, Hg 4358 Å, 5461 Å and Na 5889 Å, 5896 Å. Simplicity and flexibility are important features of this method of excitation, which is of particular value for coloured samples.

Introduction

In recent years there have been striking improvements in Raman sources, but these have been mainly confined to mercury arcs [1, 2]. In general these are only satisfactory when the lines at 2537 Å, 4047 Å or 4358 Å are used, as the other lines in the spectrum are too weak. If the sample absorbs appreciably at these wavelengths then it often proves difficult and sometimes impossible to record a Raman spectrum. We have encountered this problem in our attempt to obtain the Raman spectra of halogen molecules in various solvents. The general problem of recording the Raman scattering of absorbing samples often demands, for its solution, excitation and detection in the red and near infra-red regions. STAMMREICH [3] has recently reviewed these techniques and he and his co-workers have reported results obtained with the yellow and red lines of helium and argon in helical discharge lamps [4–7], and preliminary work with Rb and Cs lamps [3].

As an alternative to a range of conventional discharge lamps, we have made a series of annular electrodeless lamps which are powered by microwaves.* This simple type of source is well suited to the cylindrical symmetry of a scattering experiment and the possibilities of the method have been explored by making lamps containing sodium, mercury and helium. Details of the construction and performance are given below.

Experimental details

The helium lamp is an annulus made in Pyrex glass, having internal diameter 15 mm, external diameter 30 mm and length 45 mm. These dimensions were found by trial and error to be the best of several combinations which were tested. If the length of the annulus greatly exceeds half the wavelength of the microwaves used, the discharge does not fill the entire tube. The lamps are first outgassed at 200°C for 24 hr. This treatment alone is not sufficient, since the discharge releases oxygen from the walls of the tube. To complete the outgassing of the tube it is operated for half an hour and then re-evacuated: this process is repeated

* High-frequency radio waves and microwaves have been used for exciting Hg^{198} lamps [8, 9] and recently a small high-intensity Hg discharge tube for Zeeman effect work has been described [10].

VOL. 12 1958

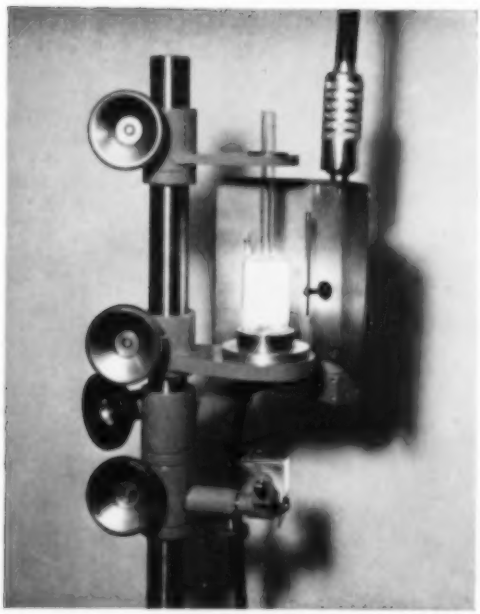

Fig. 1. Microwave-powered Raman source assembly.

VOL.
12
1958

until no atomic oxygen lines or O_2^+ bands* are visible when the lamp is run continuously for several hours. This is usually achieved after about a dozen flushings of the tube. The tube is filled with helium at about 4 mm/Hg pressure and sealed off. This pressure is low enough to favour excitation of the triplet states [3] and hence emission of the yellow line [$^3D_0$–^3P].

The mercury lamp is similar to that described above but with internal and external diameter 13 and 23 mm respectively, and length 65 mm. A drop of purified mercury is introduced into the tube, which is filled to 1 mm/Hg with neon.

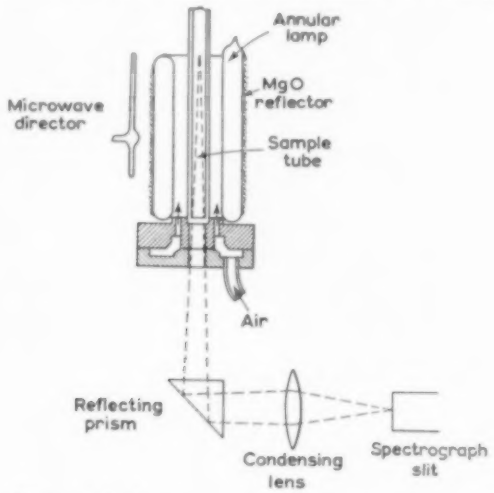

Fig. 2. Schematic diagram of microwave-powered Raman source assembly.

The sodium tube† has the same dimensions as the helium lamp. Following the same outgassing procedure as for the helium lamp, a few grams of distilled sodium are run into the tube, which is then filled to 4 mm/Hg with helium.‡ Finally the tube is mounted in an evacuated annulus. This permits the lamp to operate at about 300°C, at which temperature there is sufficient sodium-vapour pressure for efficient operation of the lamp.

To increase the amount of light falling on the sample, the outside of the annular lamp is coated with a layer of magnesium oxide about 1 mm thick [13]. This doubles the intensity of the Raman spectrum.

The experimental arrangement is shown in Figs. 1 and 2.

The Raman sample tube (i.d. 7 mm, sample volume 2 ml) is mounted vertically in front of the spectrograph (a Hilger two-prism E612 with E614 $f/5{\cdot}7$ camera) and the lamp is placed around it. The lamp and sample tube are supported on a brass block so constructed that a stream of air can be directed between the lamp

* The atomic oxygen lines at 5330·65 Å and 5435·16 Å were the most easily detected. The following prominent band heads from the First Negative oxygen bands ($^4\Sigma_g^- \rightarrow {}^4\Pi_u$ transition of O_2^+) were the most easily detected [11]: 6418·7 Å, 6351 Å, 5973 Å, 5597·5 Å and 5274·7 Å.

† Pyrex glass is not satisfactory for the sodium lamp, but can be used for about 10 hr before darkening of the glass is too serious. The use of tubing lined with a borate glass will lengthen the lamp life considerably.

‡ Neon with a small quantity of argon is normally used in commercial sodium lamps [12], but both these gases have many lines in the red region. The simpler spectrum of helium causes less interference with Raman spectra.

and the sample tube. This cooling is sufficient to remove most of the heat dissipated by the lamps. A condensing lens focuses the remote end of the tube on the spectrograph slit.

The microwave generator is a Raytheon Microtherm Model CDM4 rated at 125 W at a frequency of 2450 Mc/s ($\lambda = 12{\cdot}25$ cm). The "C-director" supplied

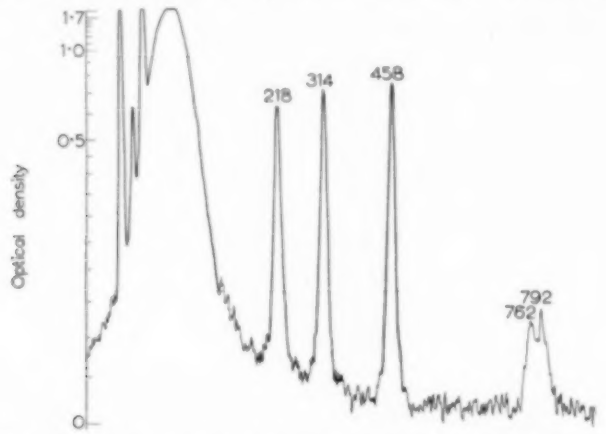

Fig. 3. Microphotometer tracing of Raman spectrum of CCl_4 obtained with mercury annular electrodeless lamp (exciting line 4358 Å). Exposure 2 min, slit-width 0·06 mm = 4 cm^{-1}, Zenith plates, sample volume 2 ml. The figures are the Raman frequencies of CCl_4 excited by Hg 4358 Å.

with the generator, which gives an ellipsoidal energy pattern, is satisfactory to maintain the discharge. The discharge is started by a Tesla coil and maintained by placing the director as close as possible to the tube. The only attempt made to couple the lamp to the coaxial cable has been to place a hemi-cylindrical sheet of copper around the lamp on the side opposite the director. This results in a gain of intensity of about 2. It is possible that further attention to the design of the coupling may markedly improve the intensity of the source. The use of microwave generators of higher output (say 2 kW) also merits investigation.

Performance of lamps

Mercury lamp

This lamp gives a spectrum with high intensity and narrow line-width. The narrow line-width can be seen from the fact that there is no self-reversal of 2537 Å and that the complex structure of the green 5461 Å line is observable on an echelle spectrograph, indicating a half-width of less than 0·05 Å. Fig. 3 shows a microphotometer tracing of a Raman spectrum of carbon tetrachloride excited by 4358 Å with an exposure of 2 min on Zenith plates. Using Ilford HPS plates, the Raman spectrum excited by the green 5461 Å line has also been recorded.

Sodium lamp

The strongest lines are the sodium *D* lines at 5889 Å and 5896 Å; the second members of the sharp and diffuse series at 6160 Å, 6154 Å and 5688 Å, 5682 Å respectively are present, but most of the other doublets are quite weak. The

VOL. 12 1958

presence of the helium yellow line indicates that a higher temperature of operation should increase the *D* line intensity. Fig. 4 shows a tracing of a Raman spectrum of CCl_4 obtained with a 2 min exposure on an HPS plate. The doublet structure of the Raman lines excited by the sodium doublet is clearly visible.

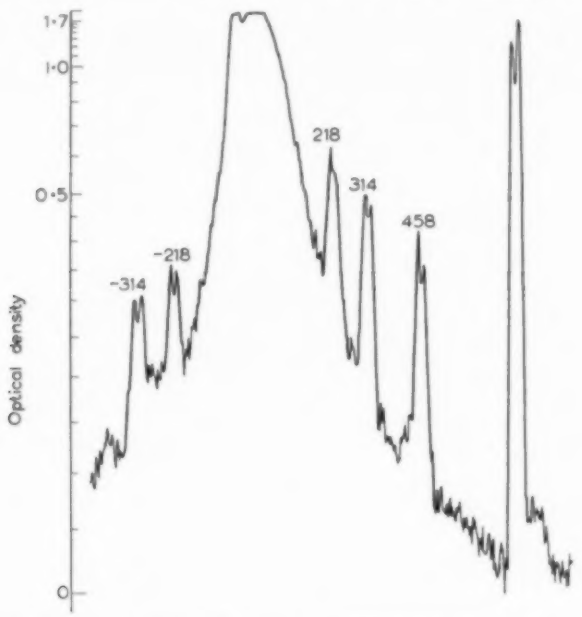

Fig. 4. Microphotometer tracing of Raman spectrum of CCl_4 obtained with sodium annular electrodeless lamp. Exposure 2 min, slit-width 0·04 mm ≡ 5·5 cm^{-1}, HPS plates, sample volume 2 ml. The figures are the Raman frequencies of CCl_4 excited by sodium doublet 5889 Å and 5896 Å.

Helium lamp

The strongest lines from the lamp in the visible region are 5876 Å and 4471 Å, both of which arise from transitions within the triplet levels of helium. The Raman spectrum of CCl_4 excited by 5876 Å is obtained on an HPS plate in 2 min. With sulphur monochloride, which is pale yellow and opaque to mercury blue light in a 1 cm layer, the strongest Raman lines excited by He 5876 Å were recorded in 5 sec: the complete spectrum, obtained in 30 sec, is shown in the tracing in Fig. 5.

Conclusion

These experiments show that microwave-powered lamps provide a simple and powerful method of exciting Raman spectra. The results with sodium indicate that it will be possible to make lamps employing other alkali metals, and the use of these,* in addition to the helium and mercury lamps, will permit a wide range in the choice of exciting frequency. This flexibility, coupled with the ease with which lamps can be interchanged, is the outstanding feature of this

* The resonance lines of the alkali metals, and hence the strongest lines in their spectra, are Li 6708 Å; Na 5889 Å, 5896 Å, K 7645 Å, 7699 Å; Rb 7800 Å, 7947 Å and Cs 8521 Å, 8943 Å.

method, and we believe it will permit the Raman spectra of many coloured compounds to be recorded. The method should prove particularly valuable when used in conjunction with the concentration–absorption effects discussed by LIPPINCOTT [14, 15] and in all work where a narrow width of exciting line is important. The microwave technique also removes the difficulties associated with Wood's method of using He 3888 Å as exciting line, with a nickel–oxide glass filter [16].

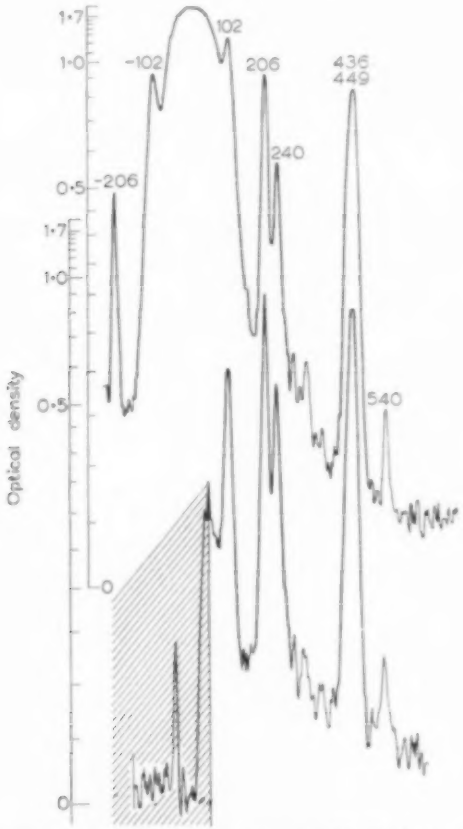

Fig. 5. Microphotometer tracing of Raman spectrum of S_2Cl_2 obtained with helium annular electrodeless lamp (exciting line 5876 Å). Exposure 30 sec, slit-width 0·04 mm ≈ 5·5 cm^{-1}, HPS plates, sample volume 2 ml. The lower tracing is of a plate in which the Rayleigh line has been reduced in intensity by placing a glass filter in the focal plane of the spectrograph. The position of the filter is indicated by the hatched region in the tracing. The figures are the Raman frequencies of S_2Cl_2 excited by He 5876 Å.

Acknowledgement—We are grateful to Mr. W. G. JONES for the construction of the annular lamps, and for technical advice.

References

[1] WELSH H. L., STANSBURY E. J., ROMANKO J. and FELDMAN T. *J. Opt. Soc. Amer.* 1955 **45** 338.
[2] STOICHEFF B. P. *Canad. J. Phys.* 1954 **32** 330.
[3] STAMMREICH H. *Spectrochim. Acta* 1956 **8** 41.

VOL. 12 1958

[4] Stammreich H. *Phys. Rev.* 1950 **78** 79; *Experientia* 1950 **6** 224.
[5] Stammreich H. and Forneris R. *Z. Naturf.* 1952 **7a** 756; *J. Chem. Phys.* 1953 **21** 944; 1954 **22** 1624; *Spectrochim. Acta* 1956 **8** 46, 52.
[6] Stammreich H., Forneris R. and Sone K. *J. Chem. Phys.* 1955 **23** 972.
[7] Stammreich H., Forneris R. and Tavares Y. *J. Chem. Phys.* 1956 **25** 580, 1277, 1278.
[8] Meggers W. F. and Westfall O. *J. Res. Nat. Bur. Stand.* 1950 **44** 447.
[9] Jacobsen E. J. and Harrison G. R. *J. Opt. Soc. Amer.* 1949 **39** 1054.
[10] Forrester A. T., Gudmundsen R. A. and Johnson P. O. *J. Opt. Soc. Amer.* 1956 **46** 339.
[11] Pearse R. W. B. and Gaydon A. G. *The Identification of Molecular Spectra* p. 197. Wiley, New York 1950.
[12] Nelson E. H. and Rigden S. A. R. *Light and Ltg.* 1956 **49** 217.
[13] Menzies A. C. and Skinner J. *J. Sci. Instrum.* 1949 **26** 299.
[14] Lippincott E. R. and Nelson R. D. *J. Chem. Phys.* 1953 **21** 1307.
[15] Fisher R. D. and Lippincott E. R. *Analyt. Chem.* 1954 **26** 435.
[16] Wood R. W. *Phil. Mag.* 1929 **7** 858.

L.
2
58

Spectrochimica Acta, 1958, Vol. 12, pp. 94 to 100. Pergamon Press Ltd., London

RESEARCH NOTES

The promise and problems of the matrix isolation method for spectroscopic studies

GEORGE C. PIMENTEL
Chemistry Department, University of California, Berkeley, California, U.S.A.

(*Received* 26 *August* 1957)

THE matrix isolation method was developed at the University of California to permit the leisurely spectroscopic study of extremely unstable species, including free radicals. In the technique it is desired to prepare a suspension of the species of interest in a suitable solid matrix, that is, in a solid material which is chemically inert, rigid with respect to diffusion, and transparent in the spectral region of interest. In these laboratories the matrix materials selected were nitrogen, argon, and xenon, since the infrared spectral region was considered to be of primary importance. In other laboratories [1, 2, 3, 4] where the technique was developed independently, interest was directed toward ultraviolet-visible studies and matrix materials used included the familiar glass-forming organic mixtures (e.g. "E.P.A.", *iso*pentane-3-methyl pentane). In our use of nitrogen or a rare-gas matrix, the solid sample is prepared by freezing quickly a gas mixture of a small amount of some material of interest in a very large amount of the matrix. Suitable coolants are liquid hydrogen (20°K) or liquid helium (4°K) but not liquid nitrogen (77°K).

In the course of experimentation it became apparent that a variety of types of study were made possible by the matrix technique. These are enumerated and examples given.

(a) *Band narrowing.* The infrared spectrum of a monomolecular dispersion of a compound in solid argon consists of very narrow lines. This reduction of band widths sometimes aids in verifying the existence of overlapping, accidentally degenerate bands. This spectral behavior is of particular importance in the study of the hydrogen stretching modes of hydrogen bonded species. The large band breadths observed in spectra of solutions prevent identification of frequencies characteristic of hydrogen bonded polymers of various sizes. In matrix studies of methanol in nitrogen, for example, it was possible to assign characteristic O—H stretching frequencies to dimers, trimers, tetramers, and higher polymers. The pattern of frequency shifts is informative of the structures of these polymers [5].

(b) *Free radicals.* Two methods are in use for the preparation of suspensions of free radicals. The free radicals may be prepared in the gas phase and quickly frozen with the matrix on a cold surface. Another technique is to produce the free radicals after deposition by photolyzing a suitable starting material. For example, hydrazoic acid has been suspended in solid nitrogen at 20°K and then photolyzed. As the HN_3 is decomposed by photolysis, various products are revealed by the appearance of new infrared bands. One of these products is certainly ammonia, suggesting that the NH radical produced in the primary dissociation extracts hydrogen atoms from other HN_3 molecules in successive secondary reactions. This scheme supports the identification of a band at 1290 cm^{-1} attributed to the bending mode of NH_2 radical [6].

VOL. 12 1958

(c) *Primary act of photolysis.* The matrix method provides a method of studying the photolytic process. In principle, the photolytic process can be stopped without secondary reactions, thus providing direct information on the primary act of photolysis. For example, studies have been made of the photolysis of methyl nitrite in solid argon. The product identified was formaldehyde in a yield of one mole per mole of methyl nitrite photolyzed. No nitric oxide was detected, but one unidentified band is in a reasonable spectral region for an absorption of HNO. The data are informative concerning the production of formaldehyde in the photolysis of gaseous methyl nitrite, for which a yield of about one half mole per mole of methyl nitrite photolyzed is obtained.

(d) *Kinetics.* The matrix method provides a means of bringing together reactive species at very low temperature as well as a means of isolating them. With spectroscopic observation, it is possible to make direct kinetic studies for reactions with unusually low activation energies, probably in the range 1–3 kcal. For example, the rate of disappearance of a band assigned to *cis*-nitrous acid has been measured at 20°K. This disappearance is attributed to the *cis* to *trans* isomerization of nitrous acid. Assuming zero entropy of activation leads to an enthalpy of activation of 1·4 kcal/mole.

In attempting to exploit these possible applications of the matrix technique, a variety of practical and interpretive difficulties have been discovered. Two of these are discussed.

In interpreting the spectra obtained by the matrix method, it is necessary to estimate the extent to which the results are determined by the matrix. The infrared spectra of a number of stable molecules in nitrogen or argon matrices have been examined and it is clear that the sharp bands obtained are very close in frequencies to the corresponding bands observed in gas-phase studies. It is implied that the matrix disturbs neither the structure nor the vibrational force constants of the suspended molecules. An exception is provided by ammonia. The symmetrical bending mode of ammonia is observed at about 975 cm^{-1} in a nitrogen matrix instead of near 950 cm^{-1} as in the gas phase. This shift, in the wrong direction for a dielectric effect, is considered to reflect the loss of inversion doubling because of constraint by the matrix.

Similarly, there is uncertainty in the interpretation of kinetic measurements. The constraints of the matrix could affect the activation thermodynamics so as to make the results of doubtful applicability to the reaction kinetics under more normal conditions. The *cis-trans* isomerization provides a striking example, since the best previous estimate of the activation energy for isomerization is 10 kcal, seven times larger than the value deduced here. Another possible kinetic measurement, diffusion, is subject to uncertainty because the nature of the solid obtained by condensing a gas is not well known.

This introduces another question of significant interest in matrix studies, the exact nature of the solid obtained in these experiments. On the one hand, the solid seems to be microcrystalline, as suggested by the high scattering of light. On the other hand, the infrared spectra of pure solids prepared in this manner often indicate imperfect development of spectral features attributable to crystalline interactions. The solid thus could be partially crystalline with vitreous "pockets" or it could be a highly imperfect crystal. The calorimetric studies of De Nordwall and Staveley [7] are pertinent. They have discovered that for each of a number of solids prepared by quickly freezing a gas there is a characteristic temperature at which heat is released during warming. This temperature, T_D, is presumed to be due to a devitrification process. We have measured spectroscopically this same temperature, T_D, as revealed by diffusion processes or by development of crystal splittings. In both types of study, the ratio of T_D to the melting point is near 0·5. For three of the four compounds for which De Nordwall and Staveley found no thermal peculiarities, it seems likely that the coolant temperature was not sufficiently low to keep the sample temperature below T_D during deposition. Combining the data of De Nordwall

and STAVELEY with the spectroscopic studies, it seems that the phenomenon of forming highly imperfect crystals or glasses on freezing a gas is a very general one. The examples include such extremes as argon, water, methylene chloride, and toluene. Neither type of study has, as yet, provided conclusive evidence of the precise nature of the solid, however.

In conclusion, it is amply clear that the matrix isolation method has wide and interesting applications, particularly with infrared spectral techniques. There remain certain problems of interpretation which are themselves of significant interest.

References

[1] LEWIS G. N., LIPKIN D. and MAGEL T. T. *J. Amer. Chem. Soc.* 1941 **63** 3005.
[2] NORMAN I. and PORTER G. *Nature, Lond.* 1954 **174** 508; *Proc. Roy. Soc.* A 1955 **230** 399.
[3] BROIDA H. and PELLAM J. *Phys. Rev.* 1954 **95** 845.
[4] SOWDEN R. G. and DAVIDSON N. *J. Amer. Chem. Soc.* 1956 **78** 1291.
[5] VAN THIEL M., BECKER E. D. and PIMENTEL G. C. *J. Chem. Phys.* 1957 **27** 95.
[6] BECKER E. D., PIMENTEL G. C. and VAN THIEL M. *J. Chem. Phys.* 1957 **26** 145–50.
[7] DE NORDWALL H. J. and STAVELEY L. A. K. *Trans. Faraday Soc.* 1956 **52** 1061–6, 1207–15.

Excitation of atomic emission lines of nitrogen in steel by means of a high-energy, single-discharge source

E. F. RUNGE and F. R. BRYAN
Scientific Laboratory, Ford Motor Co., Dearborn, Michigan, U.S.A.

(*Received* 20 *May* 1957)

VOL. 12 1958

Introduction

DURING the past twenty years both the nonferrous and ferrous alloy industries have relied heavily on spectroscopic procedures for production control analysis. For at least this same period it has been realized that a certain few essential elements in steel could not readily be determined spectroscopically. These have included the nonmetals carbon, sulfur, phosphorus, and the gases nitrogen, oxygen and hydrogen. Several major laboratories have worked on these special problems achieving some success with carbon, phosphorus and sulfur [1–3]. However, there have been relatively few published reports of successful work on the gases in steels by spectroscopic methods [4–8].

Among the literature references is one reporting success in determining nitrogen in steel by means of atomic emission spectra using a single-discharge source [6]. This report was sufficiently intriguing to warrant building an excitation source of similar characteristics to test the principle of the procedure.

Basic problems

There are two fundamental problems that must be met in the development of a spectrographic method for the determination of nitrogen in metals. First it is quite obvious that the excitation must either take place in some atmosphere other than air, or within a vacuum system. The second problem is the fact that the most sensitive lines of nitrogen occur below 1200 Å. Although there has been increasing instrumentation in recent years designed

for detecting radiation in the far ultraviolet, the major difficulties of making quantitative measurements in the 900–1300 Å region still remain. From the viewpoint of conventional spectrographic techniques, the region from 4000–6000 Å appears to offer a more reasonable possibility of practical success in the determination of nitrogen. However, in this region one is faced with the prospect of producing nitrogen lines of relatively high excitation potential (29·5 eV).

Experimental method

Excitation source. Standard types of excitation sources were found to be unsuitable for producing atomic emission lines of nitrogen in the near ultraviolet. Therefore a high-energy, single-discharge spark source was designed and constructed in this laboratory along the lines of the source described by MANDEL'SHTAM and FAL'KOVA. Using a relatively high capacitance (4·5 μF) charged to a voltage of 20 kV and discharged through an inductance of 25 μH, this source develops about 900 J of energy per discharge. The condenser charging time is about 2 min while the duration of the discharge is less than 1 msec. The resonant frequency of the circuit is approximately 15 kc/s. Table 1 summarizes the source conditions used.

Table 1. Experimental conditions for the determination of nitrogen in steel

Excitation source	Modified design after MANDEL'SHTAM and FAL'KOVA [6].
Peak voltage	20,000 V
Capacitance	4·5 μF
Inductance	25 μH
Peak current	6000 A
Analytical gap	0·5 mm
Duration of discharge	650 μsec
Carbon dioxide flow Rate	9 l/min
Spectrograph	Large Littrow quartz prism.
Spectral range	3200–6500 Å
Line pair	N 3994·99 Å/Fe 3961·15 Å
Slit width	20 μ
Length of exposure	One discharge
Emulsion	Kodak Type "M" plates

Controlled atmosphere chamber. The analytical gap is enclosed in a chamber providing an atmosphere of carbon dioxide to prevent interference from nitrogen in the air. This controlled atmosphere chamber consists of a ceramic tube 4·45 cm in diameter and 15 cm long having two opposed 0·635 cm diameter holes located midway from the ends, for insertion of the electrodes. The ends of the tube are each capped with a brass fixture which contains a quartz or glass port through which light can pass. The entrance and exit apertures for the controlled atmosphere flow are also located in these brass fixtures. A gas tight seal is accomplished between the port, the brass, and the ceramic tube by means of O-rings. An exploded view of the chamber is shown in Fig. 1.

Spectrographic equipment. The spectrograph is a standard quartz Littrow instrument having a reciprocal linear dispersion of 10·5 Å/mm at 4000 Å. (Table 1). For recording spectra in the 4000–5000 Å range, Kodak Type M emulsion was found to offer the best compromise of speed, contrast, and grain size.

Standards and samples. The type of steel used in this investigation was a high-chromium,

high-manganese, austenitic steel containing approximately 0·5 per cent nitrogen. Both the standards and samples were machined from 1·58 cm diameter bar stock which had been hot-rolled from 7 kg ingots. The standard ingots were sampled and analyzed chemically for their nitrogen content by a modified Kjeldahl procedure. The spectroscopic samples

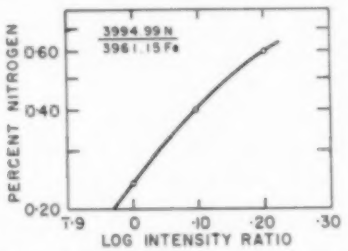

Fig. 2. Analytical calibration curve for nitrogen in steel using single-discharge excitation.

machined from this material were rod-shaped electrodes of 0·5 cm diameter, several centimeters long, and ground on one end to a conical point of 140° included angle.

Counter electrode. Counter electrodes of tungsten have been recommended [6]. However, it was found that when working at the lower nitrogen levels present in some of our alloys there was objectional pickup contamination on the surface of the tungsten from one exposure to the next. Since the tungsten must be resurfaced for each new exposure, a more easily machined material was sought. Carbon was considered, but it was felt that due to its porosity there was danger of contamination from absorbed atmospheric nitrogen. Pure copper in rod form was tried and found to be quite satisfactory. Copper, like the tungsten, must be resurfaced between discharges, but the refinishing is much more easily performed on copper.

Choice of lines. The nitrogen line at 3994·99 Å was chosen on the basis of sensitivity and freedom from interference from major constituents in the alloy. The reference line Fe 3961·15 Å was chosen from several iron lines in the vicinity of the nitrogen line being measured. The iron line selected was comparable in intensity to the nitrogen line and provided relatively reproducible intensity ratios with the nitrogen line.

The photographic photometry and intensity ratio evaluations followed standard practices. The analytical curve for the particular lines chosen is plotted in Fig. 2.

Results

It is possible to obtain an emission spectrum of nitrogen in steel, in the amount of 0·20 per cent nitrogen, using a high-energy, single-discharge spark source. The coefficient of variation, based on a single sample excited twenty times by this type of source, proved to be 17 per cent of the amount of nitrogen present.

References

[1] Kudelya, E. S. and Dem'yanchuk A. S., *Avtom. Svarka* 1935 **6** 19.
[2] Brooks L. S. and Bryan F. R., *Spectrochim. Acta* 1954 **6** 413.
[3] McNally J. R. Jr., Harrison G. R. and Rowe E., *J. Opt. Soc. Amer.* 1947 **37** 93.
[4] Fassel V. A. and Tabeling R. W. *Spectrochim. Acta* 1956 **8** 201.
[5] Runge E. F. and Bryan F. R., *J. Appl. Spectr.* 1956 **10** 68.
[6] Mandel'shtam S. L. and Fal'kova O. B. *Zavodskaya Lab.* 1950 **16** 430.
[7] Fal'kova O. B. *Izv. Akad. Nauk SSSR (ser. fiz.)*1955 **19** 149.
[8] Fal'kova O. B. *Zavodskaya Lab.* 1955 **21** 1083–7.

VOL. 12 1958

Fig. 1. End view of controlled atmosphere chamber showing ceramic tube for containing electrodes and disassembled brass cap for admission and exhaustion of gas.

VOL.
12
1958

Automatic film washer-rinser-dryer*

Louis E. Owen
Technical Division, Goodyear Atomic Corporation,
Portsmouth, Ohio, U.S.A.

(*Received* 13 *August* 1957)

Abstract—Modification of a strip-film washing device which is the subject of a previous article [1] provides for automatic washing rinsing, and drying of the emulsion. The change consists of adding a side arm inlet for compressed air at the bottom of the chamber and putting air-exit holes in the film-carrying cap.

The developed and fixed film is loaded into the washer, which is mounted flush with the workbench (Fig. 1). Tap and distilled water are valved successively into the two upper inlets of the annular chamber which furnishes a spray to the body of the washer. The

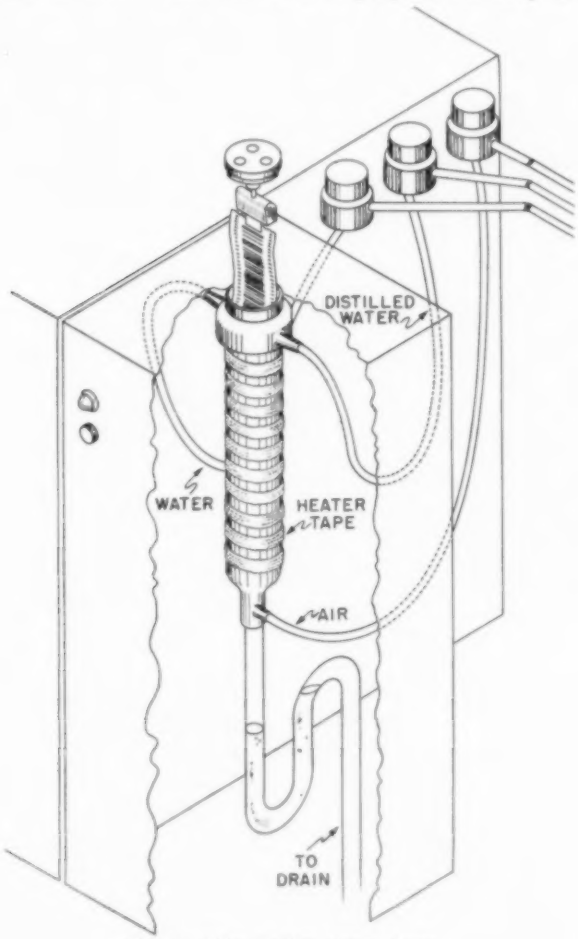

Fig. 1. Film washer–rinser–dryer.

* This work was performed under contract AT-(33-2)-1 with the United States Atomic Energy Commission.

film is washed vigorously with tap water for a pre-set period and then rinsed several times with distilled water, after which the emulsion is dried by air and radiant heat. A flexible tape heater and the compressed air line are used in the drying. A trap in the water outlet of the chamber insures proper direction of airflow over the film. Program timers are suitable for actuating the solenoid valves controlling the process steps. The circuit shown in Fig. 2 utilizes thermal time-delay relays in the simplest successful circuit tested.

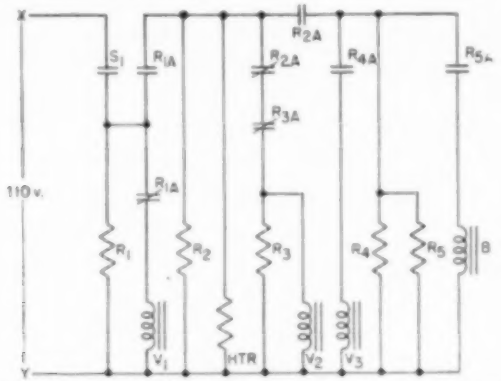

Fig. 2. Automatic film washer–rinser–dryer control circuit and component list.

Part	Function	Type
S_1	Start and stop	Toggle switch SPST.
R_1	Time wash period	Thermal time-delay relay, 60 sec.
R_2	Time rinse period	Thermal time-delay relay, 30 sec.
R_3	Pulsate rinse	Amperite relay 115F30.
R_4	Permit drain	Thermal time-delay relay, 3 sec.
R_5	Signal end of process	Thermal time-delay relay, 5 min.
V_1	Control wash water	Solenoid, 5/32 in.
V_2	Control distilled rinse	Solenoid, 3/8 in. port.
V_3	Control air	Solenoid, 1/8 in. port.
HTR	Heater	Briskheat Tape, 400 W.

Switch S_1 is thrown as the film is lowered into the wash chamber. The solenoid valve V_1 opens to begin the washing period. Relay R_1, which was simultaneously energized, actuates its contact R_{1A} after a time delay of 60 sec. Contact R_{1A} closes valve V_1 and opens the rinse valve V_2, which is pulsed by flasher relay R_3 with its contact R_{3A}. Relay R_2, which was also energized by R_{1A} at the start of the rinse period, transfers its contact R_{2A} after a delay of 30 sec to stop the rinsing and to start the time-delay relays R_4 and R_5. Relay R_4 permits the chamber to drain by delaying the drying air stream controlled by valve V_3 for 3 sec. The drying heater, which is energized at the start of the rinse period, heats sufficiently fast to be effective when the airflow begins. Relay R_5 sounds the buzzer B after 5 min to recall the operator to the darkroom, as the film is then ready for removal. Switch S_1 is opened to silence the buzzer and to reset the control for subsequent use.

If rapid recycling is required, the circuit can be modified with a holding relay at the buzzer position to permit earlier cooling of the thermal elements. Immediate recycling would require motor-driven cam switches [2] or interval-counting controllers [3] rather than regular thermal time-delay relays.

References

[1] Manning D. C. and Philips W. O. *Spectrochim. Acta* 1956 **8** 54.
[2] Owen L. E. *Rev. Sci. Instrum.* 1946 **17** 155.
[3] Owen L. E. *Photogr. Sci. Tech.* 1957 II **4** 3.

VOL. 12 1958

Spectrochimica Acta, 1958, Vol. 12, pp. 101 to 104. Pergamon Press Ltd., London

REPORTS OF MEETINGS

IUPAC Commission on Molecular Spectroscopy

THE Commission on Molecular Spectroscopy of the International Union of Pure and Applied Chemistry held three meetings in Paris, from 19 to 22 July 1957. The following were present:

H. W. THOMPSON (U.K., President), G. U. M. DUYCKAERTS (Belgium), J. A. KETELAAR (Holland), J. LECOMTE (France), R. C. LORD (U.S.A.), A. MANGINI (Italy), R. MECKE (Germany), S. MIZUSHIMA (Japan), A. N. TERENIN (U.S.S.R.), R. R. BRATTAIN (U.S.A.) and R. N. JONES (Canada).

The following attended by special invitation for discussions on particular topics:

W. R. BRODE (U.S.A.), A. R. PHILPOTTS (U.K.), E. K. PLYLER (U.S.A.).

The nomination of Professor T. URBANSKI as a Polish national representative was accepted. It was agreed that liaison with the Joint Spectroscopy Commission of the IUPAP and IAU should be maintained by exchange of Minutes and through Professor E. HERZBERG, and with the IUPAC Commission on Optical Data through Professor G. DUYCKAERTS.

The Commission discussed standard wavelengths for the infrared, the standardization of infrared intensity measurements, the documentation of infrared data, matters concerning spectroscopic units and terminology, including the millimicron ($m\mu$), and a possible symbol for the wave number (cm^{-1}), the co-ordination of nuclear magnetic resonance data, the co-ordination of spectroscopic meetings and symposia, the compilation of spectroscopic data of biochemical interest, the documentation of ultraviolet molecular data and other matters.

With regard to the *Documentation of Infrared Spectra*, pending further enquiries and decisions, it was *agreed* unanimously to make the following recommendation public:

> "The Commission has considered the desirability of obtaining some internationally acceptable form for the presentation of infrared spectra over the range 200–10,000 cm^{-1}. Although no general agreement has yet been reached on this point, some progress appears to have been made in different countries.
>
> The Commission is unanimously of the opinion that such spectra should be plotted linearly in wave number (cm^{-1}) units rather than linearly in wavelength, the scale being broken for convenience at suitable places. In any case, both wave number and wavelength scales should be shown. The Commission also feels that it may be preferable to plot decreasing wave numbers towards the right hand side, and that % transmission is at the present time the most satisfactory ordinate for general use."

A number of small working groups were set up, to report progress and make further recommendations during 1958:

(i) *On infrared wavelength standards.* R. N. JONES, J. LECOMTE, R. C. LORD, R. MECKE, E. K. PLYLER, G. HERZBERG, H. W. THOMPSON; to compile a set of acceptable data already known for the range 200–10,000 cm^{-1}, for both high and low dispersion work, and to suggest other suitable substances (gases or liquids) and arrange for measurements upon them as calibrants for prism spectrometers.

(ii) *On infrared intensity measurements.* R. R. BRATTAIN, B. C. CRAWFORD, G. V. M. DUYCKAERTS, R. N. JONES, J. A. KETELAAR, A. N. TERENIN, A. R. PHILPOTTS, H. W. THOMPSON; to investigate means of obtaining more transferable and reproducible data in

different laboratories; to suggest units and notation, to establish a set of standard substances for which band-shapes and peak extinction coefficients could be determined, using low or medium dispersion, these to include broad, medium, or sharp bands; to promote further experimental and theoretical study of the effective of slit width upon band shapes and intensities and of the correct evaluation of effective spectral slit width.

(iii) *On the documentation of infrared data.* R. R. Brattain, J. A. Ketelaar, J. Lecomte, R. Mecke, W. R. Brode, N. Wright, H. W. Thompson; to examine the possibility of unifying various national systems at present in operation, to promote a greater exchange of spectral data, to recommend the most acceptable size and format for standard spectral charts and to consider methods of access and indexing to spectral collections.

(iv) *On spectral units and terminology.* G. V. M. Duyckaerts, R. N. Jones, G. Herzberg, S. Mizushima, W. R. Brode, H. W. Thompson; to consider current questions such as the millimicron (mμ), units of wave number (cm^{-1}), or notation for molecular vibrations.

(v) *On the documentation of ultraviolet data.* R. R. Brattain, R. N. Jones, J. A. Ketelaar, A. Mangini, H. W. Thompson; to advise on current plans for the compilation of molecular ultraviolet data. The Commission *agreed to recommend at once* the use of absorbance (ordinate) against wavelength (Ångstroms) with longer wavelength to the right hand side.

The Commission intends to bring together in a Manual at the earliest possible moment its collected data on standard infrared wavelengths, band intensity values and procedures of measurement, units, symbols and terminology and other related matters, to be published under the auspices of the IUPAC.

The Commission is exploring further the better co-ordination of international spectroscopic meetings and hopes for a closer relationship between meetings of the International Spectroscopic Colloquium and the European Molecular Spectroscopy Group, alternating with corresponding meetings in the United States.

The next official meeting of this Commission will be held at Liège in September 1958, when progress of the working groups will be considered. The Commission would welcome views of pure or applied spectroscopists on any of the above aspects of its work. These should be sent to Dr. H. W. Thompson, St. John's College, Oxford, England, or to Professor B. L. Crawford, Department of Chemistry, University of Minnesota, Minneapolis, U.S.A., or to a member of the Commission resident in their own country.

VOL. 12 1958

4th Symposium on Spectroscopy in Japan, held at Tokyo, October 12–13 1957

This annual meeting is organized by the Japanese Science Council in conjunction with the Chemical, Pharmaceutical, Agricultural Chemical, Analytical Chemical and Spectroscopic Societies of Japan.

The following papers were presented:

Recent progress in the quantitative analysis by means of the infrared spectrophotometry: S. Tanaka.

Measurement of the infrared spectra of samples adsorbed on thin paper and its application to paper chromatography: G. Chihara.

Quantitative determination of methyl-, ethyl- and isopropyl-alcohols in the "alcohol for disinfection" by means of infrared absorption spectrum. T. Oba.
A cell for infrared absorption measurement at the temperature of liquid nitrogen: K. Nukada
Characteristic frequencies of acetals: K. Nukada and Y. Masiko.
New devices in the experiment of Raman effect: Y. Masiko and H. Tomita.
An anomaly in the Raman effect of the aqueous solution of dimethyl ether: Y. Masiko.
Recent progress in the apparata for infrared absorption spectroscopy: K. Kudo.
Wave-length calibration of Perkin–Elmer 112G Spectrometer and the determination of molecular constants of fundamental molecules: S. Mizushima, T. Shimanouchi, I. Ichishima, M. Tsuboi, I. Nakagawa, M. Hayashi, A. Yamaguchi, K. Fukushima, H. Kamiyama, S. Tsuchiya, J. Seto, S. Takeda, I. Suzuki and H. Takahashi.
Vibration-rotation spectra of $N^{14}H_3$ and $N^{15}H_3$: M. Tsuboi, T. Shimanouchi and S. Mizushima.
Calculation of normal vibrations of alanine and the assignment of the observed frequencies: S. Mizushima, T. Shimanouchi, K. Fukushima and T. Onishi.
Analysis of the out-of-plane motion of the hydrogen atoms in benzene, pyridine, and their alkyl derivatives and determination of their force constants: Y. Kakiuchi and T. Shimanouchi.
Conjugated double bonds in benzene and the C–H out-of-plane vibrations: N. Oi.
Absolute intensities of the absorption bands arising from the C—O stretching motions in diesters: K. Kuratani and A. Minegishi.
Special Lecture: On the nuclear magnetic resonance: S. Fujiwara.
Recent development in the infrared spectroscopy of natural organic compounds: K. Takeda.
Infrared spectra of substituted phenylsulfonyl compounds: T. Momose, Y. Ueda, and T. Shoji.
Studies on organic sulfates by means of their infrared spectra: G. Chihara.
Infrared spectra of substituted pyridines and pyrazines: H. Shindo.
Infrared spectra of pyridine- and pyrazine-carboxylic acids: S. Yoshida and M. Asai.
Infrared spectra of anthraquinones. Effects of hydroxyl, methoxyl, acetoxyl and methyl substituents: O. Tanaka.
Infrared spectra of isomers of kainic acid: H. Kamio, M. Nishikawa and T. Kanzawa.
Recent development in the infrared spectroscopy of polymers: H. Tadokoro.
Multiple bond stretching frequencies in some organic molecules with carbonyl, nitro and phenyl groups: M. Kato and M. Yamaguchi.
On the crystallization of glucose and the hydrogen bonding: S. Motoi and J. Mizuguchi.
Infrared spectra of cupper complexes of aliphatic dinitriles: I. Matsubara.
Infrared spectra of alkyl titanates and alkyl silicates: T. Yoshimoto, Y. Masiko and T. Takatani.
Cis and trans isomerization in maleic acid resin and its infrared spectrum: R. Inoue, K. Naito and H. Shima.
Infrared spectra of polyethylene irradiated by γ-ray: R. Kawai, S. Kawamatsu, Y. Harada and Y. Maeda.
Infrared pleochroism of doubly-oriented film of polyvinyl-alcohol observed by infrared microscope: H. Tadokoro, S. Seki, I. Nitta and R. Yamadera.
Special Lecture: Recent development of molecular spectroscopy in Europe: S. Mizushima.

Symposium on Spectroscopy in India

The Second Annual Symposium on Spectroscopy, organized by the Convention of Spectroscopists, was held in Madras (India) on Sunday, 5th January, 1958. The following papers were presented:

Vibrational transition probabilities review and recent trends: N. R. Tawde and N. Sreedhara Murthy, Karnatak University, Dharwar.
Spectra of P_2^+ and PH^+: N. A. Narasimham, Atomic Energy Establishment, Trombay, Bombay.
Spectra of intermetallic molecules: D. Sharma, University of Allahabad, Allahabad.

Nuclear spectroscopy of short-lived isotopes: B. V. Thosar, Tata Institute of Fundamental Research, Bombay.

Relative intensities of Raman lines in liquids: K. Venkateswarlu, Annamalai University, Annamalai Nagar.

Structural studies on organic free radicals using paramagnetic resonance spectroscopy: Balu Venkatraman, Atomic Energy Establishment, Trombay, Bombay.

A secondary standard microwave spectrograph: P. Venkateswarlu, Muslim University, Aligarh.

Explanation of the sharp and diffuse character of spectral lines: R. Satya Narayan, Osmania University, Hyderabad.

Force constants of some polyatomic molecules and ions: T. A. Hariharan, Indian Institute of Science, Bangalore.

Schmidt camera: S. L. Mallick, (Presented by Professor P. K. Kichlu), Department of Physics, Delhi University, Delhi.

The nuclear magnetic shielding in mercury compounds: S. S. Dharmatti, C. R. Kanekar and S. C. Mathur, Tata Institute of Fundamental Research, and Atomic Energy Establishment, Bombay.

Sixth Annual Southeastern Seminar on Spectroscopy, University of Florida, 8, 9, 10 January 1958

This year's spectroscopy symposium at the University of Florida maintained its reputation of informality and charm coupled with important technical discussions. The program was limited to invited papers on direct reading spectrometers. Jason Saunderson spoke on the development and basic theory of direct readers. Maurice Hasler lectured upon present trends and potentialities in direct reading instrumentation and Frederick Brech rigorously examined signal measuring systems of direct readers for their performance possibilities.

Warren Wright discussed direct reading spectrometers from the viewpoint of an industrial user and indicated their great versatility. Louis Owen also lectured on electronic circuits as used in spectrographic instrumentation.

A high light of the meeting came in the first announcement by Brech of the development of a new electromechanical pulse counting motor with 1000 pulses/sec potentialities. Early use of the component in various pulse read-out systems was indicated.

Louis E. Owen

VOL. 12 1958

Spectrochimica Acta, 1958, Vol. 12, pp. 105 to 106. Pergamon Press Ltd., London

NOTICES OF MEETINGS

Gordon Conference

THE 1958 Gordon Conference on Infrared Spectroscopy will take place from 18 to 22 August at Kimball Union Academy, Mariden, New Hampshire, U.S.A. The following programme has been arranged:

18 August

B. CRAWFORD, Jr., Chairman.

Spectra of trapped species—

J. A. A. KETELAAR: Infrared spectra of crystalline solid solutions.

G. C. PIMENTEL: Matrix methods.

Infrared spectra of adsorbed molecules—

A. TERENIN: Infrared spectra of molecules adsorbed on solid surfaces.

W. A. PLISKIN and R. P. EISCHENS: The infrared spectra of carboxylic acids chemisorbed on metals and metal oxides.

19 August

G. C. PIMENTEL, Chairman.

Measurement of vibrational relaxation times—

K. E. SHULER: Theoretical aspects.

S. H. BAUER: Experimental aspects.

Detectors for the infrared region—

E. F. DALY: Infrared detectors.

20 August

D. A. RAMSAY, Chairman.

Infrared intensities—

D. F. EGGERS, Jr.: Infrared intensities from band area measurements.

J. H. JAFFE: Infrared intensities from dispersion measurements.

Raman intensities—

M. V. VOLKENSTEIN: Theoretical aspects.

L. A. WOODWARD: Experimental aspects.

21 August

V. Z. WILLIAMS, Chairman.

The origin of group frequency shifts—

D. H. WHIFFEN: Physical effects.

L. J. BELLAMY: Chemical effects.

Group intensities—

R. N. JONES: Infrared intensities in liquid and solution phases.

22 August

Infrared: Its present needs and future directions; general discussion—

F. A. MILLER, Chairman.

L. J. BELLAMY, B. CRAWFORD, Jr., J. A. A. KETELAAR, R. C. LORD, H. W. THOMPSON, N. WRIGHT.

Requests for attendance at the Conference should be addressed to W. George Parks, Department of Chemistry, University of Rhode Island, Kingston, R.I.

International Spectroscopic Colloquium

THE Seventh International Colloquium of Spectroscopy, under the auspices of the IUPAC, will take place in Liège (Belgium) from 8 to 12 September 1958 and be organized through the Association des Ingénieurs sortis de l'Ecole de Liège (AILg).

The Fédération des Industries Chimiques de Belgique will hold at the same time also in Liège the Thirty-first International Congress for Applied Chemistry.

The opening speech will be common both to the Seventh International Colloquium for Spectroscopy and to the Thirty-first International Congress for Applied Chemistry:

A review in the field of infrared spectroscopy and its applications to industry by Dr. H. W. THOMPSON (Great Britain).

General lectures and discussions will be arranged as follows:

(1) (a) Present state and prospects in emission spectroscopy. General lecture by Dr. W. F. MEGGERS (U.S.A.).
(b) Evolution of emission spectral techniques in industrial control. General lecture by Eng. V. MATHIEN (Belgium).
(2) New ways in spectroscopic techniques. General lecture by Prof. P. JACQUINOT (France)
(3) New trends in infrared. General lecture by Dr. G. M. B. M. SUTHERLAND (Great Britain).
(4) Recent progress in Raman spectroscopy. General lecture by Dr. A. C. MENZIES (Great Britain).
(5) Reflection spectra in ultraviolet and infrared. General lecture by Prof. G. KORTÜM (Germany).
(6) Fluorescence spectra by means of X-rays and electronic rays. General lecture by Dr. S. L. BIRKS (U.S.A.).
(7) (a) Electrical quadrupole resonance. General lecture by Prof. P. GRIVET (France).
(b) Electronic magnetic resonance and nuclear magnetic resonance. General lecture by Prof. B. BLEANEY (Great Britain).

Information about attendance at the meeting can be obtained from the Secretary, Association des Ingénieurs sortis de l'Ecole de Liège (AILg), 22, rue Forgeur, Liège (Belgique).

American Association of Spectrographers

THE American Association of Spectrographers will hold its Ninth Annual Symposium on Spectroscopy at the Pick-Congress Hotel, Chicago, Illinois, U.S.A. starting Monday, June 9 and continuing through Wednesday, June 11, 1958.

Papers in the fields of Emission Spectroscopy, Flame Photometry, X-Ray Spectroscopy, Infrared, Near-Infrared, Visible and Ultraviolet Spectroscopy are invited.

The Symposium will also include an instrument display.

All correspondence concerning attendance at the Symposium as well as papers to be submitted should be directed to:

H. J. Hettel,
Symposium Coordinator,
Armour Research Foundation,
Chicago 16,
Illinois, U.S.A.

VOL. 12 1958

Spectrochimica Acta, 1958, Vol. 12, p. 107. Pergamon Press Ltd., London

Papers to be published in future issues

D. F. SMITH: Infrared spectra analysis for hydrogen fluoride

B. STEVENS: A relationship between some bond properties of diatomic molecules and the ionization potentials of their constituent atoms

L. H. SUTCLIFFE: Rydberg term tables

D. W. GRANT, D. E. GLANVILLE and G. L. STRACHAN: A simple arrangement for the measurement of absorption spectra of aqueous systems at elevated temperatures

E. G. MCRAE: Solvent effects on merocyanine spectra

R. C. HIRT: Ultraviolet absorption vapor spectra of pyrazine and chloropyrazine

D. P. STEVENSON and H. M. MCCONNELL: Ultraviolet criteria for monoaromaticity

M. TSUBOI, T. ONISHI, I. NAKAGAWA, T. SHIMANOUCHI and S. MIZUSHIMA: Assignments of the vibrational frequencies of glycine

L. H. SPINAR and J. L. MARGRAVE: Absorption spectra of gaseous alkali metal hydroxides at high temperatures

M. MACK and N. SPIELBERG: Statistical factor in X-ray intensity measurements

J. K. HURWITZ: Spectrographic analysis of segregates with a dynamic microvolume technique-II. Experimental verification of theory

D. M. W. ANDERSON, L. J. BELLAMY and R. L. WILLIAMS: The infrared spectra of some gem dihydroxy compounds and their deuterated derivatives

R. N. JONES and A. NADEAU: Cavity type micro-cells for infrared spectrometry

I. NAKAGAWA, S. MIZUSHIMA, A. S. SARACENO, T. J. LANE and J. V. QUAGLIANO: Infrared absorption spectra of inorganic co-ordination complexes—XVI. Normal vibrations of sulfamic acid, $H_3N \pm SO_3^-$

T. T. CROW and R. T. LAGEMANN: Infrared spectrum of sulfuryl bromofluoride

J. BURDON and D. H. WHIFFEN: Infrared spectra of fluoro-cyclo olefins

D. HADYI and M. PINTAR: The OH in-plane deformation and the C—O stretching frequencies in monomeric carboxylic acids and their association shifts

R. C. HIRT and R. G. SCHMITT: Ultraviolet absorption spectra of derivatives of symmetric triagine—II. Oxo-triagines and their acyclic analogs

R. C. LORD, D. W. MAYO, H. E. OPITZ and J. S. PEAKE: The preparation and vibrational spectra of disilylacetylene

G. R. BIRD, A. DANTI and R. C. LORD: Pure rotational absorption of NO_2 in the 50–200 micron region

R. MECKE und K. NOACK: Untersuchungen über die beeinflussung der frequenz und intensität der ν_{CO} und ν_{C-C} banden im IR-spektrum ungesättigter ketone durch konjugation und sterische hinderung

M. C. DE WILDE-DELVAUX et P. L. TEYSSIE: Etude spectrographique infra-rouge de quelques β-dicetones

H. STAMMREICH, D. BASSI and O. SALA: Raman spectra of the ions CrO_4 and Cr_2O_7

G. PORTER and E. STRACHAN: The electronic spectra of benzyl

C. GARRIGON-LAGRANGE, J. M. LEBAS et M. L. JOSIEU: Etude comparée des spectres de vibration des dérivés paradisubstitués du benzène—I. Région 670–1600 cm^{-1}

A. L. BLUHM: The infrared spectra and the structure of some homophthalimides

F. A. MILLER and R. B. HANNAN: The ultraviolet absorption spectrum of dicyano-acetylene

R. N. KNISELEY, V. A. FASSEL, B. B. QUINNEY, C. TREMMEL, W. A. GORDON and W. J. HAYLES: Quantitative spectrographic analysis of the rare earth elements—IX.

D. F. HORNIG, H. F. WHITE and F. P. REDING: The infrared spectra of crystalline H_2O, D_2O and HDO

ERRATUM

VELMER A. FASSEL and RAYMOND W. TABELING:

Spectrographic Determination of Oxygen in Metals—I.
Plain Carbon Steels.

Spectrochim. Acta 1956 **8** 201

IN this paper the statement is made that the oxygen triplet at 7772 Å could not be detected in spectrograms of d.c. carbon arc discharges in air. A recent re-investigation of these experiments has revealed to us that these conclusions were erroneously based on spectra actually obtained from d.c. arc discharges between *iron* and *iron–carbon* electrodes. In d.c. carbon arc discharges in air, the oxygen triplet actually exhibits moderate intensity. These observations do not alter the stated conclusions that the efficiency of exciting the oxygen triplet is enhanced by several orders of magnitude when the d.c. carbon arc is operated in rare gas atmospheres.

VOL.
12
1958

Spectrochimica Acta, 1958, Vol. 12, pp. 109 to 113. Pergamon Press Ltd., London

A simple arrangement for the measurement of absorption spectra of aqueous systems at elevated temperatures

D. W. Grant, D. E. Glanville and G. L. Strachan
Atomic Energy Research Establishment, Harwell

(*Received* 16 *November* 1957)

Abstract—Absorption spectra are measured in electrically-heated sealed glass ampoules. It is shown that quantitative measurements can be made despite distortions in the optical path arising from the cylindrical nature of the cell and the variation in the refractive index of its contents with temperature.

Methods for the measurement of absorption spectra of organic compounds in organic solvents have been described [1, 2], in which the solutions were contained in small Dewar vessels fitted with optical windows. Heating was effected either by hot air [1] or by the vapours of boiling liquids [2]. However, the authors have been unable to find any reference to the measurement of absorption spectra of aqueous solutions above the boiling point, although much useful information on ionic equilibria could be derived in this way.

The apparatus

The normal type of optical cell with thin, plane parallel optical faces cannot be used at elevated temperatures with aqueous solutions because of the high pressures involved. However a preliminary investigation showed that qualitative measurements of absorption spectra at room temperature could be made on solutions contained in Pyrex glass ampoules of normal wall thickness and of internal diameter $\simeq$3 mm [3].

The apparatus for use at high temperatures, shown in Fig. 1, consisted of a brass block B with two exactly aligned slits W ($\simeq$3·3 mm wide), which fitted into the cell carriage of a Unicam SP 600 spectrophotometer (see Fig. 3). The brass block was located in the same position with respect to the light beam for every measurement by means of a spigot L, which fitted snugly into a hole in the base of the carriage. Both the brass block and the carriage were secured to the movable cradle of the instrument by screw S. The ampoule A made from nominal 3 mm bore Pyrex tubing, fitted into a central cavity of the block, and was held fairly rigidly by PTFE formers F_2, and F_3. Screw S was countersunk deeply to allow the ampoule to sit in a depression in the latter former (this is not shown in Fig. 1). The electrical heater consisted of nichrome resistance wire strung between the PTFE formers F_1, F_2 and F_3 in such a manner as not to obstruct the light beam traversing the ampoule (see Fig. 2). The electrical leads were led in through the aperture at the base of the spectrophotometer, and were fixed to terminals T on the cell carriage from which connexion to the heater was made (see Fig. 3). The heating current was supplied from the a.c. mains through a 12 V transformer,

and was kept at a constant value in the range 0–1 A by frequent manual adjustment of a variable resistance.

The temperature within an empty ampoule was calibrated for known values of current using a chromel-alumel thermocouple. During each calibration the cell carriage was housed in the spectrophotometer to simulate as far as possible actual experimental conditions. A fairly uniform temperature will exist in any solution under observation in an ampoule, since at $\simeq 180°$ the temperature difference between the bottom of the ampoule and a point where the meniscus would be was only $\simeq 6°$. The performance of the spectrophotometer itself will be unaffected by the presence of an ampoule at elevated temperatures, since the air temperature

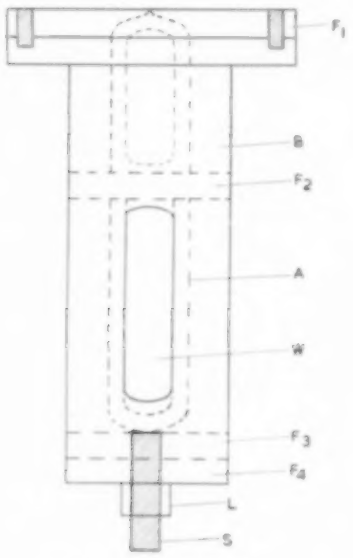

Fig. 1. Ampoule holder.

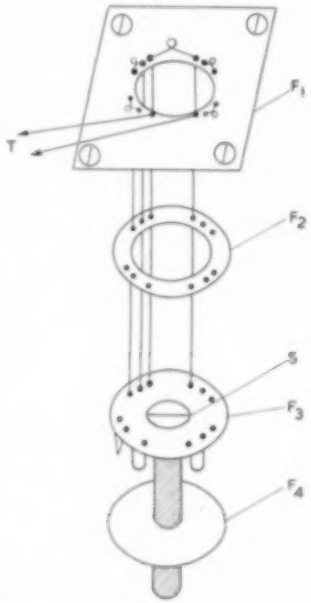

Fig. 2. Ampoule heater. For simplicity only a few heater windings are shown.

within the cell housing during operation was only a few degrees above the ambient temperature. To compensate approximately for the absorption due to the ampoule walls and the brass block, all optical densities ($D_A{}^1$) were determined with respect to a "blank" consisting of an empty 1 cm optical cell with its front face masked except for a window with similar dimensions to the slits of the brass block. Absolute optical densities due to the solute species itself (D_A) were evaluated by subtracting from the measured values the optical densities (D_B) obtained by replacing the aqueous solution with the appropriate solvent. Since ordinary glass tubing is not uniform in bore, the optical path length varies according to the orientation of the ampoule in its holder. Nevertheless optical densities were found to be reproducible to $\simeq \pm 0{\cdot}005$ units, provided care was taken to align a scratch mark on the ampoule with a mark on the top face of the brass block.

VOL. 12 1958

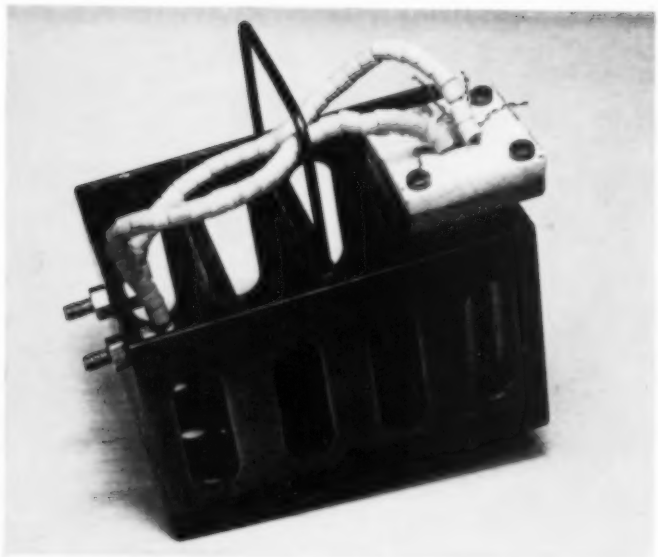

Fig. 3

VOL.
12
1958

The quality of the optical measurements at 20°

For quantitative work the measurements taken in an ampoule should satisfy the following requirements:

(1) The effective path length l_A, defined as: $D_A/D_C \times l_C$, where D_C is the optical density obtained by using a conventional optical cell of path length l_C, should be independent of the absorbing solute species and should be constant over a wide range of wavelength, and (2) D_A should vary linearly with concentration of solute. The optical densities of a solution of neodymium nitrate measured in an ampoule and a Pyrex glass optical cell of path length 10 mm, are recorded in Table 1. The values of l_A determined using equation (1) indicate that the effective path length is independent of wavelength over the range 530–890 mμ.

Table 1. The effect of wavelength on the effective path length of an ampoule

λ (mμ)	D_A[1]	D_B	D_A	D_C	l_A (mm)
528	0·085	−0·058	0·143	0·418	3·42
584	0·197	−0·060	0·257	0·754	3·41
760	0·460	+0·235	0·225	0·669	3·37
820	0·506	+0·236	0·270	0·794	3·40
893	0·338	+0·242	0·096	0·281	3·42

Linear plots of optical density against uranyl ion concentration in the solution range 0–0·6 molar were obtained for uranyl perchlorate solutions at 416, 428 and 440 mμ.

High-temperature effects

(*a*) *Solvent distillation.* The absorption spectra of a number of solutions which had been heated were found not to revert to their original states on cooling, owing to distillation of solvent on to the colder top of the ampoule with resultant concentration of the solutions. From the reproducibility of the spectra at elevated temperatures, it appears that the distilled solvent remains as a static pocket of liquid in the top of the ampoule. Thus, the change of concentration due to solvent distillation may be determined from the heights of the absorption bands at ambient temperature before and after heating. However, the effect is undesirable since the introduction of a correction factor reduces the accuracy of the measurements. Fortunately, experience has shown that the effect can be eliminated by ensuring that the ampoule fits very tightly into formers F_1, F_2 and F_3, and does not protrude from the end of its holder.

(*b*) *The refractive index effect.* The absorbancy of a perchloric acid solution was observed to decrease with increasing temperature, an effect which might be attributed to the changing refractive index of the solution with consequent changes in the optical path of the light beam traversing the ampoule. At 95° the optical density change at 500 mμ was $\simeq$0·02, while at 180° the change was $\simeq$0·08, which is consistent with a decrease in the refractive index of water of $\simeq$1 per cent at 95° and $\simeq$4 per cent at 180°. The apparent increase in absorbancy when water is replaced by liquids of higher refractive index conclusively proves the origin of the effect (see Table 2).

Table 2. The effect of refractive index on D_B at 20°

Solvent in ampoule	Refractive index (18°C)	D_B		
		360 mμ	420 mμ	500 mμ
Water	1·333	−0·041	−0·043	−0·054
Chloroform	1·446	0·121	0·147	0·165
Trichlorethylene	1·478	0·180	0·190	0·205

Table 3. The effect of perchloric acid concentration on $D_A{}^1$, D_B, D_A and l_A at 20°

		$HClO_4$ (moles/l.)								
	λ (mμ)	0·09	0·37	0·74	1·1	1·85	2·5	3·7	5·55	7·4
$D_A{}^1$	380	0·109	0·119	0·120	0·136	0·136	0·150	0·154	0·198	0·220
	416	0·422	0·430	0·433	0·450	0·448	0·461	0·471	0·502	0·522
	428	0·308	0·325	0·320	0·338	0·335	0·354	0·353	0·394	0·410
D_B	380	−0·038	−0·047	−0·060	−0·046	−0·038	−0·019	0·018	0·031	0·065
	416	−0·047	−0·058	−0·072	−0·061	−0·040	−0·030	0·003	0·024	0·053
	428	−0·046	−0·063	−0·071	−0·057	−0·039	−0·031	0·004	0·028	0·054
D_A	380	0·147	0·166	0·180	0·182	0·174	0·169	0·136	0·167	0·155
	416	0·469	0·488	0·505	0·511	0·488	0·491	0·468	0·478	0·469
	428	0·354	0·388	0·391	0·395	0·374	0·385	0·349	0·366	0·356
D_C	380	0·525	0·519	0·516	0·516	0·507	0·507	0·497	0·483	0·452
	416	1·48	1·48	1·48	1·47	1·45	1·47	1·44	1·43	1·37
	428	1·166	1·139	1·147	1·159	1·139	1·139	1·124	1·094	1·062
l_A(mm)	380	2·80	3·20	3·49	3·53	3·43	3·33	2·74	3·46	3·43
	416	3·17	3·30	3·41	3·48	3·37	3·34	3·25	3·34	3·42
	428	3·04	3·41	3·41	3·41	3·28	3·38	3·10	3·34	3·35

$l_A(\text{av})_{380_{m\mu}} = 3{\cdot}27 \pm 0{\cdot}24$ mm; $l_A(\text{av})_{416_{m\mu}} = 3{\cdot}34 \pm 0{\cdot}07$ mm; $l_A(\text{av})_{428_{m\mu}} = 3{\cdot}30 \pm 0{\cdot}11$ mm

VOL. 12 1958

The effect of temperature on an absorption spectrum is most conveniently expressed as a change in the molar extinction coefficient ε_T of the absorbing species at any temperature T,

where $$\varepsilon_T = \frac{D_A}{l_A \times C_T}$$

For moderately concentrated solutions the molar concentration at T is

$$C_T = \frac{C_{20^\circ} \times \text{density of water at } T^\circ}{\text{density of water at } 20^\circ}$$

Unfortunately, l_A is not independent of temperature because of the refractive index effect previously discussed, and cannot be determined directly at elevated temperatures. However, some idea of the magnitude of the effect of temperature on l_A can be deduced from its change with refractive index at ambient temperature. Since the molar extinction coefficient of a uranyl perchlorate solution is almost independent of the perchloric acid concentration, it is reasonable to assume that the nature of the absorbing species is unchanged. Therefore any observed variation in l_A with acidity must be attributed to a change in the refractive index of the solution. Referring to Table 3 it is seen that although D_A[1] and D_B increase markedly as the acid concentration is varied from 0·1 to 7·4 molar, D_A and l_A are relatively unaffected. As the standard mean deviations in the average values of l_A at the three wavelengths considered are comparable with the estimated experimental errors, l_A may be assumed to be independent of D_B and temperature.

The limitations of the apparatus

Measurements made using the type of ampoule described are probably limited to a temperature in the neighbourhood of 250° owing to excessive steam pressures. However, the temperature limit will vary according to the pH of the solution under consideration, and for solutions of pH $>$ 3 rapid corrosion of the ampoule walls would probably restrict measurements to below 200°. The authors have observed no perceptible attack on one ampoule used for many measurements on solutions containing 2 M perchloric or 2 M sulphuric acids at 180°.

Acknowledgement—The authors would like to express their appreciation of the valuable assistance rendered by Mr. F. W. Derrick.

References

[1] Fischer E. U.C.R.L. 3157 1955 p. 22.
[2] Hirshberg Y. and Fischer E. *J. Chem. Soc.* 1953 629.
[3] Glanville D. E. and Grant D. W. Atomic Energy Research Establishment, Harwell, Report C/R 2155 1957.

Spectrochimica Acta, 1958, Vol. 12, pp. 114 to 126. Pergamon Press Ltd., London

Ultraviolet absorption vapor spectra of pyrazine and chloropyrazine

R. C. Hirt
Research Division, American Cyanamid Company, Stamford, Connecticut, U.S.A.

(*Received* 30 *September* 1957)

Abstract—The ultraviolet absorption spectra of pyrazine vapor and of chloropyrazine vapor are analyzed in terms of ground-state and excited-state vibrational frequencies and combinations thereof. The "sharp" band systems of both pyrazine and chloropyrazine (attributed to "n-to-pi" transitions involving the nonbonding electrons of the heterocyclic nitrogen atoms) are analyzed. Only the "diffuse" system attributed to a "pi-to-pi" (benzenoid) transition of pyrazine vapor showed enough detail to permit any attempt at assignments. Extremely weak bands have been observed at lower energies in solution or liquid phases which show a substitutional "blue-shift" between pyrazine and chloropyrazine. These are attributed to a "n-to-pi" singlet–triplet transition. Infrared and Raman data for chloropyrazine are reported for comparison with the ultraviolet band spacings.

Introduction

The near-ultraviolet solution spectra of the diazines, their halogen and alkyl halide derivatives, and their behavior in various solvents have been described, along with a valence-bond treatment of the diazine π-electrons [1]. The two major band systems, called the "sharp" and the "diffuse" systems from their appearance in the vapor phase, were assigned to a nonbonding nitrogen electron transition and to a π-electron transition, respectively. The position of the zero–zero (0–0) band of the "sharp" system in the vapor phase and the approximate spacings of the principal upper-state vibrational bands have been reported for pyrazine (*p*-diazine) and for pyridazine (*o*-diazine) [2]. The vapor spectrum of pyrimidine (*m*-diazine) has been reported by Uber [3]. In this report, the details and assignments of the "sharp" and "diffuse" band systems of pyrazine vapor and of chloro pyrazine vapor are described. Since the publication of the "Letter to the Editor" [2] concerning the vapor spectra of the diazines was published, a Ph.D. thesis [4] was presented by Miss Betty Jane Fax concerning the infrared and ultraviolet spectra of the diazines and pyridine. A microfilm copy of this thesis has been examined, but no data or assignments are used from it. Recently Lord *et al.* [5] and Ito *et al.* [6] published data on the Raman spectrum of pyrazine, and Ito *et al.* [7] have published data on the "sharp" ultraviolet vapor spectrum only.

Experimental

The vapor spectrum of pyrazine and chloropyrazine were photographed with a medium Hilger quartz spectrograph having a dispersion of 163 kaysers/mm (cm^{-1}/mm) at 31,000 K (cm^{-1}), and with a large Hilger Littrow quartz spectrograph having a dispersion of 60 K/mm at 31,000 K. A water-cooled Nester hydrogen lamp operating from a regulated d.c. power supply served as the source. Fused quartz cells of 10, 20, 50, and 100 mm light path length and Eastman Kodak plates of types II-0 and III-0 were used. The vapor pressure of pyrazine and chloropyrazine were sufficiently high to allow the use of these cell lengths. The cells were stoppered but not evacuated.

VOL. 12 1958

The measurement of the bands was done on tracings of the plates prepared on a Leeds and Northrup microphotometer of the Knorr–Albers type. Wavelength calibration was effected by use of an H-3 mercury lamp and a standard Pfund iron arc. The wavelengths of the bands were corrected to vacuum and converted into wavenumbers (kaysers) by use of KAYSER's tables. From the conditions of the experiments and the measurements, the positions of the bands are probably not accurate to better than 4 K. The samples used were identical to those of the solution work [1] and had been purified by sublimation.

The vapor spectra were also measured with a Cary automatic recording spectrophotometer, Model 11, using identical samples and cells. The instrument was operated at its lowest scanning

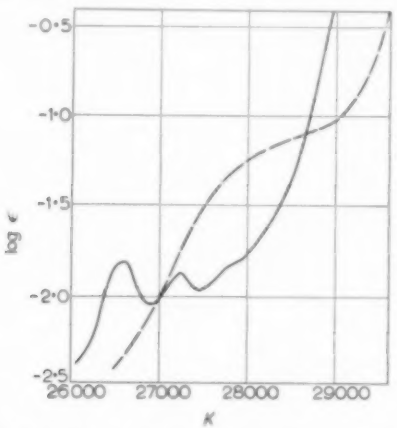

Fig. 1. Singlet–triplet absorption bands of: Pyrazine————; Chloropyrazine – – – –.

speed of 1 Å/sec and with very narrow slits (0·005 to 0·02 mm). These spectra closely resembled the microphotometer tracings, and measurement of the band positions yielded wavenumber differences in reasonably good agreement with the spectrographic data. The Cary was calibrated with a 4 W "Sterilamp" mercury lamp. The values reported in the Tables are almost entirely taken from the spectrographic data, although the Cary data were taken into consideration in making the band assignments. Solution spectra were obtained on both Cary and Beckman DU instruments, using cells of 50 and 100 mm and concentrated solutions.

The infrared bands were obtained by Mr. JOHN WHALEN on a Perkin–Elmer infrared spectrometer, Model 12C, using both NaCl and KBr optics. The solid pyrazine was melted, squeezed between two NaCl or KBr plates, and allowed to solidify before running. Chloropyrazine was run as a liquid between NaCl or KBr plates. The infrared band positions for pyrazine were in excellent agreement with those recently reported by LORD *et al.* [5] and so are not reproduced here, except where used in connection with the ultraviolet band assignments. The Raman data on chloropyrazine were obtained by Dr. R. F. STAMM, using a fast grating spectrograph [8].

Discussion

(1) *Observed electronic transitions of pyrazine and chloropyrazine*

Evidence for five electronic transitions of pyrazine has been obtained. A weak set of three bands has been observed in concentrated *cyclo*hexane solutions at 3760 Å, 3670 and 3600 Å (26,600, 27,250, and 27,800 K). The long wavelength position and extreme weakness ($\varepsilon = 0{\cdot}015$) indicate that these belong to a forbidden singlet–triplet transition. Chloropyrazine shows a shoulder at 3650 Å or 28,100 K with $\varepsilon = 0{\cdot}05$, thus displaying a substitutional "blue-shift." These bands have been assigned to an $n \rightarrow \pi^*$, singlet–triplet transition (Fig. 1) [9].

The "sharp" band system, with its zero–zero vapor band at 30,879 K, has been shown to arise from an $n \rightarrow \pi^*$ transition involving the nonbonding nitrogen electrons on the heterocycle nitrogen atoms [1]. The "diffuse" band system at shorter wavelength has similarly been explained as a $\pi \rightarrow \pi^*$ transition analogous to the familiar benzene 2600 Å system.

A fourth system indicates its presence by an upturn in the absorption curve near the short wavelength limit of the available instrumentation. Klevens and Platt [10] have published the vacuum ultraviolet spectrum of pyrazine in heptane solution, which shows the maximum of this band system to occur near 51,500 K (1940 Å), and which indicates the presence of yet another band system above 58,000 K (below 1720 Å).

Four transitions for chloropyrazine are known. A shoulder attributed to an $n \rightarrow \pi^*$, singlet–triplet transition was observed in the absorption spectrum of the liquid. Like pyrazine, there is a "sharp" band system for the $n \rightarrow \pi^*$ transition and a "diffuse" system of higher intensity for the first $\pi \rightarrow \pi^*$ (benzenoid) transition [1]. An up-turn of the solution absorption curves near 2150 Å indicates the presence of a second $\pi \rightarrow \pi^*$ transition near 2000 Å. No data in the vacuum ultraviolet are available.

(2) *Details of the ground-state vibrations of pyrazine*

The "sharp" ultraviolet band system of pyrazine vapor shows enough detail to permit a vibrational analysis and comparison with the infrared and Raman spectra [5, 11]. Pyrazine is a planar molecule of symmetry class V_h (D_{2h}). Since it has a center of symmetry, the observed infrared and Raman bands should be mutually exclusive. The Z axis was chosen perpendicular to the plane of the ring, and the Y axis through the N atoms. (This choice of axes differs from those of Lord *et al.* and Ito *et al.* [5, 7].)

The totally symmetric A_{1g} modes would be expected to appear strongly as bands to the red of the zero–zero band, and they are found with spacings of 598, 1015, and 1228 K. Observed ultraviolet bands and assignments are given in Table 1. Fitting the corresponding benzene frequencies to the pyrazine bands is aided by the knowledge that the frequencies will not have undergone very large changes from benzene to pyrazine. Other bands to the red of the zero–zero bands have been assigned to ground-state frequencies, largely because of the "fit" of their values; these are at 415, 852, 914, and 1414 K, corresponding to modes 16b, 10a, 17a, and 19b. Ultraviolet bands to the "red" side of the 0–0 arise from vibrational states which are already excited at the time of the electronic transition, and the population of these states is regulated by the Boltzman factor. Thus at ordinary temperatures very few ultraviolet bands farther than 1000 K to the red of the zero–zero band are likely to be observed. (Ito *et al.* [7] obtained bands as far as 2000 K with long-path cells at 140°.)

(3) *Details of the upper-state vibrations*

Unlike 1–0 or 1–1 transitions, 0–1 transitions are not dependent upon the Boltzman factor for their probability. Transitions from the nonvibrating ground-state to vibrating upper-states are quite probable, and prominent bands are

VOL. 12 1958

Table 1. "Sharp" bands of the ultraviolet spectrum of pyrazine

Band position (K)	Difference from 0–0 band	Estimated intensity*	Assignment
29,376	1503	vvw	
446	1433	vvw	
465	1414	vvw	0 − 1419 (19b)
507	1372?	vvw	
606	1273	vvw	
651	1228	w	0 − 1232 (9a)
687	1192	w	0 − 2 × 598
705	1174	vw	
748	1131	vw	
792	1087	vvw	
864	1015	vw	0 − 1015 (1)
915	964	vw	0 − 1015 + 53
965	914	m	0 − 914 (17a)
30,027	852	w	0 − 852 (10a)†
095	784	m	0 − 415 − 362
152	727	w	
197	682	w	
231	648	w	
244	635	w	0 − 641 (6b) or (4)
281	598	m	0 − 598 (6a)
296	583	vw	
331	548?	vw	
335	544	ms	0 − 3 × 179
390	489	m	
432	447	w	
464	415	vw	0 − 415 (16b)
487	392	vw	
517	362	s	0 − 362 (16a)‡ or 0 − 2 × 179?
551	328	m	0 − 805 + 474 (1-1 of 11)
618	261	vs	0 − 852 + 585 (1-1 of 10a)
640	239	w	
674	205	m	
700	179	vs	0 − 415 + 236 (1-1 of 16b)
734	145	m	0 − 362 + 215 (1-1 of 16a)
749	130	m	0 − 362 + 236
825	54	m	0 − 1015 + 957 (1-1 of 1)
879	0	vvs	0–0
932	53	vs	0 − 415 + 474
988	109	w	0 − 362 + 474
31,026	147	w	
094	215	m	0 + 215 (16a′)
115	236	m	0 + 236 (16b′)
178	299	m	
221	342	w	
264	385	m	C′ of Ito *et al.* [7]?§
277	398	s	0 + 585 − 179?
290	411	m	

Table 1 (*continued*)

Band position (K)	Difference from 0–0 band	Estimated intensity*	Assignment
31,325	446	w	0 + 236 + 215 or 0 + 630 − 179
353	474	s	0 + 474 (11′) or 0 + 2 × 236?
390	511	w	
404	525	w	
464	585	vs	0 + 585 (6a′)
473	594	w	
509	630	m	0 + 630 (6b′)
522	643	w	
544	665	m	0 + 665 (17a′)
562	683	vw	0 + 215 + 474
583	704	vw	0 + 236 + 474
641	762	vw	
657	778	vw	0 + 1138 − 2 × 179?
707	828	m	0 + 236 + 585
741	862	m	0 + 236 + 630
779	900	w	0 + 236 + 665
822	943	m	0 + 2 × 474 (or C′ of Ito)§
836	957	ms	0 + 957 (1′)
868	989	m	
882	1003	w	
915	1036	m	
939	1060	m	0 + 474 + 585
982	1103	ms	0 + 630 + 474
32,017	1138	m	0 + 1138 (9a′)
053	1174	vs	0 + 2 × 585
090	1211	m	0 + 630 + 585
129	1250	ms	0 + 1250 (14′)
198	1319	m	(D′ of Ito)§
228	1349	w	0 + 1138 + 236
259	1380	ms	0 + 1380 (19b′)
274	1395	m	
294	1418	m	0 + 957 + 474?
329	1450	w	0 + 1450 (8b′)?
390	1520	ms	0 + 1520 (8a′)
428	1549	w	0 + 957 + 585
457	1578	w	0 + 957 + 630
491	1612	w	0 + 1380 + 236 or 0 + 1138 + 474
529	1650	vw	
558	1679	m	0 + 1380 + 474 − 179
598	1719	w	0 + 1138 + 585
615	1736	w	0 + 1520 + 215
629	1750	m	0 + 3 × 585
642	1763	w	0 + 1520 + 236?
712	1833	w	0 + 1250 + 585
757	1878	vw	
779	1900	w	
797	1918	w	0 + 2 × 957

VOL. 12 1958

Table 1 (*continued*)

Band position (K)	Difference from 0–0 band	Estimated intensity*	Assignment
32,823	1944	m	0 + 1250 + 630
858	1974	w	0 + 1380 + 585?
902	2023	w	0 + 1250 + 665
921	2042	w	0 + 1450 + 585 or 0 + 1380 + 665
973	2094	vw	0 + 1138 + 957
33,024	2145	w	0 + 1520 + 630
076	2197	vw	
132	2253	vw	
154	2275	w	0 + 2 × 1138
203	2324	vw	0 + 1250 + 957
296	2417	vw	0 + 2 × 630 + 2 × 585
343	2462	vvw?	
432	2553	vvw?	
479	2600	vvw?	
561	2682	vvw?	
630	2751	vvw?	0 + 2 × 1380?
882	3003	vvw?	

* Key for intensities: vvw = very very weak; vw = very weak; w = weak; m = medium; ms = medium strong; s = strong; vs = very strong; vvs = very very strong.
† Lord *et al.* [5] used 10a = 753 K.
‡ Lord *et al.* estimated 16a as 340 K.
§ These assignments of Ito *et al.* [7] were inserted during preparation of the manuscript.

observed. The bands at separations of 215, 236, 474, 585, 630, 665, 957, 1138, 1250, 1380 and 1520 K from the 0–0 band have been assigned as upper-state vibrational bands. These bands and corresponding ground-state frequencies are summarized in Table 2, along with calculated and observed difference frequencies (1–1 bands). Doubtful values or assignments are marked with a question mark (?). Considerable difficulty was encountered in assigning the prominent band at 398 K above the 0–0 and at 544 K below. (Ito *et al.* have assigned these to a different, forbidden $n \rightarrow \pi^*$ transition.) The difference frequencies are used in making assignments of the less prominent bands wherever their values permit. Similarly difference frequencies which arise between different modes are used in the assignments, as well as additive combinations.

One notable feature of the pyrazine vapor spectrum is the lack of long progressions of the upper-state bands. Only a few 2× and 3× assignments could be made, and these were to rather weak bands. This lack of long progressions had been noted earlier [2] and used in the identification of the "sharp" band system with an $n \rightarrow \pi^*$ or nonbonding nitrogen electron, transition [1].

(5) *The "diffuse" band of pyrazine vapor*

Only a few maxima could be resolved from the "diffuse" band system of pyrazine vapor. These bands could not be measured with anywhere near the

precision of the bands of the "sharp" system. These data are shown in Table 3, along with the corresponding bands of the "sharp" system and tentative assignments.

Monochloropyrazine. The near ultraviolet solution spectrum of monochloropyrazine was reported [1] along with data on other diazines. The "sharp" series of bands at longest wavelengths were assigned to a nonbonding nitrogen–electron transition, and the stronger, "diffuse" bands at shorter wavelengths were assigned to a π-electron (benzenoid) transition. The ultraviolet vapor spectrum of 2-chloropyrazine has not been previously reported.

Table 2. Comparison of ground- and upper-state frequencies of the sharp bands of pyrazine
R = observed in Raman
i.r. = observed in infrared
u.v. = observed in ultraviolet

Vibration	Mode	Ground-state (K)	Upper-state (K)	Ground–upper difference	Observed difference freq. (K)
1	A_{1g}	1015 u.v., R	957	58	54
6a	A_{1g}	598 u.v., i.r.	585	13	—
8a	A_{1g}	1584 R	1520	64	—
9a	A_{1g}	1228 u.v., R	1138	90	—
16a	A_{1u}	362 u.v.†	215	147	145
17a	A_{1u}	914 u.v., i.r., R	665	249	239?
10a	B_{2g}	852 u.v.*	585?	267?	261
19a	B_{1u}	1491 i.r.	1380	111	—
6b	B_{1g}	641 R	630	11	—
11	B_{1u}	805 i.r.	474	331	328
16b	B_{1u}	415 u.v., i.r.	236	179	179
14	B_{2u}	1345 i.r.	1250	95	—
19b	B_{2u}	1414 u.v., i.r.	1380	29	—

* Lord *et al.* [5] used 10a = 753 K.
† Lord *et al.* estimated 16a as 340 K.

The infrared and Raman spectral data are summarized in Table 4, along with values for ground-state frequencies obtained from bands to the red of the zero–zero band of the ultraviolet vapor spectrum.

The bands of the ultraviolet vapor spectrum are tabulated in Table 5, along with their differences (from the 0–0 band) and the assignments where they have been made.

Ground-state vibrations of chloropyrazine. The V_h symmetry class of pyrazine is reduced to the lower symmetry class C_h or C_s, for chloropyrazine, which has but one plane of symmetry (that through the ring of the molecule). All modes become A' or A''.

Assignment of vibrational modes becomes difficult and largely empirical. The assumption is made that certain modes are changed but little by the presence of the heavy chlorine atom; if a "fit" of infrared, Raman and ground-state ultraviolet frequencies is found to correspond to one of the unsubstituted pyrazine

VOL. 12 1958

Table 3. "Diffuse" bands of the ultraviolet vapor spectrum of pyrazine

Band no.	Band position (K)	Relative intensity to 0–0	Difference from 0–0	Corresponding difference in sharp bands	Possible assignment
1	37,792	0·17	971	964	
2	37,855	0·18	908	914	914 (17a)
3	38,086	0·09	700	—	
4	38,173	0·09	590	598	0 − 609 (6a)
(5)	38,303	0·13	460	447?	
6	38,475	0·24	288	261	(1-1 of 10a)
7	38,718	0·93	45	54	(1-1 of 1)
8	28,763	1·00	0	0	0–0
9	38,833	0·93	70	—	
10	38,961	0·43	198	215?	(16a′)
11	39,274	0·36	511	511	
12	39,359	0·38	596	585	0 + 585 (6a′)
13	39,448	0·37	686	683	0 + 215 + 474
14	39,626	0·43	863	862	0 + 236 + 630
15	39,725	0·52	962	957	0 + 957 (1′)
16	39,832	0·41	1069	1060	0 + 474 + 585
17	40,021	0·30	1258	1250	0 + 1250 (14′)
18	40,250	0·18	1487	—	
19	40,698	0·14	1935	1944	0 + 1250 + 630
(20)	40,868	0·07	2105	2094	0 + 1138 + 957

frequencies, the mode is assigned to the analogous pyrazine mode. A check may be made to see if the analogous vibrational mode in benzene is one which may be pictured as the chlorine and attached carbon atom holding still while the rest of the ring vibrates (an admittedly crude picture). "Fits" of infrared, Raman and ultraviolet frequencies which do not correspond to a pyrazine frequency therefore are taken to be modes which are seriously affected by substitution; these must often remain unassigned.

In Table 6 a comparison is made of the modes and ground-state frequencies found in pyrazine with those found in chloropyrazine. Of these values, only three appeared in ultraviolet, infrared and Raman data, though nine appeared in two of the techniques. Some assignments have been made on but one source; these are necessarily questionable.

Since the probabilities or intensities of 1–0 and 1–1 type transitions depend upon the population of the vibration ground-state (determined by the Boltzman factor), ground-state frequencies higher than 1000 or 1200 K are of little or no use in assigning ultraviolet vapor spectra bands. Use has been made of only the ground-state frequencies of 336, 432, 614, 654, 793, 832, 920 and 1007 K, though a tentative assignment was made of a difference frequency using 1225 (9a). The use of 654 is somewhat doubtful, for the nearest ultraviolet band was at 661 and quite weak; however, good fits were obtained on three difference bands using 654 value.

The weak band at 1194 K to the red of the 0–0 is probably a ground-state frequency because of its occurrence in the infrared and Raman spectra, but no

Table 4. Infrared, Raman, and ultraviolet data on ground-state vibrations of chloropyrazine

Infrared band (K)	Estimated intensity	Raman line (K)	Estimated intensity	Ultraviolet band to red of 0–0	Estimated intensity
—	—	190	s	—	—
—	—	311	m	—	—
—	—	365	w	—	—
434	w	437	s	432	vw
452	w	—	—	—	—
478	m	480	w	477	vw
617	w	616	m	614	m
—	—	654	w	661	vvw
—	—	704	w	—	—
742	s	743	w	—	—
760	s	760	m	—	—
—	—	799	vw	793	vvw
828	w	—	—	832	vvw
845	s	843	w	—	—
—	—	911?	?	—	—
926	w	927	w	920?	vvw
954	w	951	w	—	—
—	—	992?	?	—	—
1013	s	1009	s	1007	vvw
1052	s	1046	s	—	—
1136	s	1135	m	—	—
—	—	1158	w	—	—
1179	m	1176	w	—	—
1192	m	1192?	?	1194	w
1198	w	—	—	—	—
1225	w	—	—	—	—
1260	w	—	—	—	—
1290	s	1287	w	—	—
1322	w	—	—	—	—
1338	w	—	—	—	—
1357	w	—	—	—	—
1390	s	1385	vw	—	—
1422	w	—	—	—	—
1462	s	1461?	?	—	—
1480	w	1482	vw	—	—
1520	s	1516	m	—	—
1561	m	1561	w	—	—
3060	s	—	—	—	—

mode could be assigned to it. It is likely a mode which has been greatly changed by the chlorine substitution.

Upper-state vibrations of chloropyrazine. By use of the ground-state frequencies, the more prominent bands to the short wavelength side of the 0–0 band, and the agreement with difference-band assignments, a set of but five reasonable upper-state frequencies were arrived at. Ground- and upper-state frequencies are compared in Tables 6 and 7.

VOL. 12 1958

Table 5. Bands and assignments for 2-chloropyrazine vapor

Band position (K)	Difference from 0–0 band (K)	Intensity (estimated)	Assignment
30,694	1374	vvw	
874	1194	w	0 − 1194?
941	1127	vvw	
31,061	1007	vvw	0 − 1007 (1)
100	968	vw	
148	920	vvw	0 − 920 (17a)
236	832	vvw	0 − 832 (10a)
275	793	vvw	0 − 793 (11)
407	661	vvw	0 − 654? (6b) Raman 654
454	614	m	0 − 614 (6a)
551	517	vw	0 + 490 − 1007 or 0 + 274 − 793
591	477	vw	
636	432	vw	0 − 432 (16b)
661	407	vw	0 + 244 − 654 or 0 + 599 − 1007?
732	336	m	0 − 336 (16a)
780	288	vw	
828	240	vw	0 + 274 − 614
856	212	w	
897	171	m	
906	162	w	0 + 490 − 654 or 0 + 274 − 432 (1-1 of 16b)
915	153	w	0 − 3 × 51
927	141	w	0 + 976 − 832
951	117	w	0 + 490 − 614
966	102	ms	0 − 2 × 51
32,017	51	m	0 + 599 − 654 (1-1 of 6b)
026	42	m	
059	9	m	
068	0	vvs	0–0
134	66	w	0 + 490 − 432?
142	74	m	
165	97	m	
182	114	w	0 + 490 + 274 − 654
191	123	m	
217	149	vw	0 + 976 − 832 or 0 + 336 + 490
252	184	vw	0 + 976 − 793
265	197	w	0 + 244 − 51?
304	236	w	
312	244	s	0 + 244 (16a′?)
324	256	m	0 + 599 + 274 − 614 (1-1 of 6a + 16b′?)
335	267	m	0 + 599 − 336
342	274	s	0 + 274 (16b′)
381	313	vw	0 + 976 − 654?
395	327	w	0 + 490 + 274 − 432 or 0 + 976 − 654?
420	352	vw	
429	361	w	0 + 976 − 614
444	376	w	0 + 1170 − 793
455	387	w	0 + 490 − 2 × 51?

Table 5 (*continued*)

Band position (K)	Difference from 0–0 band (K)	Intensity (estimated)	Assignment
32,466	398	w	
492	424	w	0 + 490 + 274 − 336
558	490	s	0 + 490 (11′?)
597	529	w	
639	571	w	0 + 976 + 599 − 1007?
667	599	s	0 + 599 (6a′)
680	613	m	0 + 1170 + 274 − 832
706	638	m	0 + 976 − 336
716	648	m	0 + 2 × 490 − 336 or 0 + 1170 + 274 − 793?
729	661	w	0 + 599 + 490 − 432
751	683	m	
771	703	m	
780	712	ms	
792	724	w	
811	743	w	0 + 1170 − 432
845	777	m	
864	796	ms	0 + 2 × 599 − 336
879	811	m	
909	841	w	0 + 244 + 599
934	866	m	0 + 1170 + 490 − 793
976	908	w	
33,008	940	w	0 + 1170 + 599 − 832
021	953	m	
044	976	ms	0 + 976 (1′)
092	1024	ms	
161	1093	m	0 + 599 + 490
238	1170	ms	0 + 1170 (9a′)
351	1283	w	
412	1344	w	
476	1408	w	0 + 244 + 1170
564	1496	w	0 + 1170 + 976 − 654
643	1575	w	0 + 976 + 599
791	1723	w	0 + 1170 + 2 × 274
945	1877	w	
34,032	1964	w	
089	2021	w	
181	2113	w	
333	2265	vw	0 + 1170 + 599 + 490
507	2439	vw	0 + 2 × 976 + 490
585	2517	vw	
903	2835	vw	0 + 2 × 1170 + 490?
35,131	3063	vw	

Only one or two multiples of upper-state frequencies could be found. Difference frequencies between upper- and lower-state were found for about twenty out of a possible forty-five combinations; only two of these were 1–1 transition of the same

VOL. 12 1958

Table 6. Comparison of modes and ground-state frequencies for pyrazine and chloropyrazine

Designation	Pyrazine mode	Chloro-pyrazine mode	Pyrazine freq.	Chloro-pyrazine freq.	Cl-found in
1	A_{1g}	A′	1015	1007	all
2	A_{1g}	A′	3055	3060	i.r.
6a	A_{1g}	A′	596	614	all
8a	A_{1g}	A′	1584	1561	i.r. and R
9a	A_{1g}	A′	1228	1225	i.r.
16a	A_{1u}	A′	362	336	u.v.
17a	A_{1u}	A′	914	920?	u.v.
10a	B_{2g}	A″	852	832	ir. and u.v.
12	B_{2u}	A′	1027	1049	i.r. and R
19a	B_{1u}	A″	1491	1481	i.r. and R
3	B_{1g}	A′	1117	1135?	i.r. and R
6b	B_{1g}	A′	641	654?	R and u.v.
8b	B_{1g}	A′	1523	1523	i.r. and R
11	B_{1u}	A″	805	793	u.v. and R
16b	B_{1u}	A″	417	432	all
4	B_{3g}	A″	755	760	i.r. and R
14	B_{3u}	A′	1345	1338?	i.r.
18b	B_{3u}	A′	1150	1158?	R
19b	B_{3u}	A′	1419	1422?	i.r.

Table 7. Comparison of ground- and upper-state frequencies for chloropyrazine

Designation	Ground-state	Upper-state	Difference	Observed difference	Remarks
1	1007	976	31	—	Too near 0–0 to be resolved
6a	614	599	15	—	Too near 0–0 to be resolved
9a	1225 i.r.	1170	55	51	
11	793	490	304	—	
16b	432	274	158	162	

mode. Persistent difference values appear to be lacking, although a few assignments of doubtful status could be made with the fifty-one differences. This is probably characteristic of a molecule of low symmetry.

Acknowledgements—The assistance of Mr. J. Whalen in obtaining the infrared spectra and of Mr. W. L. Dutton in photographing certain of the ultraviolet vapor spectra is gratefully acknowledged. Dr. R. C. Lord very kindly permitted the examination and use of the Raman spectral data on pyrazine [11] prior to the publication of these data, and Dr. R. F. Stamm very kindly furnished the Raman spectral data on chloropyrazine. The many discussions with Dr. F. Halverson were especially helpful, as were those with Dr. M. Kasha and Dr. L. Goodman; the singlet–triplet bands of pyrazine were originally observed and their assignment suggested by Dr. Kasha [9].

References

[1] Halverson F. and Hirt R. C. *J. Chem. Phys.* 1951 **19** 711.
[2] Halverson F. and Hirt R. C. *J. Chem. Phys.* 1949 **17** 1165.
[3] Uber F. M. *J. Chem. Phys.* 1941 **9** 777.
[4] Fax B. J. *Near Ultraviolet Absorption Spectra of Pyridine, Pyridine-d_5, and the Diazines under High Dispersion.* Ph.D. Thesis, Massachusetts Institute of Technology, 1950.
[5] Lord R. C., Marston A. L. and Miller F. A. *Spectrochim. Acta* 1957 **9** 113.
[6] Ito M., Shimada R., Kuraishi T. and Mizushima W. *J. Chem. Phys.* 1956 **25** 597.
[7] Ito M., Shimada R., Kuraishi T. and Mizushima W. *J. Chem. Phys.* 1957 **26** 1508.
[8] Stamm R. F. *Industr. Engng. Chem. (Anal.)* 1945 **17** 318.
[9] Goodman L. and Kasham M. *J. Mol. Spectrosc.* In press.
[10] Klevens H. B. and Platt J. R. *Survey of Vacuum Ultraviolet Spectra* Tech. Rept. ONR Contract N60RI–20, Task Order IX, Project NR 019 101, 1954.
[11] Lord R. C. Private communication Sept. 2, 1954.

VOL.
12
1958

Spectrochimica Acta, 1958, Vol. 12, pp. 127 to 138. Pergamon Press Ltd., London

Ultraviolet absorption spectra of derivatives of symmetric triazine—II

Oxo-triazines and their acyclic analogs

R. C. Hirt and R. G. Schmitt
Research Division, American Cyanamid Company, Stamford, Connecticut, U.S.A.

(*Received* 16 *December* 1957)

Abstract—The ultraviolet absorption spectra of the oxygen-containing symmetric triazines, their ions, and their acyclic analogs are correlated with their molecular structures in terms of conjugated double bonds between carbon and nitrogen atoms of the heterocyclic ring and exocyclic nitrogen and oxygen atoms. The probable structure of the positive ion of melamine (2:4:6-triamino-s-triazine) is deduced from these correlations. Spectrophotometrically determined ionization constants are reported.

Introduction

The ultraviolet absorption spectra of a number of mono-, di- and triamino derivatives of symmetric triazine were presented and discussed in Part I of this series [1]. This paper presents the spectra, structures and ionization constants of the oxygen-containing triazine derivatives ammeline, ammelide and cyanuric acid, and their acyclic analogs biguanide, guanylurea and biuret. Correlations between the observed spectra and the structures of the neutral and ionic forms of these molecules are discussed in detail. The preferred structures of these molecules are here presented:

Preferred structures of neutral molecules:

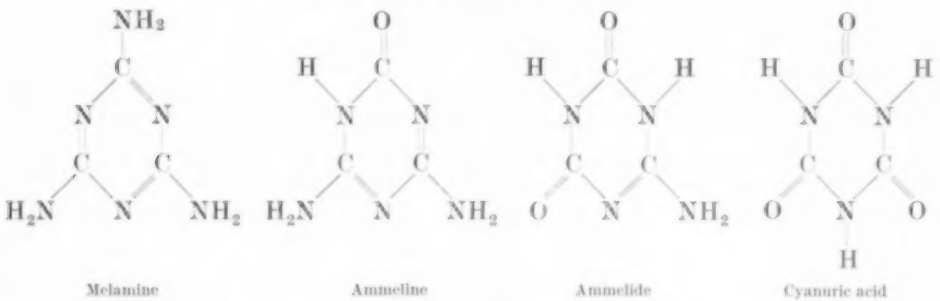

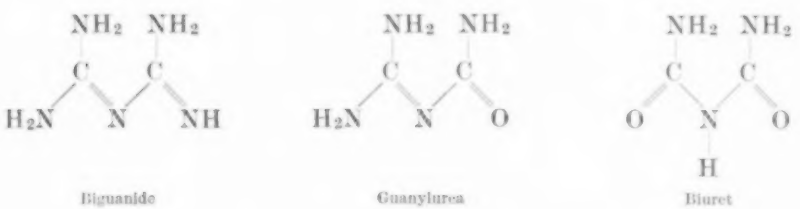

Experimental procedure

The data presented were obtained on either a Cary Model 11, or a Beckman Model DU spectrophotometer. Fused quartz cells of 1, 5, 10, 20, 50 and 100 mm light path length were used, as well as micrometer Baly cells which were adjustable from 5·00 to 0·01 mm in length [2]. Non-absorbing buffered systems, 0·1 N HCl and 0·1 N NaOH, were used as solvents. Dissociation constants were obtained spectroscopically by means of the "Spectro-titrimeter" [3].

The data are presented as plots of the log of the molar absorptivity (molar extinction) versus wave-number (kaysers, K or cm^{-1}). Beer's law was used in the form $A = (\epsilon/M) \cdot b \cdot c$, where A is the absorbance (optical density), ϵ is the molar absorptivity (molar extinction), M is the formula weight, b is the cell length in millimeters and c is the concentration in grams per 100 ml. All of the compounds mentioned were prepared by various members of these laboratories and recrystallized or resublimed to obtain a high degree of purity. In most cases, samples were identical to those in previous publications [1, 4].

Results

The observed bands of the compounds studied are summarized in Table 1. The pH range over which these positions and intensities apply and their dissociation constants are also indicated. The spectra of these compounds are shown in Figs. 1–7.

VOL. 12 1958

Discussion

It has been established that melamine (A), in the solid state and in neutral solution, exists in the symmetrical, triamino form [1, 5, 6]. A complete discussion of the ultraviolet spectrum of melamine in the un-ionized state has been given by Hirt and Salley [1]. These authors assigned the weak transition occurring at 42,500 K or 2350 Å to a symmetry-forbidden π-electron transition. Although the spectrum of the melamine ion (Fig. 1) has been reported in connection with determination of its ionization constant [7, 8, 9] and with analytical applications [10], no attempt was made to assign a structure to the ion. Melamine in acidic solution may be hydrolyzed progressively by the loss of one, two and three amino groups to ammeline, ammelide and cyanuric acid respectively. These related compounds do show similarities and progressions in their ultraviolet spectra [11] (see Figs. 2, 3, 4) which may be utilized in determining the structure of the melamine ion.

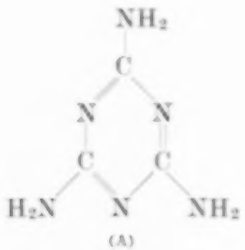

(A)

Table 1. Spectral data and ionization constants of compounds examined

Compound	pK_a	Form	Range of pH values	Maximum (Å)	Maximum (K)	Intensity (ϵ)
Melamine		2nd positive ion	below −1	2360	42,400	20,650*
	~0					
		1st positive ion	1–4	2350	42,550	10,200
	5·1					
		neutral molecule	6–13	2350-S	42,550-S	2,820
Ammeline		1st positive ion	1–3	2300	43,480	20,300
	4·5					
		neutral molecule	6–8	2300	43,480	7,650
	9·4					
		1st negative ion	11–13	2300-S	43,480-S	3,580
Ammelide		1st positive ion	below 0	no band	no band	
	1·8					
		neutral molecule	3·5–5·5	2220	45,050	14,080
	6·9					
		1st negative ion	8·5–13	2260	44,250	9,730
	~13·5					
		2nd negative ion	above 14	no data	no data	no data
Cyanuric acid		neutral molecule	1–4·5	no band	no band	
	6·5					
		1st negative ion	8–9	2140	46,730	10,170
	10·6					
		2nd negative ion	12–14	2200	45,050	6,360
Biuret		neutral molecule	1–11	no band	no band	
	13·2					
		1st negative ion	above 14·5	2160	46,300	5,670†
Guanylurea		1st positive ion	1–6	no band	no band	
	8·0					
		neutral molecule	10–13	2180	45,870	19,380
Biguanide		2nd positive ion	below 1·5	no band	no band	
	3·2					
		1st positive ion	5–10	2300	43,480	12,360
	13·3					
		neutral molecule	above 14·5	2300	43,480	8,900E

S = shoulder, E = estimated
* Value in conc. HCl
† Value at pH 13

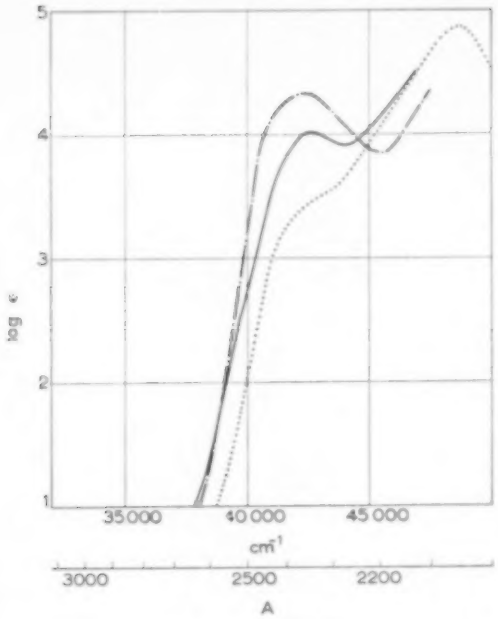

Fig. 1. Ultraviolet spectra of melamine, in water (pH > 6) ....., in 0·1 N HCl ———, in 12 N HCl · — · — · — ·.

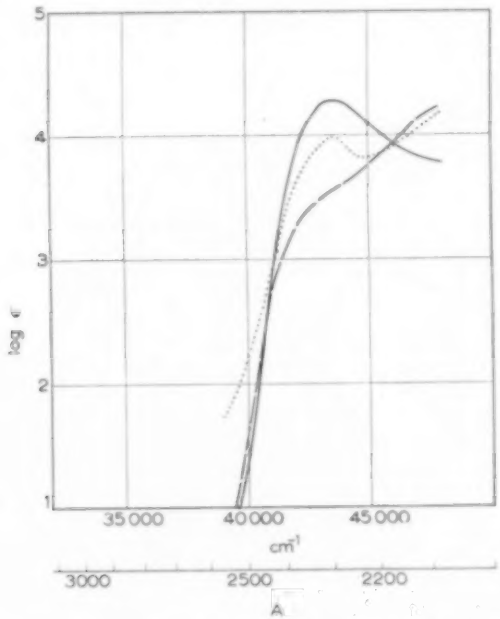

Fig. 2. Ultraviolet spectra of ammeline, in 0·1 N NaOH – – – –, in water (pH = 7) . . . ., in 0·1 N HCl ———.

VOL. 12 1958

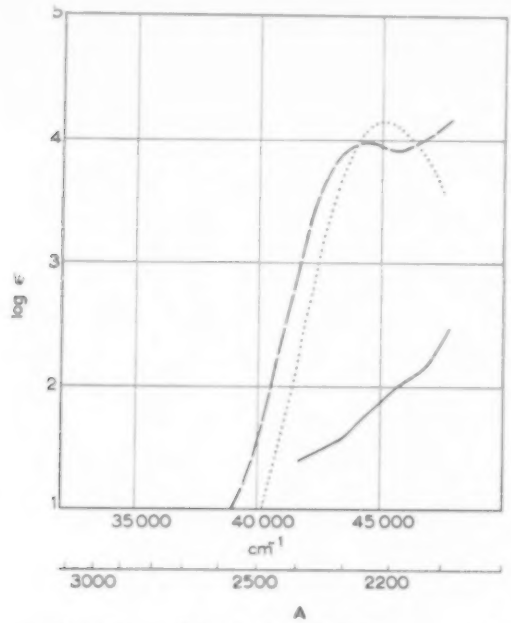

Fig. 3. Ultraviolet spectra of ammelide, in 0·1 N NaOH – – – –, in buffer (pH = 4·7) . . . ., in 1 N HCl ———.

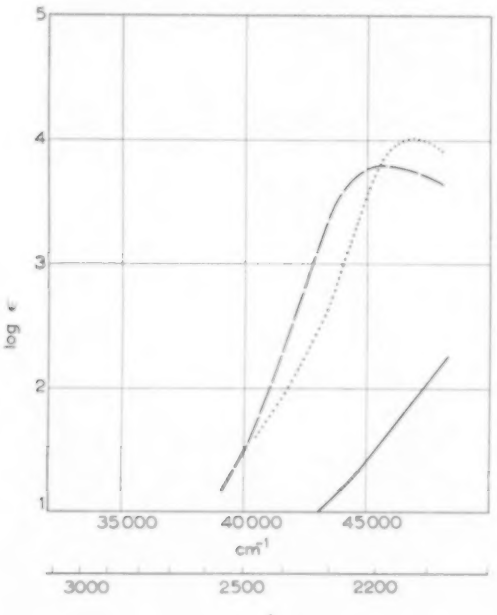

Fig. 4. Ultraviolet spectra of cyanuric acid, in NaOH (pH = 12) – – – –, in buffer (pH = 9) . . . ., in 0·1 N HCl ———.

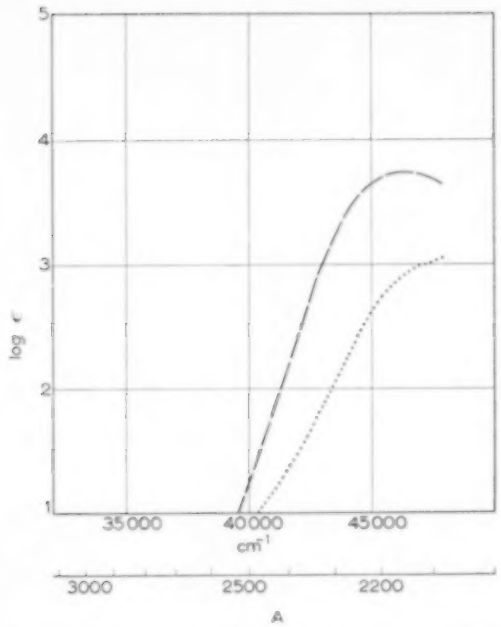

Fig. 5. Ultraviolet spectra of biuret, in 0·1 N NaOH – – – –, in buffer (pH = 8) . . . . .

VOL.
12
1958

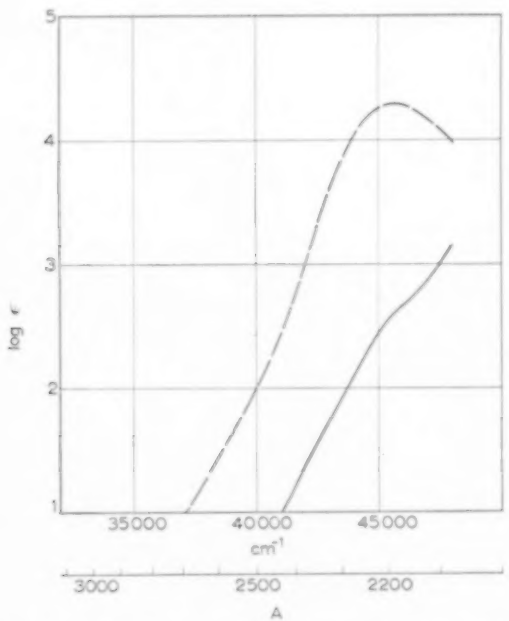

Fig. 6. Ultraviolet spectra of guanylurea, in 0·1 N NaOH – – – –, in 0·1 N HCl ———.

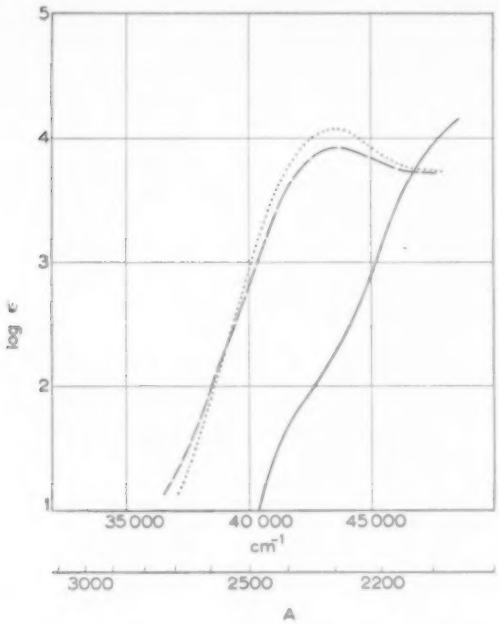

Fig. 7. Ultraviolet spectra of biguanide, in 1 N NaOH – – – –, in buffer (pH = 9) . . . ., in 0·1 N HCl ———.

There are several possible forms in which cyanuric acid can exist in the solid or un-ionized form in solution; the trihydroxy form (B), the tricarbonyl form (C), and combinations of these two (D, E, F).

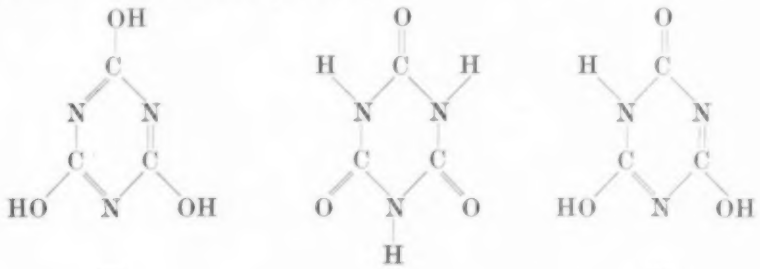

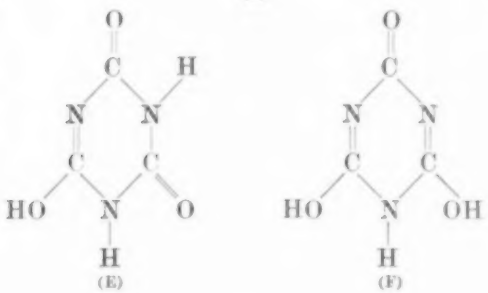

Hughes [5] presented evidence, based largely on the calculated and observed heats of formation, for the tricarbonyl form of cyanuric acid. Klotz [8] described the spectra of cyanuric acid at three pH values, and attributed the large change in intensity of absorption with pH to an ionized form having a double bond within the ring conjugated with the carbonyl group outside the ring. Thus the tricarbonyl form, which has no conjugation of the double bonds, displays weak absorption in the ultraviolet, while the anion with two conjugated double bonds has moderately strong absorption near 45,500 K (2200 Å).

The ultraviolet absorption spectrum of cyanuric acid and its pH dependence have been studied in these laboratories with samples of very high purity. Three distinct forms for cyanuric acid were observed in the pH range of from 1 to 14, the spectra of which are shown in Fig. 4. Values for pK_a of 6·5 and 10·6 were determined. The spectrum at pH 1 (0·1 N HCl) shows very weak absorption, which is in agreement with Klotz, and must be attributed to the tricarbonyl form of cyanuric acid (C) as it is the only possible nonconjugated structure. It follows then that the spectrum at pH 9 is due to the singly-ionized form and has the structure (G) and the curve at pH 12 is the doubly-ionized form, structure (H).

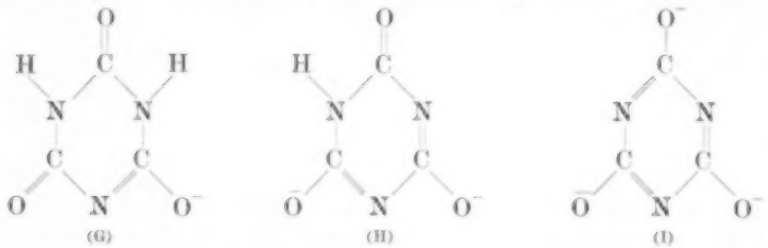

(G) (H) (I)

It is interesting to note that the doubly-ionized form of cyanuric acid absorbs at somewhat longer wave length (max. at 45,500 K) than the singly-ionized form (max. at 46,700 K or 2140 Å). The longer conjugated system in structure (H) serves as a satisfactory explanation to these observations and lends support to the conclusion that cyanuric acid exists as the tricarbonyl form in the neutral state. A third ionic form (I) may exist in the solid salt "trisodium cyanurate"; it is not observable spectroscopically in solution. It should be noted that the infrared spectrum of solid cyanuric acid shows the presence of carbonyl groups (band at 1715 K), although no statement may be made concerning the number of such groups present. This gives further confirmation of the carbonyl structure of cyanuric acid.

It seems reasonable to assume that ammeline and ammelide should have molecular structures which are intermediate between those of melamine and cyanuric acid; that is, with one and two carbonyl groups respectively [4]. The infrared spectra of solid ammeline and ammelide showed the presence of carbonyl groups. It is also interesting to note that the calculation of the heat of formation from Pauling's data [12] shows that the carbonyl form has 10 kcal/mole more than the hydroxy form. This fact was noted by Klotz in his discussion of cyanuric acid [8], and appears implicitly in the reasoning on cyanuric acid carried out by Hughes [5].

VOL. 12 1958

To illustrate the structure-spectra correlations that can be made for the neutral and ionic forms of melamine, ammeline, ammelide and cyanuric acid, Fig. 8 was prepared in which the various structures were divided into groups corresponding to the shape of their ultraviolet absorption curve. The structures for ammeline, ammelide and the ionic form of melamine are deduced from the now proven structures of cyanuric acid and its ions and the neutral form of melamine by comparing their observed spectra. There are four distinct types of spectra observed which we call "shoulder", "resolved", "peak" and "weak", corresponding to three, two, one and no double bonds in the ring. Ammeline

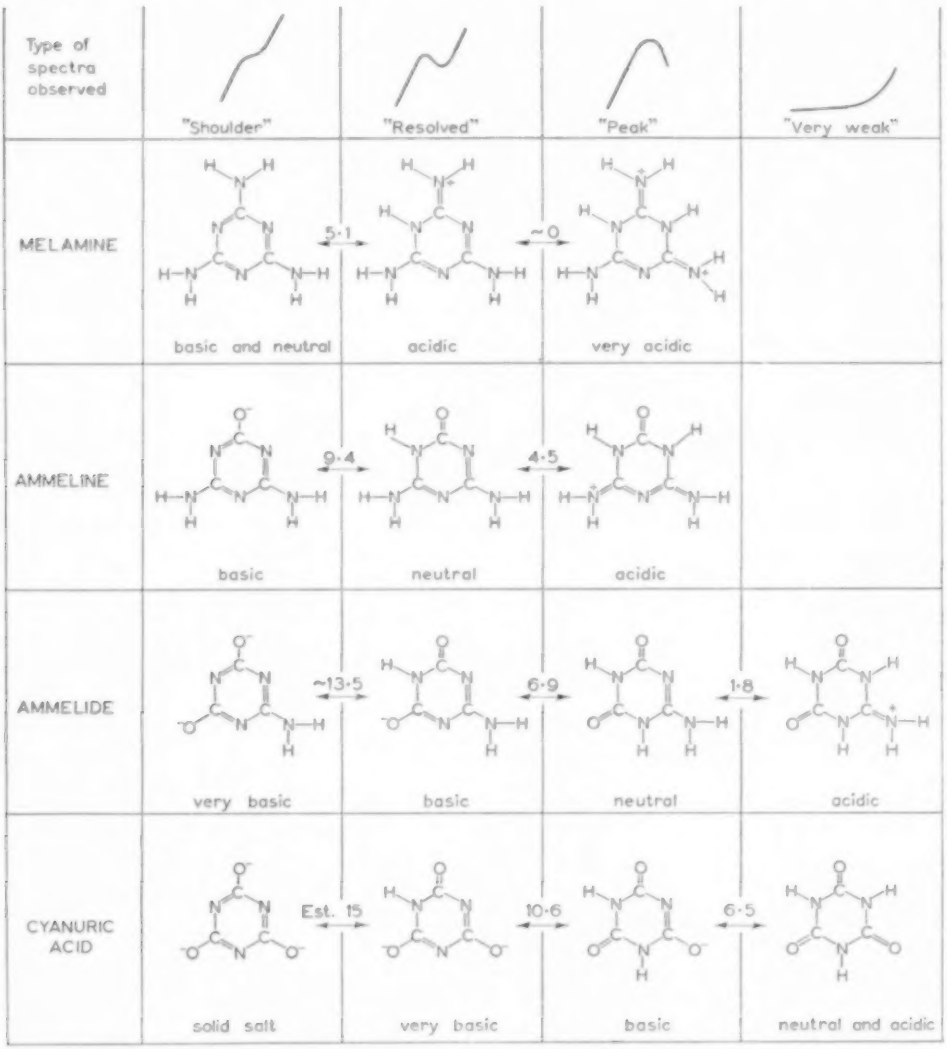

Fig. 8. Correlation between the ultraviolet absorption spectra and the molecular structures of melamine, ammeline, ammelide and cyanuric acid.

displays three forms, a neutral molecule and both a positive and a negative ion:

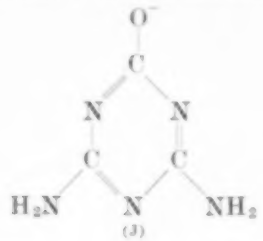

(J)

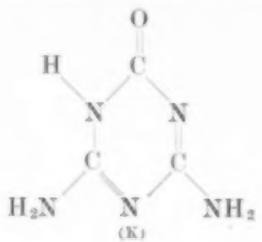

(K)

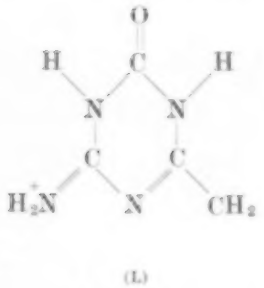

(L)

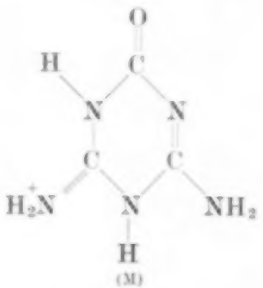

(M)

There are two possible structures for the positive ion of ammeline, (L) and (M). By comparing the wavelength maxima of ammeline at pH 1 with that of its acyclic analogs, guanylurea and biguanide (see Table 1), it becomes apparent that structure (L) with its C=N—C=N conjugated system is the more likely choice. Both the positive ion of ammeline and the positive ion of biguanide have their maximum absorption at identical energies (43,500 K or 2300 Å), whereas the neutral form of guanylurea (Y) with its C=N—C=O conjugated system absorbs at 2180 Å. The effect of the amino substituents on these three molecules should be about equal.

Ammelide was reported [11] to have a neutral form (P) and a singly-ionized negative form (O); recent work with strong NaOH and HCl solutions have shown the existence of a positive ion (Q) and have indicated the presence of a double-ionized negative form (N):

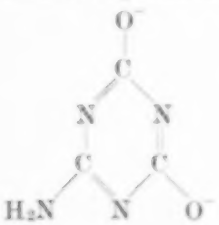

(S)

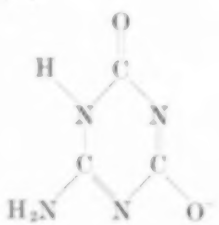

(O)

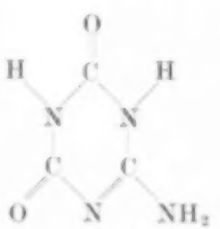

(P)

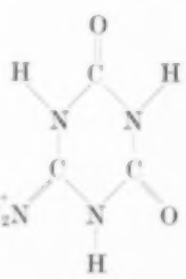

(Q)

The spectra of melamine cation (pH 1), of un-ionized ammeline (pH 7), of ammelide anion (pH 11) and the cyanuric acid double-negative ion (pH 12) are quite similar in shape and intensity. These data suggest that the positive ion

VOL. 12 1958

of melamine should be represented by an *iso*melamine type of structure (R) and not as the normal form of melamine (S).

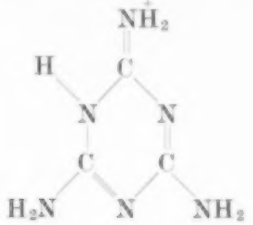

(R)

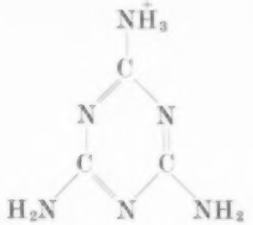

(S)

The existence of the nonconjugated forms of ammelide (Q) and of cyanuric acid (C), which did not display bands in the ultraviolet region above 2000 Å, suggested the examination of compounds having analogous structures. These were guanylurea to correspond to ammelide, and biuret to correspond to cyanuric acid in the arrangement of C, N and O atoms and their connecting bonds.

Biuret, though commonly written in a linear form with right-angle branches,

as: $H_2N—C—NH—C—NH_2$, may more realistically be written with 120° angles, as:

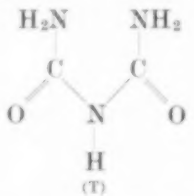

(T)

The resemblance to cyanuric acid is apparent and no bands are found. Upon ionization in basic solution, a proton is lost, and an absorption band appears at 46,300 K or 2160 Å as in Fig. 5. The structure should then be written, in a form analogous to singly ionized cyanuric acid, as:

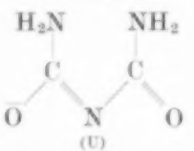

(U)

Guanylurea, which shows no bands in acid solution, must be written in a non-conjugated form, and be analogous to ammelide. If the conventional structure (V) is written for guanylurea, the ion, showing absorption at 45,870 K or 2180 Å, as in Fig. 6, would have to be written as (W):

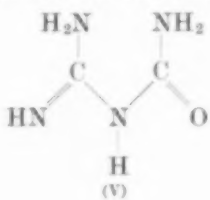

(V)

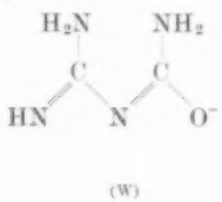

(W)

However, the presence of the strongly basic guanyl group would favor the acceptance of a proton from the water rather than the delivery of one; the structures would more likely be given as:

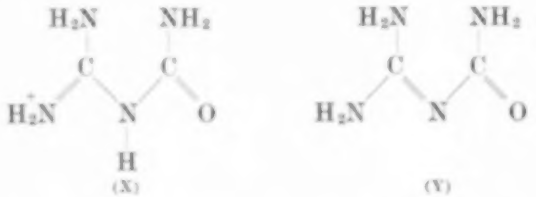

(X) (Y)

The existence in the neutral molecule of the conjugated C=N—C=O with a band at 45,800 K or 2180 Å closely corresponds to the same system in ammelide with a band at 45,000 K or 2220 Å (structure (O)); a C=N—C=N conjugated system would absorb at lower energy as in ammeline positive ion (L) with its band at 43,500 K or 2300 Å. To check this, biguanide, which can have only a C=N—C=N conjugation, was examined and found to absorb at 43,500 K, as in Fig. 7. Neutral biguanide and its positive ions are written as:

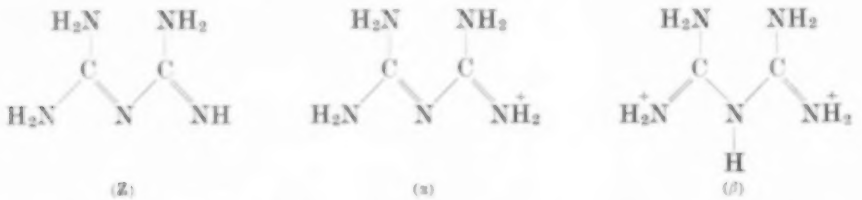

(Z) (α) (β)

It is interesting to note that the addition of a single proton to biguanide does not shift its absorption band position, but only decreases its intensity; the addition of a second proton makes a conjugated resonating system impossible, and the absorption band disappears into the vacuum ultraviolet region.

References

[1] Hirt R. C. and Salley D. J., *J. Chem. Phys.* 1953 **21** 1181.
[2] Hirt R. C. and King F. T., *Analyt. Chem.* 1952 **24** 1545.
[3] King F. T. and Hirt R. C., *Appl. Spectrosc.* 1953 **7** 164.
[4] Hirt R. C., *Appl. Spectrosc.* 1952 **6** 15.
[5] Hughes E. H., *J. Amer. Chem. Soc.* 1941 **63** 1737.
[6] Dewar M. J. S. and Paoloni L., *Trans. Faraday Soc.* 1957 **53** 261.
[7] Dixon J. K., Woodberry N. H. and Costa G. W., *J. Amer. Chem. Soc.* 1947 **69** 599.
[8] Klotz I. M. and Askounis T., *J. Amer. Chem. Soc.* 1947 **69** 801.
[9] Costa G. W., Hirt R. C. and Salley D. J., *J. Chem. Phys.* 1950 **18** 434.
[10] Hirt R. C., King F. T. and Schmitt R. G., *Analyt. Chem.* 1954 **26** 1273.
[11] Hirt R. C., Talk before *Symposium on Molecular Structure and Spectroscopy.* The Ohio State University, Columbus, Ohio, June 1950.
[12] Pauling L., *Nature of the Chemical Bond* pp. 53, 131. Columbia Univ. Press 1940.

VOL. 12 1958

Spectrochimica Acta, 1958, Vol. 12, pp. 139 to 142. Pergamon Press Ltd., London

Infrared spectra of fluoro-*cyclo*olefines

J. Burdon and D. H. Whiffen
Chemistry Department, The University, Birmingham 15

(*Received 5 February* 1958)

Abstract—The —C=C— stretching frequencies of several different types of highly fluorinated six-membered ring olefines have been measured and it has been shown that, in the vapour phase, those compounds with two fluorine atoms on the double bond absorb near 1749 cm^{-1} and those with one hydrogen and one fluorine atom, near 1719 cm^{-1}. The frequencies of related *cyclo*hexadienes are also discussed.

In this department many highly fluorinated *cyclo*hexenes and *cyclo*hexadienes have been prepared [1,2,3] by the alkaline dehydrofluorination of the polyfluoro-*cyclo*hexanes* obtained from the cobaltic fluoride fluorination of benzene. In previous reports of this work the —C=C— stretching frequencies of several olefines of this nature have been quoted [2,3,4], and the C—H stretching frequencies discussed [5]. Several correlations have now been found between type of double bond and infrared absorption frequency and a summary is reported in the tables. These correlations should be useful in the structural determination of highly fluorinated olefines since the ranges for each type of double bond do not overlap.

Highly fluorinated *cyclo*hexenes (Table 1) possessing a double bond of the type —CF=CF— and perfluoro*cyclo*pentene all absorbed strongly in the range 1745–1755 cm^{-1} (vapour phase spectra). This compares with the open chain C—CF=CF—C absorption range of 1712–1733 cm^{-1} for which, however, only two specific compounds have been reported [6–9], although Haszeldine [10] gives 1730 cm^{-1} for compounds of the type R_f·CF=CF·R (R_f is any perfluoroalkyl group, R any alkyl group).

Highly fluorinated *cyclo*hexenes with a —CF=CH— bond absorbed strongly in the range 1713–1722 cm^{-1} (vapour phase). No spectra of straight chain olefines of this type have been recorded.

The spectra of two highly fluorinated *cyclo*hexenes with —CH=CH— bonds have been measured but the absorption bands in the expected region were weak, in contrast to those reported above. There were, however in both cases, weak bands near 1688 cm^{-1}, but, from the spectrum, it is not difficult to mistake a compound of this nature for a saturated compound.

The data for the *cyclo*hexa-1:4-dienes are shown in Table 2 and two bands appear in each case. The sum of the two frequencies is about the same as, or a little higher than, the sum of the individual frequencies which the two double bonds

* The nomenclature used in this paper for the *cyclo*hexene and *cyclo*hexadiene derivatives follows that used for the inositols [S. J. Angyal and C. G. Macdonald, *J. Chem. Soc.* 1952 686; D. H. Whiffen, *Chem. and Ind.* 1956 964] as extended in the perfluoro*cyclo*hexane field [3].

Table 1. *cyclo*Hexenes

	Absorption frequency (cm^{-1})
Type —CF=CF—	
*cyclo*Hexene	
Decafluoro-[1]	1746 s
3H-Nonafluoro-[2]	1752 s
4H-Nonafluoro-[2]	1747 s
3H/4H-Octafluoro-[3]	1755 s
3H:4H/-Octafluoro-[13]	1746 s
4H/5H-Octafluoro-[3]	1755 s
4H:5H/-Octafluoro-[13]	1745 s
Mean	1749
Compare also:	
Octafluoro*cyclo*pentene [6]	1754
Hexafluoro*cyclo*butene [11]	1799
Octafluorobut-2-ene [6–9]	1733
Dodecafluorohex-3-ene [9]	1712
Type —CH=CF—	
*cyclo*Hexene	
1H-Nonafluoro-[2,4]	1714 s
1H,4H-Octafluoro-[13]	1713 s
1H,5H-Octafluoro-[13]	1717 s
1H,4H/5H-Heptafluoro-[13]	1722 s
1H,4H:5H/-Heptafluoro-[13]	1720 s
Mean	1719
Compare also:	
1H-Pentafluoro*cyclo*butene [13]	1685 s
Type —CH=CH—	
*cyclo*Hexene	
1H:2H-Octafluoro-[13]	1695 vw
1H:2H,4H-Heptafluoro-[13]	1682 w
Compare also:	
cis.1:2-bis(trifluoromethyl)-ethylene [12]	1681
1H:2H-Tetrafluoro*cyclo*butene [13]	1560 vvw

would have if they were in separate molecules and this criterion is some guide to the identification of unknown structures. The increase occurs mostly in the higher frequency as is to be expected if the two vibrational levels repel each other. The existence of two frequencies in the octafluoro*cyclo*hexa-1:4-diene and its 1H:4H-derivative suggests that these molecules are not centrosymmetric since if they were the selection rules would forbid the appearance of one of the two frequencies in the infrared. The higher frequency band is, however, much the weaker in these cases. Models suggest that the boat-shaped structures are less

VOL. 12 1958

Table 2. *cyclo*Hexadienes

	Absorption frequencies (cm^{-1})			Sum	Sum of isolated bond frequencies
*cyclo*Hexa-1:4-diene					
Octafluoro-[2]	1777 w		1741 s	3518	3498 = 1749 + 1749
1H-Heptafluoro-[3]	1771 m		1721 s	3492	3468 = 1749 + 1719
1H:2H-Hexafluoro-[13]	1770 s		1688 m	3458	3437 = 1749 + 1688
1H:4H-Hexafluoro-[13]	1737 m		1707 s	3444	3438 = 1719 + 1719
1H:5H-Hexafluoro-[13]	1744 s		1711 m	3455	3438 = 1719 + 1719
*cyclo*Hexa-1:3-diene					
Octafluoro-[2]	1746 s		1712 s	3458	3498 = 1749 + 1749
1H-Heptafluoro-[3,13]	1740 s		1676 s	3416	3468 = 1749 + 1719
2H-Heptafluoro-[3,13]	1740 s		1684 m	3424	3468 = 1749 + 1719
1H:2H-Hexafluoro-[13]	1734 s	(1698 m)	1635 s	3369	3438 = 1749 + 1688
Compare also:					
Hexafluorobuta-1:3-diene [7]	1770				

strained than the centrosymmetric flat rings. For the 1:3-dienes, also in Table 2, two bands again appear and the influence of the conjugation reduces the sum of the frequencies by about 50 cm^{-1} from the sum of the frequencies of the individual double bonds; it is the lower frequency in particular which is reduced. The ranges for the 1:3- and 1:4-dienes overlap each other, but the 1:3-dienes are readily distinguished by their strong ultraviolet absorption near 255 mμ [2,3].

Experimental

Vapour phase spectra. These were measured on either a Grubb-Parsons single-beam infrared spectrometer or a Perkin-Elmer double-beam infrared spectrometer with NaCl prisms in an 11 cm cell at vapour pressures between 10–40 mm. Duplicate spectra on these instruments were identical in all cases tested and the frequencies quoted are believed correct to ± 6 cm^{-1}. Accurate molecular extinction coefficients have not been obtained but approximate values for all frequencies measured are indicated by quoting bands of molecular extinction coefficient thus: $\varepsilon > 300$, as vvs; 300–100, vs; 100–30, s; 30–10, m; 10–3, w; 3–1 vw; < 1 vvw.

Acknowledgements—We wish to thank Professor M. Stacey, F.R.S. for his interest in this work and Dr. J. C. Tatlow for many helpful discussions. We are grateful to their colleagues, Drs. D. E. M. Evans, J. A. Godsell and R. Stephens, and Messrs. G. Fuller, E. Nield and E. H. Wiseman for providing the compounds. We also thank Miss H. Rogers for her technical assistance in making the measurements.

References

[1] Barbour A. K., Mackenzie H. D., Stacey M. and Tatlow J. C., *J. Appl. Chem.* 1954 **4**, 347.

[2] Evans D. E. M. and Tatlow J. C., *J. Chem. Soc.* 1954 3779; 1955 1184; Smith R. P. and Tatlow J. C., *J. Chem. Soc.* 1957 2505; Stephens R. and Tatlow J. C., *Chem. & Ind. (Rev.)* 1957 821.

[3] Evans D. E. M., Godsell J. A., Stephens R., Tatlow J. C. and Wiseman E. H., *Tetrahedron* 1958 **2,** 183; Godsell J. A., Stacey M. and Tatlow J. C. *Tetrahedron* 1958 **2,** 193.
[4] Roylance J., Tatlow J. C. and Worthington R. E., *J. Chem. Soc.* 1954 4426.
[5] Steele D. and Whiffen D. H., *Tetrahedron* 1958 **3,** 181.
[6] Henne A. L. and Latif K. A., *J. Amer. Chem, Soc.* 1954 610.
[7] Haszeldine R. N., *J. Chem. Soc.* 1952 4423.
[8] Haszeldine R. N. and Osborne J. E., *J. Chem. Soc.* 1956 61; Brice T. J., LaZerte J. D., Hals L. J. and Pearlson W. H., *J. Amer. Chem. Soc.* 1953 **75,** 2698.
[9] Haszeldine R. N. and Steele B. R., *J. Chem. Soc.* 1953 1592.
[10] Haszeldine R. N. *Nature, Lond.* 1951 **168,** 1028.
[11] Nielsen J. R., El-Sabban M. Z. and Alpert M., *J. Chem. Phys.* 1955 **23,** 324.
[12] Haszeldine R. N., *J. Chem. Soc.* 1952 2504; Henne A. L. and Finnegan W. G., *J. Amer. Chem. Soc.* 1949 **71,** 298.
[13] Tatlow J. C. *et al.* To be published.

VOL.
12
1958

Spectrochimica Acta, 1958, Vol. 12, pp. 143 to 146. Pergamon Press Ltd., London

Infrared spectrum of sulfuryl bromofluoride

T. T. Crow and R. T. Lagemann
Department of Physics and Astronomy, Vanderbilt University,
Nashville, Tennessee, U.S.A.

(*Received* 20 *August* 1957)

Abstract—The infrared absorption spectrum of gaseous SO_2BrF has been observed using a prism spectrometer equipped with NaCl, KBr and CsBr prisms. Of the nine fundamental vibrations eight have been observed with reasonable certainty while the remaining fundamental has possibly been observed. Several of the proposed fundamentals could not be assigned to particular modes of vibration with complete assurance since the necessary Raman data were not available.

Introduction

The infrared spectrum of sulfuryl fluoride, SO_2F_2, has been studied by Perkins and Wilson [1], and Bender and Wood [2] have studied its Raman spectrum. The Raman spectrum of sulfuryl chloride, SO_2Cl_2, has been examined by several investigators [3-5], while Martz and Lagemann [6] have obtained infrared data on this compound from 400 cm^{-1} to 5000 cm^{-1}. These appear to be the only previous infrared studies of the halogen-containing sulfuryl compounds. The present report gives the results of a study of the infrared spectrum of a similar compound, SO_2BrF, and interprets the spectrum on the basis of C_s symmetry.

The sample of SO_2BrF was prepared in this laboratory using the method of Kwasnik. Jonas [7] has described this procedure and, in addition, has given many of the physical and chemical properties of the compound. The SO_2BrF was prepared by the following chemical reaction:

$$Br_2 + 3SO_2 + BrF_3 \rightarrow 3SO_2BrF$$

Since the SO_2BrF was extremely water-reactive, it was necessary that the compound be prepared in an evacuated system. Copper tubing and monel valves were used in the construction of the system while the reaction vessel was a small steel pressure cylinder. The components were mixed, and the reaction vessel was allowed to stand in ice water for 48 hr. The product contained as impurities SO_2, SOF_2, SO_2F_2, and Br_2. By several simple distillations, using traps of fluorothene (for visibility), all impurities except bromine were essentially removed. A large part of the excess bromine was removed by agitating the remaining sample with mercury for several hours.

The infrared spectrum of the gas was observed between 2 and 25 μ using 10 cm long, Pyrex absorption cells and a model 21, Perkin-Elmer, double-beam spectrometer equipped with NaCl and KBr prisms. In the CsBr region from 15 to 38 μ, a 10 cm, brass absorption cell and polyethylene windows were used.

The observed spectrum is presented in Fig. 1 while the locations of the absorption maxima, their proposed assignment and type (for the fundamentals) are given in Table 1.

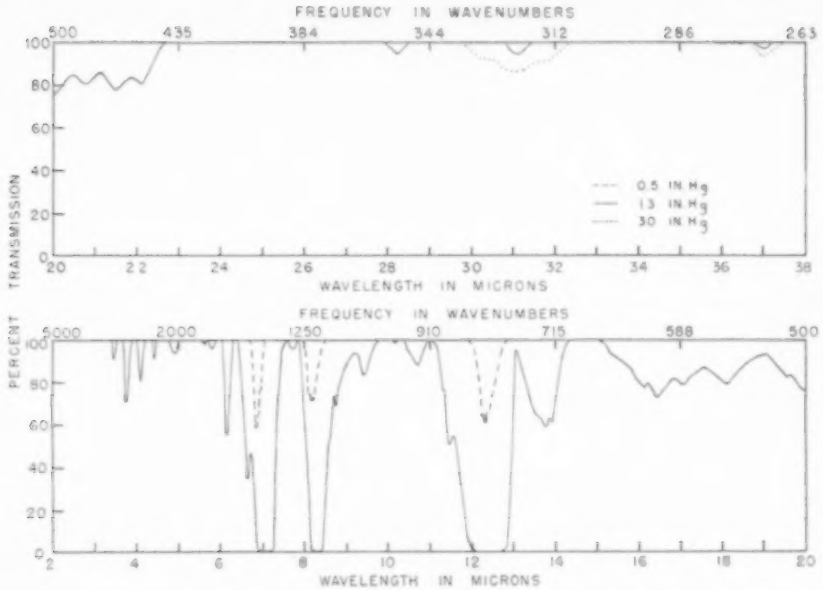

Fig. 1. Infrared spectrum of sulfuryl bromofluoride.

VOL. 12 1958

Interpretation

On the assumption of C_s symmetry for the molecule, the sulfur and oxygen atoms form one plane while the sulfur and halogen atoms form another at right angles to the first. Of the fundamental vibrations six (A') are symmetric with respect to the plane of symmetry (formed by the sulfur–halogen group) and three (A'') are asymmetric with respect to this plane. Of these fundamentals all are infrared active and all combinations and overtones are allowed.

Fig. 2. Regularities in the fundamental frequencies of SO_2F_2, SO_2BrF and SO_2Cl_2.

The band at 1460 cm^{-1} is assigned to the SO_2 asymmetrical stretch while the similar vibration occurs at 1502 cm^{-1} in SO_2F_2 [1], 1434 cm^{-1} in SO_2Cl_2 [5], and 1361 cm^{-1} in SO_2 [8]. The SO_2 symmetrical stretch is found at 1228 cm^{-1} (1269 cm^{-1} in SO_2F_2, 1205 cm^{-1} in SO_2Cl_2, and 1151 cm^{-1} in SO_2), while the SO_2 bend occurs at approximately half the stretching frequency, 608 cm^{-1} (586 cm^{-1} in SO_2Cl_2 and 524 cm^{-1} in SO_2). In SO_2F_2 the SF_2 asymmetrical stretch is assigned at 885 cm^{-1} and the SF_2 symmetrical stretch is assigned at 848 cm^{-1}. However, in SO_2Cl_2 the SCl_2 symmetrical stretch is assigned at 408 cm^{-1} and the SCl_2 asymmetrical stretch is assigned at 388 cm^{-1}. Since no other data are available on

Table 1. Absorption frequencies of SO_2BrF

Frequency (cm^{-1})	Intensity	Assignment
2890	vvw	$2 \times 1460 = 2920$
2650	vw	$1228 + 1460 = 2688$
2440	vvw	$2 \times 1228 = 2456$
2265	vvw	$1460 + 814 = 2274$
2035	vvw	$1228 + 814 = 2042$
1763	vvw	$1460 + 320 = 1780$
1713	vvw	$1228 + 497 = 1725$
1622	w	$2 \times 814 = 1628$
1511	vw	$1228 + 270 = 1498$
1460	vs	ν_7(SO_2 asymmetrical stretch—A'')
1305	vvw	$814 + 497 = 1311$
1272	sh	$814 + 461 = 1275$
1228	vs	ν_1(SO_2 symmetrical stretch—A')
1140	vvw	$814 + 320 = 1134$
1080	vvw	$814 + 270 = 1084$
1069	vvw	$608 + 461 = 1069$
1060	vvw	$608 + 450 = 1058$
984	vvw	$2 \times 497 = 994$
948	sh	$497 + 450 = 947$
930	vvw	$608 + 320 = 928$
873	vw	$608 + 270 = 878$
814	s	ν_8(rocking—A'')
728	vw	$461 + 270 = 731$
720	vw	$450 + 270 = 720$
650	sh	$2 \times 320 = 640$
608	s	ν_2(SO_2 bend—A')
551	w	$2 \times 270 = 540$
497	m	ν_3(SFBr asymmetrical stretch—A')
461	m	ν_4(SFBr symmetrical stretch—A')
450	m	ν_5(rocking—A')
353	vw	$814 - 461 = 353$
320	vw	ν_9(Torsion—A'')
(270)	vvw	ν_6(SFBr bend—A')

SO_2BrF, there is no definite procedure by which one can distinguish between the stretching frequencies. We assign the band at 497 cm^{-1} to the SFBr asymmetrical stretch and the band at 461 cm^{-1} to the SFBr symmetrical stretch. The bending frequency should occur at a lower value; hence, the SFBr bend is assigned at 270 cm^{-1} (estimated to occur at 300 cm^{-1} in SO_2F_2 and 209 cm^{-1} in SO_2Cl_2). At this point it should be noted that the band at 270 cm^{-1} is somewhat doubtful. In this region one is approaching the upper limit of usefulness of the CsBr prism, and this may account for the inability to observe the band with greater certainty. The band at 551 cm^{-1} is quite distinct and is assumed to be the first overtone of this proposed fundamental.

The torsional mode for SO_2BrF is assigned at 320 cm^{-1} and compares to 388 cm^{-1} in SO_2F_2[2] and 280 cm^{-1} in SO_2Cl_2. The two remaining fundamentals

have been assigned to the rocking modes. Fig. 2 illustrates the regularities observed in the fundamental absorption frequencies of SO_2F_2, SO_2BrF, SO_2Cl_2.

Acknowledgements—The authors wish to express their gratitude to Dr. E. A. Jones who made available the experimental equipment and who offered many helpful suggestions.

References

[1] Perkins W. P. and Kent Wilson M., *J. Chem. Phys.* 1952 **20,** 1791.
[2] Bender P. and Wood J. M. Jr., *J. Chem. Phys.* 1955 **23** 1316.
[3] Matossi F. and Aderhold H., *Z. Phys.* 1931 **68** 690.
[4] Cabannes J. and Rousset A., *Ann. Phys., Paris* 1933 **19** 229.
[5] Vogel-Högler R., *Acta Phys. Austr.* 1948 **1** 323.
[6] Martz D. E. and Lagemann R. T., *J. Chem. Phys.* 1954 **22** 1193.
[7] Jonas H., *Z. Anorg. Chem.* 1951 **265** 273.
[8] Herzberg G., *Infrared and Raman Spectra of Polyatomic Molecules.* Van Nostrand, New York 1945.

VOL.
12
1958

Spectrochimica Acta, 1958, Vol. 12, pp. 147 to 153. Pergamon Press Ltd.: London

The preparation and vibrational spectra of disilylacetylene

R. C. Lord,
Spectroscopy Laboratory, Massachusetts Institute of Technology, Cambridge 39, Mass., U.S.A.

D. W. Mayo.* H. E. Opitz† and J. S. Peake‡
Department of Chemistry, Indiana University, Bloomington, Indiana, U.S.A.

(*Received* 5 *February* 1958)

Abstract—Disilylacetylene ($H_3SiC_2SiH_3$) has been prepared by the action of silyl bromide on ethynylene magnesium bromide, and some of its physical properties determined (freezing point, −59°C; boiling point, 43°C; vapor pressure (mm): $\log_{10} p = -1434/T + 7{\cdot}417$; d_4^{25}, 0·743; n_D^{25}, 1·4234). The infrared spectrum of its vapor has been measured in the range 4000–400 cm^{-1} and its Raman spectrum (including depolarization factors) recorded photoelectrically for the liquid state. The vibrational spectra confirm the expected structure. The fundamental frequencies have been assigned with the exception of the infrared-active skeletal bending vibration estimated to lie at about 80 cm^{-1}. Only a part of one perpendicular band in the infrared was resolved, but the Q-sub-band spacing of this band shows clearly that disilylacetylene is a free internal rotator.

During a study of the structure and reactions of monobromosilane [1, 2] the preparation of disilylacetylene (DSA) appeared desirable in view of the recent spectroscopic investigations of trigonally symmetrical molecules containing free internal rotors [3–5]. In particular it was felt that the vibrational spectrum of DSA might give evidence concerning the correctness of the proposed structure for disiloxane [5]. DSA is a hitherto unknown silyl derivative, although other investigators [6–8] have previously reported substituted silyl acetylenes. It was prepared by the following reactions:

$$C_2H_5Br + Mg \rightarrow C_2H_5MgBr$$
$$2C_2H_5MgBr + C_2H_2 \rightarrow BrMgC_2MgBr + 2C_2H_6$$
$$BrMgC_2MgBr + 2SiH_3Br \rightarrow H_3SiC_2SiH_3 + 2MgBr_2$$

Experimental

The apparatus and techniques used in the preparation of DSA were those described previously [2]. With di-*n*-butyl ether as solvent, 50 g (0·46 mole) of ethyl bromide was caused to react with 11 g (0·46 mole) of magnesium turnings. Acetylene was bubbled through the resulting solution of ethylmagnesium bromide for several days to give the ethynylenemagnesium bromide. The gradual introduction of 50·4 g (0·454 mole) of monobromosilane gas produced an exothermic reaction and caused the contents of the reaction flask to thicken considerably.

Present addresses: * Materials Laboratory, Wright Air Development Center, Ohio; † Research and Development Center, Armstrong Cork Co., Lancaster, Penna. ‡ Central Research Dept., Minnesota Mining and Mfg. Co., St. Paul, Minn.

Table 1. Infrared spectrum of disilylacetylene vapor (400–4000 cm^{-1})

Freq. (cm^{-1}) (vac)	Int. and band type	Assignment	Freq. (cm^{-1}) (vac)	Int. and band type	Assignment
682	ms, perp.	ν_{14}	1101	vw, perp.	$\nu_4 + \nu_{11}$; $\nu_7 + \nu_{11}$
798 sh			1216	w, par.	$\nu_4 + \nu_7$
807	s, par.	ν_7	1358	w, par.	$\nu_4 + \nu_{13}$
817 sh			1463	vw, ?	?
908 P			1615	vw, par.	$\nu_3 + \nu_{14}$; $\nu_9 + \nu_{14}$
(912-min)	vs, par.	ν_6			
916 R			1855	vw, par.	$\nu_3 + \nu_6$
939 Q, w			1878	w, par?	$\nu_3 + \nu_{13}$
946 Q, s	m, perp.	ν_{13}	1895	vw, perp.	$\nu_9 + \nu_{13}$
953 Q, w			2170	s, par.	ν_5
960 Q, w			2190	m, perp.	ν_{12}
967 Q, s			2880	w, —	$\nu_1 + \nu_{14}$
974 Q, w			2980	w, —	$\nu_1 + \nu_7$
981 Q, w					
988 Q, s			3140	w, —	$\nu_1 + \nu_{13}$; $\nu_9 + \nu_{12}$
994 Q, w					
1000 Q, w					
1007 Q, s					

Abbreviations: m, medium; s, strong; sh, shoulder on a stronger band; v, very; w, weak; par., parallel band; perp., perpendicular band; min., minimum in absorption at center of parallel band; P, Q, R: P-branch, Q-branch, R-branch absorption maxima.

Stirring was continued for another day to ensure completeness of the reaction. The reaction flask was then attached directly to a distillation assembly having an 11-plate column, the system was flushed with nitrogen and the flask heated. DSA was taken off at a reflux temperature of 36°C at the prevailing atmospheric pressure. The yield was 35 per cent based upon the monobromosilane used.

DSA is a clear, colorless liquid which fumes slightly in air. At reflux temperatures near atmospheric pressure, it slowly decomposes and evolves silane. However, when distilled at low temperatures in a vacuum line, the compound is perfectly stable. It may be stored indefinitely if protected from traces of moisture and if kept at low temperatures. The vapor pressure of DSA was determined at different temperatures to establish the atmospheric boiling point. Vapor pressure constants for the equation $\log_{10} p$ (mm) $= -A/T + B$ were: A, −1434; B, 7·417. From this equation the boiling point is calculated as 43°C. Other properties are: freezing point, ca. −59°C; d_4^{25}, 0·743; n_D^{25}, 1·4234.

DSA proved a difficult compound to analyze by standard methods. However, determination of the silicon content (weighed as silica) gave fairly reproducible results: percentage Si found, 65 ± 2·5 (mean of three determinations); calc. for $Si_2C_2H_6$, 65.

VOL. 12 1958

Table 2. Raman spectrum of liquid disilylacetylene

Frequency (cm^{-1}) (vac)	Intensity and depolarization factor	Assignment
240	vw —	a
297	s 0·86	ν_{11}
420	m 0·2	ν_4
607	w 0·5	b; ν_{10}
946	s 0·8	ν_9 (ν_3)
2132	s 0·3	ν_2
2187	vs 0·2	ν_1; ν_8

a—Possibly ν_{11} excited by Hg-4348.
b—Partly ν_1 excited by Hg-4077, though ν_{10} also contributes to the intensity of this line.

Measurements of the infrared spectrum of the vapor of DSA were recorded with a Perkin—Elmer model 21 spectrophotometer in the region 4000–400 cm^{-1}, employing sodium chloride and potassium bromide prism-interchange units. The spectrum was obtained at pressures varying from 285 to 1 mm Hg, with a cell path length of 10 cm. Band centers are accurate to 2 cm^{-1} at wave numbers below 1500 cm^{-1}. Results are listed in Table 1.

The Raman data, including depolarization measurements, were obtained with the photoelectric instrument of BOYD, LORD and WILMOT [9]* on a liquid sample about 1 ml in volume. Recorded spectra of disilane and disilane-d_6 obtained with this instrument on larger liquid samples are shown in the recent paper of BETHKE and WILSON [10]. Precision of the frequencies listed in Table 2 is estimated as ± 2 cm^{-1}. Polarization measurements, despite the small size of the sample, gave good results.

Interpretation of the spectra

By analogy with dimethylacetylene, DSA is expected to exhibit free internal rotation. However, as pointed out by BAUMAN [11] the vibrational selection rules for a molecule of this type are indistinguishable from those of point group D_{3d}, and the spectrum of DSA can best be interpreted on this basis. Table 3 lists an assignment for the infrared and Raman frequencies based on the D_{3d} model and Table 4 gives a comparison of these frequencies with other silyl molecules belonging to this point group. [5, 10]

The assignment of the observed frequencies to the various vibrational species was made as follows:

Species A_{1g}: With one exception the totally symmetrical Raman frequencies are easily identified by their polarized lines. There can be little doubt that the pair of lines at 2187 and 2132 cm^{-1} are to be associated with the pair of vibrations arising from the symmetrical stretching of the C≡C and Si—H bonds. The Raman line at the higher frequency is very strong compared to all the other lines and by

* The basic features of the instrument are described in the Ph.D. thesis of G. B. WILMOT, Massachusetts Institute of Technology, October, 1954.

Table 3. Symmetry species, selection rules and frequency assignments of fundamentals of disilylacetylene (D_{2d} symmetry).

Species	Vibration no.	Approx. form of vibration	Selection rules		Assignment
			Raman	Infrared	
A_{1g}	1	Si—H stretching	Polarized	Forbidden	2187
	2	C≡C stretching			2132
	3	SiH_3 deformation			(930)
	4	Si—C stretching			420
A_{1u}	—	(free internal rotation)	—	—	
A_{2u}	5	Si—H stretching	Forbidden	Active; parallel bands	2170
	6	SiH_3 deformation			912
	7	SiC stretching			807
E_g	8	Si—H stretching	Depolarized	Forbidden	2187
	9	SiH_3 deformation			946
	10	SiH_3 rocking			607?
	11	Si—C≡C—Si bending			297
E_u	12	Si—H stretching	Forbidden	Active; perpendicular bands	2190
	13	SiH_3 deformation			946
	14	SiH_3 rocking			682
	15	Si—C bending			(80?)

analogy to disilane [10] is assigned to Si—H stretching despite the fact that the C≡C stretching frequency should also lie near or above this point. The low value (2132) of the latter frequency appears to imply a considerable weakening of the C≡C bond in DSA, although some of the decrease from the expected value is probably due to coupling between the two stretching motions. In fact, the two motions are doubtless mixed to an appreciable extent in both vibrations and assignment of either frequency to pure C≡C stretching or to pure Si—H stretching is an oversimplification.

The symmetrical deformation frequency of the silyl group is believed to lie at about 930 cm^{-1}. The Raman line at 946 is depolarized and must therefore be the E_g deformation. In disilane [10] these two frequencies fall close together at 909 and 929 (Table 4) and the latter, which is the degenerate mode, is much more intense in the Raman spectrum. We therefore assume that the A_{1g} deformation in DSA is hidden by the E_g Raman line, and is weak enough so that its polarized nature does not affect the observed depolarization of the E_g line. This supposition is consistent with the values observed for the corresponding deformation frequencies in the infrared at about 912 and 946 cm^{-1}.

The fourth A_{1g} vibration involves mainly the stretching motion of the Si—C bonds and is assigned with confidence to the remaining polarized line at 420 cm^{-1}.

VOL. 12 1958

Table 4. Comparison of frequencies of some silyl molecules of effective D_{3d} symmetry

Species	Description	$Si_2H_6C_2$	Si_2H_6	Si_2H_6O	Si_2D_6	Si_2D_6O
A_{1g}	SiH str.	2187	2152·0	2174	1547·5	1575
	C≡C str.	2132	—	—	—	—
	SiH_3 def.	(930)	909	1009	683·1	771
	SiX str.	420	434·2	606	407·5	555
A_{1u}	torsion	fr. rot.	forb.	fr. rot.	forb.	fr. rot.
A_{2u}	SiH str.	2170	2154·3	2169	1549·3	1575
	SiH_3 def.	912	843·5	957	624·9	713
	SiX str.	807	—	1107	—	1094
E_g	SiH str.	2187	(2155?)	2174	1569·0	1546
	SiH_3 def.	946	929·3	947	667·0	699
	SiH_3 rock	607?	625·2	716	474·7	532
	SiX bend.	297	—	—	—	—
E_u	SiH str.	2190	2187·6	2183	1585·0	1575
	SiH_3 def.	946	939·6	957	682·9	720
	SiH_3 rock	682	379·3	764	277·0	593
	SiX bend.	(80?)	—	(112?)	—	(105?)

X = C, Si, O, Si, O in colums 3–7 respectively

Species E_g: The Si—H stretching mode of this species presumably lies near 2187 cm^{-1} but was not observed. This was also the case in disilane [10], although for disilane-d_6 the E_g vibration was actually resolved and found to be some twenty times weaker than the A_{1g} vibration. On the other hand both in DSA and disilane the E_g deformation vibration is much more intense than the corresponding A_{1g} mode, as was mentioned above.

The E_g rocking mode of the silyl group is assigned to the weak Raman line at 607 cm^{-1}, somewhat displaced from the comparable infrared-active fundamental at 682. The precise location of this line is in doubt because of the fact that the very intense Raman line at 2187 as excited by Hg-4077 falls near it (cf. Table 2). In disilane the corresponding frequency is 625 cm^{-1}. The remaining E_g vibration, a bending of the molecular axis, was found as an intense depolarized line at 285 cm^{-1}. This frequency is to be compared with the analogous one in dimethylacetylene at 374 cm^{-1}, which also corresponds to an intense Raman line.

Species A_{2u}: This species contains three vibrations giving rise to parallel infrared bands. The Si—H stretching band occurs as expected near 2170 cm^{-1}, in agreement with the A_{1g} vibration. The close-lying P and R branches of this band were not resolved by the rock-salt prism spectrometer, but the broad perpendicular Si—H stretching band was noticeable at the base of the A_{2u} band.

The SiH_3 deformation vibration appears as a P—R doublet of high intensity

whose center is at 912 cm^{-1}, the weakness of the Q-branch being due to the small ratio of I_A to I_B.

The A_{2u} band due to the Si—C stretching vibration appears at 807 cm^{-1}. The narrow width of this band shows clearly that the vibration is a parallel one, but no central minimum is observed. This is probably due to the fact that the band is a superposition of fundamental and upper-stage bands arising from excited states of the very low bending frequencies ν_{15}. Since in the excited states the Si—C stretching frequency could easily be shifted by the 4 cm^{-1} necessary to cause its P-maximum (or R-maximum, as the case may be) to fall on the Q-minimum of the fundamental, such a superposition could easily wipe out the minimum if the Boltzmann factor of the first excited state is large enough. For a frequency below 100 cm^{-1}, as is estimated for ν_{15}, this condition is satisfied.

The fact that the double minimum is still observed for the 912 band can be understood if the effect of the bending mode on the frequency of the SiH_3 deformation is very small. This is physically reasonable. It is of interest to note that the structures [5] of the analogous parallel bands in disiloxane are almost exactly the same, the band due to the deformation frequency being double and that due to the anti-symmetrical Si—O—Si stretching being single with evidence of overlapping maxima. The latter band is in fact superimposable on that of DSA.

Species E_u: As previously stated, the perpendicular band due to the Si—H stretching vibration of this species appears as a broad band at the base of the parallel band. The asymmetry of the two superposed bands indicates that the center of the perpendicular band is some 20 cm^{-1} above that of the parallel band, as is to be expected from disilane [10]. The same kind of superposition is found for the bands of the deformation vibrations, but the separation of centers is somewhat larger (34 cm^{-1}) and a considerable number of the Q-sub-bands of the E_u band can be observed. These sub-bands, whose frequencies are listed in Table 1, show the expected strong–weak–weak intensity alternation. The separation of the sub-bands is 7 cm^{-1}, which shows that disilylacetylene is a free internal rotator, since no reasonable value of I_A and the zeta constant could lead to such a large separation without the additional help of free rotation.

In DSA the value of A, the reciprocal moment of inertia, should lie in the range 1·30–1·50 cm^{-1}, and the smallest possible value of zeta is -1. Hence for a hindered rotator the largest possible Q-sub-band spacing, $2A(1 - \zeta)$, is $4A$, or 6 cm^{-1}. The observed value of 7 cm^{-1} exceeds this limit and forces the conclusion that the molecule is a free rotator.

For a D_3 free rotator the Q-sub-band separation is $4A(1 - \zeta)$. If one takes $A = 1{\cdot}43$ cm^{-1}, the value found for disilane [10], a separation of 7 cm^{-1} implies a value for zeta of about $-0{\cdot}22$, which is close enough to the zeta for the analogous vibration in disilane ($-0{\cdot}31$).

The E_u silyl rocking vibration has been assigned to the broad unresolved band at 682 cm^{-1}, which compares well with values found for this vibration in disiloxane, [5], SiH_3Br [1,12] and SiH_3Cl [12].

The remaining E_u vibration has not been observed. It is an axial bending mode and would be expected to occur somewhere near 80 cm^{-1} by analogy with the comparable vibrations in disiloxane and dimethylacetylene.

VOL. 12 1958

Conclusions

(1) The vibrational spectra of the compound obtained by the action of silyl bromide on ethynylenemagnesium bromide show that this compound is the expected disilylacetylene and that the effective point-group symmetry of the molecule is D_{3d}.

(2) The rotational structure of one of the perpendicular bands (ν_{13} at 946 cm^{-1}) confirms the trigonal symmetry of the molecule and indicates that the molecule is a free internal rotator.

(3) The very close structural similarity of the parallel bands and most of the perpendicular bands of disilylacetylene to those of the analogous vibrations in disiloxane supports the conclusion [5] that the disiloxane molecule is linear or nearly so. The band in disiloxane analogous to the only resolved perpendicular band in disilylacetylene was not resolvable in disiloxane, mainly because the companion parallel band was more precisely superimposed on it. In disilylacetylene the band centers of the two bands are separated by 34 cm^{-1} whereas in disiloxane the separation is estimated to be less than 10 cm^{-1}.

Acknowledgements—The synthesis of disilylacetylene was supported in part by the Office of Naval Research [Contract Nonr-908(02)–Task NR356321 with Indiana University]. Construction of the Raman spectrometer was assisted by a Grant-in-Aid from the Owens–Illinois Glass Company to the Massachusetts Institute of Technology. The authors are indebted to Dr. D. R. J. Boyd for recording the Raman spectra.

References

[1] Mayo D. W., Opitz H. E. and Peake J. S., *J. Chem. Phys.* 1955 **23** 1344.
[2] Opitz H. E., Peake J. S. and Nebergall W. H., *J. Amer. Chem. Soc.* 1956 **78** 292.
[3] Mills I. A. and Thompson H. W., *Proc. Roy. Soc.* A 1954 **226** 306.
[4] Miller F. A. and Bauman R. P., *J. Chem. Phys.* 1954 **22** 1548.
[5] Lord R. C., Robinson D. W. and Schumb W. C., *J. Amer. Chem. Soc.* 1956 **78** 1327.
[6] Petrov A. D. and Shchukovskaya L. L., *Dokl. Akad. Nauk. SSSR* 1952 **86** 551; *Chem. Abstr.* 1953 **47** 12225h.
[7] Petrov A. D., Shchukovskaya L. L. and Egorov Y. P., *Dokl. Akad. Nauk. SSSR* 1953 **93** 293; *Chem. Abstr.* 1954 **48** 13616g.
[8] Frisch K. C. and Young R. B., *J. Amer. Chem. Soc.* 1952 **74** 4853.
[9] Boyd D. R. J., Lord R. C. and Wilmot G. B. To be published.
[10] Bethke G. W. and Wilson M. K., *J. Chem. Phys.* 1957 **26**.
[11] Bauman R. P., *J. Chem. Phys.* 1956 **24** 13.
[12] Wilson M. K. *et al.*, *J. Chem. Phys.* 1956 **24** 855.

Spectrochimica Acta, 1958, Vol. 12, pp. 154 to 161. Pergamon Press Ltd., London

A relationship between some bond properties of diatomic molecules and the ionization potentials of their constituent atoms*

BRIAN STEVENS†
The James Forrestal Research Center, Princeton University, Princeton, New Jersey, U.S.A.

(*Received* 13 *May* 1957)

Abstract—The relationship $kr_e^2 = 2N\,(I_A + I_B)$ between the force constant k, equilibrium internuclear distance r_e and bond order N of the diatomic molecule AB in its ground state, and the first ionization potentials I_A and I_B of atoms A and B, is examined. For covalent molecules with eight, ten or eleven valence shell electrons the relationship is satisfactory, but for molecules with two, twelve or fourteen electrons in the valence shell the expression must be modified by the introduction of two constants.

For the forty-nine covalent molecules examined the average deviation of calculated from observed bond length is less than 2 per cent. Bond lengths predicted for twenty-two molecules are reasonably self-consistent and the derived covalent radii are used to extend the table of values introduced by PAULING [14].

Introduction

No simple expression relating the force constant k, dissociation energy D, order N and equilibrium length r_e of a chemical bond has yet been proposed which has more than a very limited application. Recently, semi-empirical expressions have been put forward [1, 2] which relate one or more of these bond properties to the electro-negativities of the bonded atoms. These have led to further definitions of the concept introduced by PAULING [3] and MULLIKEN [4] and several tables of electro-negativities now exist [5].

WALSH [6] has pointed out the advantage of relationships between bond constants and atomic ionization potentials which are well defined and which are known with precision; he observed a linear dependence of k for the A—H bond on the second power of the first ionization potential of atom A. For restricted groups of molecules, the force constant [7], equilibrium frequency [8] and dissociation energy [9] have also been related to the first ionization potential of one or both of the bonded atoms.

The purpose of this note is to examine the empirical relationship (1) between k and r_e

$$kr_e^2 = 2N(I_A + I_B) \tag{1}$$

of the diatomic molecule AB in its ground state, and I_A and I_B, the energies required to ionize atoms A and B, all expressed in e.g.s. units. N in most cases is equal to the bond order but is more specifically defined to include those molecules in which A and B have different group valencies as the average group valency of A and B; thus for CO, NO and O_2, N has the values 3, 2·5 and 2 respectively.

* This research was supported by the United States Air Force under Contract No. AF33(038)–23976 monitored by the office of Scientific Research. ASTIA Document No. AD.126489

† Present address: Department of Chemistry, The University, Sheffield 10, England.

VOL. 12 1958

Covalent molecules

Values of r_e calculated from equation (1) are given in Table 1 together with the experimental bond lengths for seventeen molecules with eight, ten and eleven valence shell electrons*. Apart from the halogen hydrides PO, N_2 and PN, these molecules are not treated by GORDY [1] and comparison with his expression is not easily made. Use of GORDY's expression IA leads to calculated bond lengths for the molecules in Table 1 which on the average are some 13 per cent greater

Table 1. Bond lengths calculated from $kr_e^2 = 2N(I_A + I_B)$ for covalent molecules with 8, 10 and 11 valence shell electrons

Molecule	$k \times 10^{-5}$ (dyn/cm)	N	r_e (Å) Observed	r_e (Å) Calculated	% Deviation	r_e (Å)†	% Deviation
HF	9·653	1	0·917	1·015	10·7	0·919	0·2
HCl	5·160	1	1·275	1·284	0·7	1·236	3·2
HBr	4·117	1	1·414	1·407	0·5	1·397	0·9
HI	3·141	1	1·604	1·566	2·4	1·603	0·0
NO	15·94	2·5	1·151	1·189	3·3		
PO	9·41	2·5	1·449	1·447	0·2	1·482	2·3
N_2	22·96	3	1·094	1·103	0·8	1·082	1·2
P_2	5·556	3	1·894	1·948	2·9		
PN	10·17	3	1·491	1·553	4·2	1·592	6·8
CO	19·02	3	1·128	1·121	0·6		
SiO	9·242	3	1·510	1·504	0·4		
GeO	7·522	3	1·651	1·666	0·9		
SnO	5·615	3	1·838	1·893	3·0		
PbO	4·557	3	1·922	2·106	9·6		
CS	8·485	3	1·534	1·565	2·0		
SiS	4·929	3	1·929	1·897	1·7		
PbS	2·991	3	2·395	2·390	0·2		
					Avg. 2·5		Avg. 2·1

† From GORDY's expression IA.

than the experimental values. Oxygen could be included in this table, the deviation of calculated from observed value being 0·5 per cent; however, this molecule is grouped with other twelve valence electron molecules in Table 4.

In the case of hydrogen, the alkali metals and their hydrides with two valence shell electrons, r_e calculated from equation (1) is uniformly larger than the experimental value, the linear relationship being expressed by equation (2).

$$k(0{\cdot}32 + 1{\cdot}28\, r_e)^2 = 2N(I_A + I_B) \qquad (2)$$

For the eighteen molecules of this type shown in Table 2, the agreement between the observed bond lengths and those calculated from equation (2) is almost as

* Unless otherwise stated, the ionization potentials, force constants and experimental bond lengths are taken from or calculated from the data listed by HERZBERG [10,11].

Table 2. Bond lengths calculated from $k(0{\cdot}32 + 1{\cdot}28\,r_e)^2 = 2N(I_A + I_B)$ for covalent molecules with two valence shell electrons

Molecule	$k \times 10^{-5}$ (dyn/cm)	r_e (Å) Observed	r_e (Å) Calculated	% Deviation	r_e (Å)*	% Deviation
H_2	5·759	0·741	0·711	4·0	0·744	0·4
Li_2	0·254	2·672	2·630	1·6	2·558	4·3
Na_2	0·172	3·079	3·167	2·9	3·096	0·6
K_2	0·099	3·923	3·890	0·9	3·845	2·0
Rb_2	0·081	4·22†	4·24	0·5	4·22	0·0
Cs_2	0·069	4·50†	4·45	1·1	4·44	1·3
LiH	1·026	1·596	1·652	3·5	1·602	0·4
NaH	0·779	1·888	1·918	1·6	1·892	0·2
KH	0·560	2·244	2·252	0·4	2·254	0·4
RbH	0·514	2·368	2·350	0·8	2·368	0·0
CsH	0·467	2·494	2·455	1·6	2·488	0·2
LiK	0·148	3·30†	3·33	0·9	3·29	0·3
LiRb	0·129	3·50†	3·56	1·7	3·53	0·9
LiCs	0·109	3·75†	3·83	2·2	3·83	2·2
NaK	0·130	3·50†	3·53	0·9	3·47	0·9
NaRb	0·120	3·59†	3·65	1·7	3·59	0·0
NaCs	0·108	3·76†	3·79	0·8	3·75	0·3
RbCs	0·075	4·36†	4·34	0·5	4·31	1·1
				Avg. 1·5		Avg. 0·9

* From GORDY's expressions IB and IC.
† Computed from the SCHOMAKER–STEVENSON rule [12].

close as that obtained by GORDY [1] who uses a different set of constants for hydrogen and the hydrides.

Lone-pair repulsion [6] may account for the fact that experimental bond lengths for the halogens are larger than those calculated from equation (1). For these molecules with a valence shell of fourteen electrons shown in Table 3, expression (3) is satisfactory.

$$k(0{\cdot}63 + 0{\cdot}50\,r_e)^2 = 2N(I_A + I_B) \tag{3}$$

The experimental bond lengths for those molecules containing two Group VI atoms with twelve valence shell electrons are also larger than the corresponding values calculated from equation (1). In Table 4, the bond lengths calculated from equation (4)

$$k(0{\cdot}38 + 0{\cdot}69\,r_e)^2 = 2N(I_A + I_B) \tag{4}$$

are given. GORDY [1] prescribes a bond order of less than 2 for the molecules in this group.

Covalent radicals

In Fig. 1 the bond lengths calculated from expression (1) with $N = 1$ are plotted against the observed values for some diatomic hydride radicals. A regular trend is apparent and linear relationships appear to exist for the hydrides of elements in the two short periods as well as for those of the elements in a particular

VOL. 12 1958

group. As observed above, the increase in bond length calculated from equation (1) seems to depend on the number of electrons in the valence shell.

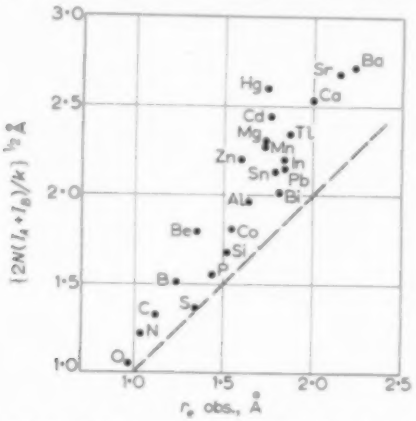

Fig. 1. Plot of r_e calculated from expression (1) with $N = 1$ against observed bond length for some diatomic hydride radicals. The dashed line is drawn through the origin with unit slope.

Ionic molecules

The combination of highly electropositive and electronegative atoms results in virtually complete electron transfer and the bond constants may be expected to depend on the electron affinity of the electronegative constituent. The deviation of r_e calculated from equation (1) from the observed value is fairly large and irregular for the typical ionic molecules in Table 5; however, the use of electronegativities in GORDY's expression does not lead to a significant improvement in the calculated bond length for the molecules chosen.

Table 3. Bond lengths calculated from $k(0{\cdot}63 + 0{\cdot}50\, r_e)^2 = 2N(I_A + I_B)$ for covalent molecules with fourteen valence shell electrons

Molecule	$k \times 10^{-5}$ (dyn/cm)	r_e (Å) Observed	r_e (Å) Calculated	% Deviation	r_e (Å)*	% Deviation
Cl_2	3·286	1·989	1·918	3·6	2·014	1·3
Br_2	2·458	2·284	2·254	1·3	2·317	1·4
I_2	1·721	2·667	2·682	0·6	2·730	2·4
ClF	4·483	1·628	1·686	3·6	1·857	14·1
BrF	4·070	1·756	1·776	1·1	1·916	9·1
IF	3·621	1·906†	1·880	1·4	1·967	3·2
BrCl	2·755	2·118†	2·136	0·9	2·210	4·1
ICl	2·383	2·321	2·286	1·5	2·323	0·1
IBr	2·064	2·439†	2·460	0·9	2·500	2·5
				Avg. 1·7		Avg. 4·2

* From GORDY's expression IA.
† Computed from SCHOMAKER–STEVENSON role by COLE and ELVERUM [13].

Table 4. Bond lengths calculated from $k(0{\cdot}38 + 0{\cdot}69\, r_e)^2 = 2N(I_A + I_B)$ for covalent molecules with twelve valence shell electrons

Molecule	$k \times 10^{-5}$ (dyn/cm)	r_e (Å) Observed	r_e (Å) Calculated	% Deviation
O_2	11·77	1·207	1·207	0·0
S_2	4·958	1·889	1·820	3·6
Se_2	3·614	2·157	2·144	0·6
Te_2	2·367	2·59	2·650	2·3
SO	7·929	1·493	1·465	1·9
			Avg.	1·7

Some predicted bond lengths

The agreement between r_e calculated from equations (1) and (4) and the experimental values shown in Tables 1 and 4 is sufficiently close to justify the prediction of bond lengths for similar molecules shown in Table 6 for which no experimental values are available. For purposes of comparison the appropriate sums of covalent radii are given in the fifth column of Table 6, these being calculated from PAULING's values or as otherwise stated in Table 7. The data in Tables 6 and 7 are reasonably self-consistent, but it appears that some revision of PAULING's double-bond radius for Ge, As and Sn is required if experimental verification of the predicted bond lengths in Table 6 is forthcoming.

Discussion

For covalent diatomic molecules in the ground state, the expression discussed above appears to be as satisfactory as that proposed by GORDY [1] which may be written as

$$(k - b)\, r_e^{1\cdot5} = aN(X_A X_B)^{0\cdot75} \qquad (5)$$

where X_A and X_B are the electro-negativities of the bonded atoms and a and b are constants with $a = 1{\cdot}67 = 2^{0\cdot75}$ in most cases. If, as WALSH has suggested [6], I_A may be taken as a rough approximation of X_A, equations (1) and (5) are of the same form with the exception that the sum and product of electro-negativities are involved respectively; moreover, if it is accepted that k is determined by the energies of the bonding electrons in their atomic orbitals [6] i.e. by the quantity $N(I_A + I_B)$, the semi-empirical derivation of expression (1) may proceed along the lines by which expression (5) is obtained.

It may be expected that the use of valence ionization potentials [4] would improve the results obtained from expression (1). As these are some 22 per cent higher than the measured ionization potentials for the halogens [6] their use in expression (1) would lead to an increase of 11 per cent in the calculated bond length for the molecules in Table 3. However, the experimental bond lengths in this case are approximately 25 per cent higher than the values calculated from expression (1) using experimental ionization potentials and it is felt that the modification of expression (1) by the introduction of empirical constants leads

VOL. 12 1958

Table 5. Bond lengths calculated from $kr_e^2 = 2N(I_A + I_B)$ for some ionic molecules

Molecule	$k \times 10^{-5}$ (dyn/cm)	N	r_e (Å) Observed	r_e (Å) Calculated	% Deviation	r_e (Å)*	% Deviation
NaCl	1·186	1	2·36†	2·21	6·4	2·51	6·4
NaBr	1·044	1	2·50†	2·28	8·8	2·71	8·8
NaI	0·938	1	2·71†	2·31	14·8	2·81	3·7
KCl	0·859	1	2·67†	2·54	4·9	3·23	24·7
KBr	0·825	1	2·82†	2·51	11·0	3·18	12·8
KI	0·704	1	3·05†	2·61	14·8	3·17	3·9
BeO	7·516	2	1·33	1·40	5·3	1·34	0·7
MgO	3·485	2	1·75	1·98	13·2	2·10	20·0
CaO	2·843	2	1·75	2·11	20·6	2·23	27·4
SrO	3·401	2	1·92	1·91	0·5	1·95	1·6
BaO	3·784	2	1·94	1·79	7·8	1·71	11·9
					Avg. 9·8		Avg. 11·0

* From Gordy's expression IA.
† Reference [15].

Table 6. Bond lengths predicted from $kr_e^2 = 2N(I_A + I_B)$

Molecule	$k \times 10^{-5}$ (dyn/cm)	N	r_e (Å) Predicted	$(r_A + r_B)$ (Å)*	% Deviation
SeO	6·444	2	1·658†	1·63	1·7
TeO	5·304	2	1·845†	1·85	0·3
AsO	7·265	2·5	1·630	1·66	1·8
SbO	5·560	2·5	1·790	1·81	1·2
BiO	4·315	2·5	1·970‡	1·93	2·0
As_2	4·069	3	2·226	2·22	0·3
Sb_2	2·612	3	2·521	2·52	0·0
Bi_2	1·835	3	2·760‡	2·76	0·0
AsN	7·929	3	1·743	1·66	5·0
SbN	6·566	3	1·842	1·81	1·8
SbBi	2·193	3	2·640‡	2·64	0·0
GeS	4·359	3	2·018	2·02	0·1
SnS	3·536	3	2·193	2·21	0·8
CSe	6·583	3	1·752	1·632	7·4
SiSe	4·094	3	2·050	2·03	1·0
GeSe	3·743	3	2·142	2·18	1·8
SnSe	3·064	3	2·314	2·37	2·4
PbSe	2·594	3	2·520	2·55	1·2
SiTe	3·130	3	2·295	2·24	2·0
GeTe	2·902	3	2·382	2·39	0·4
SnTe	2·440	3	2·537	2·58	1·7
PbTe	2·086	3	2·750	2·76	0·4
					Avg. 1·5

* Sum of covalent radii—see text and Table 7.
† Calculated from $k(0{\cdot}38 + 0{\cdot}69\, r_e)^2 = 2N\,(I_A + I_B)$.
‡ Calculated using 7·25 eV for ionization energy of Bi [16].

Table 7. Covalent radii (Å)*

	C	Si	Ge	Sn	Pb
Double-bond	0·665	1·07	1·12	1·30	
Triple-bond	0·602	1·00	1·15†	1·34†	1·52‡
	N	P	As	Sb	Bi
Double-bond	0·60	1·00	1·11	1·31	
Triple-bond	0·547	0·93	1·11§	1·26§	1·38§
	O	S	Se	Te	
Double-bond	0·55	0·94	1·08**	1·30**	
Triple-bond	0·50	0·87	1·03††	1·24‡‡	

* Values are those given by PAULING [14] unless otherwise stated.
† Obtained from XO bond length minus 0·5 Å.
‡ Obtained from PbS bond length minus 0·87 Å.
§ One half predicted bond length of X_2.
** One half observed bond length of X_2.
†† Average value of predicted XSe bond length minus r_xÅ (X = C, Si, Ge, Sn, Pb).
‡‡ Average value of predicted XTe bond length minus r_xÅ (X = Si, Ge, Sn, Pb).

VOL. 12 1958

to a more useful relationship than one employing corrected values of the related quantities to which some uncertainty is attached [6]. The dependence of these constants on the number of valence shell electrons indicates that the improvement of expression (1) will involve a correction for this factor rather than any other [17].

One disadvantage of expression (1) is its limited application to polyatomic molecules which requires that the ionization potentials of the bonded radicals are known. However, there is evidence that the electro-negativity of an atom also depends on its environment [1] which together with the possibility of interaction between non-bonded atoms imposes a similar limitation to the use of expression (5), although to a much lesser degree.

References

[1] GORDY W. *J. Chem. Phys.* 1946 **14** 305.
[2] ARNOLD J. R. *J. Chem. Phys.* 1956 **24** 181.
[3] PAULING L. *J. Amer. Chem. Soc.* 1932 **54** 3570.
[4] MULLIKEN R. S. *J. Chem. Phys.* 1934 **2** 782.
[5] PRITCHARD H. O. and SKINNER H. A. *Chem. Rev.* 1955 **55** 745; GORDY W. and THOMAS W. J. O. *J. Chem. Phys.* 1956 **24** 439.
[6] WALSH A. D. *Proc. Roy. Soc.* A 1951 **207** 13.
[7] TORKINGTON P. *Nature, Lond.* 1948 **161** 724.
[8] VARSHNI Y. P. *Z. Phys.* 1953 **135** 512.
[9] MITRA S. S. *Z. Phys.* 1954 **137** 520.
[10] HERZBERG G. *Atomic Spectra and Atomic Structure* (2nd Ed.) Dover Publications, New York 1944.
[11] HERZBERG G. *Spectra of Diatomic Molecules* (2nd Ed.) Nostrand, New York 1950.

[12] Schomaker V. and Stevenson D. P. *J. Amer. Chem. Soc.* 1941 **63** 37.
[13] Cole L. G. and Elverum G. W. *J. Chem. Phys.* 1952 **20** 1543.
[14] Pauling L. *Nature of Chemical Bond* (2nd Ed.) Oxford University Press, London 1950.
[15] Honig A., Mandel M., Stitch M. L. and Townes C. H. *Phys. Rev.* 1954 **96** 629.
[16] Rice O. K. *Electronic Structure and Chemical Binding* (Table 4) McGraw Hill, New York 1940.
[17] Williams R. L. *J. Phys. Chem.* 1956 **60** 1016.

L.
2
58

Spectrochimica Acta, 1958, Vol. 12, pp. 162 to 168. Pergamon Press Ltd., London

The OH in-plane deformation and the C—O stretching frequencies in monomeric carboxylic acids and their association shifts

D. Hadži and M. Pintar

University Chemical Laboratory and Institute "B. Kidrič", Ljubljana

(*Received* 20 *January* 1958)

Abstract—Infrared spectra of six carboxylic acids and their deuterium analogues in the vapour state at 150–160°C are reported. A possible assignment of the bands mentioned in the title is discussed on the basis of the shifts due to deuterium substitution, and of association to dimers and association with pyridine, respectively.

The spectra of monomeric carboxylic acids, with the exception of the bands due to the OH and C—O stretching, have not been studied so extensively as the spectra of the associated acids [1, 2, 3]. Moreover, the interpretation of some important bands in the former seems to be controversial [4] so that the study of a larger number of simple monomeric acids appears justified. In this paper the spectra are described of mono-, di-, and trichloroacetic acids, and of benzoic and butyric acids together with their analogues in which deuterium is substituted in the carboxyl group. The spectrum of acetic acid has been also recorded. It was published in another recent paper [5]. The discussion of these spectra is focused on the region between 1500 and 900 cm^{-1} since the data obtained for other regions have not brought out any new features.

Examination of the spectra of the carboxylic acids shown in Fig. 1, reveals two characteristic bands lying in the intervals between 1190 and 1075 cm^{-1} (strong, designated henceforth *A*) and between 1380 and 1280 cm^{-1} (medium, designated *B*). The positions of these bands change strongly with association of the acids, and the bands are replaced by new ones after deuteration. The intervals within which the latter appear (Fig. 2) are 1178 to 1315 cm^{-1} (strong, designated *C*) and 959 to 1000 cm^{-1} (medium-strong, designated *D*). It should be noted that the intervals in which these bands characteristic of the monomeric acids appear are much larger than those in which the corresponding bands of the dimeric acids [1, 2] occur, and this would be even larger if the bands of formic [4, 6] and trifluoroacetic acid [7] were included. Sometimes it is not easy to pick out these bands as they are overlapped by others, e.g. in the spectrum of butyric acid band *B* is overlaid by the δCH band and is revealed only by a slight change of the position and contour of the complex band near 1380 cm^{-1} after deuteration. Another remarkable feature of the spectra now measured is the unusually strong accentuation of skeletal or CH bands which are close in frequency to the bands of the carboxyl group. Thus band *D* of the benzoic acid is surrounded by several strong bands, due to the vibrations of the aromatic part of the molecule which are much weaker in the undeuterated compound not containing band *D*. One of the two strong

VOL. 12 1958

peaks, at 1115 and 1050 cm^{-1} respectively, in the spectrum of dichloroacetic acid is probably due to the same cause.

There is not much doubt that the bands *A*, *B*, *C* and *D* are due to the C—O stretching and the OH or OD in-plane deformation vibrations. There also seems

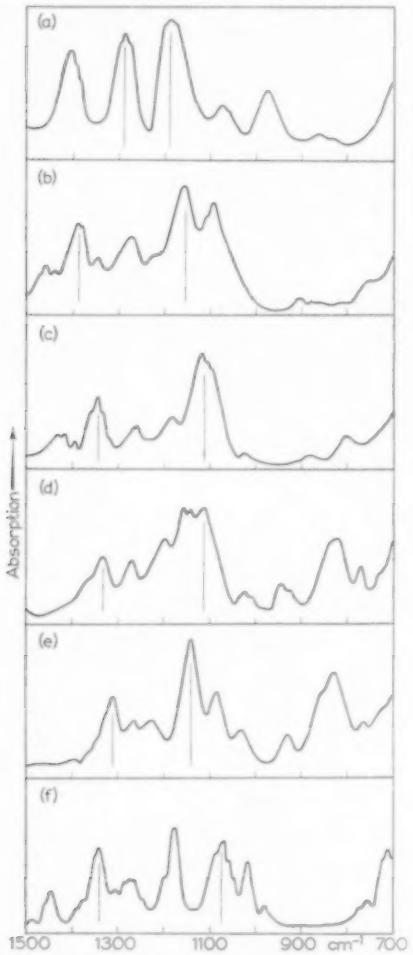

Fig. 1. Infrared spectra of some carboxylic acids in the vapour state at 150–160°. *A* acetic; *B* butyric; *C* monochloroacetic; *D* dichloroacetic; *E* trichloroacetic; *F* benzoic.

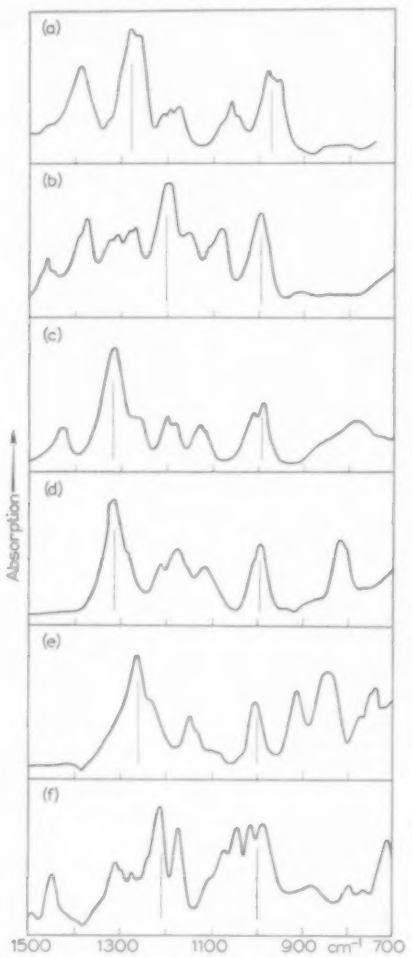

Fig. 2. Infrared spectra of some deuterated carboxylic acids. Conditions and lettering the same as in Fig. 1.

to be no disagreement with the more explicit assignment of the bands of the deuterated group, band *D* being assigned to the OD bending and band *C* to the C—O stretching vibration [3, 5]. However, two conflicting interpretations have been advanced by various authors for the bands *A* and *B* of the spectra of the undeuterated acids [4, 5, 6, 7, 8, 9]. According to Orville Thomas [6, 8] the higher frequency band in the spectrum of formic acid (1200 cm^{-1}) which corresponds

to band B of the present designation, belongs to the δOH vibration, but a strong vibrational interaction of this mode with the C—O stretching is assumed. A similar view has been advanced by Sverdlov [9, 10]. Wilmshurst on the other hand attributed band B to the C—O stretching vibration and band A to the OH deformation vibration [4]. He extended this assignment to the spectrum of acetic acid [5] and Kagarise applied the same argument to trifluoroacetic acid [7].

Two criteria for differentiating between the νC—O and OH bands of hydroxylic compounds are often used in the empirical interpretation of their spectra, namely the extent of the shifts on substituting deuterium for the hydroxylic hydrogen atom and that of the shifts upon changing the state of association. Both shifts are expected to be larger for the OH bands than for the νC—O band.

We shall consider the example of benzoic acid to test the criterion of the isotopic shifts, using the assignment analogous to that of Wilmshurst [4]. We find thus that the ratio of the frequencies B and C (1340 and 1210 cm^{-1}) is 1·107 whereas bands A and D (1075 and 980 cm^{-1}) yield a ratio of 1·097. There is an extremely small difference between these two ratios, suggesting that the motions of the hydrogen atom participate to a similar extent in both normal vibrations and that there is not much sense in calling one band δOH and the other νC—O. Benzoic acid is perhaps just an extreme example but it shows that the vibrational coupling between the bond stretching and the adjacent angle deformation vibration is very strong, which is certainly not unexpected. The degree of interaction will depend *inter alia* on the proximity of the respective frequencies. Now, the C—O stretching vibration is not a strictly characteristic vibration because it interacts with other skeletal stretching and CH deformation vibrations [11, 12]. We may expect that the proximity of frequencies of the C—O stretching and the OH deformation and hence the degree of mixing will vary from one compound to the other and may be influenced also by intermolecular factors contributing to the force field. Turning towards other examples investigated, we note that in fact the frequency ratios do not match as closely as in the case of benzoic acid, hence that one of the bands might be more entitled to the designation of δOH and the other of νC—O. Nevertheless, it appears that this cannot be decided on the basis of the isotopic shifts alone. We can easily determine whether the ratios of either of the frequency pairs, i.e. B/C and A/D or A/C and B/D, respectively, fit. For instance in trichloroacetic acid, the ratio B/C is 1·04, and A/D 1·14, in agreement with Wilmshurst's assignment [4, 5]. On the other hand, assuming that band B has mainly the character of OH bending, the ratio with the corresponding frequency D of the deuterium analogue is 1·32, which makes this correlation very plausible. The high frequency shift of the band A to C may be explained by a strong interaction of the stretching with the OH bending vibration. This would be in agreement with the conclusions from the study of the spectra of carboxylic dimers [2].

The spectra of the acids in the free state can now be compared with those of the hydrogen bonded acids in order to obtain a second criterion for the assignment. We may consider first the spectra of the deuterated acids since the assignments in this case are assumed to be clear cut. Most of the data for the dimeric acids are taken from the paper by Hadži and Sheppard [2], but some were collected during this investigation using the same criteria for the assignment as in the paper quoted.

VOL. 12 1958

Table 1. Characteristic infrared frequencies (cm^{-1}) of some carboxylic acids between 900 and 1500 cm^{-1}

Acid / Band designation	State of association	*B*	*A*	*C*	*D*
Acetic	m	1285	1190	1272	959
	d	1413	1290	1320	1059
Monochloroacetic	m	1350	1110	1315	1000
	d	1410	1290	1370	1050
Dichloroacetic	m	1335	1150	1315	995
	d	1420	1280	1380	1050
Trichloroacetic	m	1320	1143	1265	1000
	d	1410	1255	1340	1050
Butyric	m	1380	1150	1210	993
	d	1430(?)	1290(?)	1390	1090
Benzoic	m	1340	1075	1210	980
	d	1418	1290	1360	1043

The data collected in Table 1 show that the difference between the OD deformation frequencies of the free and associated deuterated acids amounts to between 50 and 100 cm^{-1} whereas it is between 50 and 150 cm^{-1} for the νC—O bands. Thus, it seems to be on the average larger for the νC—O than for the δOD bands. The direction of the shift of the angle deformation frequency is clear; it is increased because of the additional potential which opposes this motion. The same direction of the shift of the C—O stretching band, i.e. to higher frequencies, may be explained by the incipient ionization of the O—H linkage due to hydrogen bonding. This causes an electron migration from the carbonyl bond which renders the C—O bond stiffer and therefore the stretching frequency higher. If we consider the shifts observed with the OD bands together with their assignments to the undeuterated acids, we realise that band *B* exhibits smaller shifts than band *A* and may conclude that band *B* is analogous to the band near 1000 cm^{-1} of the deuterated acids (band *D*). Hence, it should have rather the character of the deformation vibration whereas band *A* would represent the stretching vibration. The relative intensities of the bands are in agreement with this correlation. However, no great weight should be given to either of these arguments and particularly not to that based on the shifts since they are of a similar order of magnitude.

The failure to obtain more evidence from the frequency changes due to carboxyl–carboxyl association may be compensated by the consideration of the changes in the spectrum of the carboxyl group when it undergoes hydrogen bonding to pyridine or related bases. The details of this investigation will be published elsewhere and only the results relevant to the present discussion will be quoted

here. It is apparent from the spectra of benzoic acid and deuterated benzoic acid mixed with pyridine (Fig. 3) that the bands due to the deformation vibrations of the COH and COD groups are very weak or completely missing. In particular, the band due to the out-of-plane vibration in the carboxylic dimers, known to be strong and broad, and appearing in the region near 900 cm^{-1}, cannot be detected in the complex with pyridine. As the hydrogen bond COOH . . . N(pyridine) is stronger than that in the carboxylic dimers (estimated by the shift of the νOH band) it is not likely that the γOH band would be of a lower frequency than in the case of dimers and lie outside the rock salt region. In the spectrum of the deuterated benzoic acid it is possible to detect besides the aromatic band at 1042 cm^{-1} a very weak band near 1047 cm^{-1}. This frequency is slightly higher than that at which the δOD band of the dimeric acid appears. Hence, the weak band may be attributed

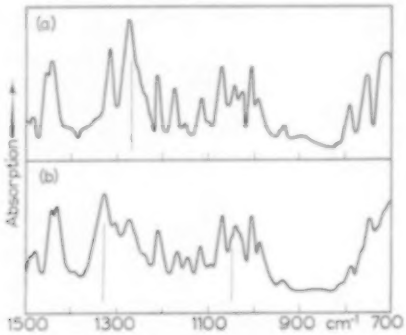

Fig. 3. Infrared spectra of benzoic acid (A) and benzoic acid-d_1 (B) mixed with pyridine 1:1. Liquid film.

to the same vibration in the acid–pyridine complex, the intensity being however much smaller. In the undeuterated acid, the band expected to appear near 1420 cm^{-1} by analogy with the spectrum of the dimeric acid is not detectable. This effect of hydrogen bonding between the carboxylic hydroxyl group and the nitrogen atom of pyridine has been observed with all the acids investigated but it is by no means a general effect of hydrogen bonding and no satisfactory explanation of it can be offered at present. In contrast with the behaviour of the deformation bands, the strong band at 1289 cm^{-1} in the spectrum of the dimeric benzoic acid has its equally strong analogue at 1275 cm^{-1} (1330 cm^{-1} with the deuterated acid) in the spectrum of the acid–pyridine complex. Considering the fact that the bands due to the deformation vibrations (both the out-of-plane and the in-plane) are of very small intensity or even non-observable in the acid–pyridine mixtures, it is safe to consider the strong band as due to the C—O stretching. These observations agree with the conclusions drawn from the study of the spectra of carboxylic dimers [2], i.e. that the higher frequency band (near 1400 cm^{-1}) is probably better described as the δOH band than that near 1300 cm^{-1}. A comment should be made on the lower frequency of the νC—O vibration in the pyridine–acid complex as compared with the carboxylic dimers. The reverse might be expected if the shifts of the δOD bands are considered which are in the same direction, but stronger in the complex.

VOL. 12 1958

However, it must be remembered that in the case of dimerization (as well as polymerization) the carbonyl group acts as an electron donor in hydrogen bonding, whereas this is not so in the pyridine–acid complex. This is of course, reflected also in the extent of the electron shift towards the C—O bond.

The possibility of attributing more definitely the character of the in-plane bending to the bands *B* and *D* respectively, and of C—O stretching to the other two in the spectra of the bonded carboxyl group is not at variance with the conclusions reached on the basis of the isotopic shifts. Hydrogen bonding may change the extent of the interaction of both vibrations, leading to the bands in the monomeric benzoic acid both having the same vibrational character, but to a much smaller interaction in the acid–pyridine complex, which permits differentiation of the bands. We hope to be able shortly to put this in a more quantitative form. For the moment, we are interested in the case of other acids than benzoic, in which even the monomeric bands could be differentiated: one as more δOH and the other as more νC—O in character. Although the assignment of the bands *A* and *B* in the associated state seems to be well established, it cannot be transferred directly to the spectra of the monomers since there are two possible ways of correlating the bands. Let us take first the case that band *A* of the monomer has not the same character as band *A* of the associated group, but that it is more δOH, as postulated by Wilmshurst; this would mean that it would have to shift about 300 cm^{-1} on association, which is much more than actually found with the deuterated acids. Moreover this correlation would give the other band (νC—O) erratic shifts, changing even the direction in various acids. Thus, with formic and acetic acids it would show a slight increase of frequency on association (5 cm^{-1}), whereas association would bring about a decrease of about 60 cm^{-1} in other acids and contrary to what was actually observed with the deuterated acids.

Conclusions

The spectra of monomeric carboxylic acids contain two bands appearing within rather wide limits and which are due to the νC—O and the δOH vibrations. From the behaviour of these two bands upon isotopic substitution it appears that the corresponding vibrations interact to such a degree as to make the explicit assignment of the bands difficult or even meaningless in some cases. However, the band shifts introduced by association and particularly the spectral changes due to hydrogen bonding with pyridine show that if a differentiation into a δOH and a νC—O band can be made at all, it is the higher frequency band (*B*) which is more liable to be called δOH, whereas the other (*A*) is rather the C—O stretching mode. This is fairly well established for the spectra of the dimeric acids, but it is made probable also for the bands of the monomeric acids.

The shifts of the δOD(δOH) and νC—O bands arising from association vary considerably with individual acids. The average shifts of the former bands are usually slightly smaller than those of the latter, both being of the order 50 to 150 cm^{-1}.

Experimental

The spectra were recorded with a Perkin–Elmer model 21 instrument, using a heated glass cell of 10 cm path length. The cell was connected through glass

joints to a small bulb containing the substance. The cell was filled by heating the bulb and sweeping it with thoroughly dried nitrogen (liquid nitrogen cooled trap). The deuterated acids were prepared by the hydrolysis of the acid chlorides with D_2O. The hydrolysis was carried out in the bulb which was connected to the gas cell after removing the deuterium chloride. By this method it was possible to obtain spectra of the heavy acids with a content of the light species estimated at less than 20 per cent and only traces of the dimeric species.

Acknowledgements—The authors are grateful to Dr. Fleš (Pliva Laboratories, Zagreb) for the sample of mono- and dichloroacetyl chloride and to the Boris Kidrič Fund for some financial assistance.

References

[1] Flett M. St. C., *J. Chem. Soc.* 1951 962.
[2] Hadži D. and Sheppard N., *Proc. Roy. Soc.* A 1953 **216** 247.
[3] Corish P. J. and Chapman D., *J. Chem. Soc.* 1957 1746.
[4] Wilmshurst J. K., *J. Chem. Phys.* 1956 **25** 478.
[5] Wilmshurst J. K., *J. Chem. Phys.* 1171.
[6] Thomas O., *Disc. Faraday Soc.* 1950 **9** 339.
[7] Kagarise R. E., *J. Chem. Phys.* 1957 **27** 519.
[8] Thomas O., *Research, Lond.* 1956**8** 15.
[9] Sverdlov L. M., *Dokl. Akad. Nauk SSSR* 1953 **91** 503.
[10] Sverdlov L. M., *Izv. Akad. Nauk SSSR (Ser. Khim.)* 1953 **17** 567.
[11] Hadži D. and Jeremić D., *Spectrochim. Acta* 1957 **9** 263.
[12] Nolin B. and Jones R. N., *Canad. J. Chem.* 1956 **34** 1392.

VOL.
12
1958

Spectrochimica Acta, 1958, Vol. 12, pp. 169 to 178. Pergamon Press Ltd., London

Statistical factors in X-ray intensity measurements

M. Mack and N. Spielberg
Philips Laboratories, Irvington-on-Hudson, New York, U.S.A.

(*Received* 29 *July* 1957)

Abstract—In X-ray intensity measurements, statistical factors result from the inherent randomness of the X-ray excitation process. The optimum division of counting times for given counting rates is discussed for various combinations of counting rates, with particular attention to the difference and the ratio of two counting rates. The influence of various confidence levels on the total time and the total counts that must be accumulated for a given precision is demonstrated. Graphical means of determining these quantities are exhibited. The relationship between the accuracy of an intensity measurement and the nominal accuracy of a spectrochemical analysis is considered.

1. Introduction

For purposes of X-ray analysis, it is often desired to determine the net peak intensity of a line above background or some quantity that involves a combination of net peak intensities of two or more lines. The development of counter tubes has made possible the measurement of X-ray intensities with a precision that, in theory, is limited only by the amount of time available. In practice, however, there are various factors to be considered in measuring a net counting rate, n, whether by a ratemeter, fixed time, or fixed count method [1]. Furthermore the time available for the measurements is limited by practical considerations. Thus if a large number of measurements are to be made, or if much time is involved in a measurement, it is desirable to know how best to divide the available time to obtain the greatest precision in the measurements. This problem and related statistical factors were discussed by Parrish [1]. The purpose of this paper is to present an expanded treatment illustrated with examples and to present graphs that will facilitate calculations.

It will be assumed that the X-ray emission process is random and fluctuates according to a Gaussian distribution for which the standard deviation is the square root of the mean [2, 3].

2. Determination of net peak intensity

(A) *General case*

The net peak intensity of a line is usually determined as the difference of two individually measured counting rates: n_1 = peak plus background ($P + B$) and n_2 = background (B), as shown in Fig. 1(a). The net peak is but one example of the determination of any quantity A as a function of two measured counting rates, n_1 and n_2

$$A = f(n_1, n_2) \tag{1}$$

The problem to be considered is: Given two counting rates, n_1 and n_2, and a limited total time, $T = t_1 + t_2$, available for their measurement, how should the

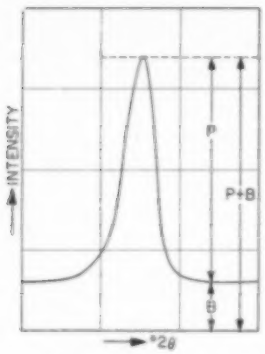

Fig. 1(a). Typical X-ray reflection with peak (P), peak plus background ($P + B$), and background (B) indicated.

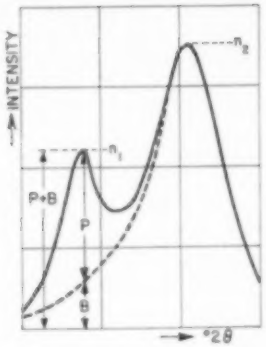

Fig. 1(b). X-ray reflection with peak (P) = n_1 and with background (B) = βn_2 due to overlapping "wing" of adjacent reflection.

measurement time be divided so that a minimum relative statistical error, ε_A, in the quantity A may be achieved?

ε_A is a function of the time spent on the measurements of n_1 and n_2:

$$\varepsilon_A = \varepsilon_A(t_1, t_2) \tag{2}$$

$$\varphi(t_1, t_2) = T - (t_1 + t_2) = 0 \tag{3}$$

The problem is to find a minimum value of (2) subject to the restraining condition (3). This may be done by the method of LaGrange multipliers [4] which yields:

$$\frac{\partial \varepsilon_A}{\partial t_1} = \frac{\partial \varepsilon_A}{\partial t_2} \tag{4}$$

(B) *Simple differences*

Consider the special case for which

$$A = d = n_1 - n_2 \tag{5}$$

This problem has been considered in great detail by other authors [5–8, 11] but the solution and results are here presented in a somewhat different form. Moreover the results here exhibited will be used in section 3 of this paper.

Let ε_1 and ε_2 be the relative errors of n_1 and n_2, respectively. The absolute errors are $n_1\varepsilon_1$ and $n_2\varepsilon_2$. The relative error of the difference is [9]:

$$\varepsilon_d = \frac{[(n_1\varepsilon_1)^2 + (n_2\varepsilon_2)^2]^{1/2}}{n_1 - n_2} \tag{6}$$

The form of equation (6) shows that there is little point in expending the effort to make the absolute error in one measurement small in order to achieve a small value of ε_d without also making the absolute error in the other measurement comparably small.

VOL. 12 1958

If Q is a constant determined by the confidence level desired [10], then $\varepsilon_1 = Q/(n_1 t_1)^{1/2}$ and $\varepsilon_2 = Q/(n_2 t_2)^{1/2}$. Therefore equation (6) may be rewritten as:

$$\varepsilon_d = \frac{Q}{n_1 - n_2}\left[\frac{n_1}{t_1} + \frac{n_2}{t_2}\right]^{1/2} \tag{7}$$

Substituting equation (7) into equation (4) yields

$$\frac{t_1}{t_2} = \left(\frac{n_1}{n_2}\right)^{1/2} = K^{1/2} \tag{8}$$

where K is the ratio of the counting rates. Equations (3) and (8) give

$$t_1 = \frac{K^{1/2}}{1 + K^{1/2}}\,T \tag{9}$$

It is often desirable to know how long a time must be expended to achieve a stipulated precision. Because it is necessary to accumulate a specific total number of counts to attain a specific precision (regardless of the counting method used), the problem may be rephrased: given two counting rates, n_1 and n_2, how many total counts, $N_1 = n_1 t_1$ and $N_2 = n_2 t_2$, must be accumulated so that the relative error of the difference will have a stipulated value? By manipulation of equations (7) and (8) it can be shown that

$$N_1 = \frac{Q^2}{{\varepsilon_d}^2} K^{3/2} \frac{(K^{1/2} + 1)}{(K - 1)^2} = \frac{Q^2}{{\varepsilon_d}^2} Z_1 \tag{10}$$

$$N_2 = \frac{Q^2}{{\varepsilon_d}^2} \frac{(K^{1/2} + 1)}{(K - 1)^2} = \frac{Q^2}{{\varepsilon_d}^2} Z_2 \tag{11}$$

In Fig. 2 the values of $Z_1 = K^{3/2}(K^{1/2} + 1)/(K - 1)^2$ and of $Z_2 = (K^{1/2} + 1)/(K - 1)^2$ are plotted as a function of K. In Fig. 3, N vs. Z is plotted for various confidence levels and percentage errors (ε_d in %). The relations $Z_1 = K^{3/2} Z_2$ and $N_1 = K^{3/2} N_2$ are useful in condensing calculations. The values of Q used for the 50, 90 and 99 per cent confidence levels are 0·67, 1·64, and 2·58, respectively. Thus for two given counting rates, the total number of counts, N_1 and N_2, necessary for a stipulated accuracy of the difference may be determined either analytically using equations (10) and (11) or graphically using Figs. 2 and 3.

Table 1 gives values of N_1, N_2, and T for some arbitrarily selected counting rates to illustrate certain typical situations for optimum division of counting times. It is clear from the table that to increase the confidence level from 50 per cent (probable error) to 90 per cent, the total time expended must be increased by a factor of $(1{\cdot}64/0{\cdot}67)^2 = 6$. Note that in examples 1 and 4, K is unchanged and therefore the corresponding values of N_1 and N_2 are identical. However, because the counting rates for the two cases differ by a factor of ten, the total time expended also differs by a factor of ten. Examples 7 and 8 demonstrate that for K greater than 50 only a very nominal determination of n_2 is required.

It is of interest to examine further the effect on the total time and on the accuracy when the time is not used in the optimum manner. Table 2 summarizes data for

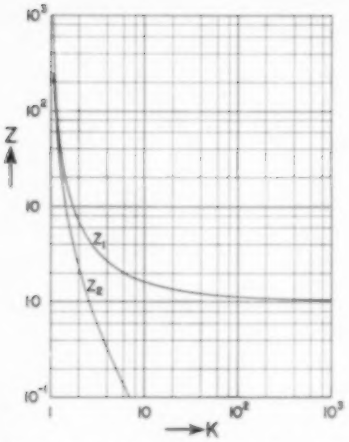

Fig. 2. Graphical solutions of the relations $Z_1 = (K^2 + K^{3/2})/(K-1)^2$ and of $Z_2 = (K^{1/2}+1)/(K-1)^2$.

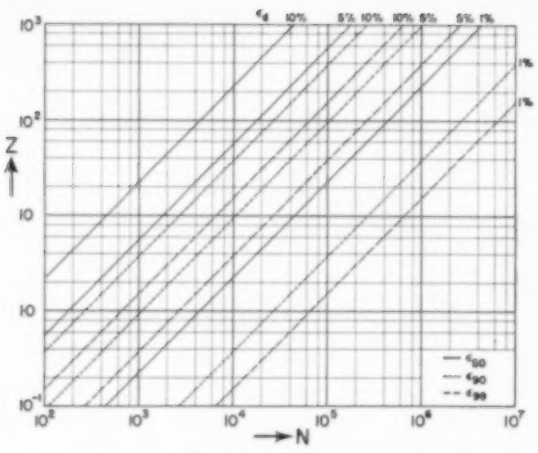

Fig. 3. Graphical solutions of equations (10) and (11) (see text) for various confidence levels and percentage errors. Confidence levels of 50, 90 and 99 per cent are indicated by the solid, dotted and dashed lines respectively. The percentage errors are given at the top of the chart. Note that for $Z = 1$, $N = Q^2/\varepsilon_d^2$.

VOL. 12 1958

Table 1. Effect of selected counting rates on statistical accuracy

Ex.	$\frac{n_1}{(P+B)}$ (c/s)	$\frac{n_2}{B}$ (c/s)	$\frac{n_1-n_2}{P}$ (c/s)	$\frac{n_1-n_2}{n_2}$ P/B	K n_1/n_2	1% accuracy					
						50% conf. level			90% conf. level		
						N_1	N_2	T (sec)	N_1	N_2	T (sec)
1	150	100	50	1 : 2	1·5	73,000	40,000	890	440,000	239,000	5300
2	60	10	50	5 : 1	6·0	9,100	620	210	55,000	3,700	1300
3	40	10	30	3 : 1	4·0	12,000	1,500	450	72,000	9,000	2700
4	15	10	5	1 : 2	1·5	73,000	40,000	8900	440,000	239,000	53000
5	1000	100	900	9 : 1	10·0	7,300	230	10	44,000	1400	58
6	500	100	400	4 : 1	5·0	10,200	910	29	61,000	5400	176
7	500	10	490	49 : 1	50·0	5,300	15	12	32,000	90	73
8	1000	10	990	99 : 1	100·0	5,000	5	5·5	30,000	30	33

Sample calculation: For $(P+B) = n_1 = 150$; $B = n_2 = 100$; $K = 1{\cdot}50$
From Fig. 2, $Z_1 = 16{\cdot}35$; $Z_2 = 8{\cdot}90$.
From Fig. 3, $N_1 = 440{,}000$; $N_2 = 239{,}000$; (1% ε_d and 90% C.L.).

$$\text{Thus, } T = t_1 + t_2 = \frac{N_1}{n_1} + \frac{N_2}{n_2} = \frac{440{,}000}{150} + \frac{239{,}000}{100} = 5300 \text{ sec.}$$

Table 2. Effect on total time and on accuracy when time is not used in the optimum manner

			A: $\frac{t_1}{t_2} = \frac{n_2}{n_1}$			B: $\frac{t_1}{t_2} = \left(\frac{n_1}{n_2}\right)^{1/2}$				C: $\frac{t_1}{t_2} = \left(\frac{n_1}{n_2}\right)^{1/2}$			
n_1 (c/s)	n_2 (c/s)	K	T (sec)	$N_1 = N_2$	ε_d (%)	T (sec)	N_1	N_2	ε_d (%)	ε_d (%)	N_1	N_2	T (sec)
200	100	2	180	12,000	3·3	180	21,000	7500	3·0	3·3	16,500	5900	142
1,000	100	10	180	16,400	1·4	180	136,000	4300	0·6	1·4	21,000	700	28
10,000	100	100	180	17,800	1·2	180	1,600,000	1600	0·14	1·2	19,000	20	2·4

such a situation for three different counting time ratios. For the data in column (A), the total time, T, is divided so that the same number of counts is accumulated in each measurement ($N_1 = N_2$). This determines both n_1 and n_2 to the same relative error. The resultant value of ε_d is to be compared with the value of ε_d in column (B), which is obtained when the same total time is used in the optimum manner (eq. 8). Column (C) gives the total time in which the value of ε_d in column (A) could have been determined if the optimum time division had been used. Note that as K increases, the disparity between ε_d of columns (A) and (B) increases. This is to be expected, for as K increases in the first case ($N_1 = N_2$) a greater proportion of the time is spent on the lower counting rate while in the second case (optimum time) a greater proportion of the time is spent on the higher counting rate.

(C) *Overlapping lines*

Occasionally the expression for net peak takes a slightly different form than that of equation (5). For example, the line whose intensity is to be determined may be situated on the "wing" of another line, and hence the background will not have the constant value assumed in Fig. 1 (a) and equation (5); but rather the situation may be represented by Fig. 1 (b), for which

$$A = n_1 - \beta n_2 \tag{12}$$

where n_2 is the counting rate at the peak of the other line and βn_2 is the value of the background at the position where n_1 is measured. The quantity β, which is determined from the spectral line shape, is a function of the instrument and is known beforehand.

$$\varepsilon_A = \frac{1}{n_1 - \beta n_2}[(n_1\varepsilon_1)^2 + (\beta n_2\varepsilon_2)^2]^{1/2} \tag{13}$$

or

$$\varepsilon_A = \frac{Q}{n_1 - \beta n_2}\left[\frac{n_1}{t_1} + \beta^2\frac{n_2}{t_2}\right]^{1/2} \tag{14}$$

Substitution of (14) in equation (4) yields

$$\frac{t_1}{t_2} = \frac{1}{\beta}\left(\frac{n_1}{n_2}\right)^{1/2} = \frac{1}{\beta^{1/2}}K'^{1/2} \tag{15}$$

where

$$K' = \frac{n_1}{\beta n_2} \tag{16}$$

Manipulation of equations (14) and (15) yields

$$N_1 = \frac{Q^2}{\varepsilon_A^2} K'^{3/2} \beta^{1/2} \frac{(K'/\beta)^{1/2} + 1}{(K' - 1)^2} = \frac{Q^2}{\varepsilon_A^2} Z'_1 \tag{17}$$

$$N_2 = \frac{Q^2}{\varepsilon_A^2} \frac{(K'/\beta)^{1/2} + 1}{(K' - 1)^2} = \frac{Q^2}{\varepsilon_A^2} Z'_2 \tag{18}$$

It is possible then to plot graphs, analogous to Fig. 2, of Z'_1 and Z'_2 as functions of K' for various values of the parameter β. As an example, when $n_1 = 500$ c/s, $\beta n_2 = 100$ c/s and $\beta = 0{\cdot}1$, it may be calculated that for $\varepsilon_r = 1$ per cent at the 50 per cent confidence level, the values of N_1 and N_2 are 8200 and 2200 respectively, with a total time expenditure of 18 sec.

Equation (12) assumes only small overlap, with no contribution to n_2 from the overlap of the line represented by n_1. If the degree of overlap is such that n_2 must be corrected, equation (12) must be divided by $1 - \alpha\beta$, where α is the overlap factor from the first line. However, the results given in equations (13) to (18) will be unaltered because $(1 - \alpha\beta)$ is a constant multiplier of A and will not affect the relative error.

3. Combination of net peak intensities

A number of net peak intensities may be combined together to determine some particular quantity of interest. For example, the analyst may be interested in the determination of the ratio of two line intensities.

The problem to be considered is: given a quantity

$$X = F(A, B, C, \ldots) \tag{19}$$

where $A, B, C, \ldots$ represent individually determined line intensities, each requiring the measurement of two rates (as in Section 2) and a limited total time available for the overall measurement, how should the total available time be distributed among the various n_i, so that a minimum relative statistical error ε_X in the quantity X may be achieved? If there are M quantities $A, B, C, \ldots$ there will be $2M$ individual n_i and $2M$ individual t_i

$$\varepsilon_X = g(\varepsilon_A, \varepsilon_B, \varepsilon_C \ldots) \tag{20}$$

$$q(t_i) = T - (t_i + t_2 + t_3 + t_4 + t_5 + t_6 + \ldots) = 0 \tag{21}$$

Jarrett [5] has shown how to derive explicit forms of ε_X.

The method of LaGrange multipliers yields the following set of equations:

$$\begin{aligned} \frac{\partial \varepsilon_A}{\partial t_1} &= \frac{\partial \varepsilon_A}{\partial t_2} \\ \frac{\partial \varepsilon_B}{\partial t_3} &= \frac{\partial \varepsilon_B}{\partial t_4} \\ \frac{\partial \varepsilon_C}{\partial t_5} &= \frac{\partial \varepsilon_C}{\partial t_6} \end{aligned} \tag{22}$$

VOL. 12 1958

and

$$\frac{\partial g}{\partial \varepsilon_A}\frac{\partial \varepsilon_A}{\partial t_1} = \frac{\partial g}{\partial \varepsilon_B}\frac{\partial \varepsilon_B}{\partial t_3}$$
$$\frac{\partial g}{\partial \varepsilon_A}\frac{\partial \varepsilon_A}{\partial t_1} = \frac{\partial g}{\partial \varepsilon_C}\frac{\partial \varepsilon_C}{\partial t_5} \tag{23}$$

There will be M equations of the type (22) and $(M-1)$ equations of the type (23). These equations plus equation (21) give sufficient equations to determine the $2M$ t_i's.

Equation (21) may be rewritten:

$$[T - (t_3 + t_4 + t_5 + t_6 \ldots)] - t_1 - t_2 = 0 \tag{24}$$

The quantity in brackets is independent of t_1 and t_2. Therefore (24) has the same form as (3). The first of the equations (22) is identical with (4); therefore it is possible to determine the relationship between t_1 and t_2 as if they were independent of the other t_i, and similarly for the other pairs of t_i. This reasoning verifies the intuitive expectation that the time allotted to each of the quantities $A, B, C, \ldots$ should be used in the optimum manner that would be found considering each quantity independently.

Consider the special case

$$X = \frac{A}{B} \tag{25}$$

The relative error in X is

$$\left.\begin{aligned} \varepsilon_X = \varepsilon_r &= [\varepsilon_A{}^2 + \varepsilon_B{}^2)^{1/2} \\ \text{and} \qquad T - (t_1 + t_2 + t_3 + t_4) &= T - (t_A + t_B) = 0 \end{aligned}\right\} \tag{26}$$

Assume that

$$A = n_1 - n_2 \tag{27}$$

$$B = n_3 - n_4 \tag{28}$$

Therefore, ε_A and ε_B may be found from equation (7). Equations (22) result in

$$\frac{t_1}{t_2} = \left(\frac{n_1}{n_2}\right)^{1/2} = K_A{}^{1/2} \tag{29}$$

$$\frac{t_3}{t_4} = \left(\frac{n_3}{n_4}\right)^{1/2} = K_B{}^{1/2} \tag{30}$$

Equations (23) yield

$$\frac{t_1}{t_3} = \left(\frac{n_1}{n_3}\right)^{1/2}\frac{n_3 - n_4}{n_1 - n_2} \tag{31}$$

Combining (29), (30), and (31) yields the division of measurement time between A and B:

$$\frac{t_A}{t_B} = \frac{t_1 + t_2}{t_3 + t_4} = \frac{n_3{}^{1/2} - n_4{}^{1/2}}{n_1{}^{1/2} - n_2{}^{1/2}} \tag{32}$$

Equations (29) and (30) are the same as equation (8). Therefore, as already pointed out, once the division of measurement time between A and B has been determined, the determination of A and B is carried out as prescribed in Section 2. It is first necessary to determine ε_A and ε_B from the stipulated ε_r and the known approximate values of n_1, n_2, n_3, n_4.

Combining equations (7), (26), (29), (30), (31), and (32) gives

$$\frac{\varepsilon_A^2}{\varepsilon_B^2} = \frac{n_2^{1/2} - n_4^{1/2}}{n_1^{1/2} - n_2^{1/2}} = \frac{t_A}{t_B} \tag{33}$$

Substitution in equation (26) gives

$$\varepsilon_A = \varepsilon_r \left[1 + \frac{t_B}{t_A}\right]^{-1/2} = \varepsilon_r \left[1 + \frac{n_1^{1/2} - n_2^{1/2}}{n_3^{1/2} - n_4^{1/2}}\right]^{-1/2} \tag{34}$$

$$\varepsilon_B = \varepsilon_r \left[1 + \frac{t_A}{t_B}\right]^{-1/2} = \varepsilon_r \left[1 + \frac{n_3^{1/2} - n_4^{1/2}}{n_1^{1/2} - n_2^{1/2}}\right]^{-1/2} \tag{35}$$

Thus for given ε_r, n_1, n_2, n_3 and n_4, ε_A and ε_B are computed from equations (34) and (35) and N_1, N_2, and N_3, N_4 are found from Figs. 2 and 3 or equations (8), (10) and (11). For example, if n_1, n_2, n_3, n_4 equal 550, 100, 150 and 100 c/s respectively, for $\varepsilon_r = 1$ per cent at the 50 per cent confidence level, the values of N_1, N_2, N_3 and N_4 will be 67,000, 6000, 86,000 and 47,000 respectively, with a total time expenditure of 2000 sec.

If n_4 and n_2 may be neglected by comparison to n_3 and n_1, equations (33), (34), (35) and (10) reduce to

$$\frac{\varepsilon_A^2}{\varepsilon_B^2} = \frac{t_A}{t_B} = \left(\frac{n_3}{n_1}\right)^{1/2} \tag{36}$$

$$\varepsilon_A = \varepsilon_r [1 + (n_1/n_3)^{1/2}]^{-1/2} \tag{37}$$

$$\varepsilon_B = \varepsilon_r [1 + (n_3/n_1)^{1/2}]^{-1/2} \tag{38}$$

$$N_1 = Q^2/\varepsilon_A^2 \tag{39}$$

$$N_3 = Q^2/\varepsilon_B^2 \tag{40}$$

The derivation given above is not rigorous, because the quantity $1/B$ does not have a Gaussian distribution. However, if $Bt > 400$ its distribution is close enough to Gaussian for these purposes. If $Bt < 400$, ε_B is already large enough that there is little point in discussing relative errors at a given confidence level, and one might just as well deal with the r.m.s. deviation from the mean. In such a case, even for $Bt = 100$ the r.m.s. deviation of $1/B$ from the mean is not significantly different from the r.m.s. deviation of B from the mean (12 per cent compared to 10 per cent).

4. Use of statistical errors in estimating chemical composition

In X-ray analysis, the composition of a given specimen is sought by means of the interpretation of characteristic line intensities. The relative error in the percentage composition is not equal to the relative error in the characteristic line

VOL. 12 1958

intensity measurement unless the composition is proportional to the line intensity. In Fig. 4, A and B represent two calibration curves of intensity (counts/sec) vs. concentration of element "i". Curve A would result for "i" in a low absorption matrix; curve B for "i" in a high absorption matrix. At point p of curve A, an error in the intensity, ε, corresponds to an approximately equal error in concentration. However, at point r, a small relative error in intensity results in a larger

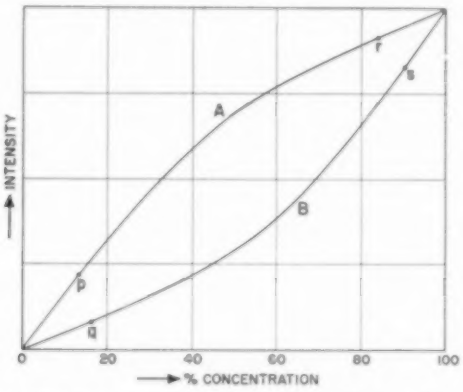

Fig. 4. Typical calibration curves of intensity (counting rate) vs. concentration.

relative error in concentration. At point q of curve B, an intensity error corresponds to an approximately equal error in concentration, while at point s a small relative error in intensity results in an even smaller relative error in concentration. It may be shown that the ratio of the relative error in intensity to the relative error in concentration at a point x is directly proportional to the ratio of the slope of the curve at the point x to the slope of the line from the origin to the point x. (Note that linear scales are assumed for the calibration curves.) This consideration assumes the greatest importance in the upper concentration region of the curve. It applies regardless of whether the intensity error is due to counting rate statistics alone or in combination with other factors.

As a note of caution, it cannot be emphasized too strongly that discussions of counting statistics in a given application are of limited value if other errors (random or systematic) that result from the experimental arrangements are not considered. It is true that significant deviations of the counting statistics from a Gaussian distribution whose standard deviation is the square root of the mean reflect some of the experimental errors [2]. However, it does not follow from the lack of such deviations that all errors have been eliminated, for there are other errors, such as systematic errors, which do not affect the distribution.

5. Conclusions

(1) In X-ray analyses that require two or more intensity measurements, it is often desirable to divide the available measuring time among the measurements in such a manner as to give a minimum error in the quantity of interest.

(2) When the quantity of interest requires the determination of two or more net line intensities in the presence of varying backgrounds, the optimum division

of the total time may be found by determining the optimum amount of time to be allotted to each individual net intensity measurement and then optimizing independently the use of the time for each individual intensity measurement.

(3) For the difference of two counting rates the optimum division of the available counting time results when the ratio of the counting times is directly proportional to the ratio of the square roots of the counting rates.

(4) For the ratio of two counting rates, the optimum division of the available counting time results when the ratio of the counting times is inversely proportional to the ratio of the square roots of the counting rates.

Acknowledgements—We are indebted to Dr. W. Parrish, who suggested this problem and reviewed the manuscript, to Mr. T. Kohler, who made several suggestions, and to several of our colleagues who reviewed the manuscript.

References

[1] Parrish W. *Philips Tech. Rev.* 1956 **17** 206.
[2] Liebhafsky H. A. Pfeiffer H. G. and Zemany P. D. *Analyt. Chem.* 1955 **27** 1257.
[3] Rainwater L. J. and Wu C. S. *Nucleonics* 1947 **1** No. 2 60.
[4] Sokolnikoff I. S. and Sokolnikoff E. S. *Higher Mathematics for Engineers and Physicists* (2nd Ed) pp. 163–167. McGraw-Hill, New York 1941.
[5] Jarrett A. A. *Statistical Measurements Used in the Measurement of Radioactivity.* AECU–262, MonP–126, U.S. Atomic Energy Commission Technical Information Division, Oak Ridge, Tennessee 1946.
[6] Loevinger R. and Berman M. *Nucleonics* 1951 **9** No. 1 26.
[7] Browning W. E. Jr. *Nucleonics* 1951 **9** No. 3 62.
[8] Freedman A. J. and Anderson E. C. *Nucleonics* 1952 **10** No. 8 57.
[9] Beers Y. *Introduction to the Theory of Error* pp. 33–34. Addison–Wesley, New York 1953.
[10] Hoel P. G. *Introduction to Mathematical Statistics* pp. 32, 130. Wiley, New York 1947.
[11] Horton W. S. *Appl. Spectrosc.* 1955 **9** 173.

VOL.
12
1958

Spectrochimica Acta, 1958, Vol. 12, pp. 179 to 182. Pergamon Press Ltd., London

Rydberg term tables

L. H. SUTCLIFFE
Department of Inorganic and Physical Chemistry, The University, Liverpool

(*Received* 22 *October* 1957)

THE expression $109{,}737{\cdot}1/(n-\delta)^2\ \mathrm{cm}^{-1}$ has been evaluated for values of the principal quantum number n ranging from 2 to 11 and for quantum defect (δ) values ranging from 0·00 to 1·00 in intervals of 0·01. Term values are listed in vertical columns beneath the principal quantum numbers; differences between term values are interposed between these columns. The value recently adopted for the Rydberg constant is 109,737·3. If maximum accuracy is sought from these tables therefore, the term value should be multiplied by the factor 1·0000018.

δ \ n	2	3	4	5	6	7	8	9	10	11
1·00	109,737·1	27,434·28	12,193·01	6858·57	4389·48	3048·26	2239·53	1714·64	1354·79	1097·37
	82,302·82	15,241·27	5334·44	2469·09	1341·23	808·72	524·89	359·85	257·42	
0·99	107,574·8	27,161·98	12,112·13	6824·40	4371·98	3038·12	2233·15	1710·36	1351·77	1095·18
	80,412·87	15,049·85	5287·73	2452·42	1333·86	804·97	522·79	358·59	256·59	
0·98	105,475·87	26,893·71	12,032·05	6790·49	4354·58	3028·03	2226·79	1706·10	1348·78	1092·99
	78,582·16	14,861·66	5241·56	2435·91	1326·55	801·24	520·69	357·32	255·79	
0·97	103,437·74	26,629·40	11,952·76	6756·84	4337·28	3018·00	2220·46	1701·85	1345·79	1090·82
	76,808·34	14,676·64	5195·92	2419·56	1319·28	797·54	518·61	356·06	254·97	
0·96	101,458·12	26,368·97	11,874·25	6723·43	4320·09	3008·01	2214·16	1697·62	1342·82	1088·64
	75,089·15	14,494·72	5150·82	2403·34	1312·08	793·85	516·54	354·80	254·18	
0·95	99,534·78	26,112·34	11,796·52	6690·27	4302·99	2998·08	2207·88	1693·41	1339·85	1086·48
	73,422·44	14,315·82	5106·25	2387·28	1304·91	790·20	514·47	353·56	253·37	
0·94	97,665·63	25,859·44	11,719·54	6657·35	4286·00	2988·19	2201·63	1689·21	1336·89	1084·32
	71,806·17	14,139·90	5062·19	2371·35	1297·81	786·56	512·42	352·32	252·57	
0·93	95,848·63	25,610·19	11,643·32	6624·68	4269·11	2978·35	2195·41	1685·03	1333·95	1082·17
	70,238·44	13,966·87	5018·64	2355·57	1290·76	782·94	510·38	351·08	251·78	
0·92	94,081·88	25,364·53	11,567·83	6592·24	4252·32	2968·56	2189·21	1680·86	1331·01	1080·02
	68,717·35	13,796·70	4975·59	2339·92	1283·76	779·35	508·35	349·85	250·99	
0·91	92,363·52	25,122·39	11,493·08	6560·05	4235·63	2958·82	2183·04	1676·70	1328·08	1077·88
	67,241·13	13,629·31	4933·03	2324·42	1276·81	775·78	506·34	348·62	250·20	
0·90	90,691·82	24,883·70	11,419·05	6528·08	4219·03	2949·13	2176·89	1672·57	1325·17	1075·75
	65,808·12	13,464·65	4890·97	2309·05	1269·90	772·24	504·32	347·40	249·42	
0·89	89,065·09	24,648·39	11,345·74	6496·36	4202·54	2939·48	2170·77	1668·44	1322·26	1073·62
	64,416·70	13,302·65	4849·39	2293·82	1263·06	768·71	502·33	346·18	248·64	
0·88	87,481·74	24,416·41	11,273·12	6464·86	4186·14	2929·89	2164·68	1664·34	1319·36	1071·50
	63,065·33	13,143·29	4808·26	2278·72	1256·25	765·21	500·34	344·98	247·86	
0·87	85,940·25	24,187·68	11,201·21	6433·59	4169·83	2920·33	2158·61	1660·25	1316·47	1069·39
	61,752·57	12,986·47	4767·62	2263·76	1249·50	761·72	498·36	343·78	247·08	
0·86	84,439·14	23,962·16	11,129·98	6402·55	4153·62	2910·83	2152·57	1656·17	1313·59	1067·28
	60,476·98	12,832·18	4727·43	2248·93	1242·79	758·26	496·40	342·58	246·31	
0·85	82,977·04	23,739·77	11,059·42	6371·73	4137·51	2901·37	2146·55	1652·11	1310·72	1065·18
	59,237·27	12,680·35	4687·69	2234·22	1236·14	754·82	494·44	341·39	245·54	
0·84	81,552·54	23,520·47	10,989·54	6341·13	4121·89	2891·96	2140·56	1648·06	1307·86	1063·08
	58,032·07	12,530·93	4648·41	2219·24	1229·93	751·40	492·50	340·20	244·78	
0·83	80,154·44	23,304·19	10,920·31	6310·76	4105·56	2882·59	2134·59	1644·03	1305·01	1060·99
	56,850·25	12,383·88	4609·55	2205·20	1222·97	748·00	490·56	339·02	244·02	

δ \ n	2	3	4	5	6	7	8	9	10	11
0·82	78,811·47	23,080·88	10,851·74	6280·60	4089·72	2873·27	2128·65	1640·01	1302·17	1058·91
	55,729·59	12,139·14	4571·14	2190·88	1216·45	744·61	488·64	337·84	243·26	
0·81	77,492·48	22,880·49	10,783·81	6250·65	4073·98	2863·99	2122·73	1636·01	1299·34	1056·83
	54,611·99	12,096·68	4533.26	2176·68	1209·99	741·16	486·72	336·67	242·51	
0·80	76,206·33	22,672·95	10,716·51	6220·92	4058·33	2854·76	2116·84	1632·02	1296·50	1054·75
	53,533·38	11,956·44	4495·50	2162·59	1203·57	737·92	484·82	335·52	247·15	
0·79	74,951·92	22,468·23	10,649·85	6191·41	4042·76	2845·58	2110·97	1628·05	1293·70	1052·69
	52,483·69	11,818·38	4458·44	2148·65	1197·18	734·61	482·92	334·35	241·01	
0·78	73,728·23	22,266·27	10,583·80	6162·10	4027·29	2836·43	2105·13	1624·09	1290·90	1050·63
	51,461·96	11,682·47	4421·70	2134·81	1190·86	731·30	481·04	333·19	240·27	
0·77	72,534·27	22,067·02	10,518·37	6133·09	4011·90	2827·34	2099·31	1620·14	1288·10	1048·58
	50,467·25	11,548·65	4385·37	2121·10	1184·56	728·03	479·17	332·04	239·52	
0·76	71,369·08	21,870·44	10,453·54	6104·10	3996·60	2818·28	2093·52	1616·21	1285·31	1046·53
	49,498·64	11,416·90	4349·44	2107·50	1178·32	724·76	477·31	330·90	238·78	
0·75	70,231·75	21,676·47	10,389·31	6075·41	3981·39	2809·27	2087·75	1612·30	1282·54	1044·49
	48,555·28	11,287·16	4313·90	2094·02	1172·12	721·52	475·45	329·76	238·05	
0·74	69,121·38	21,485·06	10,325·67	6046·92	3966·27	2800·30	2082·00	1608·40	1279·77	1042·46
	47,636·32	11,159·39	4278·75	2080·65	1165·97	718·30	473·60	328·63	237·31	
0·73	68,037·14	21,296·18	10,262·61	6018·63	3951·23	2791·38	2076·27	1604·51	1277·01	1040·43
	46,740·96	11,033·57	4243·98	2067·40	1159·85	715·11	471·76	327·50	236·58	
0·72	66,978·21	21,109·60	10,200·13	5990·54	3936·28	2782·49	2070·57	1600·64	1274·26	1038·41
	45,868·61	10,909·47	4209·59	2054·26	1153·79	711·92	469·93	326·38	235·85	
0·71	65,943·81	20,925·82	10,138·22	5962·64	3921·41	2773·65	2064·90	1596·78	1271·52	1036·39
	45,017·99	10,787·60	4175·58	2041·23	1147·76	708·75	468·12	325·26	235·13	
0·70	64 933·18	20,744·26	10,076·87	5934·94	3906·63	2764·86	2059·24	1592·93	1268·78	1034·38
	44,188·92	10,667·39	4141·93	2028·31	1141·77	705·62	466·31	324·15	234·40	
0·69	63,945·63	20,565·04	10,016·07	5907·43	3891·92	2756·10	2053·61	1589·10	1266·06	1032·37
	43,380·59	10,548·97	4108·64	2015·51	1135·82	702·49	464·51	323·04	233·69	
0·68	62,980·43	20,388·14	9955·83	5880·12	3877·31	2747·38	2048·01	1585·28	1263·34	1030·37
	42,592·29	10,432·31	4075·73	2002·81	1129·93	699·37	462·73	321·94	232·97	
0·67	62,036·92	20,213·51	9896·12	5852·99	3862·77	2738·71	2042·42	1581·48	1260·64	1028·38
	41,823·41	10,317·39	4043·13	1990·22	1124·06	696·29	460·94	320·84	232·26	
0·66	61,114·45	20,041·11	9836·95	5826·05	3848·32	2730·08	2036·86	1577·69	1257·94	1026·39
	41,073·34	10,204·16	4010·90	1977·73	1118·24	693·22	459·17	319·75	231·55	
0·65	60,212·39	19,870·91	9778·31	5799·29	3833·95	2721·48	2031·32	1573·91	1255·25	1024·41
	40,341·48	10,092·60	3979·02	1965·34	1112·47	690·16	457·41	318·66	230·84	
0·64	59,330·18	19,702·87	9720·19	5772·72	3819·65	2712·93	2025·81	1570·15	1252·57	1022·43
	39,627·31	9982·68	3947·47	1953·07	1106·72	687·12	455·66	317·58	230·14	
0·63	58,467·21	19,536·95	9662·59	5746·33	3805·44	2704·42	2020·31	1566·39	1249·88	1020·44
	38,930·26	9874·36	3916·26	1940·89	1101·02	684·11	453·92	316·51	229·44	
0·62	57,622·93	19,373·12	9605·50	5720·12	3791·31	2695·95	2014·85	1562·67	1247·23	1018·50
	38,249·81	9767·62	3885·38	1928·81	1095·36	681·10	452·18	315·44	228·73	
0·61	56,796·80	19,211·34	9548·02	5694·09	3777·25	2687·52	2009·39	1558·94	1244·58	1016·54
	37,585·46	9662·42	3854·83	1916·84	1089·73	678·13	450·45	314·36	228·04	
0·60	55,988·32	19,051·58	9492·83	5668·24	3763·28	2679·13	2003·96	1555·23	1241·93	1014·58
	36,936·74	9558·75	3824·59	1904·96	1084·15	675·17	448·73	313·30	227·35	
0·59	55,196·97	18,893·80	9437·23	5642·56	3749·38	2670·78	1998·56	1551·53	1239·29	1012·63
	36,303·17	9456·57	3794·67	1893·18	1078·69	672·22	447·03	312·24	226·66	
0·58	54,422·29	18,737·98	9382·13	5617·06	3735·55	2662·46	1993·18	1547·85	1236·66	1010·69
	35,684·31	9355·85	3765·07	1881·51	1073·09	669·28	445·33	311·19	225·97	
0·57	53,663·80	18,584·07	9327·50	5591·73	3721·81	2654·19	1987·81	1544·18	1234·04	1008·75
	35,079·73	9256·57	3735·77	1869·92	1067·62	666·38	443·63	310·14	225·29	
0·56	52,921·06	18,432·06	9273·35	5566·57	3708·14	2645·95	1982·47	1540·52	1231·43	1006·82
	34,489·60	9158·71	3706·78	1858·43	1062·19	663·48	441·95	309·09	224·61	
0·55	52,193·63	18,281·99	9219·67	5541·58	3694·54	2637·75	1977·16	1536·88	1228·82	1004·90
	33,911·73	9062·23	3678·09	1847·04	1056·79	660·59	440·28	308·06	223·92	
0·54	51,481·09	18,133·57	9166·45	5516·76	3681·02	2629·59	1971·86	1533·25	1226·23	1002·98
	33,347·52	8967·12	3649·69	1835·74	1051·43	657·73	438·61	307·02	223·25	

VOL. 12 1958

δ \ F	2	3	4	5	6	7	8	9	10	11
0·53	50,783·05	17,987·03	9113·70	5492·10	3667·57	2621·47	1966·58	1529·63	1223·64	1001·06
	32,796·02	8873·33	3621·60	1824·53	1046·10	654·89	436·95	305·99	222·58	
0·52	50,099·11	17,842·27	9091·39	5467·61	3654·20	2613·39	1961·33	1526·03	1221·06	999·15
	32,256·84	8780·88	3593·78	1813·41	1040·81	652·06	435·30	304·97	221·91	
0·51	49,428·90	17,699·25	9069·54	5443·28	3640·90	2605·34	1956·09	1522·43	1218·49	997·25
	31,729·65	8689·71	3566·26	1802·38	1035·56	649·25	433·66	303·94	221·24	
0·50	48,772·04	17,557·94	8958·13	5419·12	3627·67	2597·33	1950·88	1518·85	1215·92	995·35
	31,214·10	8599·81	3539·01	1791·45	1030·34	646·45	432·03	302·93	220·57	
0·49	48,128·20	17,418·31	8907·16	5395·11	3614·52	2589·39	1945·69	1515·29	1213·37	993·45
	30,709·89	8511·15	3512·05	1780·59	1025·13	643·70	430·40	301·92	219·92	
0·48	47,497·01	17,280·34	8856·62	5371·27	3601·43	2581·42	1940·52	1511·73	1210·82	991·57
	30,216·67	8423·72	3485·35	1769·84	1020·01	640·90	428·79	300·91	219·25	
0·47	46,878·17	17,144·01	8806·51	5347·58	3588·42	2573·52	1935·37	1508·19	1208·28	989·68
	29,734·16	8337·50	3458·93	1759·16	1014·90	638·15	427·18	299·91	218·60	
0·46	46,271·34	17,009·28	8756·83	5324·05	3575·48	2565·65	1930·24	1504·66	1205·75	987·81
	29,262·06	8252·45	3432·78	1748·57	1009·83	635·41	425·58	298·91	217·94	
0·45	45,676·21	16,876·14	8707·56	5300·67	3562·60	2557·83	1925·13	1501·14	1203·22	985·94
	28,800·07	8168·58	3406·89	1738·07	1004·77	632·70	423·99	297·92	217·28	
0·44	45,092·50	16,744·55	8658·72	5277·45	3549·80	2550·03	1920·04	1497·63	1200·71	984·07
	28,347·95	8085·83	3381·27	1727·65	999·77	629·99	422·41	296·92	216·64	
0·43	44,519·90	16,614·50	8610·28	5254·38	3537·07	2542·28	1914·97	1494·14	1198·20	982·21
	27,935·40	8004·22	3355·90	1717·31	994·79	627·31	420·83	295·94	215·99	
0·42	43,958·14	16,485·95	8562·24	5231·46	3524·40	2534·55	1909·92	1490·66	1195·70	980·35
	27,471·19	7923·71	3330·78	1707·06	989·85	624·63	419·26	294·96	215·35	
0·41	43,406·95	16,358·89	8514·61	5208·69	3511·80	2526·87	1904·89	1487·19	1193·21	978·50
	27,048·06	7844·28	3305·92	1696·89	984·93	621·98	417·70	293·98	214·71	
0·40	42,866·05	16,233·30	8467·37	5186·06	3499·27	2519·22	1899·88	1483·74	1190·72	976·66
	26,632·75	7765·93	3281·31	1686·79	980·05	619·34	416·14	293·02	214·06	
0·39	42,335·21	16,109·14	8420·52	5163·59	3486·81	2511·60	1894·89	1480·29	1188·25	974·82
	26,226·07	7688·62	3256·93	1676·78	975·21	616·71	414·60	292·04	213·43	
0·38	41,814·17	15,986·41	8374·07	5141·26	3474·41	2504·02	1889·92	1476·86	1185·78	972·98
	25,827·76	7612·34	3232·81	1666·85	970·39	614·10	413·06	291·08	212·80	
0·37	41,302·68	15,865·07	8327·99	5119·08	3462·08	2496·47	1884·97	1473·44	1183·32	971·15
	25,437·61	7537·08	3208·91	1657·00	965·61	611·50	411·53	290·12	212·17	
0·36	40,800·53	15,745·11	8282·30	5097·03	3449·81	2488·96	1880·04	1470·03	1180·86	969·33
	25,055·42	7462·81	3185·27	1647·22	960·85	608·92	410·01	289·17	211·53	
0·35	40,307·47	15,626·50	8236·97	5075·13	3437·61	2481·48	1875·13	1466·63	1178·42	967·51
	24,680·97	7389·53	3161·84	1637·52	956·13	606·35	408·50	288·21	210·91	
0·34	39,823·31	15,509·23	8192·03	5053·38	3425·47	2474·03	1870·23	1463·25	1175·98	965·69
	24,314·08	7317·29	3138·65	1627·91	951·44	604·80	406·98	287·27	210·29	
0·33	39,347·81	15,393·27	8147·44	5031·76	3413·40	2466·62	1865·36	1459·87	1173·55	963·88
	23,954·54	7245·83	3115·68	1618·36	946·78	601·26	405·49	286·32	209·67	
0·32	38,880·78	15,278·61	8103·22	5010·28	3401·39	2459·24	1860·51	1456·51	1171·12	962·08
	23,602·17	7175·39	3092·94	1608·89	942·15	598·73	404·00	285·39	209·04	
0·31	38,422·00	15,165·23	8059·36	4988·93	3389·45	2451·89	1855·67	1453·16	1168·71	960·28
	23,256·77	7105·87	3070·43	1599·48	937·56	596·22	402·51	284·45	208·43	
0·30	37,971·32	15,053·10	8015·86	4967·73	3377·57	2444·58	1850·85	1449·82	1166·30	958·49
	22,918·22	7037·24	3048·13	1590·16	932·99	593·73	401·03	283·52	207·81	
0·29	37,528·50	14,942·21	7972·70	4946·65	3365·74	2437·29	1846·05	1446·49	1163·89	956·69
	22,586·29	6969·51	3026·05	1580·91	928·45	591·24	399·56	282·60	207·20	
0·28	37,093·40	14,832·54	7929·90	4925·72	3353·99	2430·05	1841·28	1443·18	1161·50	954·91
	22,260·86	6902·64	3004·18	1571·73	923·94	588·77	398·10	281·68	206·59	
0·27	36,665·81	14,724·08	7887·44	4904·91	3342·29	2422·83	1836·52	1439·88	1159·12	953·13
	21,941·73	6836·64	2982·53	1562·62	919·46	586·31	396·64	280·76	205·99	
0·26	36,245·57	14,616·80	7845·31	4884·24	3330·66	2415·65	1831·77	1436·58	1156·74	951·36
	21,628·77	6771·49	2961·07	1553·58	915·01	583·88	395·19	279·84	205·38	
0·25	35,832·53	14,510·69	7803·53	4863·69	3319·08	2408·50	1827·05	1433·30	1154·37	949·59
	21,321·84	6707·16	2939·84	1544·61	910·58	581·45	393·75	278·93	204·78	

δ \ n	2	3	4	5	6	7	8	9	10	11
0·24	35,426·49	14,405·73	7762·07	4843·28	3307·57	2401·88	1822·34	1430·03	1152·09	947·83
	21,020·76	6643·66	2918·79	1535·71	906·19	579·04	392·31	278·03	204·17	
0·23	35,027·32	14,301·01	7720·95	4822·09	3296·11	2394·29	1817·65	1426·77	1149·65	946·07
	20,725·41	6580·96	2897·96	1526·88	901·82	576·64	390·88	277·12	203·58	
0·22	34,634·86	14,199·20	7680·15	4802·84	3284·72	2387·23	1812·90	1423·52	1147·30	944·31
	20,435·66	6519·05	2877·31	1518·12	897·49	574·24	389·47	276·22	202·99	
0·21	34,248·96	14,097·60	7639·68	4782·80	3273·38	2380·20	1808·33	1420·29	1144·95	942·56
	20,151·36	6457·02	2856·88	1509·42	893·18	571·87	388·04	275·34	202·39	
0·20	33,869·48	13,997·08	7599·52	4762·89	3262·10	2373·21	1803·70	1417·06	1142·62	940·82
	19,872·40	6397·56	2836·63	1500·79	888·89	569·51	386·64	274·44	201·80	
0·19	33,496·26	13,897·63	7559·68	4743·11	3250·88	2366·24	1799·08	1413·84	1140·29	939·08
	19,598·63	6337·95	2816·57	1492·23	884·64	567·16	385·24	273·55	201·21	
0·18	33,129·18	13,799·24	7520·15	4723·45	3239·72	2359·31	1794·49	1410·64	1137·97	937·34
	19,329·94	6279·09	2796·70	1483·73	880·41	564·82	383·85	272·67	200·63	
0·17	32,768·10	13,701·89	7480·94	4703·91	3228·62	2352·40	1789·90	1407·45	1135·66	935·61
	19,066·21	6220·95	2777·03	1475·29	876·22	562·50	382·45	271·79	200·05	
0·16	32,412·90	13,605·57	7442·02	4684·49	3217·57	2345·53	1785·34	1404·26	1133·35	933·89
	18,807·33	6163·55	2757·53	1466·92	872·04	560·19	381·08	270·91	199·46	
0·15	32,063·44	13,510·26	7403·42	4665·20	3206·58	2338·69	1780·80	1401·09	1131·05	932·17
	18,553·18	6106·84	2738·22	1458·62	867·89	557·89	379·71	270·04	198·88	
0·14	31,719·59	13,415·94	7365·10	4646·01	3195·64	2331·87	1776·27	1397·93	1128·75	930·45
	18,303·65	6050·84	2719·09	1450·37	863·77	555·60	378·34	269·18	198·30	
0·13	31,381·25	13,322·62	7327·09	4626·96	3184·76	2325·09	1771·75	1394·77	1126·47	928·74
	18,058·63	5995·53	2700·13	1442·20	859·67	553·34	376·98	268·30	197·73	
0·12	31,048·30	13,230·26	7289·37	4608·01	3173·94	2318·34	1767·26	1391·65	1124·19	927·04
	17,818·04	5940·89	2681·36	1434·07	855·69	551·08	375·62	267·46	197·15	
0·11	30,720·61	13,138·86	7251·94	4589·19	3163·17	2311·61	1762·79	1388·51	1121·92	925·33
	17,581·85	5886·92	2662·75	1426·02	851·56	548·82	374·28	266·59	196·59	
0·10	30,398·09	13,048·41	7214·80	4570·47	3152·46	2304·92	1758·33	1385·39	1119·65	923·64
	17,349·68	5833·61	2644·33	1418·01	847·54	546·59	372·94	265·74	196·01	
0·09	30,080·62	12,958·88	7177·94	4551·88	3141·80	2298·25	1753·88	1382·29	1117·39	921·94
	17,121·74	5780·94	2626·06	1410·08	843·55	544·38	371·59	264·90	195·45	
0·08	29,768·09	12,870·27	7141·37	4533·39	3131·19	2291·61	1749·46	1379·19	1115·14	920·25
	16,897·82	5728·90	2607·98	1402·20	839·58	542·17	370·27	264·05	194·88	
0·07	29,460·42	12,782·57	7105·07	4515·02	3120·64	2285·00	1745·04	1376·10	1112·90	918·57
	16,677·85	5677·50	2590·05	1394·38	835·64	539·96	368·94	263·20	194·33	
0·06	29,157·48	12,695·76	7069·05	4496·76	3110·14	2278·42	1740·65	1373·02	1110·66	916·89
	16,461·72	5626·71	2572·29	1386·62	831·72	537·77	367·63	262·36	193·77	
0·05	28,859·20	12,609·84	7033·30	4478·61	3099·70	2271·87	1736·28	1369·96	1108·43	915·22
	16,249·36	5576·54	2554·69	1378·91	827·83	535·59	366·32	261·53	193·21	
0·04	28,565·47	12,524·78	6997·83	4460·57	3089·31	2265·35	1731·92	1366·90	1106·20	913·55
	16,040·69	5526·95	2537·26	1371·26	823·96	533·43	365·02	260·70	192·65	
0·03	28,276·29	12,440·58	6962·62	4442·64	3078·97	2258·85	1727·58	1363·86	1103·99	911·89
	15,835·62	5477·96	2519·98	1363·67	820·12	531·27	363·72	259·87	192·10	
0·02	27,991·30	12,357·22	6927·67	4424·81	3068·68	2252·39	1723·25	1360·82	1101·77	910·23
	15,634·08	5429·55	2502·86	1356·13	816·29	529·14	362·43	259·05	191·54	
0·01	27,710·69	12,274·71	6892·99	4407·09	3058·44	2245·95	1718·94	1357·80	1099·57	908·57
	15,435·98	5381·72	2485·90	1348·65	812·49	527·01	361·14	258·23	191·00	

VOL. 12 1958

Spectrochimica Acta, 1958, Vol. 12, pp. 183 to 191. Pergamon Press Ltd., London

Cavity type micro-cells for infrared spectrometry*

R. Norman Jones and Armand Nadeau
Division of Pure Chemistry, National Research Council of Canada,
Ottawa, Canada

(*Received* 8 *Feburary* 1958)

Abstract—Two new types of cells suitable for the measurement of infrared absorption spectra of liquids and solutions are described:

(a) A semimicro-cell designed for use with a Perkin–Elmer Model 21 spectrophotometer.

(b) A micro-cell for use in conjunction with an infrared micro-illuminator.

In both types of cells the sample cavity is formed within a rectangular block of rock salt by conventional drilling and ultrasonic impact grinding. The absence of gasket seals eliminates the possibility of sample leakage, and, in the case of the micro-cell, provision is made for total sample transfer into the cell by including a "flask" cavity communicating directly with the optical cell cavity.

The simple construction of these cells makes it economically feasible to use them in large numbers. This allows a substantial increase in the functioning rate of the spectrometer by reducing interruptions in recording for frequent cleaning and refilling of a limited number of cells.

Introduction

The construction and design of liquid-containing cells for infrared spectrometers have undergone little modification during the past few years. With few exceptions, the cells in current use consist essentially of a pair of flat plates of optically transparent material separated by a spacer. Access to the cell cavity is provided by holes drilled through the side of the spacer or through the face of one of the windows. Unless carefully constructed and maintained, such cells are subject to leakage. If the windows and spacers are sealed with a chemical adhesive, leaks may develop through attack on the adhesive by the solvent, and products extracted from the adhesive may contaminate the sample and invalidate the spectrum. In cells of more recent design, these difficulties have been overcome by careful polishing and machining of the component parts so that a leak resistant seal between window and spacer can be achieved by the application of pressure alone. Such cells, however, are expensive to produce, and their servicing and replacement is a significant economic factor on the maintenance of an infrared spectrometer in routine operation.

The conventional type of liquid cell has the further disadvantage that no methods are available to ensure the total transfer of the sample from its containing vial into the functional part of the cell; this becomes increasingly serious as the total amount of material available for analysis diminishes. By the use of a micro-illuminator, it has been demonstrated that useful spectra can be obtained from solutions in cells having a functional volume of less than 1 mm^3, with less

* Published as Contribution No. 4753 from the Laboratories of the National Research Council of Canada. Presented, in part, at the Chemical Society Symposium on Terpenoid Compounds, Glasgow, Scotland, 12 July 1957.

than 5 μg of solute in the optical beam [1, 2]. The manipulative losses, however, are so large that many times this weight of sample material is required. In consequence of this, the trend in micro-sampling techniques has been away from solution measurements towards the use of micro-pellets in potassium bromide. This circumvents the major difficulties of semi-quantitative micro-sample transfer, but the resultant spectra are subject to complication from polymorphism, and stress effects in the disk [3–5].

In our laboratory, a variety of cells suitable for use with liquids and solutions have been constructed in which these disadvantages have been overcome by drilling or grinding the cell cavity in a single rectangular block of rock salt. A selection of these cells is shown in Fig. 1.

The feasibility of drilling cell cavities in rock salt plates was demonstrated in 1954 by Lewis, Wiggins and Wootton [6], who described a cell consisting of a cylindrical cavity drilled through a rock salt plate and stoppered at each end with tapered polythene plugs. In our experience this cell suffered from three defects. In the first place, one of the two stoppers was at the bottom of the cell when the latter was aligned in front of the spectrometer slit; this aggravated leakage difficulties and could lead to a complete loss of sample. The circular cross-section of the cell introduced critical alignment problems and made it virtually impossible to use the cell in a double-beam spectrometer compensated with a plane parallel faced variable thickness cell of conventional design. Thirdly, this design did not make provision for total sample transfer when used on the micro scale.

VOL. 12 1958

The cell we wish to describe has been developed in two basic forms. (a) A semimicro-cell suitable for use with a Perkin–Elmer Model 21, or similar spectrophotometer. (b) A micro-cell for use in conjunction with a micro-illuminator in a single beam spectrometer. Provision for total sample transfer has been built into the micro-cell, and, using this cell, spectra satisfactory for identification purposes have been obtained where the total sample available for analysis did not exceed 10 μg.

Semimicro-cells

Three forms of the semimicro-cell will be described. Types A and B are cells of 1 mm thickness suitable for use with dilute solutions, while Type C is a thinner cell of 0·1 mm thickness.

Type A

This cell is shown diagrammatically in Fig. 2. It is constructed from two rectangular blocks of rock salt. The lower block is 17 mm high by 10 mm wide by 8 mm thick. In this is formed a rectangular cavity, the sides of which are parallel with the sides of the block: the cavity is 12 mm high, 2 or 3 mm wide and 1 mm thick. This cavity opens to the upper surface of the block. To the top of this block is sealed the second rock salt block. This has the same cross-section as the lower block and contains a cylindrical hole of about 1·5 mm diameter. This hole communicates directly with the rectangular cavity of the lower block and provides the filling orifice; it can be closed with a Teflon stopper. The cell is used in the normal sample cell position of the Perkin–Elmer Model 21 spectrophotometer

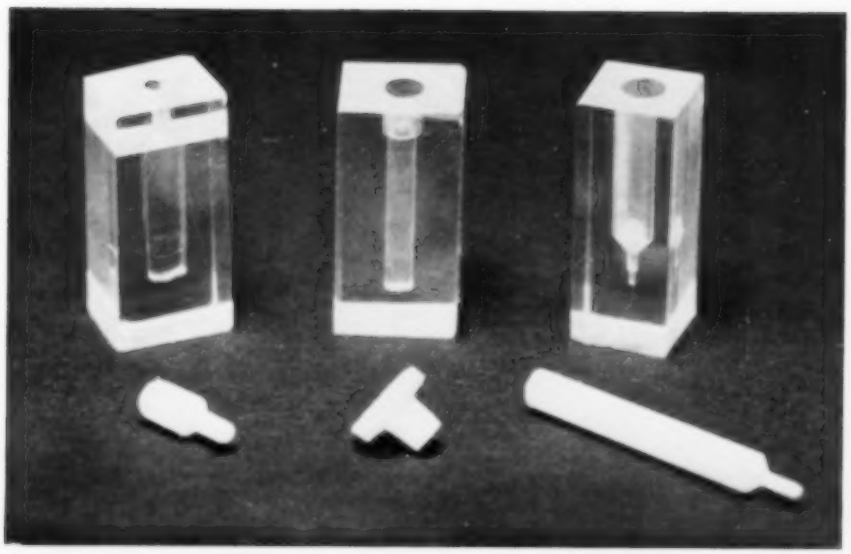

Fig. 1. Cavity type infrared absorption cells. (*Left*) Type A semimicro-cell. (*Center*) Type B semimicro-cell. (*Right*) Micro-cell with cylindrical "cell" cavity

VOL.
12
1958

in an adjustable holder arranged to provide lateral alignment with the entrance slit. Such a cell holder is illustrated on p. 312 of reference [7].

The rectangular cavity is ground out by means of an ultrasonic impact drill. The general technique for producing small cavities in brittle materials by ultrasonic impact grinding has been described by HARTLEY [8]; we employed a 50 W Mullard drill (Type E7680/2). The initial cavity can be produced in 2–3 min using a slightly undersized mild steel bit with no. 280 mesh carborundum abrasive

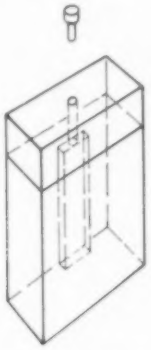

Fig. 2. Type A semimicro-cell.

suspended in absolute ethanol. The walls of the cavity so produced have a coarsely etched appearance. A preliminary polish is obtained by repeating the drilling process with a slightly larger bit and a fine emery powder (American Optical Co. no. 303½). A final smooth surface is then achieved by flushing out the cell rapidly with 50 per cent aqueous ethanol followed immediately by absolute ethanol. The circular hole in the upper block is drilled with a no. 53 machinist's drill, kept well lubricated with light machine oil. The contact surfaces of the two blocks are then smoothed with 600 mesh grinding paper, moistened with saturated aqueous sodium chloride solution, clamped under pressure and bonded by heating at 110°C for 12 hr. By this means strong bonds between rock salt plates can be obtained which will resist cleavage at temperatures at least to 200°C. The bonded surface is not optically clear, but this is immaterial as it is not in the optical beam.

A spectrum obtained with such a cell for 500 μg of etiocholane-3:17-dione in carbon disulfide solution with a Perkin–Elmer variable thickness cell in the compensating beam is shown in Fig. 3. Linear compensation within $\pm$ 0·01 units of optical density is obtained between 4000 and 700 cm^{-1}, except for small regions near 2170 and 1375 cm^{-1}. These regions are associated with the trailing edges of very strong solvent bands and are most susceptible to minor differences in the optical paths of the two beams.

Type B

A modification of the above cell is shown in Fig. 4. This contains a similar rectangular cell cavity, but the whole cell is constructed from a single rock salt block, and the seal associated with narrow filling orifice is avoided.

This cell is formed by first drilling a wider filling orifice consisting of a circular

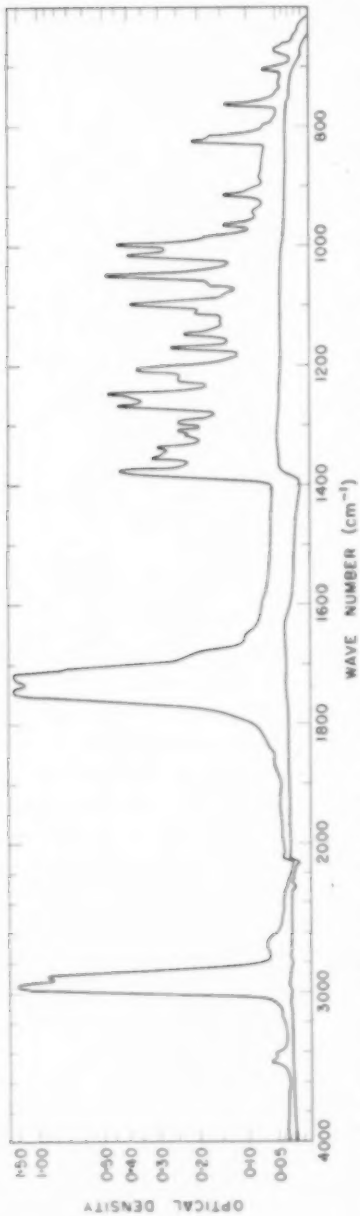

Fig. 3. Spectrum obtained with Type A semimicro-cell. (500 μg of etiocholane-3:17-dione in carbon disulfide solution using a Perkin-Elmer Model 21 spectrophotometer and variable thickness cell in the compensating beam).

VOL. 12 1958

hole 3 mm in diameter and 3–5 mm deep. The rectangular cavity is then formed from the bottom of this hole by ultrasonic impact drilling exactly as described above. A tapered Teflon stopper is employed. This form of cell is simpler and cheaper to construct than the Type A cell. It has the advantage that the larger filling orifice can be used in a similar manner to the "flask" of the micro-cell described below, to permit total sample transfer. Because of the wider neck however it is more difficult to avoid solvent evaporation and greater care must be exercised to maintain a tightly fitting stopper while the cell is in use.

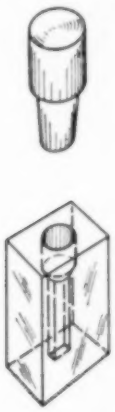

Fig. 4. Type B semimicro-cell.

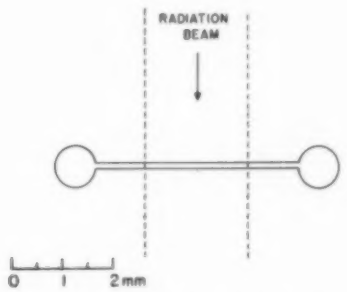

Fig. 5. Diagrammatic cross-section through Type C semimicro-cell.

Type C

Cells of Types A and B provide a sample thickness of approximately 1 mm and are therefore suitable for work with dilute solutions. It is quite feasible to form narrower slots in rock salt by the ultrasonic drilling technique; but, unless special precautions are taken, the bits become very delicate and tend to deform during the grinding process, producing curved slots that are no longer parallel with the outside faces of the cell. This difficulty can be avoided by the use of a bit of dumb-bell shaped cross-section as shown in Fig. 5. The rounded side members are formed from steel rod of approximately 0·75 mm diameter, while the cross bar that grinds the functional slot is constructed from a section of a steel feeler gauge of 0·001–0·003 in. thickness, soldered or spot-welded to the supporting bars. The cell cavity produced by this bit has the dumb-bell cross-section, and there is an appreciable parasitic volume in the lateral cylindrical chambers. This however is not critical for many purposes. The cylindrical side chambers will accept a no. 22 hypodermic needle and this permits the cell to be cleaned rapidly by flushing out with solvent. Cells of this type have been constructed with a functional thickness down to 0·1 mm.

The micro-cell

The two forms of the micro-cell are illustrated in Figs. 6 and 7. The form shown in Fig. 6 is simpler to construct and will serve as a basis for a general description.

The cell is formed from a rectangular block of rock salt, 20 mm high by 8 mm wide by 8 mm thick. It consists of three concentric cylindrical cavities of decreasing diameter, drilled down from the top. The largest and uppermost cavity (3 mm diam. by 10 mm long) constitutes the "flask"; the middle cavity (1 mm diam. by 2 mm long) is the "neck", and the lowest cavity (0·50 mm diam. by 1·5 mm long) is the "cell". The junctions between "flask" and "neck", and between "neck" and "cell" are beveled. The inner walls of the several cavities must be moderately smooth, but need not be optically polished. When the cell is

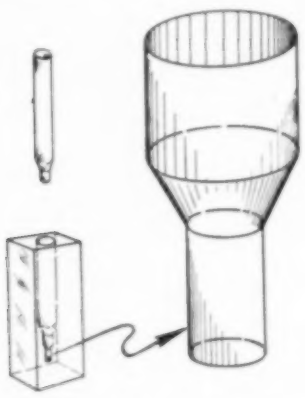

Fig. 6. Micro-cell with circular "cell" cavity.

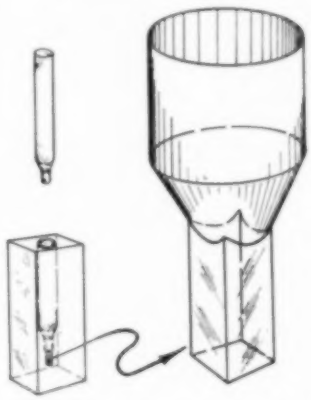

Fig. 7. Micro-cell with rectangular "cell" cavity.

in use, the "neck" is closed by a well-fitting Teflon stopper, the stem of which is long enough to extend through the "flask" section and out at the top of the cell. If the holes are bored with a sharp drill operated at 400 rev/min and lubricated liberally with light machine oil, no additional polishing is required. In order to obtain a suitable slope to the beveled sections, the drill bits are modified to have a point angle of 90° instead of the normal angle of 120°. To form the "cell" cavity a no. 76 machinist's drill is used. During the drilling process the rock salt block is supported by cementing with paraffin wax on a precision drill stand with micrometer motion in all planes. Two of the opposite outside faces of the cell are optically polished and marked so as to ensure that the cell is always repositioned with the radiation passing through in the same direction.

To fill the cell, the sample is first dissolved in a suitable volatile solvent, and transferred by syringe or micro-pipette from its containing vial into the "flask". The whole cell unit is then placed on the electrical heating plate *A* (Fig. 8). This is constructed from a brass block mounted on a Transite base. Heat is provided by a small soldering iron which is operated through a Variac, and which fits into a cavity in the brass block; another cavity holds a thermometer. The temperature is adjusted to within a few degrees of the boiling point of the solvent, and the rate of evaporation is controlled by the insertion of a micro-reflux condenser (*B*). This consists of a finned cylinder of brass or aluminum which rests lightly on the top of the cell. From the lower surface of the cylinder a projection extends down a few millimeters into the cell to touch the wall. This loosely fitting condenser

VOL. 12 1958

permits the gradual evaporation of the solvent, while promoting sufficient reflux action to wash the walls of the "flask" and prevent upward creep of the depositing solute; this can be troublesome for certain types of materials. The evaporation process is continued until a quantitative transfer of sample material from the sample vial to the "flask" has been achieved, after which the residual solvent is removed and the cell cooled. At any time during the transfer process the evaporation can be checked instantly by placing the cell on the "cold plate" (*C*) which consists simply of a brass block at room temperature.

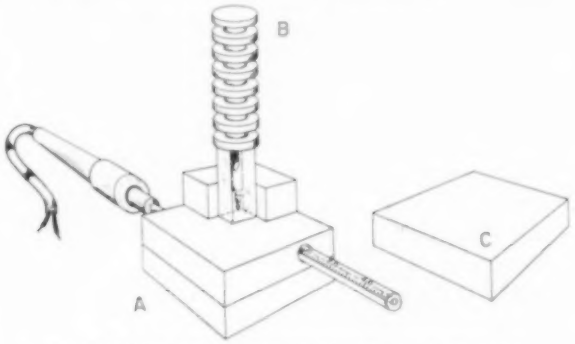

Fig. 8. Micro-cell assembly for total sample transfer.

The distribution of the solute at this stage can be checked by examination with a low power microscope, and the bulk of the material will normally be observed as a deposit on the walls of the "cell" and "neck" with relatively little on the walls of the "flask". For this transfer process the choice of solvents is not restricted to those commonly used for infrared determinations and it is often more convenient to use other volatile solvents, such as hexane or diethyl ether for this purpose.

The infrared transmitting solvent, normally carbon disulfide, carbon tetrachloride or chloroform, is now added in sufficient quantity to half fill the "flask". It will generally be observed at this stage that a small amount of air remains entrapped in the "cell". The refluxing process is recommenced and by this means the air entrapped by capillary action is released and at the same time the solute is brought into solution. Evaporation is continued until the meniscus of the solution is level with the bottom of the "neck". The micro-cell is then transferred to the cold plate and the stopper inserted. In some cases it has been found more convenient to carry out this final evaporation stage in a centrifuge at room temperature instead of on the hot plate, and centrifuging will also serve effectively to remove air entrapped in the "cell". When the micro-cell is correctly filled, the stopper should close firmly in the "neck" leaving no air bubble in the "cell". This is important, since the presence of such an air bubble will disturb the optical path when the micro-cell is in the focal plane of the micro-illuminator.

These cells have been used with a micro-illuminator of numerical aperture 0·5 placed before the entrance slit of a Perkin–Elmer Model 112 spectrometer [2]. The spectrum obtained from a 10 μg sample of tigogenin in carbon disulfide

solution under these conditions is shown in Fig. 9 and may be compared with Chart no. 282 of reference [9].

In the modified cell shown in Fig. 7, the "cell" cavity has a rectangular cross-section formed with the ultrasonic impact drill. Cells of this type have been constructed with the faces of the "cell" cavity parallel with the outer sides of the rock salt block, and also with the "cell" cavity oriented at 45° with respect to the outer sides, as shown in Fig. 7. It was anticipated that cells of these designs might transmit more energy than the cell of round cross-section. In practice,

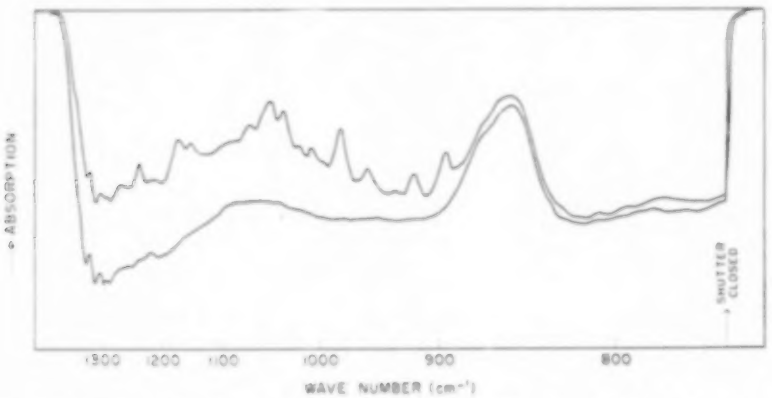

Fig. 9. Spectrum obtained with micro-cell of circular "cell" cavity for 10 μg of tigogenin in carbon disulfide solution. (*Upper curve*) solution spectrum; (*lower curve*) solvent spectrum.

however, any difference was extremely small, and the round type cell is to be preferred in view of its easier manufacture. The use of ultrasonic impact grinding does, however, permit the construction of cell cavities of almost any desired cross-section and investigation of the effect of the shape of the cell cavity on the transmission efficiency is being continued.

Conclusions

The development of a satisfactory form of semimicro cavity type infrared cell with approximately plane parallel faces has been possible only through the application of the ultrasonic impact grinding technique. Although the cells constructed in this fashion do not meet the close tolerances for optical parallelism between faces obtainable with carefully constructed cells of conventional type, they can be used satisfactorily for qualitative analysis and for quantitative work where the highest standards of absolute accuracy in intensity measurements are not required. They have the advantage of being cheap and easy to construct from small pieces of scrap rock salt, and there should be no difficulty in working in a similar fashion with other infrared transmitting optical materials. Their main advantage lies in control work, where large numbers of repetitive analyses are involved. Under these conditions it is both convenient and economic for the analyst to have large numbers of cells available as much time can be saved by eliminating the need for continuous cleaning and refilling.

VOL. 12 1958

The design and construction of micro illuminators are not yet to any degree standardized; the micro-cell described here has been designed specifically for use with a micro-illuminator of our own construction; modifications of the size and shape of the "cell" cavity would be required for optimum performance with a different micro-illuminator.

Acknowledgements—We wish to thank Dr. R. N. WILSON of the Light Division, National Physical Laboratory, Teddington, England, for his most helpful advice and assistance in preliminary work with the ultrasonic impact grinding technique. We are also grateful to Mr. A. COUTURE for technical assistance in our machine shop.

References

[1] BLOUT E. R., PARRISH N., BIRD G. R. and ABBATE M. J., *J. Opt. Soc. Amer.* 1952 **42** 966.
[2] COLE A. R. H. and JONES R. N., *J. Opt. Soc. Amer.* 1952 **42** 348.
[3] ROBERTS G., *Analyt. Chem.* 1957 **29** 911.
[4] FARMER V. C., *Spectrochim. Acta* 1957 **8** 374.
[5] BAKER A. W., *J. Phys. Chem.* 1957 **61** 450.
[6] LEWIS P., WIGGINS H. S. and WOOTTON I. D. P., *Biochem. J.* 1954 **56** 43.
[7] JONES R. N. and SANDORFY C., The application of infrared and raman spectrometer to the elucidation of molecular structure. *Technique of Organic Chemistry* (Edited by WEISSBERGER A.) Vol. IX. Interscience, New York and London 1956.
[8] HARTLEY M. S., *Electronics* 1956 **29** 132.
[9] DOBRINER K., KATZENELLENBOGEN E. R. and JONES R. N., *The Infrared Absorption Spectra of Steroids—An Atlas.* Interscience, New York and London 1953.

Spectrochimica Acta, 1958, Vol. 12, pp. 192 to 210. Pergamon Press Ltd., London

Solvent effects on merocyanine spectra*†

E. G. McRae‡
Department of Chemistry, University of Western Australia, Nedlands, Western Australia, and Department of Chemistry, Florida State University, Tallahassee, Florida, U.S.A.

(*Received* 9 *August* 1957)

Abstract—Solvent effects on the visible absorption spectra of three merocyanine dyes are described. The dyes comprise two (I and II) of exceedingly high polarity, and a third (III) less polar than I and II but still highly polar by ordinary standards.

(I)

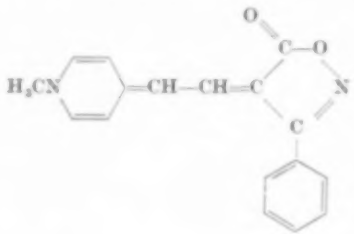

(II)

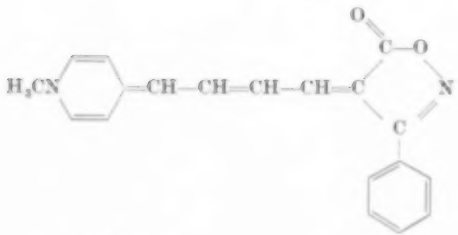

(III)

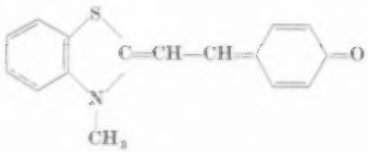

The absorption curves, values of the extinction coefficient and frequency at the absorption maxima (ϵ_{max} and ν_{max} respectively), and oscillator strengths are given for I dissolved in a number of pure solvents, and for II and III dissolved in a variety of both pure and mixed solvents. For each dye, ϵ_{max} and ν_{max} undergo pronounced solvent effects, but the oscillator strengths are insensitive to solvent perturbations. The results are discussed in terms of a simple theory in which the combining states are considered as superpositions of a polar and a nonpolar resonance structure. A more detailed theory is applied in the interpretation of the frequency shifts induced by nonhydrogen bonding solvents.

* Taken in part from a thesis submitted by E. G. McRae for the degree of M.Sc. at the University of Western Australia.

† Part of the work was carried out under a contract between the U.S. Air Force, Office of Scientific Research, ARDC, and the Florida State University.

‡ Present address: Department of Chemistry, Indiana University, Bloomington, Indiana, U.S.A.

VOL. 12 1958

1. Introduction

THE visible absorption spectra of highly polar merocyanine dyes undergo extraordinary solvent effects. The phenomena were first reported by BROOKER and his collaborators [1, 2] who studied the spectra of several merocyanines dissolved in pyridine–water mixed solvents. It was found that variation of the percentage

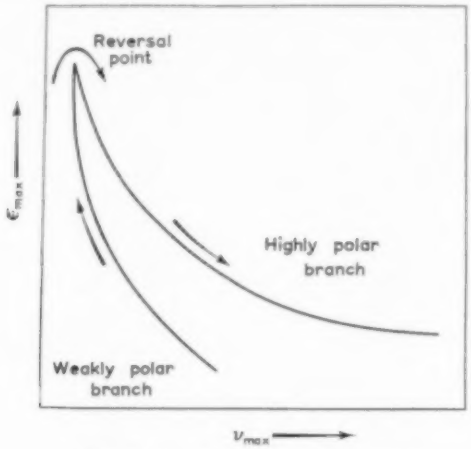

Fig. 1. ϵ_{max} vs. ν_{max} plot (schematic).

water content of the solvent gives rise to pronounced changes of both the maximum extinction coefficients, ϵ_{max}, and the corresponding frequencies, ν_{max}, at the visible absorption maxima.

The main qualitative features of the solvent effects have been described in a recent review by BROOKER [3]. For an exceedingly highly polar dye in a pyridine–water or lutidine–water mixed solvent, the progressive addition of water to the solvent leads to a shift of ν_{max} to higher frequencies, with a concomitant diminution of ϵ_{max}. The curve of ϵ_{max} vs. ν_{max} has the shape of the "highly polar" branch of the curve shown in Fig. 1. The arrow indicates the effect of adding water to the solvent. The opposite behavior is exhibited in the case of a dye which is comparatively weakly polar (but which may still be fairly highly polar by ordinary standards). Here, the plot of ϵ_{max} vs. ν_{max} resembles the "weakly polar" branch (Fig. 1). For dyes of intermediate polarity, the initial addition of water to a pure pyridine or lutidine solvent has an effect qualitatively similar to that observed with weakly polar dyes. Upon further progressive addition of water to the solvent, ϵ_{max} and ν_{max} pass through extreme values, and the subsequent differential solvent effect is qualitatively similar to that observed with exceedingly highly polar dyes.

For convenience in a subsequent discussion, we shall refer to points on the ϵ_{max} vs. ν_{max} plot as "solvent representative points" for the dye in question. The point on the plot at which ϵ_{max} attains its maximum value will be called the "reversal point," and will be thought of as the junction of the two branches.* With this nomenclature, the above description of merocyanine solvent effects

* Fig. 1 is slightly idealized in that the minimum of ν_{max} is shown to coincide with the reversal point. Actually, the two extrema do not exactly coincide, although in most but not all cases they lie quite close together.

may be summarized as follows: for exceedingly highly polar dyes, the representative points for pyridine–water or lutidine–water solvents lie on the highly polar branch, for relatively weakly polar dyes they lie on the weakly polar branch, and for dyes of intermediate polarity they straddle the reversal point.

The work reviewed by Brooker [3] is extensive in that it encompasses the spectra of dyes covering a wide range of polarity. However, the published data pertain only to the absorption maxima, and the solvents used were limited largely to pyridine–water and lutidine–water mixtures. In this paper, we give a more detailed description of solvent effects on the visible absorption spectra of three of the merocyanines previously studied by Brooker *et al.* [1, 2]. Of the three dyes, I and II, which have the same pair of end-groups, are exceedingly highly polar, while III has intermediate polarity.* The absorption curves of II in pure solvents have been given by Bayliss and McRae [4], in a preliminary report on the present work.

(I)

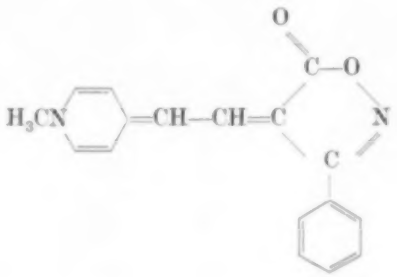

(II)

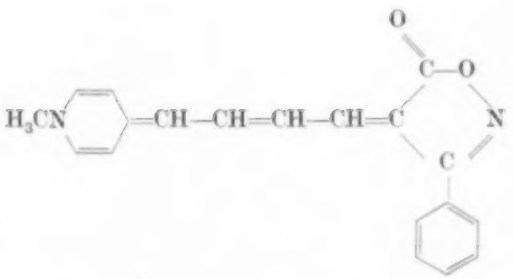

(III)

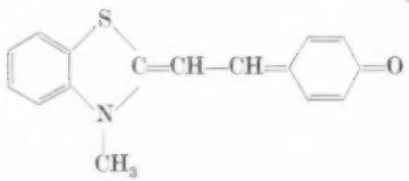

Taken together with the data previously published by Brooker *et al.* [1, 2], our results provide an overall picture of solvent effects on merocyanine band frequencies, intensities (oscillator strengths) and band shapes. This information is thought to be of particular interest in view of several recent discussions of the origins of solvent effects on merocyanine spectra [3, 4, 5–7].

* I and II are labeled XII ($n = 1$ and $n = 2$ respectively) in Ref. [1], and III is labeled V in Ref. [2.]

VOL. 12 1958

2. Experimental

Solvents. Most of the solvents used in this work have been described in a previous paper [8], and the remaining solvents are described below. Except where other references are given, the physical constants in parentheses are those quoted by TIMMERMANS [9].

Aniline of a technical grade was dissolved in hydrochloric acid, and the main impurity, nitrobenzene, was removed by steam distillation. The aniline hydrochloride was neutralized, and steam distilled. The distillate was dried with potassium hydroxide, and fractionated twice under reduced pressure. It was stored in the dark over potassium hydroxide pellets, and fractionated again immediately before use. B.P. 94°/35 mm (94/35) [10]; n_D^{20} 1·5860 (1·5863).

Dioxane of British Drug Houses technical grade was refluxed for 10 hr with one-tenth its volume of 0·1 N hydrochloric acid. It was then allowed to stand for one day over sodium hydroxide sticks, and fractionated. It was kept in the dark and used within one week of purification. B.P. 101·6° (101·4); n_D^{20} 1·4215 (1·4214).

Formamide was prepared from ethyl formate by the method of SLOBODIN *et al.* [11], and the product was fractionated under reduced pressure. The formamide was again fractionated immediately before use. B.P. 116°/39·2 mm; n_D^{20} 1·4482 (1·4475).

Pyridine of a grade conforming to British Drug Houses Analar standards (Judex analytical reagent) was allowed to stand for 1 week over sodium hydroxide sticks, refluxed for 10 hr over freshly burned calcium oxide, and fractionated. B.P. 115·2° (115·4); $n_D^{18·7}$ 1·5106 (1·5106).

Buffer solutions: for the pH range 5–8, MCILVAINE's standard buffer solutions [12] were prepared, using Analar grade reagents. The solvent of pH 9 was a 0·05 molar solution of Analar grade borax.

Merocyanine dyes. Pure merocyanine dye samples were supplied by Dr. L. G. S. BROOKER.

Solutions. In so far as permitted by the dye solubilities, the dye solutions were prepared to give a minimum transmission reading between 20 and 70 per cent. This corresponds to a dye concentration in the vicinity of 5×10^{-6} M. Where practicable, solutions of known dye concentration were prepared. Weighed 1 mg dye samples were dissolved, and the resulting solutions diluted either by volume or by weight. The latter method was used for most of the solutions in mixed solvents. Volume dilutions were carried out with a standardized 5 ml. pipette and standardized 25 ml flasks. Where weight dilution was employed, the dye molarity was calculated with the aid of the tabulated densities of the mixed solvents in question [13].

Spectra. Except in the tests of Beer's law (see below), all spectra were measured with a Beckman spectrophotometer, model DU, using matched 1 cm Corex cells.

Frequencies, ν (cm^{-1}), were obtained from the wavelength settings, no vacuum corrections being applied. The molar extinction coefficients, ϵ, were calculated according to the formula:

$$\epsilon = (1/cd) \log_{10} (100/T)$$

where c denotes the molarity, d the path length (cm), and T the percentage transmission reading. Oscillator strengths, f, were calculated from the absorption curves according to the formula [14]

$$f = 4·32 \times 10^{-9} \int \epsilon \, d\nu$$

Errors. The errors in the determination of ν_{max} ranged from 20 to 50 cm^{-1}, depending on the band width.

The errors in the measurement of absolute extinction coefficients, which were essentially concentration errors, did not exceed 5 per cent. In several cases it was not possible to measure extinction coefficients, because of sparing dye solubility. In these cases, ϵ_{max} was estimated by adjusting the area under the absorption curve to correspond to the oscillator strength of the dye dissolved in water. The justification of the procedure rests on a particular result of the present work, namely that the oscillator strengths are rather insensitive to solvent perturbations. The percentage error of ϵ_{max} determined in this way is considered not greater than the total percentage variation of oscillator strength, viz. 20 per cent (Section 3).

In merocyanine spectra, the visible absorption band is not overlapped appreciably by bands at higher frequencies; consequently the errors in the oscillator strengths were only slightly greater than those in the extinction coefficients.

In a few cases, which are noted individually in the next section, the errors were probably greater than indicated above.

In the cases in which a comparison is possible, our results agreed with those of Brooker *et al.* [1, 2], within the limits of error quoted above.

Tests of Beer's law. Beer's law tests were carried out using a Beckman spectrophotometer, model DK, with 0·1, 2·0 and 10·0 cm cells. The spectra of dyes I and III were measured in the concentration range 3×10^{-7} to 3×10^{-5} M. Most of the measurements reported in this paper (Section 3) were carried out at concentrations near the middle of this range ($\sim 5 \times 10^{-6}$ M). In the Beer's law tests, the solvents in each case were pyridine–water mixtures. The solvent for dye I contained 90 mole per cent pyridine, and that for dye III, 80 mole per cent pyridine. In both cases, Beer's law was obeyed well within the dilution error, and there was no detectable change of band shape throughout the hundredfold range of concentration.

3. Results

The solvents used in this research are listed in Table 1, together with their designations in the figures, their relevant physical properties, and the values of some derived properties thought to be of importance in the interpretation of the solvent effects (Section 4).

Table 1. Solvent designations and properties

Solvent	Designation	D*	n_D†	$F(D, n_D)$‡	$\frac{n_D^2 - 1}{2n_D^2 + 1}$
Benzene	B	2·3	1·498	0	0·23
Dioxane	D	2·2	1·421	0·03	0·20
Chloroform	CF	5·2	1·446	0·32	0·21
Nitrobenzene	NB	35	1·555	0·60	0·24
Pyridine	P	12·4	1·511	0·49	0·23
Acetone	Ac	21	1·359	0·65	0·18
Aniline	An	7·3	1·586	0·34	0·25
Ethanol	E	28	1·363	0·68	0·18
Formamide	F	109	1·448	0·71	0·21
Water	W	79	1·333	0·76	0·17

* Dielectric constant.
† Refractive index (sodium D line).
‡ $F(D, n_D) = (D - 1)/(D + 2) - (n_D^2 - 1)/(n_D^2 + 2)$

Dyes I *and* II

The results obtained with dyes I and II dissolved in pure solvents (Table 2, Figs. 2, 3) are qualitatively similar, the solvent effects being somewhat less pronounced in the case of I. In the case of dye II, the results include the effects of mixed as well as pure solvents (Table 3, Fig. 4).

The absorption bands of dyes I and II in 0·26 N hydrochloric acid lie at higher frequencies than the corresponding curves for water solvent. The absorption curves obtained at lower acid concentration passed through a well-defined isosbestic point, indicating that the higher-frequency absorption is due to the protonated dye in each case.

Frequencies. The pure solvents induce increasing shifts to higher frequencies in the order: dioxane, chloroform, nitrobenzene, pyridine, acetone, aniline, ethanol,

VOL. 12 1958

Table 2. Dyes I–III in pure solvents

Solvent	$\nu_{max} \times 10^{-4}$ (cm^{-1})			$\epsilon_{max} \times 10^{-3}$			f		
	I	II	III	I	II	III	I	II	III
Dioxane	1·864	1·559	1·838	58·0*	82·5*	53·0*	—	—	—
			1·947†			52·6*†			
Chloroform	1·883	1·570	1·773	74·0	103·5	90·4	0·65	0·74	0·82
			1·888†			50·4†			
Nitrobenzene	1·920	1·629	1·753	66·5	92·9	89·0	0·63	0·79	0·80
			1·853†			49·7†			
Pyridine	1·935	1·638	1·768	80·5	112·8	98·0	0·70	0·91	0·81
			1·883†			58·0†			
Acetone	1·970	1·681	1·804	78·0	103·6	76·0	0·74	0·94	0·74
			1·920†			50·5†			
Aniline	1·986	1·690	—	67·5	79·3	—	0·64	0·82	—
Ethanol	2·071	1·805	1·811	51·0	50·7	113·0	0·62	0·85	0·90
			2·333§			41·4§			0·82§
Formamide	2·115	1·890	2·351§	46·0	42·5	35·9§	0·62	0·82	0·73§
Water	2·292	2·132	2·028**	37·5	36·7	43·3**	0·63	0·80	0·74**
	2·615‡	2·480‡	2·463††	29·0‡	26·0‡	33·5††	0·62‡	0·80‡	0·72††

* Adjusted to conform to an oscillator strength equal to that for the same dye in water.
† Refers to a second maximum.
‡ Protonated dye. Solvent: 0·26 N HCl.
§ Protonated dye.
** Solvent: buffer solution, pH 9.
†† Protonated dye. Solvent: buffer solution, pH 6.

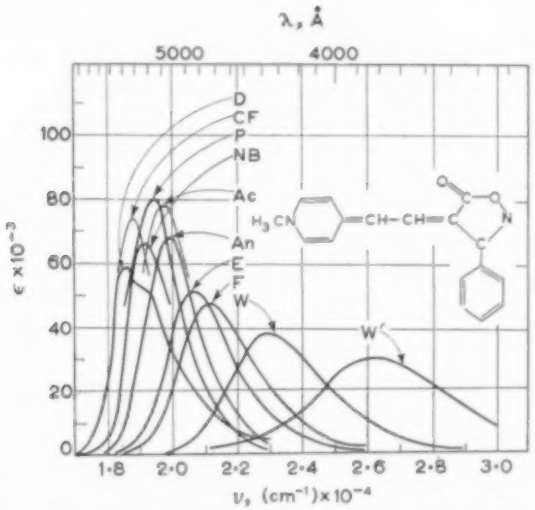

Fig. 2. Absorption curves for dye I in pure solvents. For solvent designations, see Table 1. W′ indicates the absorption curve for the protonated dye dissolved in aqueous solvent.

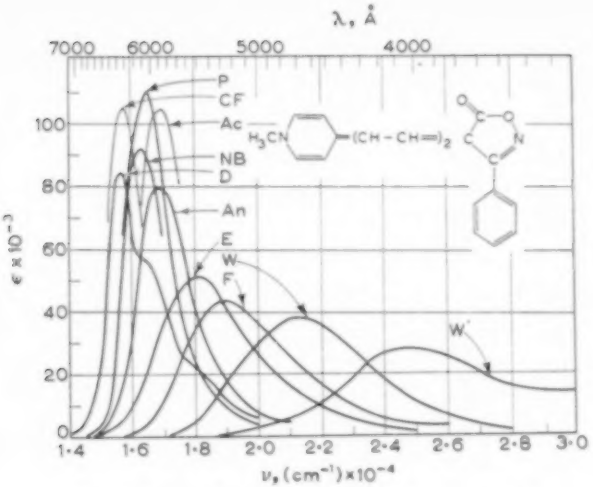

Fig. 3. Absorption curves for dye II in pure solvents.

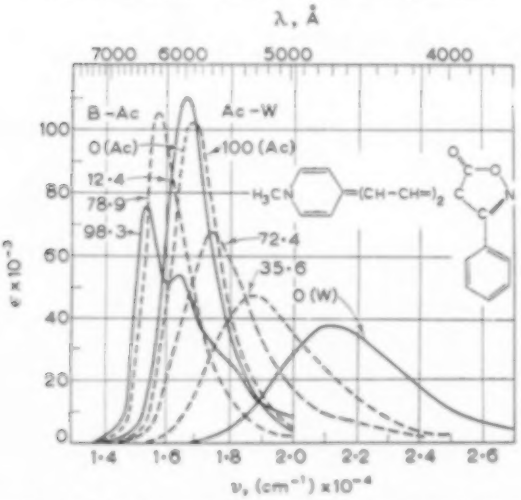

Fig. 4. Absorption curves for dye II in acetone–water and benzene–acetone mixed solvents. The numbers denote mole percentages of the first-named solvent component.

formamide, water. As has been pointed out previously [4] there is a sharp distinction between the effects of the hydrogen bonding solvents (last four members of the above sequence) and the nonhydrogen bonding solvents (first five members).*

In each case, the absorption of the protonated dye lies at a higher frequency than that of the dye itself dissolved in water.

* It is not clear whether or not chloroform should be classified as a hydrogen bonding solvent. Presumably it can form hydrogen bonds with the dyes, yet its solvent effect is intermediate between those of dioxane and pyridine. A similar result appeared in the writer's analysis of solvent effects on the spectrum of phenol blue [7]; there, it was found that the frequency shift produced by chloroform was close to that predicted for a non-hydrogen bonding solvent having the same macroscopic properties. In this paper, chloroform will be considered provisionally as a nonhydrogen bonding solvent.

VOL. 12 1958

Intensities. The band intensities do not undergo pronounced solvent effects, nor do they show an progressive variation with the band frequency. Yet, for each dye, some of the observed oscillator strengths differ significantly from the mean observed oscillator strength. For example, acetone, and to a smaller extent, pyridine, appear to cause a relative intensification. It is noteworthy that the

Table 3. Dye II in mixed solvents

Solvent	Mole %*	$\nu_{max} \times 10^{-4}$ (cm^{-1})	$\epsilon_{max} \times 10^{-3}$†	f
Dioxane–water	95·0	1·570	90·0	—
	90·0	1·590	85·5	—
	78·4	1·660	62·0	—
	64·2	1·713	59·0	—
	44·6	1·770	49·8	—
	20·0	1·885	43·0	—
	11·7	1·958	40·4	—
Benzene–pyridine	98·1	1·533	76·2	—
		1·636‡	56·4‡	
	78·2	1·554	90·7	—
	52·7	1·589	102·0	—
	24·6	1·618	90·0	—
Benzene–acetone	98·3	1·534	75·2	—
		1·631‡	53·7‡	
	94·9	1·542	81·4	—
	91·7	1·549	100·0	—
	78·9	1·573	105·2	0·84
	49·3	1·618	117·7	0·93
	37·0	1·632	109·0	0·89
	12·4	1·661	105·0	0·94
Acetone–water	99·0	1·682	106·5	0·96
	95·4	1·695	103·8	0·99
	72·4	1·750	66·4	0·89
	57·9	1·776	63·8	0·91
	35·6	1·870	47·0	0·82
	22·2	1·927	46·0	0·86
	9·4	2·010	38·4	0·77

* Refers to first-named solvent component.

† Where no oscillator strengths are given, the extinction coefficients are adjusted to conform to an oscillator strength equal to that for the same dye in water.

‡ Refers to a second maximum.

intensity of absorption of the protonated dye is nearly the same as that of the dye itself dissolved in water.

Band shapes. The absorption curves for dyes I and II in dioxane each display a definite shoulder on the high-frequency side. In the case of dye II, further structure may be discerned at still higher frequencies. With dye II, the vibrational structure is developed even more strongly in benzene-rich benzene–acetone and

benzene–pyridine mixed solvents, a second peak appearing in each case. The separation of the peaks is 1030 $\pm$ 100 cm^{-1}.*

The structureless absorption curves become progressively broader with increasing shift to higher frequencies. On plotting the corresponding solvent representative points for dye II, it is found that within the limits of error in the determination of ϵ_{max} they all lie close to a curve corresponding to the highly polar branch (Fig. 5). The values of ϵ_{max} for dioxane–water solvents were determined

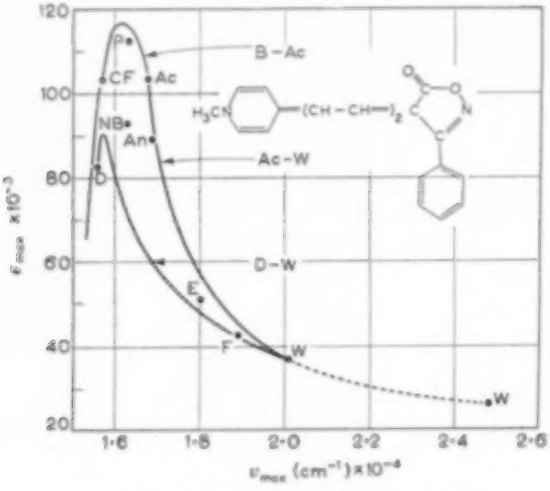

Fig. 5. ϵ_{max} vs. ν_{max} plot for dye II.

on the assumption of a constant oscillator strength. The actual values may be as much as 20 per cent higher. It is interesting that the point for the protonated dye lies near the extrapolated curve. The representative points corresponding to the absorption curves with structure lie close to a curve corresponding to the weakly polar branch, between the reversal point and the minimum of ν_{max}.

Dye III

At first sight the absorption curves for dye III in pure solvents (Table 2, Fig. 6) appear to bear no relation to those obtained with dyes I and II. However, the results are readily rationalized with reference to the absorption curves obtained with mixed solvents (Table 4, Fig. 7), and the ϵ_{max} vs. ν_{max} plot showing points for both pure and mixed solvents (Fig. 8). Again, the solvent representative points all lie close to a curve having the general shape of that shown in Fig. 1.

The visible absorption of dye III in water is the superposition of the absorption of the dye itself and a higher-frequency absorption attributed to the protonated dye. The absorption curves for the separate components (Fig. 6) were obtained in buffer solutions of pH 9 and pH 6 respectively. At intermediate pH, the composite absorption curves were found to pass through a definite isosbestic point. A similar result was obtained with the solvent ethanol, in which the composite

* The absorption curves obtained with benzene-rich mixed solvents changed slowly with time, probably because of the dye crystallizing out. They are less accurate than the other curves, but the frequencies were reproducible within the quoted limits of error.

VOL. 12 1958

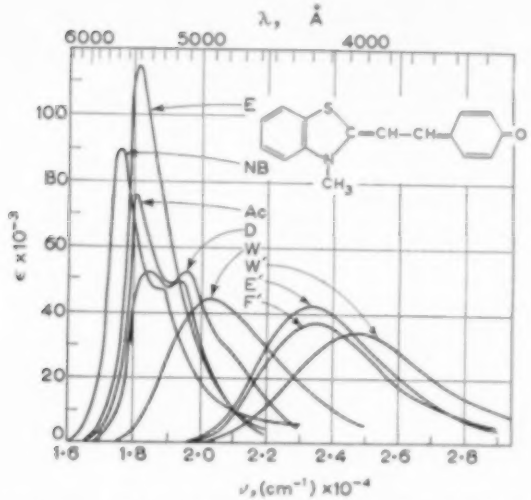

Fig. 6. Absorption curves for dye III in pure solvents. *E′* and *F′* indicate the absorption curves for the protonated dye dissolved in ethanol and formamide respectively.

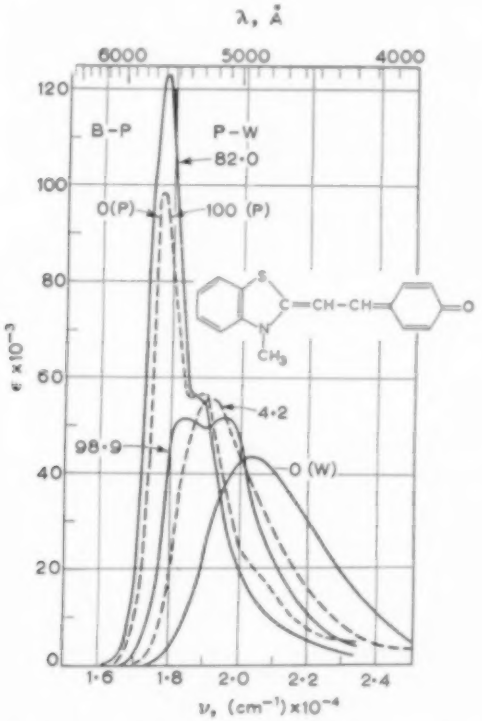

Fig. 7. Absorption curves for dye III in benzene–pyridine and pyridine–water mixed solvents.

Table 4. Dye III in mixed solvents

Solvent	Mole % *	$\nu_{max} \times 10^{-4}$ (cm^{-1})	$\epsilon_{max} \times 10^{-3}$ †	f
Dioxane–water	96·3	1·813	58·0	—
		1·925‡	50·0‡	
	88·7	1·791	75·5	—
		1·908‡	49·0‡	
	77·7	1·785	103·5	—
	61·1	1·791	107·0	—
	42·2	1·803	96·0	—
	23·1	1·835	70·0	—
	12·0	1·892	55·5	—
Benzene–pyridine	98·9	1·835	52·0	—
		1·930‡	52·4‡	
	70·3	1·798	70·5	0·83
		1·914‡	60·5‡	
	46·3	1·784	84·0	0·86
		1·895‡	60·5‡	
	22·4	1·775	93·0	0·86
		1·890‡	60·0‡	
Pyridine–water	92·3	1·766	112·0	0·84
		1·876‡	56·5‡	
	82·0	1·764	125·5	0·85
	48·4	1·785	104·5	0·80
	34·5	1·801	77·0	0·72
	4·2	1·913	55·4	0·82
	0·8	1·992	45·5	0·78

* Refers to first-named solvent component.

† Where no oscillator strengths are given, the extinction coefficients are adjusted to conform to an oscillator strength equal to that for the same dye in water.

‡ Refers to a second maximum.

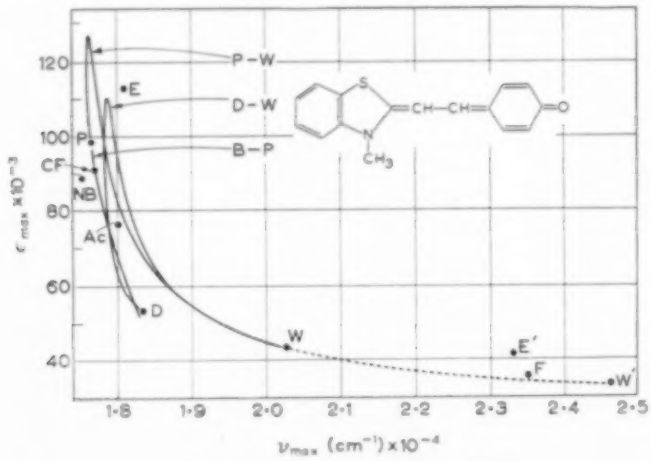

Fig. 8. ϵ_{max} vs. ν_{max} plot for dye III.

VOL. 12 1958

absorption curve varied slowly with time. By observing the absorption over a period of a few hours, it was resolved into the two curves shown in Fig. 6, the higher-frequency absorption being attributed to the protonated dye. The curves obtained with ethanol solvent are somewhat less accurate than the other curves shown in Fig. 6. The absorption observed with the solvent formamide is thought to be due to the protonated dye.

Frequencies. Of the pure solvents, ethanol has a representative point closest to the reversal point. The representative point for water definitely lies on the highly polar branch of the ϵ_{max} vs. ν_{max} curve, while the points for the nonhydrogen bonding solvents all appear to belong to the weakly polar branch. However, on the weakly polar branch the solvent order of increasing shift to higher frequencies is not the reverse of that observed with dyes I and II, as would be expected if there were a perfectly regular relationship between ϵ_{max} and ν_{max}.

The consideration of band frequencies alone affords no definite distinction between the effects of hydrogen bonding and nonhydrogen bonding solvents. Perhaps the most concise description of the effect of hydrogen bonding, in terms of experimentally observed quantities, is that it causes a displacement of the solvent representative point in the arrow direction along the ϵ_{max} vs. ν_{max} curve (Fig. 1). This does not necessarily imply a large frequency shift.

Intensities. Again, the band intensities appear to be rather insensitive to solvent perturbations, although the variation of oscillator strength from solvent to solvent slightly exceeds the experimental error in a few cases.

Band shapes. The absorption curves corresponding to representative points lying on the weakly polar branch display definite vibrational structure. A high-frequency shoulder or second peak is observed in every case, together with some less pronounced structure at still higher frequencies. As the solvent representative point moves away from the reversal point, the second peak grows up at the expense of the first, actually surpassing it in intensity in the case of a benzene–pyridine solvent. (Throughout, ϵ_{max} and ν_{max} refer to the lower-frequency peak.) The separation of the peaks is 1100 ± 100 cm^{-1} (average of observed separations).

On the high-frequency side of the reversal point, the absorption curves undergo progressive broadening similar to that observed with dyes I and II. The trend extends to the absorption curves of the protonated dye, the corresponding points lying near the extrapolated ϵ_{max} vs. ν_{max} curve (Fig. 8).

Gross features of the solvent effects

Inasmuch as the dyes I–III are typical members of the series of dyes studied by Brooker *et al.* [1, 2], the gross features of the solvent effects reported here are probably common to all merocyanine spectra. They are as follows:

(1) For a given dye, all solvent representative points lie near part of a curve having the general shape shown in Fig. 1. The particular part of the curve traced out by the points for a given series of solvents depends on the dye polarity, as indicated in Section 1.

(2) The representative points for hydrogen bonding solvents tend to be displaced in the arrow direction along the ϵ_{max} vs. ν_{max} curve (Fig. 1), compared with nonhydrogen bonding solvents.

(3) Band intensities (oscillator strengths) are almost independent of the solvent.

(4) As the solvent representative point moves away from the reversal point on the weakly polar branch, at least one new absorption peak grows up on the high-frequency side, at the expense of the lowest-frequency peak. The peak separation is 1000–1100 cm^{-1}.

4. Discussion

Frequency shifts

The gross features of the frequency shifts have been explained by Brooker [3] in terms of the relative solvent stabilization of the extreme polar and the nonpolar resonance structures (IVa and IVb respectively).

(IV)

(a) $\overset{+}{\text{N}}\!=\!(\text{C}\!-\!\text{C}\!=\!)_n\,\text{C}\!-\!\overset{-}{\text{O}}$

(b) $\text{N}\!-\!(\text{C}\!=\!\text{C}\!-\!)_n\,\text{C}\!=\!\text{O}$

Brooker has identified the reversal point with the *isoenergetic* point, i.e. the point at which the two structures have the same energy. The situation in which the polar structure is the more stable corresponds to the highly polar branch of the ϵ_{max} vs. ν_{max} curve, and the opposite situation corresponds to the weakly polar branch.

Brooker's interpretation has been elaborated by Simpson [5] who has taken into account the interactions between many resonance structure functions. However, the results of Simpson's treatment are not in agreement with experiment [4], and the treatment itself has been adversely criticized by Ooshika [15] on the ground that it is based on an oversimplified representation of the solvent–solute interaction energy. Platt [6] has pointed out the relationship between Brooker's interpretation and an alternative scheme in which the frequency shift is related to the relative magnitudes of the dipole moment of the solute in its ground and excited states.*

Recently, McRae [7] has given a general treatment of frequency shifts arising from dipole interactions. It was shown that the frequency shift may be expressed in terms of contributions to the environmental electric field at the solute dipole (all molecular dipoles being treated as point dipoles). In the case of a merocyanine dye dissolved in a polar solvent, it was proposed that as far as the relative frequency shifts induced by different solvents are concerned, the most important contribution to the environmental field is the field arising from the oriented permanent dipoles of the solvent molecules. Denoting the latter field by $\boldsymbol{R}$, and neglecting all other contributions to the environmental field, the following expression was derived for the frequency shift:

$$\nu - \nu_{ref} = (1/hc)(\boldsymbol{M}_g - \boldsymbol{M}_e)\,.\,\boldsymbol{R} + (3/2\,hc)\,(\alpha_g - \alpha_e)\,R^2 \qquad (1)$$

* Platt has attributed the latter method of interpretation to McConnell [16] and to Bayliss and McRae [17]. Actually, Platt's discussion represents an advance on the earlier work, which was based implicitly on the assumption of a rigid solute dipole.

VOL. 12 1958

Here, ν and ν_{ref} denote the band frequencies for the dye dissolved respectively in the solvent under consideration, and in a nonpolar reference solvent. On the right, h and c have the usual meanings, $\boldsymbol{M}_g$ and α_g respectively signify the permanent dipole moment and isotropic polarizability of the isolated solute molecule in its ground electronic state, and $\boldsymbol{M}_e$, α_e stand for the corresponding quantities for the excited state. The term involving R^2 represents the quadratic Stark effect.

It has been shown that, with $\alpha_g > \alpha_e$ and $\boldsymbol{M}_e$ assumed parallel to $\boldsymbol{M}_g$, Eq. 1 provides a satisfactory interpretation of the gross features of the frequency shifts in merocyanine spectra, including the order of magnitude of the shifts [7]. From a purely qualitative viewpoint, the description is exactly the same as that given previously by PLATT [6]. The important new feature of the approach based on (1) is the introduction of the field intensity, R, as a parameter to which the frequency shifts may advantageously be referred.

Probably the most serious errors inherent in (1) are those incurred through the neglect of environmental field contributions other than $\boldsymbol{R}$. This implies the neglect of dispersive interactions and interactions of the solute permanent dipole-solvent induced dipole type. In most cases apart from merocyanine spectra, these interactions make an important if not dominant contribution to the frequency shift. However, they may be expected to play a relatively small part in the case of merocyanine spectra, because of the high polarity of the merocyanines compared with ordinary molecules. The extent to which this expectation is realized is indicated in the following discussion of the results of the present work; this discussion is based at first on equation (1).

Nonhydrogen bonding solvents. In the absence of hydrogen bonding, the field intensity may be related to macroscopic properties of the solvent. On the basis of the simplest possible model for the solute in solution (point dipole at the center of a spherical cavity in a homogeneous dielectric medium), together with certain other simplifying assumptions, there results [7]

$$R = \frac{2\,M_g}{a^3}\left[\frac{D-1}{D+2} - \frac{{n_0}^2-1}{{n_0}^2+2}\right] \tag{2}$$

where a denotes the cavity radius, D the solvent dielectric constant and n_0 the refractive index of the solvent at zero frequency. Combining (1) and (2), assuming $\boldsymbol{M}_e$ parallel to $\boldsymbol{M}_g$ in (1) and denoting the expression in brackets (Eq. 2) by $F(D, n_0)$, we obtain:

$$\nu - \nu_{ref} = (2/hca^3)\,M_g\,(M_g - M_e)\,F + (6/hca^6)\,{M_g}^2\,(\alpha_g - \alpha_e)F^2 \tag{3}$$

According to (3), the band frequencies should vary regularly, though not necessarily linearly, with F.

Figures 9 and 10 show graphically the relationship between F and the observed band frequencies for dyes II and III dissolved in nonhydrogen bonding solvents. The corresponding plot for dye I is similar to that for dye II. The values of F for the pure solvents are taken from Table 1 (here and elsewhere in this paper, all refractive indices are replaced by n_D for the purpose of numerical calculation). For the benzene–pyridine mixed solvents, the dielectric constants are interpolated

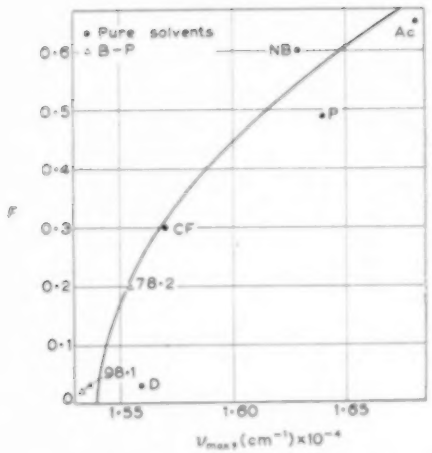

Fig. 9. Dye II: dependence of band frequency on solvent F.
$(F = (D-1)/(D+2) - (n_0^2-1)/(n_0^2+2))$.

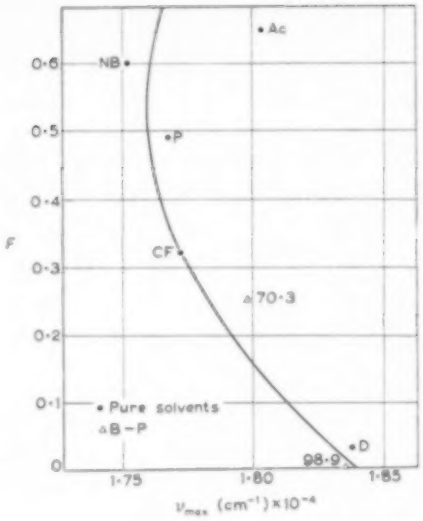

Fig. 10. Dye III: dependence of band frequency on solvent F.

VOL. 12 1958

from the data of Lange [18]. It is seen that there is a definite though imperfect correlation between the frequency shifts and the corresponding values of F. The points obtained for dye II lie near a curve having the shape expected from (1) and (2), with $M_g > M_e$ and $\alpha_g > \alpha_e$. For dye III, the trend conforms to $M_g < M_e$ and $\alpha_g > \alpha_e$.

The irregularities in the relationship between band frequency and solvent F may be discussed in terms of the superposed effects of dispersive interactions and of interactions of the dipole-induced dipole type; as noted above, both types of interaction were neglected in the derivation of (1).

Dispersive interactions invariably give rise to a shift to lower frequencies, relative to the vapor frequency (the "general red shift"). The general red shift is expected to be particularly large for strong bands such as appear in the visible spectra of dyes, and the relative magnitudes of the red shifts produced by different solvents are known to depend primarily on the solvent refractive index [7, 15, 17].*

Dipole-induced dipole interactions are expected to produce a shift to lower frequencies relative to the vapor frequency if the solute dipole moment of the dissolved dye molecule is greater in the excited state than in the ground state; otherwise, a shift to higher frequencies is expected. For a particular solute, the magnitudes of the shifts induced by different solvents are expected to depend on the solvent refractive index [7, 15, 17].

Accepting the above description of the dispersive and dipole-induced dipole effects, we conclude that the dipole-induced dipole shift augments the general red shift in the case of dye III and opposes it in the case of dye II. Upon reference

* The general red shift was called the "polarization red shift" in Ref. [17].

to Figs. 9 and 10, we find that the most noticeable irregularities occur with dye III in nitrobenzene and acetone. Now these two solvents have respectively the highest and the lowest refractive indices of the series. By virtue of the superposed effects of dispersive and dipole-induced dipole interactions, the two solvents are expected respectively to produce larger and smaller red shifts, compared with a reference solvent of intermediate refractive index, than predicted on the basis of the solvent F alone. The corresponding irregularities in the case of dye II in nitrobenzene and acetone are much less pronounced, as is expected in view of the partial cancellation of the dispersive and dipole-induced dipole shifts. A similar explanation can be advanced for most of the remaining irregularities; however, it is most likely that those irregularities merely reflect the limitations of the simple theory in which the solvent is treated as a homogeneous dielectric medium.

It is readily shown that the above discussion involves quantities of the correct order of magnitude. The curves superposed on Figs. 9 and 10 represent the behavior predicted by (3), with $M_g = 10\,D$, $a = 4$ Å, and $\alpha_g - \alpha_e = 0{\cdot}4 \times 10^{-23}$ cm^3 for each of the two dyes, $M_g - M_e = 0{\cdot}05\,D$ for dye II and $M_g - M_e = -1{\cdot}7\,D$ for dye III. It may be noticed that the curves are drawn on the assumption that the value of $(\alpha_g - \alpha_e)/a^3$ is the same for both dyes; this is to be expected in view of the general similarity of the spectra of the two dyes. It is noteworthy that the difference between the ground and excited state polarizabilities need not be particularly large to account for the observed trends. The chosen value of the difference is about one-quarter of the contribution of a strong visible transition to the ground state polarizability.

For strong transitions, such as those considered here, the general red shift is given approximately by [7]

$$\Delta\nu \text{ (dispersive)} = -2{\cdot}14 \times 10^{-14} \frac{Lf}{a^3} \frac{n^2 - 1}{2n^2 + 1}$$

where L and n respectively denote the "weighted mean wavelength" and refractive index of the solvent at the band frequency, f denotes the oscillator strength of the transition in question, and a again denotes the cavity radius. The minus sign indicates that the shift is to lower frequencies, relative to the vapor frequency. Adopting $L = 1250$ Å, $a = 4$ Å and $f = 0{\cdot}8$, we obtain

$$\Delta\nu \text{ (dispersive)} \simeq 3300 \frac{{n_D}^2 - 1}{2{n_D}^2 + 1} \tag{4}$$

as a rough estimate (cm^{-1}) of the general red shift. The literal application of the above formula (refractive indices from Table 1) accounts for a little over half the frequency separation of the points on Fig. 10 for dye III in nitrobenzene and acetone.

According to a formula given previously [7], the dipole-induced dipole shift, relative to the vapor frequency, is given by

$$\Delta\nu \text{ (dipole-induced dipole)} = \frac{{M_g}^2 - {M_e}^2}{hca^3} \frac{{n_0}^2 - 1}{2{n_0}^2 + 1}$$

Actually, the above formula does not apply accurately to the merocyanines, because it is based on the assumption of a rigid solute dipole. In a more elaborate discussion, we would have to replace M_g and M_e by appropriate expressions for the dipole moments of the dissolved dye. Bearing that in mind, the above formula suffices to show that if, for the dissolved dye, the ground and excited state dipole moments differ by less than 2 D, then the magnitude of the dipole-induced dipole shift is approximately equal to or less than that of the general red shift.

We have shown, first, that the observed frequency shifts display a definite though imperfect correlation with the solvent F, which has been defined with

reference to Eq. 2; second, that the observed behavior conforms approximately to that predicted by (3), with plausible values for the dipole moments and polarizabilities of the dyes; third, that the most noticeable discrepancies which do occur are of the nature and approximate magnitude to be expected from the superposition of dispersive and dipole-induced dipole effects. The evidence leaves little cause to doubt that the frequency shifts are caused primarily by dipole-dipole interactions, with the quadratic Stark effect playing an important or dominant role.

Hydrogen bonding solvents. Although the order in which the hydrogen bonding solvents induce shifts to higher frequencies is the same as that of increasing F, it is clear from the magnitudes of the shifts that they correspond, in a formal sense, to values of R much larger than those calculated from (2). It appears that the quadratic Stark effect makes a dominant contribution to the frequency shift.

Even when the quadratic Stark effect has been taken into account, there seems to be no simple explanation of the results in terms of hydrogen bonding. To take an extreme example, in the spectrum of dye II, the solvent water induces a shift of about 4500 cm^{-1} to higher frequencies, referred to acetone. If we allow 500 cm^{-1} for the change of F, there remains 4000 cm^{-1}, or about 12 kcal/mole, to be accounted for by hydrogen bonding. This appears to be too large a shift to be attributable to the formation of a single hydrogen bond. Again, in the case of dye II the shift induced by water is about twice as great as that induced by formamide, and about four times as great as that induced by ethanol (all referred to acetone), though the three solvents presumably form hydrogen bonds of about the same strength. On the other hand, the band frequencies for dye II in ethanol and aniline exceed by about the same amount ($\sim$1200 cm^{-1}) those expected on the basis of the solvent F alone.

We suggest that in the case of the solvent water, and possibly formamide, two solvent molecules simultaneously form strong hydrogen bonds with one dye molecule to form a complex of structure V. In each of the dyes I–III only

(V)

one dye atom can be strongly hydrogen bonded, namely the carbonyl oxygen. The formation of a second strong hydrogen bond would therefore be sterically hindered or prohibited in ethanol and aniline solvents.

This possibility has been considered previously for another solute by Pimentel, in a discussion of solvent spectral shifts [19].

Intensities. A simple theory of solvent effects on merocyanine band intensities has been proposed by McConnell [20]. The theory is based on the assumption that the ground and excited electronic state functions for the strong visible transition may be considered as linear combinations of the electronic state functions

VOL. 12 1958

appropriate to the isoenergetic point. This assumption differs only formally from that upon which BROOKER based his interpretation of the frequency shifts. There results

$$f/f_I = \nu_I/\nu \tag{5}$$

where f and ν respectively denote the oscillator strength and frequency of a band, and the subscript refers to the isoenergetic point.

The theory is not supported by the results of the present work. Whereas the frequencies of the bands of known intensity undergo a total variation of 20 per cent and 30 per cent for dyes I and II respectively, the oscillator strengths show no progressive variation with band frequency beyond the experimental error of 5 per cent. With dye III, the band frequencies do not cover a sufficiently large range to permit a valid test of the theory.

Band shapes. PLATT [6] has shown that BROOKER's interpretation of the frequency shifts can be extended to explain the concomitant changes of band width. At the isoenergetic point, the equilibrium nuclear configuration of the dye does not change upon excitation, so that only the O—O vibronic band appears strongly. As the solvent representative point moves away from the isoenergetic point, the equilibrium length of each bond in the C—C chain suffers a progressively more pronounced change upon excitation. According to the Franck–Condon principle, this should lead to the growing up of higher-frequency vibronic bands at the expense of the O—O band, with frequency separations corresponding to the C—C stretching frequency.

The above interpretation is strongly supported by the results of the present work. The absorption curves corresponding to representative points near the reversal point and on the weakly polar branch show definite vibrational structure, which changes in the predicted manner as the representative point moves away from the reversal point. The separation of the vibronic peaks (1000–1100 cm^{-1}) is in satisfactory agreement with the C—C stretching frequency. Vibrational structure does not appear in the absorption curves corresponding to points on the highly-polar branch, probably because of the blurring of structure normally associated with strong solvent–solute interaction. Nevertheless, the broadening may be attributed to changes of the relative intensity of the underlying vibronic transitions. It can be seen from the absorption curves that if it were possible to plot ϵ_{max} against the O—O frequency rather than against ν_{max}, the highly-polar and weakly-polar branches would be nearly superposed. This tends further to substantiate PLATT's interpretation, since the ground- and excited-state potential energy curves for C—C stretching are presumably nearly symmetrical near their respective minima.

Acknowledgements—Most of the work described above was carried out under the supervision of Professor N. S. BAYLISS, to whom the writer is indebted for encouragement and helpful criticism. The writer is glad to thank Dr. L. G. S. BROOKER for the gift of the merocyanine dye samples, and Professors N. S. BAYLISS and M. KASHA for reading this paper prior to publication. Financial assistance provided by the University Research Fund (University of Western Australia), including the award of a studentship, is gratefully acknowledged, as is also the award of a Hackett Studentship by the University of Western Australia.

References

[1] Brooker L. G. S., Keyes G. H., Sprague R. H., Van Dyke R. H., Van Lare E., Van Zandt G., White F. L., Cressman H. W. J. and Dent S. G., *J. Amer. Chem. Soc.* 1951 **73** 5332.

[2] Brooker L. G. S., Keyes G. H. and Heseltine D. W., *J. Amer. Chem. Soc.* 1951 **73** 5350.

[3] Brooker L. G. S., *Experientia Supplementum II–XIVth International Congress of Pure and Applied Chemistry* p. 229 1955.

[4] Bayliss N. S. and McRae E. G., *J. Amer. Chem. Soc.* 1952 **74** 5803.

[5] Simpson W. T., *J. Amer. Chem. Soc.* 1951 **73** 5359.

[6] Platt J. R., *J. Chem. Phys.* 1956 **25** 80.

[7] McRae E. G., *J. Phys. Chem.* 1957 **61** 562.

[8] Bayliss N. S. and McRae E. G., *J. Phys. Chem.* 1954 **58** 1006.

[9] Timmermans J., *Physico-chemical Constants of Pure Organic Compounds* Elsevier Publishing, Amsterdam 1950.

[10] Landolt–Bornstein, *Physikalisch-chemische Tabellen* (5th Ed.) p. 2462 (Eg. III c) Springer, Berlin 1935.

[11] Slobodin Ya. M., Zigel M. S. and Yanishevska M. V., *Zh. prikl. khim., Mosk.* 1943 **16** 280. See *Chem. Abstr.* 1945 **39** 702.

[12] *Handbook of Chemistry and Physics* (24th Ed.) p. 1374 Chemical Rubber Publishing 1940.

[13] Landolt–Bornstein, *Physikalisch-chemische Tabellen* (5th Ed.) Springer, Berlin 1935.

[14] Mulliken R. S. and Rieke C. A., *Rep. Progr. Phys.* 1941 **8** 231.

[15] Ooshika Y., *J. Phys. Soc. Japan* 1954 **9** 594.

[16] McConnell H., *J. Chem. Phys.* 1952 **20** 700.

[17] Bayliss N. S. and McRae E. G., *J. Phys. Chem.* 1954 **58** 1002.

[18] Lange L., *Z. Phys.* 1925 **33** 169.

[19] Pimentel G. C., *J. Amer. Chem. Soc.* 1957 **79** 3323.

[20] McConnell H., Quoted by Platt, Ref. [6].

VOL. 12 1958

Spectrochimica Acta, 1958, Vol. 12, pp. 211 to 223. Pergamon Press Ltd., London

Spectrographic analysis of segregates with a dynamic microvolume technique—II

Experimental verification of theory*

J. K. HURWITZ†
Physical Metallurgy Division, Mines Branch, Department of Mines and Technical Surveys, Ottawa, Ontario, Canada

(*Received* 6 *September* 1957)

Abstract—To test the theory for the microvolume analysis of segregates, traverses were carried out on artificial segregates as thin as 0·077 mm. These segregates were synthesized by clamping thin plates of high-chromium steel between thick blocks of low-chromium steel. Statistical tests indicated that there is no significant difference between the observed and theoretical results. The severe non-uniformity in microphotometer slit illumination was measured and it was shown that the effect of this non-uniformity on the traverse results in relatively small and may be neglected.

Introduction

In a previous paper [1], the theoretical development of the dynamic microvolume analysis of segregates in metals and alloys was presented. This theory accounted for the width of the segregates, the size and shape of the sparked crater, the lengths of the spectrograph and microphotometer slits and the ratio of camera speed to specimen speed. The model of a segregate was assumed to be a region of uniform composition separated by two linear boundaries from its surroundings which were different but uniform in composition.

The experimental verification of the theory would be very difficult to achieve using segregates occurring naturally in metallurgical products. Control of segregate size and distribution being impracticable and chemical analysis, especially of narrow segregates, being difficult and of doubtful value, it was necessary to synthesize them. This was done by sandwiching thin plates of one composition between thick blocks of another composition. In this way close control on the segregate's width and composition was achieved easily.

This paper presents the experimental verification of the double boundary traverse theory. Twenty different cases are investigated. Also some attention is given to the effect on the traverse results of non-uniformity in microphotometer slit illumination. It is shown that this effect is relatively small.

Experimental

The equipment for the dynamic microvolume technique has been described previously [2]. It provides for the simultaneous motion of the sample and of the camera of the spectrograph to give a continuous record of changes in composition across a selected face of the sample. The

* Published by permission of the Director, Mines Branch, Department of Mines and Technical Surveys, Ottawa, Ontario, Canada.

† Present address: Applied Research Laboratory, United States Steel Corporation, Monroeville, Pennsylvania, U.S.A.

description of the experimental procedure includes discussion of the preparation of artificial segregates, and describes the spectroscopic and traversing conditions.

(a) *Preparation of artificial segregates*

The segregates were synthesized from two secondary spectrographic steel standards. The compositions are given in Table 1. Standard 9s was rolled down to a plate 3·8 mm thick from which several thin plates ranging in thickness from 0·18 mm to 2·54 mm were produced by

Table 1. Analyses of standards

Standard	C (%)	Mn (%)	V (%)	Si (%)	Cr (%)	Mo (%)	Ni (%)	Cu (%)
9s	0·49	0·71	0·33	0·60	1·91	0·24	0·22	0·35
10s	0·46	0·77	0·07	0·16	0·24	0·33	4·51	0·42

Table 2. Spectroscopic conditions

Spectrograph	Hilger large quartz and glass littrow.
Wavelength range	2450–3500 Å with quartz optics
Analytical gap width	0·38 mm
Source to slit distance	150 mm
Slit width	25 μ
Source unit	Applied Research Laboratories Multisource
Source conditions	
capacity	2 μF
inductance	50 μH
resistance	10 Ω
discharge point control	90°
Positive upper electrode (grounded)	Sample metallographically polished, unetched.
Negative lower electrode	Silver rod, 99·99 per cent purity, $\frac{1}{8}$ in. in diameter, pointed with a 30° included angle.
Emulsion	Kodak spectroscopic plate, type 103–O.
Processing	Developed in hydroquinone developer [3] for 7 min at 68°F, rinsed in Kodak SB–1 for 30 sec, fixed in Kodak F–5 for 15 min, washed in running water for 30 min and dried in an Applied Research Laboratories plate drier after removing the excess water with a fine-pore cellulose sponge. All developing, rinsing and fixing was carried out in an Applied Research Laboratories developing machine.
Microphotometer	Hilger, non-recording.
Camera speed	8·0 mm/min
Sample speed	Variable
Spectral line pairs	Cr 2876·0/Fe 2875·3 Cr 2876·2/Fe 2875·3
Emulsion calibration	Two-line method using Cr 2876·0 and Cr 2876·2, measured intensity ratio Cr 2876·0: Cr 2876·2 = 1·32:1

VOL. 12 1958

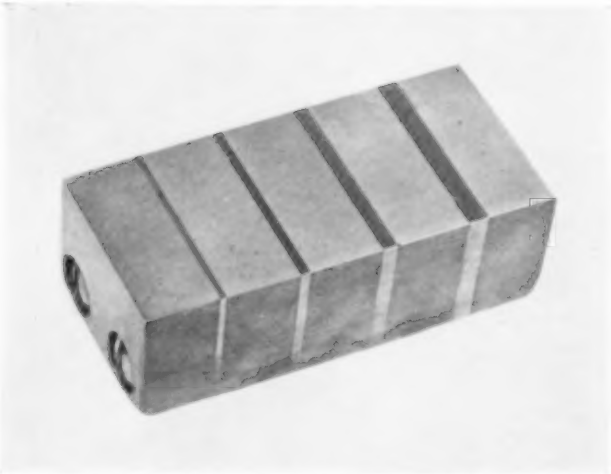

Fig. 1. Steel block assembly containing artificial segregates. Etched in 2 per cent Nital for 10 sec.

VOL.
12
1958

grinding. An additional plate was carefully hand ground from 0·18 to 0·077 mm. Five thick blocks, 24 mm × 17 mm × 9 mm, were machined and ground from standard 10s for use as the matrix surrounding the segregate. Two holes were drilled through the blocks and the thin plates were rigidly clamped between the blocks. By this means four artificial segregates of any

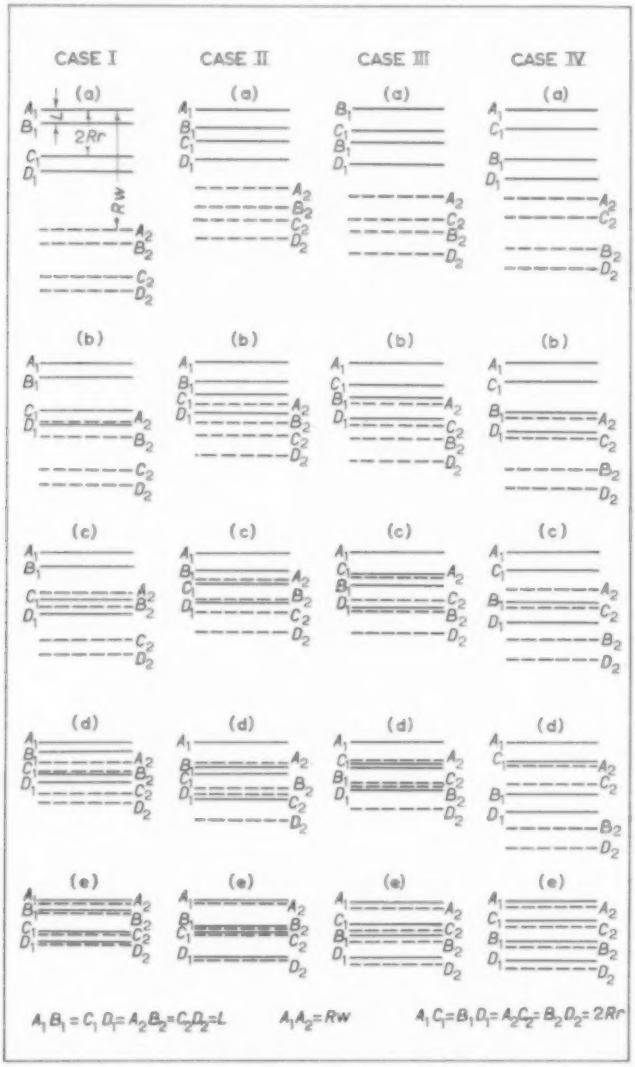

Fig. 2. Zonal diagrams drawn to scale for the traverses carried out in these experiments.

desired thickness could be prepared at a time. The assembled segregated sample is shown in Fig. 1.

(b) *Spectroscopic conditions*

Table 2 presents a summary of the spectroscopic conditions employed in all these experiments. Since the spectral lines used for analysis are also used for emulsion calibration, the indicated

emulsion calibration procedure is nearly ideal. It covers the full range of densities encountered, and the emulsion is calibrated in the wavelength region and position on the plate where the microphotometer readings are made. When a very narrow segregate was traversed, a small

Table 3. Traversing conditions

$r = 0{\cdot}3$ mm; $K/M = 1{\cdot}0$ mm; $X_1 = 0{\cdot}24$ per cent; $X_2 = 1{\cdot}91$ per cent

Case	R	L (mm)	W (mm)
I(a)	5·03	0·90	1·52
II(a)	3·36	1·23	1·52
III(a)	2·23	2·10	2·54
IV(a)	2·01	3·20	2·54
I(b)	5·03	0·90	0·76
II(b)	3·36	1·23	0·76
III(b)	2·23	2·10	1·14
IV(b)	2·01	3·20	1·75
I(c)	5·03	0·90	0·52
II(c)	3·36	1·23	0·52
III(c)	2·23	2·10	0·72
IV(c)	2·01	3·20	1·14
I(d)	3·36	0·60	0·38
II(d)	3·36	1·57	0·38
III(d)	2·23	1·58	0·52
IV(d)	2·01	3·20	0·72
I(e)	3·36	0·60	0·077
II(e)	3·36	1·57	0·077
III(e)	2·23	2·10	0·18
IV(e)	2·01	2·50	0·18

range of densities was anticipated; a second traverse across a wider segregate was therefore recorded on the same photographic plate in order to obtain a satisfactory calibration. Every plate used in these experiments was calibrated.

(c) *Traversing conditions*

All traverses were made in duplicate under the conditions summarized in Table 3. The symbols are defined as follows:

r is the radius of the sparked crater on the surface of the sample
R is the ratio of the camera speed to sample speed
L is the length of the image of the spectrograph slit on the photographic emulsion
K is the length of the microphotometer slit
M is the magnification of the microphotometer's optical system
w is the width of the segregate
X_2 is the chromium concentration in the segregate
X_1 is the chromium concentration everywhere in the sample except in the segregate.

VOL. 12 1958

The zonal diagrams for the various conditions given in Table 3 are shown in Fig. 2. The measurement of the various parameters was carried out as follows: The speed ratio R was obtained from the gear and sprocket ratios used in the moving camera and traversing spark equipment. The length of the image of the spectrograph slit was found by photographing a steel spectrum on a stationary plate and measuring the length of the chromium spectral lines used in this investigation on the microphotometer. The microphotometer slit length was measured directly on the Hilger microphotometer with the scale provided on the wedge diaphragm. To determine the magnification in the microphotometer's optical system a sheet of translucent graph paper was placed in the carriage of the microphotometer and the spacing between two lines on the graph paper of their projected images on the slit was measured. The width of each segregate was measured with a microscope of known magnification in the range 25× to 100× prior to performing the spectrographic traverse. The radius of the sparked crater in steel which had been determined previously [2] from microscopic measurements was 0·3 mm.

Table 4. Equations applicable in non-overlapped zones

Case	Zone	$C_a(s)$
$L < 2Rr$ $L > 2Rr$	A_2B_2 or A_1B_1 A_2C_2 or A_1C_1	$X_1 + \frac{Rr}{L}(X_2 - X_1)\int_{1-\frac{s}{Rr}}^{1} g(b)db$
$L < 2Rr$	B_2C_2 or B_1C_1	$X_1 + \frac{Rr}{L}(X_2 - X_1)\int_{1-\frac{s}{Rr}}^{1-\frac{s-L}{Rr}} g(b)db$
$L > 2Rr$	C_2B_2 or C_1B_1	$X_1 + (X_2 - X_1)\frac{s - Rr}{L}$
$L < 2Rr$ $L > 2Rr$	C_2D_2 or C_1D_1 B_2D_2 or B_1D_1	$X_2 + \frac{Rr}{L}(X_1 - X_2)\int_{-1}^{1-\frac{s-L}{Rr}} (1 - g(b))db$

The traverses were carried out in accordance with the conditions outlined in Tables 2 and 3. From experience in the laboratory, it was known that the concentrations of chromium used in the "segregated" specimen were within the linear portion of the working curve. Hence, in every traverse, one point on the working curve was obtained at 0·24 per cent chromium. In cases I(a), II(a), III(a) and IV(a), an additional point at 1·91 per cent chromium was also available. Plotting the logarithm of the chromium concentrations as the ordinate and the logarithm of the intensity ratios as the abscissae, a slope of 1·30 for the working curve was obtained. This slope was used throughout to determine the apparent concentrations. Each traverse was done in duplicate and two spectral line pairs (Table 2) were used.

Theoretical calculations

To compare the experimental traverse results with those predicted by theory, numerical calculations were carried out using equations developed in a previous paper [1]. The original theory assumed that both sides of the segregate were of different compositions whereas they were the same in these experiments. The equations suitable for calculation purposes are given in Tables 4 and 5 and by equations (1) and (2). Tables 6 and 7 give the tabulated values of the integrals

Table 5. Equations applicable in overlapped zones

Overlapped zone	Case	$C_a(s)$
$A_1B_1 - A_2B_2$ $A_1C_1 - A_2C_2$	I(c), II(d), II(c) III(d), III(c), IV(c)	$X_1 + \frac{Rr}{L}(X_2 - X_1)\left[\int_{1-\frac{s}{Rr}}^{1} g(b)db - \int_{1-\frac{s-Rw}{Rr}}^{1} g(b)db\right]$
$B_1C_1 - A_2B_2$	I(c), I(d), I(c) II(c), II(d), II(c)	$X_1 + \frac{Rr}{L}(X_2 - X_1)\left[\int_{1-\frac{s}{Rr}}^{1-\frac{s-L}{Rr}} g(b)db - \int_{1-\frac{s-Rw}{Rr}}^{1} g(b)db\right]$
$B_1C_1 - B_2C_2$	I(d), I(c), II(c)	$X_1 + \frac{Rr}{L}(X_2 - X_1)\left[\int_{1-\frac{s}{Rr}}^{1-\frac{s-L}{Rr}} g(b)db - \int_{1-\frac{s-Rw}{Rr}}^{1-\frac{s-Rw-L}{Rr}} g(b)db\right]$
$C_1D_1 - A_2B_2$ $B_1D_1 - A_2C_2$	I(b), II(b), I(c), II(c), II(d) III(b), III(c), IV(b), IV(c), III(d)	$X_2 + \frac{Rr}{L}(X_1 - X_2)\left[\int_{-1}^{1-\frac{s-L}{Rr}} (1 - g(b))db + \int_{1-\frac{s-Rw}{Rr}}^{1} g(b)db\right]$
$C_1D_1 - B_2C_2$	I(c), I(d), I(c), II(c), II(d), II(c)	$X_2 + \frac{Rr}{L}(X_1 - X_2)\left[\int_{-1}^{1-\frac{s-L}{Rr}} (1 - g(b))db + \int_{1-\frac{s-Rw}{Rr}}^{1-\frac{s-Rw-L}{Rr}} g(b)db\right]$
$C_1D_1 - C_2D_2$ $B_1D_1 - B_2D_2$	I(c), II(d), II(c) III(d), III(c), IV(c)	$X_1 + \frac{Rr}{L}(X_1 - X_2)\left[\int_{-1}^{1-\frac{s-L}{Rr}} (1 - g(b))db - \int_{-1}^{1-\frac{s-Rw-L}{Rr}} (1 - g(b))db\right]$
$C_1B_1 - A_2C_2$	III(c), IV(c), IV(d) III(d), III(c), IV(c)	$X_1 + \frac{Rr}{L}(X_2 - X_1)\left[\frac{s - Rr}{Rr} - \int_{1-\frac{s-Rw}{Rr}}^{1} g(b)db\right]$
$C_1B_1 - C_2B_2$	III(c), IV(d), IV(c)	$X_1 + \frac{Rw}{L}(X_2 - X_1)$
$B_1D_1 - C_2B_2$	III(c), IV(c), IV(d) III(d), III(c), IV(c)	$X_2 + \frac{Rr}{L}(X_1 - X_2)\left[\int_{-1}^{1-\frac{s-L}{Rr}} (1 - g(b))db + \frac{(s - Rw - Rr)}{Rr}\right]$

VOL. 12 1958

of $g(b)$ and $1 - g(b)$ for an effective sparked distribution which is assumed to be a paraboloid of revolution. All symbols not defined so far are as follows:

s is the distance on the photographic emulsion measured from A_1 towards D_2 in the zonal diagrams (Fig. 2)

b is the ratio of the perpendicular distance of the centre of the sparked crater from a boundary to the radius of the sparked crater. This ratio is significant only for values between -1 and $+1$

$g(b)$ is the ratio, to the total volume at any instant, of the volume represented by the effective spark distribution on the side of a boundary towards which the sparked crater is moving

$C_a(s)$ is the apparent concentration recorded on the photographic emulsion at a point which is at a distance, s, from A_1

C_a is the apparent concentration which results from a microphotometer measurement

α is the fraction of the total light passing through the microphotometer slit at any point along that slit

α_i' is the fraction of the total light passing through the ith segment of N segments into which the microphotometer slit length is divided.

The zonal diagram (Fig. 2) for a traverse across an artificial segregate is really a combination of two identical zonal diagrams (one for each boundary separating

Table 6. $\int_b^1 g(b)db$

b	0	1	2	3	4	5	6	7	8	9
1·0	0·000									
0·9	0·000	0·000	0·000	0·000	0·000	0·000	0·000	0·000	0·000	0·000
0·8	0·001	0·001	0·001	0·001	0·000	0·000	0·000	0·000	0·000	0·000
0·7	0·004	0·003	0·003	0·003	0·002	0·002	0·002	0·001	0·001	0·001
0·6	0·009	0·008	0·008	0·007	0·007	0·006	0·005	0·005	0·004	0·004
0·5	0·020	0·018	0·017	0·016	0·015	0·014	0·013	0·012	0·011	0·010
0·4	0·035	0·033	0·032	0·030	0·028	0·026	0·025	0·024	0·022	0·021
0·3	0·057	0·054	0·052	0·050	0·047	0·045	0·043	0·041	0·039	0·037
0·2	0·086	0·083	0·080	0·077	0·074	0·071	0·068	0·065	0·062	0·060
0·1	0·124	0·120	0·116	0·112	0·108	0·104	0·100	0·097	0·093	0·090
0·0	0·170	0·165	0·160	0·155	0·150	0·146	0·141	0·137	0·132	0·128
−0·0	0·170	0·175	0·180	0·185	0·190	0·196	0·201	0·207	0·212	0·218
−0·1	0·224	0·230	0·236	0·242	0·248	0·254	0·260	0·267	0·273	0·280
−0·2	0·286	0·293	0·300	0·307	0·314	0·321	0·328	0·335	0·342	0·350
−0·3	0·357	0·364	0·372	0·380	0·387	0·395	0·403	0·411	0·419	0·427
−0·4	0·435	0·443	0·452	0·460	0·468	0·476	0·485	0·494	0·502	0·511
−0·5	0·520	0·528	0·537	0·546	0·555	0·564	0·573	0·582	0·591	0·600
−0·6	0·609	0·618	0·628	0·637	0·647	0·656	0·665	0·675	0·684	0·694
−0·7	0·704	0·713	0·723	0·733	0·742	0·752	0·762	0·771	0·781	0·791
−0·8	0·801	0·811	0·821	0·831	0·840	0·850	0·860	0·870	0·880	0·890
−0·9	0·900	0·910	0·920	0·930	0·940	0·950	0·960	0·970	0·980	0·990
−1·0	1·000									

Table 7. $\int_b^1 (1 - g(b))\, db$

b	0	1	2	3	4	5	6	7	8	9
1·0	0·000									
0·9	0·100	0·090	0·080	0·070	0·060	0·050	0·040	0·030	0·020	0·010
0·8	0·199	0·189	0·179	0·169	0·160	0·150	0·140	0·130	0·120	0·110
0·7	0·296	0·287	0·277	0·267	0·258	0·248	0·238	0·229	0·219	0·209
0·6	0·391	0·382	0·372	0·363	0·353	0·344	0·335	0·325	0·316	0·306
0·5	0·480	0·472	0·463	0·454	0·445	0·436	0·427	0·418	0·409	0·400
0·4	0·565	0·557	0·548	0·540	0·532	0·524	0·515	0·506	0·498	0·489
0·3	0·643	0·636	0·628	0·620	0·613	0·605	0·597	0·589	0·581	0·573
0·2	0·714	0·707	0·700	0·693	0·686	0·679	0·672	0·665	0·658	0·650
0·1	0·776	0·770	0·764	0·758	0·752	0·746	0·740	0·733	0·727	0·720
0·0	0·830	0·825	0·820	0·815	0·810	0·804	0·799	0·793	0·788	0·782
−0·0	0·830	0·835	0·840	0·845	0·850	0·854	0·859	0·863	0·868	0·872
−0·1	0·876	0·880	0·884	0·888	0·892	0·896	0·900	0·903	0·907	0·910
−0·2	0·914	0·917	0·920	0·923	0·926	0·929	0·932	0·935	0·938	0·940
−0·3	0·943	0·946	0·948	0·950	0·953	0·955	0·957	0·959	0·961	0·963
−0·4	0·965	0·967	0·968	0·970	0·972	0·974	0·975	0·976	0·978	0·979
−0·5	0·980	0·982	0·983	0·984	0·985	0·986	0·987	0·988	0·989	0·990
−0·6	0·991	0·992	0·992	0·993	0·993	0·994	0·995	0·995	0·996	0·996
−0·7	0·996	0·997	0·997	0·997	0·998	0·998	0·998	0·999	0·999	0·999
−0·8	0·999	0·999	0·999	0·999	1·000	1·000	1·000	1·000	1·000	1·000
−0·9	1·000	1·000	1·000	1·000	1·000	1·000	1·000	1·000	1·000	1·000
−1·0	1·000									

the segregate from the rest of the sample). These zonal diagrams are displaced from each other by a distance, Rw. The equations relating apparent concentration to distance in each zone not common to both zonal diagrams are given in Table 4. Those applicable in each zone common to both zonal diagrams are given in Table 5.

When the microphotometer slit illumination is uniform, C_a is given by

$$C_a = \frac{M}{K} \int_{s-\frac{K}{2M}}^{s+\frac{K}{2M}} C_a(s)\, ds$$

and when the microphotometer slit illumination is not uniform, C_a is given by

$$C_a = \int_{s-\frac{K}{2M}}^{s+\frac{K}{2M}} \alpha\, C_a(s)\, ds$$

For purposes of calculation, the summation form of these equations is better. For uniform slit illumination:

$$C_a = \sum_{i=1}^{N} C_a(s)_i \qquad (1)$$

VOL. 12 1958

and for non-uniform slit illumination

$$C_a = \sum_{i=1}^{N} \alpha_i' \, C_a(s)_i \qquad (2)$$

where the microphotometer slit length is divided into N equal segments and $C_a(s)_i$ is the apparent concentration in the middle of the ith segment as calculated by the equations in Tables 4 and 5. Since $C_a(s)$ was calculated at intervals 0·1 mm apart and since the effective length of the microphotometer slit, K/M, used in these experiments was 1·0 mm, N is 10.

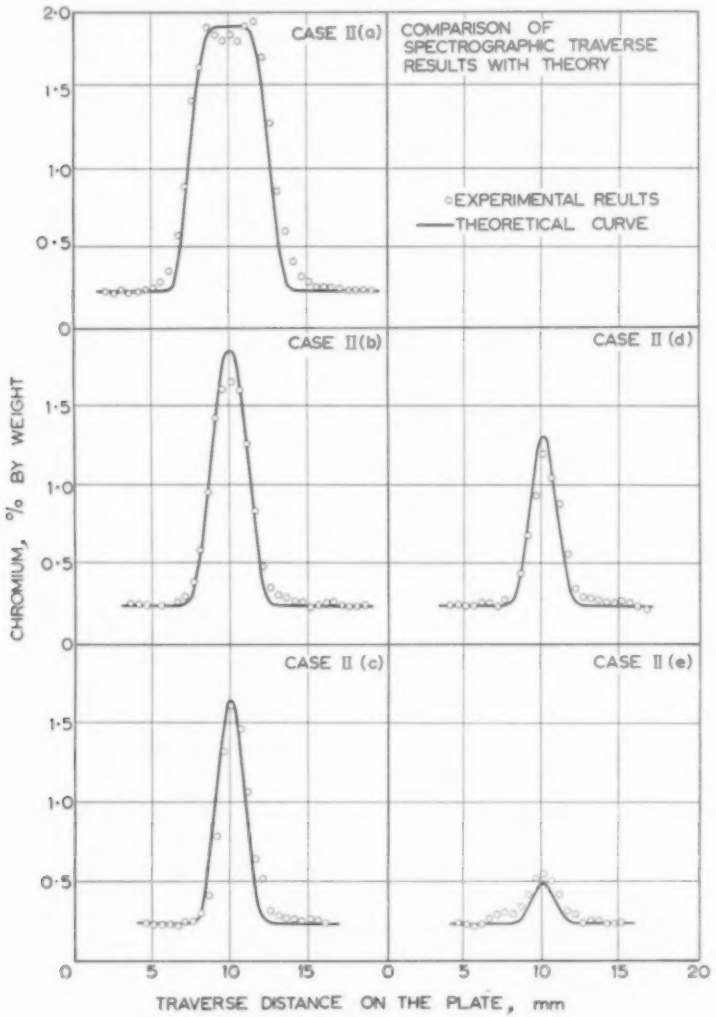

Fig. 3. Traverse results for cases II(a), II(b), II(c), II(d) and II(e).

Traverse results

Typical traverse results for cases II(a), II(b), II(c), II(d) and II(e) are plotted in Fig. 3. The curve drawn in each case is that predicted by theory assuming uniform slit illumination in the microphotometer. Generally, the observed peak concentration is slightly less than the theoretical value. This is thought to be caused by the difficulty in setting precisely on the peak density when the microphotometer measurements were made. Also the observed curves were generally wider than the theoretical curves. Microscopic examination of the segregate after a traverse indicated some preferential sparking to the segregate boundary which would account for this broadening. In practice, however, no preferential sparking has been observed so far in segregated samples submitted to the laboratory.

Fig. 4 compares the observed peak concentrations with those predicted by

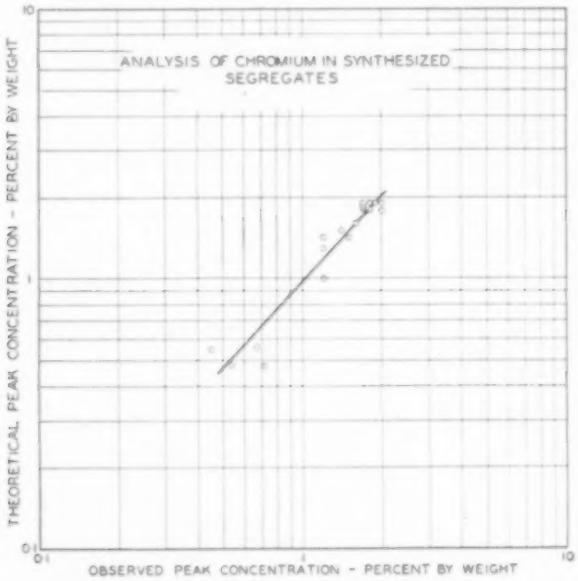

Fig. 4. Comparison of observed peak concentrations with theoretical values.

theory. The differences between the observed and theoretical peak concentrations were tested using the "student t test" under the hypothesis that the true difference was zero. The result of the test indicated that there was no justification for rejecting the above hypothesis. Hence it was concluded that on the average the results predicted by theory will be correct. The deviations of the theoretical values from the observed ones were examined and yielded a standard deviation of 0·07 per cent. Assuming that a linear expression describes the data plotted in Fig. 4, the line of best fit was computed by least squares. This line has a slope of 1·03 and an intercept on the ordinate axis of −0·026. This computed line accounts for 92·2 per cent of the total variation. Considering that the remaining 7·8 per cent of the variation included random experimental error as well as that due to high

VOL. 12 1958

powers of the observed peak concentrations, it was reasonable to conclude that the relationship is adequately described by a linear expression.

Non-uniformity in microphotometer slit illumination

To see if non-uniformity in microphotometer slit illumination introduced an appreciable error in the measurement of apparent peak concentration, and to

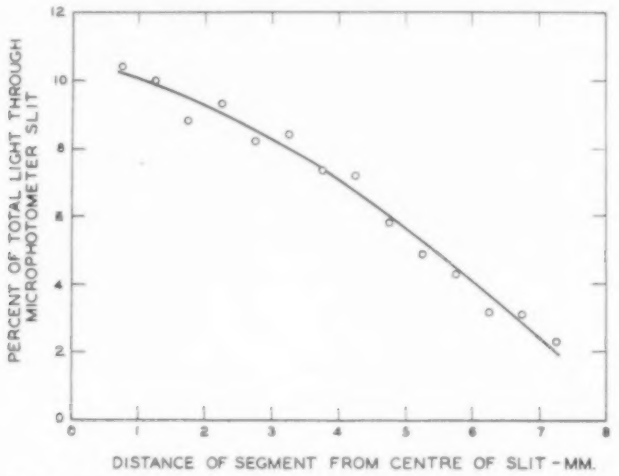

Fig. 5. Distribution of light over the length of the microphotometer slit which shows severe non-uniformity in slit illumination.

correct it if necessary the light distribution over the length of the microphotometer slit was measured as follows:

The microphotometer slit length was set at 15 mm initially by means of a wedge diaphragm, and the sensitivity of the instrument was adjusted to give 100 per cent transmission through a clear portion of an exposed and processed photographic plate. Per cent transmission readings in sextuplicate were taken after successive 1 mm reductions in slit length. The per cent of the total light passing through each pair of 0·5 mm intervals symmetrically placed on either side of the centre of the slit was calculated by subtracting successive per cent transmission readings from each other. These values were plotted against the distance of the centre of the segment from the centre of the slit divided by the magnification of the microphotometer's optical system (Fig. 5). This curve illustrates the severe non-uniformity of slit illumination.

To calculate the values of α' for use in equation (2) the following procedure was followed: the microphotometer slit length used in the traverse experiments was 12·5 mm so that K/M was 1·0 mm (Table 3). This length was divided into ten equal intervals which have been numbered from 1 to 10 in Column 1 of Table 8. The percentage of the light passing through each of the ten intervals was obtained from Fig. 5 and entered in Column 2. These values must be corrected for at 12·5 mm length. This was done by summing Column (2) and dividing each value in the

Table 8. Calculation of α'

Interval no.	Percentage of light passing through each interval	α'
1	4·3	0·057
2	6·2	0·082
3	7·9	0·104
4	9·2	0·121
5	10·3	0·136
6	10·3	0·136
7	9·2	0·121
8	7·9	0·104
9	6·2	0·082
10	4·3	0·057

Sum of column 2 = 75·8

Table 9. Theoretical peak concentrations

Case	Uniform microphotometer slit illumination (%)	Non-uniform microphotometer slit illumination (%)
I(a)	1·91	1·91
I(b)	1·91	1·91
I(c)	1·80	1·81
I(d)	1·51	1·54
I(e)	0·55	0·56
II(a)	1·91	1·91
II(b)	1·86	1·87
II(c)	1·64	1·66
II(d)	1·31	1·33
II(e)	0·48	0·48
III(a)	1·91	1·91
III(b)	1·79	1·81
III(c)	1·43	1·45
III(d)	1·30	1·32
III(e)	0·56	0·56
IV(a)	1·91	1·91
IV(b)	1·82	1·83
IV(c)	1·42	1·43
IV(d)	1·00	1·00
IV(e)	0·48	0·48

VOL. 12 1958

column by the sum. The corrected values are shown in Column 3. These values of α' apply only for the microphotometer lamp and microphotometer used and are the values for use in equation (2).

Table 9 gives a comparison between the theoretical peak concentrations for each of the traverses described in this paper calculated (a) assuming uniform slit illumination and (b) using the values of α' given in Table 8. The error involved in ignoring non-uniformity in slit illumination is very small even though this non-uniformity is severe. Hence, very little precision is sacrificed by assuming uniform illumination.

Conclusions

The double boundary traverse theory has been verified experimentally by carrying out traverses on artificial segregates for each of the twenty different cases predicted by the theory. Although the non-uniformity in microphotometer slit illumination was severe, the investigations showed that it had little effect on the results.

Traverses on segregates as narrow as 0·077 mm indicated that very small segregates may be analysed successfully, but the method is not applicable to segregation on a microscale such as grain boundary segregation in fine-grained alloys. In the practical field it is best applied to the analysis of "stringers" and inclusions in as-cast, rolled and forged products.

Acknowledgements—The author wishes to thank Dr. J. Convey and Dr. R. L. Cunningham for their interest and encouragement. He would also like to acknowledge the assistance of Mrs. B. A. Murray and Mr. F. Quinn in making the necessary measurements and the statistical work of Mr. R. C. Shnay.

References

[1] Hurwitz J. K. *Spectrochim. Acta* 1957 **9** 3.
[2] Hurwitz J. K. *J. Opt. Soc. Amer.* 1952 **42** 484.
[3] Bryan F. R. and Nahstoll G. A. *J. Opt. Soc. Amer.* 1947 **37** 311.

Spectrochimica Acta, 1958, Vol. 12, pp. 224 to 232. Pergamon Press Ltd., London

Infrared spectra analysis for hydrogen fluoride*

D. F. Smith
Technical Division, Oak Ridge Gaseous Diffusion Plant, Union Carbide Nuclear Company
Oak Ridge, Tennessee

(*Received* 21 *June* 1957)

Abstract—An equation describing the apparent absorption at the peaks of the lines of the hydrogen fluoride fundamental band is given for pure hydrogen fluoride. This equation has a single parameter which for fixed conditions is a constant. An equation describing the fractional increase in absorption when foreign gas is added is also given. This contains a parameter which is a constant for the foreign gas and the particular line at constant temperature. A table giving this parameter for five lines and twenty different foreign gases at 100°C is presented. These equations are combined so that they may be used for analysis for hydrogen fluoride.

Introduction

In the course of experiments on the effects of foreign gases on the breadths of the lines of the fundamental vibration rotation spectrum of hydrogen fluoride an expression for the apparent absorption of hydrogen fluoride in terms of the partial pressure of hydrogen fluoride and the partial pressure of the foreign gas was developed and tested. The use of this expression permits an improved analysis for hydrogen fluoride, with the analytical calibration parameters dependent on only two kinds of measurements. One kind of parameter depends on the particular experimental conditions such as cell length and spectrometer resolving power. This parameter can be measured with pure hydrogen fluoride under the conditions to be used in the analysis. The other kind of parameter is characteristic of the foreign gas present in the sample to be analyzed. It can be measured under optimum experimental conditions for the determination of this parameter, and employed when conditions or spectrometers are changed. This report will present the expression for the absorption, methods of evaluating the parameters and a list of the foreign gas parameters that have been measured.

Pure hydrogen fluoride

When the lines of the fundamental vibration band of hydrogen fluoride are examined in a cell of sufficient length (about 10 cm in most of the experiments reported here), and with a spectrometer having sufficient resolving power to isolate the lines nicely, it may be verified that the observed absorbance at the peak of the line is linear in the pressure, that is

$$A_0 = mp_{HF} \tag{1}$$

The absorbance is defined as $-\log_{10}$ (fractional energy transmitted), which is a function of the frequency. A_0 represents this absorbance at the peak of the line

* This document is based on work performed for the Atomic Energy Commission by Union Carbide and Carbon Corporation at Oak Ridge, Tennessee.

VOL. 12 1958

with a sample of pure hydrogen fluoride at a pressure p_{HF}. The parameter m is a constant for a particular set of experimental conditions. It does, however, depend on:

(1) Cell length; m increases about as the square root of the cell length.

(2) Spectrometer slit width; m increases as the slit width is narrowed. It is also dependent on the spectrometer transmission function shape, and hence depends on the characteristics of the optical components of the spectrometer and their adjustments. Thus m may differ from spectrometer to spectrometer even though the slit widths and other characteristics are similar.

Table 1. Typical values of $m = A_0/p_{HF}$, the absorbance per unit pressure for pure hydrogen fluoride at the line peak in units of [cm Hg of HF]$^{-1}$

Line	Prism*	Grating†			
	100°C	48°C	118°C	198°C	292°C
$R(0)$	0·0174	0·139	0·102	0·073	0·051
$R(1)$	0·0231	0·176	0·129	0·099	0·073
$R(2)$	0·0224	0·173	0·131	0·104	0·076
$R(3)$	0·0184	0·131	0·103	0·089	0·072
$R(4)$	0·0121	0·080	0·068	0·067	0·060
$R(5)$		0·046	0·046	0·045	0·043
$R(6)$		0·021	0·024	0·028	0·026
$R(7)$			0·012	0·015	0·017

* Perkin–Elmer model 12 C (single pass) spectrometer with lithium fluoride prism. Slit widths 29 μ resolution estimated as about 10 cm^{-1}. 100 mm cell length.

† University of Tennessee grating spectrometer 15,000 lines/in. grating. Slit widths 0·011 in. resolution estimated as 0·3 cm^{-1}. 30 mm cell length. These results obtained from Dr. G. A. Kuipers.

(3) Sample temperature; the temperature variation is not calculable. For lines of low J it decreases with temperature, while for lines of high J it increases.

For the purposes of analysis, m can be considered an experimental constant which must be evaluated for the experimental conditions to be used in the analysis. Table 1 presents values of m that have been obtained for certain experimental conditions. It is to be emphasized that these are illustrative values only, and are not to be used with other spectrometers, or even with the same spectrometer when different adjustments of the optical system have been made.

Dennison [1] and Nielsen *et al.* [2] present expressions for the absorption at the peak of a spectral line for particular assumptions as to the line shape and the spectrometer transmission function. Both equation (1) and (2) can be obtained from these particular results. If, however, equation (1) is empirically observed, (2) follows even though the line shape or spectrometer transmission function is not of the particular form assumed by them. One can conceive of certain spectrometer transmission functions with which different behavior from that indicated

by equation (1) would be found. While it is not likely that these transmission functions be encountered it is recommended that equation (1) be tested at the same time as the quantity, m, is evaluated. If equation (1) does not pertain the technique described here can not be employed.

Table 2. Measured ratio of broadening efficiencies, b/a, at 100°C

Broadening compound	HF line				
	$R(0)$	$R(1)$	$R(2)$	$R(3)$	$R(4)$
H_2	0·183	0·113	0·080	0·066	0·063
A	0·092	0·047	0·033	0·035	0·042
O_2	0·112	0·070	0·055	0·050	0·051
CH_4	0·167	0·116	0·107		
SF_6	0·153	0·104	0·084	0·085	0·102
C_2F_6	0·171	0·130	0·102	0·104	
F_2	0·177	0·122	0·094	0·072	0·071
N_2	0·198	0·152	0·127	0·106	0·101
CO	0·237	0·192	0·153	0·131	0·131
C_3F_8	0·202	0·155	0·131	0·134	0·189
UF_6	0·226	0·177	0·188	0·280	0·46
MoF_6	0·244	0·159	0·167	0·181	0·253
CS_2	0·256	0·164	0·143	0·158	0·211
$CClF_3$	0·266	0·152	0·104	0·107	0·115
Cl_2	0·293	0·169	0·142	0·131	0·151
CCl_3F	0·284	0·193	0·167	0·168	0·203
N_2O	0·336	0·206	0·150		
CO_2	0·36	0·22	0·146	0·144	0·159
ClF_3	0·48	0·254	0·186	0·182	0·222
$COCl_2$	0·541	0·239	0·174		
CH_3Cl	0·91	0·323	0·179	0·154	0·167
SO_2	0·92	0·468	0·230	0·177	0·219

Hydrogen fluoride in the presence of other gases

When a foreign gas is added to the sample of hydrogen fluoride the observed absorbance at the peak of the line is increased. This behavior is described quantitatively by the equation

$$\left(\frac{A}{A_0}\right)^2 = 1 + \frac{b}{a}\frac{p_b}{p_{HF}}. \tag{2}$$

Here A_0 is again the absorbance at the peak of the line which is obtained with pure hydrogen fluoride at a pressure p_{HF}, while A is the absorbance at the peak of

VOL. 12 1958

the line when a sample of hydrogen fluoride is present in the cell at a partial pressure p_{HF} together with a foreign gas at a partial pressure p_b. The quantity b/a is the ratio of the foreign gas broadening efficiency to the self-broadening efficiency. For the present purposes, b/a can be taken as a parameter dependent on the particular hydrogen fluoride line and the particular foreign gas. It varies only slowly with temperature. It does not depend on the spectrometer or spectrometer adjustments, and can be measured on one spectrometer and used with any other spectrometer for which equation (1) pertains. Table 2 lists the broadening efficiency ratios that have been measured at 100°C. These values should not require re-measurement for use in analysis. Table 3 presents a comparison of the values of b/a at room temperature and 100°C to illustrate the small variation in b/a.

The compounds listed in Table 2 were selected to give information as to foreign gas broadening properties, and not as compounds most likely to be encountered in analytical work.

Some compounds have been investigated on which b/a was not determined for one of a number of reasons.

(1) Some compounds such as methyl fluoride absorb in the region of the hydrogen fluoride R branch, and the corrections for this absorption are so large that b/a can not be evaluated with any precision.

(2) Some compounds when admitted to the conditioned system release hydrogen fluoride into the system making the partial pressure of hydrogen fluoride uncertain. Hydrogen chloride probably releases hydrogen fluoride by reaction with the fluorides on the surface, while carbon tetrachloride probably does this by driving hydrogen fluoride off the walls.

(3) Some compounds such as diethyl ether, acetone, methanol and dioxane complex with hydrogen fluoride in the vapor phase, and appreciable amounts of the hydrogen fluoride may be bound in the complex hence not absorbing the infrared radiation as monomeric hydrogen fluoride.

The values of b/a presented in Tables 2 and 3 were obtained by first filling a cell to a pre-assigned pressure of hydrogen fluoride, usually 50·0 or 100·0 mm and measuring A_0. The foreign gas was then added, increasing the pressure. The partial pressure of the foreign gas was taken to be the total pressure p, less the initial pressure of hydrogen fluoride. The foreign gas was added in four or five increments of pressure until the total pressure was about 1 atm, and A measured after each increment. This procedure then was used to test the validity of equation (2) in each case. For a few cases where the values of b/a are small the foreign gas was added to a total pressure of about 3 atm. Table 4 illustrates a determination of b/a.

In the measurement of b/a, it was verified that equation (2) pertained in almost every instance. The exceptions were for the $R(0)$ line of hydrogen fluoride broadened with sulfur dioxide or methyl chloride. This breakdown can result from either a drastic change in line shape (which has been observed at high resolution for the $R(0)$ line broadened with sulfur dioxide), or from excessive values of $(b/a)(p_b/p_{HF})$.

The considerations on which equation (2) were obtained limit the range of validity to small values of $(b/a)(p_b/p_{HF})$. For the hydrogen fluoride lines observed

with a 10 cm absorption cell, the absorbance of the $R(2)$ line is noticeably less than that computed from equation (2) when $(b/a)(p_b/p_{HF})$ exceeds about 400. For the weaker lines it is less at even smaller values. The absorbance A, for $R(4)$ is less than that computed with equation (2) for values of $(b/a)(p_b/p_{HF})$ in excess of about 100.

Table 3. Broadening efficiency ratios, b/a, at two temperatures

Compound	Temperature (°C)	$R(0)$	$R(1)$	$R(2)$	$R(3)$	$R(4)$
N_2	25	0·170	0·139	0·119	0·102	0·096
	100	0·198	0·152	0·127	0·106	0·101
C_3F_8	25	0·176	0·133	0·126	0·144	0·190
	100	0·202	0·155	0·131	0·134	0·190
CCl_3F	25	0·23	0·15	0·14	0·16	0·21
	100	0·284	0·193	0·167	0·168	0·203
Cl_2	25	0·24	0·149	0·117	0·119	0·137
	100	0·293	0·169	0·142	0·131	0·151
SO_2	25	0·78	0·37	0·21	0·20	0·27
	100	0·92	0·47	0·23	0·18	0·22

Table 4. $R(2)$ line of hydrogen fluoride with sulfur dioxide at 100°C.

$$\frac{b}{a} = \left[\left(\frac{A}{A_0}\right)^2 - 1\right]\frac{p_{HF}}{p - p_{HF}}$$

Prism 50 mm HF		Prism 80 mm HF	
$p - p_{HF}$	b/a	$p - p_{HF}$	b/a
176·3	0·224	149·8	0·223
305·0	0·229	270·2	0·228
436·1	0·234	402·1	0·230
558·0	0·233	535·1	0·233
672·2	0·230	654·3	0·232
	Mean 0·230		

Equation (2) pertains to a sample containing hydrogen fluoride and a single foreign gas. It can be used for a mixture of foreign gases if an effective value of (b/a) is employed:

$$\left(\frac{b}{a}\right)_{\text{effective}} = \sum_i c_i \left(\frac{b}{a}\right)_i \qquad (3)$$

VOL. 12 1958

where c_i is the mole fraction of the ith component and $(b/a)_i$ is the broadening efficiency ratio for this component. This substitution has not yet been experimentally tested.

Analysis

Equations (1) and (2) when combined yield

$$\left(\frac{A}{mp_{\mathrm{HF}}}\right)^2 = 1 + \frac{b}{a}\cdot\frac{p_b}{p_{\mathrm{HF}}}$$

and for a mixture of a single foreign gas with hydrogen fluoride, $p_b = p - p_{\mathrm{HF}}$, so that

$$\left(\frac{A}{mp_{\mathrm{HF}}}\right)^2 = 1 + \frac{b}{a}\frac{(p - p_{\mathrm{HF}})}{p_{\mathrm{HF}}} \tag{4}$$

This is a quadratic equation in the partial pressure of hydrogen fluoride, p_{HF}. When solved for p_{HF} it yields

$$p_{\mathrm{HF}} = \frac{-b/a}{2(1 - b/a)}\,p + \tfrac{1}{2}\left[\left(\frac{b/a}{1 - b/a}\,p\right)^2 + \frac{4A^2}{m^2(1 - b/a)}\right]^{1/2} \tag{5}$$

The mole fraction of hydrogen fluoride present in the sample is then

$$C = \frac{p_{\mathrm{HF}}}{p} = \frac{-b/a}{2(1 - b/a)} + \tfrac{1}{2}\left[\left(\frac{b/a}{1 - b/a}\right)^2 + \frac{4A^2}{m^2p^2(1 - b/a)}\right]^{1/2} \tag{6}$$

For low concentration of hydrogen fluoride, $(b/a)(p_b/p_{\mathrm{HF}})$ is large compared with unity, and

$$C(\mathrm{HF}) \simeq \frac{A^2}{m^2p^2(b/a)} \tag{7}$$

For a mixture of several foreign gases, it is necessary to analyze for the other components separately to determine their concentration. The effective value of b/a given by equation (3) is then employed.

Equations (6) and (7) are then in a form that can be used for analysis. There are advantages in using such expressions. Firstly, it is not necessary to make an empirical calibration relating the concentration of hydrogen fluoride to the sample pressure, composition and absorbance over the range contained in the specific sample to be analyzed. Secondly, since b/a can be determined with reasonably high pressures of hydrogen fluoride, it is not necessary to obtain a sample of the foreign gas entirely free of hydrogen fluoride. Thirdly, the use of these expressions permits an estimate of the concentration of hydrogen fluoride present in the sample used for calibration, so that corrections to the parameter b/a can be made for this concentration. For values of b/a reported in Table 3, these corrections were negligible.

The advantages are of consequence, because in some cases the precision of the analysis using empirical calibration has been limited by the uncertainty of the hydrogen fluoride concentration in the foreign gas used in the calibration. In effect, one could not be certain how much hydrogen fluoride was present in the synthetic samples prepared for calibration.

It should be clear that for low concentrations of hydrogen fluoride, when the major portion of the experimental error is in the measurement of the absorbance A, the precision will be best at the highest available sample pressure. From equation (7) this absorbance at constant concentration varies as the square of the total pressure.

Expressions (5) and (6) have been employed in analysis for hydrogen fluoride in samples of uranium hexafluoride and fluorine. The samples were taken directly in the infrared cell. The cell was well conditioned before attaching to the sampling

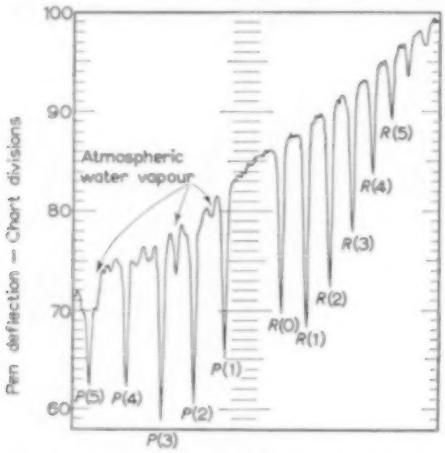

Fig. 1. Tracing of scan of hydrogen fluoride fundamental vibration band. Perkin–Elmer model 12-C (single pass, single beam) spectrometer with lithium fluoride prism. Slits 29 μ. Cell length 10 cm. Calcium fluoride windows on cell, Globar source, thermocouple detector. Cell at 100°C. Sample prepared by adding fluorine to hydrogen fluoride at 25·0 mm Hg pressure until total pressure was 749 mm Hg.

port. The leads and the cell were brought into equilibrium with the sample when possible by flowing the sample through the cell for a one half-hour period. When there was no provision at the sampling site for flowing the sample, the cell was filled and after about 5 min evacuated, and this filling procedure repeated at least four times. The cell was then valved closed, removed from the sampling manifold and removed to the infrared spectrometer, where the spectrum was recorded. The sampling procedure was used in order to minimize such effects as sample reaction with the unconditioned leads which can produce hydrogen fluoride, or the adsorption or desorption of hydrogen fluoride on the cell walls. On the one hand it has not been established that this procedure is adequate nor on the other hand that less time-consuming procedure would be adequate.

In scanning the spectrum, even with the slowest available scanning speed, the hydrogen fluoride lines are not recorded with the full deflection that would be obtained with an infinitely slow scan. Rather than reduce the scanning speed, which would require a longer time to scan the spectrum, the spectrometer has been manually adjusted to the peak of the line. The background has been determined by interpolation of the deflections between the lines.

Fig. 1 shows a chart record of a sample prepared by adding fluorine to hydrogen

VOL. 12 1958

fluoride at a pressure of 25·0 mm, until the total pressure of 749 mm was obtained. Table 5 presents the parameters used in the analysis and the results of an analysis based on equations (4) and (6).

Summary

For the lines of the fundamental vibration rotation band of hydrogen fluoride the following equations pertain:

$$\left(\frac{A}{A_0}\right)^2 = 1 + \frac{b}{a}\frac{p_b}{p_{HF}}$$

and

$$A_0 = mp_{HF}$$

A_0 is the absorbance at the peak of a line for a sample of pure hydrogen fluoride at a pressure p_{HF}.

Table 5. Analysis of synthetic sample prepared by adding fluorine to 25·0 mm of hydrogen fluoride until the total pressure was 749 mm. $C(HF) = 3{\cdot}3^4$ mole per cent

Line	Deflection* background (interpolated)	Deflection† at peak	Absorbance	b/a‡	m§ $(\text{mm Hg})^{-1}$	p_{HF} Calculated (mm Hg)	Concentration of HF (mole per cent)
$R(0)$	87·1	68·0	$0{\cdot}108_1$	0·177	$1{\cdot}74(10)^{-3}$	25·0	$3{\cdot}3_4$
$R(1)$	88·5	66·5	$0{\cdot}124_8$	0·122	$2{\cdot}31(10)^{-3}$	25·7	$3{\cdot}4_3$
$R(2)$	90·7	70·8	$0{\cdot}108_2$	0·094	$2{\cdot}24(10)^{-3}$	25·1	$3{\cdot}3_5$
$R(3)$	92·4	76·6	$0{\cdot}082_1$	0·072	$1{\cdot}84(10)^{-3}$	25·8	$3{\cdot}4_4$
$R(4)$	94·1	82·8	$0{\cdot}056_2$	0·071	$1{\cdot}21(10)^{-3}$	27·4	$3{\cdot}6_5$
					Mean	25·4	$3{\cdot}4_4$

* Interpolated on scan in Fig. 1.
† From manually setting on line peak.
‡ From Table 2.
§ Spectrometer conditions as for Table 1.

A is the absorbance at the peak of the line for an identical sample of hydrogen fluoride at the sample partial pressure, p_{HF}, when mixed with a foreign gas at a partial pressure p_b.

m depends upon the particular experimental conditions.

b/a is the ratio of the foreign gas broadening efficiency to the self broadening efficiency. It is not dependent on the experimental conditions except for a small variation with temperature.

The equations can be used for an analysis for hydrogen fluoride. The parameters m can be determined using pure hydrogen fluoride and the particular experimental conditions to be used in the analysis. The parameters b/a can be measured with different experimental conditions. A table of values of b/a for twenty different foreign gases including uranium hexafluoride, chlorine trifluoride and fluorine is presented.

By the use of this analysis the necessity of preparing calibration samples for

each set of sample conditions has been eliminated. The precision of the analysis has been improved by the elimination of uncertainties of the effect of an hydrogen fluoride impurity in the foreign gas sample used for calibration.

Acknowledgement—Requisite to this work has been a knowledge of adequate procedures for handling hydrogen fluoride and observing its spectrum. These procedures have been developed over a considerable period with contributions by Mr. T. G. Burke, Dr. D. W. Magnuson and Dr. G. A. Kuipers, and helpful advice from Dr. W. Davis, Jr.

The author would also like to thank Professor A. H. Nielsen for helpful discussion and for the use of the University of Tennessee grating spectrometer.

References

[1] Dennison D. M. *Phys. Rev.* 1928 **31** 503.
[2] Nielsen J. R., Thornton V., and Dale E. B. *Rev. Mod. Phys.* 1944 **16** 307.

VOL.
12
1958

Spectrochimica Acta, 1958, Vol. 12, pp. 233 to 238. Pergamon Press Ltd., London

The infrared spectra of some gem dihydroxy compounds and their deuterated derivatives

D. M. W. Anderson,* L. J. Bellamy† and R. L. Williams†

(*Received* 8 *February* 1958)

Abstract—The spectra of a number of compounds having two hydroxyl groups at the same carbon atom have been studied, together with their deuterated derivatives. This series has some advantages over simple alcohols for the study of the in-plane OH deformation frequencies. The results confirm earlier suggestions that this vibration occurs in the 1400–1300 cm^{-1} region in normal alcohols, and that it is liable to interact with CH deformation frequencies. Marked changes occur also in the 1200–1000 cm^{-1} region in this series and the reasons for this are discussed.

Introduction

There has been much controversy over the assignments of the OH in-plane deformation mode in alcohols, both in the monomeric and associated forms. Associated alcohols show five bands which are to some extent sensitive to deuteration and which change on dissociation to the monomer. These have been listed by Stuart and Sutherland [1] as falling near 3300 cm^{-1}, 1400 cm^{-1}, 1330 cm^{-1}, 1110 cm^{-1} and 650 cm^{-1}. The first and last of these are clearly the OH stretching and out-of-plane deformation vibrations but the assignment of the remainder is a matter of some difficulty. Some authors [2–5] regard the in-plane deformation mode as falling in the 1100–1000 cm^{-1} region and associate the higher frequencies with C–O stretching motions. Others reverse these assignments [1, 6, 7] and Krimm *et al.* [7] have suggested that the multiple absorptions in the 1400–1300 cm^{-1} range arise from interactions between the δOH mode and the deformation vibrations of hydrogen atoms attached to the same carbon atom. This is supported by the observation that only a single band appears in this region in tertiary alcohols, and also by Hadži's [8] work on the molecule CH_3CD_2OH which behaves similarly. Tarte and Deponthiere [9] have recently made an extensive study of the corresponding monomeric bands in normal and hydrated alcohols. Their conclusions follow those of Stuart and Sutherland [1] and the monomeric OH in-plane deformation frequency is assigned near 1270 cm^{-1}. However, they point out that in many cases the number of bands which disappear on deuteration is not the same as the number of new bands produced. This has led them, in common with some other workers [10, 11] to suggest that rotational isomerism may play an important part in determining the numbers and positions of these absorptions in some cases.

In the course of a recent investigation [12] we have had occasion to study the spectra of a small number of *gem* dihydroxy compounds produced by the addition of water across a suitably activated carbonyl group. It occurred to us that such

* Department of Chemistry, University of Edinburgh, Edinburgh 9.
† ERDE Ministry of Supply, Waltham Abbey, Essex.

systems might have a number of advantages over simple alcohols for the study of this problem; not only are the deuterated analogues very easily prepared but the products are crystalline solids in which rotational isomerism cannot occur. Further, unlike the simple alcohols, the strengths of the hydrogen bonds formed on association vary widely so that systematic shifts should occur in the positions of the δOH modes in the opposite direction to the shifts of the OH stretching absorptions. Finally a number of these compounds, such as hexachloroacetone hydrate, and ninhydrin hydrate, contain no methylene groups and will therefore be free from

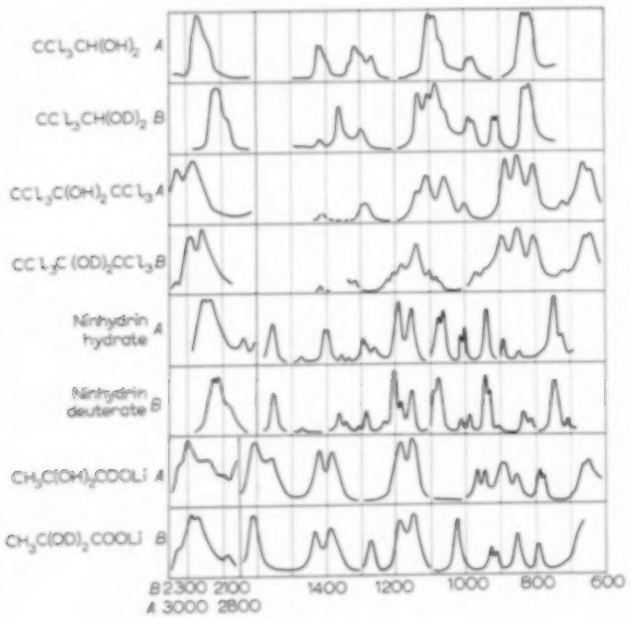

Fig. 1.

coupling effects with this particular group. We have accordingly examined a number of such compounds in both the H and D forms and have compared their spectra with those of the original carbonyl compound. The results are discussed below, and some typical spectra are illustrated in Fig. 1.

Experimental

Spectra were measured with either a Grubb Parsons double beam S.3A spectrometer or with a Hilger double beam H.800 instrument. Sodium chloride prisms were used in both cases. Specimens were prepared as mulls in paraffin oil or perfluorokerosene. The hydrates and deuterates were prepared, in most cases by the addition of the calculated quantity of water or D_2O to the carbonyl compounds. The deuterated hydrates of ninhydrin and of lithium pyruvate were however obtained by the repeated recrystallization of the normal hydrates from heavy water.

VOL. 12 1958

Results and discussions

(a) *Chloral hydrate:* $CCl_3C(OH)_2H$

This compound shows a strong OH stretching band at 3330 cm^{-1} (OD 2439 cm^{-1} ratio 1·37). The band is however somewhat asymmetric and it is possible that the two hydroxyl groups are not quite equivalently bonded. The results from the remainder of the spectrum support this. In the 1400–1300 cm^{-1} region the original aldehyde shows only a single absorption at 1355 cm^{-1} due to the deformation mode of the isolated CH group. This band appears at the same point in the OD compound but is missing from the spectrum of the normal hydrate where it is replaced by a doublet at 1418, 1410 cm^{-1} and another band at 1300 cm^{-1}. This can best be interpreted as being due to the interaction of two slightly different δOH frequencies with the aldehydic CH deformation along the lines suggested by KRIMM *et al.* [4] and is supported by the appearance of a new doublet in the deuterated material at 913 cm^{-1} and 905 cm^{-1}. If the original uncoupled δOH modes are assumed to fall near 1350 cm^{-1} these correspond to ratios of 1·48 and 1·49.

In addition to these changes however a new band appears on deuteration at 1130 cm^{-1} along with the two other bands in this region (1085 cm^{-1} and 1102 cm^{-1}) which are common to both hydrates. This band has no counterpart at higher frequencies in the normal hydrate. None of these bands appears in the spectrum of the original ketone and they are probably associated with C–O stretching motions coupled with the C–C skeletal mode. These bands are known to be particularly sensitive to their environment. In the sterols a single band near 1050 cm^{-1} is shown by equatorial 3-hydroxy groups whereas axial substitution leads to two bands. In the triterpenes a hydroxy group at the 3 position leads to three bands in some cases and two in others [13]. It would therefore seem reasonable to suppose that the additional 1130 cm^{-1} band in the present case results from an accidental alteration in the degree of degeneracy of these coupled modes. As will be seen below this is supported by the similar behaviour of many of the other compounds studied.

(b) *αα′β-Trichlorobutyraldehyde hydrate:* $CH_3CHClCCl_2CH(OH)_2$

This compound behaves very similarly to chloral hydrate. The original aldehyde absorbs at 1370 cm^{-1} due to the aldehydic CH deformation mode. This band vanishes in the hydrate and is replaced by a doublet at 1448 and 1439 cm^{-1}, and another band at 1282 cm^{-1}. These can be assigned to coupled OH and CH deformation modes. In the deuterate the 1370 cm^{-1} CH band reappears and a new absorption is shown at 906 cm^{-1} corresponding to the OD in plane deformation.

As before, there are also marked changes on deuteration in the 1150–1000 cm^{-1} region, in which additional bands appear at 1171 cm^{-1} and 1000 cm^{-1}. These can be regarded as arising in the same way as the similar bands in deuterated chloral.

(c) *Dichloroacetaldehyde hydrate:* $CHCl_2CH(OH)_2$

The OH stretching frequency of this compound occurs at 3270 cm^{-1} (OD 2440 cm^{-1} ratio 1·34), so that the in-plane deformation is to be expected in the same region as in chloral hydrate. In the original aldehyde two separate CH deformation modes appear associated with the two different hydrogen atoms. One of these, at

1370 cm^{-1}, remains on hydration, but the other (1361 cm^{-1}) vanishes. This latter is presumably the aldehyde CH which is now coupled with the OH deformation, and new bands appear at 1408 cm^{-1}, 1333 cm^{-1} and 1292 cm^{-1}. These are not shown by the deuterate which however shows changes in the 900 cm^{-1} region. The hydrate has a single band at 940 cm^{-1} whilst the deuterate has two weaker absorptions at 963 cm^{-1} and 922 cm^{-1}. These could well arise from an accidental coupling between the OD in-plane frequency and the original 940 cm^{-1} absorption.

In the 1150–1000 cm^{-1} range there are again marked changes. The hydrate has two strong bands at 1107 cm^{-1} and 1046 cm^{-1} whereas the deuterate has three, at 1158 cm^{-1}, 1080 cm^{-1} and 1055 cm^{-1}. No higher frequency absorption corresponding to the 1158 cm^{-1} band can be traced in the hydrate and a change in the degree of coupling of the sketelal modes appears to offer the best explanation. One small additional change occurs on deuteration, in that a weak band at 1250 cm^{-1} in the hydrate moves to 1278 cm^{-1} in the deuterate where it remains weak. This change would also appear to be unlikely to be associated with an OH or OD frequency.

(d) *Hexachloracetone hydrate:* $(CCl_3)_2C(OH)_2$

This is a particularly interesting compound, partly because it contains no CH groups capable of interaction with the δOH mode and partly because the OH stretching frequencies are abnormally high compared with simple associated alcohols, presumably owing to steric hindrances to hydrogen bonding. Two sharp OH stretching bands occur at 3460 cm^{-1} and 3356 cm^{-1} suggesting that the two hydroxyl groups are not equivalently bonded, and these are paralleled by the OD frequencies which occur at 2577 cm^{-1} (ratio 1·34) and 2519 cm^{-1} (ratio 1·33). The high OH stretching frequencies would be expected to correspond to δOH in plane vibrations at lower frequencies than before and nearer to those of monomeric systems. In fact two bands appear in the spectrum of the hydrate at 1299 cm^{-1} and 1282 cm^{-1} which are absent from both the original ketone and from the deuterate. We would associate these with the δOH modes of the two OH groups and this is supported by the presence of a corresponding pair of bands at 966 cm^{-1} (ratio 1·35) and 930 cm^{-1} (ratio 1·38) in the deuterate.

In the 1150–1000 cm^{-1} region a number of remarkable changes occur on deuteration. Where the hydrate shows four bands in this range, the deuterate has six which differ widely in frequency and intensity. It is difficult to see how changes of this order could be accounted for in terms of OH and OD modes and it would seem more probable that changes in the degree of coupling between C–C and C–O stretching modes are again involved. In this connexion it is noteworthy that the number of such linkages is now greater than in the previous cases and more complex interactions may be expected. In acetals and ketals it is known that upwards of four absorption bands can occur in this region due to such coupled modes [10, 14].

(e) *Ninhydrin hydrate*

This is another compound in which there is no possibility of coupling between OH and CH vibrations. The OH stretching frequencies again appear as a doublet (3300 cm^{-1} and 3247 cm^{-1}) with the OD bands in corresponding positions (2439

VOL. 12 1958

cm^{-1} ratio 1·35, 2410 cm^{-1} ratio 1·36). These frequencies are close to those of simple alcohols so that the δOH modes can be expected to be more nearly normal. A pair of bands occurs at 1399 cm^{-1} and 1389 cm^{-1} in the hydrate which are absent from the deuterate, which contains instead two bands at 941 cm^{-1} and 930 cm^{-1}. The 941 cm^{-1} band cannot be positively identified with an OD vibration however as the hydrate has itself a medium intensity band at 943 cm^{-1}. A weak band at 1253 cm^{-1} in the hydrate also vanishes on deuteration and the reasons for this are not clear. In the 1200–1000 cm^{-1} range the hydrate has six sharp bands. These are all reproduced in the deuterate with only minor frequency changes although the relative intensities change considerably. In addition the deuterate contains a new strong absorption at 1200 cm^{-1}. As before it is difficult to see how changes of this magnitude could originate in OH modes and it would seem more logical to associate these bands with coupled sketal frequencies.

(f) *Lithium pyruvate hydrate:* $CH_3C(OH)_2COOLi$

This material has been shown previously to exist wholly in the *gem* dihydroxy form [12] whereas the sodium salt does not form a hydrate at all and retains its carbonyl character. Owing to the strongly electronegative COO^- group the hydroxyl functions are very strongly bonded and the stretching absorption occurs as a single broad band at 3000 cm^{-1} (o.d. 2250 cm^{-1} ratio 1·33). The δOH in plane frequency should therefore occur at appreciably higher frequencies than in the previous cases and we find that a medium strength band at 1551 cm^{-1} does in fact vanish on deuteration, being replaced by another band of similar intensity at 1023 cm^{-1} (ratio 1·54). Two bands occur in the 1200–1000 cm^{-1} region in both the hydrated and deuterated compounds at 1185 cm^{-1} and 1150 cm^{-1}, but the deuterated product has also a new band at 1273 cm^{-1}. This is rather higher than would be expected to arise from coupling between C–C and C–O modes and its origin is not clear. The spectra also show minor differences of position in the 1500–900 cm^{-1} region and the hydrate contains an absorption at 897 cm^{-1} which is absent from the deuterate. This last is possibly the δOH out of plane frequency. This would normally occur in the 750–650 cm^{-1} range but would be expected to shift to higher frequencies under the influence of the abnormally strong hydrogen bonding.

(g) *Tetrachloroacetone hydrate:* $CCl_2H\ C(OH)_2CCl_2H3H_2O$

It is not possible to obtain this compound free from water of crystallization. In addition the deuterated product exchanges rapidly with atmospheric moisture so that we were unable to obtain any sample wholly free from OH absorptions. The value of the OH stretching region is therefore diminished owing to the uncertainties in the position of the free water bands. However bands present in the hydrate at 1389 cm^{-1} and 1351 cm^{-1} diminished sharply in intensity on partial deuteration and these are probably due to the δOH mode. In agreement with this a new band appears at 970 cm^{-1} in the deuterated material. This corresponds to a ratio of 1·4 based on a mean value. As with hexachloroacetone hydrate, the frequency and intensity changes in the 1200–1000 cm^{-1} range following deuterium exchange are considerable. The two strong bands of the hydrate at 1110 cm^{-1} and 1087 cm^{-1} remain in substantially the same positions but alter in relative intensities; a new

strong band appears at 1176 cm^{-1} and a band at 1005 cm^{-1} is replaced by a series of four new bands in the range 1040–1000 cm^{-1}. Changes in the coupling of skeletal modes is again the most likely explanation of this behaviour.

Conclusions

As in the cases of simple associated alcohols, the materials studied all show multiple shifts on deuteration which cannot be simply interpreted in terms of vibrations of the OH group alone. Of the two possible regions to which the δOH in-plane frequency might be assigned, the 1400–1300 cm^{-1} range would seem to be a much more likely choice than the alternative range of 1150–1000 cm^{-1}, because of the appearance of corresponding OD bands in the 1000–900 cm^{-1} region which are in a correct ratio to the higher frequency bands. On the other hand no similar absorption can be found at lower frequencies which could be related to the 1150–1000 cm^{-1} bands. The higher frequency assignment is also very strongly supported by the systematic shifts shown by these absorptions in relation to the OH stretching frequencies. In hexachloroacetone hydrate in which the OH stretching frequencies are unusually high for an associated alcohol, the bands assigned to the OH deformations are then corresponding low. On passing to compounds such as chloral hydrate the OH stretching frequencies fall and the deformations rise as expected. Finally in the hydrate of lithium pyruvate the abnormally low OH stretching frequency is accompanied by a high deformation frequency. No similar systematic behaviour can be traced in any of the bands in the alternative 1150–1000 cm^{-1} range. The commonest effect of deuteration in this region is the appearance of additional bands which are in many cases on the high frequency side. No corresponding OH bands can be found with which these might be associated, and the extent of the changes themselves is such as to suggest that something more than simple changes in OH absorptions is involved. The fact that all samples were studied in the solid phase eliminates the possibility that rotational isomerism is responsible for these effects and the suggestion given above that coupled skeletal modes are involved would seem to be the most satisfactory alternative.

This work was carried out during the tenure by one of us (D. M. W. A.) of a vacation consultancy of the Ministry of Supply.

References

[1] Stuart A. V. and Sutherland G. B. B. M., *J. Chem. Phys.* 1956 **24** 559.
[2] Quinan J. R. and Wiberley S. E., *J. Chem. Phys.* 1953 **21** 1896.
[3] Quinan J. R. and Wiberley S. E., *Analyt. Chem.* 1954 **26** 1762.
[4] Borden A. and Barker E. V., *J. Chem. Phys.* 1938 **6** 553.
[5] Davies M., *J. Chem. Phys.* 1948 **16** 267.
[6] Noether H. D., *J. Chem. Phys.* 1942 **10,** 693.
[7] Krimm S., Liang C. Y. and Sutherland G. B. B. M., *J. Chem. Phys.* 1956 **25** 778.
[8] Hadži D. and Jeramic D., *Spectrochim. Acta.* 1957 **9** 263.
[9] Tarte P. and Deponthiere R., *Bull. Soc. Chim. Belg.* 1957 **66** 525.
[10] Badger R. M. and Bauer S. H., *J. Chem. Phys.* 1936 **4** 711.
[11] Maclou M. and Henry L., *C. R. Acad. Sci., Paris* 1957 **244** 1494.
[12] Bellamy L. J. and Williams R. L., *Biochem. J.* 1958 **68** 81.
[13] Allsop I. L., Cole A. R. H., White D. E. and Willix R. L. S., *J. Chem. Soc.* 1956 4868.
[14] Bergmann E. and Pinchas S., *Rec. Trav. Chim. Pays-Bas* 1952 **71** 161.

VOL. 12 1958

Spectrochimica Acta, 1958, Vol. 12, pp. 239 to 243. Pergamon Press Ltd., London

Infrared absorption spectra of inorganic co-ordination complexes—XV*

Normal vibrations of sulfamic acid, $H_3N^+—SO_3^-$

Ichiro Nakagawa, San-ichiro Mizushima,† A. J. Saraceno, T. J. Lane and J. V. Quagliano

(*Received* 10 *February* 1958)

Abstract—Normal vibrations of the zwitter ion model of sulfamic acid have been calculated. For the skeletal vibrations, the L matrices and the potential energy distribution among symmetry co-ordinates for each normal mode of vibration have been calculated. Based on the result, complete assignment of the infrared and Raman frequencies has been made.

Introduction

In another paper on sulfamato-platinum (II) complexes [1], an assignment of the infrared and Raman frequencies of sulfamic acid, differing to some extent from that made by Vuagnat and Wagner [2], was reported. This paper presents the normal vibration calculation of the zwitter ion model of the acid, $H_3N^+—SO_3^-$, in order to confirm the correctness of that assignment.

According to the X-ray investigation of Kanda and King [3], the three S—O bonds in sulfamic acid do not have exactly the same length and the bond angles are not equal. However, the actual site symmetry may be considered as C_{3v} and the observed spectra can be explained by using the C_{3v} model from which the normal vibration calculation was made, assuming all the bond angles to be tetrahedral.

Experimental

Sulfamic acid (G. Frederick Smith Chemical Company), having a purity assay of 99·98 per cent when dried over P_2O_5 for 24 hr, was used.

Absorption measurements. The infrared spectra were obtained by means of a Perkin–Elmer infrared spectrophotometer model 21 employing sodium chloride, calcium fluoride and caesium bromide prisms over their regions of greatest resolution. The spectra were obtained by the potassium bromide disk technique [4] and checked in Nujol mulls.

Discussion

The potential function used in this calculation is of the Urey–Bradley type [5, 6]:

$$V = \tfrac{1}{2}\Sigma K\,(\Delta r)^2 + \tfrac{1}{2}\Sigma H r_0^2\,(\Delta\alpha)^2 + \tfrac{1}{2}\Sigma F(\Delta q)^2 + (\text{linear terms})$$

where r's are the bond lengths, α's the bond angles and q's the distances between non-bonded atoms, and K, H, and F are the stretching, deformation and repulsive force constants respectively.

The normal vibrations of $H_3N^+—SO_3^-$ can be divided into two groups: the

* For paper XIV in series see *J. Amer. Chem. Soc.* 1958 **80** 527. Contribution from the Department of Chemistry, University of Notre Dame. Notre Dame, Indiana, U.S.A.

† Visiting Professor from the Faculty of Science, Tokyo University.

vibrations of the skeleton $(N^+H_3)SO_3^-$ regarded as five-bodied and the hydrogen vibrations. The G and F matrices are constructed in the usual manner [7]. The values of the force constants and bond lengths used in this calculation are shown in Table 1.

Table 1. Values of force constants (in 10^5 dyn/cm) and intramolecular tensions (in 10^{-11} dyn/cm) [5], and bond lengths of $H_3N^+—SO_3^-$

$K_{NS} = 2{\cdot}2$, $K_{SO} = 7{\cdot}5$	
$H_{NSO} = 0{\cdot}30$, $H_{OSO} = 0{\cdot}43$, $H_{HNH} = 0{\cdot}54$, $H_{HNS} = 0{\cdot}073$	
$F_{S\cdots(S)\cdots O} = 0{\cdot}30$, $F_{O\cdots(S)\cdots O} = 0{\cdot}76$, $F_{H\cdots(N)\cdots H} = 0{\cdot}060$	
$F_{H\cdots(N)\cdots S} = 0{\cdot}80$	
$\kappa(NSO_3) = 0{\cdot}30$, $\kappa(SNH_3) = -0{\cdot}10$	
$r_{SS} = 1{\cdot}73$ Å, $r_{SO} = 1{\cdot}48$ Å, $r_{NH} = 1{\cdot}00$ Å	

The symmetry co-ordinates [8] for the skeletal vibrations are listed in Table 2 (see also Fig. 1).

The calculated frequencies are compared with those observed in Table 3. The vibrational modes listed in the first column have been determined from the calculation of potential energy distribution among symmetry co-ordinates to be explained below.

The agreement between the observed and calculated frequencies listed in Table 3 shows that the assignment made in the previous paper [1] is correct.

VOL. 12 1958

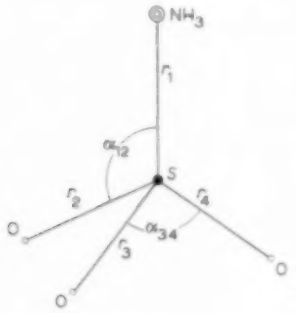

Fig. 1.

Comparison of the present work with that of Vuagnat and Wagner [2] shows the greatest difference in the assignment of the SO_3 symmetric deformation vibration assigned by them to the band at 1066 cm^{-1}, this being higher by 500 cm^{-1} than our calculated value. The band at 1066 cm^{-1} is assigned by us to the SO_3 symmetric stretching vibration which they assigned to a shoulder band at 1262 cm^{-1}.

There is some difference between the calculated and observed frequencies of the SO_3 degenerate stretching and NH_3 rocking vibrations, which can be explained

Table 2. Symmetry co-ordinates for the skeletal vibrations

Species	Symmetry co-ordinates	Modes
A_1	$S_1 = \Delta r_1$	SN stretching
	$S_2 = \frac{1}{\sqrt{3}}\Delta(r_2 + r_3 + r_4)$	SO_3 symmetric stretching
	$S_3 = \frac{1}{\sqrt{6}}\Delta\begin{pmatrix}\alpha_{12} + \alpha_{13} + \alpha_{14} \\ -\alpha_{34} - \alpha_{42} - \alpha_{23}\end{pmatrix}$	SO_3 symmetric deformation
E	$S_{4a} = \frac{1}{\sqrt{6}}\Delta(2r_2 - r_3 - r_4)$ $S_{4b} = \frac{1}{\sqrt{2}}\Delta(r_3 - r_4)$	SO_3 degenerate stretching
	$S_{5a} = \frac{1}{\sqrt{6}}\Delta(2\alpha_{12} - \alpha_{13} - \alpha_{14})$ $S_{5b} = \frac{1}{\sqrt{2}}\Delta(\alpha_{13} - \alpha_{14})$	SO_3 rocking (SN bending)
	$S_{6a} = \frac{1}{\sqrt{6}}\Delta(2\alpha_{34} - \alpha_{23} - \alpha_{24})$ $S_{6b} = \frac{1}{\sqrt{2}}\Delta(\alpha_{23} - \alpha_{24})$	SO_3 degenerate deformation

Table 3. Calculated and observed frequencies of $H_3N^+—SO_3^-$ (cm^{-1})

Vibrational mode	Calculated	Observed
ν_1 (A_1) SO_3 symmetric stretching	1084	1066
ν_2 (A_1) SN stretching	688	688
ν_3 (A_1) SO_3 symmetric deformation	505	534
ν_4 (A_1) NH_3 symmetric deformation	1402	1445
ν_5 (E) SO_3 degenerate stretching	1195	1310
ν_6 (E) SO_3 degenerate deformation	538	534
ν_7 (E) SO_3 rocking (SN bending)	380	374
ν_8 (E) NH_3 degenerate deformation	1548	1540
ν_9 (E) NH_3 rocking	1050	1003

as follows. We have calculated the skeletal vibrations and hydrogen deformation vibrations, separately. The coupling between these two vibrations, which are close to each other in frequency, will be considerable. Due to the coupling, the frequency of the SO_3 degenerate stretching vibration will be raised and that of the NH_3 rocking vibration will be lowered when compared with those values calculated above. Thus the improvement of the calculation will yield frequency values close to those observed.

Table 4. L-matrices of the skeletal vibrations of $H_3N^+—SO_3^-$*

(A_1)	Q_1	Q_2	Q_3
S_1	−0·078	0·264	0·118
S_2	*0·270*	0·011	0·001
S_3	0·114	−0·256	*0·234*
(E)	Q_5	Q_6	Q_7
S_4	*0·322*	−0·016	0·007
S_5	−0·120	−0·093	*0·255*
S_6	0·135	*0·287*	0·092

* Calculations have been made with bond lengths in Å, bond angles in radians and masses in atomic weight units. It should be noted that the dimension of L for the stretching co-ordinates is different from that for the deformation co-ordinates. The deformation displacement of each atom can be obtained by multiplying by the equilibrium bond length in Å units.

Table 5. The potential energy distribution $F_{ii}L_{ii}^2$ among symmetry co-ordinates for each normal mode of vibration*

(A_1)	r_1	r_2	r_3
S_1	0·018	*0·204*	0·041
S_2	*0·708*	0·001	0·000
S_3	0·022	0·110	*0·092*
(E)	r_5	r_6	r_7
S_4	*0·844*	0·002	0·000
S_5	0·018	0·011	*0·080*
S_6	0·031	*0·142*	0·014

* Values of force constants are given in 10^5 dyn/cm.

To determine the nature of the skeletal vibrations in more detail [8, 9], we have calculated the relative amplitude for each of the internal symmetry co-ordinates in a given normal mode of vibration.

The internal symmetry co-ordinates, S, are related linearly to the normal co-ordinates, Q, through the matrix expression [5],

$$S = LQ$$

VOL. 12 1958

If, therefore, the elements of the L matrix for a given normal vibration are calculated, relative amplitudes for symmetry co-ordinates can be determined. Such calculations have been made for all the skeletal vibrations and the results are shown in Table 4, where the italicized figures refer to the larger amplitudes.

In some of these vibrations the amplitude for a symmetry co-ordinate is nearly the same as that for another and, therefore, the determination of the nature of the vibration is not simple. To make a more reasonable assignment in such a case, as well as to distinguish between stretching and deformation vibrations, we have calculated the distribution of energy among internal symmetry co-ordinates for each normal vibration. The potential energy (V) of the whole molecule for a given normal mode of vibration (Q_λ), may be expressed as [10]:

$$V = \tfrac{1}{2}Q_\lambda^2 \sum_{ij} F_{ij}L_{i\lambda}L_{j\lambda}$$

where $F_{ii}L_{i\lambda}^2$ is the distribution of energy in a symmetry co-ordinate, S_i, in a normal mode of vibration (Q_λ). The result of the calculation of the potential energy distribution, $F_{ii}L_{i\lambda}^2$, for each normal mode of vibration, is shown in Table 5, where the italicized figures refer to the largest terms. In this way the nature of each normal vibration can be determined reasonably as shown in Table 3.

This investigation was supported in part by a research grant H-2218(C) from the Department of Health, Education and Welfare, Public Service.

References

[1] Saraceno A. J., Mizushima S., Lane T. J. and Quagliano J. V., *Abstracts of Papers*, 132nd Meeting of the Amer. Chem. Soc. New York, September 1957 22B.
[2] Vuagnat A. M. and Wagner E. L., *J. Chem. Phys.* 1957 **26** 77.
[3] Kanda F. A. and King A. J., *J. Amer. Chem. Soc.* 1951 **73** 2315.
[4] Stimson M. M. and O'Donnell M. J., *J. Amer. Chem. Soc.* 1952 **74** 1805; Faust J. P. and Quagliano J. V., *J. Amer. Chem. Soc.* 1954 **76** 5346.
[5] Shimanouchi T., *J. Chem. Phys.* 1949 **17** 245, 743, 848.
[6] Mizushima S., *Structure of Molecules and Internal Rotation*. Academic Press, New York 1954.
[7] Wilson E. B., Jr., *J. Chem. Phys.* 1939 **7** 1047; 1941 **9** 76.
[8] Nakagawa I. and Mizushima S., *Bull. Chem. Soc. Japan* 1955 **28** 589.
[9] Mizushima S., Nakagawa I. and Quagliano J. V., *J. Chem. Phys.* 1955 **23** 1367.
[10] Nakagawa I., *J. Chem. Soc. Japan* 1953 **74** 243. Morino Y. and Kuchitsu K., *J. Chem. Phys.* 1952 **20** 1809. Sweeny D. M., Nakagawa I., Mizushima S. and Quagliano J. V., *J. Amer. Chem. Soc.* 1956 **78** 889.

Spectrochimica Acta, 1958, Vol. 12, pp. 244 to 246. Pergamon Press Ltd., London

Absorption spectra of gaseous alkali metal hydroxides at high temperatures

L. H. Spinar and J. L. Margrave
Department of Chemistry, University of Wisconsin, Madison, Wisconsin

(*Received* 1 *October* 1957)

Abstract—A modified Perkin–Elmer Model 81 single-beam recording infrared spectrometer has been used for studies of gaseous hydroxides at temperatures up to 1000°. Characteristic absorptions have been found for the equilibrium gases over NaOH, KOH and RbOH at wavelengths in agreement with predictions made on the basis of a gaseous ionic model for $[MOH]_x$ (g).

Gases over LiOH, NaOH and KOH were examined in the visible and ultraviolet regions, but no absorption spectra were found. Na (g), in equilibrium with $[NaOH]_x$ (g), was first detectable at about 850°.

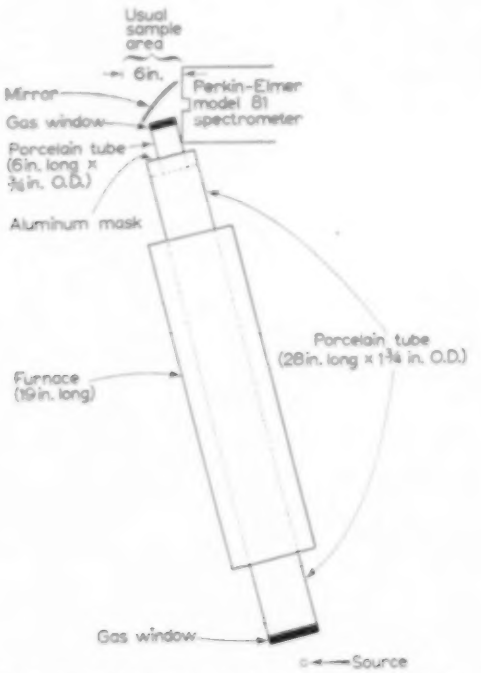

Fig. 1. Modification of the Perkin–Elmer Infrared Spectrometer for high temperature studies (dimensions are in inches).

When alkali metal hydroxides are heated to 700–900°, extensive vaporization occurs. The gaseous species present in the vapor are mainly the $[MOH]_x$ (g) molecules, where $x = 1$ or 2, as reported from flame and mass spectrographic studies [1–3]. Various regions of the spectrum have been surveyed in a search for characteristic absorption spectra of gaseous hydroxides.

VOL. 12 1958

Ultraviolet and visible absorption spectra were sought from 2000 to 7400 Å with a small Hilger quartz spectrograph and various standard light sources. The alkali metal hydroxides were contained in silver or MgO boats and heated in a wire-wound furnace so that an absorption path of 6 to 8 in. was available. LiOH, NaOH and KOH were examined in this study, but no absorptions characteristic of molecules were observed.

It was observed that LiOH appeared to vaporize completely at this temperature and examination of the white solid which condensed in cool parts of the tube showed X-ray patterns and equivalent weights characteristic of LiOH and $LiOH.H_2O$. This is in contrast to the expected dehydration reaction

$$2\ LiOH\ (s \text{ or } l) = Li_2O\ (s) + H_2O\ (g)$$

which should leave a residue in the boat of nonvolatile Li^2O [4] and form only water in the gas. NaOH vapors showed the sodium D-absorption at temperatures of 850° and above. No spectra were observed for KOH.

Equilibrium vapors over LiOH, NaOH, KOH, RbOH and CsOH at 800–900° were examined in the infrared with a NaCl-prism from 6–13 μ and with a CsBr-prism from 16–33 μ. The modified Perkin–Elmer Model 81 single-beam recording infrared spectrometer used a spherical, aluminum-surfaced mirror, which covered a solid angle of 0·003 sterad through the absorption tube, as shown in Fig. 1. Entrance of air and water vapor to the absorption cell was minimized by means of a "gas" window, which consisted of a brass ring machined to fit the absorption tube and slotted to direct a stream of helium across the end of the tube. This effectively isolated the gaseous hydroxides from air, carbon dioxide and water vapor but did not interfere with transmission of infrared radiation.

Radiation from about half of the hot walls of the absorption tube was masked from the spectrometer slit by an aluminum disc. All connections were made with asbestos cord packing. The modification of the absorption path was tested by taking an absorption spectrum of naphthalene. No effort was made to eliminate the air gaps in the path which allowed a background of water and CO_2 absorption bands.

Gaseous $[NaOH]_x$, $[KOH]_x$ and $[RbOH]_x$ were detected in the infrared region. The $[NaOH]_x$ absorption at 22·7 to 23·1 μ (433–440^{-1}), which was the strongest, is shown in Fig. 2. The $[KOH]_x$ absorption fell in the region 24·4 to 24·7 μ (405–410 cm^{-1}) and the $[RbOH]_x$ absorption in the region 27·2 to 27·6 μ (362–368 cm^{-1}). No spectra were detected for $[LiOH]_x$ (expected to fall around 13 μ) probably because of the high absorption of the NaCl prism. The $[CsOH]_x$ absorption was expected at approximately 29 μ but in this region there was a high absorption.

These bands are located in good agreement with the predictions which one would make on the basis of an ionic model for the gaseous hydroxides in which the main binding energy arises from electrostatic attraction of M^+ for OH^-. A similar model has been used for alkali halides by RITTNER [5] and for other gaseous halides and hydrides by MARGRAVE [6]. A comparison of the observed vibrational frequencies and those calculated and observed for the alkali fluorides is given in Table 1.

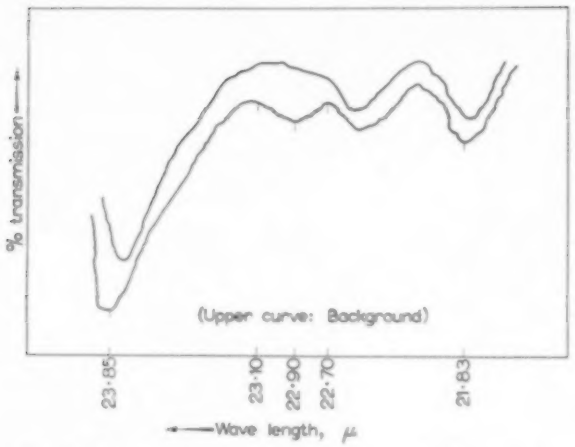

Fig. 2. Infrared absorption spectrum of equilibrium gases over liquid NaOH at 850°. Upper curve is spectrum of background.

Table 1. Vibrational frequencies of the gaseous alkali hydroxides* and halides

	ν obs. (cm^{-1})		ν obs.[7] (cm^{-1})	ν calc.[5] (cm^{-1})
$[LiOH]_x$	—	LiF	—	773
$[NaOH]_x$	437 ± 10	NaF	—	477
$[KOH]_x$	408 ± 10	KF	405	410
$[RbOH]_x$	365 ± 20	RbF	390	361
$[CsOH]_x$	—	CsF	385	345

* The linear MOH molecule should have three vibrational frequencies: one for the M-OH stretch, one for the O-H stretch and one (doubly degenerate) for bending. The first of these is the vibration concerned in this study.

Acknowledgement—This work was supported by a grant from the Wisconsin Alumni Research Foundation.

References

[1] Smith H. and Sugden T. M. *Proc. Roy. Soc.* A 1952 **211** 31 58.
[2] Smith H. and Sugden T. M. *Proc. Roy. Soc.* A 1953 **219** 204.
[3] Schoonmaker R. C. and Porter R. F. Private communication 1957.
[4] Margrave J. L. and Brewer L. *J. Phys. Chem.* 1955 **59** 421.
[5] Rittner E. S. *J. Chem. Phys.* 1951 **19** 1030.
[6] Margrave J. L. *J. Phys. Chem.* 1954 **58** 258.
[7] Barrow R. F. and Caunt A. D. *Proc. Roy. Soc.* A 1953 **219** 120.

VOL. 12 1958

Spectrochimica Acta, 1958, Vol. 12, pp. 247 to 252. Pergamon Press Ltd., London

Pure rotational absorption of NO_2 in the 50–200 micron region

G. R. Bird,* A. Danti and R. C. Lord
Spectroscopy Laboratory, Massachusetts Institute of Technology,
Cambridge 39, Mass., U.S.A.

(*Received* 25 *January* 1958)

Abstract—The pure rotational infrared absorption spectrum of nitrogen dioxide gas has been investigated with a small grating spectrometer in the spectral range 50–200 μ (200–50 cm^{-1}). Nine lines have been found which occur at the positions expected for a prolate symmetrical top with large centrifugal distortion. The observed frequencies of these lines are in excellent agreement with the frequencies calculated from the microwave value of 7·573 cm^{-1} for the rotational constant $A - (B + C)/2$, provided the centrifugal distortion constant D_k is taken as $-2{\cdot}24 \times 10^{-3}$ cm^{-1}. The resolution achieved by the spectrometer was not sufficient to separate the fine structure of the lines due to electron spin, but an upper limit of 1 cm^{-1} has been set for the spacing of the spin components.

Nitrogen dioxide is unique among simple molecules in being a polyatomic free radical stable in the gas phase [1]. The vibrational spectrum of NO_2 has been investigated under high resolution by Moore [2] and by Keller and Nielsen [3]. The isotopic molecule $^{15}NO_2$ has been investigated by Weston [4]. Precise moments of inertia for the ground state have been obtained from these infrared observations and refined by a microwave study of NO_2 [5]. The ONO angle of 134° 15′ is unusually large, and leads to a large value for A, the greatest reciprocal moment of inertia. The molecule is a nearly prolate symmetric top, with the $\nu_2(a_1)$ infrared band having an easily-resolved fine structure suggestive of a simple symmetric top. While the microwave spectrum is greatly complicated by the magnetic interactions among electron spin, molecular rotation, and nuclear spin, only one possible indication of magnetic splitting has been observed in the infrared. This is the peculiar splitting of $2\nu_1 + \nu_3$ observed by Moore [2] and attributed by him to either asymmetry or spin splitting. The latter explanation seems more probable to us.

Experimental

The far infrared spectrum of NO_2 has been observed with the small grating instrument described by Lord and McCubbin [6]. The gas was contained at pressures slightly below one atmosphere in a 10 cm stainless steel cell with polyethylene windows. Ordinary tank NO_2 was dried over P_2O_5 and admitted to the cell. Of the other gases present with NO_2 from this source, only H_2O has a resolvable rotational spectrum, and traces of it always remain in the purged spectrometer housing. N_2O_4 is present in equilibrium with NO_2, but has no far infrared absorption. The absorption cell was heated to about 45°C to shift the equilibrium towards NO_2. Provided the gas has been sufficiently dried, its corrosive effects upon the cell are not serious. Due to the small permanent dipole (0·33 D) in NO_2, the bands are rather narrow even at the high pressures used, and the absorption is

* Present address: Department of Chemistry, Rice Institute, Houston, Texas.

weak as compared to that of gases like HCl or NH_3 at about 40 mm pressure and the same path length.

The observed lines are given in Table 1 and some of them are shown in Fig. 1. All of the observed lines, with the exception of the last one, were observed in the

Table 1. Rotational Q-branch absorptions of NO_2

K_L	Observed frequency (cm^{-1} (vac))	Calculated frequency using $D_K = -2{\cdot}24 \times 10^{-3}$ for non-rigid molecule	Calculated frequency for rigid molecule	Half-width of band (cm^{-1})
0		7·571	7·573	
1		22·69	22·72	
2		37·72	37·86	
3	52·77	52·62	53·01	
4	67·36	67·32	68·15	0·76†
5	81·72	81·80	83·30	0·77†
6	95·90	95·96	98·44	1·04†
7	109·67	109·79	113·59	1·41†
8	123·16	123·21	128·73	
9	136·17	136·18	143·88	1·90‡
10	(148·8)*	148·62	159·02	
11	160·76	160·52	174·17	
12		171·79	189·32	
13		182·38	204·46	

* Heavily masked by strong H_2O absorption at 149 cm^{-1}.

† All four lines were run under the same conditions with a mechanical slit of 1·85 mm. These measurements were made on the lower curve in the illustration.

‡ Mechanical slit was 1·35 mm.

first order of the 8 grooves-per-mm grating blazed at 9·0 cm^{-1}. The last line (160·8 cm^{-1}) was observed in the second order and in the optimum portion of the KCl reststrahlen region. This line is quite weak, since it is considerably removed from the region of maximum intensity, and was only observed because of the optimum conditions. No trace of the 172 or 183 cm^{-1} lines was apparent.

The observed frequencies reported in Table 1 are expected to be correct to within 0·15 cm^{-1} or better. Above 90 cm^{-1} the region was calibrated with the mercury green line, a new line appearing about every 0·6 cm^{-1}. The 50–115 cm^{-1} region was calibrated by using the absorption spectrum of H_2O. The frequencies were calculated from the energy levels given by Benedict, Claassen, and Shaw [7] following the assignments of Randell, Dennison, Ginsburg and Weber [8]. These two methods of calibration, overlapping for the 96 and 110 cm^{-1} lines, agreed to within about 0·15 cm^{-1}. The values reported in Table 1 for these two lines represent the average of the two measurements.

Some of the lines which were recorded at fast speed ($\sim$1 cm^{-1}/min) may appear to show signs of just resolvable fine structure (see Fig. 1). Comparison of different scans disposes of this interpretation. Moreover, careful examination of

VOL. 12 1958

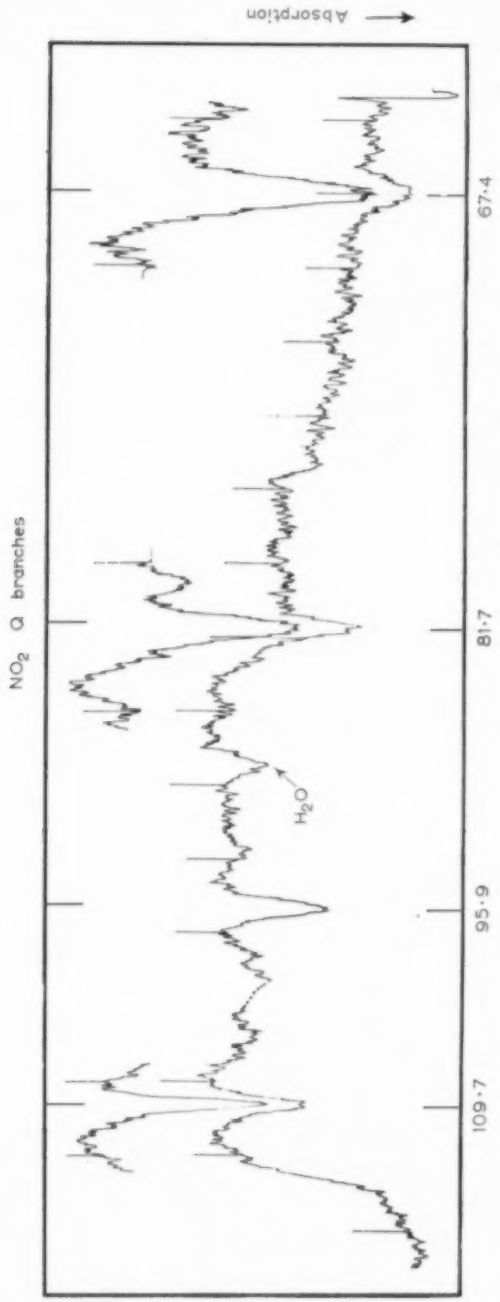

Fig. 1. Original tracings of NO_2 absorption.
The lower spectrum was recorded as follows: source, AH-4 Hg-arc; 2 mm soofed-quartz transmission filter plus KRS-5 reflection filter; KBr chopper; slit width, 1·85 mm. For instrumental details, see ref. [6]. Cell length, 10 cm, total NO_2-plus N_2O_4-pressure, ~1 atm. The traces of individual lines (upper spectrum) were recorded with higher amplifier gain and different slit widths (2·8 mm for 67 cm^{-1} line, 2·6 mm for 82 cm^{-1} line, 1·35 mm for 110 cm^{-1} line).

the smooth contours recorded at slow speed (~0·1 cm^{-1}/min) revealed no indication of magnetic splitting. The resolution achieved by the spectrometer varied considerably because of the large changes in grating angle and mechanical slit width. It is estimated to increase from about 0·4 to 1·8 cm^{-1} over the range 50–125 cm^{-1} in the first order. This continued increase in spectral slit width is primarily responsible for the increasing half-widths of the bands in the direction of higher frequency (see Table 1). The magnetic spin-rotation interactions were expected to be small from the simple rotational fine structure of the ν_2 infrared band, so that the absence of observable splitting is hardly surprising. The observed half-widths of the lines set an upper limit of about 1 cm^{-1} for the splitting of each line into its principal magnetic components.

Discussion of results

In the absence of observable magnetic interactions, the rotational spectrum of NO_2 may be treated to a satisfactory degree of approximation as a simple asymmetric-top spectrum. Thus the observed lines are a series of Q branches with the selection rules $\Delta N = 0$, $\Delta K_{-1} = +1$, $\Delta K_{+1} = -1$. Each line is actually a composite of all transitions with $N > K_{-1}$ arising from states $N_{K-1,K+1}$ having appreciable thermal population. In the above notation N is the total rotational angular momentum exclusive of electron and nuclear spin and K_{-1} is the limiting prolate symmetric top quantum number. For example, the 95·9 cm^{-1} line is composed of the transitions:

$$7_{71} \leftarrow 7_{62}, \quad 8_{71} \leftarrow 8_{62}, \quad 9_{73} \leftarrow 9_{64}, \quad 10_{73} \leftarrow 10_{64}, \quad \text{etc.}$$

Only states with the sum of $K_{-1} + K_{+1}$ even are permitted because of the zero nuclear spin of the ^{16}O nuclei symmetrically located about the twofold axis of symmetry. The states making the greatest contribution to the intensity of these lines are those with N about 20, while states with $N > 40$ have essentially zero thermal population at ordinary temperatures.

The appearance of these Q-branches depends on the fact that NO_2 is a very nearly prolate symmetric top. The Wang asymmetry parameter obtained from microwave studies is:

$$b_p = \frac{C - B}{2[A - (B + C)/2]} = -1{\cdot}52 \times 10^{-3}$$

The effect of this small but finite asymmetry is calculable from the table of Wang expansion coefficients prepared by Schwendeman [9], and is seen to be greatest for low K_{-1} and high N. For the K_{-1} values observed here, the asymmetry correction is much less than the instrumental precision and resolution except for $N > 40$, or for $K_{-1} < 6$ and $N > 30$. Thus consideration of NO_2 as a rigid symmetric top predicts a series of sharp Q-branches having frequencies given within experimental error by the limiting symmetric top formulae:

$$W = \frac{B + C}{2} N(N + 1) + \left[A - \frac{B + C}{2}\right] K_{-1}^2 \qquad (1)$$

$$\nu_Q = \left[A - \frac{B + C}{2}\right](2K_L + 1) \qquad (2)$$

VOL. 12 1958

Here K_L is the lower value of K_{-1} for the transition. This prediction is not completely satisfied, for the microwave value of :

$$\left[A - \frac{B+C}{2}\right] = 227{,}020 \pm 40 \text{ mc or } 7{\cdot}573 \text{ cm}^{-1} \tag{3}$$

predicts lines at 98·4 cm^{-1}, 128·7 cm^{-1} and 143·9 cm^{-1}, for example, as shown in Table 1, column 4.

The discrepancy between the predicted and observed spectrum is obviously associated with centrifugal distortion. A complete calculation of this effect by the method of KIVELSON and WILSON [10] seems unwarranted in the absence of high-resolution infrared data on isotopic NO_2 or reliable microwave values for the hypothetical rotational frequencies corrected for magnetic fine structure. Instead, centrifugal distortion may be treated by the symmetric top formula $W(N, K) = BN(N+1) + (A-B)K^2 + D_J N^2(N+1)^2 + D_{JK}N(N+1)K^2 + D_K K^4$ with the hope that the D's obtained will bear some resemblance to the four independent centrifugal distortion constants of NO_2. For transitions with $\Delta N = 0$, there is no contribution from D_J, and D_{JK} causes a broadening of the line, a skew shape and a shift away from the rigid rotor frequency. This broadening cannot now be separated from the effects of unresolved magnetic fine structure and instrumental slit width, but D_{JK} appears small. The principal effect is introduced through D_K, and a value of $D_K = -2{\cdot}24 \times 10^{-3}$ cm^{-1} is obtained by taking the observed frequency 136·17 cm^{-1} ($K_{-1} = 10 \leftarrow 9$), the microwave value of $A - (B+C)/2$ and $D_{JK} = 0$. This is to be compared with KELLER and NIELSEN's value of $D_K = -2{\cdot}65 \times 10^{-3}$ cm^{-1} and contrasted with MOORE's value of $-5{\cdot}8 \times 10^{-3}$ cm^{-1} obtained from rotational fine-structure analysis.

With the value for D_K of $-2{\cdot}24 \times 10^{-3}$ and the relationship

$$\nu_Q = \left[A - \frac{(B+C)}{2}\right](2K_L + 1) + D_K(4K_L{}^3 + 6K_L{}^2 + 4K_L + 1) \tag{4}$$

the frequencies listed in column 3 of Table 1 were calculated. The agreement with the observed frequencies is excellent and well within the experimental error estimated above for all lines except that at 160·76 cm^{-1}. In view of the fact that this line should be most sensitive of those observed to the effect of D_K, it may be stated that from this line alone, one obtains $D_K = -2{\cdot}20 \times 10^{-3}$. In view of the close agreement of the lower lines for the slightly higher value of D_K, we prefer the higher value.

Comparison of the frequencies given by equation (4) with those calculated from the rigid-rotor equation (2) (Table 1, column 4) demonstrates clearly the large effect of centrifugal distortion. Such a large effect is not surprising when the unusually wide bond angle of 134° 15′ and small moment of inertia I_A of NO_2 are considered. The reciprocal moment A is thus large and quite sensitive to small changes of bond angle.

The fact that no magnetic splittings were observed in this work is of course no indication that such cannot be observed, and it would be desirable to investigate the far-infrared spectrum of NO_2 with a spectrometer having higher resolving

power than the present instrument. It does not seem likely that magnetic effects would be more easily observed on going to the lower-frequency Q-lines, for the effect of molecular asymmetry is to broaden these increasingly. Indeed, the peculiar appearance of the $K_{-1} = 1 \leftarrow 0$ and $2 \leftarrow 1$ Q-branches mentioned by Keller and Nielsen is probably due to the fact that the asymmetry enters in first-order for the state $K_{-1} = 1$, thus both broadening the Q-branches and introducing marked band-heads in the associated P and R branches.

Note added in proof: It can be calculated with the help of the formulation of centrifugal distortion by S. R. Polo (*Canad. J. Phys.* 1957 **35** 880) and from available potential constants [4] that the distortion constant D_K should have the value $2{\cdot}01 \times 10^{-3}$ cm^{-1}, and D_{JK} a much smaller value ($1{\cdot}60 \times 10^{-5}$ cm^{-1}), in good argeement with the foregoing results. A complete treatment of centrifugal distortion in the microwave and far infrared spectra of NO_2 will appear in a forthcoming paper by one of us [G. R. B.]. The molecules SO_2 and O_3 are now under far infrared study in this Laboratory.

Acknowledgement—The authors are grateful to the Engineer Research and Development Laboratories, U.S. Army Corps of Engineers (Contract DA-44-009-eng-3126) and the National Science Foundation (Grant G-1892) for financial support of this work.

References

[1] Verhoek F. M. and Daniels F., *J. Amer. Chem. Soc.* 1931 **53** 1250; Giauque W. F. and Kemp J. D., *J. Chem. Phys.* 1938 **6** 40.
[2] Moore G. E., *J. Opt. Soc. Amer.* 1953 **43** 1045.
[3] Keller F. L. and Nielsen A. H. *J. Chem. Phys.* 1956 **24** 636; *Bull. Amer. Phys. Soc.* 1957 II, **2**, 285.
[4] Weston R. E., Jr. *J. Chem. Phys.* 1957 **26** 1248.
[5] Bird G. R. *J. Chem. Phys.* 1956 **25** 1040. See also his later unpublished work reported by Anderson, Baird and Bird in paper K-5 at the 1957 Ohio State Symposium on Molecular Structure and Spectroscopy.
[6] Lord R. C. and McCubbin T. K. Jr. *J. Opt. Soc. Amer.* 1957 **47** 689.
[7] Benedict W. S., Claassen H. H. and Shaw J. H. *J. Res. Natl. Bur. Stand.* 1952 **49** 91.
[8] Randall H. M., Dennison D. M., Ginsberg N. and Weber L. R. *Phys. Rev.* 1937 **52** 160.
[9] Schwendeman R. H. *J. Chem. Phys.* 1957 **27** 986.
[10] Kivelson D. and Wilson E. B., Jr. *J. Chem. Phys.* 1953 **21** 1229 and 1236.

VOL.
12
1958

Spectrochimica Acta, 1958, Vol. 12, pp. 253 to 261. Pergamon Press Ltd., London

Assignments of the vibrational frequencies of glycine

Masamichi Tsuboi, Takaharu Onishi, Ichiro Nakagawa,
Takehiko Shimanouchi and San-ichiro Mizushima
Faculty of Science, Tokyo University, Hongo, Tokyo, Japan

(*Received* 13 *December* 1957)

Abstract—Infra-red spectra of α-glycine, α-glycine-D_3, glycine-hydrochloride, glycine-hydrochloride-D_3, Na-glycinate, and Na-monochloroacetate have been compared in the NaCl region. Infra-red spectra of α- and γ-glycine and α- and γ-glycine-D_3 have been observed in the KBr region. A dichroic measurement has been made on the single crystal of γ-glycine, in which all the glycine molecules are arranged almost in the same direction. Based on the results a complete assignment has been made of the fundamental vibrational frequencies of glycine observed in the 1800–400 cm^{-1} region.

Introduction

The Raman and infra-red spectra of glycine have been measured by several investigators [1–6], but the assignment of the observed frequencies is not completed. The normal vibration calculation of this molecule is not easy, since it is a ten-body problem. However, as we have calculated the vibrations of many simple molecules related to glycine in structure [7], the result helps us in making the assignment of the glycine spectra. Furthermore, we have remeasured the infra-red spectra of glycine and the related compounds in the NaCl region, extended the measurement to the KBr region, and also made dichroic measurement on the single crystal of γ-glycine. Based on these results we have made a complete assignment of the fundamental vibrational frequencies of glycine observed in the 1800–400 cm^{-1} region.

Experimental

Samples

α-Glycine-D_3. α-Glycine was dissolved in heavy water (99·7 per cent), and the sealed tube containing the solution was kept at 80° for 3 days. The sample obtained by evaporation of the solution was shown to be almost deuterated by the measurement of the absorption at 3–5 μ region. An X-ray investigation showed the crystal to have the α-form.

Glycine hydrochloride. α-glycine was added to the equivalent amount of the 10% hydrochloric acid and the solution was kept in a sealed vessel for several hours. The sample was obtained by evaporation of the solution.

Glycine hydrochloride-D_3. The sample was obtained according to a procedure similar to that for glycine-D_3.

Sodium glycinate. A volume of 3% sodium alcoholate was added to α-glycine (in an amount little less than equivalent) and the solution was kept in a sealed vessel for several days, being stirred frequently. The sample was prepared by evaporation of the solution.

γ-glycine and γ-glycine-D_3. γ-Glycine (a polymorphic form of glycine) was obtained by recrystallizing α-glycine from aqueous solution of acetic acid at about 1° [8]. Deuterated γ-glycine was obtained by dissolving deuterated α-glycine in D_2O and by recrystallizing it at about 0°. An X-ray measurement showed that the samples were completely in γ-form.

Preparation of the section

Of a single crystal of γ-glycine of the approximate dimensions of 4 × 3 × 2 mm, a crystal face parallel to the *c*-axis was ground and polished. The polished face was pasted on the surface of an NaCl plate with paraffin. Then, the opposite face of the crystal was ground parallel to

the pasted face until a proper thickness was reached. The thickness was measured in two different ways.

First, the retardation of the section was measured by means of a polarizing microscope and a quartz wedge as $R = 200 \pm 50$. The refractive indices of this crystal were determined by the immersion method as $\omega = 1{\cdot}586$ and $\varepsilon = 1{\cdot}614$. From these, the thickness, d, was calculated as:

$$d = \frac{R}{\varepsilon - \omega} = 7 \pm 2\,\mu$$

Second, the infra-red absorption intensity of several bands of the section was measured. The absorption coefficients of these bands were determined by the intensity measurements for KBr tablets whose thicknesses and whose γ-glycine contents are known. The thickness of the section was calculated as $7 \pm 3\,\mu$.

Spectroscopic measurements

The infra-red spectra were obtained by means of a Baird Infra-red Spectrophotometer, Perkin–Elmer Spectrophotometers (models 21 and 112) and a Hilger Spectrometer (H–800), with NaCl and KBr prisms.

The samples of α-glycine, glycine hydrochloride, sodium monochlorate were measured as a solid film spread on the NaCl plate which was prepared by evaporation of the ethanol–water solution. Nujol and hexachlorobutadiene mull measurements were made for α- and γ-glycine, α- and γ-glycine-D_3 and sodium glycinate. For α- and γ-glycine and α- and γ-glycine-D_3 the KBr disk method was also applied.

For dichroic measurements, two AgCl polarizers were used and both the sample and the reference-beams (Perkin–Elmer 21) were polarized. To change the direction of the electric vector of the incident radiation, the polarizers were rotated.

VOL. 12 1958

Comparison of the spectra of glycine with those of related compounds in the NaCl region

We observed the infra-red spectra of glycine $H_3^+NCH_2COO^-$, glycine-D_3 $D_3^+NCH_2COO^-$, glycine hydrochloride $Cl^-H_3^+NCH_2COOH$, glycine hydrochloride-D_3 $Cl^-D_3^+NCH_2COOH$, sodium glycinate $H_2NCH_2COO^-Na^+$ and sodium monochloroacetate $Cl\,CH_2COO^-Na^+$ in NaCl region. In Table 1 are listed the observed frequencies and intensities.

α-Glycine shows two strong absorption bands at 1610 and 1585 cm^{-1}, one of which disappears on deuteration. Glycine hydrochloride, sodium glycinate and sodium monochloroacetate show only one band in this frequency region. These facts can be explained by assigning the band at 1610 cm^{-1} to the COO^- antisymmetric stretching vibration, and the remaining one at 1585 cm^{-1} to an NH_3^+ deformation frequency.

The bands observed for glycine hydrochloride and the deuterated compound at 1740 and 1720 cm^{-1} respectively, can undoubtedly be assigned to the carbonyl frequency of the O=C—OH group.

The band of glycine at 1500 cm^{-1} which is also observed for glycine hydrochloride and disappears on deuteration can be assigned to a NH_3^+ deformation vibration. In analogy to the $—CH_3$ deformation vibrations [9], this band is assigned to the symmetric deformation vibration and the other at 1585 cm^{-1} to the degenerate deformation vibration. The corresponding ND_3^+ deformation vibrations appear at 1170 and 1270 cm^{-1} respectively.

Table 1. Assignment of observed frequencies (cm^{-1}) of glycine and related compounds in the NaCl region

α-Glycine		α-Glycine-D_3	Glycine hydrochloride	Glycine hydrochloride-D_3	Sodium glycinate	Sodium monochloroacetate	Assignment
Infra-red	Raman (4)						
			1740 s	1720 s			C=O stretch.
1610 s		1600 s			1600 sb	1600 s	COO^- antisym. str.
1585 s			1605 s				NH_3^+ deg. def.
1500 s			1500 s				NH_3^+ sym. def.
					1490 w		
1450 s	1440 (2)	1450 s			1435 m		CH_2 bend.
			1430 s	1420 s			
1415 s	1395 (4b)	1405 s			1415 s	1420 s	COO^- sym. str.
1335 s	1325 (9)	1325 s	1340 m	1335 m	1335 m		CH_2 wag.
					1305 m		
		1270 m		1280 sb			ND_3^+ deg. def.
					1270 w		
	1240 (1)		1235 s	1215 s		1250 s	CH_2 twist.
		1170 m		1170 m			ND_3^+ sym. def.
		1160 m		1160 m			
					1155 m		
{1130 m			{1125 m				NH_3^+ rock.
{1115 m	1115 (1b)		{1110 w				
1030 m	1035 (1)	1045 m	1045 m	1040 m	1045 m		CCN antisym. str.
		1000 w			1005 w		
		905 w					
910 m		885 w	905 s	930 m	930 w	930 m	CH_2 rock.
895 m	895 (10)	825 s	855 sb	855 m	890 m		CCN sym. str.
			860 w		825 m	850 m	
		770 m		{765 m			ND_3^+ rock.
				{760 m			
						770 s	CCl str.

s: strong, m: medium, w: weak, b: broad.

The band at 1450 cm^{-1}, which is not shifted on deuteration of the NH_3^+ group, can be assigned to the —CH_2— bending vibration. All the molecules containing —CH_2— group are known to show this frequency.

The band at 1415 cm^{-1}, which is also exhibited by glycine-D_3, sodium glycinate and sodium monochloroacetate, can be assigned to the —COO^- symmetric stretching vibration.

The band at 1335 cm^{-1} can be assigned to the —CH_2— wagging vibration, according to the result of one of our previous papers [9].

The two bands of glycine at 1130 and 1115 cm^{-1} which also appear in glycine hydrochloride and disappear on deuteration can be assigned to NH_3^+ rocking vibrations. The corresponding ND_3^+ vibration is observed at 770 cm^{-1}.

In the frequency region from 850 to 1050 cm^{-1} we expect to observe absorption bands arising from C—N and C—C stretching vibrations and —CH_2— rocking vibrations. The Raman line corresponding to the absorption band at 895 cm^{-1} is very strong and, therefore, this is assigned to the C—C—N in-phase stretching vibration. Of the two bands at 1030 and 910 cm^{-1}, the latter can be assigned to

the —CH_2— rocking vibration from the frequency value. The band at 1030 cm^{-1} can, therefore, be assigned to the C—C—N out-of-phase vibration.

Absorption spectrum of glycine in the KBr region and the deuteration effect

Results of our measurements in the KBr region on the Nujol mulls of α- and γ-glycine* and α- and γ-glycine-D_3 are shown in Fig. 1. The frequencies observed are listed in Table 2 together with the Raman frequencies observed by Baba, Mukai, Shimanouchi, and Mizushima [4].

Table 2. Assignment of observed frequencies (cm^{-1}) of glycine and glycine-D_3 in the low-frequency region

Glycine in neutral aq. soln.	α-Glycine		α-Glycine-D_3	γ-Glycine	γ-Glycine-D_3	Assignment
Raman	Raman	Infra-red	Infra-red	Infra-red	Infra-red	
665 (2)	695 (1)	694 s	667 s	686 s	659 s	COO^- wag.
585 (2)	603 (1)	607 m	597 s	607 m	587 s	COO^- sym. bend.
		516 m		557 m		NH_3^+ torsion.
510 (4)	500 (2)	504 s	493 s	503 s	494 s	COO^- rock.
415 (1)	420 (0)					CCN bend.
	360 (0)					
325 (1)	320 (0)					C—C torsion.
	270 (0)					
	103 (5)					

s: strong, m: medium.

In the region below 700 cm^{-1} we expect the appearance of six vibrational modes of the glycine molecule as given in the last column of Table 2. According to our previous paper [4] the C—C—N bending and C—C torsional motions are assigned to the observed Raman lines at 420 and 320 cm^{-1}, respectively. It is reasonable to assign the Raman line at 500 cm^{-1} to the —COO^- rocking motion, on the basis of our calculation of the skeletal vibrations of glycine [4]. Furthermore, this is compatible with the assignment of the band at 465 cm^{-1} of CH_3COO^- to the same mode [10].

The band at 516 cm^{-1} of α-glycine and that at 557 cm^{-1} of γ-glycine disappear on deuteration. (Probably they are shifted to frequencies lower than 400 cm^{-1}). Therefore, they can be assigned to the NH_3^+ torsional motion in α- and γ-glycine, respectively.

The two frequencies, 694 and 607 cm^{-1} (in γ-glycine, 686 and 607 cm^{-1}), which are shifted by only 10–27 cm^{-1} on deuteration, are assigned to the two —COO^- vibrations, i.e. —COO^- wagging (out-of-plane) and symmetric bending motions. The distinction between the two vibrations can be made by the dichroic measurement to be described below.

* For γ-glycine, see the following section.

VOL. 12 1958

Dichroic measurement on the single crystal of γ-glycine

γ-Glycine is a polymorphic form of glycine discovered by ITAKA [8] and has trigonal hemihedral symmetry (P_{3_1} or P_{3_2}). The crystal structure was determined by ITAKA [11] as shown schematically in Fig. 2. Here, all the C—C bonds in the crystal are nearly parallel to the crystallographic c-axis. A unit cell of γ-glycine contains three glycine molecules, each consisting of ten atoms. Hence, a unit cell

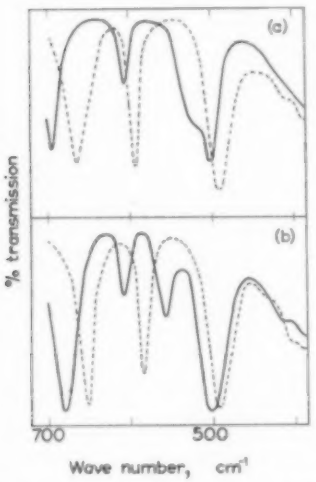

Fig. 1. Absorption spectra of (a) α-glycine (full line) and α-glycine-D_5 (broken line), and (b) γ-glycine (full line) and γ-glycine-D_5 (broken line).

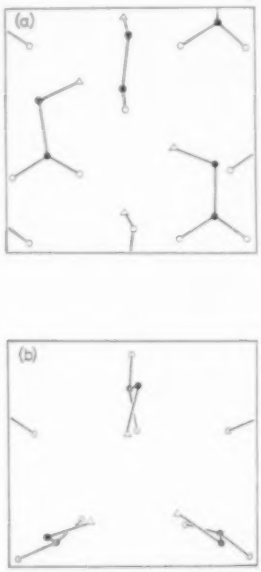

Fig. 2. The crystal structure of γ-glycine (a) viewed from a perpendicular direction to the c-axis, (b) viewed along the c-axis. ● : carbon; ○ : oxygen; △ : NH_3^+.

has altogether 90 degrees of freedom, 18 of which correspond to overall translations, and inter-molecular vibrations (or lattice vibrations). The remaining 72 refer to the intramolecular vibrations. An analysis according to the method of BHAGAVANTUM and VENKATARAYUDU [12] shows that these internal vibrations consist of 24 A-type vibrations (totally symmetric vibrations with respect to the crystal symmetry, C_3), and 24 E-type (degenerate) vibrations. The transition moments of the A-type vibrations ($\parallel$ type vibrations) are all directed along the c-axis and those of the E-type vibrations ($\perp$ type vibrations) are all directed perpendicular to it. If the interaction among the molecules in the crystal is weak, we may find for each of these A-type vibrations a corresponding E-type vibration with a slight frequency difference, and we may consider that each of such twenty-four pairs of vibrations corresponds to a vibration of the fictitious free glycine molecule, which has 24 degrees of vibrational freedom.

In other words, the normal vibrations of a glycine molecule in the crystal may be considered to be similar to those of a free molecule, except that there are certain phase relations among the vibrations of the molecules in the crystal:

namely, in the A-type vibrations the three molecules in the unit cell vibrate in phase, while in the E-type vibrations they vibrate with 120° phase difference from one another.

If a normal vibration of a free molecule has the transition moment directed nearly along the C—C bond (which is nearly parallel to the c-axis in the crystal), the corresponding A-type vibration in the γ-glycine crystal would give a strong absorption band, whereas the corresponding E-type vibration would give only a very weak absorption band. On the other hand, if its transition moment is

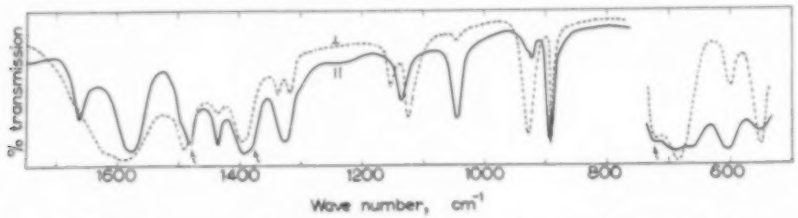

Fig. 3. Infra-red spectrum of γ-glycine. Full line: electric vector parallel to the c-axis, broken line: electric vector perpendicular to the c-axis. The arrows indicate the absorptions due to paraffin.

directed nearly perpendicular to the C—C bond (or to the c-axis of the crystal), the intensity relation would be reversed. The intensity ratio of an A-type band to the corresponding E-type band depends largely upon the angle, θ, between the transition moment of the fictitious free glycine molecule and the c-axis of the crystal. It depends also upon the intermolecular interaction, but this would not be very large. If, for the moment, we neglect the latter, we may express the intensity ratio as

$$I_A/I_E = 2\cos^2\theta/\sin^2\theta$$

therefore

$$I_A/I_E \geqslant 1, \text{ if } \theta \leqslant 55°$$

Thus, we determined the direction of the transition moment for each of the fundamental modes of the free glycine molecule. In order to obtain the intensity ratio I_A/I_E for γ-glycine, polarized infra-red absorption measurements were made of a thin section (about 7 μ in thickness) of the single crystal which is parallel to the c-axis.

The results are shown in Fig. 3, in which the full line shows the transmission of the radiation with the electric vector parallel to the c-axis and the dotted line shows that with the electric vector perpendicular to the c-axis. The minima in the former must be due to the A-type absorptions and those in the latter due to the E-type absorption.

In Table 3, frequencies of the observed A-type and E-type bands are given in the first and second columns, respectively. As is expected, most of the A-frequencies have their corresponding E-frequencies in their vicinities, and each of these pairs corresponds to a frequency of α-glycine (see Tables 1 and 2). In the third column of Table 3, are given the assignments which were made to these corresponding frequencies of α-glycine in the preceding sections (see Tables 1 and 2).

VOL. 12 1958

Based on the crystal structure of γ-glycine as determined by ITAKA [11], and assuming that the vibrations are as described in the third column of Table 3 and that there is no interaction among the molecules in the crystal, we can calculate angles between the c-axis and the dipole oscillation directions of the molecules. These are given in the fourth column of Table 3. Intensity ratios of the A-type bands to the E-type bands are calculated by equation (1) with results given in the fifth column in a qualitative manner. The exact figures of the ratios are not significant, since the assumption made is not strictly valid.

Table 3. Assignment of observed frequencies and dichroism of γ-glycine

Frequency (cm^{-1})		Approximate description of the vibrational mode	Angle between the direction of the dipole oscillation and the c-axis	Dichroism expected	Dichroism observed
A-type (∥)	E-type (⊥)				
—	1620	COO^- antisym. str	90°	extreme ⊥	extreme ⊥
1660	~1660	NH_3 deg. def.	—	—	∥
1575	1585				⊥
—	1492	NH_3 sym. def.	68	⊥	extreme ⊥
1435	1435	CH_2 sym. bend.	58	slight ⊥	∥
1389	1397	COO^- sym. str.	8	extreme ∥	∥
1324	1340	CH_2 wag.	33	∥	strong ∥
	1317				
1135	1154	NH_3^+ rock.	—	—	⊥
	1126				⊥
1044	1050	CCN antisym. str.	31	∥	strong ∥
924	929	CH_2 rock.	81	extreme ⊥	strong ⊥
893	888	CCN sym. str.	58	slight ⊥	slight ⊥
684	689	COO^- wag.	81	extreme ⊥	slight ⊥
607	602	COO^- sym. bend.	8	extreme ∥	strong ∥
560	557	NH_3^+ torsion.	—	—	⊥

In the last column of Table 3, observed intensity ratios (or observed dichroism) are also given in a qualitative way. Let us discuss the observed and expected dichroism in relation to the assignment of the vibrational frequencies.

At 1620 cm^{-1} a strong E-type band is observed while no A-type band is found in this frequency region. This band is reasonably assigned to the —COO^- antisymmetric stretching vibration, whose dipole oscillation should be almost perpendicular to the C—C bond in the free molecule, and therefore to the c-axis of the crystal.

At 1660 and 1575 cm^{-1}, two A-type bands are clearly observed, while corresponding E-type bands are not distinct probably due to the superposition of the strong 1620 cm^{-1} band. The two bands may be assigned to the NH_3^+ degenerate deformation vibration. Both of the bands show neither strong parallel nor perpendicular dichroism, and this fact does not disagree with the assignment.

The absorption band at 1492 cm^{-1} is found only in the measurement with the radiation polarized in the direction perpendicular to the c-axis. This is not contradictory to the assignment of the band to the NH_3^+ symmetric deformation vibration, since the dipole oscillation of this mode may occur along the C—N bond

which makes an angle of about 68° with the c-axis, and this angle is much larger than 55°.

The A-type band at 1435 cm^{-1} is stronger than the E-type band at 1435 cm^{-1}. At first sight this fact does not seem to agree with our assignment of this frequency to the $—CH_2—$ bending mode, since the direction of dipole oscillation of this mode should make an angle of about 58° with the c-axis. However, the fact that the frequency of this A-type band is exactly equal to that of the E-type band suggests that practically the vibration is not affected by the intermolecular force. Thus the above assignment will be justified. However, we should like to note that the $—CH_2—$ bending vibration is slightly coupled with the— COO^- symmetric stretching motion, whose frequency is very close to the frequency under consideration and whose dipole oscillation occurs nearly parallel to the c-axis. The transition moment may be affected greatly by small motions of the charged atoms such as $—COO^-$, so that its direction may make an angle with the c-axis smaller than 55°.

The A-type band at 1389 cm^{-1} is stronger than the E-type band at 1397 cm^{-1}. Hence, these bands are reasonably assigned to a mode which is mainly $—COO^-$ symmetric stretching.

At 1324 cm^{-1}, a strong A-type band is observed, while only weak E-type absorptions* are found around here. Therefore, this may mainly arise from $—CH_2—$ wagging motion, whose dipole oscillation occurs in a direction making an angle of about 33° with the c-axis.

The spectral feature in the region from 1120 to 1160 cm^{-1} is rather complicated. In any way we observed here both A-type and E-type absorptions of comparable intensity. This fact is not contradictory to our assignment of these frequencies to the NH_3^+ rocking mode, which is almost degenerate in the free molecule and whose dipole oscillation occurs on the plane of the three hydrogen atoms.

The A-type band at 1044 cm^{-1} is much stronger than the E-type band at 1050 cm^{-1}. This is compatible with our assignment of these bands to a mode in which C—C and C—N stretching motions occur with the 180° phase difference.

At 924 cm^{-1} a strong E-type band is observed, while the corresponding A-type band is much weaker. This fact is in agreement with the assignment of the frequency to $—CH_2—$ rocking mode whose dipole oscillation is directed nearly perpendicular to the c-axis.

In the 890 cm^{-1} region, we observed an E-type band whose peak intensity (at 888 cm^{-1}) is somewhat greater than that of the corresponding A-type band. Therefore, it is reasonable to assign the frequency observed in this region to the mode in which the C—C and C—N stretching motions occur in phase.

Of the two observed frequencies, 686 and 607 cm^{-1}, one has been assigned to the $—COO^-$ wagging mode and the other to the $—COO^-$ symmetric bending (see the preceding section). For the former mode we expect extreme perpendicular dichroism whereas for the latter mode extreme parallel dichroism. Actually, dichroism observed in the 686 cm^{-1} region is slightly perpendicular, while that in the 607 cm^{-1} region is almost parallel. Therefore, the former frequency can be

* The doubling of the E-type absorption is yet to be explained.

VOL. 12 1958

assigned to the —COO^- wagging vibration (although not pure), and the latter to the —COO^- symmetric bending vibration.

The E-type band at 557 cm^{-1} has a comparable intensity with the A-type band at 560 cm^{-1}. Therefore, these frequencies may be assigned to the NH_3^+ torsional motion.

Thus we can assign all the frequencies of glycine observed in the region from 1800 to 400 cm^{-1} based on two independent groups of experimental data as explained in this paper. We believe this is the best assignment available at present.

Acknowledgements—A part of the experiment on γ-glycine was carried out in the H. M. Randall Laboratory of Physics, University of Michigan by one of the authors (M. T.) during his stay there. He wishes to express his sincere thanks to Professor G. B. B. M. Sutherland and to Dr. D. L. Wood for their kind help and valuable suggestions. Our thanks are also due to Mr. Iitaka who presented us many data on γ-glycine before publication and also to Dr. T. Miyazawa for helpful discussions.

References

[1] Edsall J. T. *J. Chem. Phys.* 1936 **4** 1; 1937 **5** 508.
[2] Wright N. *J. Biol. Chem.* 1939 **127** 137.
[3] Klotz I. M. and Gruen D. M. *J. Phys. Chem.* 1948 **52** 961.
[4] Baba H., Mukai A., Shimanouchi T., and Mizushima S. *J. Chem. Soc. Japan* 1949 **70** 333.
[5] Kuratani K. *J. Chem. Soc. Japan* 1949 **70** 453.
[6] Thompson H. W., Nicholson D. L., and Short L. N. *Disc. Faraday Soc.* 1950 **9** 222.
[7] Mizushima S. *Structure of Molecules and Internal Rotation* Academic Press, New York 1954; *A Selection of Reprints of Publications on Structure of Molecules*, Vol. II. Laboratory of Physical Chemistry, Tokyo University 1955.
[8] Iitaka Y. *Proc. Imp. Acad. Japan* 1954 **30** 109.
[9] Nakagawa I. and Mizushima S. *Bull. Chem. Soc. Japan* 1955 **28** 589.
[10] Jones L. H. and McLaren E. *J. Chem. Phys.* 1954 **22** 1796.
[11] Iitaka Y. *Acta Cryst., Camb.* To be published.
[12] Bhagavantam S. and Venkatarayudu T. *Theory of Groups and Application to Physical Problems* (2nd. Ed.) p. 127. Andhra University, Waltair, India 1951.

Spectrochimica Acta, 1958, Vol. 12, pp. 262 to 274. Pergamon Press Ltd., London

Ultraviolet criteria for monoaromaticity

D. P. Stevenson and H. M. McConnell *
Shell Development Company, Emeryville, California

(*Received* 5 *December* 1957)

Abstract—Consideration of the ultraviolet absorption spectra (2000–4000 Å) of monoaromatic hydrocarbons of a wide range of structure and substitution type permits the enunciation of three general criteria that the spectrum of a substance or a mixture of substances must satisfy in order that it may be classified as a spectroscopically pure monoaromatic hydrocarbon. The bases for the formulation of these criteria of purity are described and discussed and the mode of application is exemplified.

Introduction

Ultraviolet absorption spectra have been used for many years for studies of molecular structure and for the quantitative analysis of more or less complex mixtures of substances possessing absorption bands at suitable wave lengths. The primary requisite for the analytical application of this (or any other) spectroscopic technique is a library or catalogue of spectra of pure compounds. In order for such a catalogue to be fully usable it is necessary that there exist reliable criteria for the spectroscopic purity of the substances whose spectra appear in the catalogue. Such criteria are often based on empirical spectral regularities which are established from a limited but representative set of compounds whose spectroscopic purity is known to be high. There are already known many examples of such empirical spectral regularities in the ultraviolet spectra of hydrocarbons. For example, the statement that "no saturated hydrocarbon shows appreciable light absorption in a 1·00 cm light path for wave lengths between 2100 and 6000 Å", is a good and extremely useful regularity and is moreover a sensitive criterion as to the purity of saturated hydrocarbons.

As is already well known, the ultraviolet absorption spectra of aromatic hydrocarbons exhibit many regularities which are extremely valuable for the qualitative identification of aromatic types and for the quantitative analysis of mixtures of aromatic hydrocarbons [1–3]. Many regularities in the spectra of aromatics are well described through Clar's classification of these spectra into three band types: ortho-alpha, para and ortho-beta [4]. In other words, an individual aromatic hydrocarbon typically shows three types of absorption bands, and each type has its own characteristics of intensity, wave length, vibrational fine structure, sharpness, wave length and intensity changes on substitution, etc.

By and large, many of the regularities now in use by the ultraviolet absorption spectroscopist as criteria for purity and hydrocarbon-type were originally developed in connection with the theoretical interpretation of ultraviolet spectra. This is especially true, for example, in the classification of aromatic absorption bands into various types, by Clar [4], and later by Platt [5] and others. On the other

* Present address: California Institute of Technology, Pasadena, Calif.

VOL. 12 1958

hand, many empirical regularities in the ultraviolet absorption spectra can be found which are of little direct theoretical interest but which are nonetheless of considerable analytical value. In point of fact, we shall be, in the present paper, concerned with regularities in the ultraviolet absorption spectra of monoaromatic hydrocarbons (2100–6000 Å) which form extremely useful criteria of the purity of individual monoaromatic hydrocarbons and monoaromatic mixtures. Moreover, we shall show that these regularities permit the semiquantitative identification of impurities likely to be present in aromatic mixtures encountered in the separation and processing of petroleum.

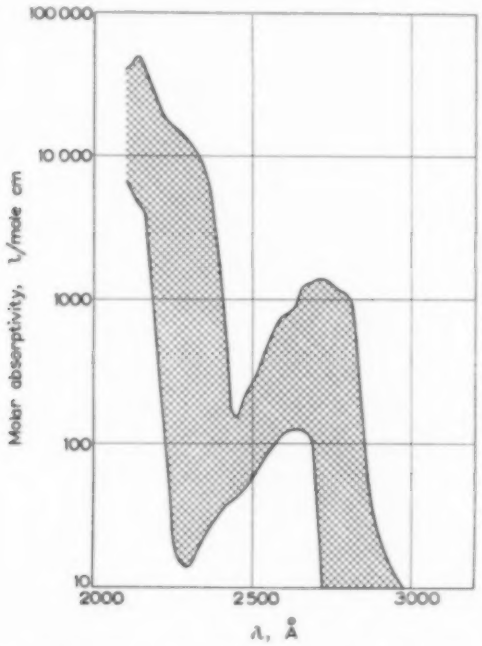

Fig. 1. General spectral region of monoaromatic hydrocarbon absorption.

General criteria for monoaromaticity

We shall consider a *monoaromatic hydrocarbon* to be a hydrocarbon derivative of benzene which contains no other unsaturated group. The ultraviolet spectra of such monoaromatics generally show an ultraviolet absorption band in the region 2500–2800 Å with peak intensity, $A \sim 100$–1500 l./mole cm, where A the molal absorbtivity is $\frac{1}{cl}\log_{10}\frac{I_0}{T}$ (Clar's ortho-alpha band.) A second more intense absorption band (the para band) is centered in the 1950–2100 Å range with peak intensity, $A \sim 8000$–$50{,}000$ l./mole cm. The difficulties that confront one in establishing general criteria for monoaromaticity are suggested by the wide ranges of intensity and wave lengths that we have used in describing the ortho-alpha and para bands. These difficulties are made more apparent in Fig. 1.

The shaded region in Fig. 1 was constructed by drawing on a single graph all the absorption spectra available to us which we know to be spectroscopically pure.* The extrema in absorption at each wave length then define the shaded zone in Fig. 1. Two extremes in the ortho-alpha and para bands of monoaromatics are illustrated in Fig. 2. As a criterion for monoaromaticity, Fig. 1 is useful in that (almost certainly) all monoaromatic hydrocarbon spectra must lie within the shaded region in Fig. 1. On the other hand this criterion is also extremely weak in that obviously, the spectra of many mixtures of monoaromatics with

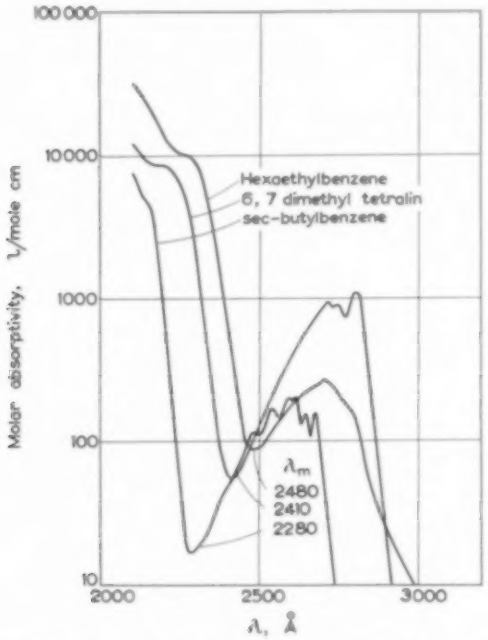

Fig. 2. Ultraviolet absorption spectra of representative monoaromatic hydrocarbons.

large impurity concentrations can also lie within this shaded zone. In particular, the spectra of monoaromatic mixtures contaminated with chemically significant concentrations of saturates, olefins, thiophenes and even polyaromatics may lie within the shaded region in Fig. 1.

Special criteria for the monoaromaticity of substances and mixtures

The first special criterion for the monoaromaticity of substances and mixtures follows directly from Fig. 1, namely that the molar absorptivities of pure monoaromatics at wave lengths greater than or equal to 3000 Å are less than 10 l./mole cm. This criterion for the spectroscopic purity of monoaromatics is similar to the previously stated criterion for spectroscopic purity of saturated hydrocarbons.

* A spectroscopically pure sample may be defined as one whose spectrum can not be made to change to within the experimental error by any further purification. In this Fig. 1 and throughout this paper the absorption spectra refer to those in *iso*-octane or similar nonpolar solvent.

VOL. 12 1958

Furthermore, it should be noted that this first criterion for monoaromaticity is not overly restrictive, since a wide variety of aliphatic hydrocarbons and their derivatives, including alkanes, *cyclo*alkanes, olefins, alkenes, ketones, etc. satisfy this criterion for monoaromaticity.

The second special criterion for monoaromaticity which we call the S-curve criterion, can be understood by reference to Fig. 2. We note that in Fig. 2 the wave length of minimum light absorption between the ortho-alpha and para bands λ_m, increases regularly with the number of substituents in the series, *sec.*-butyl

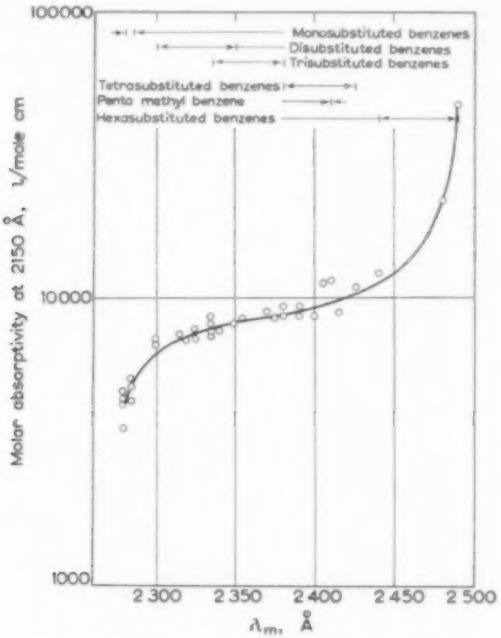

Fig. 3. "S-curve" for pure monoaromatic hydrocarbons.

benzene ($\lambda_m = 2280$ Å), 6,7-dimethyltetralin ($\lambda_m = 2410$ Å) and dodecahydrotriphenylene ($\lambda_m = 2490$ Å). This increase in λ_m is due to the larger bathochromic shift (and possibly intensification) of the more intense para-band, relative to the ortho-alpha band. At the same time the molar absorptivities at 2150 Å, A_{2150}, also increase with increasing λ_m: *sec.*-butyl benzene ($A_{2150} = 4600$), 6,7-dimethyltetralin ($A_{2150} = 9100$) and dodecahydrotriphenylene ($A_{2150} = 47{,}000$). This regular increase in A_{2150} with increasing λ_m holds not only for these three compounds but also holds approximately for some forty other pure monoaromatic substances. This regularity is demonstrated in Fig. 3 which shows a plot of A_{2150} vs. λ_m for these compounds. All the points in Fig. 3 lie on the smooth curve, the S-curve, to within 3–10 per cent in A_{2150}.

We note that this second special criterion for monoaromaticity is much more restrictive than the first, given above. Implicit in the application of this criterion for monoaromaticity to an ultraviolet absorption spectrum is that the spectrum

satisfy the general criterion for monoaromaticity, namely, fall in the general type defined by the shaded zone of Fig. 1.

The third and final special criterion for monoaromaticity is concerned with the regular increase of the absorptivity, A_m, with that of the wave length, λ_m, of the absorption minimum between the ortho-alpha and para bands. It may be seen in Fig. 2 that the absorption minima in the three spectra lie on an approximately (logarithmically) straight line. In Fig. 4 there are shown the points,

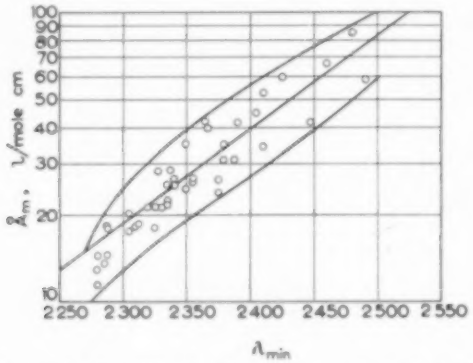

Fig. 4. Spectral points (A_m, λ_m) for pure monoaromatic hydrocarbons.

(A_m, λ_m), for the forty pure compounds considered in constructing Fig. 3, and it is seen that the points are uniformly distributed in a band about the line:

$$\ln A_m = 0{\cdot}00323\,\lambda_m - 6{\cdot}141$$

with the limitation, 2275 Å $\leq \lambda_m \leq$ 2500 Å. Although the width of the band, ± 25 per cent of A_m, may seem wide, it will be seen below that this width is small compared to the changes effected by relatively small concentrations of certain impurities.

It must finally be noted that the criteria for monoaromaticity that have been stated above, the general one and the three special ones, are by their nature necessary conditions for monoaromaticity, and that the satisfaction of no one of the criteria, nor any combination of the criteria is a sufficient condition for monoaromaticity of a substance.

Classification of impurities according to the special criteria of purity

The possible contaminants of monoaromatic substances or mixtures may be classified in terms of the effects of the impurities on the ultraviolet spectral criteria of purity defined above. The first broad group of possible impurities or contaminants, that may be termed diluents, is comprised of those substances that are more or less transparent to radiation of wave length greater than 2000–2100 Å. This group includes alkanes, alkenes, *cyclo*alkanes, *cyclo*alkenes, aliphatic alcohols and ethers, etc. The presence of such substances admixed with monoaromatics has no effect on the wave length of minimum light absorption λ_m, but causes both absorptivities, A_{2150} and A_m, to be lower than in their absence. The fact that the

VOL. 12 1958

characteristic spectral points (A_{2150}, λ_m) and (A_m, λ_m), will lie below the S-curve and below the "band" (of Fig. 4) when diluents are present in the monoaromatic, suggests that we might alternately designate these impurities as "negative" with respect to the second and third criteria. Since monoaromatics are essentially transparent to light of wave lengths greater than 3000 Å, the diluents have no effect with respect to the first criterion for monoaromaticity. Thus we may symbolize the diluents as (nil, −, −,), where the position in the parenthesis (1, 2, 3) indicates the special criterion, first, second and third.

The magnitude of the negative deviation of the spectral point, (A_m, λ_m), of either the second or third criterion, resulting from the presence of a diluent in a monoaromatic, will be directly proportional to the molar concentration of the diluent. Since the breadth of the S-curve is in the range, 3–10 per cent, while the breadth of the band about the (A_m, λ_m) of the third criterion is ± 25 per cent, the second criterion is the more sensitive as a basis for semiquantitative estimates of the magnitude of the concentration of diluents in monoaromatics.

The second class of impurities or contaminants of monoaromatics as defined by their effects on the criteria, are those substances that have a single broad absorption band in the range, 2100–2400 Å, with peak absorptivity in the range, 5000–40,000 l./mole cm. This class includes conjugated alkadienes and *cyclo*-alkadienes, thiophenes, and vinyl aromatics such as the styrenes and indenes. The presence in monoaromatics of substances with such broad and medium to strong absorption bands results in a filling in of the absorption minimum between the monoaromatic ortho-alpha and para bands in such a manner that λ_m usually increases with the concentration of the impurity. Since the peak absorptivity associated with such impurities is less than or equal to that of the aromatic para band, and the impurity band tends to extend to longer wave lengths than the para band, λ_m increases while A_{2150} remains unchanged or decreases and A_m increases with concentration of these impurities. Substances of this class are also essentially transparent to light of wave lengths greater than 3000 Å, thus the criteria symbol for these impurities is, (nil, −, +).

Since the absorptivities of substances in this second class of impurity are usually quite large for wave lengths in the range, 2200–2400 Å, where the monoaromatics are relatively transparent, while their absorptivities at shorter wave lengths are of the magnitude of or less than that associated with the para band of the monoaromatics, the third criterion, (A_m, λ_m), is the most sensitive one for semiquantitative estimation of the concentration of this class of impurity.

The general sensitivity of the third criterion for the detection and estimation of the second group of impurities of monoaromatics is illustrated in Fig. 5. In this figure there are shown the loci of the points, (A_m, λ_m), for various concentrations of styrene in ethyl benzene, indene in indane, and of 1,2-dihydronaphthalene in tetralin. It will be noted that as little as 0·5 per cent M of the Group 2 impurity (nil, −, +), causes the point, (A_m, λ_m) to move out of the zone taken as the third purity criterion.

The third group of impurities of monoaromatics that may be defined, is comprised of naphthalenes and benzothiophenes. These substances have the same set of absorption bands, ortho-alpha, para and ortho-beta that characterize the

electronic spectra of the monoaromatics, but shifted in various degree toward longer wave lengths. The bathochromic shifts are such that they exhibit strong absorption from wave lengths of 2100 Å to greater than 3000 Å. They may be designated by the criterion symbol (+, −, +). The negative deviation of the second criterion again results from the fact that the bathochromic shift of λ_m with concentration of these impurities is more effective than the change that can result in A_{2150}. For substances of this class, the first criterion is the most sensitive

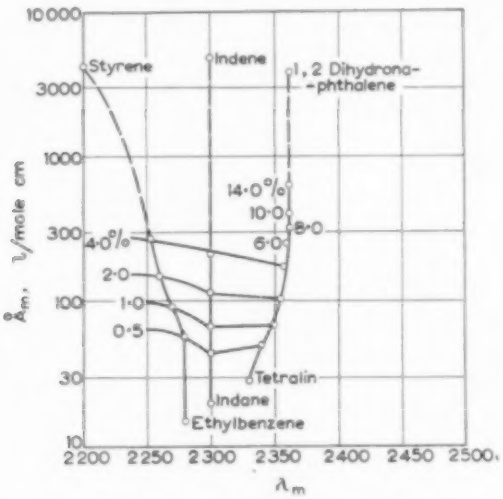

Fig. 5. The effect of impurities on the spectral points (A_m, λ_m) of ethylbenzene, indane and tetralin.

for semiquantitative estimation of the concentration of the (+, −, +) impurities.

To a good approximation the molar absorptivities of alkyl substituted naphthalenes and benzothiophenes are the same and equal to 2150 l./mole cm at 3040 Å. Thus the sum of the concentrations of (+, −, +) impurities in monoaromatics is given by:

$$(+, -, +) = (A_{3040}/21{\cdot}5) \text{ per cent M}$$

a formula that may be stated to be reliable to ±25 per cent of the concentration of (+, −, +).

The fourth class of monoaromatic contaminants is composed of the multiphenyl alkanes. The ultraviolet absorption spectra of substances of this class are essentially like those of the monoaromatics, if they are reduced to a per benzene ring basis. Thus their effect on the purity criteria may be represented by the symbol (nil, +, +). The magnitude of the deviations from the S-curve, or the (A_m, λ_m) zone, produced by these substances is directly proportional to their molar concentration and as for the diluents, (nil, −, −), the deviations from the S-curve provide the most sensitive semiquantitative measure of their concentration.

The fifth and last class of impurities of monoaromatics that we shall consider are the alkyl (or *cyclo*alkyl-) biphenyls. The strong, broad absorption band(s) of these substances in the 2000–3000 Å range causes positive deviations with

VOL. 12 1958

respect to all three special criteria, hence the symbol (+, +, +). For semi-quantitative estimation of the biphenyls, the deviations from the monoaromatic zone, (A_m, λ_m), are the most sensitive. As may be seen by reference to Fig. 6, as little as 0·6 per cent M biphenyl is readily detectable in a monoaromatic by means of the third criterion.

It has been implicit in the foregoing discussion that mixtures of monoaromatic hydrocarbons behave as do the pure individual hydrocarbons with respect to the special criteria of purity. To the extent that this situation obtains it is apparent

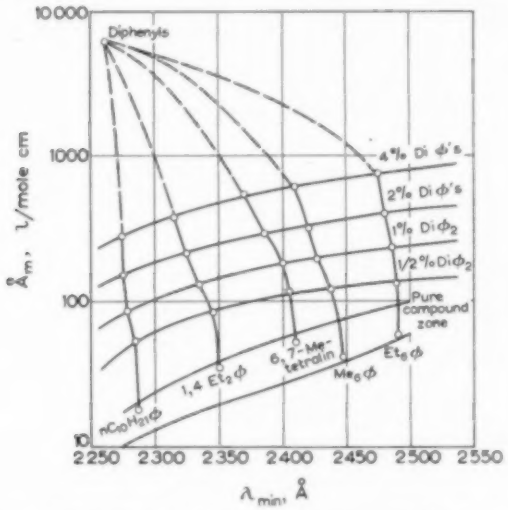

Fig. 6. The effect of "diphenyl" impurities on the spectral points (A_m, λ_m) of various monoaromatic hydrocarbons.

that the criteria of purity, as applied to pure compounds, can not provide evidence concerning the possible presence or absence of isomers and/or homologues in a particular monoaromatic. In fact even an unconjugated olefinic benzene would not be detected by the application of the criteria to a spectrum.

Under certain, very unlikely circumstances, binary or ternary mixtures of monoaromatics result in spectra that violate the purity criteria. Referring to Figs. 3 and/or 4, it will be noted that the value of λ_m characteristic of the ultraviolet absorption spectrum of a substituted benzene is primarily determined by the number of substituents. Mixtures of monoaromatics with different numbers of substituents will in general have λ_m intermediate to the λ_m of the individual substances. However, the λ_m of the mixtures are usually *not* simple additive functions of the λ_m of the individual substances, nor are the absorptivities, A_m, of the mixtures additive functions of the A_m of the individual substances. The deviations from additivity of the λ_m and A_m of the mixtures increase as the difference in the degree of substitution of the individual substances increases. Thus, for example, the "points" (A_m, λ_m), for binary mixtures of 1,2-diethyl benzene and 6,7-dimethyl tetralin lie within the pure compound zone for all possible relative concentrations. On the other hand, in the case of mixtures of *n*-dodecyl

benzene and hexa-ethyl benzene, for concentrations of the latter substance in the range, 1–40 per cent M in the former, the points (A_m, λ_m), lie above the pure compound zone. The addition of 1 per cent M hexa-ethyl benzene to *n*-dodecyl benzene shifts (A_m, λ_m) from (18,2280) to (63,2397). Such effects as this last cited are not likely to be of practical importance. In synthetic work aimed at preparing pure substances, isomers differing markedly in degree of substitution are highly unlikely impurities. In the separation of monoaromatic aggregates from petroleum there is generally expected to be encountered mixtures with a virtually continuous

Table 1. Spectral classification of monoaromatic impurities

Class of impurity	Deviation from criterion no. 1	2	3	Most sensitive criterion	Limit of detection (%)
Diluents: includes alkanes, alkenes, etc.	nil	−	−	2	3–10
Dienes: includes 1,3-alkadienes, 1,3-*cyclo*alkadienes, thiophenes, and vinyl aromatics, etc.	nil	−	+	3	0·5
Diaromatics: includes naphthalenes and benzothiophenes.	+	−	+	1	0·01
Multi-phenyl alkanes, etc.	nil	+	+	2	3–10
Biphenyls	+	+	+	3	0·5

distribution in degree of substitution (from one to six), and such mixtures behave, with respect to the criteria, as do monoaromatic substances.

The foregoing discussion of the classification of monoaromatic impurities or contaminants in terms of the special spectral criteria of purity is summarized in Table 1.

Discussion

As was indicated in the introduction, the need for criteria of spectroscopic purity arises in connection with the evaluation of the reliability of spectra of model compounds (or model mixtures of compounds) obtained as reference standards for analytical purposes. With respect to model monoaromatics the methods of synthesis that are employed are such that the most likely impurities that are of spectroscopic importance are vinyl aromatics which are in the impurity class (nil, −, +). This statement is illustrated by consideration of the spectra of certain monoaromatic hydrocarbons reported in the A.P.I. Project 44, *Catalogue of Ultraviolet Spectra*.

The spectra of the eicosylbenzenes form a particularly interesting set for the present purposes. There are shown in Table 2 the wave lengths, λ_m, and the corresponding absorptivities, A_m, for the six different eicosylbenzenes reported in the

VOL. 12 1958

A.P.I. 44 catalogue. From reliable spectra of the various butyl- and amyl-benzenes it may be inferred that λ_m should be in the range, 2280–2290 Å, and that A_m should lie in the range, 14–19 l./mole cm. For the eicosylbenzenes the reported λ_m are slightly greater in most of the cases, lying between 2290 and 2300 Å, and the A_m are in the range 30–260 l./mole cm. Referring to Fig. 5, where there is shown the effect of concentration of styrene in ethylbenzene on (A_m, λ_m) we see that the A_m of the eicosylbenzenes correspond to impurity concentration in the range, 0·2–4·0 per cent M. Since on the spectra the measurements did not extend

Table 2. Purity criteria data, eicosylbenzenes

Compound	No. *	λ_m	A_m (l./mole cm)	Impurity (% M) †
1-Phenyleicosane	7	2295 Å	36	0·2
2-Phenyleicosane	8	2290	30	0·2
3-Phenyleicosane	156	2300	158	2·0
5-Phenyleicosane	9	2290	152	2·0
5-Phenyleicosane	157	2290	158	
7-Phenyleicosane	158	2280	263	4·0
9-Phenyleicosane	10	2290	49	0·5
9-Phenyleicosane	159	2290	55	

* A.P.I. Project 44, *Ultraviolet Spectral Catalogue*, Serial Number.
† Calculated as (*i*)-Phenyl-*i*-eicosene.

to 2150 Å we can not assert with surety that the impurities in the specimens was eicosenylbenzene, but this is a reasonable inference from the methods of synthesis.

Similarly it may be concluded that the samples of the various 6-alkyltetralins, and 6,7-dialkyltetralins for which spectra are reported, A.P.I. 44, serial numbers 287 through 295 inclusive, contained from 9 to 15 per cent M impurity, primarily of the type, 1,2-dihydronaphthalene.

For the group or type analysis of heavier petroleum fractions, distillates or residues, by such methods as have been described by Burdett, Taylor and Jones [3] the necessary spectral calibration data must be obtained from model mixtures prepared by suitable separation methods, say distillation and chromatography, from petroleum. This necessity arises from the fact that in order to synthesize spectra for such complex mixtures from data on pure compounds it would be necessary to have available spectra for all the spectral types that occur in the complex mixtures, along with information on the frequency of occurrence of the spectral types, and neither of these conditions is satisfied. The three spectral criteria of monoaromaticity have been found to be of inestimable value in following the various stages of separation of representative monoaromatic aggregates from petroleum fractions that now serve as calibration standards for quantitative ultraviolet "type analyses".*

In order to apply the methods of high molecular weight mass spectrometry [6] to the determination of the distribution in empirical formula, i.e. naphtheno-ring

* See for example, Fig. 8 of ref. [3].

number, among the monoaromatics in the heavier fractions of petroleum, it is particularly important to have a reliable measure of the quality of the separation of the monoaromatics from "diaromatics", i.e. the naphthalene and benzothiophene derivatives that form an important portion of most oils. The particular necessity for clean separation from the benzothiophenes arises from the coincidence in the molecular weight of benzothiophenes and alkyl benzenes. In this connection

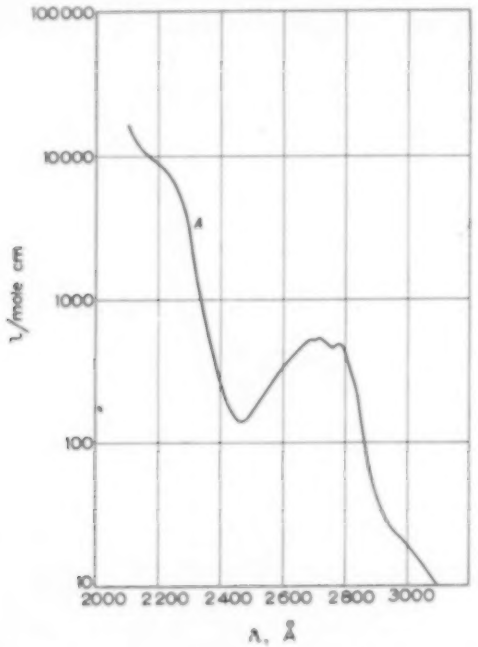

Fig. 7. Ultraviolet absorption spectrum of a monoaromatic aggregate from a lubricating oil base stock. Average molecular weight of the aggregate ca. 400, and average composition C_nH_{2n-8}. The filled in minimum (λ_m) and long wavelength absorption ($\lambda > 3000$ Å) due to about 0·9 per cent benzothiophenes.

the high sensitivity of the ultraviolet spectral criteria of purity of monoaromatics is particularly useful.

There is shown in Fig. 7, the ultraviolet absorption spectrum, 2100–3500 Å, of a monoaromatic aggregate* separated from a mid-continent lubricating oil distillate. The effect of 0·5, 1·0, 2·0, and 4·0 per cent M of thiophenes, benzothiophenes, naphthalenes and diphenyls on the spectral points, (A_{2150}, λ_m) and (A_m, λ_m) of the aggregate are shown in Fig. 8.

It is of interest to examine the applicability of the criteria of purity to other than hydrocarbon derivatives of the monoaromatics, such as halides, phenols, etc. The limited data that are available indicate that the first and third special criteria of purity are applicable to both fluoro- and chlorobenzenes and we believe it very likely that these two criteria also apply to fluoro- and chlorotetralins,

* This aggegate, with an average molecular weight of 400 and empirical formula approximating C_nH_{2n-8}, is a portion of the material whose far ultraviolet spectrum is shown in Fig. 8 of ref. [3].

VOL. 12 1958

indans, etc. The S-curve criterion does not apply to these substances. Due to the fact that the wave length associated with excitation of the nonbonding halogen electrons shifts into the range greater than 2100 Å in the cases of bromo- and even more so iodo-compounds, none of the criteria are applicable to such derivatives of the monoaromatics.

The situation in the case of phenols and phenyl-ethers is ambiguous. The first criterion is certainly applicable, i.e. $A_{3000} < 10$ l./mole cm, for these substances. The S-curve criterion is inapplicable. With respect to the third criterion,

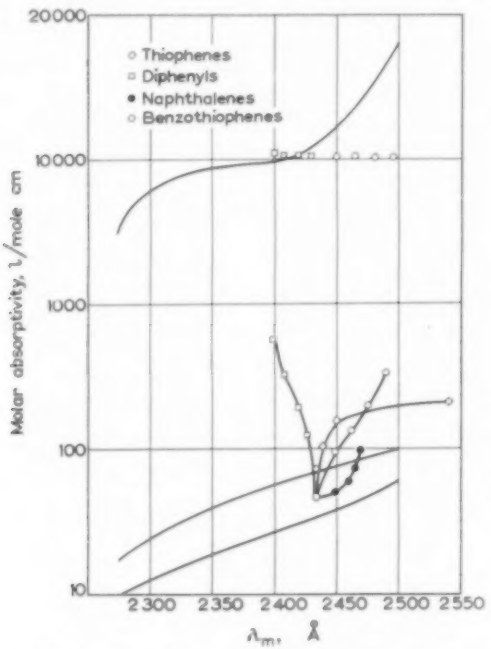

Fig. 8. The effect of various impurities on the spectral points (A_{2150}, λ_m) and (A_m, λ_m) of a monoaromatic aggregate.

the location of the spectral point (A_m, λ_m), only that of 3-ethyl-phenol, with $A_m = 40$ and $\lambda_m = 2390$ Å (A.P.I. project 44, serial no. 441), lies within the monoaromatic zone. However there are definite indications that it may be extremely difficult to obtain a true absorption spectrum of a phenol because of the ease of oxidation of these substances to quinoid structures that have an extremely strong absorption band in the 2200 to 2600 Å range. For example, it has been found in these laboratories [7] that for 2-methyl-phenol, $A_m = 68$ and $\lambda_m = 2380$ Å, while on curve no. 429 of the A.P.I. 44 catalogue there is reported $A_m = 120$ and $\lambda_m = 2385$ Å. Similarly for 3-methyl-phenol there has been reported $A_m = 106$ and $\lambda_m = 2420$ Å. All spectroscopic experience would lead to the expectation that there should be little or no difference in the spectra of the homologues, 3-methyl- and 3-ethyl-phenol.

On the basis of the cited observations and some other like anomalies, we

postulate that with the exception of 3-ethyl-phenol there has not been reported the ultraviolet absorption spectrum of a spectroscopically pure alkyl phenol, or phenyl ether. That there is more than sufficient oxygen present in ordinary spectroscopic solvents to permit significant oxidation of labile substances such as the phenols to strongly absorbing substances follows from the solubility of oxygen in the commonly used solvents. For example, McKeown and Hibbard [8] give for the solubility of oxygen in isooctane, 0·014 moles/l. at 25°. The general level of the absorptivity of monoaromatics in the 2100–3000 Å range of wave lengths is such that the spectra are obtained of solutions containing the order of 0·01 to 0·05 moles/l. Thus a solvent only 1 per cent saturated with air contains sufficient O_2 to oxidize the order of 0·1 to 1·0 per cent of a phenol. Since the peak absorptivity of such substances as *p*-benzoquinone is of the order of 50,000 l./mole cm in the vicinity of 2400 Å. as little as 0·05 per cent oxidation of a phenol would be expected to double the absorptivity in the region of λ_m.

References

[1] Gillam A. and Stern E. S., *Electronic Absorption Spectroscopy* Arnold, London 1954.

[2] Friedel R. A. and Orchin M., *Ultraviolet Spectra of Aromatic Compounds* Wiley, New York 1951.

[3] Burdett R. A., Taylor L. W. and Jones L. C., *Molecular Spectroscopy* pp. 30–42 The Institute of Petroleum, London 1955.

[4] Clar E., *Aromatische Kohlenwasserstoffe* Edward Bros., Ann Arbor, Mich. 1944.

[5] Platt J. R., *J. Chem Phys.* 1949 **17,** 484.

[6] Clerc R. J., Hood A. and O'Neal M. J., *Analyt. Chem.* 1955 **27** 868.

[7] Tunicliff D. D., Private communication.

[8] McKeown A. B. and Hibbard R. R., *Analyt. Chem.* 1956 **28** 1490.

VOL. 12 1958

Spectrochimica Acta, 1958, Vol. 12, pp. 275 to 283. Pergamon Press Ltd., London

RESEARCH NOTES

Spectrum tables used for wavelength identification in the Schuman region

(*Received* 15 *June* 1957)

THE use of the spectral range beyond 2000 Å towards the shortest wavelengths is becoming increasingly useful in both research and analytical work. To the best of the writer's knowledge, however, no tables or atlases are available, so far, that could be used as reference in identifying the wavelengths of the spectrum lines in this field. This entails considerable trouble, notably in the case of the spectra under examination having been obtained by the use of prism spectrographs, where dispersion varies according to a function which is not simple. Consequently, every researcher is now compelled to prepare his own tables, i.e. to perform a more or less useless but always lengthy and tiresome task in identifying the lines of a comparison spectrum on the basis of wavelength values already tabulated for a few metal elements [1].

It was therefore deemed advisable to publish the following tables which should considerably assist the researcher in his identification of wavelengths of unknown spectra.

The spectrum used for comparison is the emission spectrum of carbon monoxide. This spectrum shows sharp and easily identified band-heads that make it very typical, and offers the added advantage of being readily obtainable from a simple discharge tube filled with carbon dioxide flowing under a pressure in the order of 1 mm Hg, while a considerably more complex equipment is needed in the case of emission spectra (e.g. spark spectra) of metal elements for which the necessary wavelength determinations may have already been performed.

The following tables were obtained from spectra that were recorded using the vacuum spectrograph of the "Istituto Superiore di Sanità" Rome—an instrument previously described in detail by the writer [2]. It is equipped with a 1 m concave grating of 12,000 grooves/cm (or 30,000 lines/in.) having a 40 × 80 mm ruled area, and a total practical resolving power of approximately 40,000 with an average dispersion of 8·2 Å/mm approximately.

The spectrum was photographed in the first order and then enlarged twenty times. As starting point, to be used as guidance in identifying the band-heads, the measurements provided by the existing literature [3] were used. The spectrum was, however, thoroughly remeasured, the exact diagram of the dispersion of the grating used being calculated and plotted first. Although the dispersion, as expressed in Å/mm, is nearly linear, in the case of high-accuracy determinations, the fact should not be disregarded that incidence and diffraction angles are fairly removed from the normals, as also is the angle of incidence on the photographic plate. Dispersion varies from one end of the spectrum to the other, the range on the original plate going from 8·129 Å/mm at 2300 Å to 8·314 Å/mm at 1350 Å.

The individual band-heads were measured with a 20 enlargement optical projector [4] offering an accuracy of ±0·005 mm on the plate, this being the equivalent of the average resolving power of the photographic plates used (Ilford's extra-thin "Q-1"). The consequence of this uncertainty in the measurement, considering the spectrograph's own

dispersion, is that the measured wavelength measurements may be inaccurate to $\pm 0{\cdot}04$ Å, this being the reason why they were rounded off to the nearest tenth of Å.

For convenience, notably in absorption work, each measured band-head has been identified with the corresponding wave number (ν vac.). The tables, eight in number, cover the region between 2300 and 1350 Å in portions of about 150 Å for each table.

As example part of a table is reproduced full size in Fig. 1.*

Acknowledgements—My best thanks are due to Messrs. Optica, Milan, who very kindly collaborated in the final preparation of these tables.

Laboratorio di Chimica,
Istituto Superiore di Sanità,
Rome, Italy

G. Milazzo

References

[1] Wilkinson P. G., *J. Opt. Soc. Amer.* 1955 **45** 862.
[2] Milazzo G., *Ric. Ist. Sup. Sanit.* 1956 **19** 1167. *Spectrochim. Acta* Colloquium Spectroscopicum Internationale VI, Amsterdam 1956, p. 474.
[3] Estey R. S., *Phys. Rev.* 1930 **35** 309; Headrick L. A. and Fox G. W., *Ibid.* 1930 **35** 1033; Read D. N., *Ibid.* 1934 **46** 571.
[4] Intonti R. and Milazzo G., *Chim. e Industr.* 1939 **21** 662.

VOL. 12 1958

A method of mounting micro samples in infrared spectrometry†

(*Received* 8 *November* 1957)

Reflecting microscopes have been designed and used with infrared spectrometers by various workers [1–11]. With such microscopes, infrared spectra were obtained with only a few micrograms or less of substance in the light path. However, a larger sample is required because of losses in the preparation and mounting of the material [6, 8, 12]. To minimize these problems, special cells and techniques have been employed [3, 8, 12–16], but there is still need for a method of handling small samples of substances that are insoluble in solvents useful in infrared spectrometry. The following method of mounting small solid samples of 5 μg, or even less, is therefore described.

The sample, either pure or mixed with powered KBr, is pressed as a window in a piece of metal foil, which is then used to hold the sample in the light path. A hole, $0{\cdot}3 \times 0{\cdot}7$ mm or smaller, is punched near the centre of a small piece of aluminum foil, which is then folded (Fig. 1) so that the sample is sandwiched between two layers of foil in which there is no hole. This arrangement precludes lateral motion of the centre layer with respect to the other layers and thereby prevents scattering the sample across the lower layer during subsequent manipulations. By the use of a suitable press or vice, the folded piece of foil enclosing the sample is pressed between flat plates with a total force of approximately 8000 lb. After a minute, the foil is removed from the press, carefully unfolded, and mounted with the sample at the focal point of the microscope. The infrared spectrum is then recorded in the usual manner.

Certain details of the technique merit additional comment. Aluminium foil is convenient to use, but any plastic or metal sheet could be used as long as the material is sufficiently

* Photographic copies may be obtained from the Author.

† This investigation was supported in part by a research grant, C-2545, from the National Cancer Institute, Public Health Service.

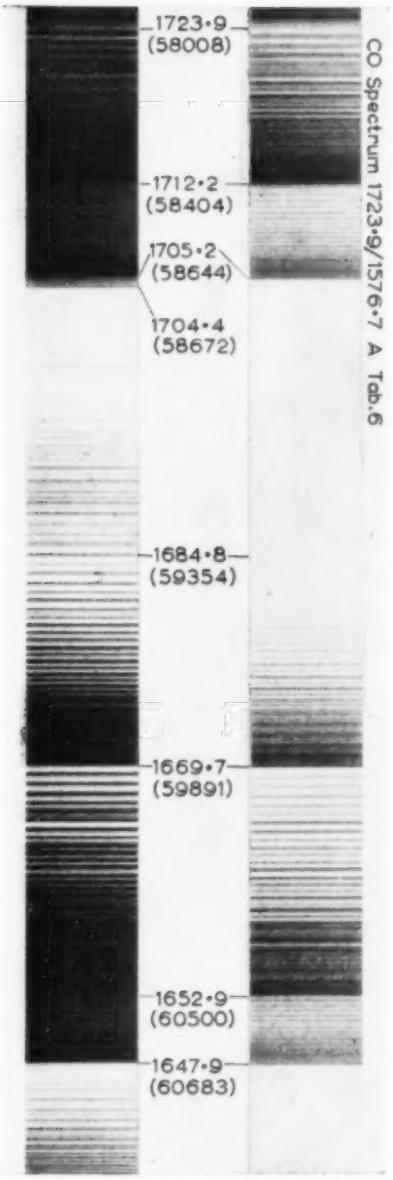

Fig. 1. Part of one table of the atlas for wavelength identification in the Schuman region in full size

VOL.
12
1958

rigid, thin, and inert towards the sample. A hypodermic needle of suitable gauge, with the end cut off at right angles and flattened, serves admirably as a punch, providing both a small end for punching the hole and a large end for conveniently handling the tool. Transferring a 5 μg sample of pure steroid into the aperture in the aluminum foil must be done with great care; otherwise, the effort to press a good window will fail. However, grinding the sample with a few micrograms of KBr in a mortar gives a larger volume, which is more easily manipulated.

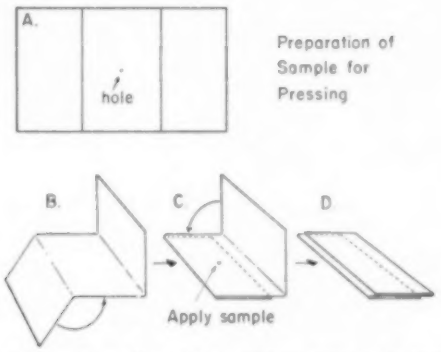

Fig. 1. Steps in folding foil to enclose sample for pressing.

The method of sample mounting described above is used with the Perkin–Elmer Model 13 Infrared Spectrometer with a Model 38A microscope [10] but the same technique could probably be used with various microscopes, whether infrared or ultraviolet, and with spectrometers and beam condensing systems such as that devised by Anderson and Miller [17].

Dale A. Clark
Anton P. Boer

Veterans Administration Hospital, McKinney, Texas
Department of Biochemistry, University of Texas, Southwestern Medical School Dallas, Texas

References

[1] Burch C. R. *Proc. Phys. Soc. Lond.* 1947 **59** 41.
[2] Barer R., Cole A. R. H. and Thompson H. W. *Nature, Lond.* 1949 **163** 198.
[3] Gore R. C. *Science* 1949 **110** 710.
[4] Blout E. R., Bird G. R. and Gray D. S. *J. Opt. Soc. Amer.* 1950 **40** 304.
[5] Wood D. L. *Rev. Sci. Instrum.* 1950 **21** 764.
[6] Blout E. R. and Bird G. R. *J. Opt. Soc. Amer.* 1951 **41** 547.
[7] Mellors R. C. *J. Opt. Soc. Amer.* 1952 **42** 283.
[8] Cole A. R. H. and Jones R. N. *J. Opt. Soc. Amer.* 1952 **42** 348.
[9] Fraser R. D. B. *J. Opt. Soc. Amer.* 1953 **43** 929.
[10] Coates V. J., Offner A. and Siegler E. H., Jr. *J. Opt. Soc. Amer.* 1953 **43** 984.
[11] Blout E. R. and Abbate M. J. *J. Opt. Soc. Amer.* 1955 **45** 1028.
[12] Blout E. R., Parrish M., Jr., Bird G. R. and Abbate M. J. *J. Opt. Soc. Amer.* 1952 **42** 966.
[13] Friedel R. A. and Pelipetz M. G. *J. Opt. Soc. Amer.* 1953 **43** 1051.
[14] Davison W. H. T. *J. Opt. Soc. Amer.* 1955 **45** 227.
[15] Mebane A. D., cited by Müller R. H. *Analyt. Chem.* 1956 **28** No. 7 37A.
[16] Black E. D., Margerum J. D. and Wyman G. M. *Analyt. Chem.* 1957 **29** 169.
[17] Anderson D. H. and Miller O. E. *J. Opt. Soc. Amer.* 1953 **43** 777.

Ein Elektrodenheizblock zur Lösungsspektralanalyse

(*Received* 10 *January* 1958)

Abstract—A heating device is described for rod shaped electrodes used in the spectral analysis of solutions, which permits rapid working and small electrode consumption.

Verwendet man nach Scheibe und Rivas [1] bei der Lösungsspektralanalyse vorerhitzte Stabelektroden, so müssen diese zwecks Erzielung wohl definierter und reproduzierbarer Arbeitsbedingungen mittels einer Heizquelle stets auf die gleiche Temperatur erhitzt werden. Zu diesem Zweck fand in einigen Arbeiten [2–4] zum Erhitzen von 1·5–2 cm langen Grafitelektroden (5 mm ϕ) der Mikro-Universalheizblock* nach Gorbach [5] mit Spezialaufsatz Anwendung. Da dieser aber zum Erhitzen längerer Elektroden nicht geeignet ist, wurde der nachfolgend beschriebene, auf den Mikro-Universalheizblock passende Spezialaufsatz entwickelt.

Der Spezialaufsatz erlaubt das Erhitzen von 200 mm langen Elektroden beliebigen Durchmessers und gewährleistet ein rasches Arbeiten und eine möglichst günstige Ausnützung der Elektroden. Nach der hier beschriebenen Arbeitsweise können im Vergleich mit der oben erwähnten Arbeitsmethodik rund dreimal soviel, nämlich 13–18 Lösungsspektralanalysen mit einer 200 mm langen Grafitelektrode durchgeführt werden. Der entwickelte Elektrodenheizblock erfordert eine geänderte Arbeitstechnik. Zwei Elektroden von 5 mm ϕ und 200 mm Länge werden an je einem Ende mit der Elektrodenspitzmaschine (Fa. A.R.L.) plan abgedreht und deren Leerspektrum aufgenommen. Danach wird das abgedrehte und abgefunkte Ende der unteren Elektrode im Elektrodenheizblock erhitzt, die Probelösung aufgebracht und nach dem Eindampfen der Lösung die Elektrode im Funkenstativ wieder eingespannt. Nach dem Abfunken werden die gebrauchten Elektrodenenden in einer Länge von etwa 5–7 mm mittels einer Schnabelzange abgebrochen, die Bruchflächen mit der Spitzmaschine wieder abgedreht und wie vorhin angegeben fortgefahren.

Die Arbeitsweise des Elektrodenheizblockes ist aus Abbildg. (1) ersichtlich. Der unbewegliche Teil (b) ist mit dem zylindrischen Teil des Spezialaufsatzes fest verbunden, während der bewegliche Teil (c) entlang der Führungsstifte (f) bewegt werden kann. Die Elektrode wird durch den Haltestift (d) festgehalten. Der Haltestift (d) und der bewegliche Teil (c) werden durch Federn in Richtung gegen den unbeweglichen Teil (b) gedrückt. Der Haltestift (d) ragt etwa 1 mm in den Bohrungsraum hinein. Da die Länge der Grafitelektrode zu Beginn grösser als die Höhe des Elektrodenheizblockes ist, empfiehlt es sich, den Elektrodenheizblock am Tischrand oder auf einem Sockel erhöht aufzustellen, sodass die Elektroden an der Tischplatte nicht anstossen. Der Spezialaufsatz ist ebenso wie der Mikro-Universalheizblock aus Aluminium hergestellt, der Haltestift (d) aus Stahl oder Messing. Bei Anregung im Hochspannungsfunken konnte eine Verunreinigung der Grafitelektroden durch den Elektrodenheizblock nicht festgestellt werden. Falls es sich aber bei einer empfindlicheren Anregungsart als notwendig erweisen sollte, so können der Haltestift (d) und die Bohrung ohne weiteres aus einem anderen Metall hergestellt bzw. mit einem solchen ausgekleidet sein.

In der von uns gewählten Ausführung weist der Elektrodenhalter (a) eine Bohrung von 5 mm auf, es können aber auch bequem zwei Bohrungen angebracht werden, wenn auf beide Elektroden gleichzeitig Probelösung aufgebracht wird oder z.B. 5 mm und 6 mm für Elektroden verschiedenen Durchmessers. Weiterhin besteht noch die Möglichkeit bis zu sechs weitere Elektrodenhalter für andere Elektrodendurchmesser kranzförmig um

* Fa. P. Haack, Wien IX, Garnisongasse 3, Österr.

VOL. 12 1958

den Mittelteil des Spezialaufsatzes anzubringen. Die Bohrung des Elektrodenhalters (a) ist um etwa 0·1 mm weiter als die Grafitelektrode, damit der bewegliche Teil (c) auch bei in die Bohrung eingeführter Elektrode völlig auf dem unbeweglichen Teil (b) aufliegt. Damit wird ein guter Wärmeübergang und ein rasches Erhitzen der Elektrode gewährleistet.

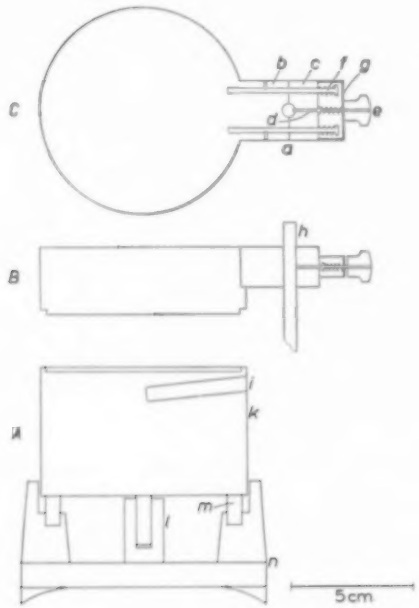

Abb. 1. Elektrodenheizblock zur Lösungsspektralanalyse; A Mikro-Universalheizblock, *B* und *C* Spezialaufsatz zum Erhitzen langer Stabelektroden, (a) Elektrodenhalter, (b) unbeweglicher Teil von (a), (c) beweglicher Teil von (a), (d) Haltestift, (e) Griff, (f) Führungsstift, (g) Halterbügel, (h) Grafitelektrode, (i) Thermometerbohrung, (k) Heizplatte, (l) elektrischer Anschluss, (m) Stiftstützen aus Porzellan, (n) Heizkörperfuss.

Das Erhitzen der Grafitelektroden wird wie folgt durchgeführt. Wenn der Heizblock auf die gewünschte Temperatur gebracht ist, zieht man den am Haltestift (d) befestigten Griff (e) zurück, wobei sich zuerst der Haltestift (d) fortbewegt bis er am Bügel (g) anschlägt, worauf auch der bewegliche Teil (c) weggezogen wird. Daraufhin führt man die abgedrehte Grafitelektrode mit einer Pinzette von oben in die Bohrung ein und lässt den Griff (e) aus, worauf sich die beweglichen Teile durch den Federdruck in umgekehrter Reihenfolge zurückbewegen. Die Elektrode muss etwa 1 cm über die Oberfläche des Elektrodenhalters herausragen. Nach etwa 1 Min ist die Elektrode auf die gewünschte Temperatur erhitzt, die Probelösung wird aufgetragen, nach dem Eindampfen die Grafitelektrode mit der Pinzette nach oben aus der Bohrung genommen und im Funkenstativ eingespannt. Die Temperatur des Mikro-Universalheizblocks (max. 360–370°C erreichbar) wird durch einen Regelwiderstand mit Hilfe eines in einer seitlichen Bohrung des Heizblockes eingeführten Thermometers so eingestellt, dass die in Tropfen von etwa 5 μl aufgebrachte Probelösung innerhalb von 5–10 Sek ohne zu spritzen verdampft. Bei der beschriebenen Ausführung erwies sich eine Temperatur von 130°C am günstigsten.

Beim Aufbringen von 200 μg Eisen in Form von 20 μl salzsaurer Eisenlösung auf die oben beschriebene Weise konnte nach dem Abfunken und Abbrechen von 5 mm der

Grafitelektrode beim Abfunken der neuen Bruchfläche im Hochspannungsfunken kein Eisen gefunden werden, das von evtl. eingedrungener Probelösung stammmen könnte. Unsere Erfahrungen beziehen sich auf RWI-Grafitelektroden (200 mm lang, 5 mm ϕ, Ringsdorff-Werke, Bad Godesberg-Mehlem), die wir bei unseren Routinearbeiten verwenden.

S. Meyer and O. G. Koch

Hauptlaboratorium der
Neunkircher Eisenwerk A.G.,
Neunkirchen/Saar, Germany

Literatur

[1] Scheibe G. und Rivas A., *Z. angew. Chem.* 1936 **49** 443.
[2] Gorbach G. und Vioque-Pizarro A., *Fette u. Seif.* 1954 **56** 177.
[3] Pohl F. A., *Z. anal. Chem.* 1954 **142** 19.
[4] Koch O. G., *Mikrochem. Acta* 1958 **92** 151.
[5] Gorbach G., *Mikrochemisches Praktikum.* Springer, Berlin, Göttingen, Heidelberg 1956.

The stretching frequency as a function of the interatomic distance in straight hydrogen bonds

(*Received* 2 *January* 1958)

VOL. 12 1958

It is generally accepted that there exists some interdependence between the stretching frequency, the energy and the length of a bond. Several empirical and semi-empirical quantitative relationships have been proposed [1, 2, 3]. Morse [4] stated that for a diatomic molecule the stretching frequency:

$$\nu \simeq \frac{l}{L^3} \tag{1}$$

where l is a constant of about 3000 cm^{-1} $Å^3$ and L is the bond length; this equation can be extended to more complicated molecules. For the bond energy, a similar inverse cube relationship has been proposed [5]:

$$E = \frac{k}{L^3} \tag{2}$$

where k is a constant which depends on the bonded atoms only and not on the type of bond. Obviously the two equations can be combined to give:

$$\nu \simeq \frac{l}{k} E \tag{3}$$

Equations (1) and (3) can be verified by application to the case of the C—H bond in hydrocarbons. In Table 1 the relevant data are assembled. It will be seen that both νL^3 $(= l)$ and ν/E $(= l/k)$ are constant within the experimental error.

Since the Morse constant l varies from 3000 to 4000 for polyatomic molecules, it can be used only for a very rough estimate of the stretching frequency. On the other hand, it can be seen from Table 1 that for the same type of bond l is constant and the stretching frequency can be calculated accurately. This is useful for the case of straight hydrogen bonds X—H···Y where the interatomic distances vary considerably.

Table 1. Interdependence of the energy, distance and stretching frequency of various C—H bonds

Compound	E [5]	L_{C-H} [5]	ν_{C-H}*	νL^3	$\frac{r}{E}$
Methane	98·19	1·093	**3020**	**3943**	**30·8**
Ethane	96·86	1·102	2872	3844	29·7
			2962	**3964**	**30·6**
Ethylene	102·35	1·071	2990	3673	29·2
			3019	3709	29·5
			3108	**3818**	**30·4**
Acetylene	107·05	1·058	**3287**	**3893**	**30·7**
			3374	3996	31·5
Benzene	102·05	1·084	3047	3879	29·8
			3062	3900	30·0
			3099	**3947**	**30·4**

* R. N. Jones and C. Sandorfy, *The Application of Infrared and Raman Spectrometry to the Elucidation of Molecular Structure* in *Chemical Applications of Spectroscopy*. Interscience, New York 1956.

The greatest number of experimental data available are for the O—H···O bridge. The effect of the hydrogen bonding on the O—H stretching frequency is twofold: (1) The equilibrium distance between the hydrogen and oxygen atom is increased. (2) The potential function has a much broader minimum than usual (even after allowing for the first effect).

It is, therefore, not surprising that in this type of bond the stretching frequency is not proportional to the inverse third power of the equilibrium distance l/L^3_{O-H}. If however, this value is reduced by the amount due to the H···O bond $l/L^3_{O\cdots H}$, the calculated results agree surprisingly well with the experimentally determined frequencies.

$$\nu = \frac{l}{L^3_{O-H}} - \frac{l}{L^3_{H\cdots O}} \tag{4}$$

It has been shown elsewhere [6] that for the hydrogen bonded system the following equation also holds:

$$E = \frac{k}{L^3_{O-H}} + \frac{k}{L^3_{H\cdots O}} \tag{5}$$

where E is the total binding energy of the O—H···O system.

From equations (4) and (5)

$$\nu = l\left(\frac{2}{L^3_{O-H}} - \frac{E}{k}\right) \tag{6}$$

E/k has been shown [6] to equal 1·20; only one parameter, the Morse constant l for the

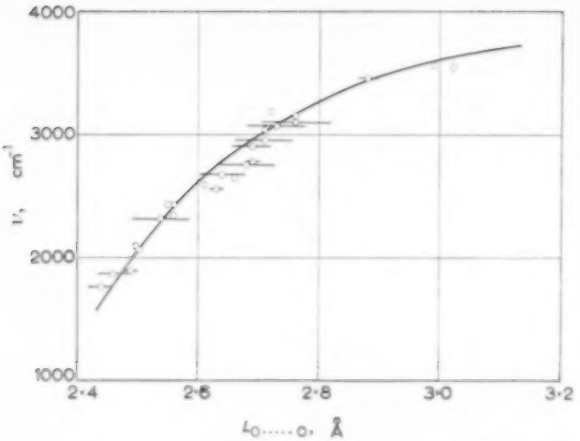

Fig. 1. Comparison of the calculated curve for the stretching frequency with the experimental data.

O—H···O system must be determined. A good fit is obtained when $l = 3750$. This is a very reasonable value when compared with the value obtained for the C—H bond above.

Though L_{O-H} is known in relatively few cases, many data on $L_{O\cdots O}$ have been collected. Using equation (5) and $E/k = 1{\cdot}20$, the value of L_{O-H} corresponding to each value of $L_{O\cdots O}$ has been calculated (Table 2).

Table 2. The O—H distance as a function of the O···O distance in straight O—H··O bonds

$L_{O\cdots O}$	L_{O-H}	$L_{O\cdots O}$	L_{O-H}	$L_{O\cdots O}$	L_{O-H}	$L_{O\cdots O}$	L_{O-H}	$L_{O\cdots O}$	L_{O-H}
2·40	1·105	2·52	1·040	2·64	1·010	2·75	0·994	3·05	0·973
2·42	1·085	2·54	1·034	2·66	1·006	2·80	0·989	3·10	0·971
2·44	1·072	2·56	1·029	2·68	1·003	2·85	0·984	3·15	0·969
2·46	1·062	2·58	1·024	2·70	1·000	2·90	0·981	3·20	0·967
2·48	1·053	2·60	1·019	2·72	0·997	2·95	0·978	3·25	0·965
2·50	1·046	2·62	1·014	2·74	0·995	3·00	0·975	3·30	0·963

Using equation (6) and Table 2 the O—H···O stretching frequencies for a number of compounds have been calculated and compared with the experimentally determined values [2]. The results are plotted in Fig. 1. It will be seen that the agreement is good though only one free parameter has been used.

Extension of this treatment to other straight hydrogen bonds is obvious. Experimental data are however too scarce to test the method.

H. Feilchenfeld

Petrochemistry Laboratory of the Research Council of Israel and the Dept. of Physical Chemistry, Hebrew University, Jerusalem, Israel

VOL. 12 1958

References

[1] Lippincott E. R. and Schroeder R., *J. Chem. Phys.* 1955 **23** 1099.
[2] Nakamoto K., Margoshes M. and Rundle R. E., *J. Amer. Chem. Soc.* 1955 **77** 6480.
[3] Welsh H. K., *J. Chem. Phys.* 1957 **26** 710.
[4] Morse P. M., *Phys. Rev.* 1929 **34** 57.
[5] Feilchenfeld H., *J. Phys. Chem.* 1957 **61** 1133.
[6] Feilchenfeld H., *J. Phys. Chem.* 1958 **62** 117.

L.
2
58

Spectrochimica Acta, 1958, Vol. 12, pp. 284 to 285. Pergamon Press Ltd., London

Book reviews

W. Brügel: **Einführung in die Ultrarot Spektroskopie.** (Zweite ausgabe) Steinkopff, Darmstadt, 1957. 404 S., 48 D.M.

The fact that a second edition of this book has been called for so soon after the appearance of the first is itself an indication of the interest which it has aroused, and the basic pattern of this work will already be familar to many readers of this review. It aims to provide a balanced introduction to all those aspects of infra-red spectroscopy which are of importance to the practising commercial spectroscopist. It begins with a group of seven chapters on basic theory which give a succint account of rotation–vibration spectra in small molecules and provide the groundwork for what is to follow. The second section is devoted wholly to instrumentation and covers topics such as sources, detectors, monochromators, gas analysers etc. and includes a very useful and balanced review of all the commercial spectrometers at present available. The third section deals with applications in structural diagnosis, qualitative and quantitative analysis and the uses of polarization, reflection and microscopic techniques. Documentation of spectra is also discussed and the various types of punched card systems are described and illustrated. Finally there is a group of chapters dealing in more detail with frequency correlations for some selected groups such as the carbonyl, olefinic and aromatic groups, and with the spectra of high polymers and of inorganics. Special applications in hydrogen bonding, rotational isomerism, crystal effects, etc. are also briefly discussed.

It will be seen that the scope of the book is very wide so that the treatment of some of those subjects is necessarily brief. Nevertheless the author has succeeded extremely well in providing a much needed introduction to the subject and sufficient references are given to enable the reader to pursue further any selected topic. A comparison with the earlier edition shows that the revision has been carried out with great care. Some subjects, such as commercial instrumentation, and applications of intensity studies have needed considerable expansion but in general the alterations are usually small but very numerous. Some 200 new references are included and all the important recent advances in the field have been built into the text.

The commercial demand for infra-red spectroscopists has for many years greatly exceeded the supply of graduates trained in research in this field and the need for the basic training of larger numbers is reflected in the growth in the U.S.A. of a number of highly successful summer schools. Nevertheless, until Dr. Brügel's book appeared there was no single text which could be recommended to students seeking an adequate introduction to all aspects of practical infra-red spectroscopy and on this ground alone the appearance of a new edition is very welcome. It is a pity that no similar book is yet available in the English language. The book is well produced and lavishly illustrated. The only serious criticism which can be made of it is the price.

L. J. Bellamy

Francis A. Jenkins and Harvey E. White: **Fundamentals of Optics.** (Third edition) McGraw-Hill, New York, London, Toronto, 1957. 637 pp., $8.50.

The first edition of this book was published in 1937 and since then it has enjoyed wide popularity as a standard text-book for the teaching of optics at the undergraduate level. This has been due to the systematic arrangement of the material which has been fitted into a modern background wherever possible. The second edition included geometrical as well as physical optics and filled the students' need of a single text covering both these subjects. It also included a chapter on "quantum optics" with the object of reconciling the wave properties with the photon character of light.

VOL. 12 1958

The third edition has been prepared in the interest of simplification and further modernization. The notions of wave packet, line width and coherence length are given more prominence because of their importance in quantum mechanics. Brief descriptions of the latest measurements of the velocity of light, developments in multilayer films, the echelle grating, Cerenkov counters etc. are included and references given to fuller accounts of these topics. The 637 pages of the book are only adequate to form an introduction to the subject and it would take another volume of equal length to deal satisfactorily with its many new aspects. The aim of the writers of text-books should be to discard what has become redundant, to preserve what is fundamental and to weld it on to modern concepts and developments. This has been achieved in this book within the limits prescribed by its size. The problems which are appended to each chapter are invaluable as no subject can be absorbed without exercise in its principles.

W. C. Price

F. Burriel-Martí and J. Ramírez-Muñoz: **Flame Photometry (A manual of methods and applications)**. First Edition, Elsevier, Amsterdam, London, New York and Princeton, 1957 531 pp. 99 diagrams, 65 s.

Despite the considerable popularity of the flame photometric method of analysis, few systematic discussions of this field have appeared. This is the first full length treatise on the subject in English, being a translation from the original Spanish. The principal portions of the text are concerned with instrumentation, both commercial and non-commercial, the possibilities and limitations of the method, experimental techniques, and a number of particular applications.

This work will be of special value to those with little or no experience in flame photometry. Large portions of the volume are devoted to practical information on such subjects as preparation of samples and standards, prediction of interferences, calculation of results, and instrument maintenance. The information is presented in sufficient detail to enable a novice to gain a reasonably good understanding of flame photometric techniques.

More than 100 pages of the text are concerned with particular applications. This section will be useful even for experienced workers because of the thorough consideration of methods which may be unfamiliar to the particular reader. The same information is, of course, available in the original papers, but it is helpful to have it collected for ready reference.

Several important sections of the book are difficult to read. The sentence structure is often so complex that certain paragraphs may have to be re-read several times before the meaning is clear. In addition, the authors use an unusual and complex system of notation that often seems to confuse more than to clarify. For example, the following sentence appears on p. 219: "Where $pL_L > pD - 2$, the useful range will be less than the previous (L_u to $L_u/10$) and reduced to L_u to L_u/n, where n fulfils the condition $1 < n < 10$." The context of this sentence could probably be expressed more clearly in less mathematical terms. There is also an exceptionally large number of footnotes, so that the continuity of the discussion is often impaired. Very few typographic or factual errors were found.

A valuable portion of this work is an extensive bibliography of more than 900 references. This is keyed to the text and to the subject index, so that pertinent papers in a particular field may be quickly located.

M. Margoshes

Spectrochimica Acta, 1958, Vol. 12, pp. 286 to 287. Pergamon Press Ltd., London

Papers to be published in future issues

M. C. DE WILDE-DELVAUX et P. L. TEYSSIE: Étude spectrographique infra-rouge de quelques β-dicetones

G. PORTER and E. STRACHAN: The electronic spectra of benzyl

C. GARRIGOU-LAGRANGE, J. M. LEBAS et M. L. JOSIEN: Étude comparée des spectres de vibration des dérivés paradisubstitués du benzène—I. Région 670–1600 cm^{-1}

A. L. BLUHM: The infrared spectra and the structure of some homophthalimides

F. A. MILLER and R. B. HANNAN: The ultraviolet absorption spectrum of dicyano-acetylene

R. N. KNISELEY, V. A. FASSEL, B. B. QUINNEY, C. TREMMEL, W. A. GORDON and W. J. HAYLES: Quantitative spectrographic analysis of the rare earth elements—IX

D. F. HORNIG, H. F. WHITE and F. P. REDING: The infrared spectra of crystalline H_2O, D_2O and HDO

M. TSUBOI, T. SHIMANOUCHI and S. MIZUSHIMA: Analysis of P and R branches of the 950 cm^{-1} band of $N^{14}H_3$

A. YAMAGUCHI, I. ICHISHIMA and S. MIZUSHIMA: Polarization of the reflected infrared radiation from an echelette grating

D. C. MCKEAN: Force constants, interbond angle and solid state spectrum of disiloxane

R. ANDRISANO and G. PAPPALARDO: Absorption spectra in the near ultra-violet of some α- and β-monosubstituted derivatives of thiophene

B. BAK and D. CHRISTENSEN: Infrared absorption spectra of deuterated vinyl fluorides

O. BOTSCHKOWA, T. FRISCH und E. SCHREIDER: Quantitative Spektralanalyse von Gasgemischen

P. T. GILBERT: Determination of indium by flame photometry

D. B. POWELL and N. SHEPPARD: Infrared spectra and vibrational frequencies of co-ordinated ethylene

H. BEVAN, S. V. DAWES and R. A. FORD: The electronic spectra of titanium dioxide

F. MEDA: Infrared absorption spectra of α-halogenated keto-steroids

L. J. BELLAMY: The origin of group frequency shifts—I. Abnormal frequencies in multiple bonds

F. F. BENTLEY, E. F. WOLFARTH, N. E. SRP and W. R. POWELL: Analytical applications of far infrared spectra—I. Historical review, apparatus and technique

S. MIZUSHIMA, I. NAKAGAWA, M. J. SCHMELZ, C. CURRAN and J. V. QUAGLIANO: Infra-red absorption spectra of inorganic co-ordination complexes—XVII

T. P. SCHREIBER and D. L. FRY: Spectral character as a function of spark source parameters

A. MIYAKE, I. NAKAGAWA, T. MIYAZAWA, I. ICHISHIMA, T. SHIMANOUCHI and S. MIZUSHIMA: Infrared and raman spectra of dichloroacetyl chloride in relation to rotational isomerism

P. TARTE: Réchérches sur les frequences de déformation OH—I. Spectra infra-rouge des sels basiques de cuivre

D. A. SINCLAIR and R. N. WHITTEM: Apparent rectification in tesla sparks

A. DANTI and R. C. LORD: Rotational analysis and upper-stage transitions of parallel absorption bands in benzene, Sym-benzene-d_3, benzene-d_6 and pyridine

B. BAK, D. CHRISTENSEN, L. HANSEN-NYGAARD and J. RASTRUP-ANDERSEN: The structure of vinyl fluoride

H. STAMMREICH, D. BASSI, O. SALA and H. SIEBERT: The vibrational spectrum of the dichromate ion

VOL. 12 1958

Papers to be published in future issues

D. M. Shaw, O. Wickremasinghe and C. Yip: A simple device for the spectrochemical analysis of minerals in an inert atmosphere using the Stallwood jet

A. D. E. Pullin: The variation of infrared vibration frequencies with solvent

E. A. V. Ebsworth, J. R. Hall, M. J. MacKillop, D. C. McKean, N. Sheppard and L. A. Woodward: Vibrational spectra and structure of trisilylamine and trisilylamine-d_9

E. A. V. Ebsworth and N. Sheppard: The infra-red spectra of some methylammonium iodides: angle deformation frequencies of $\overset{+}{N}H$ and $\overset{+}{N}H_2$ groups

K. Laqua and U. Luoto: Ein thyratrongesteuertes Schaltgerät für Wechselstromabreissbögen

G. L. Caldow and H. W. Thompson: Vibrational bands of isothiocyanates, thiocyanates and isocyanates

J. P. Jesson and H. W. Thompson: Vibrational band intensities of the C≡N group in aliphatic nitriles

P. E. B. Butler, D. R. Eaton and H. W. Thompson: Vibration–rotation bands of keten

H. W. Thompson and D. A. Jameson: Vibrational frequency and band intensity of the carbonyl group

PUBLISHER'S NOTICE

THE publishers regret that owing to an oversight it was not made clear that the *Proceedings of the Colloquium Spectroscopicum Internationale VI, Amsterdam, May 1956*, which was supplied to subscribers as part of their 1957 subscription, was intended as Volume XI of *Spectrochimica Acta*. The publishers wish to apologise for any inconvenience caused by this oversight. In order to avoid any further confusion in libraries, etc., a sticker is enclosed which may be affixed to the spine of the *Proceedings* volume.

VOL.
12
1958

Spectrochimica Acta, 1958, Vol. 12, pp. 289 to 293. Pergamon Press Ltd., London

Etude spectrographique infra-rouge de quelques β-dicétones

M. C. DE WILDE-DELVAUX et PH. TEYSSIÉ*
Laboratoire de Chimie Macromoléculaire, Université de Louvain, Belgique

(*Received* 24 *February* 1958)

Abstract—The infra-red spectra, in the region 1800–1500 cm^{-1} of some new β-diketones (methacroylacetone and its polymer, 2:heptyl-, 2:heptyl-4:methyl-, 2:pentyl- and 4:methylcyclohexane-1:3-dione) are discussed and compared to acetylacetone. The keto–enol equilibrium is a function of the polarity of the solvent; for the derivatives of *cyclo*hexane-1:3-dione it is a function of dilution, indicating that the hydrogen bonds are intermolecular. The C=O band of the ketonic form is nearly always double.

Introduction

PLUSIEURS études des spectres infra-rouges de β-dicétones et surtout de leurs complexes métalliques ont paru ces dernières années, notamment de l'acétylacétone et de ses complexes, du benzoylméthane, de la benzoylacétone et de quelques-uns de leurs complexes, de différentes β-dicétones fluorées, etc. [1–7]. Mais les différentes données ne concordent pas toujours, les auteurs utilisant tantôt des solutions, tantôt les produits à l'état solide.

Tout récemment, HOLTZCLAW et COLLMAN [8], ont présenté une nouvelle étude spectrométrique sur une série de β-dicétones et de leurs complexes métalliques. Ils les ont examinés en suspension dans l'huile de paraffine et quelques uns à l'état pur.

Nous nous proposons de compléter et de confirmer certaines de leurs observations en étudiant, dans divers solvants, quelques nouvelles β-dicétones récemment synthétisées dans ce laboratoire [9]: la méthacroylacétone et son polymère, quelques dérivés de la *cyclo*hexane-1:3-dione et certains de leurs complexes. L'acétylacétone a été utilisée comme substance de référence.

La région spectrale particulièrement étudiée pour les β-dicétones, est celle de la double liaison (C=O et C=C), où la chélation entraîne des perturbations importantes; celle-ci diminue le caractère de double liaison du groupe carbonyle et du groupe C=C, et provoque ainsi d'importants glissements de fréquence des bandes d'absorption:

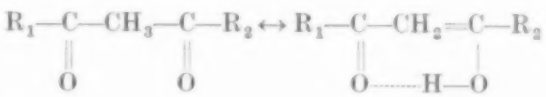

Acétylacétone

Le spectre de l'acétylacétone a déjà été décrit et discuté à plusieurs reprises. Il est cependant intéressant de mentionner ici un fait négligé par de nombreux auteurs, mais rapporté par MECKE et FUNCK [10] dans une intéressante étude sur l'acétylacétone, et observé indépendamment par nous: la présence de deux bandes

* Nouvelle adresse: Département de Chimie, Université Lovanium, BP 2158, Léopoldville, Congo Belge.

d'absorption, à 1705 et 1727 cm^{-1}, au lieu d'une dans la région C=O. Elles sont attribuables aux deux groupes carbonyles de la forme cétonique; un doublet analogue se retrouve en effet dans le spectre du malonate d'éthyle, à 1737 et 1754 cm^{-1}, et résulte de l'interaction entre les deux groupes C=O attachés au même carbone.

Ces deux bandes sont très faibles dans le spectre de l'acétylacétone en solution dans le tétrachlorure de carbone, mais deviennent de plus en plus importantes dans les spectres des solutions chloroformique et dioxanique et le spectre du liquide pur; la bande carbonyle, à 1610 cm^{-1} de la forme énolique varie en sens inverse, indiquant un déplacement de l'équilibre céto–énolique sous l'influence de la polarité du milieu. MECKE et FUNCK obtiennent des résultats analogues en utilisant l'hexane n ($\pm$90% énol) et l'acétonitrile ($\pm$45% énol) comme solvants. A l'état solide (−30°C) ils observent la disparition totale de la forme cétonique. HOLTZCLAW et COLLMAN [8] mentionnent également ces deux bandes pour diverses β-dicétones à l'état liquide ou solide.

Pour le sel cuivrique de l'acétylacétone, il importe de signaler que dans le spectre de la solution chloroformique, la bande carbonyle perturbée, à 1580 cm^{-1}, semble double: elle présente un coude imparfaitement résolu vers 1570 cm^{-1}. Par contre, dans le spectre de la solution dioxanique, la bande est simple. La seconde bande caractéristique des chélates métalliques, attribuée à la double liaison perturbée, à 1530 cm^{-1} est normale.

VOL. 12 1958

Méthacroylacétone et son polymère

La double liaison vinylique conjuguée à l'un des groupes carbonyles dans la méthacroylacétone

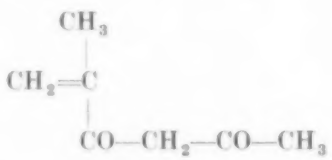

entraîne évidemment quelques perturbations dans le spectre de l'acétylacétone.

Les spectres du liquide pur, et des solutions dioxaniques et chloroformiques sont pratiquement identiques. Les deux bandes C=O de la forme cétonique sont plus éloignées l'une de l'autre et se situent à 1720 et 1667 cm^{-1}, cette dernière étant attribuée au groupe C=O conjugué à la double liaison.

La bande vinylique elle-même apparaît à 1633 cm^{-1} et la bande C=O du céto–énol se situe à 1583 cm^{-1}.

Dans le spectre de la solution dans le tétrachlorure de carbone, les deux bandes carbonyles de la forme cétonique sont très faibles, indiquant une énolisation presque complète. La bande céto–énol présente un coude vers 1610 cm^{-1}, attribuable très probablement à la double liaison de l'énol. Dans les autres cas, cette bande n'est pas séparée de la bande céto–énol, qui est assez large.

Tous les spectres présentent une bande assez large vers 1435 cm^{-1}, que Lecomte attribue au C—O de l'énol. On la retrouve également vers 1415 cm^{-1} dans l'acétylacétone.

Dans le polymère correspondant, l'action perturbatrice de la double liaison disparaît et le groupe carbonyle de l'énol se situe à nouveau vers 1605 cm^{-1}, la bande étant fort évasée. L'énolisation est très poussée, les bandes C=O de la forme cétonique, à 1693 et 1720 cm^{-1} étant très faibles, aussi bien pour une solution dans le dioxane que pour une solution chloroformique (le polymère est insoluble dans le CCl_4).

Les deux bandes (C=O et C=C perturbées) du complexe cuivrique du monomère et du polymère se situent vers 1570 et 1517 cm^{-1}. Le spectre du complexe cuivrique du monomère, en solution dans le tétrachlorure de carbone, présente un doublet à 1560 et 1570 cm^{-1}.

Il faut remarquer que le spectre du complexe cuivrique du polymère présente encore de faibles bandes C=O cétonique et céto–énol. Ce complexe contient, en effet, de faibles quantités de fonctions non complexées, dont la teneur a été évaluée à 3% au départ d'un dosage de cuivre.

Dérivés de la cyclohexane-1:3-dione

Les dérivés de la *cyclo*hexane-1:3-dione, soit le 2:heptyl (I), le 2:heptyl-4:méthyl (II), le 2:pentyl(III) et le 4:méthyl (IV) ont été obtenus par condensation de méthylalcoylcétones sur des esters acryliques ou méthacryliques. Leur comportement spectrographique est pratiquement identique à celui de la 5:5-diméthyl-*cyclo*hexane-1:3-dione ou dimédon(V) dont le spectre est décrit par Rasmussen et ses collaborateurs et par Bellamy et Beecher [1,5]:

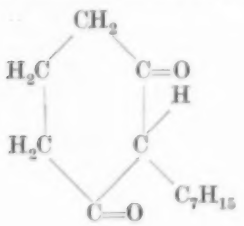

(I)

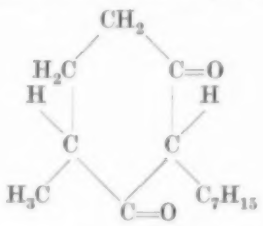

(II)

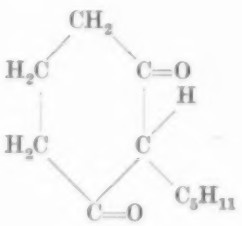

(III)

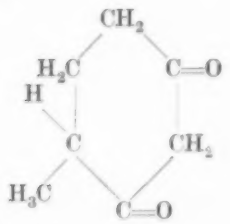

(IV)

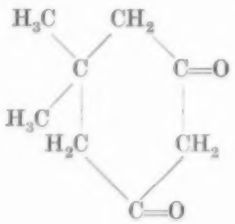

(V)

Les spectres de tous ces dérivés présentent de fortes bandes d'absorption à 1733, 1707 et 1603 cm^{-1} pour les solutions chloroformiques, et à 1737, 1715 et 1597 cm^{-1} pour les solutions dans le tétrachlorure de carbone. On trouve des maxima d'absorption à 1732, 1710, 1645 et 1609 cm^{-1} dans les spectres des solutions dans le dioxane.

BELLAMY et BEECHER attribuaient la bande vers 1706 cm^{-1} du dimédon au C=O du céto–énol libre (unchelated enol); nous préférons l'attribuer, avec la bande à 1733 cm^{-1}, de même que celles des dérivés précités, aux deux groupes C=O de la forme cétonique, par analogie avec l'acétylacétone et autres β-dicétones linéaires.

L'intensité de ces deux bandes augmente avec la dilution, tandis que celle du C=O céto–énol, vers 1600 cm^{-1}, diminue, ce qui indique un notable déplacement de l'équilibre énolique en faveur de la forme cétonique. Par contre, les deux bandes cétoniques ont complètement disparu dans le spectre du dimédon à l'état solide. Ceci n'est possible que dans le cas de ponts hydrogènes intermoléculaires: des effets stériques empêchent en effet les liaisons intramoléculaires de se former dans tous les dérivés de la *cyclo*hexane-1:3-dione.

Dans le cas de l'acétylacétone et autres β-dicétones, où les ponts hydrogènes sont intramoléculaires, les bandes ne varient pas avec la dilution, mais uniquement avec la nature du solvant.

Dans le spectre des solutions dans le tétrachlorure de carbone, la double liaison de l'énol apparaît à nouveau comme un coude assez marqué vers 1617 cm^{-1} de la bande C=O énol à 1603 cm^{-1}.

La bande à 1645 cm^{-1}, qui apparaît dans les spectres des solutions dioxaniques, peut sans doute être attribuée au groupe C=O du céto–énol libre, dont parle BELLAMY. Il est d'ailleurs vraisemblable que cet énol n'apparaisse libre que dans des solvants tels que le dioxane. Ce comportement est comparable à celui des acides carboxyliques, dont le spectre en solution dioxanique indique également une forme monomère non-associée.

Le spectre du dimédon à l'état solide présente encore dans la même région deux bandes d'absorption supplémentaires, à 1580 et 1520 cm^{-1}. On retrouve ces deux bandes dans le spectre d'une solution saturée dans le dioxane, où des cristaux de dimédon se sont formés; elles disparaissent par chauffage ou dilution de la solution. La fréquence d'absorption de ces deux bandes correspond exactement à celle d'un complexe métallique. La disposition spatiale du dimédon à l'état cristallin correspond donc vraisemblablement à la structure cristalline des complexes métalliques créant une modification semblable du caractère non saturé du groupe carbonyle.

Conclusions

Des observations précédentes on peut conclure quelques règles valables pour les dicétones en général:

(1) La bande C=O de la forme cétonique est presque toujours double, eu égard à l'interaction des deux groupes C=O attachés au même carbone.

(2) La bande d'absorption de la double liaison du céto–énol est généralement confondue avec celle du groupe carbonyle de céto–énol, vers 1600 cm^{-1}, qui est large et intense. En solution diluée dans le tétrachlorure de carbone, elle peut apparaître comme un coude de la bande principale.

(3) Dans le cas spécial de dérivés de la *cyclo*hexane-1:3-dione, les liaisons hydrogène sont intermoléculaires. Pour des solutions dioxaniques, une bande apparaît à 1645 cm^{-1} qui peut être attribuée au C=O de l'énol libre.

VOL. 12 1958

Partie expérimentale

Les spectres ont été enregistrés au spectromètre infra-rouge à double faisceau Perkin-Elmer, modèle 21. Les composés ont été étudiés en solution de 5 et de 0·5% dans le tétrachlorure de carbone, le chloroforme et le dioxane, et dans certains cas, à l'état liquide ou à l'état solide, en suspension dans l'huile de paraffine. Le spectre du malonate d'éthyle a été obtenu à grande résolution. La synthèse des nouvelles β-dicétones étudiées ici est décrite par TEYSSIÉ et SMETS [9].

Résumé

Quelques nouvelles β-dicétones, soit la méthacroylacétone et son polymère, la 2:heptyl-, la 2:heptyl-4-méthyl-, la 2:pentyl- et la 2-méthyl-*cyclo*hexane-1:3-dione et certains de leurs complexes métalliques ont été étudiées spectrographiquement dans la région 1800–1500 cm^{-1} et comparées à l'acétylacétone. L'équilibre céto–énol est fonction de la polarité du solvant; pour les dérivés de la *cyclo*hexane-1:3-dione, elle est fonction de la dilution, indiquant ainsi que les liaisons hydrogènes sont intermoléculaires.

La bande C=O de la forme cétonique est presque toujours double.

Acknowledgements—Les auteurs remercient l'Union Minière du Haut Katanga pour les subsides accordés au laboratoire, de même que le Professeur G. SMETS pour les nombreuses discussions.

Bibliographie

[1] RASMUSSEN R. S., TUNNICLIFF D. D. et BRATTAIN R. R., *J. Amer. Chem. Soc.* 1949 **71** 1068.
[2] DUVAL C., FREYMANN R. et LECOMTE J., *Bull. Soc. Chim.* 1952 **19** 106.
[3] PARK J. D., BROWN H. A. et LACHER J. R., *J. Amer. Chem. Soc.* 1953 **75** 4753.
[4] BELLAMY L. J., SPICER G. S. et STRICKLAND J. D. H., *J. Chem. Soc.* 1952 4653.
[5] BELLAMY L. J. et BEECHER L., *J. Chem. Soc.* 1954 4487.
[6] BELLAMY L. J. et BRANCH R. F., *J. Chem. Soc.* 1954 4491.
[7] BRATOZ S., HADZI D. et ROSSMY G., *Trans. Faraday Soc.* 1956 **52** 464.
[8] HOLTZCLAW H. F. JR. et COLLMAN J. P., *J. Amer. Chem. Soc.* 1957 **79** 3318.
[9] TEYSSIE P. et SMETS G., *J. Amer. Chem. Soc.* In press.
[10] MECKE R. et FUNCK E., *Z. Elektrochem.* 1956 **60** 1124.

Spectrochimica Acta, 1958, Vol. 12, pp. 294 to 298. Pergamon Press Ltd., London

Polarization of the reflected infrared radiation from an echelette grating

A. YAMAGUCHI, I. ICHISHIMA and S. MIZUSHIMA
Chemical Laboratory, Faculty of Science, Tokyo University, Hongo, Tokyo, Japan

(*Received* 17 *March* 1958)

Abstract—Intensity ratio of the two components of the reflected infrared radiation was measured with the Perkin–Elmer 112G instrument, one component being polarized parallel to the grooves of the grating and the other perpendicular to them. The ratio was found to depend considerably on the direction of the incident beam with respect to the surface of the grating and to be quite different from that obtained in a similar measurement with prism spectrometer.

Introduction

THE absorption of polarized infrared radiation has been measured by many investigators in order to study the structure of single crystals or oriented high polymers. Remarks on several sources of error have been made for prism spectrophotometers, [1, 2]. However, no dichroic measurement by use of a grating spectrophotometer has been reported.

Recently MEECHAM *et al.* [3, 4] theoretically treated the reflection of radiation from the surface of an echelette grating, and proved the result to be in agreement with that obtained experimentally in the microwave region. However, they did not report the dependence of the intensity of diffracted light upon the direction of the polarization of the initial radiation.

In the present investigation the dependence was studied using Perkin–Elmer 112G echelette grating spectrophotometer. The result was found to be quite different from that for a prism spectrophotometer.

Imperfection of a new type polarizer

When an infrared beam passes through a normal transmission polarizer consisting of a pile of several plates of silver chloride, an appreciable displacement of the beam arises from the refraction on each surface of the plates. When the polarizer is placed in such a way as the electric vector of the polarized beam is perpendicular to the length of the slit, the intensity of the transmitted beam may amount only to 15 per cent of that of the incident beam. In order to avoid this disadvantage, a polarizer consisting of six plates of silver chloride of 0·2 mm thickness were constructed as shown in Fig. 1.

This polarizer can be used at the same position as the normal one without losing the intensity of the beam. The imperfection of the polarization of the transmitted beam was measured by the method to be described in the next paragraph.

As shown in Fig. 2, the imperfection depends on frequency, but the value is less than 0·067 reported by CHARNEY for six plate polarizer of normal type [1]. This value is reasonable, because it is not much different from the square of 0·19, which is the imperfection for the three plate polarizer.

VOL.
12
1958

Polarization of the reflected radiation from an echelette grating

Perkin–Elmer 112G grating spectrophotometer consists of a KBr fore-prism and a 75 line/mm echelette grating blazed at 12 μ as shown in Figs. 3 and 4. The blaze angle is 26° 45′. The polarizer was placed between the light source unit and fore-prism unit. The intensity of the polarized beam transmitted by the spectrophotometer was measured at constant slit width in two cases where the

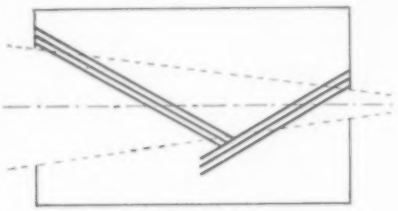

Fig. 1. Polarizer.

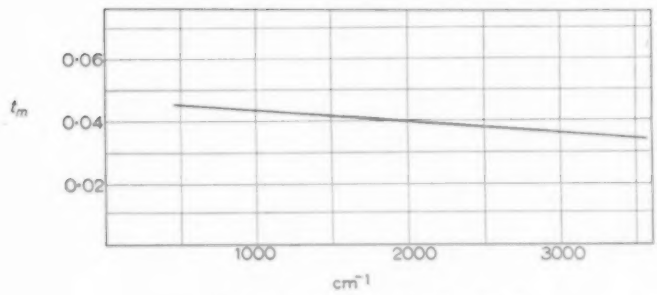

Fig. 2. Imperfection of the polarizer.

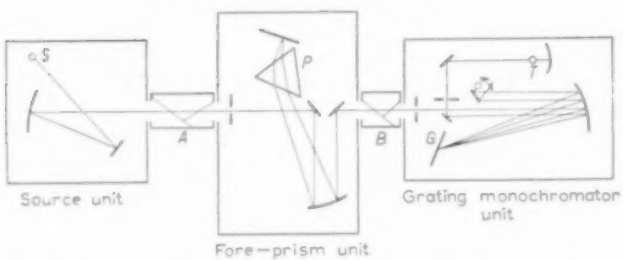

Fig. 3. Perkin–Elmer 112G fore prism-grating spectrophotometer. *S*, light source; *P*, prism; *G*, echelette grating; *T*, thermocouple detector; *A*, polarizer *A*; *B*, polarizer *B*.

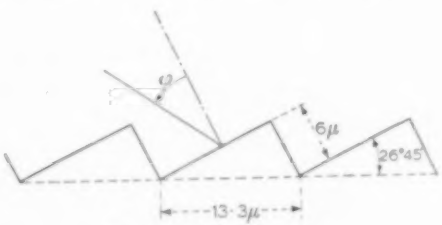

Fig. 4. Echelette grating.

direction of polarization is parallel and perpendicular to the length of the slit as shown in Fig. 5.

The intensity depends on the reflection from the surface of the grating, the prism and mirrors of the spectrophotometer, and on the absorption by the polarizer, sensitivity of the detector and also on the intensity of the light source. Except for the reflection on the surfaces, the effect on the transmitted intensity does not depend on the direction of the polarization of the incident radiation. As the reflection from the surface of a mirror cannot be considered to depend so much on

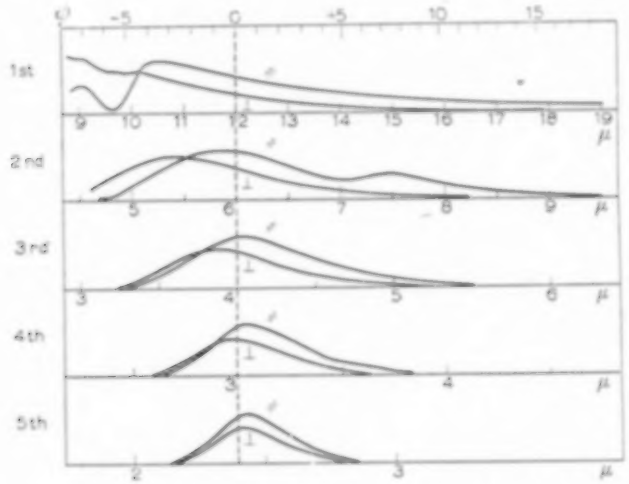

Fig. 5. Intensity distribution of the polarized beam transmitted by the spectrophotometer. ∥: Electric vector is parallel to the length of the slit; ⊥: Electric vector is perpendicular to the length of the slit.

the direction of the polarization, the difference between the two cases described above mainly arises from the reflection on the surface of the prism and the grating.

Furthermore, some anormalies in the intensity of the reflected beam were observed, when the incident ray is polarized in the direction perpendicular to the length of the slit. In the first order diffraction a pronounced anormaly appears at 9·7 μ, where the grating is rotated by $-5°$ from the normal to the blazed surface. In the second order diffraction less pronounced anormaly is observed at 7 μ, where the grating is rotated by $5°$.

Ratio of the transmittance of the polarized radiation

First let us put a polarizer A between the light source unit and the fore-prism unit. Let the intensity of the incident unpolarized beam be I_0, and that of the partially polarized beam transmitted by the polarizer by I. This consists of two components I_1 and I_2. The component I_2, whose electric vector is perpendicular to that of I_1, is due to the imperfection of the polarizer.

Let t_m be the transmission coefficient of the polarizer for the component I_2,

VOL. 12 1958

and γ_m be the reduction factor of the polarizer, then we have:

$$I = I_1 + I_2 \tag{1}$$

$$I_1 = \tfrac{1}{2}\gamma_m I_0 \tag{2}$$

$$I_2 = \tfrac{1}{2}\gamma_m I_0 t_m \tag{3}$$

t_m is a measure of the imperfection of the polarizer.

Furthermore, let $t_\parallel$ and $t_\perp$ be the transmission coefficients of the spectrophotometer for the polarized beam, whose electric vectors are parallel and perpendicular to the length of the slit, respectively, and θ be the angle formed by the electric vector of I_1 and the length of the slit, then the intensity of the beam transmitted by the polarizer and the spectrophotometer are given by:

$$I(\theta) = \tfrac{1}{2}\gamma_m I_0\{(t_\perp + t_\parallel t_m)\sin^2\theta + (t_\parallel + t_\perp t_m)\cos^2\theta\} \tag{4}$$

The intensity of the transmitted light for $\theta = 0°$ and $90°$ is, therefore, expressed as:

$$I(0°) = \tfrac{1}{2}\gamma_m I_0(t_\parallel + t_\perp t_m) \tag{5}$$

$$I(90°) = \tfrac{1}{2}\gamma_m I_0(t_\perp + t_\parallel t_m) \tag{6}$$

Next let us put a polarizer A between the light source unit and the fore-prism unit and another polarizer B between the fore-prism unit and the grating unit, the direction of the polarization of the latter polarizer being perpendicular to the length of the slit. The intensity $I'(\theta)$ of the transmitted beam was measured by rotating the former polarizer. We have the following relations (7), (8) and (9), corresponding to the previous relations (4), (5) and (6) previously obtained:

$$I'(\theta) = \tfrac{1}{2}\gamma_m{}^2 I_0\{(t_\perp + t_\parallel t_m{}^2)\sin^2\theta + (t_\perp + t_\parallel)t_m\cos^2\theta\} \tag{7}$$

$$I'(0°) = \tfrac{1}{2}\gamma_m{}^2 I_0(t_\perp + t_\parallel)t_m \tag{8}$$

$$I'(90°) = \tfrac{1}{2}\gamma_m{}^2 I_0(t_\perp + t_\parallel t_m{}^2) \tag{9}$$

The ratio $t_\parallel/t_\perp$ of the transmission coefficients of the spectrophotometer is obtained as:

$$t_\parallel/t_\perp = \frac{A - t_m}{1 - At_m}$$

from equations (5) and (6) and as:

$$t_\parallel/t_\perp = \frac{B - t_m}{t_m(1 - Bt_m)}$$

from equations (8) and (9).

Here $A = I(0°)/I(90°)$ and $B = I'(0°)/I'(90°)$.

The intensities $I(0°)$, $I(90°)$, $I'(0°)$ and $I'(90°)$ were measured in the frequency region from 550 to 5000 cm^{-1}. The values of $t_\parallel/t_\perp$ and t_m were obtained as shown in Figs. 6 and 2. The observed ratio $t_\parallel/t_\perp$ includes the part due to the reflection on the surface of the prism. Therefore this part must be removed from the observed value in order to obtain the ratio due to the grating alone. This part or the ratio $(t_\parallel/t_\perp)_p$ for KBr prism alone was determined independently and was found to be 0·73 to 0·70 in the frequency region from 500 to 1100 cm^{-1}. That for NaCl prism was found to be 0·70 to 0·66 in the region from 750 to 1750 cm^{-1}.

The ratio $(t_\parallel/t_\perp)_g$ for the grating obtained by correcting the observed ratio in this way was found quite different from that obtained in the case of a prism spectrophotometer.

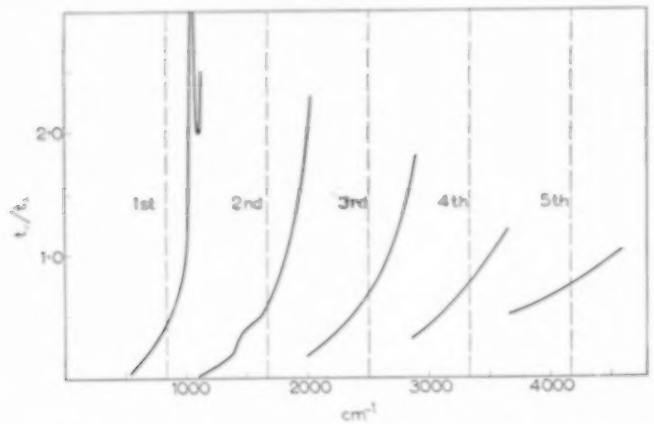

Fig. 6. Ratio of the transmission coefficients of the spectrophotometer for the polarized beam. Dotted lines indicate the frequencies at the brazed angle.

Results

From the results of our measurement, it is apparent that the intensity of the reflected beam from the surface of the grating depends considerably on the direction of the polarization of the incident beam. When the angle ϕ formed by the direction of the beam and the normal to the blazed surface of the grating is large, the ratio $t_\parallel/t_\perp$ becomes very small and is less than 0·1. However, the ratio becomes larger with decreasing ϕ and is almost equal to 1 for $\phi = 0°$. For the negative values of ϕ, the ratio becomes greater than 1 and increases rapidly. The ratio at the same value of ϕ becomes larger for the higher order diffraction, for which the wavelength becomes shorter as compared with the distance between the rulings.

The information obtained by us for the grating is very useful for the study of dichroism by the grating spectrophotometer. Even if the unpolarized beam is used for the absorption measurement of a crystal or an oriented film, the absorption intensity will depend considerably on the orientation of the sample. This should be borne in mind for the intensity measurement with a grating spectrophotometer.

References

[1] Charney E., *J. Opt. Soc. Amer.* 1955 **45** 980.

[2] Eliott A., Ambrose E. J. and Temple R., *J. Opt. Soc. Amer.* 1948 **38** 212; Newman R. and Halford R. S., *Rev. Sci. Instrum.* 1948 **19** 270; Hyde W. L., *J. Opt. Soc. Amer.* 1948 **38** 663; Šimon I., *J. Opt. Soc. Amer.* 1951 **41** 336; Frazer R. D. B., *J. Chem. Phys.* 1953 **21** 1511.

[3] Meecham W. C., *J. Appl. Phys.* 1956 **27** 361; Meecham W. C. and Peters C. W., *J. Appl. Phys.* 1957 **28** 216.

[4] Stamm R. F. and Whalen J. J., *J. Opt. Soc. Amer.* 1946 **36** 2; Hatcher R. D. and Rohrbaugh J. H., *J. Opt. Soc. Amer.* 1956 **46** 104.

VOL. 12 1958

Spectrochimica Acta, 1958, Vol. 12, pp. 299 to 304. Pergamon Press Ltd., London.

The electronic spectra of benzyl

G. Porter
Department of Chemistry, University of Sheffield

and

Emma Strachan
British Rayon Research Association

(*Received* 7 *March* 1958)

Abstract—Studies of spectra of the photolysis products of toluene and related molecules in low temperature rigid glasses have confirmed the assignment of the 3053 Å system to benzyl. A new absorption system has been observed, with maximum at 4527 Å. The two absorption systems are in excellent agreement with recent molecular orbital calculations and with emission spectra previously assigned to this radical.

Information concerning the electronic spectra of benzyl is now available from three sources:

(1) Emission spectra obtained by Schuler and collaborators [1] and by Walker and Barrow [2] in mild electrical discharges through mixtures of aromatic vapours and inert gases.

(2) Absorption spectra obtained by Porter and Wright [3] following flash photolysis of aromatic vapours, by Porter and Windsor [4] following flash photolysis of aromatic molecules in solution and by Norman and Porter [5] by photolysis of rigid solutions at low temperatures.

(3) Theoretical calculations of Dewar, Longuet-Higgins, Pople [6, 7] and of Bingle [8].

The emission spectra lie in the region of 4477 Å whilst the absorption spectra have maxima at 3053 Å, 3178 Å and 3187 Å in the gas phase, in paraffin solution at room temperature and in rigid E.P.A. glass at −197°C respectively. These findings may be explained in three ways:

(1) The emission or the absorption or both spectra have been incorrectly assigned to benzyl.

(2) Owing to operation of the Franck-Condon principle the spectra, although of the same electronic transition, are widely separated in emission and absorption. This is very improbable in view of the small number of bands and the clear evidence of progression limits.

(3) Both spectra are due to benzyl but they correspond to separate electronic transitions.

Schuler and Michel [9] have recently supported the third of these possibilities and here we present new data which confirm this interpretation.

Assignment of spectra to benzyl

We have repeated and extended the measurements of Norman and Porter on the spectra of the products of photochemical dissociation of aromatic molecules

in rigid glasses using, in the first place, identical techniques. Our results leave no doubt that the 3187 Å system is to be assigned to the benzyl radical. Some of our earlier results were used by PORTER and WRIGHT in making this assignment and further details of our measurements will be published shortly. For the present purpose it is sufficient to note two confirmations of this assignment which we have obtained in addition to that which is referred to by PORTER and WRIGHT.

(1) The series toluene, ethyl benzene, *iso*propyl benzene and *tert*-butyl benzene give radical spectra in E.P.A. which are almost identical in structure. Taking into account the energetic limitations the only possible assignments are as follows:

Molecule	λ_{max} of radical (Å)	Radical
ϕCH_3	3187	ϕCH_2
ϕCH_2CH_3	3222	$\phi CHCH_3$
$\phi CH(CH_3)_2$	3242	$\phi(CH_3)_2$
$\phi C(CH_3)_3$	3242	$\phi(CH_3)_2$

(2) The series toluene, diphenyl methane (and benzhydrol) and triphenyl methane give radical spectra with similar structure with maxima as follows:

Molecule	λ_{max} of radical	Radical
ϕCH_3	3187	ϕCH_2
ϕCH_2 (and $\phi_2 CHOH$)	3355	$\phi_2 CH$
$\phi_3 CH$	3415	$\phi_3 C$

The assignments given are the only self-consistent set and here, in addition, one of the radical spectra, that of triphenyl methyl, is already well established, indeed it was the first free radical to be detected and the first recorded radical spectrum. The 3187 Å system must therefore be considered established as part of the benzyl spectrum and in view of the experimental conditions the transition must involve the ground state.

The assignment of the 4477 Å emission system to benzyl is less certain owing to the complexity of excitation conditions in the gaseous discharge. It has been assigned to other species by WALKER and BARROW and also by SCHÜLER and his collaborators, although SCHÜLER and MICHEL have recently supported the assignment to benzyl. They pointed out that this assignment was not necessarily inconsistent with the fact that the absorption system appears at much shorter wavelengths. It is well known from fluorescence studies that the emission spectra of polyatomic molecules consist almost exclusively of combinations between the lowest excited state and the ground state. Furthermore, if the transition probability of this system is low, it may be much weaker in absorption than transitions to higher levels so that the lower transition would appear only in emission and the

VOL. 12 1958

upper system only in absorption. Evidence that benzyl has two transitions in the region investigated, the lower of which has low transition probability, is derived from two sources; first from analogy with the well-known spectra of the related radical triphenyl methyl, which shows a weak visible system and a strong system in the ultraviolet, and secondly by theoretical calculations which will be referred to later.

Proof that the carrier of the 4477 Å system of SCHÜLER is benzyl would be given if the same system could be found from the benzyl radical in absorption. Although the 3187 Å system may never appear in emission the 4477 Å system must, if it is due to benzyl, appear in absorption provided a sufficient density of benzyl can be attained. Careful examination of all our plates of the benzyl spectra showed no visible absorption bands. If the ratio of extinction coefficients of the visible and ultraviolet systems was comparable with that of triphenyl methyl a tenfold increase in benzyl radical concentration should be sufficient to make detection of the visible system possible. Previous experience had shown that the optimum concentration of benzyl attainable by photochemical methods had already been attained and therefore the only means of obtaining increased absorption was by increasing the path length above that of the 1 cm cell used in all experiments so far described.

Long cell for irradiation of low temperature glasses

The cell used was 20 cm long and of the design shown in Fig. 1. It, and the surrounding Dewar vessel, were constructed entirely of quartz and the Dewar, which was unsilvered, had double quartz flats in the base. The reaction vessel was filled with solution to a point well above the middle window so that, when contraction took place on cooling, no miniscus was formed in the optical path. The whole length of the frozen glass was irradiated by two U-shaped low pressure mercury vapour lamps and the spectrum was examined by means of a hydrogen or tungsten source and a small Hilger prism spectrograph.

This arrangement has been used many times without damage to the cell, the frozen solvent being in all cases M.P. (*iso*pentane three parts, methyl *cyclo*hexane two parts). It is anticipated from experience with other arrangements that more trouble might be encountered if E.P.A. were used as the solvent.

Absorption spectra of benzyl in the long path

Traces of the spectra obtained from photolysis of a 10^{-2} molar solution of toluene in M.P. at $-197°C$ and in the 20 cm cell are shown in Fig. 2. The 3178 Å system now appears with very high intensity and, in addition, a weak but very sharp series of bands is present in the visible region. The two systems appear together on irradiation and disappear on warming the glass. The positions of the main band maxima, are given in Table 1.

Both systems consist of a series of rather sharp bands with one strong band at long wavelengths. The strong band at 4527 Å must lie close to the origin of the visible system and is therefore to be compared with the maxima of the shortest wavelength band in the emission system, at 4477 Å. The shift of 50 Å to longer wavelengths in solutions is quite normal, the corresponding shift in the U.V.

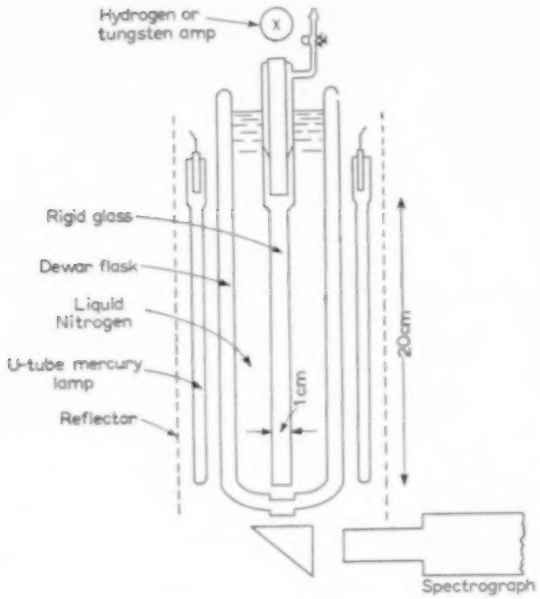

Fig. 1. Arrangement for irradiation and spectroscopy of low temperature solutions in 20 cm path.

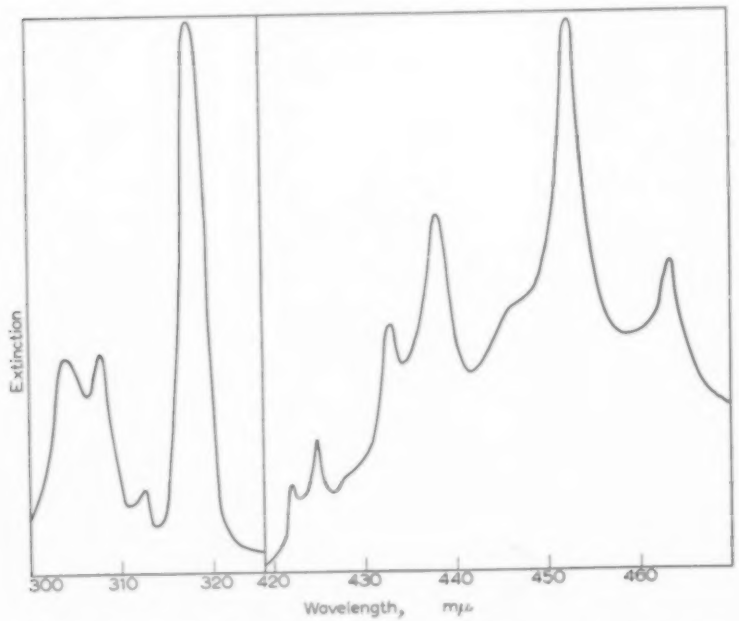

Fig. 2. Densitometer traces of spectra of benzyl obtained from 10^{-2} molar solutions of toluene in M.P. at $-197°C$ using a 20 cm path.

VOL.
12
1958

Table 1. Absorption spectra of benzyl in M.P. glass

U.V. system (Å)	U.V. system (cm^{-1})	Visible system (Å)	Visible system (cm^{-1})
3178	31,470	4635	21,580
3125	32,000	4527	22,090
3078	32,480	4460	22,420
3039	32,900	4375	22,850
		4330	23,090
		4245	23,550
		4220	23,700

system being 134 Å. There is some uncertainty as to what should be taken as the origin of the emission bands and the true origin of the absorption system is probably the weaker 4635 Å band, in which case the shift from the strongest emission band becomes 158 Å. If we consider only the main progression, in both emission and absorption, we obtain the following scheme of vibrational levels.

$v'v''$	2,0		1,0		0,0		0,1		0,2
Absorption (glass)	23,550	(700)	22,850	(760)	22,090		—		—
Emission (gas)	—				22,330	(944)	21,386	(933)	20,453

Of course v' and v'' do not necessarily refer to the same vibrational mode in emission and absorption. In spite of uncertainties as to the exact origin of the band systems there can be little doubt that the emission and visible absorption spectra involve the same transition and that both are to be assigned to benzyl.

Comparison with molecular orbital calculations.

The appearance of a weak transition in the visible and a strong one in the near ultraviolet is fully in accordance with molecular orbital calculations. Benzyl is an alternant hydrocarbon radical with seven π electrons, the three lowest configurations of which will be:

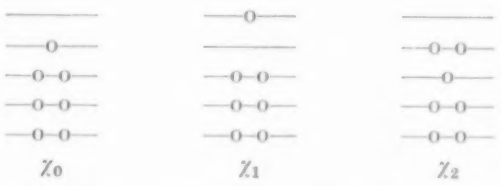

As pointed out by DEWAR and LONGUET–HIGGINS the configurations χ_1 and χ_2 are degenerate in the first approximation but when configuration interaction is introduced we obtain the wave functions $\Psi_1 = (1/\sqrt{2})(\chi_1 + \chi_2)$ and $\Psi_2 = (1/\sqrt{2})(\chi_1 - \chi_2)$.

The former has the lower energy and the transition from the ground state is weak. Calculations of the energies of these levels have been made by LONGUET-HIGGINS and POPLE and similar calculations have been given by BINGEL using both molecular orbital and free electron approaches. The results of these calculations and the experimental data from emission and absorption are compared in Fig. 3.

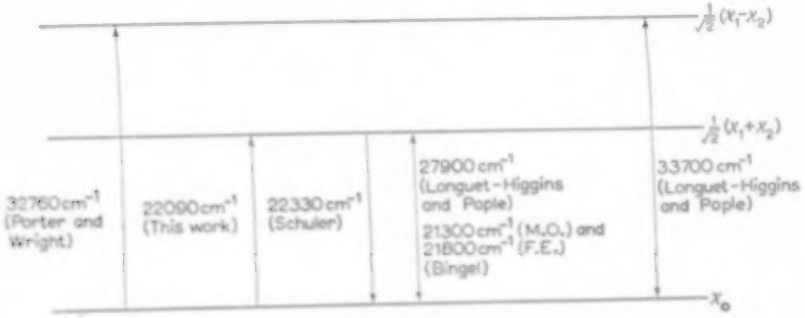

Fig. 3. Scheme of observed and calculated electronic transitions in benzyl.

The agreement is very satisfactory and lends support both to the assignments and to the methods of calculation.

Acknowledgement—The work described in this paper forms part of a programme of fundamental research being carried out by the British Rayon Research Association.

References

[1] SCHÜLER H., REINEBECK L. and KÖBERLE R., *Z. Naturf.* 1952 **7a** 421.
[2] WALKER S. and BARROW R. F., *Trans. Faraday Soc.* 1954 **50** 541.
[3] PORTER G. and WRIGHT F. J., *Trans. Faraday Soc.* 1955 **51** 1469.
[4] PORTER G. and WINDSOR M. W., *Nature, Lond.* 1957 **180** 187.
[5] PORTER G. and NORMAN I., *Proc. Roy. Soc. A* 1955 **230** 399.
[6] DEWAR M. J. S. and LONGUET-HIGGINS H. C., *Proc. Phys. Soc. Lond. A* 1954 **67** 795.
[7] LONGUET-HIGGINS H. C. and POPLE J. A., *Proc. Phys. Soc. Lond. A* 1955 **68** 591.
[8] BINGEL W., *Z. Naturf.* 1955 **10a** 462.
[9] SCHÜLER H. and MICHEL P., *Z. Naturf.* 1955 **10a** 459.

Spectrochimica Acta, 1958, Vol. 12, pp. 305 to 320. Pergamon Press Ltd., London

Etude comparée des spectres de vibration des dérivés paradisubstitués du benzène—I

Region 670–1600 cm^{-1}

CHANTAL GARRIGOU-LAGRANGE, JEANNE-MARIE LEBAS et MARIE-LOUISE JOSIEN
Centre de Physico-Chimie Structurale de la Faculté des Sciences de Bordeaux

(*Received* 24 *February* 1958)

Abstract—The infrared spectra of thirty-four paradisubstituted benzene derivatives have been obtained between 1600 cm^{-1} and 670 cm^{-1}. The interpretation of these spectra is discussed taking into account the corresponding Raman spectra as reported in the literature.

Introduction

UN très grand nombre de dérivés paradisubstitués du benzène a été examiné d'une part en spectroscopie Raman par KOHLRAUSCH et son école [1–6], d'autre part en infrarouge par LECOMTE [7–9]. Ces auteurs, dégageant l'idée de "suites" de fréquences* et guidés par des considérations théoriques, ont été amenés à faire un certain nombre d'attributions, surtout dans les régions inférieures à 1600 cm^{-1}. *Dans le même domaine spectral,* RANDLE et WHIFFEN *[11] ont donné des fréquences moyennes et proposé, pour les suites de bandes les plus caractéristiques, une attribution basée sur leur intensité et, dans le cas de fréquences Raman, sur l'intensité et l'état de polarisation des raies [57].*

Les autres travaux effectués sur les dérivés paradisubstitués du benzène sont relatifs, soit à une classe bien définie de composés [12–26], soit à une zone étroite de fréquences [27–36].

Les résultats concernant les dérivés monosubstitués du benzène [37–39], nous ont amené à examiner s'il existait aussi, dans le cas des composés paradisubstitués, des relations entre les petites variations de fréquences observées à l'intérieur d'une suite et les différentes propriétés de la molécule. Envisageant cette étude non seulement pour les fréquences de valence C—H aromatiques, mais encore pour l'ensemble des suites que l'expérience nous permettait d'atteindre, nous essaierons de dégager des conclusions générales.

LECOMTE n'a pas publié de valeurs numériques de fréquences et KOHLRAUSCH n'a utilisé que la spectroscopie Raman. Les tableaux de RANDLE et WHIFFEN, intéressants pour la distinction des divers types de benzènes substitués, sont insuffisants pour le but que nous nous proposons. Aussi a-t-il été indispensable d'enregistrer les spectres d'une série de composés dans des conditions identiques entre elles et appropriées au but poursuivi.

L'examen de cet ensemble de résultats expérimentaux a été guidé par les données déjà acquises pour le benzène, et par des considérations de symétrie. Il nous a

* Les "suites" sont des séries de bandes d'absorption ou de raies de diffusion que l'on peut attribuer en première approximation "à des vibrations du noyau benzénique auxquelles prend plus ou moins part le groupement substitué considéré comme une masse ponctuelle." LECOMTE, [10].

conduit à des attributions que nous comparerons avec celles trouvées dans la littérature: trois articles y seront consacrés. Dans un quatrième mémoire, nous aborderons l'étude des relations entre les petites variations de fréquences à l'intérieur d'une suite et les propriétés de la molécule.

Théorie

Si on fait l'approximation de considérer chaque substituant comme une masse unique concentrée sur l'axe, les dérivés paradisubstitués du benzène se classent en deux catégories de symétrie différente D_{2h} et C_{2v}, selon que les substituants sont identiques ou non*; ils possèdent trente vibrations fondamentales toutes distinctes.

Les Tableaux 1 et 2 indiquent le nombre de vibrations appartenant à chaque mode de symétrie et leur activité en spectroscopies Raman et infrarouge. Les composés du type p-$C_6H_4X_2$ possèdent quinze vibrations fondamentales actives en spectroscopie Raman, treize actives en infrarouge, aucune ne pouvant se manifester à la fois en Raman et en infrarouge; par ailleurs, deux sont complétement interdites. Au contraire, toutes les vibrations des composés du type p-C_6H_4XY, à l'exception de trois oscillations interdites en infrarouge, sont actives simultanément en spectroscopies Raman et infrarouge.

Les Fig. 1 et 2 donnent les schémas et les modes de symétrie des vibrations fondamentales des composés étudiés; le trièdre de référence choisi pour les déplacements comprend la direction de la liaison C—H ou C—X et deux directions perpendiculaires, l'une d'elles étant située dans le plan de la molécule. Pour faciliter la discussion, on a rappelé les types de vibration du benzène ainsi que leurs notations selon WILSON [40].

Les Tableaux 3 et 4, à double entrée, indiquent les modes de symétrie des combinaisons binaires pour les deux groupes de composés D_{2h} et C_{2v}. Ainsi, une combinaison d'une vibration B_{1g} avec une vibration B_{2u} des dérivés D_{2h} a les caractères de symétrie du mode B_{2u} (Tableau 3); elle est donc inactive en Raman, active en infrarouge, avec une variation de moment parallèle à l'axe des X (Tableau 1).

Conditions expérimentales

Une trentaine de dérivés paradisubstitués du benzène† ont été étudiés après vérification de leur pureté.‡

Un Spectromètre Perkin–Elmer 12 C simple passage§ a été utilisé; il était muni d'un prisme de chlorure de sodium pour la région 667–1400 cm^{-1} et d'un prisme de fluorure de calcium, pour la région 1350–1600 cm^{-1}.

Les fentes employées correspondent aux largeurs spectrales suivantes:

Région 667–1400 cm^{-1}: environ 5–6 cm^{-1}

Région 1350–1600 cm^{-1}: environ 3 cm^{-1}

---

* Nous verrons que cette approximation n'est plus acceptable dans le cas de molécules telles que le p-$C_6H_4(O\,CH_3)_2$. En outre, il parait probable que l'état condensé peut entrainer de légères déformations des molécules.

† En provenance des maisons Prolabo et Eastman Kodak.

‡ Nous remercions Madame VALADE qui a bien voulu se charger de cette vérification.

§ Cet appareil appartient à l'Institut du Pin. Nous remercions bien vivement Mr le Doyen BRUS de l'avoir mis à notre disposition.

VOL. 12 1958

Tableau 1. Dénombrement des vibrations des dérivés p-XC_6H_4X—Symétrie D_{2h} direction des axes C_2^x et C_2^y est celle indiquée dans la Fig. 2 le troisième axe C_2^z leur étant perpendiculaire.

Mode	Eléments principaux			Degrés de liberté		Mouvements d'ensemble	Nombre de vibrations	Activité	
	C_2^z	C_2^x	σ_z	$\tilde{\omega}_z$ 2 familles	α_x 2 familles			Raman	I.R.
A_g	s	s	s	2	1		6	P	i
A_u	s	s	a	1	0		2	i	i
B_{1g}	s	a	s	2	1	R_z	5	Dp	i
B_{1u}	s	a	a	1	1	T_z	3	i	M_z
B_{2g}	a	s	a	1	0	R_x	1	Dp	i
B_{2u}	a	s	s	2	1	T_x	5	i	M_x
B_{3g}	a	a	a	1	1	R_y	3	Dp	i
B_{3u}	a	a	s	2	1	T_y	5	i	M_y

Tableau 2. Dénombrement des vibrations des dérivés p-XC_6H_4Y—Symétrie C_{2v}

Mode	Eléments principaux		Degrés de liberté		Mouvements d'ensemble	Nombre de vibrations	Activité	
	C_2^z	σ_z	$\tilde{\omega}_z$ 4 familles	α_x 4 familles			Raman	I.R.
A_1	s	s	2	1	T_x	11	P	M_x
A_2	s	a	1	0	R_x	3	Dp	i
B_1	a	s	2	1	R_z T_y	10	Dp	M_y
B_2	a	a	1	1	R_y T_z	6	Dp	M_z

A: modes de vibration symétriques par rapport à tous les axes de la molécule au repos.
B: modes de vibration antisymétriques par rapport à un ou plusieurs axes.
g: (gerade), mode symétrique par rapport au centre.
u: (ungerade), mode antisymétrique par rapport au centre.
1, 2, 3: indices permettant une différentiation plus détaillée.
R_x, R_y, R_z: rotation autour de l'axe $0x$, $0y$, $0z$.
T_x, T_y, T_z: translation parallèlement à $0x$, $0y$, $0z$—
i: vibration inactive.
P: vibration active polarisée.
Dp: vibration active dépolarisée.
M_x, M_y, M_z: vibration active en infrarouge—la variation de moment étant respectivement parallèle aux axes $0x$, $0y$, $0z$.
$\tilde{\omega}_z$: atomes situés dans le plan de symétrie σ_z et hors de tout autre élément de symétrie.
α_x: atomes situés sur l'axe C_2^x.

Des références internes ont servi au repérage des fréquences: bandes de l'eau à 1617 et 1507 cm^{-1} [41]; du gaz carbonique considéré comme étant à 668·5 cm^{-1}. Les erreurs absolues sur les mesures des fréquences des bandes fines sont voisines de 1 cm^{-1} entre 667 et 1000 cm^{-1} et de 2 cm^{-1} dans les autres régions.

Les solutions ont été faites avec des solvants non polaires: le sulfure de carbone entre 667 et 1400 cm^{-1}; le tétrachlorure de carbone entre 1350 et 1600 cm^{-1}. Elles ont été examinées en maintenant approximativement constant le produit

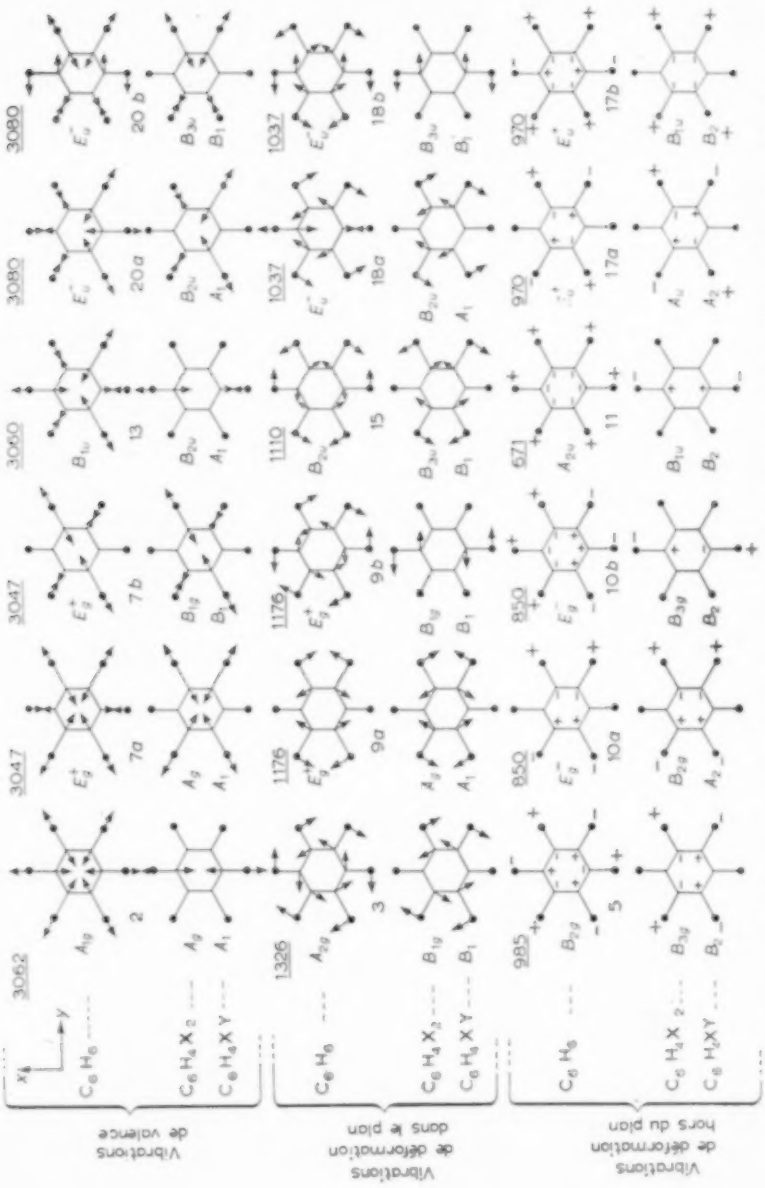

Fig. 1. Types de vibration du benzène et de ses dérivés paradisubstitués—vibrations CH et CX. Au voisinage de chaque type de vibration du benzène sont indiquées la fréquence de la vibration, son mode de symétrie et sa notation selon WILSON [40]. Pour les composés substitués figurent les modes de symétrie correspondant aux catégories p-$C_6H_4X_2$ et p-C_6H_4XY.

VOL. 12 1958

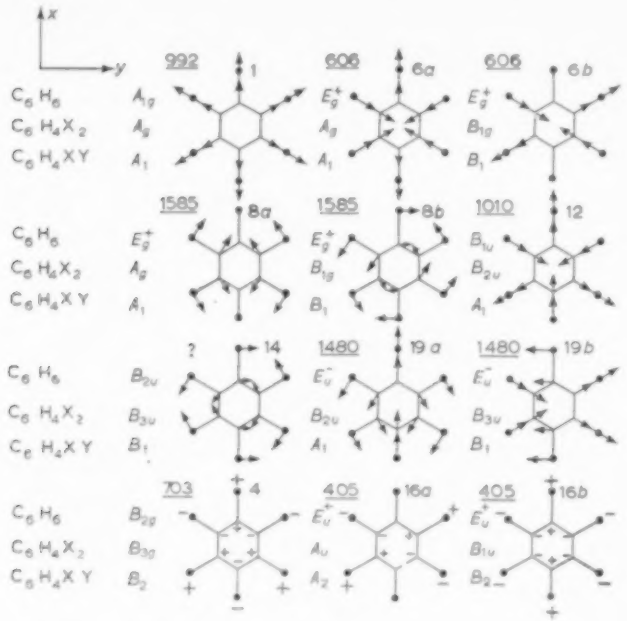

Fig. 2. Types de vibrations du benzène et de ses dérivés paradisubstitués—vibrations de noyau. Auprès de chaque type de vibration sont notés la fréquence correspondante, le mode de symétrie et la notation suivant WILSON [40] pour le benzène et les modes de symétrie pour les deux catégories p-$C_6H_4X_2$ et p-C_6H_4XY.

Tableau 3. Modes de symétrie des combinaisons binaires—dérivés D_{2h}

	A_g	A_u	B_{1g}	B_{1u}	B_{2g}	B_{2u}	B_{3g}	B_{3u}
A_g	A_g	A_u	B_{1g}	B_{1u}	B_{2g}	B_{2u}	B_{3g}	B_{3u}
A_u	A_u	A_g	B_{1u}	B_{1g}	B_{2u}	B_{2g}	B_{3u}	B_{3g}
B_{1g}	B_{1g}	B_{1u}	A_g	A_u	B_{3g}	B_{3u}	B_{2g}	B_{2u}
B_{1u}	B_{1u}	B_{1g}	A_u	A_g	B_{3u}	B_{3g}	B_{2u}	B_{2g}
B_{2g}	B_{2g}	B_{2u}	B_{3g}	B_{3u}	A_g	A_u	B_{1g}	B_{1u}
B_{2u}	B_{2u}	B_{2g}	B_{3u}	B_{3g}	A_u	A_g	B_{1u}	B_{1g}
B_{3g}	B_{3g}	B_{3u}	B_{2g}	B_{2u}	B_{1g}	B_{1u}	A_g	A_u
B_{3u}	B_{3u}	B_{3g}	B_{2u}	B_{2g}	B_{1u}	B_{1g}	A_u	A_g

Cl dans lequel C est la concentration de la solution, l la longueur de la cellule employée. D'autre part, afin d'éliminer au maximum les interactions entre molécules de soluté, on a utilisé, en général, des dilutions de 0·1 mole/l. De plus, les spectres des liquides ont été enrégistrés sous forme de film, et ceux des solides très peu solubles en suspension dans le nujol ou dispersés dans le bromure de potassium.

Tableau 4. Modes de symétrie des combinaisons binaires—dérivés C_{2v}

	A_1	A_2	B_1	B_2
A_1	A_1	A_2	B_1	B_2
A_2	A_2	A_1	B_2	B_1
B_1	B_1	B_2	A_1	A_2
B_2	B_2	B_1	A_2	A_1

Résultats

Le Tableau 5 groupe les résultats infrarouge et Raman en "suites" numérotées par ordre croissant de fréquence.

Les écarts, faibles en général, entre les fréquences que nous avons mesurées et celles publiées antérieurement, peuvent être imputés aux différences de conditions d'enregistrement et de précision de lecture.

Analyse des résultats

Les suites de fréquences comprises entre 670 et 1600 cm^{-1} seront successivement examinées,* puis nous discuterons la position des bandes propres aux substituants. Pour permettre une vue d'ensemble, nous avons rassemblé dans le Tableau 6 les principales attributions tirées de la littérature; nous y avons joint celles que nous proposons. Avant de justifier ces dernières, nous essaierons de dégager les caractéristiques essentielles des travaux cités dans le tableau.

KOHLRAUSCH ayant réuni par spectroscopie Raman un grand nombre de résultats expérimentaux, en a tenté l'interprétation à l'aide d'une représentation mathématique de l'état vibratoire des molécules, en s'inspirant des travaux de TRENKLER [55] sur la molécule hypothétique $p - C_6X_2$.

En 1939, KOHLRAUSCH [3] calcule les fréquences des vibrations planes de quelques modèles p-C_6X_2(X = CH_3, Cl, Br, m_x = 15, 35·5, 80); il prend pour la constante de force f de la liaison C—X une valeur égale aux 6/5 de la constante de force correspondante dans les composés aliphatiques. Il considère en outre les

* Dans cette première analyse, il ne sera question que des suites que nous croyons attribuables à des vibrations fondamentales. Nous nous proposons de revenir ultérieurement sur la question des fréquences de combinaison.

deux cas: $m_x = 0, f = \infty$ et $m_x = \infty, f = 0$. L'auteur répartit ensuite les valeurs numériques obtenues pour les fréquences aux différents types de vibrations d'un même mode de symétrie, ce qui le conduit à admettre des transformations dans le type des vibrations. Ainsi, par exemple, une vibration de valence ν(CH) pourrait se changer en une vibration de noyau, une vibration de noyau en une vibration de déformation δ(CH) ou δ(CX)....

Tableau 6. Attribution des suites de la région 670–1600 cm^{-1}

No des suites	Région	d'après Kohlrausch [1, 5, 6]	d'après Lecomte [7, 9]	d'après Randle et Whiffen [11, 33]		Présent travail
				Notation des auteurs [7]	Vibrations correspondantes	
I	680	17 *a*	5	$B_{3g}\phi$(C—C)	4	4
II	700–850	d[1]	—[5]	d[1]	—	d[1]
III	790–880	—[2]	17 *b*	$B_{1u}\gamma$(C—H)	11 et 17 *b*	17 *b* ou 11
IV	830	10 *ab*	—[6]	$B_{2g}\gamma$(C—H)	10 *a*	10 *a*
V	930	—[3]	—	A_u ou $B_{3g}\gamma$(C—H)	17 *a* ou 5 et 10 *b*	5
VI	1010	18 *a*	12	$B_{2u}\beta$(C—H)	18 *a*	18 *a*
VII	1060–1300	e[1]	2 et 19 *b*	e[1]	—	e[1]
VIII	1060–1300	e'[1]		e'[1]	—	e'[1]
IX	1100	—[4]	18 *a*	$B_{3u}\beta$(C—H)	15 et 18 *b*	15
X	1170	9 *a*	9 *a*	$A_g\beta$(C—H)	9 *a*	9 *a*
XI	1300	3	15	$B_{1g}\beta$(C—H) ou $B_{3u}\nu$(C—C)	9 *b* et 3 ou 14 et 19 *b*	3
XII	1400	—	3	—	—	14
XIII	1450	—	19 *a*	$B_{3u}\nu$(C—C)	14 et 19 *b*	19 *b*
XIV	1490	—	8 *b*	$B_{2u}\nu$(C—C)	19 *a*	19 *a*
XV	1570	—	8 *a*	$B_{1g}\nu$(C—C)	8 *b*	8 *b*
XVI	1590	—	7 *b*	$A_g\nu$(C—C)	8 *a*	8 *a*

Le signe—signifie que la suite n'a pas été observée par l'auteur.

[1] Pour la signification des notations: *d*, *e*, *é* et l'utilisation que nous en faisons, voir la discussion des suites *II*, *VII* et *VIII*.
[2] Kohlrausch situe la vibration 17 *b* à 740 cm^{-1} [6]
[3] Kohlrausch confond les vibrations 10 *a* et 10 *b* et admet que la vibration 5 se transforme en vibration γ(C—X) [6].
[4] Kohlrausch place la vibration 15 à 1400 cm^{-1} environ [6]
[5] La vibration 1 étant rigoureusement interdite en infrarouge pour les dérivés symétriques, Lecomte estime qu'elle possède dans les dérivés dissymétriques, une intensité trop faible pour être observée [7].
[6] Lecomte situe la vibration 10 *a* à 750 cm^{-1} [7].
[7] Ces auteurs notent ϕ C—C une vibration de déformation du noyau hors du plan, βCH une vibration de déformation du vibrateur CH dans le plan, γCH une vibration de déformation du vibrateur CH hors du plan, ν CC une vibration de noyau dans le plan.

Dans une seconde étape, Kohlrausch [4, 5] adopte une valeur fixe: $f = 5{\cdot}1.10^5$ dyn/cm pour la constante de force de la liaison C—X et considère la masse comme seule variable. Il trace les courbes des fréquences en fonction de l'expression $\sqrt{(1/m)}$; ces courbes sont continues, et celles qui appartiennent à un mode donné ne se coupent pas.

Cette analyse mathématique conduit dans certains cas à des "contradictions manifestes", comme KOHLRAUSCH l'a lui-même noté. C'est ainsi qu'en 1946 les attributions proposées par cet auteur pour les vibrations de déformation hors du plan γ(CH) et dans le plan δ(CH) ne sont pas basées sur les résultats théoriques précédents [6].

LECOMTE a réalisé la première étude systématique par spectroscopie infrarouge des dérivés paradisubstitués du benzène. Pour l'analyse de ses résultats, il tient compte des données de la spectroscopie Raman. En outre, il s'inspire des résultats théoriques de KOHLRAUSCH; c'est ainsi qu'il est amené à faire glisser une vibration ν(CH) à 1600 cm^{-1} et à déplacer vers les fréquences inférieures les vibrations de noyau 8 *ab* et 19 *ab*.

En 1955, RANDLE et WHIFFEN ont rassemblé les résultats antérieurs obtenus en spectrométries Raman et infrarouge. Ces données, nécessairement hétérogènes, étaient cependant suffisantes pour le but d'analyse spectroscopique des dérivés benzéniques qu'ils poursuivaient. Elles leur ont permis, en outre, de préciser un grand nombre d'attributions qui paraissent définitives.

Avant de commencer la discussion de chaque suite, nous indiquerons en cm^{-1} les valeurs extrêmes des fréquences qui la composent ainsi que les substituants correspondants.

Suite I (Cl, CN: 674; OC_2H_5,OC_2H_5: 724). A 703 cm^{-1}, existe pour le benzène la vibration 4. Dans les dérivés de symétrie D_{2h}, cette vibration appartient au mode B_{3g} actif seulement en spectroscopie Raman; pour les composés de symétrie C_{2v}, elle est active dans les deux phénomènes. En fait, la plupart des spectres Raman présentent une faible raie dépolarisée vers 700 cm^{-1} et on observe dans les spectres infrarouges des dérivés dissymétriques une bande d'intensité variable correspondant à la raie Raman. Comme cela a déjà été signalé dans le cas des dérivés monosubstitués du benzène [38], la faible montée des fréquences avec les substituants électropositifs, est en faveur d'une attribution à une vibration de noyau plutôt qu'à une vibration de déformation hors du plan γ (CH). Nous attribuerons donc cette suite à la vibration 4. Dans le cas des molécules p-$C_6H_4(OCH_3)_2$ et p-$C_6H_4(OC_2H_5)_2$, une fréquence infrarouge a été rangée dans la suite *I* parce que, pour le premier de ces composés, dont le spectre Raman est connu, elle coincide avec celle de la raie Raman; l'activité infrarouge de la vibration 4 pour ces deux dérivés s'explique par la diminution de symétrie due au substituant.

Suite II. (I, I: ~690; CH_3, F et CH_3, NH_2: 844). Nous avons rangé dans la suite *II* des raies Raman très intenses et fortement polarisées; nous y avons ajouté pour les dérivés dissymétriques des bandes infrarouges, les unes parce qu'elles coincident avec les raies Raman, les autres, en l'absence de spectre Raman, par analogie. Si l'intensité Raman et l'état de polarisation des raies suggèrent l'attribution de cette suite à une vibration totalement symétrique telle que la vibration 1 du benzène, par contre la grande variation de fréquence avec le substituant pose un problème.

Cette suite correspond aux raies *d* étudiées par KOHLRAUSCH en 1936 [1]. L'auteur les affecte à un type de vibration particulier, une vibration de noyau à laquelle participeraient les liaisons C—X et C—Y. (Fig. 3).

KOHLRAUSCH établit la relation empirique: $\omega_d^2 = A + B\omega_0^2$ entre la fréquence

expérimentale ω_d des raies d et une fréquence calculée $\omega_0 = 2\pi\sqrt{(f/\mu)}$($f$, constante de force de la liaison H_3C—X; μ, masse réduite calculée par l'équation $1/\mu = 1/12 + 1/m_x$; m_x, masse du substituant X). Dans cette relation, A et B sont des constantes relatives à un substituant Y fixe, et ω_0 se rapporte à un substituant X variable.

Fig. 3. Vibration "d" d'après KOHLRAUSCH [1].

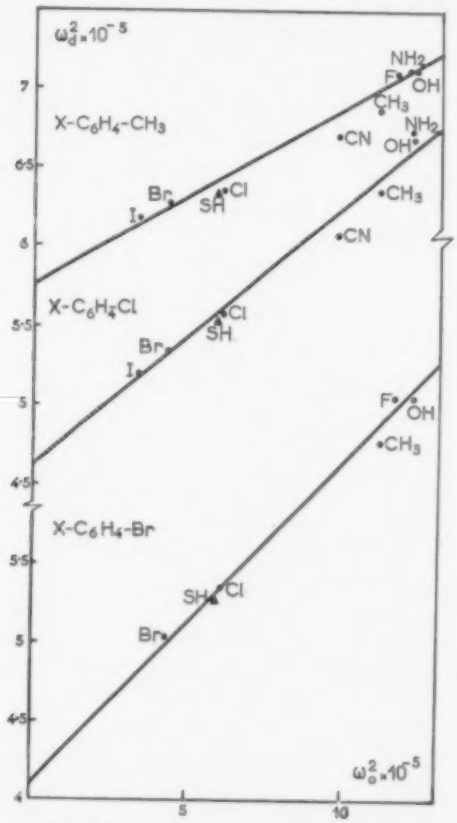

Fig. 4. $\omega_d^2 = f(\omega_0^2)$●: ω_d du tableau 8(a) ▲: ω_d du tableau 8(b)

Les représentations graphiques de la fonction $\omega_d^2 = f(\omega_0^2)$ relatives aux substituants Y = CH_3, Cl et Br (Fig. 4), obtenues en utilisant pour ω_d les fréquences expérimentales de la suite *II* et pour ω_0 les valeurs publiées par KOHLRAUSCH [1] illustrent la linéarité de cette fonction; elles donnent, pour A et B, des nombres très voisins de ceux de KOHLRAUSCH. Inversement, les fréquences ω_d calculées à partir des valeurs, A, B et ω_0 de KOHLRAUSCH sont en accord avec les résultats expérimentaux de cet auteur. [(Tableaux 7 et 8 (a)].

L'existence de la relation $\omega_d^2 = A + B\omega_0^2$ conduit aux applications suivantes:

(1) Calcul de la fréquence ω_d pour des composés dont les spectres Raman ne sont pas connus. Ce calcul a été effectué pour quatre benzènethiols (X = SH; Y = CH_3, Cl, Br, I); la fréquence obtenue coïncide avec celle d'une absorption infrarouge que nous avons alors classée dans la suite *II* [Tableau 8 (b)].

Tableau 5. Composés $p\text{-}XC_6H_4Y$—Fréquences d'absorpti

	p-X C_6H_4 Y		I	II	III	IV	V	VI	VII	VIII	IX	
1	NO_2, NO_2 (3)	α γ δ	710 820* 836	673			994	1012	1073	1105 δ 1108	1190	1169
2	Cl, Cl (3,7)	α γ δ	674 744 2(0,06) 780 806 747 22(0,06)	615 747 22(0,06)	811 (0,65)	605 860 890 855	942	968 1068	1014	1080 1075 1030 0(0,10)	1080 1104 1105 12(0,05)	1114
3	Br, Br (3)	α γ δ	711 743 797 709 19	697 709 19	809 00	855 897	932 964	999 1036 1040	1066 12	1068	1080 1102 1138 1150	
4	I, I (3)	α γ δ	660 ~650 706 784 0	801 ~690	~690	822 925 1	975 980 986 1041	1045 5	1050	1007 1001 1103 1140 1170		
5	OCH_3, OCH_3 (3)	α γ δ	711 713 10(0,72) 710 788 792 0	834 820 10(0,09)	843 1(p)	932 1035 (0,27)	1036 1040	1063 1000 8(0,12)	1030 1035 2(0,10)	1104 1121 1150 1164 2(0,17)		
6	OC_2H_5, OC_2H_5	α	667 736 731 790 797 796	614 831 542 880 927 1086 1025 1060	1107 1030 1105 1110 1154							
7	CH_2Br, CH_2Br	α	736 761 702	838 1022	1014 1090							
8	CH_3, CH_3 (42,2)	α β γ δ	743 671 702 3 2	705 707 829 410(0,06)	810 100(p)	885 904 887 936 0 971 2 1091 2	982 1022 1023 1035 3	1041 1042 1104 1205 325(0,65)	1116 1120 1120			
9	NO_2, COCl (43)	α γ δ	691 706 794 800	855 889 908 1016 1027 1190 1100 1	1106 1110							
10	Cl, NO_2 (43)	α γ δ	677 691 690 1 741 785 829 732 3 732 5	847 935 953 965 1014 1044 1064 1066 1097 1108 935 912 1 4 6 1	1109 1121							
11	Cl, CN (43)	α γ δ	674 706 758 770 811 756 6	828 874 947 968 1010 1017 1044 1070 1092 1090 1100 5 5	1111 1130							
12	Cl, SH	α	689 744 809 917 935 953 1007 1015 1009 (1097) (1097)	1105								
13	Cl, Br (5,2)	α γ δ	686 737 739 748 764 635 739 68(0,05) 10(0,09)	727 814 820 936 951 980 1011 739 0(0,54) 10(0,09)	1000 1071 8(0,16) 1000 1080 12(0,12)	1089						
14	NO_2, OH (5)	α γ δ	676 684 751 780 847 864 1005 1075 1091 9	1111								
15	NO_2, NH_2	α	675 690 741 751 827 845 854 950 1015 1049 1005 1203 1110	1124 1105								
16	Br, SH	α	689 727 755 727 805 917 935 952 991 1004 1012 1070 (1100) (1100)	1159 1166								
17	Br, F (19)	α β γ δ	689 738 751 806 751 760 689 710 m(0,80) 697 813 813 810 FF(0,1)	822 823 831 m(0,30) 850 887 913 911 930 947 970 986 1011 1014 927 944 960 986 ff(dp) ff(dp) fff(dp) f. large ff(dp)	1016 1017 1015 m(0,55) 1060 1044 m(0,50)	1086 1080 1080 FF(0,4) 1031 1032 1028 F(0,50)	1027 1001 1000 m(0,05) 1103 1101 1102 ff(dp)	
18	Cl, I (43)	α γ δ	686 722 729 748 722 729 8	810 936 955 980 1006 1036 1052 5 1061 1066 7 1067 1001 1103	1103							
19	I, SH	α	686 710 709 722 801 915 960 986 1007 1050 (1100) 1082 (1100) 1108 1105									
20	Br, $COCH_2Br$	α	697 706 761 769 777 805 811 880 821 950 968 1006 1023 1071 1107 1108 1117									
21	CH_3, NO_2 (43)	α γ δ	681 736 744 822 692 3 756 739 6,8 855 859 862 0 954 967 1017 1040 1066 1106 8 1109 1084 4 1110 1133									
22	Cl, OCH_3 (5,2)	α β γ δ	675 689 707 790 800 797 12(0,07) 829 1(0,27) 963 965 1035 1040 1046 1036 3(0,24) 1073 1004 1002 1001 9(0,09) 1045 1040 1044 1(0,25) 1102 1104 1100 1 1114 1116 1153 4(0,14)									
23	CH_3, F (44,2)	α β γ δ	694 728 758 738 695 740 1,1(0,63) 728 0,90 744 744 742,5 61(p) 814 816 844 844 825 58 844 842,5 61(p) 906 fff 927 961 1000 931 927 1000 923 1003 6,35 1017 1041 1041 1061 fff 1017 1040 fff fff 1045 1053 1054 1054 1111 1102 1099 0,51 1111 1110 58 1,1(p)									
24	CH_3, CN (44)	α γ δ	671 688 705 711 760 797 705 1 810 8 810 946 997 999 1023 1035 α large 1039 1101 1107 1094 4 1111 1130 1109									
25	Cl, NH_2 (5,2)	α γ δ	694 716 711 821 6(0,10) 816 836 6(0,10) 889 00 923 939 00 944 1007 1032 1(0,24) 1013 1060 1071 1004 1000 9(0,11) 1076 1079 4(0,22) 1120									
26	Cl, OH (5)	α γ δ	686 697 734 752 801 818 8 824 836 6 926 935 00 945 1010 1008 1 1071 (1095) 1091 8 1110 1066 1056 3 1160									
27	Br, OH (43)	α γ δ	694 697 o large 801 810 10 821 825 5 927 945 1011 1007 2 1033 1039 1064 9 1050 1052 3 1092 1150									
28	CH_3, OCH_3 (5,2)	α β γ δ	689 709 730 721 707 704 2(0,07) 810 819 835 835 9(0,00) 835 6(0,00) 922 940 960 991 1015 1017 1011 1 1041 1041 1039 1(0,45) 1066 1065 1 1104 1050 1206 2(0,10) 1112 1111 1116 1139 1151 1154 0 d									
29	CH_3, Cl (5,2)	α β γ δ	682 692 710 747 782 797 10(0,09) 805 807 822 819 2(0,22) 933 935 955 1011 1010 1040 1042 1070 1072 1091 1080 1080 10(0,09) 1110 1114 1106 7(0,09)									
30	CH_3, SH	α	696 (796) (796) 914 934 967 980 1005 1015 1039 1070 1090 1090 1114									
31	CH_3, Br (5,3)	α γ δ	692 730 773 702 5 801 835 2 840 00 894 958 1000 1015 1012 2 1019 1020 1089 7(0,05) 1080 1090 6(0,09) 1080 1130 1(0,									
32	CH_3, OH (5,2)	α β γ δ	699 730 749 804 702 219,67) 842 842 844 23(0,07) 817 810 823 5(0,15) 842 842 844 23(0,07) 932 939 940 965 1010 1017 1016 1 1045 1043 1070 1073 1054 1215 6(0,09) 1101 1105 1113 1115 1110 1180 (1170) (1170) (11 11 4(0,									
33	CH_3, I (5)	α γ δ	699 734 757 708 9(0,09) 797 810 1(p) 827 986 948 1000 1008 1049 1060 1055 4(0,12) 1097 1249 5(0,12) 1099 1111 1180 11 11 1(0,									
34	CH_3, NH_2 (5,2)	α γ δ	700 741 740 698 1(0,60) 9 844 22(0,05) 810 817 36(p) 844 22(0,05) 922 945 980 990 0 1020 1014 0(p) 1041 1070 1071 1070 1210 7(0,10) 1120 11 11 0(0,									

Les fréquences ont été classées par valeurs numérique
(1) Quand elles ont été attribuées simultanément à deu
(2) Quand elles font partie d'une suite dont la positi
fréquences (nombres en italiques).

α: Fréquences infrarouges—solution; les valeurs sou
fortes. β: Fréquences infrarouges—liquide pur. γ: Fréq
δ: Intensité des raies Raman suivie, quand il est connu
*: Fréquences infrarouges observées uniquement à l'éta

Caractères
gras: Fréquences attribuées à des vibrations pa

sception infrarouge et de diffusion Raman entre 670 et 1600 cm^{-1}

X							XI							XII		XIII			XIV				XV	XVI		
1170	1198		1234		1257					1322	1327	1379	1395		1407	1462		1479*			1530*	1570*			1 α γ δ
1170 1160 5(0,36)	1220 1		1230		1264		1221 3(0,55)	1286		1345		1379 1(0,54)	1390		1420			1470					1574 12(0,67)	1617	2 α γ δ
1170 1173 5			1210		1257		1276 1290 1	1320		1313	1330	1371 1386 1	1395		1410			1469	1500				1565 6	1610 0	3 α γ δ
1161 1179 5		1195	1215	1249	1270	1297	~1290			1326		1385 1			1422	1468	1468						~1560	1623	4 α γ δ
1174 5(0,17)	1179		1213		1230 1235 2(0,16)	1263 1286 4(0,12)	1292 1294 0	1300		1313 1310 3(0,19)		1433	1442	1455 1454 1,5(0,8)	(1466)	(1468)			1500	1516			1594	1615 1614 3(0,56)	1652	5 α γ δ
1170	1233		1230		1285		1302	1360		1394		1425	1444	1450	(1470)	(1478)			1507	1521	1562		1592	1609	1616	6 α
	1197		1214		1240								1431	1462	(1461)	(1461)			1515						1656	7 α
1167 1170 61(3)	1204 2(0,06)		1218 1230		1240 1250 1245 0	1266	1312 30(0,51)	1319		1350 1380 1379 104(0,95)	1441 15	1455 (0,45)	1468 ~1490		1480	1498			1516 1517				1581 10(0,51)	1618 140(dp)	1630 1628	8 α β γ δ
1175	1190		1226				1302	1324		1350 1355 6			1396	1396	1410	1457			1499	1523		1537 1504 9		1598	1607 1601 8		9 α γ δ
1162 1178 3	1207 1214 3		1228					1279		1311	1342 1343 20 large	1364	1395 1390 3		1424 1419 5				1479 1474 5	1498	1526 1520 4	1543	1556	1569	1570 1575 10	1606	10 α γ δ
1172 1178 5	1191 1192 6		1225		1254	1270	1290 1301 0				1364 1350 0		1400		1404				1495	1494			1576	1586 1598 7	1651	11 α γ δ
1172	1221			1205			1302			1346		1380	1394		1417	1454	1473		1478						1602	12 α
1161 1172 3(0,13)	1210		1227		1261		1302 1290 5(0,56)	1341		1366 1375 6(0,45)			1395		1415	1468			1473	1496			1570 5(0,7)	1588 1(0,7)	1631	13 α γ δ
1163	1178		1221	1264	1275 1291 9		1308			1341 1350 45			1391*		1436*				1499*	1506*			1594*	1613*		14 α γ δ
1175				1221		1264		1263		1334		1371	1380		1446*	1474*			1492*	1507*	1570*		1587*	1596*	1631*	15 α
1170	1219		1260				1306			1342	1363		1391		1413	1466			1475	1494					1625	16 α
1173 1167 1165 F(0,3)	1177 1174 HF	1161 1164 fff	1206 1210 f(0,50)	1217	1231 1232 1255 F(0,50)	1261	1276 1274 m(0,65)	1280 1280 m(0,65)	1303	1320 1323 fff	1356 1364 ff	1377 f(0,50)	1402 1402 1400 f(0,60)		1427 1427 fff	1450 fff			1487 1486 1485 m(0,60)	1505	1515	1571 ff		1587 1587 1586 F(0,90)	1596 1596 1597 m(dp)	1622 ff	17 α β γ δ
1173 1172 1	1192 1196 0	1198	1216	1257		1276	1302 1297 0			1326	1337	1382 1370 6,5	1387		1413	1467			1472	1504			1565 1564 6	1572	1630	18 α γ δ
1161	1191		1217	1260			1296	1340		1371			1398	1394	1430				1473	1478	1522			1575	1617	19 α
1172	1197		1206	1221		1250		1275		1304		1346 1391	1399	1421	(1427)	(1427)	1470		1486				1567	1587	1629	20 α
1172 1172 3	1200 1208 3			1236			1296 1300 1	1296		1315	1345 1342 30	1364 1360 4	1389	1422 1419 1	(1430)	(1430)	1471 1470 1		1497 1499 2	1515 1517 0,5 large			1569	1602 1596 6	1607	21 α γ δ
1161 1177 1161 4(0,18)	1189 1188 1188 4(0,18)		1240 1249 1244 6(0,14)					1280 1264 1283 3(0,19)		1324					1410 1404 1		1432	1443 1440 3	1457 1469 3(0,86)	1483	1493 1492 1(0,45)	1522			1562 1560 5	1596 1594 5(0,62)	1619	22 α β γ δ
1175 1170 11(0,1)	1178	1200	1211 2R(p)	1243 1254 1227 25	1259	1276 fff	1296 1290 3(0,47)	1314 1311			1333 1363 1353 fff	1383 3(0,45)	1404 ff	1430 1433 fff	(1456) (1455) ff(0,70)	(1456) (1455) ff(0,70)		1495 f	1509 1508 1506 ff	1515		1502 1501	1602 1602 1601 6,5(0,73)	1615 1613 1614 3(0,73)		23 α β γ δ
1173 1175 19	1197 1194 d		1218	1238	1262	1266	1310 1300 60					1393 1378 2	1413		(1450 1445 0	(1450 1445 0		1490	1510	1524			1569	1611 1604 10	1621	24 α γ δ
1170 1171 2(0,37)							(1276 1279 4(0,23)	(1276 1279 4(0,23)		1315		1382 60	1426					1459	1496				1574	1601 1602 5(0,56)	1621 1621 2	25 α γ δ
1161 1166 2	1179		1205	1244		1250 1255 3	1264 1264 1	1302		1319		1373	1426		1434	1462	1460	1479	1494 1492 2	1505	1522		1592 1588 5	1610 1604 3	1650	26 α γ δ
1166	1173 1166 3		1206	1235		1230 1255 3	1281 1276 3 large	1302		1321		1398 1373	1424 1415 60		1437	1478			1489	1505			1599 1593 5 large	1601	1624	27 α γ δ
1173 1166 6 double (0,18)	1177 1177		1210	1246 1250 1240 3(0,10)			(1296 1300 1295 3(0,19)	(1296 1300 1295 3(0,19)		1360 1362 1379 3(0,58)		(1444)	(1444)	1456 1455 1456 3(0,79)	(1466)	(1468)		1498 0	1512 1512	1524		1573	1586 1586 1584 2(0,72)	1614 1613 1°11 7(0,65)	1639	28 α β γ δ
1174 1179 1175 2	1204 1212 1205 7(0,09)		1220	1274			1290 1296 2(0,84)	1340				1393 1377 3(0,45)	1403		1415 1404 1	~1456 1422 1(0,81)			1490	1508			1575 1574 5(0,66)	1599 1596 3(0,66)	1617	29 α β γ δ
1170	1209		1220	1232		1266	1312					1391	1403		1420	1450	1453		1496	1506			1570	1600	1627	30 α
1170 1170 1(0,36)	1198	1209 1200 5(0,09)		1230		1266	1313 1300 1(0,69)	1354				1391 1370 6(0,59)	1396		1413	1454 1440 9(0,80)			1490	1496				1591 1588 7(0,71)	1628	31 α γ δ
(1170) (1172) 1171 4(0,34)	1205	1212 1215 0(0,09)		1230 1235	1254 1254 2(0,07)	1264	1302 1308 1296 1(0,55)		1308	1338 1343	1368 1364	1382	1420		(1460)	(1460)			1515			1570	1598 1596 4(0,74)	1618 1614 6(0,74)	1634	32 α β γ δ
1170 1180 1(0,38)	1207 1210 3(0,17)		1227			1265	1301 1302 0(0,58)					1383 1378 3(0,37)	1390		1410	1450	1475		1496	1495			1564	1585 1592 3(0,73)	1597	33 α γ δ
1174 1170 6(0,33)	1216 7(0,19)		1244 1			1271 1272 3(0,09)	1296 1292 1	1312 1304 1	1321			1381 1378 7(0,60)	(1430)		(1450)	(1460 1452 1(dp)			1518				1567	1610 1594 1(0,57)	1620 1615 10(0,57)	34 α γ δ

ériques croissantes. Certaines fréquences sont répétées:
à deux suites (nombres mis entre parenthèses).
position ne correspond pas avec l'ordre croissant des

re soulignées correspondent aux bandes moyennes ou
: Fréquences Raman, tirées de la référence mentionnée.
connu, du facteur de dépolarisation, entre parenthèses.
à l'état solide. ~: fréquences Raman approximatives.

ons propres du substituant.

(2) *Détermination graphique de nouvelles constantes A et B.* Pour $Y = SH$, on trouve $A = 0{\cdot}464.10^6$, $B = 0{\cdot}155$ et pour $Y = OH$, $A = 0{\cdot}620.10^6$, $B = 0{\cdot}082$.

(3) Calcul des valeurs A, B et ω_0 pour le substituant OCH_3 à partir des fréquences Raman des p-$OCH_3C_6H_4Cl$, p-$OCH_3C_6H_4CH_3$ et p-$C_6H_4(OCH_3)_2$. On obtient $A = 0{\cdot}581.10^6$, $B = 0{\cdot}0999$, $\omega_0 = 1037$. Cette valeur de ω_0 est comprise entre les deux fréquences ν_{C-O} de l'oxyde de méthyle.

Tableau 7. Constantes utilisées pour le calcul de ω_d [1]

Substituant	ω_0	$A.10^{-6}$	B
NH_2	1099	0·627	0·079
OH	1102	—	—
F	1077	0·619	0·081
CH_3	1052	0·574	0·109
CN	987	—	—
SH	766	—	—
Cl	775	0·463	0·157
Br	654	0·410	0·202
I	578	0·380	0·222

Dans le cas des composés nitrés, un calcul analogue est théoriquement possible; mais, faute de données Raman suffisantes, il subsiste un certain doute sur les raies des composés placées dans la suite *II*.

L'existence de la relation discutée ci-dessus est en faveur de l'hypothèse de KOHLRAUSCH qui fait de la suite *II* une vibration de noyau à laquelle participe la vibration C—X. Cependant, dans le cas des composés où les substituants sont lourds (halogènes et SH) les fréquences deviennent voisines dans certains cas des fréquences de valence C—X et on peut se demander si elles ne correspondent pas surtout à ces vibrations de valence. Les données expérimentales dont nous disposons nous paraissent insuffisantes pour résoudre actuellement le problème.

Suite III (CH_3, CH_3: 795; NO_2, No_2: 873). La suite *III* correspond à des bandes infrarouges extrêmement intenses, de fréquence sensible à l'influence des substituants et auxquelles ne correspondent pas de raies Raman. Nous l'affecterons en accord avec la plupart des auteurs à une vibration de déformation hors du plan γ (CH) pouvant être rapprochée des vibrations 11 et 17 b du benzène qui mettent en jeu de grandes variations de moment dipolaire.*

Suite IV (Br, Br: 809; OCH_3,OCH_3: 843). Composée presque uniquement de raies Raman, elle est attribuable à la vibration 10 a du benzène, interdite en infrarouge pour des composés de symétrie D_{2h} et C_{2v}. Des valeurs infrarouges ont cependant été classées dans cette suite dans le cas des molécules p-$C_6H_4(OC_2H_5)_2$ et p-$BrC_6H_4COCH_2Br$ pour lesquelles il y a disparition de toute symétrie. Pour le p-$CH_3C_6H_4Cl$, l'absorption observée uniquement dans le spectre du liquide pur

* On attendrait la vibration 17 a, permise seulement en spectrométrie Raman pour les composés de symétrie C_{2v} vers 970 cm^{-1}, position de la vibration 17 ab du benzène. Bien qu'aucune fréquence Raman n'ait été relevée dans cette région, l'éxistence d'une suite aux environs de 960 cm^{-1} expliquerait l'apparition de bandes de combinaison vers 1700 et 1800 cm^{-1} [56].

est probablement due à l'état condensé. En ce qui concerne les composés nitrés, on peut penser que la raie Raman correspondant à la vibration 10 *a* est contenue dans la raie intense, spécifique des dérivés nitrés aromatiques, située vers 850 cm^{-1}.

Suite V. (CH_3, NH_2: 922; No_2, COCl: 968). La suite *V* est constituée de raies Raman et de bandes infrarouges peu intenses, les raies Raman existant seules pour les composés symétriques. De préférence à la vibration 17 *a*, nous attribuons cette

Tableau 8. Comparaison des fréquences calculées ω_i et des fréquences observées

	Composés p-XC_6H_4Y	Fréquence calculée		Fréquence observée suite II	
				I.R.	Raman
(*a*)		A partir de ω_0 (liaison CX)			
	Cl, Cl	746·5		—	747
	Br, Br	704·5		—	709
	I, I	674		—	~690
	CH_3, CH_3	833		—	829
		A partir de ω_0 liaison (CX)	liaison (CY)		
	Cl, CN	—	786·7	780	776
	Cl, Br	728	728	731	730
	Br, F	808	803	813	810
	Cl, I	717	718	722	720
	CH_3, F	842	837	844	842·5
	CH_3, CN	—	825	—	819
	Cl, NH_2	822	808	—	821
	Cl, OH	—	808	—	818
	Br, OH	—	809	—	810
	CH_3, Cl	798	799	—	797
	CH_3, Br	796	788	792	792
	CH_3, OH	—	840	843	844
	CH_3, I	791	781	787	786
	CH_3, NH_2	845	840	—	844
(*b*)					
	Cl, SH	—	745	744	—
	Br, SH	—	727	727	—
	I, SH	—	714	718	—
	CH_3, SH	—	799	796	—

Le signe—signifie que la valeur correspondante n'a pas pu être calculée, ou observée.

suite à la vibration de déformation hors du plan γ (CH) dérivée de la vibration 5 du benzène; en effet, la seconde est théoriquement active en spectroscopie infrarouge dans le cas des dérivés de symétrie C_{2v}, tandis que la première ne l'est pas.*

* On admet que les deux vibrations de déformation hors du plan γ (CH) 11 et 10 *b* du benzène (ou 17 *b* et 10 *b* suivant l'attribution retenue pour la suite *III*) deviennent les deux vibrations γ(CX) et γ(CY), dont les fréquences sont inférieures à notre domaine d'observation.

Suite VI (I, I: 996; OCH_3, OCH_3: 1026). Elle groupe des fréquences de bandes infrarouges d'intensité très variable. Quelques raies Raman, très faibles et polarisées, ont été observées pour les composés dissymétriques à une fréquence correspondant à celle de la bande infrarouge. Nous proposons l'attribution de cette suite à une vibration de déformation dans le plan δ(CH), voisine de la vibration 18 *a* du benzène.

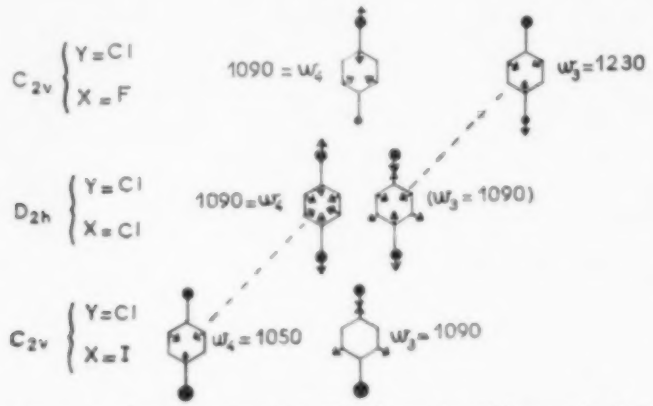

Fig. 5. Schémas de vibration permettant d'expliquer les déplacements de fréquences attribuées ω_3 et ω_4 (d'après KOHLRAUSCH [6]).

Suites VII (I, I: 1045; OCH_3,OCH_3: 1263); *Suite VIII*. (I, I: 1050; NO_2, NH_2: 1303). Les fréquences de ces suites varient beaucoup. Dans le cas des composés du type *p*-$C_6H_4X_2$, à l'exception du *p*-diméthoxybenzène et de l'αα′dibromoparaxylène, la suite *VII* est constituée uniquement de raies Raman, la suite *VIII* de bandes infrarouges. Pour les dérivés dissymétriques, la théorie permet de classer dans chacune de ces deux suites des bandes infrarouges et des raies Raman de fréquence voisine ou identique, correspondant à la même vibration. La forte polarisation et la grande intensité de ces raies Raman pour l'ensemble des composés imposent de les affecter à des vibrations totalement symétriques. Dans la majorité des cas, nous pensons que les suites *VII* et *VIII* correspondent aux vibrations de valence [YC_6H_4]—X et [XC_6H_4]—Y, les fréquences étant proches de celles attribuées habituellement aux vibrations C—X et C—Y des composés aliphatiques [46, 47]; cependant, dans le cas des benzènethiols et des dérivés halogénés et nitrés, la valeur élevée des fréquences ne permet pas de les assigner simplement à une vibration de valence.

Comme pour la raie *d*, KOHLRAUSCH [6] donne une explication originale de ces suites qu'il note *e* et *e*′. Pour lui, il y a interaction entre les vibrations de noyau 1 et 12 (ω_3 et ω_4 selon KOHLRAUSCH) avec les vibrations de valence CX et CY. Il imagine que cette interaction varie avec la masse du substituant, ainsi que l'illustre la Fig. 5. Cette interprétation se rapproche de celle donnée par LECOMTE et MANNEBACK [48] lorsque, à propos des éthylènes tétrasubstitués, ces auteurs envisagent un couplage variable entre une vibration C—X et une vibration de squelette. Dans le cas des dérivés paradisubstitués du benzène, il ne nous parait pas actuellement

possible de résoudre définitivement le problème de l'attribution des suites *VII* et *VIII*.

Suite IX (I,I: 1067; CH_3,NH_2: 1123). La suite *IX* groupe des bandes infrarouges souvent fortes. On peut, semble-t-il, les attribuer à une vibration de déformation dans le plan δ(C—H), voisine de la vibration 15 du benzène. Pour les composés dissymétriques, on doit attendre des raies Raman faibles; ces dernières apparaissent effectivement dans quelques cas; pour certains autres composés, elles sont peut-être dissimulées par les raies intenses des suites *VII* et *VIII*.

Suite X (Br, F: 1154; CH_3,CH_3: 1183). Cette suite comprend des raies Raman très intenses et fortement polarisées, ainsi que des bandes infrarouges correspondant à des raies Raman, pour la plupart des dérivés dissymétriques. Des bandes infrarouges, de fréquences très voisines des fréquences Raman, apparaissent aussi, contrairement aux règles de sélection, pour presque tous les dérivés symétriques; remarquons cependant qu'elles sont le plus souvent très faibles par rapport à celles attribuées à la vibration 18 *a*. Randle et Whiffen [11] ont expliqué l'éxistence de ces bandes par l'action du sulfure de carbone utilisé comme solvant. Nous avons vérifié que le même phénomène se produit pour les solutions dans le tétrachlorure de carbone.

En accord avec l'ensemble des auteurs, nous attribuons la suite *X* à une vibration de déformation dans le plan δ(C—H) totalement symétrique, dérivée de la vibration 9 *a* du benzène. En 1953, Nielsen [16, 17, 18] avait cependant placé cette vibration aux environs de 830 cm^{-1} et attribué les bandes de cette suite *X* à la vibration 3.

Suite XI (Br,F: 1276; CH_3,CH_3: 1313). Dans cette région, on attend une quatrième vibration de déformation dans le plan δ(C—H) se rapprochant de la vibration 3 du benzène, et active uniquement en spectroscopie Raman, pour les composés symétriques. Nous lui avons attribué les faibles raies Raman qui constituent la suite *XI*. Les dérivés dissymétriques présentent souvent une bande infrarouge faible dont la fréquence, voisine de celle observée en Raman, a été classée dans cette suite.*

Suite XII (I,I: 1377; CH_3,CH_3: 1463); *suite XIII* (I,I: 1402; CH_3,CH_3: 1480): *suite XIV* (I,I: 1467; CH_3,NH_2: 1518). Ces suites groupent des fréquences de bandes infrarouges intenses auxquelles correspondent parfois, dans le cas des dérivés dissymétriques de faibles raies Raman dépolarisées. Cependant, l'observation est souvent gênée pour les composés présentant des vibrateurs C—H aliphatiques par les absorptions de ces derniers dans cette région.

Par comparaison avec les dérivés monosubstitués du benzène, il semble que les deux suites *XIII* et *XIV* correspondent aux deux composantes de la vibration de noyau dégénérée du benzène 19 *ab*. La considération des schémas de vibration laisse prévoir pour la vibration 14 une fréquence peu différente de celles de la vibration 19 *b* (Fig. 2). C'est pourquoi, nous proposons de lui attribuer la suite *XII* dont les bandes sont comparables, en position et en intensité aux bandes de la suite *XIII*. Nous rappellerons cependant que l'attribution de la vibration 14 a été très discutée:

* Comme pour les vibrations γ(C—H) 11 et 10 *b*, on admet que les vibrations du benzène, 18 *b* et 9 *b*, se transforment dans le cas des dérivés paradisubstitués en vibrations de déformation dans le plan δ(C—X) et δ(C—Y).

LECOMTE [9] la situe à 1600 cm^{-1}, RANDLE et WHIFFEN [11] proposent 1300 cm^{-1}, NIELSEN indique 1437 cm^{-1} dans le *p*-difluorobenzène [16] 1614 cm^{-1} dans le *p*-fluorotoluène [18] et 1290 cm^{-1} dans les *p*-fluorohalogénobenzènes [19].

Suites XV et XVI (I,I: 1560; CH_3, CH_2: 1618). Ces suites sont formées de fréquences de raies Raman souvent intenses et très proches. Il arrive qu'une seule raie soit visible, on est alors amené à supposer qu'elle en contient deux, non résolues; la même remarque a été faite précédemment dans le cas de dérivés monosubstitués du benzène [49]. Comme pour ces derniers composés, cette hypothèse est confirmée par l'existence de deux bandes infrarouges, voisines des raies Raman, dans les spectres de la plupart des molécules *p*-C_6H_4XY. Nous attribuons les suites *XV* et *XVI* respectivement aux types de mouvement 8 *b* et 8 *a* issus de la vibration de noyau 8 *ab* du benzène. La diminution de symétrie due aux substituants dans le cas du *p*-diméthoxybenzène et du *p*-diéthoxybenzène se manifeste encore ici par l'apparition de bandes infrarouges.

Bandes propres aux substituants

Nous avons mentionné les vibrations de valence ν(C—X) dans la discussion des suites VII et VIII, il reste à considérer les principales fréquences caractéristiques des groupements substitués [46, 47].

Groupements contenant des CH aliphatiques [46, 47]

Dans la région des fréquences CH de déformation, les toluènes présentent des absorptions bien connues à 1380 et 1450 cm^{-1} dues respectivement aux vibrations $\delta(CH)_3$ symétrique et dégénérée. De plus, les spectres possèdent une bande très constante en position vers 1040 cm^{-1} qui a été attribuée à une vibration d'ensemble du groupe CH_3 ("rocking") [50].

Les spectres des anisoles contiennent trois ou quatre bandes dans la région de 1450 cm^{-1}, mais il est difficile de distinguer des bandes du noyau 14 et 19 *b* celles qui sont attribuables au groupement OCH_3. Aucune absorption n'est observée à 1380 cm^{-1}; enfin, une bande intense vers 1185 cm^{-1} semble caractériser la chaine C—O—C.

Les composés à groupement CH_2 ont un spectre complexe dans la région de 1450 cm^{-1} et possèdent de plus des bandes intenses vers 750 cm^{-1}.

Autres substituants

Les composés nitrés sont responsables de fortes absorptions vers 1520 et 1350 cm^{-1}; en outre, des raies Raman et des bandes infrarouges très intenses, situées près de 850 cm^{-1}, ont été attribuées aux vibrations C—(NO_2) dans les composés aromatiques [51].

Les anilines présentent une bande très intense à 1620 cm^{-1} caractéristique de la vibration de déformation $\delta(NH)_2$ [46, 47] et une autre vers 1050 cm^{-1} qui a été attribuée à une vibration d'ensemble (rocking) du groupement NH_2: $\rho(NH_2)$.

Les phénols présentent des absorptions vers 1180, 1210, 1330 et 1360 cm^{-1} qui ont été affectées au vibrateur (OH) libre et associé [53].

La vibration de déformation δ(SH) des benzènethiols se situe vers 915 cm^{-1} et est très fixe en position [54].

VOL. 12 1958

Bibliographie

[1] Kohlrausch K. W. F. *Phys. Z.* 1936 **37** 58.
[2] Paulsen O. *Mh. Chem.* 1939 **72** 244.
[3] Kohlrausch K. W. F. et Paulsen O. *Mh. Chem.* 1939 **72** 268.
[4] Herz E. et Wagner J., *Mh. Chem.* 1946 **76** 93.
[5] Herz E., Kohlrausch K. W. F. et Vogel R. *Mh. Chem.* 1946 **76** 200.
[6] Kohlrausch K. W. F. *Mh. Chem.* 1946 **76** 231.
[7] Lecomte J. *J. Phys. Radium* 1938 **9** 13.
[8] Delay A. *C.R. Acad. Sci., Paris* 1944 **219** 238.
[9] Depaigne-Delay A. et Lecomte J. *J. Phys. Radium* 1946 **7** 38.
[10] Lecomte J. *J. Phys. Radium* 1937 **8** 489.
[11] Randle R. R. et Whiffen D. H. *Molecular Spectroscopy* p. 111. Institute of Petroleum, London 1955.
[12] Lord R. C. et Andrews D. H. *J. Phys. Chem.* 1937 **41** 149.
[13] Herzfeld N., Hobden J. W., Ingold C. K. et Poole H. G. *J. Chem. Soc.* 1946 272.
[14] Bailey C. R., Carson S. C., Gordon R. R. et Ingold C. K., *J. Chem. Soc.* 1946 288.
[15] Delsemme A. H. *J. Chem. Phys.* 1950 **18** 1680.
[16] Ferguson E. E., Hudson R. L., Nielsen J. R. et Smith D. C. *J. Chem. Phys.* 1953 **21** 1457.
[17] Ferguson E. E., Mikkelsen L., Nielsen J. R. et Smith D. C. *J. Chem. Phys.* 1953 **21** 1731.
[18] Ferguson E. E., Hudson R. L., Nielsen J. R. et Smith D. C. *J. Chem. Phys.* 1953 **21** 1736.
[19] Narasimham N. A., El-Sabban M. Z. et Nielsen J. R. *J. Chem. Phys.* 1956 **24** 420.
[20] Thompson H. W. et Temple R. B. *J. Chem. Soc.* 1948 1432.
[21] Pitzer K. S. et Scott D. W. *J. Amer. Chem. Soc.* 1943 **65** 803.
[22] McMurry M. L. et Thornton V. *Analyt. Chem.* 1952 **24** 318.
[23] Turkevich J., McKenzie H. A., Friedman L. et Spurr R., *J. Amer. Chem. Soc.* 1949 **71** 4045.
[24] Van Dyke Tiers G. *J. Chem. Phys.* 1951 **19** 1072.
[25] Sponer H. et Kirby Smith J. S. *J. Chem. Phys.* 1941 **9** 667.
[26] Plyler E. K., Allen Jr., H. C. et Tidwell E. D. *J. Res. Nat. Bur. Stand.* 1957 **58** 255.
[27] Whiffen D. H. et Thompson H. W. *J. Chem. Soc.* 1945 268.
[28] Cole A. R. H. et Thompson H. W. *Trans. Faraday Soc.* 1950 **46** 2 103.
[29] Schimanouchi T., Kakiuti Y. et Gamo I. *J. Chem. Phys.* 1956 **25** 1245.
[30] Margoshes M. et Fassel V. A. *Spectrochim. Acta* 1955 **7** 14.
[31] Kross R. D., Fassel V. A. et Margoshes M. *J. Amer. Chem. Soc.* 1956 **78** 1332.
[32] Bellamy L. J. *J. Chem. Soc.* 1955 2818.
[33] Randle R. R. et Whiffen D. H. *Trans. Faraday Soc.* 1956 **52** 9.
[34] Young C. W., Duvall R. B. et Wright N. *Analyt. Chem.* 1951 **23** 709.
[35] Whiffen D. H. *Spectrochim. Acta* 1955 **7** 253.
[36] Kakiuti Y. *J. Chem. Phys.* 1956 **25** 777.
[37] Josien M. L. et Lebas J. M. *Bull. Soc. Chim. Fr.* 1956 53.
[38] Josien M. L. et Lebas J. M. *Bull. Soc. Chim. Fr.* 1956 57.
[39] Lebas J. M. et Josien M. L. *Bull. Soc. Chim. Fr.* 1956 62.
[40] Wilson E. B. *Phys. Rev.* 1934 **45** 706; 1934 **46** 146.
[41] Jones L. H. *J. Chem. Phys.* 1956 **24** 1250; 1957 **27** 1229.
[42] Bazhulin P. A., Uholin S. A., Liberman A. L. Novikov S. S. et Kazanskii B. A. *Izv. Akad. Nauk. SSSR. otdel khim. nauk* 1950 501.
[43] Magat M. *Effet Raman, Tables Annuelles des Constantes et Données Numériques* Vol. XII, Sect. 26. Hermann et Cie, Paris 1937.
[44] *American Petroleum Institute, Research Project* 44. Catalogue of Raman Spectra.
[45] Magat M. *Effet Raman, Tables Annuelles de Constantes et Données Numégriues* fascicule extrait du Vol. XI. Gauthiers–Villars, Paris.
[46] Bellamy L. J. *The Infrared Spectra of Complex Molecules. Methuen,* London 1954.

[47] Jones R. N., et Sandorfy C. *Infrared and Raman Applications. En Chemical Applications of Spectroscopy.* Interscience, New York 1956.
[48] Manneback C. et Lecomte J. *J. Phys. Radium* 1952 **13** 428.
[49] Lebas J. M., Garrigou-Lagrange C. et Josien M. L. *Cah. Phys.* 1956 **73** 31.
[50] Randle R. R. et Whiffen D. H. *J. Chem. Soc.* 1955 3497.
[51] Randle R. R. et Whiffen D. H. *J. Chem. Soc.* 1952 4153.
[52] Califano S. et Moccia R. *Gazz. Chim. Ital.* 1957 **87** 805.
[53] Barchewitz P. *C.R. Acad. Sci., Paris* 1953 **237** 237.
[54] Kohlrausch K. W. F. et Wittek H. *Mh. Chem.* 1941 **74** 1.
[55] Trenkler F. *Phys. Z.* 1936 **37** 338.
[56] Résultats personnels non publiés.
[57] Après l'envoi de notre manuscrit, nous avons eu connaissance des deux nouveaux articles de Whiffen relatifs aux dérivés paradihalogénés du benzéne: Stojiljkovic A. et Whiffen D. H. *Spectrochim. Acta* 1958 **12** 47; 1958 **12** 57.

VOL.
12
1958

Spectrochimica Acta, 1958, Vol. 12, pp. 321 to 331. Pergamon Press Ltd., London

The ultraviolet absorption spectrum of dicyanoacetylene*

F. A. MILLER and R. B. HANNAN, Jr.†
Mellon Institute, and Department of Chemistry, University of Pittsburgh, Pittsburgh 13, Pa.

(*Received* 19 *March* 1958)

Abstract—The ultraviolet absorption spectrum of dicyanoacetylene, N≡C—C≡C—C≡N, is reported for the first time. It was measured in solution, and in the vapor at both low and high resolution. There are two band systems:

	Wavelength	ε_{max} in *iso*octane	f	Vibrational structure	Postulated transition
1	2800 Å	8·4	$\sim 2 \times 10^{-5}$	Numerous sharp bands about 20 cm^{-1} apart	$^1\Sigma_g^+ \rightarrow {}^1\Sigma_u^-$
2	2680 Å	171	$\sim 4 \times 10^{-3}$	Four groups of six bands each, plus other weaker bands	$^1\Sigma_g^+ \rightarrow {}^1\Delta_u$

A vibrational analysis of the 2680 Å system is given which shows quite convincingly that the transition, which is electronically forbidden, is made vibrationally allowed by π_g vibrations. This is compatible with either $^1\Sigma_u^-$ or $^1\Delta_u$ symmetry for the upper state. The analogy to BEER's work on the polyacetylenes suggests strongly that the transition is $^1\Sigma_g^+ \rightarrow {}^1\Delta_u$, and that $^1\Sigma_u^-$ is the upper state for the other band system at 2800 Å.

DICYANOACETYLENE (N≡C—C≡C—C≡N, hereafter termed DCA) is an interesting molecule because it is the simplest example of three conjugated triple bonds. In earlier papers we have described its infrared and Raman spectra [1, 2] and an X-ray determination of its molecular structure [3]. This paper contains a description of the near ultraviolet absorption spectrum and a vibrational analysis of one of the two observed band systems.

Experimental procedures and results

The preparation of the sample has been described [1]. The ultraviolet spectrum was first obtained in *iso*octane solution with a Cary model 11 spectrophotometer. Concentrations ranged from 0·2 to 3·0 g/l. for 1 cm cells. The solution spectrum, shown in Fig. 1A, consists of four prominent bands below 2700 Å and one much weaker one near 2860 Å. The molar absorptivities for the band maxima are listed in Table 1.

Few molecules exhibit this much structure in their solution spectra, so we were encouraged to examine the spectrum of the vapor. This also was recorded

* A portion of a thesis submitted by R. B. HANNAN, JR. in partial fulfillment of the requirements for the degree of Doctor of Philosophy at the University of Pittsburgh, June 1952.

† Present address: Research Department, Standard Oil Co. of Indiana, Whiting, Indiana.

initially with the Cary instrument. Vapor pressures were 30 and 90 mm Hg in a 5 mm cell. The spectrum at 30 mm is shown in Fig. 1B. Upon going from solution to vapor there is a shift of 870 cm^{-1} toward higher frequencies, and each

Table 1. Molar absorptivities for the ultraviolet band maxima. *iso*Octane solution

λ (Å)	ε_{max} (l./mole cm)
2280	166
2400	162
2530	171
2680	97
2860	8·4

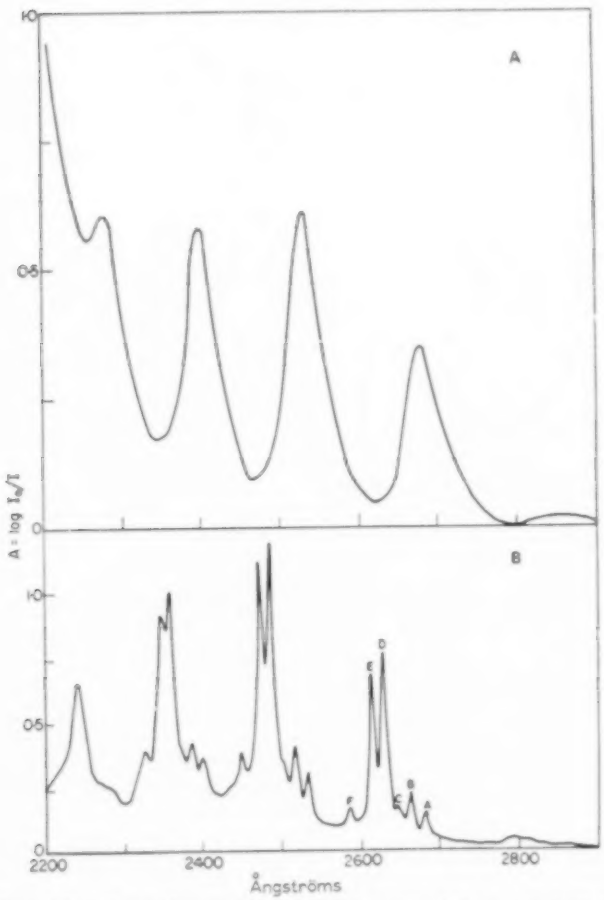

Fig. 1. Ultraviolet absorption spectrum of dicyanoacetylene. A. *iso*Octane solution, 0·275 g/l., 1 cm cell. B. Vapor, 30 mm celpressure, 5 cml.

VOL. 12 1958

of the four prominent bands in solution becomes six bands in the vapor. (See a later comment concerning the resolution of the low wavelength one.)

The added vibrational structure was in turn an incentive to measure the vapor spectrum with higher dispersion and resolving power. This was done with the first order of an Applied Research Laboratories' 2-meter grating spectrograph, which has a 24,400 line/in. concave grating (61,000 lines in all) in a Paschen mounting. The reciprocal dispersion at the film is 5·2 Å/mm.

Table 2. Observed frequencies for the 2680 Å band system of dicyanoacetylene, and their explanation

Group	Notn.	Obsd. (cm^{-1})	Estd. precision (±)	$\nu_{00}+\nu_1'+\nu_6'+\nu_7'+\nu_8'+\nu_9'+\nu_3'-\nu_6''-\nu_7''-\nu_8''-\nu_9''=$	Calcd. (cm^{-1})	Diff.
1	A_1^1	37,301	1	37,814 1 2 1 1 1	37,302	1
	A_1^2	309	1	37,814 1	310	1
	B_1^1	545	1	37,814 1 1 1	543	−2
	B_1^2	552	1	37,814 1	551	−1
	C_1^1	776	3	37,814 1 1	768	−8
	C_1^2	794	1	37,814 1 1	785	−9
	D_1	38,074	3	37,814 1	38,074	0
	E_1	272	3	37,814 1	272	0
	F_1^1	665	3	37,814 1 1	665	0
	F_1^2	690	3	37,814 2 1 1	690	0
	F_1^3	699	1	37,814 2	698	−1
2	A_2^1	39,492	1	37,814 1 2 1 2	39,486	−6
	A_2^2	502	1	37,814 1 1 1 1	494	−8
	A_2^3	511	1	37,814 1 1	502	−9
	B_2	753	5	37,814 1 1	743	−10
	C_2^1	938	5	37,814 1	?	
	C_2^2	39,954	>5	37,814 1	?	
	C_2^3	966	3	37,814 1 1 1	960	−6
	C_2^4	976	1	37,814 1 1 1	977	1
	D_2	40,266	3	37,814 1 1	40,266	0
	E_2	464	5	37,814 1 1	464	0
	F_2^1	853	1	37,814 1 1 1 1 1	849	−4
	F_2^2	862	1	37,814 1 1 1	857	−5
3	A_3	41,685	5	37,814 2 1	41,679	−6
	B_3	935	5	37,814 2 1	920	−15
	C_3	42,147	>5	37,814 2 1 1	137	−10
	D_3	444	5	37,814 2 1	443	−1
	E_3	640	5	37,814 2 1	641	+1
	F_3	43,028	>5	37,814 2 1 1	42,034	+6

Vibrational frequencies from Table 5.
′ = Upper state.
″ = Lower state.

Light from a Beckman hydrogen lamp was focused by a quartz condensing lens through the absorption cell and onto the slit. The cell was a Pyrex tube 40 cm long and 4·5 cm in diameter with quartz windows sealed on with Glyptal. An exposure time of 30 min was required with Eastman 103F film.

Two different fractions of the sample were vaporized into the cell, and spectra were recorded for each at 1, 20, and 80 mm Hg. An iron arc reference spectrum partially overlapped each absorption spectrum. The two spectra were scanned consecutively with a Leeds and Northrup recording densitometer, and wave-

lengths were determined by interpolation. Tests showed that the error of re-setting to the starting point between the two scans was less than 0·1 Å, or 1·4 cm^{-1}.

Higher resolution clearly demonstrated the presence of two band systems. The more intense one begins about 2680 Å (37,300 cm^{-1}) and extends toward lower wavelengths. It consists of the four well-spaced groups of bands with six major bands in each group. The bands are degraded to the red, showing that the moment of inertia is larger in the excited state. The frequencies are listed in Table 2, together with an estimate of the precision of measurement. Higher

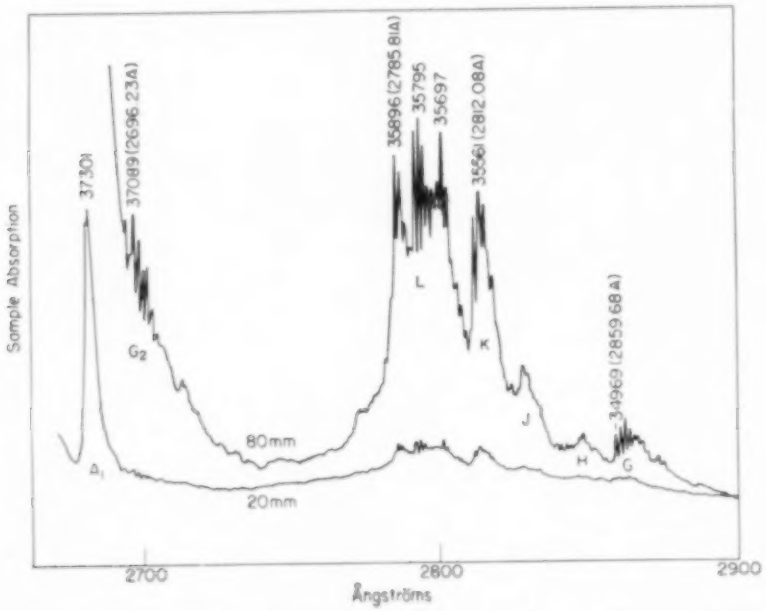

Fig. 2. Densitometer tracing of the 2800 Å band system of dicyanoacetylene; 80 and 20 mm pressure, 40 cm cell.

resolution also revealed measurable satellites for some of the six major bands. There are about fifteen other bands which can be seen on the tracings but cannot be measured with enough accuracy to warrant listing them. All six bands of the fourth, or high frequency group, were clearly evident but unfortunately could not be measured reliably. They were not resolved by the Cary instrument (Fig. 1B) because its slit widths were too wide in this region.

The other band system is centered near 2800 Å (35,700 cm^{-1}), and is shown in Fig. 2. Its main feature is a group of five or six bands, each having a further remarkable fine structure of relatively sharp bands with a separation of roughly 20 cm^{-1}. Their half intensity band widths are 10 cm^{-1}. The frequencies of the thirty-five sharp bands which could be measured are given in Table 3; still others can be seen on the densitometer trace. This band system partially overlaps the other one, as can be seen from the fine structure around 2700 Å in Fig. 2. It is much weaker than the other system. A vapor pressure of 80 mm is required to

VOL. 12 1958

Table 3. Observed frequencies for the weak 2800 Å band system of dicyanoacetylene

Band and intensity	ν (cm^{-1})	$\Delta\nu$	Band and intensity	ν (cm^{-1})	$\Delta\nu$
G (w)	34,878				
		13		716	19
	891				22
		19		738	
	910				19
		20		757	
	930				21
		21		778	
	951				17
		18		795	
	969				19
				814	
		386			22
				836	
J (w)	35,355				25
				861	
		132			18
				879	
K (m)	35,487				17
		20		896	
	507				24
		12		920	
	519				
		15			1081
	534				
		6	G_2 (w)	37,001	
	540				24
		21		025	
	561				21
				046	
		57			20
				066	
L (s)	35,618				23
		18		089	
	636				35
		25		124	
	661				
		18			
	679				
		18			
	697				

Relative intensities within the system: w = weak; m = medium; s = strong.

show it properly, whereas 1 mm brings out all the main features of the first system.

Although it is possible that this weak system may be due to an impurity, we shall assume that it really belongs to DCA. If the fine structure is rotational, a small moment of inertia must be involved. This implies either a very slightly bent DCA in the excited state, or a small impurity molecule.

The oscillator strengths of the two band systems have been measured crudely. We find for the 2680 Å system $f \simeq 4 \times 10^{-3}$, and for the 2800 Å system, $f \simeq 2 \times 10^{-5}$.

A brief, unsuccessful attempt was made to obtain the fluorescence spectrum. An unfiltered high pressure mercury arc (General Electric type AH-6) produced marked decomposition of the sample. With filters, no fluorescence was observed.

Symmetry of the electronic states

It is certain from the intensities that both band systems are due to forbidden transitions—the 2680 Å one being moderately forbidden, and the 2800 Å one strongly so. We now consider what electronic states are involved.

Our earlier work [1, 2, 3] has shown that the molecule is linear and symmetrical in its normal state. The ground electronic state therefore has symmetry $^1\Sigma_g^+$ of $D_{\infty h}$. (HERZBERG's notation [4] will be used throughout.)

When considering the electronic symmetry of the excited state, one must at the same time consider the symmetry of the nuclei. Does DCA remain linear and symmetrical, does it become linear but unsymmetrical, or is it bent in the upper state? This is not easy to answer, because in the last few years it has become apparent that the nuclear symmetry often—perhaps usually—changes in going from the ground electronic state to an excited one. Thus acetylene [5] and carbon disulfide [6] are linear in the ground state and bent in an excited state, while the converse is true for NO_2 [7] and the NH_2 radical [8]. Formaldehyde changes from planar to slightly nonplanar when absorbing in the near ultraviolet [9]. The best-known example where nuclear symmetry is preserved is benzene, which retains its D_{6h} configuration in several excited states; however it has the added geometrical restraint of ring closure. More pertinent to our present case is diacetylene, which has the same nuclear symmetry in the ground and in two excited states [10].

We were unable to get any clue from the spectrum in determining either the nuclear symmetry or the symmetry of the electronic wavefunction in the upper state. A paper by BEER on the polyacetylenes [11] provided the needed suggestion. BEER's conclusions concerning the four observed band systems of dimethyltriacetylene, $CH_3—C{\equiv}C—C{\equiv}C—C{\equiv}C—CH_3$ (hereafter termed DMTA), are summarized in Table 4. DCA has the same conjugated bond system as DMTA, plus a pair of non-bonding electrons on each nitrogen atom. It should therefore exhibit all the π–π transitions of DMTA, and in addition may show n–π transitions [12]. Actually we have observed fewer, not more, transitions for DCA, and we assume that n–π transitions are not among them.

Table 4 shows that there is a striking similarity between the two band systems of DCA and two of those for DMTA—in intensity, vibrational structure, and

VOL. 12 1958

relative positions. Therefore by analogy to BEER's conclusions for DMTA, we postulate that the very weak 2800 Å absorption is a $^1\Sigma_g^+ \rightarrow {}^1\Sigma_u^-$ transition. Unfortunately we have not been able to deduce any further information about this system, and it will not be discussed further.

Table 4. Electronic transitions for dimethyltriacetylene (DMTA)* and dicyanoacetylene (DCA)

Transition	Characteristics	DMTA (cm^{-1})	DMTA (Å)	DMTA f	DCA (cm^{-1})	DCA (Å)	DCA f
$^1\Sigma_g^+ \leftarrow {}^3\Sigma_u^+$	Phosphorescence	22,300	4500	8×10^{-9}	Not studied		
$^1\Sigma_g^+ \rightarrow {}^1\Sigma_u^-$	Extremely weak	30,340	3300	2×10^{-5}	35,700	2800	2×10^{-5}
$^1\Sigma_g^+ \rightarrow {}^1\Delta_u$	Vibrational structure in soln., $\varepsilon_{max} \simeq 150$†	32,700*	3060	5×10^{-3}	37,300	2680	4×10^{-3}
$^1\Sigma_g^+ \rightarrow {}^1\Sigma_u^+$	Vibrational structure in soln., $\varepsilon_{max} > 135{,}000$†	48,300*	2090	- -	Not studied		

* Reference [11].
† Ethanol solution data for DMTA from Armitage, Cook, Jones, and Whiting, J. Chem. Soc. 1952, 2010.
f = Oscillator strength.

On the same grounds we postulate that the 2680 Å band system is due to a $^1\Sigma_g^+ \rightarrow {}^1\Delta_u$ transition. This is admittedly only an educated guess at this stage, but it serves as a working hypothesis. We shall see shortly what further information the vibrational analysis provides.

Vibrational structure of the 2680 Å system

Selection rules

The general requirement for spectroscopic activity of a transition is that $\psi' \times \psi''$ shall have the same symmetry as one of the components of a translation, where ψ' and ψ'' are wavefunctions for the upper and lower states respectively. The pure electronic transition $^1\Sigma_g^+ \rightarrow {}^1\Delta_u$ is therefore forbidden. It is an example of what PLATT terms a "momentum forbidden, or orbitally forbidden" transition, with an oscillator strength of 10^{-1}–10^{-3} for condensed ring systems [12].

Such electronically-forbidden transitions may be made "vibrationally-allowed" by a simultaneous change in both electronic and vibrational energy. The symmetry requirement is that the symmetry of the product $\psi'_{el}\psi'_{vib}\psi''_{el}\psi''_{vib}$ shall be that of a component of the translation. Let us consider the case of absorption from the ground state for DCA. Then the requirement is that $^1\Delta_u \times (\psi'_{vib}) \times {}^1\Sigma_g^+ \times \sigma_g^+ = \Sigma_u^+$ or Π_u. This can be fulfilled only if ψ'_{vib} has the symmetry π_g. Thus if our postulate concerning the upper electronic state is correct, we should find that electronic transitions which start from the ground state are accompanied by an odd-quantum change in a π_g vibration. The same requirement will hold for transitions which start from excited vibrational levels of the lower state and terminate in the ground vibrational level of the upper state.

The fundamental vibration frequencies of DCA are summarized in Table 5 [1, 2].

Vibrational analysis

The chief feature of the 2680 Å band system is a group of six bands which is repeated at 2192 cm^{-1} and then again at 2177 cm^{-1} toward higher frequencies.

Table 5. Fundamental vibrational frequencies of dicyanoacetylene

Species	Notn.	Ground state (cm^{-1})	Upper state (cm^{-1})
σ_g^+	1	2290	$1r_1 = 2192$ $2r_1 = 2192 + 2177 = 4369$
	2	2119	—
	3	692	591 ?
σ_u^+	4	2241	—
	5	1154	—
π_g	6	504	458
	7	263	260
π_u	8	472	443 ?
	9	107	99

This is obviously a v' progression of the totally-symmetric vibration r_1 whose value in the ground state is 2290 cm^{-1}. From the two values $r_1' = 2192$ and $2r_1' = 4369$ one finds the anharmonic term $x_e r_e$ to be approximately 7·5 cm^{-1}. It is curious that no progression was found for either of the other two totally symmetrical vibrations.

The six major bands of a group will be designated A, B, ... F in order of increasing frequency (cf. Fig. 1B). Bands of the first, or lowest frequency, group are given subscript 1, those of the second group subscript 2, and so on. When a major band has several components, they will be given superscripts as, for example, A_1^1 and A_1^2. Table 2 gives for each measured band the notation, the measured frequency, and our explanation of it. It is noteworthy that bands D and E appeared to be single in each of the groups.

The origin of the band system is clearly somewhere in the lowest-frequency group, and we now consider the spacings within this group. The strongest lines should involve a change of one quantum in a π_g vibration in addition to the change in electronic energy. There are only two π_g fundamental vibrations; in the ground electronic state they are $r_6 = 504$ and $r_7 = 263$ cm^{-1} (Table 5). Thus the four transitions $r_{0,0} - 504$, $r_{0,0} - 263$, $r_{0,0} + r_7'$, and $r_{0,0} + r_6'$ should be prominent. These are shown in Fig. 3 as A, B, D, and E respectively.

It will be noted that $B - A$ should be $504 - 263 = 241$. This spacing is indeed observed. There is a complication, however, because in the first group

VOL. 12 1958

both A and B are double bands with separations of 8 and 7 cm^{-1} respectively (Table 2). One finds that $B_1^1 - A_1^1 = 244$ and $B_1^2 - A_1^2 = 243$ cm^{-1}. It is not easy to choose which pair corresponds to the simple transitions of Fig. 3, but there are two weak arguments in favor of the latter one. Both are based on the premise that vibrational frequencies will be smaller in the upper electronic state than in the lower.

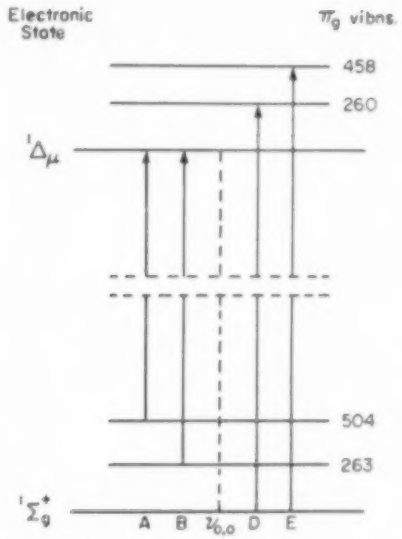

Fig. 3. 2680 Å band system: the four principal transitions within a group.

(1) If the "extra" components are on the low frequency side, they can be explained as "hot bands" involving the 107 cm^{-1} fundamental ν_9. Thus A_1^2 would be thought of as $\nu_{0,0} - 504$, and A_1^1 as $\nu_{0,0} - 504 - (\nu_9 - \nu_9')$. Incidentally this fixes $(\nu_9 - \nu_9')$ as 8 or 9 cm^{-1}, which gives $\nu_9' = 99$ cm^{-1}.

(2) The analogue of the 263 cm^{-1} frequency can now be calculated for the upper state. It is $D - B = 263 + \nu_7'$. If B_1^1 is used, $\nu_7' = 266$, which is slightly larger than the lower state value of 263. On the other hand B_1^2 gives $\nu_7^1 = 259$, which is slightly smaller.

These reasons are certainly weak, but they have led us to adopt A_1^2 and B_1^2 as the simple transitions of Fig. 3. A_1^1 and B_1^1 are considered to be hot bands as described above. The *origin of the band system* (ν_{00}) will then be given by $A_1^2 + 504$ or $B_1^2 + 263 = 37{,}814$ cm^{-1}. Finally, the upper state analogue of the 504 cm^{-1} fundamental can now be evaluated from $E_1 = \nu_{00} + \nu_6'$, from which $\nu_6' = 458$ cm^{-1}.

The upper state vibrational frequencies have also been included in Table 5. Table 2 gives the detailed explanation of each band, and a comparison of the calculated with the observed frequencies.

It will be noted that the intensities are consistent with this explanation of bands A, B, D, and E. Fig. 1B shows that bands A and B, which start from excited vibrational levels, are less intense than bands D and E which start from

the ground level. Also A is less intense than B, as befits the smaller population of its starting level.

The next features to be explained are the bands designated F. The strongest component, F_1^1, is displaced from ν_{00} by 851 cm^{-1}. There are several possible explanations for it, because it may be any of the allowed transitions A, B, D, or E plus another totally-symmetrical vibrational change. The one which we favor is $D + 591$, where $591 = \nu_3'$, the totally symmetric C—C stretch in the upper state (692 in the ground state.)

The other two components F_1^2 and F_1^3 are at higher frequency, and are separated by 9 cm^{-1}. This reminds one of the separations in A and B. We shall therefore try to account for F_1^3, and then explain F_1^2 as a hot band. One possibility is $F_1^3 = \nu_{00} + 885 = \nu_{00} + 2 \times \nu_8'$. This transition is allowed, since the pure electronic change plus two quanta of a π_g or two quanta of a π_u vibration has the correct symmetry. Then $2\nu_8' = 885$, and $\nu_8' \simeq 443$. (This obviously needs verification.) F_1^2 would then be $F_1^3 - (\nu_9 - \nu_9') = F_1^3 - 8$.

There remains band C, the weakest of the six. Actually it consists of two components displaced downward from the band origin by 38 and 20 cm^{-1}. We explain this as a v–v transition of a π_g or a π_u vibration superimposed on the electronic transition.

This is allowed, but it is expected to be weak. There are four possibilities:

$$\nu_{00} - 504 + 458 = \nu_{0,0} - 46$$
$$\nu_{00} - 263 + 259 = \nu_{0,0} - 4$$
$$\nu_{00} - 472 + 443 = \nu_{0,0} - 29\ (?)$$
$$\nu_{00} - 107 + 99 = \nu_{0,0} - 8$$

The second stage hot bands, $\nu_{00} - 2\nu_i + 2\nu_i'$, are also allowed. The most probable one is $\nu_{00} - 2(107 - 99) = \nu_{00} - 16$. Unfortunately none of these is really close to the observed $\nu_{00} - 38$ or $\nu_{00} - 20$. However one can understand qualitatively how very weak bands can appear at frequencies slightly lower than ν_{00}.

The second group of six bands repeats the same pattern at higher frequencies. D_2 and E_2 are 2192 cm^{-1} higher in frequency than D_1 and E_1. (These were used because they are single and sharp.) Therefore the "secondary origin" for this group is $\nu_{00} + 2192 = 40{,}006$ cm^{-1}. The only real difference is that the number of satellite bands is different; there are now three lines at A, four at C, and only two at F. Our explanations follow along the same lines as for group 1, but the numerical agreement is somewhat less good. They are summarized in Table 2. The four C bands are displaced downward from the secondary origin of the group by 68, 52, 40, and 30 cm^{-1}, and we can not account for the first two.

The third group is displaced by an additional 2177 cm^{-1}, and here no satellites were observed. Unfortunately no reliable measurements were made for the fourth group. The numerical agreement between predicted and observed frequencies shown in Table 2 is not as good as one would wish. It is difficult to measure some of the bands precisely because of their shape, and any errors in locating the "secondary origin" of a group will introduce errors into all the calculated frequencies for that group.

VOL. 12 1958

Conclusions

The results for the 2680 Å band system can be summarized as follows:

(1) The transition is moderately forbidden, as shown by its intensity.

(2) One quantum of a π_g vibration, and only π_g, makes the transition allowed. The evidence for this is threefold. (a) The separation $504 - 263 = 241$ is found in the spectrum as $B - A$. (b) The intensities are exactly what one would expect for this. Those for A, B, D, and E have already been mentioned. The moderately strong F and the very weak C fit in perfectly. (c) All the main features can be reasonably explained on this basis.

(3) Unfortunately this does not suffice to prove that the upper electronic state is $^1\Delta_u$. One finds that *exactly* the same symmetry requirements hold if the upper state is assumed to be $^1\Sigma_u^-$! Transitions to both are made allowed by π_g vibrations. In both cases the transition moment is perpendicular to the molecular axis. We see no basis for preferring one or the other except the analogy to the polyacetylenes in Table 4. This analogy, if valid, clearly points to $^1\Delta_u$.

(4) Finally, there is no need to postulate a bent molecule in the upper state to account for the observations made so far. A retention of the $D_{\infty h}$ nuclear configuration, with a $^1\Delta_u$ wavefunction (or, less probably, a $^1\Sigma_u^-$ wavefunction) is indicated.

Acknowledgement—One of the authors (F. A. M.) is most appreciative to the John Simon Guggenheim Memorial Foundation for the grant of a fellowship during which this material was prepared for publication.

References

[1] Miller F. A. and Hannan R. B., Jr., *J. Chem. Phys.* 1953 **21** 110.
[2] Miller F. A., Hannan R. B., Jr. and Cousins L. R., *J. Chem. Phys.* 1955 **23** 2127.
[3] Hannan R. B., Jr. and Collin R. L., *Acta. Cryst.* 1953 **6** 350.
[4] Herzberg G., *Infrared and Raman Spectra* p. 119. Van Nostrand, New York 1945.
[5] Ingold C. K. and King G. W., *J. Chem. Soc.* **1953** 2702.
[6] Kleman B., *Abstracts of Symposium on Molecular Structure and Spectroscopy* p. 33. Department of Physics and Astronomy, Ohio State University, Columbus, Ohio 1956.
[7] Robinson G. W., *Abstracts of Symposium on Molecular Structure and Spectroscopy* p. 53. Department of Physics and Astronomy, Ohio State University, Columbus, Ohio 1957.
[8] Ramsay D. A., *J. Chem. Phys.* 1956 **25** 188.
[9] Robinson G. W., *Canad. J. Phys.* 1956 **34** 699.
[10] Callomon J. H., *Abstracts of Symposium on Molecular Structure and Spectroscopy* p. 12. Department of physics and Astronomy, Ohio State University, Columbus, Ohio 1955.
[11] Beer M., *J. Chem. Phys.* 1956 **25** 745.
[12] Platt J. R., *J. Opt. Soc. Amer.* 1953 **43** 252.

Spectrochimica Acta, 1958, Vol. 12, pp. 332 to 337. Pergamon Press Ltd., London

Quantitative spectrographic analysis of the rare earth elements—IX

Determination of rare earth impurities commonly associated with purified samarium, gadolinium, terbium, and yttrium*

R. N. Kniseley, V. A. Fassel, B. B. Quinney, C. Tremmel, W. A. Gordon, and W. J. Hayles
Institute for Atomic Research and Department of Chemistry, Iowa State College, Ames, Iowa

(*Received* 18 *December* 1957)

Abstract—Emission spectrometric methods are described for the following quantitative determinations: neodymium and gadolinium in samarium; neodymium, samarium, terbium, europium, yttrium, dysprosium and holmium in gadolinium; samarium, gadolinium, terbium, dysprosium, holmium, and erbium in yttrium; and samarium, gadolinium, yttrium and dysprosium in terbium. These methods cover the concentration range from the detection limit up to 1 per cent. The basic method involves the direct-current carbon arc excitation of rare earth oxide–graphite mixtures, utilizing the unique similarity in excitation behavior of many of the rare earths to provide a high degree of internal standardization. The coefficient of variation is less than ±5 per cent in all instances.

VOL. 12 1958

Introduction

This article is an extension of previously published emission spectrometric procedures [1, 2, 3] for the determination of rare earth impurities in purified rare earth matrices. In this paper pertinent details are presented for the determination of impurities in purified samarium, gadolinium, terbium, and yttrium. Since impurity concentrations above 1 per cent can usually be determined by spectrophotometric [4, 5, 6] and other spectrometric procedures [7, 8, 9], the methods described cover the concentration ranges from the detection limits up to 1 per cent.

Apparatus

The spectrograph, external optical system, excitation source, electrode assembly, photographic processing, and microphotometry employed in these investigations have been previously described [1]. The pertinent information is summarized in Table 1.

Excitation conditions

The considerations involved in the selection of direct current carbon arc excitation of the samples in the form of rare earth oxide–graphite mixtures have been given in detail [1]. Briefly stated, these factors were as follows: the desirability of exciting the samples under conditions requiring a minimum of preliminary

* Contribution No. 564. Work was performed in the Ames Laboratory of the U.S. Atomic Energy Commission.

Table 1. Equipment and operating conditions

Spectrograph	Jarrell-Ash 3·4 m Wadsworth grating spectrograph
Sample charge	15 mg, 50% sample, 50% graphite; 30 mg, 50% sample, 50% graphite for determination of impurities in Y_2O_3
Electrode	Anode: 18 mm length of 6 mm diameter graphite rod with 2 mm deep cavity and wall thickness of $\frac{1}{2}$ mm, supported on a 3 mm diameter graphite rod
	Cathode: 40 mm length of 3 mm graphite rod pointed on one end
Excitation	D.c. arc; 250 V, 18 A, 4 mm analytical gap
Exposure time	Complete sample consumption + approximately 10 sec.*
Emulsions	Spectrum Analysis No. 1 (3000–4200), Kodak M (3800–4500)
Wave length	3200–4400 Å second order
Slit width	40 μ
Emulsion calibration	Two-step sector preliminary curve method
Densitometer	Applied Research Laboratories Comparator-Densitometer

* The precision for the element pair Dy/Tb was greatly improved by terminating the exposure after 60 sec. This eliminates the portion of the exposure during which the intensity ratio is changing rapidly (see Fig. 1).

sample preparation, consequently the oxide form as obtained from most fractionation procedures was used; the convenience and sensitivity of the d.c. carbon arc for exciting the spectra of refractory oxides; the enhanced stability of the discharge on the addition of powdered graphite to the electrode charge; and the high degree of internal standardization obtainable from rare earth systems because of the unique similarity in excitation behavior among many of the rare earths.

Selection of line pairs

In selecting analysis lines, a concerted effort was made to select the strongest impurity line free of interference from lines of the matrix and from lines of other rare earth impurities which may occur simultaneously in the sample. Because of uncertainties in matrix purity, the differentiation of persistent lines of an impurity rare earth from weak lines of the matrix presented a serious problem. As previously outlined [2], visual observation of line intensities and densitometric measurements of selected line pairs in successive samples from ion-exchange column fractions of highly purified rare earths provided an excellent method for the selection of analysis lines. The analysis lines selected were necessarily a compromise between maximum sensitivity of detection and minimum spectral interference. In many cases less sensitive alternate analysis lines were selected for use in instances where interferences from other rare earth impurities prohibit the use of the more sensitive analysis lines. Likewise, it was often necessary to select more than one internal standard line in order to cover the desired concentration range with minimum spectral interference.

In each case the selected line pair was subjected to a variation in excitation current covering the range from 10 to 19 A. Only the line pairs which showed a negligible change ($< \pm 5$ per cent) in intensity ratio over this current range were selected.

Moving plate studies were conducted in all cases in order to determine the relative volatilities of the impurity elements with respect to the matrix and thereby

Table 2. Data on analytical line pairs

Matrix	Line pair (Å)*	Detection limit (%)	Useful conc. range (%)	Conc. index (%)	Background correction	Remarks
Gd_2O_3	Ho 3453·14	0·02	0·05–1·0	0·3	Yes (below 0·1%)	
	Gd 3394·18*					
	Eu 4435·53	0·02	0·05–2·0	0·13	No	
	Gd 4437·45*					
	Nd 4012·250	0·02	0·05–1·0	0·45	No	Very weak Gd line under Nd 4012. Equivalent to ~0·01% Nd_2O_3.
	Gd 3391·705					
	Dy 3385·027	0·01	0·05–1·0	0·25	No	Weak Ho line under Dy 3385·027 interferes at Ho_2O_3 concentrations >0·5%.
	Gd 3394·18*					
	Dy 3978·573	0·1	0·10–1·0	0·25	Yes	
	Gd 3984·803				No	
	Y 3628·706	0·05	0·10–2·0	0·34	No	
	Gd 3637·742					
	Sm 3634·271	0·05	0·10–2·0	0·50	No	
	Gd 3637·742					
	Tb 3324·40	0·01	0·02–2·0	0·20	Yes (below 0·1%)	A neighboring Gd line may interfere with Tb 3324·40 unless high dispersion (2·5 Å/mm) is used.
	Gd 3321·7*					
Sm_2O_3	Nd 4303·57	0·02	0·05–1·0	0·28	Yes	
	Sm 4300·19*					
	Gd 3439·990	0·02	0·05–1·0	0·25	Yes	
	Sm 3500·008					
Tb_4O_7	Dy 3898·544	0·02	0·05–1·0	0·5	Yes	High dispersion (2·5 Å/mm) is necessary to separate these lines sufficiently for quantitative use.
	Tb 3898·734		0·20–1·0	0·6	No	
	Y 3982·595	0·005	0·02–1·0	0·18	Yes	
	Tb 3986·970		0·10–1·0	0·14	No	
	Sm 4280·779	0·03	0·05–1·0	0·23	Yes	
	Tb 4249·05		0·10–1·0	0·15	No	

VOL. 12 1958

	Gd 3350·480 / Tb 3347·27	0·01	0·03–0·5 0·10–1·0	0·11 0·067	Yes No	
	Gd 3350·480 / Tb 3347·8*	0·01	0·10–1·0	0·06	No	
Y_2O_3	Sm 4334·149 / Y 4291·034	0·05	0·10–2·0	0·8	No	Weak Dy line interferes with Sm at Dy_2O_3 concentrations $>0·1\%$.
	Gd 3350·482† / Y 3377·711	0·005	0·04–2·0	0·23	No	A weak Dy line falls at the low wavelength side of Gd 3350 ($\sim$0·05 Å). Unless sufficient resolution is available this line interferes at Dy_2O_3 concentrations $>0·5\%$.
	Gd 4327·104 / Y 4291·034	0·05	0·10–2·0	1·4	No	
	Tb 3218·93 / Y 3182·42	0·02	0·04–2·0	0·79	No	
	Tb 4318·85 / Y 4315·46	0·05	0·10–2·0	1·5	No	Sm 4318·935 interferes at Sm_2O_3 concentrations $>0·2\%$.
	Dy 3407·80 / Y 3450·95	0·005	0·05–2·0	0·5	No	There is a very weak Y line interference (equivalent to $\sim$0·005% Dy_2O_3) with Dy 3407·80. A weak Y line at slightly lower wave-length ($\sim$0·25 Å) may be used as an internal standard line for the visual estimation of Dy at low concentrations. When the intensity ratio is $\sim$1 the Dy content is $\sim$0·01%. When the intensity ratio is 0·8 the Dy content is $<0·005\%$.
	Dy 3407·80 / Y 3469·43*	0·005	0·01–2·0	0·04	No	
	Ho 3453·13 / Y 3450·95	0·007	0·05–2·0	1·0	No	La 3453·168 interferes but La is very seldom present. Y 3453·45 does not interfere but may be mistaken for Ho 3453·13 unless care is taken.
	Ho 3453·13 / Y 3469·43*	0·007	0·02–0·2	0·09	No	
	Er 4007·967 / Y 3955·095	0·005	0·01–2·0	0·5	No	
	Er 4007·967 / Y 3987·497	0·005	0·01–2·0	0·29	No	

* Wavelengths marked with an asterisk were measured by the authors; all other wavelengths were taken from the MIT wavelength tables.

† Recent experiments indicate that Gd 3422·466 is more sensitive provided the cyanogen band interference is removed by utilizing a nitrogen free atmosphere for excitation.

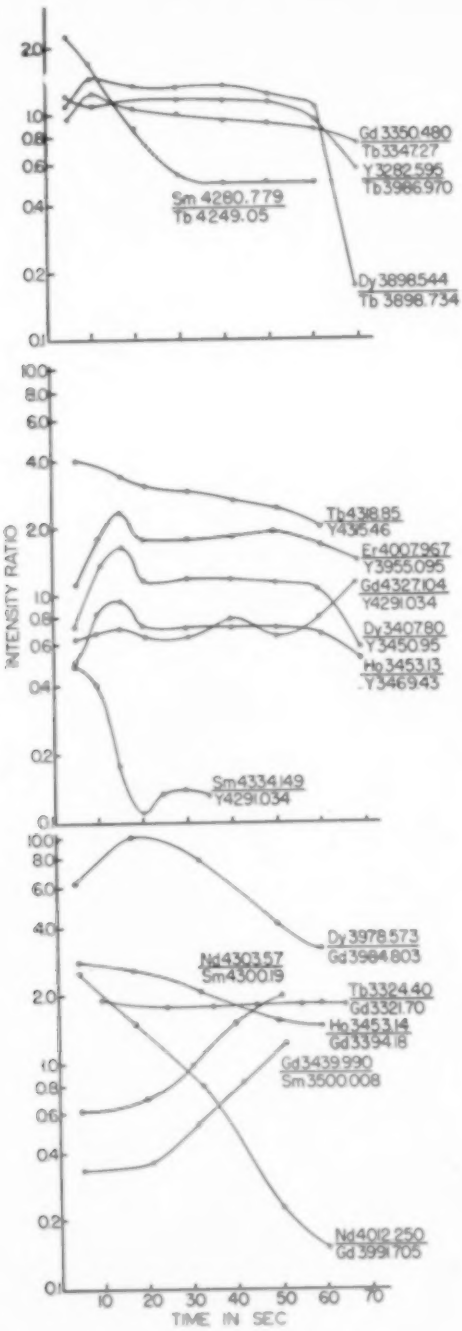

Fig. 1.

VOL. 12 1958

estimate the degree of internal standardization. The results of these studies are reproduced in Fig. 1.

The line pairs selected are presented in Table 2 along with the analytical data concerning these lines. Table 2 also lists the important interferences which may cause difficulty when these line pairs are employed. In cases where background corrections were necessary, readings were restricted to those steps where the background under both lines was between 70 and 85 per cent transmission. This restriction minimized the errors inherent in making background corrections.

While no extensive precision studies were made, replicate exposures of the standards over the entire concentration range and on individual plates showed that in no case did the percentage deviation from the mean exceed 5 per cent. It is interesting to note that even though the element pairs Sm/Y and Nd/Gd show a considerable dissimilarity in their vaporization behavior the reproducibility of their intensity ratios is not seriously impaired. This is reminiscent of the total energy method in which the net relative intensity of the analysis line is related to the concentration without reference to an internal standard. In the case of these two line pairs the internal standard lines probably serve only as a correction for errors in weighing and slight optical changes which would effect the results if only the net relative intensities of the analysis lines were used.

The lack of other methods for the determination of these impurities at the concentration levels involved precluded the verification of the analytical results obtained by the spectrographic methods. However, the results from a series of recovery experiments indicated that the accuracy was within the limits of the reported precision.

Acknowledgements—The authors wish to express their appreciation to Dr. F. H. Spedding and his associates for providing the rare earth materials used in these investigations and to Mr. C. F. Lentz for his many helpful suggestions during the course of this work.

References

[1] Fassel V. A. and Wilhelm H. A., *J. Opt. Soc. Amer.* 1948 **38** 518.
[2] Fassel V. A., Cook H. D., Krotz L. C. and Kehres P. W., *Spectrochim. Acta* 1952 **5** 201.
[3] Fassel V. A., Quinney B. B., Krotz L. C. and Lentz C. F., *Analyt. Chem.* 1955 **27** 1010.
[4] Moeller T. and Brantley J. C., *Analyt. Chem.* 1950 **22** 433.
[5] Prandtl W. and Scheiner K., *Z. anorg. Chem.* 1952 **220** 107.
[6] Rodden C. J., *J. Res. Nat. Bur. Stand.* 1941 **26** 557; 1943 **28** 265.
[7] Fassel V. A., *J. Opt. Soc. Amer.* 1949 **39** 187.
[8] Norris J. A. and Pepper C. E., *Analyt. Chem.* 1952 **24** 1399.
[9] Heidel R. H. and Fassel V. A., *Analyt. Chem.* 1958 **30** 1761.

Spectrochimica Acta, 1958, Vol. 12, pp. 338 to 349. Pergamon Press Ltd., London

The infrared spectra of crystalline H_2O, D_2O and HDO*

D. F. Hornig,† H. F. White and F. P. Reding‡
Metcalf Chemical Laboratories, Brown University, Providence, Rhode Island

(*Received* 20 *March* 1958)

Abstract—The infrared spectra of normal and deuterated ice prepared by freezing the liquid or by condensing the vapor were studied at temperatures down to −190°C. No important spectral differences between the various specimens were found. The infrared spectra of H_2O, HDO and D_2O at −190°C were compared and the spectrum of crystalline HOD identified. Starting from the HOD spectrum the spectra of H_2O and D_2O could be clarified. The band at 2230 cm^{-1} in ice is identified as the second overtone of a librational mode. The stretching region of ice consists of $2\nu_2$ at about 3150 cm^{-1}, ν_2 at about 3240 cm^{-1} and ν_1 at about 3350 cm^{-1}; D_2O is analogous. The cross-over between the frequency of ν_1 and ν_3 in passing from gas to solid is caused by a change in the stretch–stretch interaction constant. Its magnitude in ice, $f_{12} = 0{\cdot}3$ cm dyn/Å, can be roughly explained on electrostatic grounds. The spectrum of the overtone region shows that the barrier to proton transfer in ice is greater than 27 kcal/mole.

VOL. 12 1958

Despite the simplicity of its component molecules, the spectrum of ice has resisted satisfactory interpretation, partly because of problems relating to the structure of ice and partly because of certain difficulties which occur in the spectra themselves. We have attempted to clarify the situation by a careful study of the infrared spectra of crystalline H_2O, D_2O and HDO, by utilizing the method of dilute isotopic substitution to isolate the effects of the static crystalline field, and by conducting our studies at several temperatures on samples prepared in different ways.

The structure of the oxygen lattice in ice at temperatures above −80°C has long been established [1, 2, 3, 4]. As a result of recent neutron diffraction studies it now appears that the positions of the protons as well are known [5, 6] and correspond to those predicted by the Pauling model [7]. In this model each oxygen atom is surrounded tetrahedrally by other atoms at a distance of 2·76 Å; it is also surrounded by four protons on the O· · · · O lines, two at 1·02 Å and two at 1·74 Å, but there are no preferred orientations for the "near" and "distant" protons. One of the questions in which we were interested was the effect of this proton disorder on the spectrum. A related question concerns the effect on the spectrum of the probable potential minimum along each O · · · O line corresponding to the possibility of proton transfer in the process:

$$2H_2O \rightarrow OH_3^+ + OH^-$$

When water vapor is condensed at temperatures between −80°C and −140°C a cubic phase is deposited [8, 9, 10, 11, 12]. In the cubic phase each oxygen atom is surrounded tetrahedrally by oxygen atoms at a distance of 2·75 Å and the

* Based in part on Ph.D. theses submitted in partial fulfillment of the requirements for the Ph.D. degree at Brown University by F. P. Reding, June 1951 and H. F. White, October 1952.
† Present address: Dept. of Chemistry, Princeton University, Princeton, N.J.
‡ Present address: Union Carbide Chemicals Co., Charleston, W. Va.

protons may be disordered, exactly as in the "ordinary" hexagonal phase. One way of viewing the difference is that the six bonds radiating from the two oxygen atoms at the ends of a given O · · · · O axis are "opposed" in the hexagonal form and "staggered" in the cubic form. It seems unlikely that the two crystalline phases can be distinguished spectroscopically since the nearest neighbor geometry is identical in the two forms.

All of the electron and X-ray diffraction investigations have also found that when water vapor is deposited on a base maintained at a temperature below about −140°C a solid is formed which gives only a diffuse diffraction pattern [8, 12, 13, 14]. Calorimetric investigations have found evidence of a phase change at about −130°C with a very small heat of transition, between 2 and 7 cal/g according to PRYDE and JONES [15], or "not less than 6 cal/g" according to STARONKA [16]. It is not yet clear whether this low temperature material is microcrystalline or glassy but the present evidence seems to favor the latter [11].

The region of the fundamental vibrations in the infrared spectrum of ice was carefully studied near the freezing point by FOX and MARTIN [17] who found broad bands corresponding to the bending (ν_2) and stretching (ν_1 and ν_3) of the H_2O molecules at 1644 and 3256 cm^{-1}. Their spectra show an unresolved shoulder on the high frequency band at ca. 3400 cm^{-1} and a secondary peak in the low frequency band at 1530 cm^{-1}. Since our work was started GIGUERE and HARVEY have reported the infrared spectrum of solid H_2O and D_2O [18]. In addition to those previously reported, they found strong bands at 850 cm^{-1} in H_2O (−170°C) and 630 cm^{-1} in D_2O, similar to those observed by REDING [19] at 812 and 605 cm^{-1}, which presumably originate in the liberational motions of the H_2O molecules. The overtone region, which is important with regard to the question of proton transfer, has only been slightly studied [20, 21, 22].

Experimental

The infrared spectra were obtained on a Perkin-Elmer Model 83 spectrometer modified for double beam operation as described previously [23]. Most of the specimens were prepared by freezing distilled water in a glass tube, connecting it to a vacuum system, degassing the ice, and then allowing it to warm very slowly so that vapor passed to the absorption cell, where it was condensed slowly on a carrier plate of KBr, CaF_2, AgCl or KRS-5 in a low temperature cell similar to those described previously [24]. A few specimens were also prepared by freezing water in a cell consisting of two AgCl plates separated by strips of Pt 0·048 mm thick or strips of AgCl 0·250 mm thick. The plates were fused at the edges with a hot glass rod, leaving a small hole on one edge for filling.

The 100 per cent transmission line was determined before each run by taking the spectrum of the cell with carrier plate but no sample. The spectra reported are with respect to this baseline. Stray radiation was reduced in the region beyond 1000 cm^{-1} with a scattering filter made from a KBr plate etched in ethanol [25] and in the KRS-5 region with a reflection filter made from stainless steel ground with AO 103 grinding compound. The stray radiation amounted to 16 per cent at 400 cm^{-1}, 40 per cent at 300 cm^{-1} and rose rapidly to about 50 per cent at 273 cm^{-1}. However, in the KRS-5 region the samples were corrected

for stray radiation by taking a spectrum both of the sample and of the sample plus a $\frac{1}{4}$ in. thick NaCl plate which would pass only stray radiation. The difference was taken as the true absorption.

Results

The solid lines in Fig. 1 show the absorption spectrum of ice formed above $-78°C$ and studied at $-78°C$ in the region 700 to 3700 cm^{-1}. The solid curve

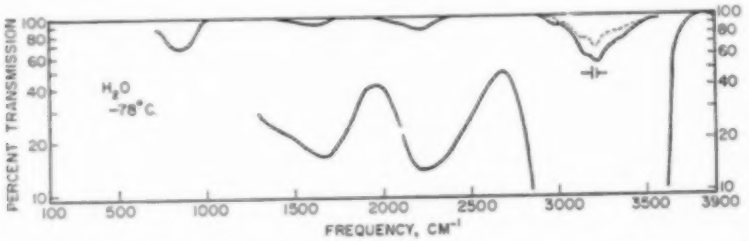

Fig. 1. The infrared absorption spectrum of ice deposited from the vapor at $-78°C$. Solid curve obtained at $-78°C$. and dotted curve at $-190°C$.

showing high absorption was obtained by freezing ice in the 0·048 mm thick AgCl cell and cooling to $-78°C$; the other solid curve was obtained by condensation from the vapor at $-78°C$. The dotted line shows the spectrum when the previous sample was cooled to $-190°C$. Figure 2 shows curves obtained with films deposited from the vapor at $-190°C$.

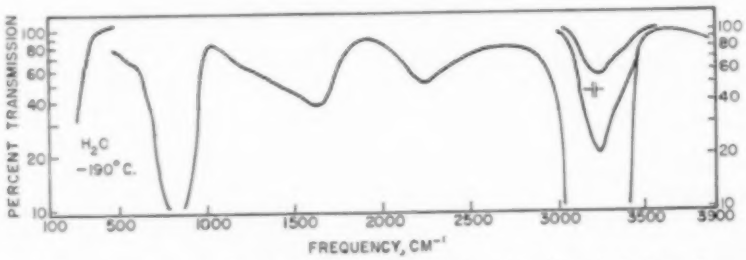

Fig. 2. The infrared absorption spectrum at $-190°C$ of ice deposited from the vapor at $-190°C$.

Several points emerge from these spectra. In the first place, the two at $-78°C$ are in reasonable agreement. The peak of the bending band (1620 cm^{-1}) is at a slightly higher frequency in the film deposited from the vapor at $-78°C$ than in that produced by freezing the liquid, but it is doubtful whether differences of the order of 20 cm^{-1} are significant in such a broad band. In the second, the frequencies found in the film produced at $-190°C$ do not differ appreciably from those produced at $-78°C$ or above, so that if a different phase is produced the effect on the spectrum is small, except in one point, the intensity reversal between the 1600 cm^{-1} and 2200 cm^{-1} bands. On the other hand, even this point is in doubt since Fox and Martin, who produced their specimens by freezing the liquid, found the 1600 cm^{-1} band to be more intense at $-7°C$ than the 2250 cm^{-1} band, as did Giguere and Harvey with specimens at $-55°C$.

VOL. 12 1958

The ice produced at −78°C or above was certainly hexagonal ice; the ice produced at −190°C was presumably either the cubic ice, the glass or a mixture of the various forms such as was found by SHALLCROSS and CARPENTER [12]. The slightly better resolution of the components of the stretching band found in the "ordinary ice" suggests that the low temperature specimens may have been glasses or mixtures. Since except for the intensity reversal the spectra

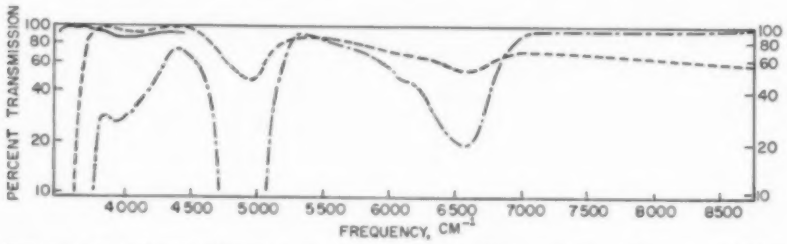

Fig. 3. The infrared absorption spectrum of ice in the overtone region at −190°C.

of Fig. 2 and Fig. 1 are in agreement, all of the rest of our work was done on ice produced at −190°C.

The spectra in the overtone region of two films frozen from water are shown in Fig. 3. It is interesting that the 250 μ thick specimen scattered practically no light whereas the 50 μ sample scattered 40 per cent of the incident beam at 8500 cm^{-1}, showing the importance of good specimens.

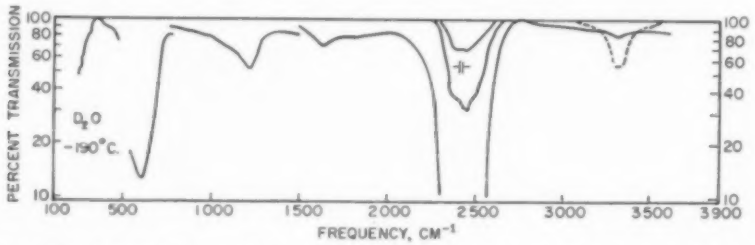

Fig. 4. The infrared absorption spectrum at −190°C of solid D_2O deposited from the vapor at −190°C.

The infrared absorption spectrum of D_2O produced and studied at −190°C is shown in Fig. 4. The band at 605 cm^{-1} appears more intense than it actually is since the cell was outfitted with NaCl windows whose absorption is superimposed on the D_2O absorption. By comparing the O—H stretching band at 3310 cm^{-1} with the O—D stretching band at 2436 cm^{-1} it is seen that the sample contained much less than 1 per cent H_2O. Very similar results were obtained by MAISCH in this laboratory [26] who froze D_2O liquid samples between AgCl plates and studied their spectra at temperatures down to −190°C.

These observations and earlier ones are summarized in Table 1, together with our assignments. Some of the previous Raman studies [27–32] are summarized in Table 2.

Table 1. Infrared spectra of H_2O and D_2O (cm^{-1})

Assignment	H_2O				D_2O	
	Ref. [17] (−7°)	Ref. [18] (−55°)	This work (−78°)	This work (−190°)	Ref. [17] (−55°)	This work (−190°C)
$\nu_L - \nu_T$				520		385
ν_L		820	830	812	610	605
$2\nu_L$	1530	1500	—	—		
ν_2	1644	1650	1620	1620	1210	1212
$3\nu_L$	2222	2240	2230	2230	1620	1627
	—	—	ca. 3020	—		
$2\nu_2$			3140	(3170)*		(2380)*
ν_3	3256	3240	3220	3240	2440	2440
ν_1	ca. 3400	—	3400	(3380)*		(2520)*
$\nu_3 + \nu_L$		4150	4050			
$\nu_1 + \nu_2, \nu_3 + \nu_2$		5000	4940		3720	
$2\nu_1, 2\nu_2, \nu_1 + \nu_3$						
$\nu_1 + 2\nu_2$			6100			
$\nu_3 + 2\nu_2$			6580			
ν_{OH} (HDO)†					3295	3310

* Estimated.
† 3285 cm^{-1}, according to ref. [26].

Table 2. Raman frequencies of crystalline H_2O and D_2O

H_2O		D_2O	
Previous*	Ref. [26]	Ref. [26]	Ref. [32]
3147	3159	2347	2330
3258	3275		2445
3348	3370	2514	2500
			2690

* Averaged from ref. [27, 28, 29, 30 and 31].

Table 3. Infrared spectra of mixtures of H_2O, HDO and D_2O at −190°C (cm^{-1})

$\%H_2O$	100	69	23	2	0
%HDO	0	28	50	26	1
$\%D_2O$	0	3	27	72	99
	520	—	—	—	385
	—	—	620	620	605
	812	790	790	800	—
	—	—	1220	1210	1212
	—	1470	1470	1480	—
	1620	1620	1630	1610	1627
	—	1950	1925	—	—
	2230	2220	—	—	—
	—	2440	2440	2440	2440
	3240	3250	3290	3300	3310

VOL. 12 1958

Since in both H_2O and D_2O the first overtone of the liberational frequency falls on the bending frequency, and the first overtone of the bend falls on the stretch, the various frequencies may be located with much more certainty in HDO where this does not occur. The spectra of a series of compositions of H_2O–D_2O are illustrated in Fig. 5 and the absorption frequencies listed in Table 3. These mixtures were made by mixing distilled H_2O with a known volume of

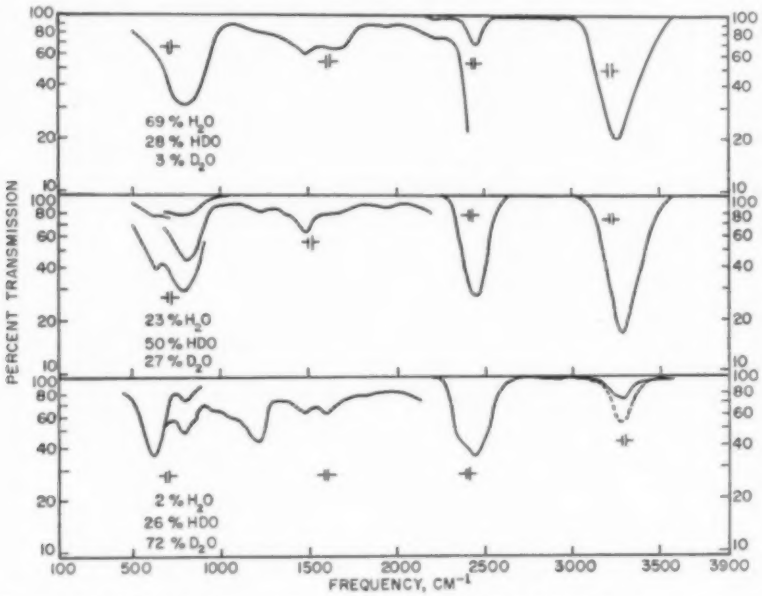

FIG. 5. The infrared absorption spectrum of solid H_2O–HDO–D_2O mixtures at −190°C.

99·75 per cent D_2O. Each mixture was shaken for a period of from 5 to 15 min to insure equilibrium before the samples were attached to the vacuum system and degassed. They were later analyzed gravimetrically. All of the films were condensed from the vapor at −190°C.

Liberational frequencies

Since it seems likely that some features of the ice spectrum have been misunderstood in the past, a number of points merit discussion. In the first place it is clear that the low frequency absorption must be ascribed to the librational motion of the molecules in the lattice. All three molecules (H_2O, HDO, D_2O) may have three librational frequencies. Except for the loss of symmetry resulting from crystalline perturbations, two of these should be active in H_2O and D_2O and one, libration about the two-fold axis, should be inactive in the infrared spectrum. Since the two active modes both involve rotation of the total molecular dipole moment they ought to be of about equal intensity. Furthermore, if the external field in which each proton lies is cylindrically symmetrical about the O—H · · · · O it is easily shown that to a good approximation the three frequencies would be equal [33].

It seems likely, therefore, that in both the H_2O and D_2O spectra the two active frequencies are unresolved and lie beneath the intense absorption peaks at 812 and 605 cm^{-1}. In that case the weak peaks at 520 cm^{-1} (H_2O) and 385 cm^{-1} (D_2O) may correspond to librations about the two-fold axis. The activity presumably arises then because the axis of libration does not coincide exactly with the two-fold axis or because local electric fields in the crystal polarize the molecule.

In HDO all three frequencies may be active. Since one of the principal axes lies close to the O—D bond (7°) and one fairly close to the O—H bond (14°), one of the libration frequencies must be only slightly higher than in D_2O and another slightly lower than in H_2O. That this is the fact is clearly seen in Fig. 5 and Table 3. The third libration in HDO is about an axis perpendicular to the symmetry plane and should have an intermediate frequency. The three HDO frequencies should be roughly in the ratio $1 : 2/\sqrt{3} : \sqrt{2}$ so it should be found at about 670 cm^{-1}. However, no clear indication of its presence can be found in our spectra.

Information about the librations can also be obtained from another source. It has been customary to ascribe the band at 2230 cm^{-1} in H_2O to a combination of the bending vibration at 1620 cm^{-1} with a libration. A corresponding band is observed at 1627 cm^{-1} in D_2O where the bending vibration occurs at 1212 cm^{-1}. With the usual interpretation, the libration frequencies involved are 610 and 415 cm^{-1}. In HDO the bend is found at 1470 cm^{-1} so the analogous interpretation requires a lattice frequency of 455 cm^{-1} to explain the band at 1925 cm^{-1}. These lattice frequencies do not coincide with any of those observed experimentally so it must be concluded that this explanation is incorrect.

These difficulties are resolved if in fact these bands in all three molecules are the second overtone of the librations. In that case the librational frequencies in D_2O, HDO and H_2O are 540, 648 and 743 cm^{-1} if no allowance is made for anharmonicity. The ratios of the frequencies, 0·73 : 0·87 : 1·00, are not far from the expected values, 0·71 : 0·82 : 1·00, if the libration involved is that about the axis perpendicular to the symmetry plane. If the anharmonicity were taken into account the fundamental frequencies would certainly be slightly higher so that these infrared active modes undoubtedly contribute considerably to the intense low frequency peaks in the spectra.

If this analysis were complete we could conclude that the three librational frequencies of HDO occur at about 620, 650 and 790 cm^{-1}, that the two infrared active librations of H_2O occur in the region 750–900 cm^{-1} and of D_2O in the region 550–650 cm^{-1}, and that the librations about the two-fold axes (infrared inactive) occur at 520 and 385 cm^{-1} in H_2O and D_2O respectively. In order to test these conclusions we can note that to the extent that these librational frequencies are decoupled from molecular vibrations and from translational lattice vibrations (and they are probably quite well decoupled) the isotope product rule can be applied to them to yield.

$$\frac{\prod_i \nu_{Li}^{H_2O}}{\prod_i \nu_{Li}^{HDO}} = 1{\cdot}70 \qquad \frac{\prod_i \nu_{Li}^{D_2O}}{\prod_i \nu_{Li}^{HDO}} = 0{\cdot}64$$

VOL. 12 1958

The previously mentioned frequencies do not satisfy the relationships at all. In particular, if it is assumed that the HDO frequencies are approximately correct and two of the H_2O frequencies are near 800 cm^{-1}, then the third should lie above 800 cm^{-1}; similarly, if two D_2O frequencies are near 600 cm^{-1}, the third ought to be also. Unless an HDO frequency with strong infrared activity exists in the region between 400–500 cm^{-1}, and this seems unlikely both from the spectra and on theoretical grounds, we are forced to conclude that the weak bands at 520 cm^{-1} (H_2O) and 385 cm^{-1} (D_2O) are not librational fundamentals, despite the fact that their frequency ratio is correct. The only alternative is that they are difference bands involving the librations and the translational modes which occur at about 210 cm^{-1} in both H_2O [27, 28, 30, 32] and D_2O [32].

We conclude, then, that all three librational modes in H_2O have frequencies near 800 cm^{-1}, and in D_2O near 600 cm^{-1}, and that in HDO the frequencies are about 620, 650 and 790 cm^{-1}.*

The bending mode

Another problem which concerned us was whether the absorption peaks at 1620 and 1212 cm^{-1} have been ascribed correctly to the bending vibrations, which occur at 1595 cm^{-1} and 1179 cm^{-1} in gaseous H_2O and D_2O. Our doubts arose from two sources; (a) the peaks in question are just at the position expected for the overtone of the librational frequency and (b) it might have been anticipated that the large hydrogen bonding forces in the crystal could cause a considerable increase in the frequency of ν_2 in going from gas to crystal. For example, if the slight displacement of the oxygen atom from the center of gravity is neglected, and it is assumed that the bending force constant f_g is the same in ice as in gaseous H_2O, but that the protons are in an external potential field characterized by a force constant f_l, then it is found straightforwardly [17] that the bending frequency in the crystal is given by:

$$\lambda_c = \lambda_l + \lambda_g$$

where $\lambda = 4\pi^2\nu^2$, λ_g is the value in the gas phase and λ_l is derived from the librational frequency.

Utilizing the value, 800 cm^{-1}, for the approximate value of the librational frequency in ice, the predicted value of the bending frequency would be 1780 cm^{-1}.

In HDO the overtones of the librations ought not to overlap the bending vibration and the bending frequency at 1470 cm^{-1} is found to be a relatively sharp peak compared to the extended bands in pure H_2O and D_2O. This frequency is quite consistent with 1620 cm^{-1} in H_2O and 1212 cm^{-1} in D_2O. However, in the absence of a good potential function in the crystal it does not allow an exact prediction of the H_2O and D_2O frequencies. The structure on the low frequency side of these bands in the pure crystals must be the band arising from the overtone band of the coupled librations and the maximum found by Fox and Martin at

* It has been pointed out to us by Dr. C. Haas (who has managed to observe the splitting due to intermolecular coupling in the stretching region) that if the proton–proton interaction is as great in the librational as in the stretching modes these conclusions need modification. In this case the band width arising from intermolecular coupling would exceed 200 cm^{-1} so that not only would each mode be broadened but the three modes would be strongly mixed. This would not affect our conclusions in H_2O and D_2O but might obliterate the distinctions in HDO.

1530 cm^{-1} suggests a librational frequency of 765 cm^{-1}, consistent with our previous findings.

We may then ask why all these bending frequencies are so much lower than those estimated by the hydrogen bonding argument. At least one possibility is that these vibrations are much more anharmonic in the crystal than in the gas and this possibility is supported by our analysis of the stretching regions.

Stretching vibrations

The region of the O—H stretching vibrations in ice has presented a persistent puzzle. There is evidence of structure in the main infrared peaks of both H_2O and D_2O at 3240 cm^{-1} and 2440 cm^{-1}, and three peaks, a sharp low frequency peak and two more diffuse peaks, have been reported in the Raman spectra of both substances (see Table 2).

The Raman peaks were originally thought to be characteristic of H_2O molecules with different degrees of coordination [28] but this explanation can no longer be considered valid in the light of modern neutron diffraction and X-ray studies which show all H_2O molecules to be 4-co-ordinated [1–12]. It appears that the three peaks must instead be essentially $2\nu_2$, ν_1 and ν_3.

An explanation along these lines is complicated by several factors. In the first place Fermi resonance may take place between $2\nu_2$ and ν_1. Secondly, the entire region may be overlapped by the third overtone of the lattice vibration. In the third place, the intermolecular coupling of the O—H oscillations may be so strong as to make the ν_1, ν_3 distinction unclear. It is quite possible that this is the case since in boric acid, for example, the intermolecular OH · · · · OH interaction force constant is −0·09 m dyn/Å [34]. As a result the splitting produced by the coupling of the motion of adjacent molecules may be of the same order of magnitude as the ν_1–ν_3 splitting.

These difficulties can be circumvented by studying dilute solutions of HDO in either H_2O or D_2O. In the first case the O—D oscillator has a frequency removed from any of those of the H_2O host lattice; in the second the same can be said of the O—H vibration. Furthermore, neither is overlapped by overtones of the bending or librational modes of HDO.

From the O—H band in the spectrum of 99 per cent D_2O, the uncoupled O—H stretching frequency is 3310 cm^{-1}* and the width at half maximum absorption about 100 cm^{-1}. In contrast to either pure H_2O or pure D_2O, the peak is symmetrical, as would be expected from a single vibration. Similarly, in the 3 per cent D_2O, 28 per cent HDO, 69 per cent H_2O specimen, a symmetrical O—D stretching peak with a width of about 75 cm^{-1} is observed at 2440 cm^{-1}, although this D_2O concentration is already high enough so that many of the HDO molecules have deuterium containing neighbors. The conclusion seems inescapable that the much wider bands in the pure compounds ought not to be associated with the individual OH · · · · O hydrogen bonds, as is usually done, but rather with the coupling of the motions of the molecules in the disordered crystals and overlapping of the several peaks in this region.

From the HDO spectra one can compare the O—H and O—D stretching frequencies in the three phases as follows [35]:

VOL. 12 1958

	Gas	Liquid	Solid
O—H	3707	3405	3310
O—D	2727	2520	2440

The intramolecular coupling of these vibrations leads to the usual ν_1–ν_3 splitting, the intermolecular coupling to a further splitting of each which, as we have pointed out before, is of the same order of magnitude. Although we have not carried out a detailed analysis, it can be anticipated that in a disordered structure in the intermolecular coupling will yield symmetrical structureless bands so that the resultant spectrum should consist of two overlapping bands, symmetrical about the uncoupled frequency, and with a separation about equal to their width, so that they should be unresolved or just barely resolved. From this argument it follows that in H_2O the two Raman peaks at about 3250 cm^{-1} and 3350 cm^{-1} must be associated with the O—H oscillations and the peak at 3148 cm^{-1} with $2\nu_2$.

In D_2O the interpretation is not quite as clear. Gross and Val'kov have found four Raman peaks at 2330 cm^{-1}, 2445 cm^{-1}, 2500 cm^{-1} and 2690 cm^{-1} [32]. In a low resolution study with a photoelectric Raman spectrometer, Maisch [26] found a strong sharp peak at 2347 cm^{-1} and a broader asymmetric peak at 2514 cm^{-1}. Since Maisch's peaks correspond to the first and third reported by Gross and Val'kov, it appears that there is a calibration difference of about 15 cm^{-1} between the two investigations but otherwise general agreement. The sharp peak at 2330 cm^{-1} is clearly analogous to the ice peak at 3148 cm^{-1} and must therefore be $2\nu_2$. From the coupling arguments, the pair at 2445 cm^{-1} and 2500 cm^{-1} must be the two O—D stretching vibrations. The peak at 2690 cm^{-1} is very weak and was not observed by Maisch. It may well be a combination of the translational lattice vibration at about 210 cm^{-1} [32] with the O—D stretching mode at 2500 cm^{-1}.

The shape of the infrared peaks in both ordinary and low temperature ice suggests secondary peaks on both sides of the main maximum. Their estimated positions are included in Table 1 and they correlate roughly with the Raman peaks, particularly if it is noted that the Raman measurements were made at 0°C and a shift to lower frequencies might be expected at −190°C.

Any detailed analysis of this region, particularly of the intensity distribution, must also take account of the Fermi resonances. Our failure to observe the overtone of the bending mode of HDO shows that its intrinsic intensity is low. The fact that this is not the case in H_2O or D_2O must be ascribed to a strong Fermi interaction in these cases. Nevertheless, a consistent picture is now obtained. In both H_2O and D_2O there is a strong sharp Raman peak which must be ascribed to the overtone of the bending vibration and a pair which originates in the stretching motion. In both cases the low frequency member of the pair is weak in the Raman spectrum but dominates the infrared spectrum so it is probably chiefly the ν_3 motion, whereas the reverse is true of the high frequency peak, which is probably chiefly ν_1.

It might be objected that the symmetric frequency, ν_1 is lower in the gas phase than is the antisymmetric frequency, ν_3. If coupling to the bending mode is neglected, the separation of the two is given by:

$$\nu_1 - \nu_3 = 2(g_{11}f_{12} + g_{12}f_{11})$$

where g and f have their usual significance [36]. This relation, to a good approximation, can be written:

$$\frac{\lambda_1 - \lambda_3}{\lambda_1 + \lambda_3} = \frac{f_{12}}{f_{11}} + \frac{g_{12}}{g_{11}}$$

f_{11} is approximately $6{\cdot}1 \times 10^5$ dyn/cm in these molecules so if $f_{12} = 0{\cdot}30 \times 10^5$ dyn/cm, the observed splittings are reproduced to within the experimental error. The inversion is apparently caused, therefore, by the change in the stretch–stretch interaction force constant.

The potential function in ice

Because of the importance of the hydrogen bond it would be interesting to know more about the potential in which the proton moves in the O—H $\cdots$ O system. It is usually thought to show two minima of unequal depth separated by a potential maximum. The second minimum corresponds to the transfer of a proton and the difference in energies corresponds to the heat of the reaction $2H_2O \rightarrow OH^- + OH_3^+$ in the ice crystal. The spectra allow certain partial conclusions to be reached. In the vicinity of 6000–6500 cm^{-1} three levels are expected, which would be identified as $2\nu_1$, $2\nu_3$ and $\nu_1 + \nu_3$ if the system were reasonably harmonic. The expected absorption is observed so that the maximum in the barrier must be considerably higher. The fact that no absorption is observed in the region between about 6700 cm^{-1} and 8000 cm^{-1} implies that the barrier is still higher since otherwise the levels $3\nu_3$ and $3\nu_1$ would drop into this region. Consequently we conclude that the barrier to proton transfer in ice is greater than 9600 cm^{-1} or 27 kcal/mole.

The other point of interest concerns the positive sign of f_{12}. It was observed by Fox and Martin that the intensity of the O—H stretching band was greater in ice than in water or the gas, corresponding to a greater effective charge on the protons. This is reasonable since polarization of the O—H bond by the oxygen atom to which it is hydrogen bonded would be expected. If the interaction term, f_{12}, resulted from the electrostatic repulsion between the effective charges on the two protons in a given H_2O molecule, its magnitude would be:

$$f_{12} = \frac{-e^2 r_{O-H}^2}{r_{H-H}^5}[4\cos\phi + \cos^2\phi + 3]e'^2$$

where e is the electron charge, e' the ratio of effective charge to the electronic charge, r_{O-H} and r_{H-H} the O—H and H—H distances and ϕ the H—O—H angle. If the angle is approximately tetrahedral, $\cos\phi = -\frac{1}{3}$ and

$$f_{12} = 0{\cdot}62\, e'^2 \times 10^5 \text{ dyn/cm}$$

The observed value of f_{12}, $0{\cdot}30 \times 10^5$ dyn/cm, would therefore be reproduced if $e' = 0{\cdot}7$. This seems a little high but is consistent with the high intensities found

VOL. 12 1958

by Fox and Martin. It parallels the evidence for a high degree of polarization of the HCl and HBr molecules in their low temperature crystalline phases [37].

References

[1] Dennison D. M., *Phys. Rev.* 1921 **17** 20.
[2] Bragg W. H., *Proc. Phys. Soc.* 1921 **34** 98.
[3] Barnes W. H., *Proc. Roy. Soc.* A 1919 **125** 670.
[4] Megaw H. D., *Nature, Lond.* 1934 **134** 900.
[5] Wollan E. O., Davidson W. L. and Shull H. G., *Phys. Rev.* 1949 **75** 1348.
[6] Peterson S. W. and Levy A. A., *Phys. Rev.* 1953 **92** 1082.
[7] Pauling L., *J. Amer. Chem. Soc.* 1935 **57** 2680.
[8] Koenig H., *Z. Krist.* A 1944 **605** 229.
[9] Lisgarten N. D. and Blackmann M., *Nature, Lond.* 1956 **128** 39.
[10] Honjo G., Kitamura N., Shimaoka K. and Mihama K., *J. Phys. Soc., Japan* 1956 **11** 527.
[11] Blackmann M. and Lisgarten N. D., *Proc. Roy. Soc.* A 1957 **238** 93.
[12] Shallcross F. V. and Carpenter G. B., *J. Chem. Phys.* 1957 **26** 782.
[13] Burton E. F. and Oliver W. T., *Nature, Lond.* 1935 **135** 505.
[14] Vegard L. and Hilleslund S., *Avh. norske Vidensk Akad.* 1924 **8** 1.
[15] Pryde J. A. and Jones G. O., *Nature, Lond.* 1952 **170** 685.
[16] Staronka L., *Roczn. Chem.* 1939 **19** 201.
[17] Fox J. J. and Martin A. E., *Proc. Roy. Soc.* A 1940 **174** 234.
[18] Giguerre P. A. and Harvey K. B., *Canad. J. Chem.* 1956 **34** 798.
[19] Reding F. P., Thesis, Brown University 1951.
[20] Bode G., *Ann. Phys., Lpz.* 1909 (4) **30** 326.
[21] Ganz E. *Ann. Phys., Lpz.* 1937 (5) **28** 445.
[22] Plyler E. K., *J. Opt. Soc. Amer.* 1924 **9** 545.
[23] Hornig D. F., Hyde G. E. and Adcock W. A., *J. Opt. Soc. Amer.* 1950 **40** 497.
[24] Wagner E. L. and Hornig D. F., *J. Chem. Phys.* 1950 **18** 296.
[25] McGovern J. J. and Friedel R. A., *J. Opt. Soc. Amer.* 1947 **37** 660.
[26] Maisch W. G., Thesis, Brown University 1956.
[27] Hibben J. H., *Chem. Rev.* 1933 **13** 345; *J. Chem. Phys.* 1937 **5** 166.
[28] Cross P. C., Burnham J. and Leighton P. A., *J. Amer. Chem. Soc.* 1937 **59** 1134.
[29] Bosschieter G. and Errera J., *C. R. Acad. Sci., Paris* 1937 **205** 560.
[30] Rao I. R. and Kateswaram P., *Indian J. Phys.* 1938 **12** 13.
[31] Narayanaswamy P. K., *Proc. Indian Acad. Sci.* A 1943 **27** 311.
[32] Gross E. P. and Vol'kov V. I., *Dokl. Acad. Nauk. S.S.S.R.* 1950 **74** 453; 1951 **81** 761.
[33] Blue R. W., *J. Chem. Phys.* 1954 **22** 280.
[34] Hornig D. F. and Plumb R. C., *J. Chem. Phys.* 1957 **26** 637.
[35] Waldron F. D., *J. Chem. Phys.* 1957 **26** 809.
[36] Wilson E. B., Jr., Decive J. C. and Cross P. C., *Molecular Vibrations.* McGraw Hill, New York 1955.
[37] Hornig D. F. and Hiebert G. L., *J. Chem. Phys.* 1957 **27** 852.

Spectrochimica Acta, 1958, Vol. 12, pp. 350 to 354. Pergamon Press Ltd., London.

Absorption spectra in the near ultraviolet of some α- and β-monosubstituted derivatives of thiophene*

R. Andrisano and G. Pappalardo
Department of Pharmaceutical and Toxicological Chemistry, University of Parma, Italy

(*Received* 25 *January* 1958)

Abstract—The near ultraviolet absorption spectra in solution of some α-monosubstituted thiophenes have been discussed in relation to the analogous derivatives of furan and thiophene. An electron-acceptor substituent modifies the first excited level of the molecule more in furan than in benzene, thiophenes being intermediate, since the transition energy decreases in the series furan > thiophene > benzene. This order in the series is similar to that expected from the resonance energies.

The absorption spectra of some β-substituted derivatives of thiophene have been described and compared with α-derivatives and with the analogous compounds of furan. In these compounds too the substituent is more conjugated when in the α-position.

VOL. 12 1958

The results reported in this paper, already briefly mentioned in a preliminary note [1], concern the spectroscopic properties of some α-monosubstituted derivatives of thiophene (C_4H_3S—X) in comparison with the related α-monosubstituted furanes (C_4H_3O—X) and benzenes (C_6H_5—X). X being an electron-acceptor group, such as —CO—, COOR, $CONH_2$.

We have also studied β-substituted derivatives of thiophene, in order to see

Table 1. Near ultraviolet absorption spectra (ethanol solutions)†

X =	C_6H_5—X				C_4H_3S—X—α				C_4H_3O—X—α(5)			
	λ_{max} (Å)	log ε	λ_{max} (Å)	log ε	λ_{max} (Å)	log ε	λ_{max} (Å)	log ε	λ_{max} (Å)	log ε	λ_{max} (Å)	log ε
H	2545	2·25	2035	3·87(1)	2310	3·77	—	— (a)	2000	4·00(6)	—	—
CHO	2800	3·20	2440	4·20(2)	2850	3·85	2600	4·02(b)	2720	4·12	2270	3·48
$COCH_3$	2790	3·03	2420	4·08(3)	2820	3·84	2600	3·98(c)	2700	4·11	2255	3·57
	2685	2·80										
COOH	2780	2·71	2245	3·97(3)	~2640	3·76	2460	3·93(d)	2425	4·03	—	—
	2725	2·96										
$COOCH_3$	2800	2·85	2290	4·05(3)	2680	3·86	2480	3·97(e)	2505	4·13	—	—
	2720	2·90										
$COOC_2H_5$	2800	2·85	2290	4·08(3)	2690	3·89	2490	3·95(f)	2510	4·13	—	—
$CONH_2$	2650	2·70	2250	3·95(4)	2720	3·87	2480	3·78(g)	2480	4·06	2140	3·73

* Contribution from C.N.R.

† Numerals in parentheses refer to spectral data previously recorded; letters refer to preparations.

(1) Doub L. and Vandenbelt I. M., *J. Amer. Chem. Soc.* 1947 **69** 2714. (2) Gillam A. E. and Stern E. S., *An Introduction to Electronic Absorption Spectroscopy* (Edited by Arnold E.), p. 126 1954. (3) Andrisano R. and Pappalardo G., *Atti accad. Lincei* 1953 (8) **15** 64. (4) Ley H. and Specker H., *Ber. dtsch. Chem. Ges.* 1939 **72** 192. (5) Andrisano R. and Pappalardo G., *Gazz. Chim. Ital.* 1955 **85** 1430. (6) Gillam A. E. *loc. cit.* p. 132. (a) Commerical product subjected to additional purification. (b) King and Nard, *J. Org. Chem.* 1948 **13** 635. (c) Hartough H. D. and Kosak A. J., *J. Amer. Chem. Soc.* 1947 **69** 3093. (d) Hartough H. D. and Conley L. I., ibid. 1947 **69** 3096. (e) b.p. 82°C.; found: S = 21, 97; $C_6H_6O_2S$ requires S = 22, 52. (f) Selenk W. and Ochs R., *Ber. dtsch. Chem. Ges.* 1915 **48** 678. (g) Nahnsen R., *Ber. dtsch. Chem. Ges.* 1884 **17** 2192. ~ flex.

whether the sequence found in the furan series [2] (namely conjugation in $\alpha \gg$ conjugation in β) is also followed in the thiophene series.

(I) (II)

Experimental

The derivatives of thiophene were prepared by known methods (see footnotes of Tables 1 and 2) and purified by crystallization or distillation *in vacuo*.

Table 2. Near ultraviolet absorption spectra (ethanol solutions)*

X =	C_4H_3S—X—β		C_4H_3O—X—β(1)	
	λ_{max} Å	log ε	λ_{max} Å	log ε
H	2310	3·77	2000	4·00
$COCH_3$	2395	3·80(a)		
COOH	2390	3·79(b)	2320	3·36
$COOCH_3$	2405	3·95(c)	2380	3·40
$COOC_2H_5$	2400	3·95(c)	2380	3·38
$CONH_2$	2410	3·89(a)		

* See footnote of Table 1.

(1) Andrisano R. and Pappalardo G., *Gazz. Chim. Ital.* 1953 **83** 340.

(a) Campaigne E. and Le Seur W. M., *J. Amer. Chem. Soc.* 1948 **70** 1555. (b) Rinkers I., *Rec. Trav. Chim.* 1936 (4) **55** 991. (c) Rinkers I., *Rec. Trav., Chim.* 1934 (4) **53** 643.

Spectroscopic measurements (see Tables 1 and 2; Figs. 1 and 2) were made with a Unicam Spectrophotometer SP 500 in the range 2100–3000 Å, in ethanolic solutions 1 : 100·000, reading every 20 Å, and for the important regions every 10 Å (Beer's law is applicable throughout).

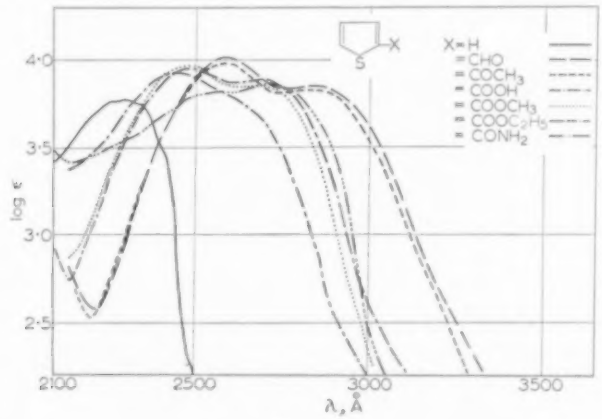

Fig. 1.

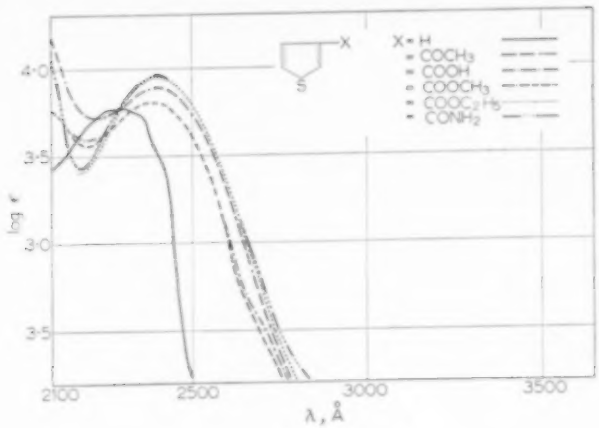

Fig. 2.

Discussion

We may first examine the first transition of benzene, thiophene and furan, which falls at 2500, 2310 and 2000 Å respectively. As the data in Table 1 show, the transition energy in every case decreases in the series:

$$\text{furan} > \text{thiophene} > \text{benzene}$$

With acetyl derivatives, for example, we have the values given in Table 3.

The series derived from the spectroscopic data is parallel to that which was obtained from the resonance energy, and this may imply that the two phenomena are related.

Table 3. Change of the transition energy (ΔE, kcal/mol) due to substituent X in the compounds Ar—X

Ar = \ X =	H	$COCH_3$	ΔE (kcal/mol)
	E (kcal/mol)	E (kcal/mol)	
C_4H_3O—α	143 (λ = 2000 Å)	106 (λ = 2700 Å)	37
C_4H_3S—α	124 (λ = 2310 Å)	101 (λ = 2820 Å)	23
C_6H_5—	112 (λ = 2550 Å)	102 (λ = 2790 Å)	10

If this hypothesis is correct, it might be concluded that the substituent modifies the first excited level of the molecule much more in the case of furan than in that of benzene, thiophene being intermediate.

If the spectral changes due to the same substituent in the α- or β-position are compared, there is an obvious analogy with the furan series [2], i.e. the changes of the spectroscopic characteristics with α-substituents are more marked than those with the β-substituents (see Figs. 3 and 4).

VOL. 12 1958

Moreover in the case of the α-substituents a second band arises in this region of the spectrum, while the β-substitution causes only a small bathochromic shift of the original thiophene or furan band: this may arise because of greater conjugation in the α- than in the β-form.

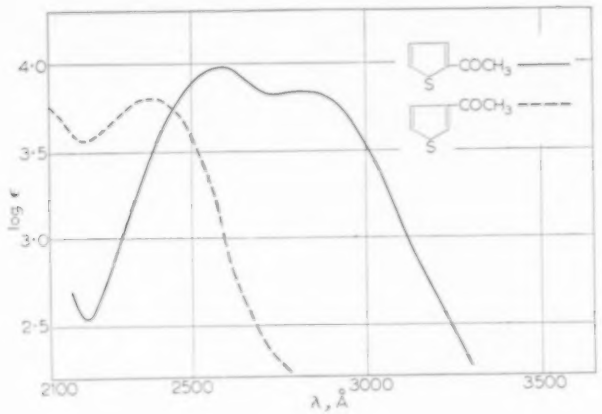

Fig. 3.

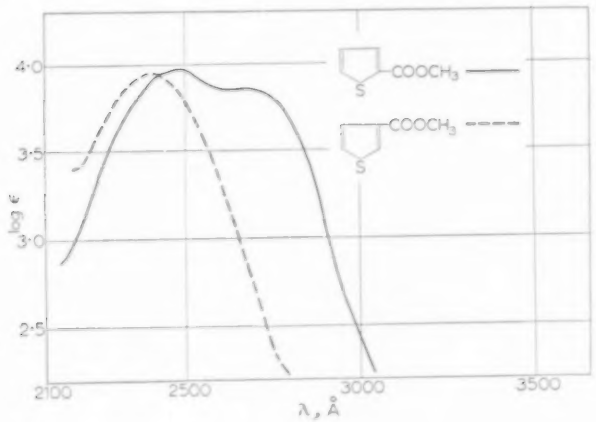

Fig. 4.

For example, the values obtained with carbomethoxy group as substituent are given in Table 4.

From the values reported in Table 4, we may infer that:

(1) The decrease of transition energy in the β-derivatives follows the same order furan > thiophene. This is another experimental fact which may be correlated with the greater aromatic character of the thiophene nucleus compared with that of furan.

(2) The greatest change in the transition energy occurs in every case with the

Table 4. Change of the transition energy (ΔE, kcal/mol) due to substituent X, in the Ar—X compounds, when it occupies the α- or β-position

Ar = \ X =	H	$COOCH_3$		ΔE (kcal/mol)
	E (kcal/mol)	Position of substituent	E (kcal/mol)	
C_4H_3O—	143 (λ = 2000 Å)	α	114 (λ = 2505 Å)	29
		β	120 (λ = 2380 Å)	23
C_4H_3S—	124 (λ = 2310 Å)	α	106·5 (λ = 2680 Å)	17·5
		β	118·5 (λ = 2405 Å)	5·5

α-substituent. These results provide further experimental evidence for the conclusions of Schomaker and Pauling [3] and are consistent with the observation that the α-substituent induces a conjugation through all the perimeter of the ring (Ia), while for the β-substituent the conjugation is limited (IIa).

References

[1] Andrisano R. and Pappalardo G., *Bol. Soc. chim. ind. Bologna* 1956 **14** 100.
[2] Andrisano R. and Pappalardo G., *Gazz. Chim. Ital.* 1953 **83** 340.
[3] Schomaker and Pauling, *J. Amer. Chem. Soc.* 1939 **61** 1769 1881.

VOL. 12 1958

Spectrochimica Acta, 1958, Vol. 12, pp. 355 to 369. Pergamon Press Ltd., London

Infrared absorption spectra of deuterated vinyl fluorides

B. Bak and D. Christensen
Chemical Laboratory of The University of Copenhagen, Denmark

(*Received* 24 *April* 1958)

Abstract—Infrared absorption spectra of vinyl fluoride and its seven deuterated derivatives have been taken. The assignment of fundamental vibrational frequencies for vinyl fluoride originally given by Torkington and Thompson must be slightly modified. A final assignment for all eight isotopic species is suggested.

Introduction

In connexion with a recent study of the structure of vinyl fluoride by microwave technique all the deuterated vinyl fluorides were prepared. The isotopic purity of the samples was checked by infrared spectra. The curves obtained revealed the possibility of altering the assignment of fundamental vibrational frequencies for vinyl fluoride given in the pioneer work by Torkington and Thompson [1], the change in view being partially due to the accessibility of the spectra of deuterated derivatives, and partially due to the fact that a somewhat larger spectral region could be investigated.

Experimental

About 100 cm³ (1 atm, 20°C) quantities of each of the gases vinyl fluoride(I), CH_2CDF(II), the *cis–trans* mixture CHDCHF(III), the *cis–trans* mixture CHDCDF(IV), CD_2CHF(V) and CD_2CDF(VI) were prepared. A detailed account of the preparations will be given elsewhere [2]. Suffice it to mention that the final purification was performed gas-chromatographically on a dry silica-gel column. Neither the infrared nor the microwave spectra showed impurities other than isotopic. In the majority of cases the latter were absent but when present they constituted less than 5–10 per cent so that only easily identifiable "foreign" lines (belonging to the strongest in the spectra of the contaminants) occurred. Such lines are omitted in Table 1 below.

The spectrograph was a Perkin–Elmer 21 double beam instrument. The length of the gas-cell mostly used was 10 cm (in a few cases 100 cm). Generally, runs were taken with the gases in the 10 cm cell at $p \sim 300$, 100 and 30 mm pressure. For sake of brevity the optical densities, recorded in Table 1, have been "normalized" to cell-length 10 cm and 100 mm pressure, extra- or interpolating from actually observed optical densities by assuming proportionality with cell-length and pressure. The classification of observed lines according to their intensity so obtained is not completely reliable but thought to be useful.

KBr, NaCl and CaF_2 optics were used in the appropriate spectral regions. All measurements were carried out at room temperature. The nomenclature used

Table 1. Observed infrared absorption frequencies and "normalized" optical densities of vinyl fluoride and seven deuterated species in the 400–3500 cm^{-1} region. Substances in gas phase at 30–300 mm pressure and room temperature.

Compound	Observed peak frequency	Normalized optical density	Band type	Interpretation
CH_2CHF				
	470	0·143	P	
	483	0·105	Q A/B	Fund. $\nu_1 = 483$
	498	0·155	R	
	711	0·4	C	Fund. $\nu_2 = 711$
	729	0·4	C	
	863	2·7	C	Fund. $\nu_4 = 863$
	913	2·3	P	
	929	3·0	Q A/B	Fund. $\nu_6 = 929$
	944	2·4	R	
	1142	3·46	P	
	1156	3·23	Q A/B	Fund. $\nu_3 = 1156$
	1170	3·77	R	
	1292	0·113	P	
	1306	0·13	Q A/B	Fund. $\nu_7 = 1306$
	1319	0·116	R	
	1365	0·135	P	
	1380	0·125	Q A/B	Fund. $\nu_9 = 1380$
	1394	0·200	R	
	1414	0·11	A/B?	
	1560	0·16	P	
	1572	0·16	Q A/B	$\nu_2 + \nu_4 = 1574$
	1586	0·20	R	
	1643	3·23	P	
	1654	3·14	Q A/B	Fund. $\nu_8 = 1654$
	1658	3·95	R	
	1741	0·051	A/B?	$\nu_{11} - \nu_6 = 1735$
	1778	0·053	P	
	1791	0·043	Q A/B	$\nu_4 + \nu_5 = 1803$
	1804	0·068	R	
	1848	0·132	P	
	1856	0·120	Q A/B	$2\nu_6 = 1858$
	1866	0·137	R	
	2065	0·069	P	
	2075	0·069	Q A/B	$\nu_3 + \nu_6 = 2085$
	2085	0·088	R	
	2287	0·047	P	
	2302	0·057	Q A/B	$2\nu_3 = 2312$
	2315	0·082	R	
	2440	0·0137	P	
	2453	0·0098	Q A/B	$\nu_2 + \nu_7 = 2462$
	2465	0·0146	R	
	2555	0·032	P	
	2570	0·030	Q A/B	$\nu_6 + \nu_9 = 2583$
	2580	0·033	R	
	2785	0·022	P	
	2798	0·020	Q A/B	$\nu_3 + \nu_8 = 2810$
	2810	0·025	R	
	2980	0·024	P?	
	3010	0·032	R? A/B?	$\nu_8 + \nu_9 = 3034$

VOL. 12 1958

Table 1 (*continued*)

Compound	Observed peak frequency	Normalized optical density	Band type	Interpretation
CH_2CHF				
	3080	0·112	Overlapping bands of A/B type	Fund. $\nu_{10} = 3080$
	3115	0·167		Fund. $\nu_{11} = 3115$
	3150	0·102		Fund. $\nu_{12} = 3150$
	3290	0·020		
	3315	0·024	A/B?	$2\nu_9 = 3108$
CH_2CDF				
	464	0·41	P	
	477	0·28	Q A/B	Fund. $\nu_1 = 477$
	492	0·43	R	
	519	0·21	C	$\nu_1 + \nu_6 - \nu_5 = 512$
	610	0·08	C?	$\nu_2 + \nu_4 - \nu_5 = 607$
	617	0·10	C?	$\nu_2 + \nu_6 - 2\nu_1 = 631$
	678	0·15	C	$\nu_1 + \nu_7 - \nu_4 = 671$
	683	0·25	C	Fund. $\nu_2 = 683$
	730	0·08	C	$\nu_4 + \nu_6 - 2\nu_1 = 739$
	771	0·06	C?	$\nu_1 + \nu_7 - \nu_2 = 779$
	791	0·17	C	Fund. $\nu_4 = 791$
	867	1·4	C	Fund. $\nu_5 = 867$
	888	0·56	P	
	902	0·53	Q A/B	Fund. $\nu_6 = 902$
	916	0·42	R	
	972	0·68	P	
	985	0·45	Q A/B	Fund. $\nu_7 = 985$
	1000	0·64	R	
	1072	0·022	P	
	1085	0·043	Q A/B	$\nu_6 + \nu_8 - \nu_3 = 1103$
	1098	0·041	R	
	1148	0·78	P	
	1165	0·8	Q A/B	Fund. $\nu_3 = 1165$
	1177	0·75	R	
	1203	0·107	Q A/B	$\nu_1 + \nu_9 - \nu_6 = 1203$
	1212	0·088	R	
	1348	0·40	P	
	1362	0·42	Q A/B	Fund. $\nu_8 = 1362$
	1373	0·43	R	
	1366	0·50	A/B?	$2\nu_2 = 1366$
	1382	0·47	C?	$\nu_3 + \nu_6 - \nu_2 = 1384$
	1451	0·069	Over-	
	1459	0·064	Q? lapping	$\nu_1 + \nu_7 = 1462$
	1468	0·10	Q? bands of	$\nu_2 + \nu_4 = 1474$
	1480	0·085	A/B type	
	1534	0·13	P	
	1548	0·17	Q A/B	$\nu_2 + \nu_5 = 1550$
	1561	0·17	R	
	1613	2·6	P	
	1628	3·2	Q A/B	Fund. $\nu_9 = 1628$
	1639	3·2	R	
	1718	0·086	Q A/B?	$\nu_7 + \nu_9 - \nu_6 = 1711$

Table 1 (*continued*)

Compound	Observed peak frequency	Normalized optical density	Band type	Interpretation
CH_2CDF				
	1728	0·093	P	
	1740	0·080	Q } A/B	$2\nu_5 = 1734$
	1752	0·078	$R + P$	
	1765	0·085	Q A/B	$\nu_{11} - \nu_8 = 1754$
	1778	0·076	$R + P$	
	1798	0·025	Q } A/B	$\nu_{12} - \nu_8 = 1784$
	1812	0·044	R	
	1866	0·029	P	
	1883	0·027	Q } A/B	$\nu_6 + \nu_7 = 1887$
	1896	0·024	R	
	1950	0·068	P	
	1966	0·058	Q } A/B	$2\nu_7 = 1970$
	1980	0·071	R	
	2040	0·019	P	
	2055	0·020	Q } A/B	$\nu_3 + \nu_6 = 2067$
	2067	0·022	R	
	2120	0·041	P	
	2135	0·041	Q } A/B	$\nu_3 + \nu_7 = 2150$
	2150	0·042	R	
	2295	0·17	Overlapping	
	2310	0·13	bands of A/B	Fund. ν_{10} = ca. 2310
	2325	0·23	type	
	2500	0·044	P	
	2517	0·042	Q } A/B	$\nu_3 + \nu_8 = 2533$
	2528	0·047	R	
	2593	0·019	P	
	2605	0·020	Q } A/B	$\nu_7 + \nu_9 = 2613$
	2618	0·022	R	
	2695	0·006	} A/B?	$2\nu_5 = 2732$
	2720	0·007		
	2760	0·022	P	
	2775	0·014	Q } A/B	$\nu_3 + \nu_9 = 2793$
	2787	0·027	R	
	3120	0·054	Overlapping	Fund. ν_{11} = ca. 3120
	3150	0·061	bands of A/B type	Fund. ν_{12} = ca. 3150
	3240	0·017	} A/B?	$2\nu_9 = 3256$
	3260	0·022		
	3453	0·017		
	3465	0·014	} A/B?	$\nu_3 + \nu_{10} = 3475$
	3482	0·020		
CD_2CHF				
	ca. 414	ca. 0·12	Q } A/B	Fund. ν_1 = ca. 414
	429	0·15	R	
	519	0·032	C?	$\nu_1 + \nu_6 - \nu_4 = 525$
	564	0·105	C	Fund. $\nu_2 = 564$
	575	0·050	C?	$\nu_3 - \nu_2 = 573$
	693	2·25	C	Fund. $\nu_4 = 693$

VOL. 12 1958

Table 1 (*continued*)

Compound	Observed peak frequency	Normalized optical density	Band type	Interpretation
CD_2CHF	730	0·72	C	$\nu_9 - \nu_5 = 732$
	791	0·95	P	
	804	1·20	Q A/B	Fund. $\nu_6 = 804$
	816	1·00	R	
	888	1·40	C	Fund. $\nu_5 = 888$
	991	0·30	P	
	1005	0·35	Q A/B	Fund. $\nu_7 = 1005$
	1016	0·23	R	
	1126	0·68	P	
	1137	0·88	Q A/B	Fund. $\nu_3 = 1137$
	1148	0·78	R	
	1206	0·128	P	
	1217	0·141	Q A/B	$\nu_1 + \nu_6 = 1218$
	1229	0·122	R	
	1245	0·125	P	
	1258	0·131	Q A/B	$\nu_2 + \nu_4 = 1257$
	1272	0·148	R	
	1298	0·187	P	
	1312	0·131	Q A/B	Fund. $\nu_8 = 1312$
	1324	0·102	R	
	1370	0·064	P	
	1384	0·043	Q A/B	$2\nu_4 = 1386$
	1396	0·050	R	
	1435	0·038	P	
	1448	0·043	Q A/B	$\nu_2 + \nu_5 = 1452$
	1460	0·033	R	
	1535	0·033	P A/B?	$\nu_1 + \nu_3 = 1551$
	1546	0·053	Q	
	1586	1·35	P	
	1596	2·92	Q A/B	$2\nu_6 = 1608$
	1607	3·23	$R + P$	
	1620	2·77	Q A/B	Fund. $\nu_9 = 1620$
	1631	2·54	R	
	1693	0·069	P	
	1702	0·104	Q A/B	$\nu_1 + \nu_8 = 1726$
	1714	0·089	R	
	1755	0·137	P	
	1768	0·131	Q A/B	$2\nu_5 = 1776$
	1780	0·140	R	
	1921	0·043	P	
	1935	0·066	Q A/B	$\nu_3 + \nu_6 = 1941$
	1946	0·066	R	
	1996	0·0143	P	
	2010	0·0186	Q A/B	$2\nu_7 = 2010$
	2022	0·0186	R	
	2243	0·211		
	2250	0·211	Overlapping	Fund. ν_{10} = ca. 2250
	2258	0·195	bands of A/B-	
	2265	0·239	type	Fund. ν_{11} = ca. 2265
	2270	0·245		

Table 1 (*continued*)

Compound	Observed peak frequency	Normalized optical density	Band type	Interpretation
CD_2CHF				
	2407	0·040	P	
	2425	0·030	Q A/B	$\nu_3 + \nu_8 = 2449$
	2435	0·036	R	
	2732	0·036	P	
	2745	0·030	Q A/B	$\nu_3 + \nu_9 = 2757$
	2755	0·037	R	
	ca. 3073	0·183		
	ca. 3085	0·145	A/B	Fund. ν_{12} = ca. 3085
	ca. 3100	0·211		
	3195	0·024		
	3210	0·018	A/B?	$2\nu_9 = 3240$
	3225	0·024		
	ca. 3365	0·024	?	$\nu_3 + \nu_{10} = 3387$
CD_2CDF				
	ca. 410	ca. 0·2	Q A/B	Fund. ν_1 = ca. 410
	425	0·34	R	
	563	0·098	C	Fund. $\nu_2 = 563$
	675	2·6	C	Fund. $\nu_4 = 675$
	728	0·35	C	Fund. $\nu_5 = 728$
	782	0·66	P	
	794	0·80	Q A/B	Fund. $\nu_6 = 794$
	804	0·74	R	
	954	0·68	P	
	967	0·86	Q A/B	Fund. $\nu_7 = 967$
	984	1·5	$R + P$	
	1001	0·90	Q A/B	Fund. $\nu_8 = 1001$
	1012	0·67	R	
	1128	2·72	P	
	1142	2·68	Q A/B	Fund. $\nu_3 = 1142$
	1154	3·03	R	
	1191	0·22	P	
	1203	0·24	Q A/B	$\nu_1 + \nu_6 = 1204$
	1212	0·19	R	
	1280	0·13	P	
	1291	0·17	Q A/B	$\nu_2 + \nu_5 = 1291$
	1303	0·17	R	
	1330	0·090	P	
	1346	0·039	Q A/B?	$2\nu_4 = 1350$
	1358	0·040	R	
	1390	0·11	P	
	1403	0·11	Q A/B	$\nu_4 + \nu_5 = 1403$
	1415	0·125	R	
	1447	0·067	P	
	1460	0·060	Q A/B	$2\nu_5 = 1456$
	1469	0·069	R	

VOL. 12 1958

Table 1 (*continued*)

Compound	Observed peak frequency	Normalized optical density	Band type	Interpretation
CD_2CDF				
	1562	2·5	P	
	1574	3·8	Q	A/B $2\nu_6 = 1588$
	1584	4·2	$R + P$	
	1596	4·5	Q	A/B Fund. $\nu_9 = 1596$
	1607	3·4	R	
	1693	0·043	P	
	1704	0·070	Q	A/B $\nu_9 + \nu_4 - \nu_2 = 1708$
	1713	0·057	R	
	1746	0·041	P	
	1759	0·057	Q	A/B $\nu_6 + \nu_7 = 1761$
	1774	0·046	R	
	1916	0·050	P	
	1928	0·060	Q	A/B $2\nu_7 = 1934$
	1941	0·057	R	
	1975	0·024	P	
	1982	0·031	Q	A/B? $2\nu_8 = 2002$
	1996	0·024	R	
	2085	0·037	P	
	2098	0·041	Q	A/B $\nu_3 + \nu_7 = 2109$
	2110	0·046	R	
	2227	0·150	P	
	2240	0·145	Q	A/B Fund. ν_{10} = ca. 2240
	2255	0·228	$P + R$	
	2273	0·130	Q	A/B Fund. ν_{11} = ca. 2273
	2287	0·140	R	
	2310	0·156	Overlapping bands of A/B-type	Fund. ν_{12} = ca. 2325
	2330	0·182		
	2380	0·094	P	
	2395	0·054	Q	A/B $\nu_6 + \nu_9 = 2390$
	2412	0·062	R	
	2555	0·0096	P?	
	2570	0·0082	Q?	A/B? $\nu_8 + \nu_9 = 2597$
	2590	0·0082	R?	
	2715	0·063	P	
	2727	0·041	Q	A/B $\nu_3 + \nu_9 = 2738$
	2738	0·044	R	
	3142	0·024	P	
	3155	0·023	Q	A/B $2\nu_9 = 3192$
	3170	0·026	R	
	3250	0·024	?	$\nu_8 + \nu_{10} = 3241$
CDHCHF				
	420	0·089	P	
	434	0·082	Q	A/B Fund. $\nu_1 = 434$
	445	0·130	$R + P$	
	ca. 455	ca. 0·1	Q?	A/B Fund. $\nu_1{}^* = $ ca. 455
	469	0·090	R	

Table 1 (*continued*)

Compound	Observed peak frequency	Normalized optical density	Band type	Interpretation
CDHCHF				
	520	0·025	*C*?	$\nu_2^* + \nu_4^* - \nu_5^* = 517$
	576	0·17	*C*	Fund. $\nu_2 = 576$
	642	0·16	*C*	Fund. $\nu_2^* = 642$
	677	0·168	*C*	$\nu_1^* + \nu_3^* - \nu_5^* = 682$
	785	2·64	*C*	Fund. $\nu_4^* = 785$
	815	1·60	*C*	Fund. $\nu_4 = 815$
	864	0·61	*P*	
	878	0·85	*Q* *A*/*B*	Fund. $\nu_6 = \nu_6^* = 878$
	890	0·90	*R*	
	910	0·90	*C*	Fund. $\nu_5^* = 910$
	926	2·12	*C*	Fund. $\nu_5 = 926$
	1073	1·84	*P*	
	1084	2·24	*Q* *A*/*B*	Fund. $\nu_7^* = 1084$
	1098	2·08	*R*	
	1123	2·28	*P*	
	1137	2·32	*Q* *A*/*B*	Fund. $\nu_3 = \nu_3^* = 1137$
	1150	2·72	*R*	
	1221	0·72	*P*	
	1235	0·68	*Q* *A*/*B*	Fund. $\nu_7 = 1235$
	1248	0·71	*R*	
	1270	0·18	*P*	
	1284	0·13	*Q* *A*/*B*	$2\nu_2^* = 1284$
	1295	0·13	*R*	
	1306	0·12	*P*	
	1318	0·10	*Q* *A*/*B*	Fund. $\nu_8 = 1318$
	1328	0·073	*R*	
	1382	0·076	*Q* *A*/*B*	Fund. $\nu_9^* = 1382$
	1404	0·058	*P*?	
	1420	0·025	*Q*? *A*/*B*	$\nu_2^* + \nu_4^* = 1427$
	1430	0·018	*R*?	
	1550	0·11	*Q* *A*/*B*	$\nu_3^* + \nu_5^* = 1552$
	1566	0·13	*Q* *A*/*B*	$2\nu_4^* = 1570$
	1620	3·00	*P*	
	1630	3·92	*Q* Overlapping bands of	Fund. $\nu_9 = 1630$
	1635	2·92	*Q* *A*/*B* type	Fund. $\nu_9^* = 1637$
	1642	3·33	*R*	
	1709	0·117	*P*	
	1719	0·131	*Q* *A*/*B*	$\nu_4 + \nu_5 = 1741$
	1729	0·146	*R*	
	1742	0·142	*P*	
	1757	0·160	*Q* *A*/*B*	$2\nu_6 = 2\nu_6^* = 1756$
	1782	0·106	*R*	
	1798	0·062	*P*	
	1813	0·058	*Q* *A*/*B*	$2\nu_5^* = 1820$
	1826	0·055	*R* + *P*	
	1844	0·029	*Q* *A*/*B*	$2\nu_5 = 1852$
	1854	0·025	*R*	

VOL. 12 1958

Table 1 (*continued*)

Compound	Observed peak frequency	Normalized optical density	Band type	Interpretation
CDHCHF				
	1930	0·025	P	
	1938	0·033	Q } A/B	$\nu_5 + \nu_2 + \nu_1 = 1936$
	1948	0·040	$R + P$	
	1959	0·044	Q } A/B	$\nu_{12} - 2\nu_8 = 1943$
	1968	0·029	R	
	2090	0·018	P	
	2105	0·019	Q A/B	$\nu_7 + \nu_8 - \nu_1 = 2119$
	2115	0·016	R	
	2145	0·020	P	
	2160	0·020	Q A/B	$2\nu_7^* = 2168$
	2170	0·024	R	
	2215	0·007	A/B?	$\nu_3^* + \nu_7^* = 2221$
	ca. 2250	0·045	?	
	2265	0·058	Q	Fund. ν_{10} = ca. 2265
	ca. 2278	0·091	? Overlapping	
	2295	0·093	Q bands of	$2\nu_3 = 2\nu_3^* = 2274$
	2305	0·096	Q A/B type	
	2315	0·109	Q	Fund. $\nu_{10}^* =$ ca. 2315
	ca. 2325	0·098	?	
	2445	0·018	P	
	2460	0·020	Q } A/B	$2\nu_7 = 2470$
	2475	0·022	$R + P$	
	2493	0·014	Q } A/B	$\nu_3^* + \nu_8^* = 2519$
	2508	0·016	R	$\nu_6 + \nu_9 = 2508$
	2692	0·018	P	
	2707	0·018	Q A/B	$\nu_1 + \nu_{10} = 2699$
	2720	0·030	R	
	2750	0·014	P	
	2763	0·015	Q A/B	$\nu_1^* + \nu_{10}^* = 2770$
	2778	0·020	R	
	2935	0·011		
	2963	0·014	?	$\nu_6 + \nu_9 = 2948$
	2985	0·010		
	3080	0·167	Overlapping	
	3095	0·153	bands of A/B	Fund. $\nu_{11}^* = \nu_{12}^* = \nu_{11} = \nu_{12} =$
	3107	0·193	type	ca. 3095
	3235	0·018	A/B?	$2\nu_9 = 3260$
	3265	0·025		$2\nu_9^* = 3270$
CHDCDF				
	ca. 418	0·14	P	
	428	0·11	Q } A/B	Fund. $\nu_1^* = 428$
	ca. 440	0·14	$R + P$	
	ca. 449	0·092	Q? } A/B	Fund. $\nu_1 = 449$
	ca. 462	0·074	R	
	519	0·054	C?	$3\nu_2^* - \nu_8^* = 521$
	539	0·26	C	$2\nu_4 - \nu_5 = 546$
	575	0·23	C	Fund. $\nu_2^* = 575$
	610	0·162	?	$2\nu_2^* + \nu_1^* - \nu_7^* = 604$

Table 1 (*continued*)

Compound	Observed peak frequency	Normalized optical density	Band type	Interpretation
CHDCDF				
	617	0·146	?	$\nu_3^\bullet - \nu_2^\bullet = 629$
	639	0·31	*C*	Fund. $\nu_2 = 639$
	675	0·43	*C*	$\nu_2^\bullet + \nu_5^\bullet - \nu_4^\bullet = 693$
	695	0·90	*C*	Fund. $\nu_4 = 695$
	726	0·35	*C*	Fund. $\nu_4^\bullet = 726$
	770	0·41	*C*	$\nu_9^\bullet - \nu_5^\bullet = 771$
	796	0·60	*A*/*B*	$2\nu_5 - 2\nu_1 = 790$
	824	1·0	*C* and *A*/*B* type bands mixed	Fund. $\nu_6 = 824$
	844	0·9		Fund. $\nu_5 = \nu_5^\bullet = 844$
	866	1·0		Fund. $\nu_6^\bullet = 866$
	956	0·78	*P*	
	969	0·89	*Q* 2 *A*/*B*-type bands	Fund. $\nu_7 = 969$
	974	0·98	*Q*	Fund. $\nu_7^\bullet = 974$
	986	0·91	*R*	
	1054	1·11	*P*	
	1067	1·22	*Q* *A*/*B*-type bands	$\nu_{10}^\bullet - \nu_8^\bullet = \nu_{10} - \nu_8 = 1081$
	1071	1·02	*Q*?	$\nu_4 + \nu_5 - \nu_1 = 1090$
	1082	1·33	*R*	
	1130	1·35	*P*	
	1145	1·71	*Q* *A*/*B*	Fund. $\nu_3 = \nu_3^\bullet = 1145$
	1156	1·71	*R*	
	1194	0·42	*P*	
	1204	0·45	*Q* *A*/*B*	Fund. $\nu_8 = \nu_8^\bullet = 1204$
	1213	0·51	*R*	
	1274	0·48	? Overlapping bands	$2\nu_2 = 1278$; $\nu_1 + \nu_6 = 1273$, $\nu_1^\bullet + \nu_6^\bullet = 1294$, $\nu_2^\bullet + \nu_4^\bullet = 1301$
	1284	0·61	?	
	1298	0·60	?	
	1330	0·40	?	$\nu_2 + \nu_4 = 1334$
	1364	0·09	*A*/*B*?	$\nu_{11}^\bullet - \nu_7^\bullet = 1351$
				$\nu_{11} - \nu_7 = 1356$
	1390	0·07	*A*/*B*?	$2\nu_4 = 1390$
	1410	0·07	*P*	
	1421	0·06	*Q* *A*/*B*	$\nu_2^\bullet + \nu_5^\bullet = 1419$
	1440	0·08	*R* + *P*	
	1449	0·06	*Q* *A*/*B*	$2\nu_4^\bullet = 1452$
	1455	0·06	*R*	
	1502	0·068	*P*	
	1518	0·077	*Q* *A*/*B*	$\nu_4 + \nu_5 = 1539$
	1530	0·089	*R*	
	1590	2·3	*P*?	
	1603	4·1	*Q* 2*A*/*B*-type bands	Fund. $\nu_9 = 1603$
	1615	4·3	*Q*	Fund. $\nu_9^\bullet = 1615$
	1625	2·7	*R*?	
	1704	0·39	?	$2\nu_1 + \nu_6 = 2\nu_1^\bullet + \nu_6^\bullet = 1722$
	1719	0·40	? Overlapping bands	$\nu_2^\bullet + \nu_8^\bullet = 1779$
	1760	0·128	?	$\nu_6 + \nu_7 = 1793$
	1778	0·110	?	
	1934	0·0034	*A*/*B*	$2\nu_7 = 1938$

VOL. 12 1958

Table 1 (*continued*)

Compound	Observed peak frequency	Normalized optical density	Band type	Interpretation
CHDCDF				
	1943	0·0034	A/B	$2\nu_7^* = 1948$
	2015	0·0013	P	
	2030	0·0019	Q A/B	$\nu_6 + \nu_8 = 2028$
	2040	0·0019	R	
	2090	0·0020	P	
	2105	0·0030	Q A/B	$\nu_2 + \nu_7 = 2114$
	2113	0·0033	$R + P$	
	2125	0·0030	Q A/B	$\nu_2^* + \nu_7^* = 2119$
	2135	0·0025	R	
	2275	0·11	?	
	2285	0·13	? Overlapping	
	2300	0·19	? bands of	Fund. $\nu_{10} = \nu_{10}^* =$ ca. 2285
	2325	0·15	? A/B-type	Fund. $\nu_{11} = \nu_{11}^* =$ ca. 2325
	2340	0·21	?	
	2445	0·0030	P	
	2457	0·0023	Q A/B	$\nu_6^* + \nu_9^* = 2481$
	2467	0·0017	R	
	2645	0·0017	P	
	2660	0·0015	Q A/B	$\nu_{12}^* - \nu_1^* = 2667$
	2675	0·0017	R	
	2730	0·0013	P	
	2745	0·0013	Q A/B	$\nu_1 + \nu_{11} = 2774$
	2760	0·0017	R	
	2965	0·0008	P	
	2985	0·0011	Q A/B	$\nu_6 + \nu_7 + \nu_8 = 2997$
	3010	0·0008	R	
	3080	0·043	Overlapping	
	3095	0·038	bands of	Fund. $\nu_{12} = \nu_{12}^* =$ ca. 3095
	3100	0·045	A/B type	

in referring to a definite component in one of the *cis–trans* mixtures is shown in Fig. 1.

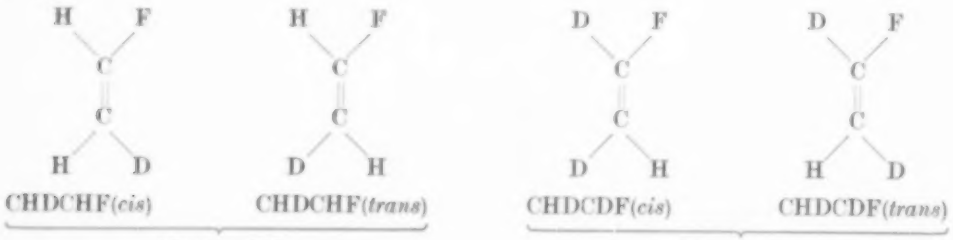

Fig. 1. Nomenclature for components of *cis–trans* mixtures.

Table 1 gives our experimental spectra and their interpretation.

Assignment of frequencies

I. *Planar vibrations (symmetry class A')*

The class contains nine fundamentals. In agreement with Torkington and Thompson we shall designate the lowest fundamental of the class by ν_1 throughout the whole series of spectra of isotopic species. Likewise, the fundamental near 1150 cm^{-1} (the *C–F* "group" frequency) will consistently be called ν_7. The fundamental in the 1600–1650 cm^{-1} region (the C=C stretching frequency) is called ν_9, the hydrogen, resp. deuterium stretching fundamentals are called ν_{10}, ν_{11} and ν_{12}. The remaining fundamentals are called ν_6, ν_7 and ν_8 *in increasing order of magnitude*, no attempt being made to localize, for example, a CH_2, resp. CDH or CD_2 "group" frequency in the spectra and calling this frequency ν_8.

The assigned fundamentals are collected in Table 2. For the compounds I, II, V and VI the assignment is straightforward. All the thirty-six bands involved are of correct band type, they are intense and the frequencies obey the product rule and sum rules (Table 3). The interpretation for (I) is identical with Thompson and Torkington's.

Table 2. Assignment of normal vibration frequencies for vinyl fluoride and its seven deuterated derivatives (frequencies in cm^{-1})

Compound		A'-class								A''-class		
		ν_1	ν_2	ν_3	ν_4	ν_5	ν_6	ν_{10}	ν_{11}	ν_{12}	ν_2	ν_3	ν_4
CH_2CHF	(I)	483	1156	929	1306	1380	1654	ca. 3080	ca. 3115	ca. 3150	711	863	(940)
CH_2CDF	(II)	477	1165	902	985	1366	1628	ca. 2310	ca. 3120	ca. 3150	683	791	867
CHDCHF (*cis*)	(III)	ca. 455	1137	878	1084	1382	1635	ca. 2315	ca. 3095	ca. 3095	642	785	910
CHDCHF (*trans*)	(III)	434	1137	878	1235	1318	1630	ca. 2265	ca. 3095	ca. 3095	576	815	926
CHDCDF (*trans*)	(IV)	ca. 449	1145	824	969	1204	1603	ca. 2285	ca. 2325	ca. 3095	639	695	844
CHDCDF (*cis*)	(IV)	428	1145	866	974	1204	1615	ca. 2285	ca. 2325	ca. 3095	575	726	844
CD_2CHF	(V)	ca. 414	1137	804	1005	1312	1620	ca. 2250	ca. 2265	ca. 3085	564	693	888
CD_2CDF	(VI)	ca. 410	1142	794	967	1001	1596	ca. 2240	ca. 2273	ca. 2325	563	675	728

For the isotopic mixture (III) no reasonable doubt can exist with respect to the assignment of ν_1, ν_3, ν_9, ν_{10} and ν_{12}, except what concerns the *cis–trans* problem. The expected positions for ν_6, ν_7, and ν_8 according to the Raileigh rule are: two lines (one *cis*, one *trans*) in the 804–929 cm^{-1} interval, two lines between 1005 and 1306, and two lines between 1312 and 1380 cm^{-1}. The two latter are obviously the lines at 1318 and 1382 (ν_8). In the 1005–1306 interval, by far the best candidates are the lines at 1084 and 1235. Without specifying *cis* and *trans* we shall, therefore, take these as ν_7. In the 804–929 interval the only *A/B* type band of suitable intensity is 878. We shall take this as ν_6, common to *cis* and *trans*. As demonstrated in Table 3 it proved possible to subdivide the fundamentals selected above into two groups, each obeying the product and sum rules.

In the spectrum of the isotopic mixture IV obviously $\nu_1 = \begin{cases}428\\449\end{cases}$, $\nu_3 = 1145$, $\nu_9 = \begin{cases}1605\\1603\end{cases}$, $\nu_{10} = 2285$, $\nu_{11} = 2325$ and $\nu_{12} = 3095$. The Rayleigh rule indicates three intervals where to look for ν_6(794–878), ν_7(967–985) and ν_8(1001–1382 for

VOL. 12 1958

Table 3. Calculated and observed product rule ratios (τ) and sums of frequencies S_i* for vinyl fluoride and its seven deuterated derivatives.

	τ				S_i	
	A'-class		A''-class		A'-class	A''-class
	Calc.	Obs.	Calc.	Obs.		
CH_2CHF					$S_1' = 8{\cdot}778.10^6$	$S_1'' = 21{\cdot}338.10^5$
CH_2CDF	0·5219	0·5334	0·8128	0·8121	$S_2' = 7{\cdot}885.10^6$	$S_2'' = 18{\cdot}438.10^5$
CHDCHF (*cis*)	0·5262	0·5279	0·7981	0·7951	$S_3' = 8{\cdot}029.10^6$	$S_3'' = 18{\cdot}565.10^5$
CHDCHF (*trans*)	0·5332	0·5337	0·7543	0·7537	$S_4' = 8{\cdot}171.10^6$	$S_4'' = 18{\cdot}535.10^5$
CHDCDF (*trans*)	0·2744	0·2806	0·6381	0·6506	$S_5' = 7{\cdot}150.10^6$	$S_5'' = 16{\cdot}037.10^5$
CHDCDF (*cis*)	0·2777	0·2809	0·6116	0·6108	$S_6' = 7{\cdot}251.10^6$	$S_6'' = 15{\cdot}701.10^5$
CD_2CHF	0·2794	0·2720	0·6019	0·6018	$S_7' = 7{\cdot}466.10^6$	$S_7'' = 15{\cdot}869.10^5$
CD_2CDF	0·1455	0·1454	0·4800	0·4797	$S_8' = 6{\cdot}584.10^6$	$S_8'' = 13{\cdot}026.10^5$

* In all S_i's, contributions from hydrogen and deuterium *stretching* frequencies have been omitted [3]. The differences:
$(S_1' + S_8') - (S_2' + S_7') = (15{\cdot}362 - 15{\cdot}351) \cdot 10^6 = 0{\cdot}011 \cdot 10^6$
$(S_1' + S_7') - (S_3' + S_4') = (16{\cdot}244 - 16{\cdot}200) \cdot 10^6 = 0{\cdot}044 \cdot 10^6$
$(S_2' + S_6') - (S_3' + S_8') = (14{\cdot}469 - 14{\cdot}401) \cdot 10^6 = 0{\cdot}068 \cdot 10^6$
should be zero if the sum rule is fulfilled exactly. The agreement is satisfactory.

the *trans*-isomer, 1001–1318 for the *cis*-isomer). Obvious candidates in the lowest region are the lines at 824 and 866. In the 967–985 interval the beautiful double band with Q-branches at 969 and 974 must be *cis–trans* ν_7. Possibilities in the 1001–1382 interval (ν_8) are 1067, 1204, 1274, 1284, 1298 and 1330 cm^{-1}. Now, the Rayleigh rule indicates that ν_1(*trans*) must be the line at 449, ν_1(*cis*) the line at 428. ν_6(*trans*) could be either 824 or 866. In the first case $\nu_8 = 1204$ if the product rule is to be obeyed. If ν_6 (*trans*) = 866 one computes 1146 cm^{-1} for ν_8. None of these possibilities can be excluded. Exactly the same consideration applies to the *cis*-spectrum. In view of the fact that one fundamental (ν_3) has already been placed at 1145, we have (somewhat arbitrarily) chosen to put $\nu_8 = 1204$ cm^{-1} for both isomers. An apparent default in the assignment is, that it leaves the strong band at 1067 unassigned as a fundamental. In the numerous combinations tested by us, and having 1067 as a fundamental, serious conflict with the product rule or the appearance of the remaining spectrum has always resulted. Its interpretation as a combination band is given in Table 1.

II. *Non-planar vibrations* (*symmetry class* A″)

The class has three fundamentals which will be called ν_2, ν_4 and ν_5 *in increasing order of magnitude*. For vinyl fluoride the correct assignment of fundamentals has been a matter of discussion between Cole and Thompson [4] on one side and Pitzer and Freeman [5] on the other. The former workers chose 715, 732 and 860 as the three fundamentals, whereas 715, 860 and 924 were suggested by the American authors, mainly based on comparisons between potential functions of

related ethylene derivatives. Cole and Thompson [4] showed that the band at 924 is of the hybrid (A/B) type, thus excluding its use as an A''-class fundamental. They also showed that the bands at 715, 732 and 860 are of the "C"-type which is a *necessary* condition if they are to be A''-fundamentals (one or both could be combination bands of the "C"-type).

The spectra of the isotopic species presented here seem to solve the problem. It is beyond doubt that for CD_2CDF two of the A''-frequencies are at 563 and 675. These bands simply have no observed qualified competitors.

Recently, Gullikson and Nielsen [6] have shown that vinyl bromide and vinyl chloride both have fundamentals in the A''-class at 940 cm^{-1}. Hence it seems reasonable to guess that vinyl fluoride should also possess a fundamental near 940 cm^{-1} (as previously proposed by Pitzer and Freeman). We shall try to verify this guess. First of all the observed CH_2CHF-spectrum does not exclude the possibility, since the region at 940 cm^{-1} is heavily occupied by the strong ν_6 band with its extensive R-branch. A weak A''-fundamental could easily be hidden here. Taking 711, 863 and the hypothetical 940 cm^{-1} as the A''-fundamentals in CH_2CHF, the lacking A''-fundamental in the CD_2CDF-spectrum should be expected at $0{\cdot}4800 \times (711 \times 863 \times 940)/(563 \times 675) = 728{\cdot}5$ cm^{-1}. Actually, a "C"-type band is observed at exactly this position, somewhat unfavourably situated on the slope of the R-branch of the 675-band. The idea of a "C"-type fundamental in the spectrum of CH_2CHF as high as 940 cm^{-1} is further supported by the experimental result that intense bands of "C"-type structure appear at 910 and 926 in the spectrum of (III) and at 888 in the spectrum of (V).

VOL. 12 1958

Accordingly, the three A''-fundamentals in the spectrum of CH_2CDF are to be looked for in the intervals 563–711, 675–863, and 728–940. If we let measured intensities guide us, two qualified candidates are the lines at 683 and 867. Using the product rule, the third fundamental is precalculated to be at $0{\cdot}8128 \times (711 \times 863 \times 940)/(683 \times 867) = 791$ cm^{-1}. Here, a rather intense "C"-type band is actually observed, inferior in intensity only to the band at 519 (and, of course, to the 683 and the 867 bands). The band at 519 lies outside any acceptable frequency range.

In the spectrum of CD_2CHF, the *intense* bands at 564, 675, and 888 cm^{-1} almost automatically are assigned as A''-fundamentals by their unusually well-developed "C"-type character. Their positions are in agreement with the product rule (Table 3). We can now make a sum-rule test by trying if:

$$S_1'' + S_8'' - S_2'' + S_7'' \sim 0$$

The assignment given in Table 2 gives $15{\cdot}365 - 15{\cdot}351 = 0{\cdot}014$ which is satisfactory.

The spectrum of CHDCHF (*cis*) ought to show one A''-line in each of the intervals 564–711, 693–863, and 888–940. The corresponding intervals for the *trans*-isomer are the same. In the high-frequency interval there are no other candidates than lines at 910 and 926 cm^{-1}. Suitable lines to be placed in the 693–863 domain are only 785 and 815. The product rule now permits the precalculation of the missing frequency in the spectra of both isomers. There is only one way of subdividing into *cis* and *trans* lines if the product rule is to be

obeyed. This is the assignment of Table 2. The product rule picked out the two strongest of the remaining "*C*"-type bands.

For the three A''-fundamentals in the spectrum of CHDCDF(*cis*) the intervals to be scanned are 563–576, 675–791, and 728–867. For the *trans*-isomer the intervals are 563–642, 675–785, and 728–867. The one, strong line observed at 575 ("*C*"-type structure) could, therefore, be $\nu_2(cis)$ or ν_2 coinciding for *cis* and *trans*. For $\nu_5(cis)$, there are observed lines at 726, 770, and 844 of correct type and not unreasonable intensity. If one of these were the second fundamental (the first being 575) the third should be situated at, respectively, 844, 796, and 726 cm^{-1}. If we are guided by intensity considerations, 844 must be a fundamental (Table 2).

For $\nu_2(trans)$ there may be lines at 575, 610, 617, and 639 with emphasis on the last possibility if one wants to avoid having 575 double and, thereafter, chooses the most intense band. Suitable candidates for the position as second fundamental are: 675, 695, 726, and 770. Candidates for the third fundamental are: 726, 770, and some line in the 824–866 region. Intensity considerations makes it desirable to have one of the fundamentals at 695. The line observed there cannot be a "*cis*" line.

We can now test by the product rule if 575 can be the second fundamental. In this case the third fundamental should be at 921 cm^{-1} which is excluded by the Rayleigh rule—thereafter, 639 is tried. Taking two fundamentals at 639 and 695, the third must be in the 824–866 region. This is by no means incompatible with the spectrum. We shall, therefore, take $\nu_5(trans) = 844$ cm^{-1}, counting this line as occurring in the spectrum of both the *cis*- and the *trans*-isomer. Various ways of testing the sum rule may now be applied. The differences:

$$(S_1'' + S_8'') - (S_2'' + S_7'') = (34{\cdot}364 - 34{\cdot}307)\ 10^6 = 0{\cdot}057\ 10^6$$
$$(S_1'' + S_7'') - (S_3'' + S_4'') = (37{\cdot}207 - 37{\cdot}100)\ 10^6 = 0{\cdot}107\ 10^6$$
$$(S_2'' + S_8'') - (S_5'' + S_6'') = (31{\cdot}464 - 31{\cdot}738)\ 10^6 = -0{\cdot}274\ 10^6$$

should be zero for exact fulfilment. They agree satisfactorily.

Discussion

The assignment of frequencies given in this paper is thought to be the best possible at present but fresh experimental evidence may still change it slightly. We want to emphasize that so far neither the Raman spectrum nor the infrared spectrum of *liquid* vinyl fluoride has been studied. The final assignment of fundamentals must wait for this important work to be done.

References

[1] Torkington P. and Thompson H. W., *Trans. Faraday Soc.* 1945 **41** 236.
[2] Bak B. and Christensen D., *Acta Chem. Scand.* 1958 (in press).
[3] Brodersen S. and Langseth A., *Mat. Fys. Dan. Vid. Selsk.* 1956 **1** 1.
[4] Cole A. R. H. and Thompson H. W., *Proc. Roy. Soc.* A 1951 **206** 17.
[5] Pitzer K. S. and Freeman N. K., *J. Chem. Phys.* 1946 **14** 586.
[6] Gullikson C. W. and Nielsen J. R., *J. Mol. Spectr.* 1957 **1** 158.

Spectrochimica Acta, 1958, Vol. 12, pp. 370 to 390. Pergamon Press Ltd., London

REPORT OF MEETING

9th Annual Pittsburg Conference on Analytical Chemistry and Applied Spectroscopy

THE conference was held from March 3 to 7, 1958. Of the 150 papers presented, some 82 of them covered subjects of spectroscopic interest.

Techniques for obtaining the infrared spectra of micro amounts of solids, liquids and gases were featured in the sessions on infrared spectroscopy.

In the field of analytical emission spectroscopy, the simultaneous direct-reading determination of all elements of interest in carbon and low alloy steels, including C, P and S was discussed. Direct-reading attachments for several commercial spectrographs and recent developments in the determination of the gaseous element content of metals were also described.

A panel discussion and open forum on X-ray spectroscopy occupied a prominent part of the program in this field. Other important developments discussed were electron probe microanalysis, and a polychromator for the simultaneous determination of as many as 22 elements.

"Space-age" spectroscopy was represented on the program by papers on rocket-borne mass spectrometers for upper atmosphere research, sodium in the upper atmosphere, and the X-ray region of the solar spectrum as observed from rocket measurements.

The subjects of review papers in spectroscopy presented at the meeting were vibrational spectra of M_2H_6 molecules (M. K. Wilson), applications of the theory of molecular electronic transitions (M. Kasha), spectroscopic techniques for studying functional groups at solid-gas interfaces (R. S. McDonald) and the place of infrared spectroscopy among modern methods (N. Wright).

The Spectroscopy Society of Pittsburgh 1958 award was presented to Dr. Norman Wright in recognition of his contributions to infrared spectroscopy.

Abstracts of papers presented at the spectroscopic session were as follows:

Infrared Spectroscopy

Hydrogen bonding in organophosphoric acids:* D. F. PEPPARD, J. R. FERRARO and G. MASON.

Association in organophosphoric acids due to hydrogen bonding appears to be as general as that in carboxylic acids. Molecular weights obtained by freezing point studies show that the following monobasic phosphoric acids are dimeric in benzene and naphthalene: bis-(2-ethylhexyl), bis-(phenyl), bis-(2,6-dimethylheptyl-4), bis-(p-octylphenyl) and bis-(n-butyl). The dibasic phosphoric acids, mono-(2-ethylhexyl) and mono-(p-octylphenyl), were found to be polymeric. Infrared studies of these acids in carbon tetrachloride show that no non-associated OH spectra appear in the fundamental and overtone regions. Monomeric molecular weights are obtained in acetic acid, but here evidence is presented for strong interaction between solute and solvent.

* Based on work performed under the auspices of the U.S. Atomic Energy Commission.

VOL. 12 1958

Determination of the position of the double bond in some unsaturated fatty acids by solid state infrared spectroscopy: H. Susi, Eastern Regional Research Laboratory,* Philadelphia, Pa.

In monounsaturated straight chain C_{18} carboxylic acids with trans configuration, the position of the double bond can be determined by counting the equally spaced absorption bands occurring in the 1175–1350 cm^{-1} region. The number of bands in this "band progression" is related to the length of the chain segment between the carboxyl group and the double bond. No difficulties were encountered due to polymorphism. The 1300 cm^{-1} carboxyl band does not interfere. The beginning of the band progression can be determined by simple polarization measurements and by applying the criteria of approximately equal spacing and roughly uniform intensities. The spectra in the 1175–1350 cm^{-1} region of mono-unsaturated acids are compared with spectra of saturated acids with a total chain length equal to the first segment of the unsaturated acids. They show marked similarities. The assignment of the progression bands is briefly discussed in light of our results on unsaturated acids and previously reported data on saturated acids.

Near-infrared analysis of mixtures of primary and secondary aromatic amines: Kermit Whetsel, William E. Roberson and Max W. Krell, Tennessee Eastman Co., Division of Eastman Kodak Co., Kingsport, Tenn.

The analysis of mixtures of primary and secondary aromatic amines by near-infrared spectroscopy was investigated. By utilizing the N–H overtone and combination bands near 1·49 and 1·97 microns respectively, methods were developed for the determination of aniline and N-ethylaniline in mixtures covering the entire concentration range and for the more precise determination of small amounts of the primary amine. The standard deviation is about $\pm 0{\cdot}5\%$ for the determination of both amines and $\pm 0{\cdot}1\%$ for the determination of aniline only. Aliphatic amines and tertiary aromatic amines do not interfere. Similar methods may be used to analyze other mixtures of primary and secondary aromatic amines.

Infrared spectrophotometric method for assay of 3° meta para cresol: M. F. Kranc and D. J. Kadavy, Pittsburgh Coke & Chemical Company, Neville Island, Pittsburgh 25, Pa.

An infrared method for the assay of meta para cresol has been developed that is far more reliable than the standard chemical method. Infrared analysis of typical plant material has repeatedly shown a ratio of almost 2 to 1 meta to para isomer content while the accepted figure is 1·5 to 1.

Infrared determination of tar acid content of tar acid oils: M. F. Kranc, D. J. Kadavy and C. M. Fialon, Research and Development Department, Pittsburgh Coke & Chemical Co., Pittsburgh 25, Pa.

An infrared method has been developed for the precise measurement of the 2·76 micron hydroxyl band height and the conversion of this measurement into an estimation of tar acid content. Calibration mixtures were made from phenol and cresols and the non-hydroxyl containing, caustic washed tar acid oils. The phenol-cresol ratio of the mixtures approximated the ratio in typical tar acid oils as analyzed by gas liquid chromatography. A comparison is given between the IR data and results obtained by two accepted chemical methods. Statistical evaluation of the results shows the standard deviation of the test method to be 2% relative.

Micro gas cell for infrared spectroscopy: J. U. White, N. L. Alpert and S. Weiner, The White Development Corp., Stamford, Conn. and W. M. Ward and W. S. Gallaway, Beckman Instruments, Inc., Fullerton, Calif.

In the analysis of liquid samples by gas chromatography, it is often difficult to identify the different fractions separated by the column. To make it possible to measure the infrared

* A laboratory of the Eastern Utilization Research and Development Division, Agricultural Research Service, United States Department of Agriculture.

absorption spectra of the gases directly as they emerge from the column, a micro gas absorption cell of the multiple traversal type has been built. A one meter path length has been folded into a volume of 22 ml by taking 24 traversals of a 4·17 cm distance. This gives about fifty times more absorption than would result from the same amount of sample in a standard 10 cm gas cell. The new cell may be heated to prevent condensation of gases with high boiling points. It fits in the sample space of the Beckman IR-4, 5 and 6 infrared spectrophotometers. The construction of the cell will be described and its performance illustrated.

Design and performance of an automatic, double-beam prism grating, infrared spectrophotometer: Joseph Ashley and William M. Ward, Beckman Instruments, Inc., Fullerton, Calif.

A new fore-prism grating instrument which is an outgrowth of the IR-4 infrared spectrophotometer will be described. The substitution of a grating for the prism of the second monochromator gives improved resolution as compared to a double prism monochromator. Resolution of 0·3 cm^{-1} at 1000 cm^{-1} will be demonstrated and the possibility of exchanging this resolution for increased speed or signal to noise. A unique automatic order changing system permits continuous scanning from 600 to 4000 cm^{-1} and preserves linear wavenumber presentation. All other features of the IR-4 have been maintained.

Quantitative analysis using the Perkin-Elmer model 137 infracord spectrophotometer: Fred Behnke and Robert Anacreon, The Perkin-Elmer Corp., Norwalk, Conn.

The quantitative analysis of gases, liquids, and solids is evaluated on the Perkin-Elmer Model 137 infracord spectrophotometer.

Analysis of gases using a long-path gas cell and of liquids and solids using a small volume microcell allows accurate measurement of trace quantities.

A study also was made of the precision with which data may be interchanged from one infracord to another. A fixed standard sample was run on 50 instruments and absorption coefficients at various wavelengths compared on a statistical basis.

VOL. 12 1958

Polyethylene capillary tubes as ultra-micro liquid cells for infrared spectroscopy: W. S. Molnar and V. A. Yarborough, Development Department, Union Carbide Chemicals Company, P.O. Box 8004, South Charleston, WVa.

A novel and simple technique for obtaining the infrared spectra of minute amounts of liquids is presented. The undiluted sample is enclosed in a small capillary tubing of polyethylene. The tube is mounted on the stage of the Perkin-Elmer infrared microscope attachment. The spectrum is recorded by the conventional techniques for the study of textile fibers. The construction of the polyethylene capillaries and the techniques used to obtain spectra by this technique are described in detail.

A unique cold-trap has been designed for sampling directly from gas chromatographic equipment with the polyethylene tubes. The polyethylene capillary technique has been used to obtain infrared spectra of minor components trapped from the gas chromatograph or recovered from other micro-methods of separation. Satisfactory infrared spectra have been recorded with less than five micrograms of liquid enclosed in the polyethylene capillary. Several spectra representative of those obtained with this new technique are presented.

Micro infrared-gas chromatography techniques as applied to complex organic systems: William S. Gallaway, Theron Johns, Donald G. Tipotsch and William F. Ulrich, Beckman Instruments, Inc.

The quantitative interpretation of the infrared spectra of complex organic mixtures is especially difficult when the identification of minor constituents is uncertain. The use of gas chromatography, therefore, appears highly desirable as a means for isolating and concentrating impurities prior to the infrared analysis.

Unfortunately, the advantages attained with this procedure often are not easily realized because of sample size restrictions. For this reason, various methods for collecting micro samples

and obtaining their infrared spectra have been developed and tested. The simplicity of these techniques is demonstrated with fractional microliter samples. Applications showing the characterization of essential oils such as clove, rose, orange, and apple essence; and the identification of impurities in hexadecane and absolute alcohol are presented. Extension of the microtechnique to include handling the sample in gaseous form is shown to have certain advantages.

Spectroscopic techniques for studying functional groups at solid-gas interfaces: Robert S. McDonald, General Electric Research Laboratory, Schenectady, N.Y.

Every solid surface has a chemical functionality which derives from its history—how it was prepared, what substances it has been in contact with, in what order and under what conditions. Infrared spectroscopy stands almost alone among the techniques of surface chemistry in allowing direct observation of surface functional groups. Apparatus and techniques which have been found useful in exploring surface functionality will be described. The advantages and limitations of spectroscopic techniques and their relationship to other techniques of surface chemistry will be discussed.

The infrared spectra of substituted anilines: Ernest J. Kaatz and Edward J. O'Reilly, Jr., Department of Chemistry, University of North Dakota, Grand Fork, N.D.

The infrared spectra of 2,6-di-X-4-Y-anilines are reported in the region 1600–400 cm^{-1}. The substituents X, Y are the hydrogen, methyl, methoxy, chloro, and bromo groups. These spectra are correlated with respect to the nature and position of the substituents. Spectral changes in going to the isomeric form 3,5-di-X-4-Y-aniline are discussed.

Detection and determination of hydroxyl by near infrared spectrophotometry: Robert F. Goddu, Research Center, Hercules Powder Company, Inc., Wilmington, Del.

The near infrared region (1·0 to 3·0 microns) is particularly valuable for the determination of hydroxyl compounds. By using the fundamental free O—H stretching vibration at 2·7 to 2·85 microns excellent sensitivity and selectivity may be obtained. Applications of this region to the determination of alcohols, acids, hydroperoxides, and phenols will be discussed. Particular emphasis will be placed on the wavelengths of the absorption maxima of various types of hydroxyl compounds and on the variation of molar absorptivity with structure or type of hydroxyl group. The effect of intramolecular hydrogen bonding and its utility in analytical work will also be described. Instrumental variables and their effect on analytical work, in particular spectral slit width, will be discussed in some detail. All work was carried out on a Beckman Model DK-2 spectrophotometer.

Infrared absorption spectra of some transition metal chelates of glycine: Anthony J. Saraceno, Brother Columba Curran, c.s.c., S. Mizushima and J. V. Quagliano, University of Notre Dame, Notre Dame, Ind.

The infrared absorption spectra of metal chelates of glycine with Cu(II), Ni(II), Co(III), Zn(II), Pt(II) and Pd(II) have been measured in the 2–15 micron region and compared with potassium glycinate, ethylglycine and glycine hydrochloride. The spectra reveal that essentially covalent metal-to-nitrogen bonds are present in the metal complexes as evidenced by the shift of the N—H stretching frequency to lower values on coordination. Retention of the carboxylate antisymmetric stretching vibration at about 1600 cm^{-1} indicates the resonance structure of the carboxylate group is essentially maintained and that the bond between the metal and carboxylate group is for the most part ionic. Significant differences in the spectra of geometrical isomers of platinum(II) and cobalt(III) were observed. The assignment of observed bands for the coordination compounds has been made based on the study of normal vibrations of glycine, mercuric amido halides and 1,2-dichloroethane. Interesting dehydration effects have been observed for some of the metal complexes, especially for bis-(glycino)-zinc(II) monohydrate.

A computer for determining wave number, intensity and line width of maxima in the infrared spectrum: Murray Eden, Frank Noble and Joseph Hayes, National Heart Institute, Bethesda, Md.

A special purpose analogue computer has been developed for the analysis of experimental curves resulting from the statistical distribution of some variable in a molecular population—e.g. molecular absorption spectra and spatial diffusion patterns. This device electronically generates up to five distribution functions—Lorentz or Gaussian. The amplitude, relative position and width of each function is independently variable. The linear sum of these functions is displayed on an oscilloscope screen. By adjusting the parameters of each function any experimental curve which is the sum of such a set of functions can be simulated and matched. The numerical values of the parameters characterizing the experimental curve can then be obtained directly from the instrument.

The ease with which numerical data can be extracted suggests that the computer will facilitate the storage and interpretation of these data, as well as to increase the resolution presently obtainable when there is extensive overlap of peaks in the spectrum.

Near-infrared spectra of primary aromatic amines: Kermit B. Whetsel, William E. Roberson and Max W. Krell, Tennessee Eastman Co., Division of Eastman Kodak Co., Kingsport, Tenn.

The near-infrared absorption spectra of 25 primary aromatic amines were measured with particular attention being given to the positions and intensities of the N—H bands occurring between 800 and 2600 mμ. The combination bands involving N—H bending and stretching modes varied in position from 1960 to 1983 mμ and had molecular extinction coefficients ranging from 1·23 to 2·95. The first overtone bands of the N—H symmetric stretching vibrations occurred between 1485 and 1503 mμ, and the extinction coefficients varied from 1·18 to 1·53. Asymmetric first overtone stretching bands having extinction coefficients of 0·14 to 0·43 were found between 1433 and 1460 mμ, and second overtone stretching bands with extinction coefficients of about 0·03 occurred in the 1012- to 1026-mμ region. Many of the variations in position and intensity of the N—H bands can be correlated with the structure of the amines. Some interesting correlations can also be made between the structure of an amine and the relationships among the various N—H bands in its spectrum. The effect of concentration upon the positions and intensities of near-infrared N—H absorption bands will also be discussed.

VOL. 12 1958

Analytical Emission Spectroscopy

Extraction and flame spectrophotometric determination of aluminum: Howard C. Eshelman* and John A. Dean, Department of Chemistry, University of Tennessee, Knoxville, Tenn., with Oscar Menis and T. C. Rains, Analytical Chemistry Division, Oak Ridge National Laboratory, Oak Ridge, Tenn.

A rapid, sensitive, and direct flame spectrophotometric method has been developed for aluminum. Aluminum is extracted from an acetate buffered solution adjusted to pH 5·5 to 5·7 with a 0·1 M solution of TTA in 4-methyl-2-pentanone and aspirated directly into an oxy-hydrogen or an oxy-acetylene flame. The emission intensity of aluminum is increased 100-fold as compared with the emission from an aqueous solution. At a slit opening of 0·030 mm, operating conditions are easily adjusted to provide sensitivities of 0·25γ of aluminum per ml. per instrument scale division. Both the stronger atomic line at 394·4 mμ and the oxide band system at 484 mμ are satisfactory for the determination of aluminum; the intensity of the former is one-half the intensity of the band system. The calibration curve is linear from 5 to 20γ of aluminum per ml. Tolerance limits for a wide diversity of ions have been determined. When necessary, preliminary separation methods have been devised to remove interfering ions. The method has been successfully applied to a variety of NBS samples.

* Present address: Chemistry Department, Southwest Louisiana Institute, Lafayette, La.

Spectrochemical determination of trace amounts of cerium in ferrous materials: Rudolph Rust and Wm. J. Edgar, Manufacturing Engineering Office Manufacturing Staff, Ford Motor Co., Dearborn, Mich.

In this study the method describes how to achieve quantitative spectrographic analyses for cerium concentrations normally below the threshold of detectability in an iron matrix. Analytical determinations of cerium in the range (0·001% to 0·010%) are accomplished in aqueous solution using the rotating carbon electrode. The investigation is carried out using high precision spark excitation to excite high energy cerium lines near 2200 Å. The main interest is to appraise the techniques necessary to determine trace amounts of cerium, quantitatively. Chemical sample preparation, high energy precision spark excitation, and photographic plate sensitivity are combined in the method. The preparation of synthetic standards is discussed. The spectrographic precision of the method is evaluated.

Effect of source damping on matrix effects and repeatability: T. P. Schreiber and R. F. Majkowski, Research Staff, General Motors Corporation, Detroit, Mich.

The multisource condition which yields a "black burn" has been found to minimize matrix effects (Goldblatt, Spectrochim Acta, IX, 3, p. 25). A study was made of this type source condition by varying the resistance from 1·5 to 5 ohms (other parameters; 10 μF; 60 to 100 μH depending upon resistance; sample positive; 120° pointed graphite counter electrode).

Oscilloscope traces of discharge current indicate it to be critically damped at 2·5 ohms. This value is lower than theory predicts because of the reignition voltage of the analytical gap.

Spectral intensity varied over a wide range with resistance changes, being high at low values, 100 at 1·5 ohms (underdamped), falling sharply to a minimum 15 at 2·5 ohms (critically damped), and then rising slowly to 30 at 5 ohms (overdamped).

With resistance values of 2·0, 2·5 and 3·0 ohms, combined analytical curves were plotted for low alloy steel, stainless steel, tool steel, and cast iron. The least matrix effect was exhibited by the 2·0 ohm condition.

Repeatability studies indicated that in general the 2·0 ohm condition was best although specific elements in particular alloys were better with the 3·0 ohm condition.

Spectrometric standard samples for ingot iron and low-alloy steel: Robert E. Michaelis and Bourdon F. Scribner, National Bureau of Standards, Washington 25, D.C.

A set of eight standard samples has been prepared for the spectrometric analysis of ingot iron and low-alloy steel to cover an extended range of concentrations for 22 elements. The standards are now available with values certified for 13 elements: C, Mn, P, Si, Cu, Ni, Cr, V, Mo, Sn, Ti, B, and As; additional elements will be certified later. Melting, casting, fabricating, and testing procedures were investigated to ensure proper gradation of concentrations and high homogeneity in the final product. Details of the preparation and the results of chemical and spectrometric tests of homogeneity are given. The standards were finished to two sizes: rods $\frac{7}{32}$ in. in diameter, 4 in. long; and disks $1\frac{1}{4}$ in. in diameter, $\frac{3}{8}$ in. thick, the latter being suitable for both optical and X-ray spectrometry. Applications of the standards are discussed and typical analytical curves, including carbon and phosphorus, are presented.

Direct reading analysis of steel solutions using a reservoir-cupped center post electrode: L. C. Flickinger,* E. W. Polley and F. A. Galletta, Chemical Department, Campbell Works, Youngstown Sheet & Tube Co., Youngstown, Ohio.

A rapid and accurate direct reading spectrometric method for the analysis of steel solutions has been developed using a reservoir-cupped center post electrode and a high voltage spark excitation. The method is especially useful when analyzing finished steel products which vary in physical form and metallurgical history. Steel is analyzed for molybdenum, silicon, lead, acid soluble aluminum, copper, nickel, manganese and chromium.

* Deceased.

Point to plane spectrographic analysis employing alloy grey iron standards and method of casting: Orren G. Clark, Cleveland Diesel Engine Division, General Motors Corp., Cleveland, Ohio.

A method is presented describing foundry technique for homogeneous alloy cast iron spectrographic point to plane standards.

Spectrographic and source unit conditions are given, showing analytical curves for the various elements analyzed. Comparison tables showing wet chemical results versus spectrography results are shown.

Metallurgical history of cast iron samples illustrated by photomicrographs is discussed. Accurate spectrographic results are obtained regardless of the metallurgical structure (quenched iron, chilled iron, soft iron) of the iron under the specific casting and spectrographic conditions used. There is no shift in the analytical curve.

Application of the Quantovac to provide complete, high speed, low alloy steel analysis: J. M. Carrol, G. Andermann and M. F. Hasler, Applied Research Laboratories, Lausanne, Switzerland and Glendale, Calif.

The production version of the Quantovac allows use of the ultraviolet spectrum from 1600–3300 Å as one of its operating ranges. Up to twenty-four multiplier phototubes can be utilized with the new box type head. This allows simultaneous analysis of all elements of interest in carbon and low alloy steels. These elements include C, P, S, and As among the nonmetallics, and Mn, Cr, Ni, Si, Cu, Mo, Sn, etc., among the metallics.

By the use of argon in the arc-spark chamber instead of nitrogen, as originally reported, enhanced line intensities and line-to-background ratios are obtained for most elements. This allows carbon and low alloy steels to be completely analyzed with a single discharge, which provides adequate sensitivity for residuals and excellent accuracy for alloying elements. Complete details are provided.

VOL.
12
1958

Steel quality control by using the A.R.L. quantometer: Harold C. Brown, Armco Steel Corp., Butler Works, Butler, Pa.

This paper describes the precision and accuracy of the A.R.L. quantometer in the analyses of stainless, silicon, and plain carbon steels produced at the Butler Works of the Armco Steel Corporation over the past five years. The procedure employed to determine the accuracy of the instrument and a comparison of quantometric determinations with referee chemical determinations will be discussed. Scope of control, concentration ranges, and allowable tolerances will also be discussed.

Other factors which influence the precision and accuracy of the instrument, such as, the surface preparation of standard and unknown samples, grade of graphite electrodes used, and so forth, will be described. Number of breakdowns causing furnace delays will also be given.

Spectrographic determination of carbon in sedimentary rocks using direct-current arc excitation: William H. Dennen, Cabot Spectrography Laboratory, Massachusetts Institute of Technology, Cambridge, Mass.

Carbon may be determined in its various compounds by direct-current arc emission spectrography. When samples are excited in copper electrodes, the carbon in the sample combines with atmospheric nitrogen to form cyanogen, and the bandhead CN 3883 Å is measured. Cathode excitation at 6 A and ~50 V provides the best sensitivity for graphitic carbon and carbonates. A coefficient of variation of 13% is obtained. Marked differences of relative intensity are related to the nature of the carbon compound, to the excitation conditions, and to the presence of silica. These matrix variations are controlled by comparing unknown samples with chemically similar standards, maintaining uniform arcing conditions, and diluting samples with quartz. Separate determinations for different compounds of carbon are required.

A field method of spectrographic analysis for use in geochemical exploration—An improved technique: U. Oda, A. T. Myers and E. Cooley, U.S. Geological Survey, Denver, Colo.

A semiquantitative spectrographic method of rock and soil analysis reported at the Pittsburgh Conference in 1956 was found to give erratic results for the more volatile elements.

The method previously reported utilizes powder standards to determine as many as 32 elements. In it, ten (10) mg of standard or sample powder are mixed with 20 mg of graphite powder, arced a predetermined time, and the spectra recorded by means of a small grating spectrograph; for estimation of element concentration, the sample spectrum is compared with a standard by using a visual comparator. The modification of this method is the addition of 20 mg of a $CaCO_3$-graphite mixture (1 : 5) on top of the sample-graphite powder. This addition gives a smoother burning arc and minimizes sample loss during arcing, so that the former variability of results is also minimized. The improved technique has been tested in a truck-mounted spectrographic laboratory constructed and used by the U.S. Geological Survey in geochemical exploration.

Data are presented on about 30 samples analyzed by the Bureau of Standards or the U.S. Geological Survey. The accuracy of this new technique shows substantial improvement over the earlier method when compared with quantitative results.

Determination of barium, calcium, and strontium in celestite: Dorris M. Doyle and A. B. Chandler, Foote Mineral Company, Research and Development Laboratory, Box 576, Berwyn, Pa.

Barium, calcium and acid insolubles are determined in celestite ($SrSO_4$) by first converting the strontium, calcium and barium sulfates to carbonates by fusion with sodium carbonate, leaching and washing out the water soluble carbonates.

The calcium is determined by flame photometry using calcium standards containing strontium. Barium is determined by double precipitation as a chromate in a buffered glacial acetic acid solution first at a pH of 6 and the second precipitation at a pH of 5·8. Residual sodium is determined by flame photometry. Silica and acid insolubles are determined in the untreated celestite. Strontium is obtained by difference.

The flame photometry was done on the Beckman B and DU obtaining identical results.

Approximately a day of elapsed time is required for the conversion of the celestite to carbonates. The celestite as carbonate is allowed to dry overnight and the analysis completed the second day. The method of analysis is precise and accurate with an indicated standard deviation of 0·5 per cent.

Spectrochemical determination of strontium to calcium ratios in food, milk, cream, blood, feces, and urine of cows: George V. Shalimoff, John G. Conway and Ann E. Pitzer, Radiation Laboratory, University of California, Berkeley, Calif.

A d.c. carbon-arc spectrochemical method has been developed for the determination of strontium to calcium ratios in the food, milk, cream, blood, feces, and urine of cows. A marked dependence of the line intensities of the two elements by the amount of each present was observed, especially with very small amounts. To overcome this matrix effect, sodium is added to the samples to produce uniformly enhanced and reproducible spectral lines in the range of 10^{-4} to 5×10^{-2} strontium to calcium ratios. The results of analysis of the products of three cows and their food are given with a precision of $\pm 12\%$.

Spark in flame spectroscopy: William A. Straub, S. H. Bauer and W. D. Cooke, Baker Laboratory of Chemistry, Cornell University, Ithaca, N.Y.

A light source consisting of a flame crossed by a high voltage spark has been reinvestigated for possible use in solution analysis. This combination was found to possess the convenience of the flame photometric method coupled with the sensitivity of a spark technique. Good reproducibility was obtained due to the stabilizing action of the flame on the spark.

Line intensities were measured by a photomultiplier-tuned amplifier-recorder circuit in conjunction with a wavelength scanning spectrometer.

Samples were introduced as a spray in the flame. Most elements excited by the source were detected at the 1 p.p.m. level or lower. Especially good sensitivity was shown for Zn, Cd, Mg and Ca. Experimental parameters affecting sensitivity and precision were investigated and optimum conditions were selected. Interferences were noted and partially corrected for by employing a "radiation buffer."

A study in oxy-cyanogen flame photometry: PAUL GILBERT, JR., Beckman Instruments, Inc., Fullerton, Calif.

As the oxygen–cyanogen flame, burning at 4560°C, offers the hottest conveniently available chemical source of heat, its use as a spectrochemical source has been suggested. An instrument has been assembled comprising a concentric atomizer, heated spray chamber, aerosol divider, and platinum-tipped burner for burning the premixed flame, and quartz lens and concave backing mirror for focusing the light upon the slit of a Beckman DU spectrophotometer provided with blue- and red-sensitive multiplier phototubes, electronic power supply, wavelength drive, energy recording attachment and recorder. With a cyanogen flow of 200 ml/min, operation is economical and attended with negligible hazard. Sample is consumed at about 0·3 ml/min. Emission characteristics of the flame itself and a number of elements have been studied. Most of the spectra are simple and free from bands or continua, and intensities are so great that the spectrophotometer can be operated at maximum resolution.

Automation in spectrometric recording and computation: BOURDON F. SCRIBNER and ROBERT E. MICHAELIS, National Bureau of Standards, Washington 25, D.C.

The application of high-speed electronic read-out systems in emission spectrometric measurements offers advantages of reduction of transcription errors and marked improvement in speed, particularly when the data are to be treated statistically. A system is described in which the output from a spectrometer is fed to digital electronic storage and subsequently read into an IBM card. Information is printed and punched on the card for intensity measurements on 18 chemical elements, plus sample identification and a serial number, all recorded within 10 seconds after the exposure is completed. The recording of data in a form suitable for immediate submission to an electronic computer simplifies the application of computer methods, for example, analysis of variance may be obtained within 15 minutes after spectrometric observations are completed. Applications to studies of homogeneity of alloys and investigations of experimental methods will be described.

VOL. 12 1958

Simplification in spectrochemical measuring systems: FREDERICK BRECH, Jarrell-Ash Company, Newtonville, Mass.

It is well known that Atomcounter type Direct Readers employ a measuring system based on the conversion of the transduced d.c. signal energy to pulses that are summed simultaneously in each channel for the duration of a predetermined internal standard channel count. A marked simplification of the measuring circuit has been achieved by the use of pulse actuated motors capable of driving speeds of 400 c/s. The utility of the system, its precision, sensitivity and stability in spectrochemical analysis, for both X-ray and optical spectroscopy will be described. Since the read out is provided by the rotation of the motor armature, power—albeit in inch/ounces—is available. The unusual feature of a high sensitivity measuring system having work energy available as a bonus will be discussed in terms of designs utilizing this feature.

New direct reading attachment for twenty inch camera three meter concave grating spectrograph: L. O. EIKREM, Engineering Department, Baird-Atomic, Inc., 33 University Road, Cambridge, Mass.

A direct reading attachment for the Baird-Atomic three meter concave grating spectrograph is described. The 20-inch plate-holder is replaced by a "DR Box", an assembly containing focal curve, exit slits, and photomultiplier tubes. Rapid setting of exit slits is facilitated by use of an electronic slit setting attachment. A separate cabinet contains high and low voltage

power supplies, the measuring circuitry, and the clock type reading units. The concentrations of eight different elements may be read simultaneously. Approximately three hours is required to set up a DR box on a new problem. Photographic work may proceed with the DR box placed in standby status, and approximately ten minutes is then required to return to direct reading on the problem previously set up. Stability of optical alignment is assured by the use of a servo monitor which automatically and continuously keeps the spectrum lines precisely aligned with the exit slits.

A direct-reading attachment for the Jarrell-Ash convertible Ebert spectrograph: R. K. Brehm and George Benzie, Jarrell-Ash Company, Newtonville, Mass.

A direct-reading attachment for the Jarrell-Ash 3·4 meter convertible Ebert spectrograph is discussed. The attachment consists of a housing containing exit-slits and multiplier phototubes on special focal curves mounted permanently in the instrument. To make photographic work compatible with the direct-reading assembly, a movable 30″ × 2″ × 45 degrees reflecting mirror is provided. The camera track and slide, normally located at the primary focus is relocated on the side of the instrument. The direct-reading attachment incorporates standard Jarrell-Ash "Atomcounter" or Hilger & Watts "Polychromator" electronics. Data on precision of alignment and instrumental stability are given.

The design principles of high precision spark sources: A. Bardocz, Hungarian Academy of Sciences, Central Research Institute of Physics, Department for Spectroscopy, Budapest, Hungary.

High precision spark sources are built up today as a combination of electronic elements and spark gaps. The high precision in time which is required for the production of time resolved spark spectra can be achieved with the aid of electrically pre-stressed and pre-ionized spark gaps and with application of a sudden high voltage rise. The sufficient pre-ionization and at the same time the necessary de-ionization of the spark gaps can only be achieved when the charging and discharging processes of the working condenser are completely separated. This separation at higher sparking frequencies can be achieved best by using specially constructed transformers.

The NSL intermediate direct reader: H. M. Bedell, H. Buckert and J. T. Rozsa, National Spectrographic Laboratories, Inc., Cleveland, O.

With over two years field experience, NSL is now ready to report on their direct reader. The unit, designed by H. Buckert, has a number of unusual innovations. While 55 channels, maximum, are possible, the electronic circuitry is unusually simple. Relays and switches in the measuring circuit have been eliminated. The read out system utilizes the new modern impulse counters with digital display. The spectrometer utilizes a 2 meter plane grating mounting. Details of the unit and performance data will be presented.

Recent developments in the analytical spectroscopy of the rare earth elements: Richard N. Kniseley, Velmer A. Fassel, Carl G. Tremmel and Raymond J. Jasinski, Institute for Atomic Research and Department of Chemistry, Iowa State College, Ames, Iowa.

This paper will summarize recent developments in applying spectroscopic techniques to the analysis of rare earth mixtures. The subjects to be discussed include: (a) pertinent data on purity determinations of the heavy rare earths by emission spectroscopy; (b) line misidentifications in the emission spectra of the rare earths; (c) analytical applications of flame spectra; (d) near infrared absorption spectra of aqueous solutions of the rare earths; and (e) emission spectrometric determination of thorium in cerium.

The spectrochemical determination of zirconium in plutonium: Roy Ko, General Electric Company, Hanford Laboratories Operation, Richland, Wash.

The spectrographic analysis of plutonium for impurity elements is not without difficulties due to the complex emission spectrum of plutonium and to its toxicity. Separating the plutonium

from the elements of interest would reduce the spectral interference and also the health hazard. In the determination of zirconium in plutonium reported here, the plutonium was separated from zirconium by retaining the plutonium as a nitrate complex on the anion exchange resin, Dowex–1, while collecting the zirconium in the effluent and wash solution. The combined effluent and wash solutions were evaporated to a small volume and the resulting solution analyzed for zirconium by graphite spark excitation using cobalt as the internal standard. Concentrations as low as 20 parts per million of zirconium in plutonium have been determined with a precision of $\pm 17\%$ (95% C.L.) for a single measurement.

Ion exchange—Spectrographic method for determination of impurities in uranium and plutonium:* James K. Brody, John P. Faris, Robert F. Buchanan and J. Goleb, Argonne National Laboratory, Lemont, Ill.

The application of an anion exchange procedure was investigated for the separation of impurities from plutonium and subsequent spectrographic determination by the copper spark method. In the initial experiments, 1 g of uranium used as a stand-in for plutonium, was dissolved in concentrated HCl plus a few drops of HNO_3 and placed on a resin column. The impurities were washed through the column, concentrated in a small volume and estimated by the copper spark method.

The investigation was undertaken to determine the concentrational sensitivity of the impurities, limitations due to contamination from solvents, resin and laboratory ware and also to explore any advantages from the standpoint of safety in manipulating plutonium in solution rather than the dry finely divided form required by the carrier distillation method.

Comparison between ion exchange-copper spark method and the carrier distillation procedure will be shown as well as some recovery experiments. Some advantages and disadvantages of the method applied to plutonium will be discussed.

VOL. 12 1958

Recent developments in the emission spectrometric determination of oxygen and nitrogen in metals: Velmer A. Fassel, William A. Gordon, Raymond Jasinski, Monte Evens and Lawrence Altpeter, Institute for Atomic Research and Department of Chemistry, Iowa State College, Ames, Iowa.

The progress made during the past year on applying emission spectrometric techniques to the determination of oxygen and nitrogen in metals will be summarized. Among the topics to be discussed are recent developments in: (a) the determination of oxygen in zirconium, niobium, vanadium, and the rare earths; (b) determination of nitrogen in steels; and (c) non-spectroscopic techniques for measuring gases evolved during the arcing process.

The spectrographic analysis of zircaloy: J. Allen Wheat, Analytical Chemistry Division, Savannah River Laboratory, E. I. du Pont de Nemours & Co., Aiken, S.C.

Tin, iron, chromium, and nickel which are present as alloying constituents in zircaloys can be determined by the point-to-plane spark method of spectrographic analysis. Under appropriate conditions this method can be applied to the analysis of rolled sheet and thin-walled tubing as well as massive blocks. Analysis for the elements listed can be completed in an hour and precision is adequate to determine whether a sample meets the specifications of composition for the alloy.

X-ray Spectroscopy

Progress in X-ray spectroscopy: L. S. Birks, U.S. Naval Research Laboratory, Washington, D.C.

The present state of X-ray spectroscopy will be reviewed. Subjects to be considered include improvements in instrumental components, limits of detection under various conditions, and the electron probe micro-analyzer for point by point analysis.

Investigation of inter-elemental effects in X-ray fluorescence analysis of stainless steels: James W. Cunningham, Cannon-Muskegon Corp., Muskegon, Mich.

The investigation of inter-elemental effects has been a part of the Cannon-Muskegon

* Based on work performed under the auspices of the U.S. Atomic Energy Commission.

Corporation program to use X-ray fluorescence spectroscopy in the analysis of production heats of more than 150 different iron, nickel, and cobalt base alloys that they produce for the investment casting industry. The need to limit the number of standard samples required, and to use those standards to analyze alloys not in regular production, has resulted in melting and analyzing samples of compositions suited for studying the effects of the other elements present on the intensity of the wavelength being measured.

The report will include slides of graphs and tables of the results of those measurements, primarily in the effects of nickel on chromium measurement under different operating conditions. Slides will be included to show sampling methods, as well as the melting equipment used.

X-ray fluorescent analysis of titanium in a high temperature alloy (M-252): Robert F. Stoops and Keith H. McKee, Metallurgical Products Department, General Electric Company, Detroit, Mich.

Most of the difficulties encountered in the analysis of titanium in high temperature alloys can be attributed to segregation of titanium bearing phases. This segregation is much greater in as-cast material than in converted bar stock which indicates that heat treating and/or working helps to distribute titanium more uniformly.

In preparing standards or working curves, the very same surfaces must be analyzed by X-ray fluorescence and wet chemistry to obtain satisfactory agreement. For routine analyses the samples must be selected carefully to obtain results which represent the average titanium content of the material. The standard deviation from the averages in both the X-ray fluorescence and wet chemistry analyses was approximately 1% of the amount of titanium present. When results of X-ray determinations were compared to the averages of wet chemistry determinations, a standard deviation of only 1·1% of the amount present was obtained.

Analysis of yttrium in ores by X-ray fluorescence: C. G. Schultz, R. R. Freeman, Jr., and A. B. Whitehead, Michigan Chemical Corp., St. Louis, Mich.

A method has been devised for the rapid, quantitative determination of yttrium in ores and minerals by X-ray fluorescence. Strontium nitrate was used as internal standard, and no prior separation of the rare earth fraction is necessary. The method has been checked against spectrographic analysis, by addition and dilution experiments, and by material balances. The effects of different matrices have been evaluated for both direct scaling and internal standard methods, and the superiority of the latter is demonstrated.

Interference effects were investigated. Line interference by rubidium was found to be significant, and correction curves have been prepared. The absorption edge interference due to the presence of niobium is not significant at niobium concentrations less than 10%.

Determination of yttrium and zirconium by X-ray fluorescence aqueous solution method: Louis Silverman, Lavada Moudy and William Houk, Atomics International, A Division of North American Aviation, Inc., Canoga Park, Calif.

The wet laboratory procedures for the quantitative determination of yttrium and zirconium in certain types of alloys involve the usual separation procedures and are time-consuming. A fluorescent X-ray spectrographic procedure was investigated in order to develop a rapid quantitative method for the determination of yttrium and zirconium in a large number of samples without prior separations.

The alloy samples were dissolved in hydrochloric and hydrofluoric acids and diluted to volume with water. The fluorescence data were obtained for specific K-alpha lines of the elements and for the background at 0·872 Å. The counting rate of the element corrected for background at 0·872 Å was compared to a standard plot in order to determine the percentage of the element present in the sample.

Yttrium has been quantitatively determined in concentration range of 40 to 250 micrograms per ml and zirconium in the concentration range of 0·25 to 6·0 milligrams per ml. A single pair of determinations can be made in 30 minutes.

Comparison of power supplies and X-ray tubes for X-ray spectrochemical analysis: Nathan Spielberg and Marian Mack, Philips Laboratories, Irvington-on-Hudson, N.Y.

The paper reports results of an experimental investigation of the effects on the X-ray fluorescence intensity of the mode of operation of the X-ray tube, and of the window-anode distance and window diameter, which determine the effective size of the primary cone of radiation. The data show that the gain from the use of constant potential increases rapidly with critical excitation voltage as expected. Two X-ray tubes, one rated at 1 kW with a small anode to window distance, and another rated at 2·5 kW with a larger anode to window distance, were compared. The data illustrate the importance of a minimum window-anode distance for obtaining maximum intensities. The effect of the primary wavelength distribution in exciting fluorescence radiation is discussed. The λ^3 law does not always hold, and conclusions drawn from experiments with pure elements must be applied with care. An experimental comparison is made of the intensities emitted by different target X-ray tubes and the results used to explain an experimental comparison of these same tubes for fluorescence excitation of pure element specimens.

The PXQ, a direct reading X-ray polychromator: E. Davidson, A. W. Gilkerson and J. W. Kemp, Applied Research Laboratories, Glendale, Calif.

A production control X-ray quantometer has been designed for the rapid and accurate analysis of all elements with atomic number above 11. Simultaneous determinations of as many as 22 elements, compared to a common standard, can readily be achieved.

The basic geometry employs the principles of curved crystal optics with the inherent advantages in resolution and sensitivity.

Special emphasis has been placed on instrumental stability, unitized design features, and versatility of applications.

Various combinations of slit widths, crystals, detectors, and optical paths allow optimum choices for any individual problem.

A selection of sample cartridges permits the analysis of solids, liquids, and powders.

Determination of sulfur in petroleum liquids by X-ray fluorescence: T. C. Yao, Research Department, Standard Oil Company (Indiana), Whiting, Ind.

X-ray fluorescence can determine sulfur in such petroleum stocks as gasolines, distillate fuels, residual fuels, and lube-oil additives. A commercial spectrometer, equipped with a rock-salt crystals, helium path, flow-proportional counter, and pulse-height analyzer, is used. The minimum sulfur concentration for analysis is 0·02 weight per cent. With one calibration curve, the X-ray method is as accurate as the ASTM Lamp, Bomb, and Induction Furnace methods and covers the whole range of sulfur concentrations normally determined by them. It also is faster than any of the three; elapsed time per analysis is about ten minutes.

Geochemical (trace) analysis of soil, water and plant samples by fluorescent X-ray spectrography: Merlyn L. Salmon, FLUO-X-SPEC Analytical Laboratory, Denver, Colo.

The objective of this program was to develop a method for soils and other types of samples and a NORELCO 3-position spectrograph with a scintillation detector, pulse height analyzer, and FA-60 tungsten target X-ray tube was used. Minor modifications were made in the amplifier and scaler-ratemeter circuits.

Plastic cups with slip rings and a Mylar window are used as individually-sealed sample containers for the sequential analysis of large numbers of samples with no loss of instrument time for sample loading.

Plant and soil samples are checked as loosely packed powders and liquids are checked directly with no evaporation or other pre-concentration methods.

The experimental results are presented in sequential series of single-element peaks on chart recordings with direct readings of p.p.m. per unit of peak height. These results are suitable for geochemical prospecting and the X-ray method offers some advantages over chemical methods.

VOL. 12 1958

One spectrographer with a 3-position unit can produce results for 6 to 10 times the number of samples per day that can be analyzed by a chemist and the cost of the spectrographic work is about one-half to three-quarters the cost per sample for chemical work. The spectrographic costs include operation, maintenance, and depreciation expense.

Preliminary studies of selective oxidation in molten metals by fluorescent X-ray spectrography: Melvin Leon* and William J. Campbell, Eastern Experiment Station, Bureau of Mines, U.S. Department of the Interior, College Park, Md.

A fluorescent X-ray spectrograph has been constructed in which the sample holder is a resistance wound furnace. Although the oxidizing surface of the metal is approximately 0·5 inches from the X-ray tube window the unit has been operated above 600°C. Conventional flat crystal X-ray optics are used to follow changes in surface composition.

Preliminary studies on arsenic and antimony as impurities in lead indicate that this spectrograph will be very useful for oxidation rate studies, particularly for trace amounts of their elements for which thermogravimetric methods are insensitive.

Selective oxidation may be very useful for trace analysis since the high concentration of the impurity element in the surface increases its detectability to parts per million as compared to parts per thousand in the original sample.

Improvements in the determination of uranium by X-ray absorption: Stancil S. Cooper, James O. Hibbitts and Mary R. Menke, General Electric Company, Aircraft Nuclear Propulsion Dept., Cincinnati 15, Ohio.

Several publications have appeared in the literature concerning the determination of uranium in solution by X-ray absorption. It has been indicated that, as a general rule, frequent recalibration of the X-ray photometer is necessary because of changes in instrument response. This presentation will describe a means of overcoming the difficulties of daily calibration with uranium solutions. The method to be described, using aluminum blocks as the calibrating material, has been found to be both rapid and accurate. The instrument can be calibrated daily in 15 minutes or less. The method has been found to have an L.E. of $\pm 2{\cdot}5\%$ at the 95% confidence level, for a single determination. The difficulty of obtaining cells matched for X-ray absorption work will also be described. The latter point is one which has not been sufficiently stressed previously.

Electron probe microanalysis: R. M. Fisher and R. K. Lewis, Edgar C. Bain Laboratory for Fundamental Research, U.S. Steel Corp., Research Center, Monroeville, Pa.

The various design features of electron probe microanalyzers will be discussed, such as: requirements on the electron optical system used to produce a very fine probe, the light optical viewing system, the stage mechanism, and the X-ray spectrometer. The sensitivity of the method and the accuracy of quantitative analysis will be described and illustrated by typical applications to metallurgical problems. Results of microanalysis of sub-micron precipitates by extraction replica procedures will be shown and the problems involved in extending electron probe microanalysis to elements of atomic number lower than magnesium outlined.

The X-ray region of the solar spectrum from rocket measurements: Herbert Friedman, U.S. Naval Research Laboratory, Washington, D.C.

Photoelectric measurements of solar X-rays have been made in isolated wavelength bands from 1–8 Å, 8–18 Å, 44–60 Å and 44–100 Å. Data obtained during the period of sunspot minimum (1953–1955) can be explained in terms of a half million degree gray body general emission from the corona with a short wavelength limit near 15 Å. Superposed on this background are local hot regions which contribute emissions down to about 6 Å, characterized by temperatures as high as 2 million degrees. The variations in X-ray emission show a definite

* Now on General Electric Fellowship, Physics Department, Cornell University.

correlation with coronal emission lines in the visible spectrum. Recent measurements, at the peak of the solar cycle show an increase in X-ray emission consistent with the increase in ionospheric electron density.

A remarkable increase in hardness of the X-ray spectrum has been observed over the region of a solar flare. In a class 3+ flare the X-ray spectrum extended to 2 Å. The X-ray flux from flares appears to be intense enough to account for most of the accompanying ionospheric disturbances.

Ultraviolet Spectroscopy

Ultraviolet and visible absorption spectra of coals and other carbonaceous materials: R. A. Friedel and J. A. Queiser, U.S. Bureau of Mines, Pittsburgh 13, Pa.

Quantitative determinations of the ultraviolet and visible spectra of thin sections of coal vitrain and of KBr pellets of vitrains and other carbonaceous materials will be described. It has not been possible to obtain quantitative data throughout the ultraviolet region on coal vitrain thin sections because of the difficulty of preparing sufficiently thin, hole-free specimens. The preparation of KBr pellets of coal vitrains for successful quantitative work in the ultraviolet depends mainly on very long grinding times.

The ultraviolet and visible spectra of coal vitrains* and other carbonaceous materials have been investigated in an attempt to measure possible concentrations of polynuclear condensed aromatics. The absorption intensities (specific extinction coefficients, K) of these materials are small compared to the large K values of the principal absorption bands of various polynuclear condensed aromatics. The weakness of absorption intensity and lack of fine structure in the ultraviolet and visible spectra of coals and other presumably highly aromatic substances place severe limitations on the amounts of polynuclear condensed aromatics that can be present in these substances.

VOL. 12 1958

The absorption spectra and stabilities of the complexes of some divalent cations of the first transition series with thioglycolate: D. L. Leussing, University of Wisconsin, Madison 6, Wis.

The stabilities and absorption spectra of the complexes of thioglycolate with Mn(II), Fe(II), Co(II), Ni(II) and Zn(II) have been investigated. It has been found that stable mono- and bis-thioglycolate complexes are formed. The complexes are somewhat unusual in that those of Zn(II) have relatively high stability compared with those of the other metal ions of the series. The optical spectra of various complexes show both d-level and charge-transfer transitions. The behavior of these energy transitions in the series of metal ions studied will be discussed.

Halogen exchange in potassium halide disks, palladium(II) and platinum(II) complexes: Sister Mary Quintin Ryan, O.S.J., Sister Ann Gertrude Hill, O.S.U., and Brother Columba Curran, C.S.C., University of Notre Dame, Notre Dame, Ind.

Ultraviolet absorption spectra have been obtained for complexes of palladium(II) and platinum(II) halides with halide ions, ammonia, triphenylphosphine and 1,2-bis-(methylmercapto)-ethane at concentrations of about 0·1 mole per cent in KCl, KBr, and KI disks. The data reveal that for both the palladium and platinum complexes at these concentrations M—Cl and M—Br covalent bonds are practically completely replaced by M—I bonds, reversible exchange occurs between M—Cl bonds and bromide ions, and M—I bonds react very little or not at all with chloride or bromide ions. The presence or absence of halogen exchange is also indicated by the colors of the disks, although absorption in the visible region is weaker and less characteristic than in the ultraviolet. The spectra suggest that electronic transitions within the iodine atom in iodo complexes occur more readily in potassium iodide than in potassium bromide or chloride disks.

Molecular weight determination by spectrophotometry: V. I. Siele and J. P. Picard, Explosives Research Section, Picatinny Arsenal, Dover, N.J.

It is possible to determine the molecular weight of amines by the use of spectrophotometry

* Nature, 179, 1237 (1957).

in the visible region. This is accomplished by studying the light absorption of the picrate and styphnate derivatives. The method is remarkable in its applicability to a large variety of amines, i.e. primary, secondary, tertiary, alkyl, aryl, and heterocyclic amines. There appears to be no significant difference between the values obtained when either picrates or styphnates are used, however, it is important that these salts be of high purity. The per cent error is no greater than $\pm 1\%$, as good as any of the methods now used to determine molecular weight.

Optical Fluorescence Spectroscopy

Linear energy spectrophotofluorimeter: WALTER SLAVIN, The Perkin-Elmer Corp., Norwalk, Conn.

Spectrophotofluorimetric data obtained on conventional equipment depends upon the instrument parameters. Numerous factors affect this data, most notably the variation of source luminosity and detector sensitivity with wavelength. This variation can affect peak wavelength as well as curve shape, and data obtained even on equipment of similar design may vary considerably.

A thermocouple detector responds linearly to energy and this fact has been utilized to design an instrument which records fluorescence in energy units. A portion of the energy from the excitation monochromator is directed to the thermocouple. A servo coupled to the excitation monochromator slits acts to keep the signal constant, which provides constant energy on the sample when the excitation wavelength is scanned. A second servo controls the slits of the fluorescent monochromator so that the detector, a 1P28 photomultiplier, will produce a signal linearly related to energy. This servo is controlled by an adjustable electrical cam and accounts for monochromator dispersion, detector sensitivity, etc. It is easily set by using the first monochromator as a constant energy source.

Merits and performance characteristics of the system will be discussed and some preliminary data will be presented.

Fluorescence and absorption spectra of estrogens in sulfuric acid studied with recording spectrofluorometers: WILLIAM S. BAULD, Department of Metabolism and McGill University Clinic of the Montreal General Hospital, Montreal, Quebec, Canada; LEWIS L. ENGEL, John Collins Warren Laboratories of the Massachusetts General Hospital, Boston, Mass.; and JOSEPH GOLDZIEHER, Department of Endocrinology, South-west Foundation for Research & Education, San Antonio, Texas.

Two automatic recording spectrofluorometers have been designed. Their features will be described and compared to a commercially available instrument.

This instrumentation has made possible a study of the optimum conditions for the development of fluorescence in sulfuric acid of mircoquantities of estrogenic steroids. Absorption spectra were determined in a ratio recording UV spectrophotometer; fluorescence spectra were studied with respect to excitation wavelength, acid concentration, ethanol concentration, time and temperature of fluorescence development. Estrone estradiol-17b, estriol, 16-epiestriol, 16a-hydroxyestrone, 16-ketoestradiol-17b, 16-ketoestrone and 2-methoxyestrone were studied in this fashion. Estrone, estradiol-17b and the epimeric estriol fall into one group, which absorbs maximally around 450 mμ and has a fluorescence peak around 480 mμ. The other estrogens, which have a lower fluorescence yield, absorb maximally around 500 mμ and have a fluorescence peak around 530 mμ. The 436 mμ mercury line was the best excitation source in all instances.

Spectrofluorometric studies on some mono- and di-hydroxy naphthalenes: DAVID M. HERCULES* and L. B. ROGERS, Department of Chemistry and Laboratory for Nuclear Science, Massachusetts Institute of Technology, Cambridge, Mass.

The absorption and fluorescence spectra in the near ultraviolet region have been investigated for 1- and 2-naphthol and for 1,3- 1,4- 1,5- 1,6- 2,3- 2,6- and 2,7-naphthalenediols. The fluorescence spectra of most of these compounds have been reported for the first time.

* Present address: Department of Chemistry, Lehigh University, Bethlehem, Pa.

Molecular and Electronic Spectra

Vibrational spectra of M_2H_6 molecules: M. Kent Wilson, Chemistry Department, Tufts University, Medford, Mass.

The infrared and Raman spectra of Ge_2H_6 and Ge_2D_6 have been obtained and analyzed. All fundamental vibrations with the exception of the inactive tortional mode have been identified. These spectra are compared with those previously reported for C_2H_6, Si_2H_6, and related compounds. Some attention is given to the force fields which obtain for these molecules.

Applications of the theory of molecular electronic excitation: M. Kasha, Department of Chemistry, Florida State University, Tallahassee, Fla.

The chief molecular parameters responsible for the photoexcitation behavior of molecules will be analyzed. Special reference to the theory of radiationless processes involving spin-orbital coupling will be made.

The detailed application of the parameters deduced from the above considerations will be made to the various observed electronic energy level patterns. In particular, the variation of molecular excitation behavior with the orbital-type and multiplicity of electronic excited level will be illustrated.

The extension of the results of the spin-orbital coupling theory to inter-molecular cases will be made by a description of three types of inter-molecular perturbation recently observed. In addition, the quantum-mechanical ideas involved in inter-molecular energy migration will be formulated and applied to some recent observations on photoexcitation in molecular composite systems.

The treatment will be largely descriptive rather than mathematical. The applications discussed will include analytical spectroscopy, photosensitization, and more briefly, radiation chemistry and scintillation counters.

VOL. 12 1958

Ultraviolet Spectrophotometry

Extraction and colorimetric determination of chromium in situ with diphenylcarbazide: John A. Dean and Mary Lee Beverly, Department of Chemistry, University of Tennessee, Knoxville, Tenn.

A rapid, selective, and accurate colorimetric determination of chromium is based upon the solvent extraction of chromium(VI) from aqueous 1 N hydrochloric acid with 4-methyl-2-pentanone and development of the red-violet color of the chromium-diphenylcarbazide complex in the extract. The absorbance of the color body is measured at 540 mμ 10 minutes after mixing. Beer's law is followed. The optimum concentration range extends from 0·5 to 10·0γ of chromium in 6 ml of solution. Very large amounts of iron and moderate amounts of vanadium offer no interference. The method is particularly applicable to cast iron and steel samples whose chromium content is low.

Expansion of the transmittance scale of a spectrophotometer: Robert Bastian, Richard Weberling and Frank Palilla, Research Laboratories, Sylvania Electric Products, Inc., Bayside, N.Y.

Recent emphasis has been given to a modified method of using colorimeters intended to increase the precision of concentration measurements. In this method the zero per cent transmittance point on the instrument is made to correspond to a finite amount of light rather than darkness. This is accomplished on the Beckman DU spectrophotometer by unbalancing the dark current and more effectively by using the zero suppression circuit. A study is made of the expansion of the transmittance scale as a function of zero suppression and sensitivity settings. Part of this expansion results from allowing more light to strike the photocell than the maximum that can be used normally, and part from utilizing the limit of detection of the electrical circuit. The latter is accomplished more satisfactorily by installing a longer transmittance slide wire. The advantages and disadvantages of zero-suppression methods versus high absorbance differential spectrophotometry employing a normal transmittance zero are discussed.

Continuous colorimetric analyzers for on-stream control: George Schneider, Pratt Johnson, and Hans Fuhrmann, Milton Roy Company, Philadelphia 18, Pa.

This paper will discuss the chemical, optical, mechanical and electrical aspects of continuous colorimetric analyses.

Employing the principles of the Beer-Lambert law, Quantichem analyzers automatically and continuously determine concentrations of specific materials in liquid or vapor process streams. Repeating timed cycles, these instruments are miniature laboratories which perform all steps of an analysis from flushing the sample cells to recording the results and initiating corrective control action.

Using a single light source, Quantichem analyzers meter stream samples and reagents to two cells in order to produce two solutions—one colored in accordance with the concentration of the specific material and the other colored in accordance with the complete absence of the material. The difference in light transmitted through these colored solutions is measured by phototubes which are variable resistances in a modified Wheatstone bridge circuit. A resulting electrical signal activates the recorder.

The earliest analyzers were for total hardness in the range of 0 to 3 p.p.m. and silica concentration in the range of 0 to 0·05 p.p.m. Present development work is concentrating on Quantichem analyzers for dissolved iron, phosphates and oxygen. This method is, of course, applicable to any standard analysis in which concentration is proportional to color intensity.

Ultraviolet stream analyzer: M. H. Axler, Axler Associates, Inc., Corona 68, N.Y.

An ultraviolet flow analyzer developed by Axler Associates upon the specific request of the Pulp and Paper Research Institute of Canada is described along with a few of its potential applications.

The Axler flow analyzer embodies two distinct differences from already existing on stream analyzers, i.e. the wavelength being used for absorption measurements is at 205 millimicrons and a specifically designed sample dilution stage has become intermediary between process stream and the analyzer.

Several models are presently in use both in Canada and the United States on sulfite and kraft pulping digesters as a means for more efficient cooking control. The simplicity of operation and modification renders the instrument versatile for allied process control problems.

Spectrophotometric determination of traces of lead in igneous rocks: C. E. Thompson and H. M. Nakagawa, U.S. Geological Survey, Denver, Colo.

Ferric dithizonate has been extracted from alkaline solutions and found to exhibit a maximum absorbance at 435 millimicrons. This dithizonate of iron has prevented accurate determinations of lead in mafic igneous rocks containing 10% or more iron. Extraction of iron and zinc thiocyanates from an acid solution with ethyl acetate eliminates the interference of iron and zinc inherent in other dithizone procedures. Using an aqueous sample solution that contains 20 per cent ammonium citrate prevents the precipitation of calcium or magnesium phosphate and of aluminum hydroxide that otherwise would occur at the optimum pH for the dithizone extraction of lead. The repeatability of the method is $\pm 3\%$. The method permits the determination of 1 p.p.m. lead in igneous rocks.

A field method for the determination of small quantities of tin in soils and rocks: A. P. Marranzino and F. N. Ward, U.S. Geological Survey, Denver, Colo.

A rapid, relatively simple, and moderately accurate method for the determination of small quantities of tin in soil and rocks is based on the volatilization of the stannic iodide accomplished by heating the sample with ammonium iodide and on subsequent reaction of quadrivalent tin with 4,5-dihydroxyfluorescein. The proposed procedure is applicable to samples containing from 5 to 100 p.p.m. of tin; with modifications it can be used on samples containing larger amounts. The organic reagent is not available commercially, but is prepared by condensing pyrogallol and phthalic anhydride. After purified and stable acetonic solution of the reagent has been added to

a sample solution, the resulting tin complex is extracted at a pH of 2·3 with a mixture of cyclohexanone and *o*-dichlorobenzene. The maximum absorbance of the complex occurs at 500 millimicrons and follows Beer's law in the concentration range of 0·1 to 2 micrograms of tin per ml. Approximately 60 determinations can be made per man day in a camp-site laboratory.

Spectrophotometric determination of traces of mercury in soils and rocks: F. N. Ward, U.S. Geological Survey, Denver, Colo.

A rapid, moderately accurate method for determining traces of mercury in soils and rocks was needed to (1) make possible the number of determinations required in a commodity study, and (2) serve as a reference method to facilitate development of a field method for geochemical exploration. The sample solution is effected by a short digestion of the finely powdered sample in a test tube with hot 9 M sulfuric acid and bromine, the latter generated in place. In an acetate medium containing EDTA, mercury(II) reacts with dithizone to form a complex extractable into a small volume of an immiscible solvent that absorbs maximally at 490 millimicrons. The system follows Beer's law in the concentration range of 0·04 to 3 micrograms per ml. The reaction of interfering elements—such as gold, platinum, silver, copper and bismuth—is prevented by either valence changes, complexation with EDTA, or decomposition of the dithizonates with thiocyanate. Recoveries of added mercury are generally better than 80 per cent, and the accuracy using small aliquots compares favorably with assay methods. More than 50 determinations can be made per man day.

Spectrophotometric determination of iron in niobium and tantalum: C. Albright and T. Clay, Kawecki Chemical Co., Boyertown, Pa.

A spectrophotometric method for the determination of trace amounts of iron in niobium and tantalum is suggested using 4,7-dihydroxy-1,10-phenanthroline (Snyder's reagent). The samples are taken into solution with nitric and hydrofluoric acids, complexed with tartaric acid and made alkaline with ammonium hydroxide. Iron is reduced with sodium hydrosulfite and its color developed in the presence of the fluoride with a solution of Snyder's reagent. The iron content is determined by measuring the absorbance of the red iron complex at 520 mμ.

VOL. 12 1958

Simultaneous spectrophotometric determination of niobium and tungsten: B. McDuffie, Washington & Jefferson College, Washington, Pa. and W. R. Bandi, U.S. Steel Corp. Research Center, Monroeville, Pa.

A thiocyanate method has been developed for the simultaneous spectrophotometric determination of niobium and tungsten in steel. The method is applicable in the presence of tantalum, titanium, and molybdenum.

After preliminary reduction of tungsten(VI) to tungsten(V), the total absorbancy of the niobium(V) and tungsten(V) thiocyanates is measured at 405 mμ, 20 volume per cent acetone being used to stabilize and intensify the niobium-thiocyanate color. Then oxalate ion is added to complex the niobium and thus bleach its thiocyanate color, after which the absorbancy due to the tungsten-thiocyanate complex alone is measured. The difference in absorbancies gives the niobium concentration. Careful control of the temperature is essential for accurate niobium analyses, since the absorbancy of the niobium-thiocyanate complex is temperature dependent, decreasing 1·5 per cent per degree rise in temperature at 25°C.

The spectrophotometric determination of copper in titanium and other metals with dicyclohexanone oxalyldihydrazone: W. K. Murray, Watertown Arsenal, Watertown, Mass.

Dicyclohexanone Oxalyldihydrazone has been applied to the direct spectrophotometric determination of copper in titanium alloys and other metals. This reagent reacts in alkaline solution with copper to form an intense blue colored complex which exhibits maximum absorption at a wave length of 600 mμ. The molar absorbtivity of the complex is approximately 16,000. Other metals do not form colored complexes thus allowing the direct determination of copper without extraction or preliminary separations. Data are given comparing this method with other methods in range, accuracy and precision.

Photometric determination of aluminum in steel: U. T. Hill, Inland Steel Company, East Chicago, Ind.

In a recent paper from this laboratory a direct photometric method for aluminum in iron ores was described. This eriochrome cyanine-R method is applicable to carbon and low alloy steels when the aluminum content is approximately 0·1% or higher. When aluminum determinations are made in lower concentrations and in high alloy steels, a chemical separation must be made. Of the number of methods available for the separation of iron and aluminum the sodium hydroxide method is the most attractive because of its speed and simplicity. The shortcomings of incomplete separation of aluminum from iron and contamination from glassware usually encountered in a caustic separation are overcome by employing a carrier element to effect a complete separation of aluminum from iron while employment of polyethylene beakers eliminates contamination from glassware. Interference from residual iron which may accompany aluminum is eliminated by complexing. Results are accurate and the method is applicable to a wide variety of alloy steels.

Photometric determination of sulfur in steels and high temperature alloys: John Penkrot, Westinghouse Electric Corp., East Pittsburgh, Pa.

An accurate and rapid method for the photometric determination of sulfur in amounts of less than 0·01% in steels and high temperature alloys has been developed. A single determination requires approximately five minutes. In this method, the sample is burned in oxygen in a high frequency unit. The sulfur is oxidized to sulfur dioxide which in turn will bleach the blue color of the starch-iodine complex. The extinction of the blue color is proportional to the concentration of sulfur present in the sample. From a curve prepared by analyzing steels of known sulfur content, the percentage of sulfur can be calculated. The method has been successfully applied to samples containing as low as 0·005% sulfur. The method is also applicable to samples containing over 0·01% sulfur.

Photometric determination of boron in steels and high temperature alloys: John Penkrot, Westinghouse Electric Corp., East Pittsburgh, Pa.

Since the rate of solution of steels and high temperature alloys in phosphoric acid is very slow, a new method of solution in various concentrations of sulfur acid has been developed. Sample weights of one to five grams can be put into solution within three hours. Thus ten boron determinations can be made by an analyst per day. The methyl alcohol distillation procedure is used in conjunction with relatively inexpensive simplified apparatus. Thus, the analysis is finished by the boron-curcumin procedure.

Determination of traces of sulfur in naphthas by lamp combustion and spectrophotometry: R. W. Klipp and J. E. Barney, II, Research Department, Standard Oil Company (Indiana), Whiting, Ind.

A rapid, sensitive method has been developed for determining 1 to 400 p.p.m. sulfur in naphthas. The sample is burned in the ASTM lamp in an atmosphere of carbon dioxide and oxygen, and the sulfuric acid formed is determined by a barium chloranilate spectrophotometric method. The two absorption peaks of chloranilic acid solutions, at 330 mμ and 530 mμ, give satisfactory sensitivity for the entire concentration range. A buffer of acetic acid and sodium acetate simplifies the spectrophotometric determination by eliminating the need to adjust pH. Most common anions do not interfere. Ten to twelve absorber solutions can be analyzed in one hour.

Rapid spectrophotometric determination for manganese, triethanolamine and peroxide complexes of manganese(III): E. R. Nightingale, Jr., Ethyl Corp., Detroit, Mich.

In alkaline triethanolamine solutions, manganese(II) is air oxidized to form a green manganese(III)-triethanolamine complex. At 438 mμ, the molar absorbancy index of the complex is 199. The spectrophotometric measurement of the manganese(III)-triethanolamine complex in alkaline solution offers a rapid and highly selective method for determining manganese.

Evidence is presented for the existence of a manganese(III)-peroxide complex in alkaline solution.

Solution color determination for products of corn: R. J. Smith and C. R. Colburn, George A. Moffett Research Laboratories, Corn Products Refining Company, Argo, Ill.

Solution color evaluation in the corn wet-milling industry has traditionally been accompanied by a variety of visual and instrumental methods. The results have not been suited to direct comparison, nor have they been related to any absolute standard. The spectrophotometric study described here provides a method for direct and accurate comparison of tinctorial power of many different materials. The method also permits color specification on the basis of the internationally-accepted C.I.E. system. This is accomplished by means of transmittance determinations at only three wavelengths, followed by reference to graphs, tables, or equations for conversion to estimates of dominant wavelength, excitation purity, and luminous transmittance. Alternatively the same data can be used to calculate color level on the one-dimensional NBS scale. The method appears to apply equally well to products of the sucrose industry.

The colorimetric determination of amine antioxidants in miscellaneous rubber stocks: C. L. Hilton, United States Rubber Company, Research Center, Wayne, N.J.

A spectrophotometric method for the identification and estimation of most of the commercially available amine antioxidants is described. The rubber stock is extracted with ethanol (or one of the other common extraction solvents) in an Underwriter's Extractor for a period of sixteen hours. A suitable aliquot is treated with a coupling reagent consisting of a diazotized aromatic amine in a mixture of methanol and concentrated hydrochloric acid. The visible absorption spectrum of the coupled color is then determined using a suitable spectrophotometer. The shape of the spectrum identifies the antioxidant and the intensity indicates the amount present.

The accuracy and precision of the method have been found to be satisfactory for routine analyses.

Advantages of the new method over existing procedures include: (1) Identification and estimation of the antioxidant can be made with the same absorption spectrum. (2) Considerable savings in man-hours per determination are effected. (3) Smaller volumes of solvents are required.

Spectrophotometric determination of microgram quantities of chloride and fluoride in metal oxides, salts, and solutions: B. D. La Mont and B. W. Conroy, Westinghouse Electric Corp., Atomic Power Department, Pittsburgh 30, Pa.

Nuclear reactors and high pressure boilers constructed of stainless steel are subject to stress corrosion in the presence of chloride and fluoride in oxygenated systems. Consequently, determinations were requested for chloride (0·5 to 15 micrograms) and fluoride (0·5 to 50 micrograms). A procedure involving bleaching of the mercury (1) diphenylcarbazone complex is used to determine chloride. Fluoride is measured by the bleaching of the thorium "thorin" complex. These procedures were successfully applied to samples of metal oxides, salts, and solutions.

Spectrophotometric determination of traces of copper, iron, and nickel in zinc-cadmium sulfide phosphors: James W. Hunter and Gerrit Dragt, Lamp, Wire, and Phosphors Department, General Electric Company, Cleveland, Ohio.

Methods have been developed for the determination of trace quantities of copper, iron, and nickel in zinc-cadmium sulfide phosphors. The sample is dissolved in hydrochloric acid and converted to the sulfate. The aqueous solution of the sulfate is analyzed by spectrophotometric procedures employing reagents specific for each element. Copper is determined as the cuprous neo-cuproine complex, iron as the iron-Nitroso-R-salt complex, and nickel as nickelic dimethylglyoxime. Interferences are minimized or eliminated without recourse to separation techniques. The methods were developed for copper, iron, and nickel through the range 0 to 10 p.p.m. Higher concentrations as impurities are not normally encountered in these luminescent materials. Results are accurate to within $\pm$0·3 p.p.m.

VOL. 12 1958

Spectrochimica Acta, 1958, Vol. 12, pp. 391 to 405. Pergamon Press Ltd., London

RESEARCH NOTES

Untersuchungen über die Beeinflussung der Frequenz und Intensität der $\nu_{C=O}$- und $\nu_{C=C}$-Banden im I.R.-Spektrum ungesättigter Ketone durch Konjugation und sterische Hinderung

(*Received* 1 *March* 1958)

Abstract—Conjugated unsaturated ketones can be subdivided into two classes according to the frequencies and intensities of their $\nu_{C=O}$- and $\nu_{C=C}$-bands in the I.R. spectrum:

(a) Those with $\nu_{C=O}$-frequencies <1690 cm^{-1} and higher intensities than the mean value of six saturated ketones and relatively high $\nu_{C=C}$-frequencies.

(b) Those with $\nu_{C=O}$-frequencies between 1700 and 1690 cm^{-1} and lower intensities than the saturated ketones and lower $\nu_{C=C}$-frequencies than class (a).

The ketones of the class (a) show no steric hindrance in the planar *s-trans*-configuration, those of the class (b) show steric hindrance or have a fixed *s-cis*-configuration. In all cases examined the *s-cis*-configuration is not sterically hindered.

Im Infrarot- und Ramanspektrum bewirkt eine Konjugation von C=O- und C=C-Gruppen eine Frequenzerniedrigung der beiden Valenzschwingungen um 30–40 cm^{-1}, bezogen auf Verbindungen mit isolierten C=O und C=C-Doppelbindungen [1].

Im Ultraviolettspektrum haben konjugiert ungesättigte Ketone eine charakteristische Bande (*K*-Bande) bei 2100–2500 Å ($\varepsilon_{max} \sim 13{,}000$). Sterische Hinderung der ebenen *s-trans*-Konfiguration (II) macht sich oftmals in einem Absinken des ε_{max} ohne merkliche Veränderung des λ_{max} bemerkbar [2, 3].

Über systematische Untersuchungen der Beeinflussung der Frequenzen und besonders der Intensitäten der $\nu_{C=O}$- und $\nu_{C=C}$-Banden im I. R.-Spektrum von 36 gesättigten, unkonjugiert und konjugiert ungesättigten Ketonen durch die Konjugation und sterische Hinderung soll hier berichtet werden.

Es zeigte sich, was auch nicht überraschend ist, dass sowohl die Intensitäten als auch die Frequenzen der $\nu_{C=O}$-Banden in gesättigten und unkonjugiert ungesättigten Ketonen sehr nahe beeinander liegen. Der Mittelwert aus 6 gesättigten Ketonen ergab sich zu $\nu_{max} = 1719$ cm^{-1}, $A' = 5{\cdot}45$ cm^3/Mol.*

Zum selben Ergebnis führten auch Messungen der Ramanintensitäten von Michel und Duyckaerts [4]: Der Mittelwert der $\nu_{C=O}$-Intensität von 13 gesättigten Ketonen beträgt dort 0·123, bezogen auf die CCl_4-Bande bei 459 cm^{-1}.

In der folgenden Tabelle wurden diese Intensitätswerte der $\nu_{C=O}$-Banden der gesättigten Ketone jeweils als Einheiten für die übrigen Intensitäten gewählt. Die U.V.-Spektren sind in Cyclohexan-Lösung gemessen und die I.R.-Spektren in C_2Cl_4-Lösung mit dem Spektrometer Mod. 112 von Perkin–Elmer mit CaF_2-Prisma aufgenommen. Bei den gesättigten Ketonen nimmt nur das 2 : 2 : 4 : 4-Tetramethylpentanon-3 mit $\nu_{max} = 1687$ cm^{-1} und einer relativen Intensität der $\nu_{C=O}$-Bande von 0·87 eine Sonderstellung ein.

* Die Integration über die Wellenlänge liefert einen Intensitätswert, der dem Anteil der betr. Absorptionsbande an der Verschiebungs-polarisierbarkeit proportional ist. Umrechnung in die üblichen, über der Frequenz integrierten Intensitäten nach:

$$A' = 1/c \cdot l \cdot \int \ln(I_0/I) \cdot d\lambda = \lambda^2 \cdot 1/c \cdot l \cdot \int \ln(I_0/I) \cdot d\nu$$

Tabelle 1. U.V. Absorption. Mittelwerte der Frequenzen und relativen Intensitäten im I.R. -und Ramanspektrum $\nu_{C=O}$- und $\nu_{C=C}$-Banden

Gruppe	Anzahl	R_1 R_2 R_3	U.V. λ_{max}	U.V. ε_{max}	I.R. ν_{max}	I.R. $I_{C=O}$	I.R. ν_{max}	I.R. $I_{C=C}$	Ra [4] $I_{C=O}$	Ra [4] $I_{C=C}$
I	1	H H H	—	—	1723	0·96	1639	0·16	0·92	2·85
unkonj.	2	CH_3 H H	—	—	1719	0·94	1648	0·20		
	2	CH_3 H CH_3	—	—	1718	1·00	1667	0·04		
	1	H CH_3 CH_3	—	—	1722	1·00	1685	0·03		
II	1	H H H	2080	8200	1706 / 1686	0·93	1618	0·13	4·51	5·20
konj.	1	CH_3 H H	2140	7900	1684	1·20	1630	0·12	5·45	4·06
s-trans	4	H H Alkyl	2175	12,800	1702 / 1682	1·23	1630	0·42	9·18	6·25
	2	Alkyl H Alkyl	2245	13,200	1675	1·17	1644	0·25		
	3	Phenyl	2460	13,600	1688	1·20	—	—		
III	2	H Alkyl H	2235	9600	1698	0·70	1617	0·47		
konj.	3	Alkyl Alkyl H	2385	7300	1693	0·82	1624	0·60		
s-cis	2	H Alkyl Alkyl	2320	12,600	1693	0·73	1624	1·05	2·28	15·4
	3	Alkyl Alkyl Alkyl	2420	6600	1687	0·91	1623	0·51		
Aldehyd. konj.	1	H—CO—CH=CH_2	2080	9000	1703	1·33	1620	0·04	6·42	3·09
Arom., sterisch gehindert	1	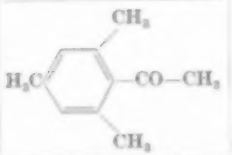	2430	3100	1705	1·25	—			

R_4 = CH_3 oder Alkylreste

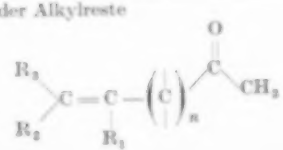

(I) unkonjugiert

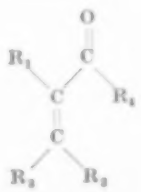

(II) *s-trans*

(III) *s-cis*

Die konjugiert ungesättigten Ketone kann man nach ihrer $\nu_{C=O}$-Intensität und -Frequenz in zwei Gruppen einteilen: Solche mit relativen Intensitäten > 1 und Frequenzen < 1690 cm^{-1}, und solche mit relativen Intensitäten < 1 und Frequenzen zwischen 1700 und 1690 cm^{-1}. An Stuartmodellen ist leicht zu sehen, dass bei den Verbindungen der ersten Gruppe, zu denen auch das Butenon hinzugenommen wurde, keine sterische Hinderung der ebenen

VOL. 12 1958

s-trans-Konfiguration (II) besteht, während bei denen der zweiten Gruppe die ebene *s-trans*-Konfiguration infolge der Überlappung der Alkylreste R_2 und R_4 sterisch gehindert ist. Die *s-cis*-Konfiguration (III) ist dagegen spannungsfrei realisierbar. In die zweite Gruppe wurden drei Ketone mit durch die Struktur festgelegter *s-cis*-Konfiguration hinzugenommen (Äthyliden-*cyclo* hexanon, Butyliden-*cyclo* hexanon und Pulegon). Die Übereinstimmung ihrer Eigenschaften mit denen der anderen Verbindungen dieser Gruppe lässt vermuten, dass auch bei diesen entgegen der Ansicht Braudes [2] die sterisch unbehinderte *s-cis*-Konfiguration vorliegt.

Die Intensität der $\nu_{C=C}$-Bande wird fast bei allen Verbindungen durch die Konjugation erhöht, bei der Gruppe der Verbindungen mit *s-cis*-Konfiguration mehr als bei den *s-trans*-Verbindungen, jeweils verglichen mit ebenso an der C=C-Doppelbindung substituierten unkonjugiert ungesättigten Ketonen.

Beim 2:4:6-Trimethylacetophenon, dessen U.V.-Spektrum auf eine starke Störung der Konjugation infolge sterischer Hinderung schliessen lässt, ist nur die Frequenz der $\nu_{C=O}$-Bande erhöht, nicht aber ihre Intensität erniedrigt. Hier ist keine sterisch ungehinderte *s-cis*-Konfiguration wie bei den Äthylenketonen möglich.

Die Tabelle gibt ferner zum Vergleich einige Messungen der Ramanintensitäten [4], bezogen auf den Mittelwert der $\nu_{C=O}$-Intensität der gesättigten Ketone als Einheit. Durch die Konjugation wird die Intensität der $\nu_{C=O}$- und $\nu_{C=C}$-Banden im Ramanspektrum weit mehr vergrössert als im I.R.-Spektrum. Aber der Gang ist derselbe: Bei sterischer Hinderung der *s-trans*-Konfiguration, d.h. bei *s-cis*-Verbindungen, ist die $\nu_{C=O}$-Intensität kleiner, die $\nu_{C=C}$-Intensität aber grösser als bei den konjugiert ungesättigten Verbindungen mit unbehinderter *s-trans*-Konfiguration.

Eine ausführliche Darstellung und Diskussion der Ergebnisse erfolgt demnächst an anderer Stelle.

Zusammenfassung

Konjugiert ungesättigte Ketone lassen sich nach der Frequenz und Intensität ihrer $\nu_{C=O}$- und $\nu_{C=C}$-Banden im I.R.-Spektrum in zwei Gruppen unterteilen:

(a) Solche mit $\nu_{C=O}$-Frequenzen <1690 cm^{-1} und höheren Intensitäten als der Mittelwert aus 6 gesättigten Ketonen und relativ hohen $\nu_{C=C}$-Frequenzen.

(b) Solche mit $\nu_{C=O}$-Frequenzen zwischen 1700 und 1690 cm^{-1} und niedrigeren Intensitäten als die gesättigten Ketone und niedrigeren $\nu_{C=C}$-Frequenzen als Gruppe (a).

Bei den Verbindungen der Gruppe (a) zeigt die ebene *s-trans*-Konfiguration keine sterische Hinderung, bei denen der Gruppe (b) ist sie sterisch gehindert oder die ebene *s-cis*-Konfiguration festgelegt. Die ebene *s-cis*-Konfiguration zeigt bei den Verbindungen beider Gruppen keine sterische Hinderung.

R. Mecke und K. Noack

Institut für physikal. Chemie,
Freiburg i. Br.

Literatur

[1] Jones R. N. and Sandorfy C. *Technique of Organic Chemistry* (Edited by A. Weissberger). Interscience, New York and London, 1956 p. 481.
[2] Turner R. B. and Voitle D. M. *J. Amer. Chem. Soc.* 1951 **73** 1403.
[3] Braude E. A. and Timmons C. J. *J. Chem. Soc.* 1955 3766.
[4] Michel G. and Duyckaerts G. *Spectrochim. Acta* 1958 **10** 259.

On the problem of calcium depression by phosphorus in flame photometry

(*Received* 30 *March* 1958)

In spite of the many investigations on the problem of Ca-depression by the phosphate-ion in flame photometry (cf. [1–5]), some essential features of this interference remained to be explained. We have made some additional measurements by spraying $CaCl_2$ solutions, with added phosphoric acid, into an acetylene-air and propane-air flame, at various Ca- and P-concentrations, with the height in the flame as a (significant) parameter. No Ca-depression was found when Ca and P were sprayed separately, by means of two sprayers in parallel, into the same flame. The outcome of these and other measurements has led us to a detailed hypothesis on the mechanism of this type of anion interference, which satisfactorily explains, among other things, its dependence on Ca concentration, height in the flame, flame temperature and size of the spray-droplets as well as the well-known occurrence of a saturation in the extent of the depression. Conclusions could be drawn as to the reduction or elimination of this depressing effect, which may be useful in practical analysis. In the light of these results, the problem of Ca-depression by added aluminium was also reviewed. A more extensive report will be published elsewhere [6].

Physisch Laboratorium,
Rijksuniversiteit, Utrecht,
Holland

C. T. J. Alkemade
M. H. Voorhuis

References

[1] Baker G. L. and Johnson L. H., *Analyt. Chem.* 1954 **26** 465.
[2] Dippel W. A., Thesis, Princeton University 1954.
[3] Leyton L., *Analyst* 1954 **79** 497.
[4] Margoshes M. and Vallee B. L., *Analyt. Chem.* 1956 **28** 180.
[5] Tsuchikashi S. and Sekido E., *J. Chem. Soc. Japan*, 1956 **77**, 708.
[6] Alkemade C. T. J. and Voorhuis M. H., *Z. anal. Chem.* To be published.

VOL. 12 1958

Spin-forbidden transitions in the electronic spectrum of acetaldehyde*

(*Received* 7 *May* 1958)

The electronic spectrum of formaldehyde has recently received considerable experimental [1, 2, 3, 4, 5] and theoretical [6, 7, 8] study. In comparison, acetaldehyde has been neglected, the only attempt at analysis of the near ultraviolet vapour spectrum being due to Walsh [9] using Schou's data [10]. Cohen and Reid [2] observed three weak β bands (f approx. 10^{-8}) at 26,380, 25,740 and 25,220 cm^{-1} in absorption in formaldehyde which they suggested were $^1A_1 \rightarrow {}^3A_2$. More recent work [4, 5] has revealed that this system consists of nine double-headed bands of which the four longest wavelength components are probably "hot" bands associated with transitions from a ground state in which the 1746 cm^{-1}, ν_2, vibration is excited. We have attempted to detect the analogous transition in acetaldehyde.

Acetaldehyde (reagent grade), was purified in diffuse light by multiple fractional distillation under nitrogen using a 12 in. column of $\frac{1}{8}$ in. diameter glass helices. Fractionation was to $\pm 0{\cdot}1$°C. The boiling point, refractive index and infrared spectrum [11] all

* The experimental work discussed here was carried out in the Research Laboratories of British Nylon Spinners Ltd., Pontypool, England.

showed the material to be pure. However the most severe test was the reproducibility of the ultra-violet absorption spectrum on repeated fractionation. Only under these conditions was the spectrum considered to be intrinsic. After purification the material was stored in the dark. Fig 1 shows the spectrum recorded with a 100 mm path of pure liquid, using a Unicam S.P.500. Under these conditions with acetaldehyde (approx. 18 molar) peak optical density readings in the 24,000 cm^{-1} region were 0·022. Since biacetyl absorbs around 24,000 cm^{-1}, the spectrum was recorded from red to blue so as to minimize any

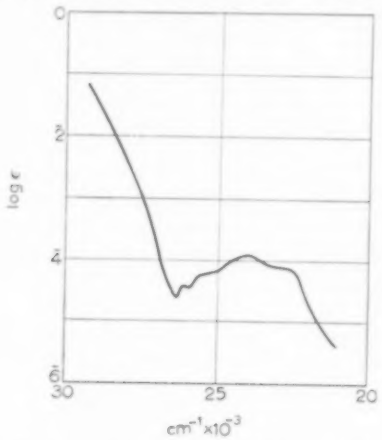

Fig. 1. Absorption spectrum of acetaldehyde using a 100 mm path length.

photochemical formation of biacetyl in the spectrometer. Repeatable results were obtained by two independent operators. The 24,000 cm^{-1} transition shows some diffuse fine structure with inflexions at 26,100, 25,500, 24,400, 23,900 and 22,700 cm^{-1}, but this is insufficient to allow any analysis. However it may be noted that it is different from the biacetyl absorption in this region [12]. The low intensity, f approx. $1{\cdot}7 \times 10^{-9}$, clearly points to the transition being spin-forbidden.

Strictly acetaldehyde possesses no symmetry except for certain special angles of rotation of the methyl group that are probably unimportant. However the great similarity shown by the spectra of all saturated aldehydes and ketones suggests that one is justified in considering the effective symmetry to be C_{2v}. For convenience we shall do so. Then the lower triplet states of acetaldehyde which are likely to be important are $^3A_1$, $^3A_2$ and $^3B_2$ resulting from $\pi_1 \rightarrow \pi_2$, $n \rightarrow \pi_2$ and $n \rightarrow \sigma_{z_2}$ excitations respectively. Table 1 summarizes the allowed spin-orbit perturbations of these states and the properties of the optical transitions between the intermediate states and the $^1A_1$ ground state.

With formaldehyde the parallel type of the β bands [2] shows the transition to be z-axis polarized so the perturbing singlet state must have $^1A_1$ symmetry. This leaves us with two alternatives for the assignment of the triplet state, $^3A_2$ and $^3B_2$. However consideration of the singlet–triplet separations for these transitions leads one to prefer $^3A_2$. Erdmanis and Robinson [5] have located the O—O band of the $^1A_1 \rightarrow {}^1A_2$ transition at 28,190 cm^{-1} and the suggested origin of the β band system is at 25,243 cm^{-1} [4]. This gives an S–T separation of 2947 cm^{-1} which is in good agreement with values for $n \rightarrow \pi$ transitions in other carbonyl molecules, notably glyoxal [13], biacetyl [14] and camphorquinone [15], where the values are remarkably similar, all falling between 2000 and 3000 cm^{-1}. On the other hand the S–T separation for the $n \rightarrow \sigma_{z_2}$ transition would be 26,000 cm^{-1} giving an exceptionally high value for the M.O. exchange integral $K_{n\sigma}$. Therefore Cohen and Reid's assignment seems to be the most reasonable one.

Table 1. Intercombination processes in acetaldehyde

Triplet state	Intermediate state	Spin-orbit coupling component	Transition between ground and intermediate state		
				Transition moment axis	Active vibrations
$^3A_2\,{}^3B_2$	$^1A_1$	$z\,x$	allowed	z	A_1
$^3A_1\,{}^3B_2$	$^1A_2$	$z\,y$	forbidden	y / x	B_1 / B_2
$^3A_1\,{}^3A_2\,{}^3B_2$	$^1B_1$	$y\,x\,z$	allowed	x	A_1
$^3A_1\,{}^3A_2$	$^1B_2$	$x\,y$	allowed	y	A_1

With acetaldehyde, in the absence of polarization data a study of solvent effects would have helped in the assignment of the lowest triplet state but this was not possible because of the low intensity. However the similarity to formaldehyde, both in relative position and in intensity, which is about correct for an overlap forbidden inter-combination process, strongly suggests that we are dealing with the $^1A_1 \rightarrow {}^3A_2$ transition. No definite statement can be made about the perturbing singlet state until the polarization of the 24,000 cm^{-1} transition has been determined. On energetic grounds one might expect mixing with the $^1A_1 \rightarrow {}^1B_2$ transition to be most important, leading to polarization in the y-axis. In fact, McClure [16] has suggested that $^1B_2$ is the principal perturbing state in acetone and other aliphatic ketones because of the parallel effect of methyl substitution on the phosphorescent lifetime and the intensity of the 51,000 cm^{-1}, $n \rightarrow \sigma_{z_2}$ transition.

Finally, if we consider the 24,000 cm^{-1} transition in acetaldehyde to be analogous to the β band system in formaldehyde, methyl substitution appears to cause a red shift of about 1000 cm^{-1}, whereas we might expect a blue shift. This suggests that configuration and spin-orbit interaction may be greater in acetaldehyde than formaldehyde.

Acknowledgements—The technical assistance of Mr. S. V. Dawes is gratefully acknowledged.

R. A. Ford

Mullard Research Laboratories,
Salfords, Redhill, England

References

[1] Brand J. C. D., *J. Chem. Soc.* 1956 858.
[2] Cohen A. D. and Reid C., *J. Chem. Phys.* 1956 **24** 85.
[3] Robinson G. W., *Canad. J. Phys.* 1956 **34** 699.
[4] Hodges S. E., Henderson J. R. and Coon J. B., *Presented at Ohio State Spectroscopy Conference, June*, 1957. Abstract published in *Spectrochim. Acta*, 1957 **10** 230.
[5] Erdmanis V. and Robinson G. W., *Presented at Ohio State Spectroscopy Conference, June* 1957. Abstract published in *Spectrochim. Acta*, 1957 **10** 230.
[6] Parks J. M., Ph.D. Thesis, Carnegie Institute of Technology 1956.
[7] Sidman J. W., *J. Chem. Phys.* 1957 **27** 429.
[8] Pople J. A. and Sidman J. W., *J. Chem. Phys.* 1957 **27** 1270.
[9] Walsh A. D., *J. Chem. Soc.* 1953 2318.
[10] Schou S. A., *J. Chim. Phys.* 1929 **26** 27.
[11] Kindly recorded by Mr. C. G. Cannon of British Nylon Spinners Ltd., Pontypool.
[12] Forster L. S., *J. Amer. Chem. Soc.* 1955 **77** 1417.
[13] Brand J. C. D., *Trans. Faraday Soc.* 1954 **50** 431.
[14] Sidman J. W. and McClure D. S., *J. Amer. Chem. Soc.* 1955 **77** 6461.
[15] Ford R. A. and Parry F. *Spectrochim. Acta* 1958 **12** 78.
[16] McClure D. S., *J. Chem. Phys.* 1949 **17** 905.

VOL. 12 1958

Determination of indium by flame photometry*

(*Received* 30 *January* 1958)

Abstract—The flame spectrum of indium has been observed in air–hydrogen and oxy–hydrogen flames; the lines at 4511 and 4102 Å are strongest, followed by 3256 and 3039 Å. The 4511 line in oxy–hydrogen is best for quantitative determination, providing a detection limit of 0·01 p.p.m. in aqueous solution, with a Beckman flame spectrophotometer equipped with multiplier phototube. The emission of indium at this wavelength is exactly proportional to concentration up to at least 100 p.p.m. Hydrochloric acid increases the background radiation and depresses the indium emission. In the determination of indium in the range 10–250 μg, the precision was 1 per cent or better, attaining 0·1 per cent under suitable conditions.

Introduction

THE brilliant blue-violet colour of an indium-containing flame has long been known. The air–acetylene flame [1] excites the lines 4511, 4102, 3256, 3039, 2754, and 2710 Å, in decreasing intensity. The first to use the flame for quantitative determination of indium were RUSANOV and co-workers [2–6]. They used air–acetylene and oxy–acetylene, and either 4511 or 4102 Å; the best detection limit was 5 p.p.m. and the accuracy about 10 per cent. More recently, MELOCHE *et al.* [7] have determined indium with the oxy–hydrogen flame in copper–aluminium alloys containing 0·5 to 2·5 per cent indium. The standard error was 0·3 p.p.m. in the range 0–100 p.p.m. indium in solution, in the presence of Cu, Al, Zn, Pb, and Fe, and the detection limit was judged to be about 0·2 p.p.m.

The present application was developed in connexion with a problem in neutron flux measurement [8], requiring determination of indium in the microgram range. A detection limit of 0·01 p.p.m. indium in solution and a precision of 0·3 per cent were attained. The time required amounted to a few minutes per sample.

Instrument

The instrument used was a Beckman DU spectrophotometer with Model 9200 flame attachment and 1P28 multiplier phototube. The instrument was focused for peak response with an indium solution spraying, and the hydrogen pressure was simultaneously adjusted for peak response. A point in the flame slightly below the most luminous, as thus located, generally gave somewhat steadier emission. Focusing of the mirror was particularly important in the range below 1 p.p.m. to provide a maximal ratio of net indium to background emission. The 4511 Å line was carefully located on the wavelength scale. The slit width was 0·1 mm for the lowest concentrations, and narrower for higher concentrations. The sensitivity control on the DU and the photomultiplier voltage were adjusted to obtain a compromise between galvanometer sensitivity and shot-effect noise. When precision was required over a 100-fold range of concentration, the instrument was set to read full-scale on the strongest solution with the selector switch in the "1·0" position. For the lower end of the range the switch was turned to "0·1".

Materials

The samples of indium were in the form of pure metallic films evaporated upon small plates of glass or, in some cases, other substances. The indium weighed from 0·01 to 0·25 mg. The film was dissolved with 4 ml of 1 : 1 hydrochloric acid and diluted to 25 ml, to give a solution containing from 0·4 to 10 p.p.m. indium. Standards were prepared similarly from pure indium, the stock containing 100 p.p.m.; this was diluted to make standards ranging

* Presented before the American Chemical Society, New York, September 1954.

down to 1 p.p.m. The same concentration of HCl was used as in the samples, viz. 3·5% HCl by weight.

At these low concentrations, appreciable errors may result from adsorption of indium on the glassware. Such effects were revealed by comparison of fresh and aged standards. In one instance, the same samples after a lapse of several days showed apparent changes of about 2 per cent. To avoid these effects, Desicoted glassware [9] should be used for handling the solutions, and the standards should be stored in polyethylene; however, loss of water

Table 1. Indium flame spectrum

Flame:	Oxy–hydrogen			Oxy–hydrogen			Air–hydrogen		
Slit width:	0·02 mm			0·05 mm (calc.)			0·05 mm		
Wavelength (Å)	Intensity	Background	Line/background ratio	Intensity	Background	Line/background ratio	Intensity	Background	Line/background ratio
4511	350	5½	65	1400	35	40	195	3	65
4102	180	5	35	720	32	22	100	3	35
3256	14	8	2	55	(50)	(1)	15	5	3
3039	3	5½	½	12	(35)	(0·3)	4	3	1½

Values in parentheses uncertain owing to flame bands.

through the polyethylene may occur over long periods. In the present work both the dilute standards and the samples were prepared just before analysis.

Emission characteristics of indium

In order to establish the best operating conditions, the indium spectrum was measured in oxy-hydrogen and air-hydrogen flames. Table 1 shows the intensities for 100 p.p.m. To permit direct comparison, the oxy-hydrogen data were recalculated to a 0·05 mm slit, with allowance for the 0·03 mm equivalent bandwidth broadening due to aberrations, slit mismatch, etc. Air–hydrogen, with its greater indium/background ratios, would be preferable with a more sensitive instrument, but the present instrument does better with oxy–hydrogen, which yields greater absolute intensities. Clearly 4511 Å is the strongest line; but in the event of interferences at this wavelength, 4102 Å would also give excellent sensitivity, while even 3256 Å would be entirely practical for determinations down to 1 p.p.m.

As shown in Fig. 1, the emission at 4511 Å in the oxy–hydrogen flame was strictly proportional to concentration at least up to 100 p.p.m., in agreement with MELOCHE. These data were obtained from 3·5% HCl solutions. It was found, however, that free HCl increased the background and depressed the indium emission, most strongly in that part of the flame in which the indium/background ratio was greatest. HCl at 3·5% raised the background by 5 to 5½ per cent as compared with water, and reduced the net indium light at 4511 Å by 4·4 per cent at 10 p.p.m. Judging from the linearity of the working curve, this 4·4 per cent reduction was independent of concentration between 1 and 100 p.p.m.

Precision and sensitivity

In the analysis of samples, instrumental drift was often unavoidable. For instance, in one set of triplicate analyses on a set of nine samples, two standards, and a blank, a downward drift of 0·66 per cent per cycle of twelve readings was established. The thirty-six

VOL. 12 1958

readings were therefore recalculated to the time of the first reading, to permit averaging the three readings for each solution. Such a set required from 10 to 20 min. In this and other sets, the mean deviations of the individual readings from the mean for each solution averaged 0·34 per cent of the mean. These readings averaged less than half-scale, and expressed as scale divisions the mean deviations averaged only 0·1, that is, 0·1 per cent of full-scale.

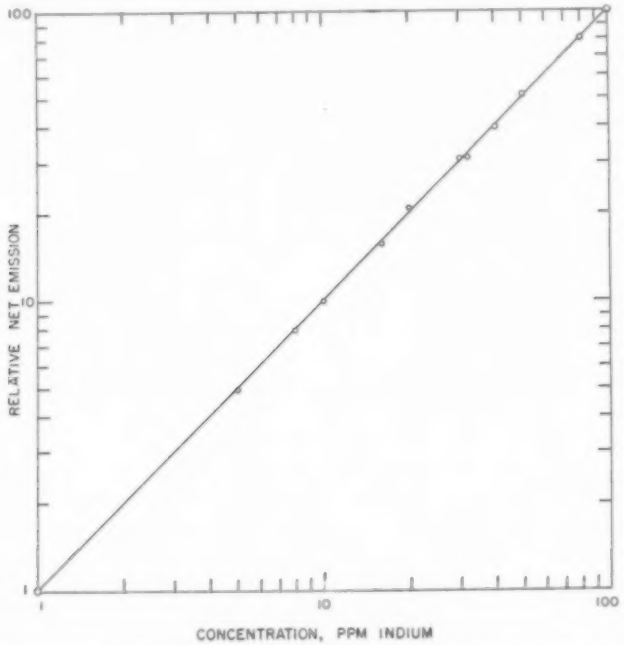

Fig. 1. Emission-concentration curve for the determination of indium. Oxy-hydrogen flame, wavelength 4511 Å.

Under the instrumental conditions employed, the mean deviation was equivalent to 0·012 p.p.m. indium. Thus, in the analysis of a set of solutions, four or five repetitions will yield results in which the probable error of the mean is only 0·1 per cent, provided the samples and standards contain at least 5 p.p.m. and the readings are nearly full scale.

Accuracy could not be directly checked, because no other method was available for determining such small quantities of indium with precision approaching that of the flame photometer. Microbalance weighings were done on the plates before and after evaporation of the indium, but the precision was not adequate, as the plates weighed far more than the indium. A somewhat better independent test was made by taking into account the geometry of the vacuum evaporator, and comparing the quantities of indium simultaneously evaporated upon plates in different positions. The agreement here averaged about 5 per cent; this was really not a test of the accuracy of the flame determination, but rather a test of the isotropy of evaporation.

Acknowledgement—The development of this analytical method was incidental to a project in charge of R. L. Koontz [8], and for the opportunity thus afforded the author wishes to express his gratitude. Mr. Koontz prepared the evaporated indium samples and assisted in the flame

determinations. The solutions and standards were prepared by Mrs. JUANITA K. TAYLOR. The project was under the support of the U.S. Atomic Energy Commission.

P. T. GILBERT JR.*

North American Aviation Inc.,
Downey, California.†

References

[1] LUNDEGÅRDH H., *Die quantitative Spektralanalyse der Elemente*, Vol. II. Fischer, Jena 1934.
[2] RUSANOV A. K., *Bull. acad. sci. URSS, Sér. phys.* 1940 **4** 195.
[3] RUSANOV A. K. and ALEKSEEVA V. M., *Zavodskaya Lab.* 1940 **9** 66.
[4] RUSANOV A. K. and BODUNKOV B. I., *Zavodskaya Lab.* 1938 **7** 573.
[5] RUSANOV A. K. and KUNINA S. I., *Zavodskaya Lab.* 1937 **6** 836.
[6] RUSANOV A. K. and SOLODOVNIK S. M., *Redkie Metal.* 1937 **6** 5–6 29.
[7] MELOCHE V. W., RAMSAY J. B., MACK D. J. and PHILIP T. V., *Analyt. Chem.* 1954 **26** 1387.
[8] GREENFIELD M. A., KOONTZ R. L., JARRETT A. A. and TAYLOR J. K., *Nucleonics* 1957 **15** 3 57.
[9] GILBERT P. T., JR., *Science* 1951 **114** 637.

* Present address, Beckman Instruments, Inc., Fullerton, Calif.
† Nuclear Engineering and Manufacturing Dept., now Atomics International, Canoga Park, Calif.

Correction de l'intensité des raies Raman pour l'absorption du milieu diffusant

(*Received* 19 *May* 1958)

VOL. 12 1958

AVEC l'emploi de l'enregistrement photoélectrique, il apparaît nettement que la détermination du coefficient de diffusion réel d'une raie Raman exige l'application aux intensités mesurées d'un certain nombre de corrections qui ont été discutées par BERNSTEIN et ALLEN [1] et par BRANDMÜLLER et SCHRÖTTER [2].

L'absorption éventuelle du milieu diffusant doit aussi être prise en considération et nous nous proposons de montrer ici comment il est possible d'en tenir compte.

On peut montrer que, dans le cas d'un tube Raman droit placé dans l'axe d'une lampe hélicoïdale du type Toronto, dans l'hypothèse d'un éclairage uniforme, l'intensité apparente mesurée $I_a(\nu)$ est liée à l'intensité réelle $I(\nu)$ par la relation approchée suivante:

$$I(\nu) = I_a(\nu)\,\frac{E(\nu)\cdot l}{1-\exp\{-E(\nu)\cdot l\}}\cdot\exp\{E(\nu_0)\cdot\beta\cdot d\} \tag{1}$$

$E(\nu)$, $E(\nu_0)$ étant l'extinction sous 1 cm d'épaisseur du liquide absorbant aux fréquences de la raie Raman et de la raie excitatrice; l et d sont respectivement la longueur et le diamètre du tube Raman, β est un facteur empirique destiné à corriger le terme approximatif d'absorption de la raie excitatrice.

La détermination du coefficient de diffusion se fait plus facilement en solution dans une substance étalon, par ex. le CCl_4, comme nous l'avons déjà fait pour des substances incolores [3] en nous servant de la relation:

$$k^A(\nu) = I^A(\nu)/I^{CCl_4}(\nu')\cdot N_{CCl_4}/N_A \tag{2}$$

N_{CCl_4} et N_A étant les nombres de môles des deux constituants du mélange.

Dans le cas d'une substance absorbante A en solution, on obtient à partir des équations (1) et (2) la relation suivante:

$$k^A(\nu) = I_a{}^A(\nu)/I_a^{CCl_4}(\nu')\cdot\frac{[1-\exp\{-E(\nu')\cdot l\}]}{[1-\exp\{-E(\nu)\cdot l\}]}\cdot E(\nu)/E(\nu')\cdot N_{CCl_4}/N_A \tag{3}$$

nous supposons que la loi de Lambert–Beer est applicable.

Tableau 1. Benzène + quinone, $\nu = 992\ \text{cm}^{-1}$, $\bar{\beta} \simeq 0{\cdot}8$, $E(\nu)/E(\nu_0)_{\text{moyen}} = 1{\cdot}05$

$E(\nu)$	$E(\nu_0)$	$\frac{I_a(\nu)}{I(\nu)}$ mesuré	$\frac{I_a(\nu)}{I(\nu)}$ calculé	Δ	Écarts relatifs (%)
$0{\cdot}042_7$	$0{\cdot}040_4$	0·673	0·661	0·012	1·8
$0{\cdot}042_7$	$0{\cdot}040_9$	0·671	0·661	0·010	1·5
0·059	0·058	0·589	0·561	0·018	3·2
0·079	0·078	0·494	0·472	0·024	5·1
0·098	0·093	0·413	0·407	0·006	1·5
0·099	0·095	0·410	0·402	0·008	2·0
0·101	0·095	0·412	0·396	0·016	4·0
0·125	0·109	0·350	0·337	0·013	3·9
0·126	0·120	0·338	0·332	0·006	1·8
0·163	0·157	0·254	0·260	0·006	2·3
0·163	0·157	0·254	0·260	0·006	2·3
0·198	0·189	0·202	0·212	0·010	4·7
0·199	0·192	0·196	0·211	0·005	2·4
0·199	0·193	0·210	0·210	0·000	0
0·264	0·251	0·147	0·154	0·007	4·5
0·264	0·251	0·143	0·154	0·011	7·1
0·239	0·232	0·161	0·172	0·011	6·4
0·310	0·297	0·115	0·126	0·011	8·7
0·310	0·285	0·120	0·128	0·008	6·2
0·310	0·297	0·114	0·126	0·012	9·5

Écart relatif moyen ±4% Écart relatif maximum 9·5%

Tableau 2. C_6H_6 + *p*-azoxyanisole $= 992\ \text{cm}^{-1}$ $\bar{\beta} \simeq 0{\cdot}6$ $E(\nu)/E(\nu_0) = 0{\cdot}29$

$E(\nu)$	$E(\nu_0)$	$\frac{I_a(\nu)}{I(\nu)}$ mesuré	$\frac{I_a(\nu)}{I(\nu)}$ calculé	Δ	Écarts relatifs (%)
0·039	0·140	0·661	0·640	0·021	3·3
0·042	0·146	0·644	0·619	0·023	3·8
0·046	0·159	0·615	0·598	0·017	2·8
0·044	0·164	0·616	0·609	0·007	1·2
0·047	0·171	0·602	0·588	0·014	4·2
0·066	0·244	0·460	0·480	0·02	4·2
0·069	0·261	0·448	0·457	0·009	2·0
0·069	0·274	0·437	0·460	0·023	5·0
0·076	0·285	0·436	0·433	0·003	6·9
0·092	0·345	0·373	0·371	0·002	5·4
0·084	0·326	0·372	0·354	0·018	5·1
0·113	0·430	0·288	0·305	0·017	5·6
0·106	0·416	0·308	0·322	0·016	5·0
0·119	0·443	0·285	0·292	0·007	2·4
0·115	0·437	0·274	0·301	0·027	9·0
0·125	0·464	0·252	0·278	0·026	9·3
0·154	0·593	0·194	0·216	0·022	10·2
0·172	0·639	0·187	0·212	0·025	11·5
0·205	0·740	0·143	0·153	0·010	6·5
0·218	0·759	0·135	0·142	0·007	4·9
0·209	0·750	0·135	0·148	0·013	8·7

Écart relatif moyen ±4·7% Écart relatif maximum 11·5%

Vérification des formules proposées

Nous avons choisi le benzène pour son spectre intense et nous avons fait la vérification de la formule (1) en mesurant l'intensité de la raie 992 cm^{-1} sur la substance pure et sur la substance additionnée d'un colorant.

Nous avons réalisé une première série d'expériences avec la quinone comme colorant et enfin une seconde série avec le mélange benzène-*p*-azoxyanisole.

Tableau 3

Mélange n°	$E(\nu)$	$E(\nu')$	$E(\nu)/E(\nu')$	$I_a(992)$	$I_a(458)$	$k(992)$ apparent	$k(992)$ corrigé
1	0·059	0·054	1·083	123·9	83·2	2·99	3·09
2	0·142	0·126	1·120	60·4	42·4	2·85	3·11
3	0·193	0·176	1·097	43·8	30·9	2·83	3·08
4	0·227	0·209	1·086	37·3	27·0	2·76	2·99
5	0·367	0·338	1·086	20·2	14·5	2·78	3·02
Pur	0	0		198·5	130·9	3·04	

Nous avons mesuré les extinctions des solutions aux fréquences ν et ν_0 au moyen d'un spectrophotomètre Beckman B en utilisant des cellules de 5 cm, tandis que nous enregistrions sur notre spectromètre photoélectrique [4] la raie 992 cm^{-1} du benzène pur et de la solution colorée; nous avons de la sorte calculé le β moyen de la formule (1) sachant que $l = 20$ cm et $d = 1$ cm:

benzène + quinone: $\bar{\beta} \simeq 0{\cdot}8$, $E(\nu)/E(\nu_0)_{\text{moyen}} = 1{\cdot}05$

benzène + *p*-azoxyanisole: $\bar{\beta} \simeq 0{\cdot}6$, $E(\nu)/E(\nu_0)_{\text{moyen}} = 0{\cdot}29$

Connaissant les β moyens, nous sommes ensuite partis de la formule (1) et des valeurs de $E(\nu)$, de l et de d pour calculer un rapport $I_a(\nu)/I(\nu)$ que nous avons comparé au rapport $I_a(\nu)/I(\nu)$ mesuré: ces résultats sont rassemblés dans les tableaux 1 et 2.

La vérification de la formule 3 a été faite sur un mélange approximatif de $\frac{1}{3}$ mole de benzène pour $\frac{2}{3}$ mole de tétrachlorure de carbone ($N'/N = 2$), auquel nous avons ajouté des quantités croissantes de quinone (voir tableau 3).

Le mélange pur, c'est à dire sans quinone nous donne un $k(992) = 3{\cdot}04$; nous voyons par le tableau 3 que la concordance des $k(992)$ corrigés est meilleure (dispersion de $\pm 2\%$ au lieu d'une erreur systématique de 9% environ).

Remerciements—Nous tenons à remercier le Professeur G. Duyckaerts qui nous a aidé par ses discussions constructives.

G. Michel

Service de chimie analytique,
Université de Liège,
Belgique

Bibliographie

[1] Bernstein H. J. et Allen G., *J. Opt. Soc. Amer.* 1955 **45** 237.
[2] Brandmüller J. et Schrötter H., *Z. Phys.* 1957 **149** 131.
[3] Michel G. et Duyckaerts G., *Spectrochim. Acta* 1958 **10** 259.
[4] Michel G. et Duyckaerts G., *Spectrochim. Acta* 1957 **8** 356.

VOL. 12 1958

Raman spectrum and force constants of the chromate ion

(*Received* 27 *May* 1958)

NEARLY all tables of vibrational spectra of regular tetrahedral molecules and ions (symmetry point group T_d) report the four fundamentals of the chromate ion as observed by VENKATESWARAN [1] on the Raman spectra of sodium, potassium and ammonium chromate in the solid state and in aqueous solutions. There exist however indications that some of the data given by VENKATESWARAN have to be corrected, namely the frequency-values of 481 and 503 cm^{-1} assigned to the bending modes of vibration ν_2 and ν_4 (of species E and F_2 respectively) seem considerably too high. This may be concluded immediately from the table of force constants given, since the value of the bending force constant of the chromate ion appears to be abnormally large as compared with the corresponding constant of similar ions.

The same conclusion may be drawn from an analysis of the infrared spectra of a number of chromates reported by DUVAL and LECOMTE [2]. The authors measured absorptions in the spectral range accessible with a NaCl-prism-spectrometer and found—as to be expected—only one band that has to be ascribed to a fundamental vibration, namely to the triply degenerate stretching vibration ν_3 (of species F_2) at about 860–880 cm^{-1}. All the other observed bands in the region studied have to be assigned to overtones or combinations. The band of lowest frequency was found at about 670–680 cm^{-1} and has to be assigned to $2\nu_4$ or to $\nu_3 + \nu_4$ since $F_2 \times F_2$ and $E \times F_2$ are the only infrared-active binary combinations to be considered here. This situation indicates clearly that the frequency of at least one of the two bending vibrations of the molecule should be expected to be 350 cm^{-1} or lower.

We attempted therefore to obtain the Raman spectrum of the $(CrO_4)^{=}$-ion by making use of an experimental arrangement for excitation of Raman spectra in the red and near infrared by helium-radiations, as described previously by one of us [3]. In the present case He 5875·6 Å was used for excitation and we registered approximately sixty spectra of samples of aqueous solutions of potassium, sodium and ammonium salts in concentrations ranging from 5 per cent to saturation.

Some spectra were taken with a fairly high dispersion of 9 Å/mm, corresponding to 25 wave-numbers/mm in the 6000 Å region. Since the spectra were obtained without any particular difficulties and measurements of the Raman shifts agreed in all spectra within the limit of experimental errors which is estimated to be ± 1 cm^{-1} for sharp lines, we shall omit further details. Table 1 gives our results on the frequencies (in wave-numbers), estimated intensities, state of polarization, etc., of the observed Raman shifts as compared with the values reported by VENKATESWARAN.

Whereas our measurements of the stretching frequencies agree fairly well with the observations of VENKATESWARAN we found the frequencies of the two bending vibrations to be 133 cm^{-1} and 135 cm^{-1} lower than indicated by this author. We believe that the origin of the discrepancy is an erroneous identification of a reference line in the iron arc spectrum used by VENKATESWARAN as comparison spectrum for his wavelength measurements. His Raman spectra of chromates were excited by Hg 5461 Å: the strongest iron lines in the region of the shifts corresponding to the bending modes of vibration ν_2 and ν_4 are Fe 5572·8 Å and Fe 5615·7 Å. The two Raman shifts are found close to the first of these iron lines whose separation in wave-numbers is 136 cm^{-1}. Apparently VENKATESWARAN has mistaken Fe 5572·8 Å for Fe 5615·7 Å and has consequently obtained values for ν_2 and ν_4 that are 136 cm^{-1} higher than they should be.

We believe it worthwhile to call attention to this mistake since the data of VENKATESWARAN were subsequently used by various authors in calculations of the force constants of

Table 1. Raman spectrum of $(CrO_4)^{=}$ and assignment

Assignment	ν_1 (A_1)	ν_2 (E)	ν_3 (F_2)	ν_4 (F_2)
VENKATESWARAN	859	481	877	503
This work	847 (10)l	348 (5b)	884 (3vb)	368 (2b)

Table 2. Force constants of $(CrO_4)^{=}$ (mdyn/Å)

	f_d	f_{dd}	f_α	$f_{\alpha\alpha}$	$f_{d\alpha}$
VENKATESWARLU and SUNDARAM	6·95	—	1·00	0·13	1·21
This work	6·76	—	0·61	0·12	1·19
SIEBERT	5·23	0·56	0·84	0·06	—
This work	5·48	0·43	0·42	0·02	—

the $(CrO_4)^{=}$-ion based on assumptions of different force fields; the numerical results of these calculations are now corrected.

Recently VENKATESWARLU and SUNDARAM [4] evaluated the force constants of a number of radicals and molecules of the type XY_4 belonging to the T_d symmetry point group by making use of WILSON's F–G matrix method and available Raman data. Their expressions for the potential energy of the system contain the following force constants: f_d (associated with the X–Y stretching mode of vibration), f_α (Y–X–Y bending), $f_{d\alpha}$ (stretching–bending interaction) and $f_{\alpha\alpha}$ (bending–bending interaction).

Previously to the mentioned paper SIEBERT [5] communicated a set of equations for the frequencies of tetrahedral molecules taking into account the stretching–stretching interaction (represented by the force constant f_{dd}) and the interaction between adjacent angles ($f_{\alpha\alpha}$), neglecting consequently the interaction between the stretching and bending modes of vibration. It seems that this treatment applies in a more satisfactory manner to molecules possessing a heavy central atom and light external atoms such as is the case in the chromate ion. A subsequent paper of SIEBERT [6] gives the numerical evaluation of the force constants of $(CrO_4)^{=}$ obtained from his expressions and from VENKATESWARAN's Raman data.

We recalculated the force constants of the chromate ion given by VENKATESWARLU and SUNDARAM and by SIEBERT using the Raman frequencies reported in this paper; the results are given in Table 2 and show—as expected—a pronounced decrease of the bending constant f_α as compared with the previous values.

These force constants were calculated using our frequency-assignment of Table 1, based upon the assumption that the lower frequency of the two bending modes of vibration corresponds to the species E as tabulated for nearly all tetrahedral molecules and especially for ions of the type $(XO_4)^{n-}$. It should be noted, however, that the Raman spectrum alone provides no evidence for the correct assignment of the two low frequencies to the respective

VOL. 12 1958

modes of vibration of species E and F_2. The frequency of the infrared absorption band observed by DUVAL and LECOMTE [2] at 670–680 cm^{-1} fits best with our results when ascribed to the first overtone of the lowest fundamental and not to the combination $\nu_2 + \nu_4$. Since only the harmonics of species F_2 are infrared-active whereas those of species E are forbidden, the Raman shift 348 cm^{-1} should be assigned, possibly, to $\nu_4\,(F_2)$ and 368 cm^{-1} to $\nu_2\,(E)$. However, the eventual inversion of the frequencies assigned to ν_2 and ν_4 affects the values of the principal force constants only in an insignificant manner. The values of f_d, f_{dd} and $f_{d\alpha}$ remain practically unchanged, f_α decreases by about 10 per cent.

Regarding the question of the dependence of the frequencies corresponding to the two bending modes of vibration on the relative masses of the central atom and the external atoms in tetrahedral molecules, we refer to KOHLRAUSCH [7] who discussed the case in terms of a simple valence force model.

Acknowledgements—The authors wish to express their gratitude to Dr. S. SUNDARAM, Annamalai University, India, and to Dr. H. SIEBERT, Academy of Mining, Clausthal-Zellerfeld, Germany, for helpful discussions. They feel indebted to the Conselho Nacional de Pesquisas, Rio de Janeiro, who supported this work.

H. STAMMREICH
D. BASSI
OSWALDO SALA

Dept. of Physics,
University of São Paulo,
São Paulo, Brazil.

References

[1] VENKATESWARAN C. S., *Proc. Indian Acad. Sci.* 1938 **7** 144.
[2] DUVAL C. and LECOMTE J., *Bull. Soc. Chim. France* 1947 **14** 106.
[3] STAMMREICH H., *Spectrochim. Acta* 1956 **8** 41.
[4] VENKATESWARLU K. and SUNDARAM S., *J. Chem. Phys.* 1955 **23** 2365.
[5] SIEBERT H., *Z. anorg. allg. Chem.* 1953 **273** 21.
[6] SIEBERT H., *Z. anorg. allg. Chem.* 1954 **275** 225.
[7] KOHLRAUSCH K. W. F., *Ramanspektren* pp. 154–156. Leipzig 1943.

Spectrochimica Acta, 1958, Vol. 12, p. 406. Pergamon Press Ltd., London

Book review

CHARLOTTE E. MOORE: **Atomic Energy Levels.** Vol. III. National Bureau of Standards Circular No. 467, 1958. xxxviii + 245 pp. $2.50.

THIS compilation of atomic structure data is compiled from the analyses of optical spectra, and is a sequel to two previous volumes dealing with elements of lower atomic number; Vol. III deals with the elements from molybdenum to actinium, excluding the rare earth group Ce to Lu. Like the previous volume it includes not only published data, but work specially done for this volume in the laboratories of the National Bureau of Standards, Princeton University, Madrid, Amsterdam, Jerusalem and elsewhere.

Analytical spectroscopists will use it chiefly for the revised table of the ionization potentials of all the elements in each state of ionization, and as a source of references for details about emission spectra. All readers will be impressed by the careful and extensive work involved in its preparation, in particular by the eight pages of additions and corrections to the two earlier volumes which contribute to bringing the work as a whole up to date early this year.

A bibliography of papers dealing with the rare earth spectra has been included, pending the completion of Vol. IV which will deal with these elements and the group from thorium through fermium.

ERNEST VAN SOMEREN

VOL.
12
1958

Spectrochimica Acta, 1958, Vol. 12, pp. 407 to 408. Pergamon Press Ltd., London

Papers to be published in future issues

A. L. Bluhm: The infrared spectra and the structure of some homophthalimides

M. Tsuboi, T. Shimanouchi and S. Mizushima: Analysis of P and R branches of the 950 cm^{-1} band of $N^{14}H_3$

D. C. McKean: Force constants, interbond angle and solid state spectrum of disiloxane

O. Botschkowa, T. Frisch und E. Schreider: Quantitative Spektralanalyse von Gasgemischen

D. B. Powell and N. Sheppard: Infrared spectra and vibrational frequencies of co-ordinated ethylene

H. Bevan, S. V. Dawes and R. A. Ford: The electronic spectra of titanium dioxide

F. Meda: Infrared absorption spectra of α-halogenated keto-steroids

L. J. Bellamy: The origin of group frequency shifts—I. Abnormal frequencies in multiple bonds

F. F. Bentley, E. F. Wolfarth, N. E. Srp and W. R. Powell: Analytical applications of far infrared spectra—I. Historical review, apparatus and technique

S. Mizushima, I. Nakagawa, M. J. Schmelz, C. Curran and J. V. Quagliano: Infra-red absorption spectra of inorganic co-ordination complexes—XVII

T. P. Schreiber and D. L. Fry: Spectral character as a function of spark source parameters

A. Miyake, I. Nakagawa, T. Miyazawa, I. Ichishima, T. Shimanouchi and S. Mizushima: Infrared and raman spectra of dichloroacetyl chloride in relation to rotational isomerism

P. Tarte: Réchérches sur les frequences de déformation OH—I. Spectra infra-rouge des sels basiques de cuivre

D. A. Sinclair and R. N. Whittem: Apparent rectification in tesla sparks

A. Danti and R. C. Lord: Rotational analysis and upper-stage transitions of parallel absorption bands in benzene, Sym-benzene-d_3, benzene-d_6 and pyridine

B. Bak, D. Christensen, L. Hansen-Nygaard and J. Rastrup-Andersen: The structure of vinyl fluoride

H. Stammreich, D. Bassi, O. Sala and H. Siebert: The vibrational spectrum of the dichromate ion

D. M. Shaw, O. Wickremasinghe and C. Yip: A simple device for the spectrochemical analysis of minerals in an inert atmosphere using the Stallwood jet

A. D. E. Pullin: The variation of infrared vibration frequencies with solvent

E. A. V. Ebsworth, J. R. Hall, M. J. MacKillop, D. C. McKean, N. Sheppard and L. A. Woodward: Vibrational spectra and structure of trisilylamine and trisilylamine-d_9

E. A. V. Ebsworth and N. Sheppard: The infra-red spectra of some methylammonium iodides: angle deformation frequencies of $\overset{+}{N}H$ and $\overset{+}{N}H_2$ groups

K. Laqua and U. Luoto: Ein thyratrongesteuertes Schaltgerat für Wechselstromabreissbögen

G. L. Caldow and H. W. Thompson: Vibrational bands of isothiocyanates, thiocyanates and isocyanates

J. P. Jesson and H. W. Thompson: Vibrational band intensities of the C≡N group in aliphatic nitriles

P. E. B. Butler, D. R. Eaton and H. W. Thompson: Vibration–rotation bands of keten

H. W. Thompson and D. A. Jameson: Vibrational frequency and band intensity of the carbonyl group

G. C. Cannon and B. C. Stace: ν OH of trifluoroethanol and the Kirkwood–Bauer reaction

H. W. Thompson and D. J. Jewell: Effect of solvent upon vibration bands

Carlos Gual, Ralph I. Dorfman and Harris Rosenkrautz: Infrared absorption spectra of ring D steroid lactones—I. Intense hydrogen bonding in estrololactone

L. W. Dausch: Infrared group of frequencies versus electronegativity

---

VOL.
12
1958

ERRATA

Llewellyn H. Jones: Systematics in the vibrational spectra of uranyl complexes *Spectrochimica Acta*, 1958, Vol. X, pp. 395 to 403.

1. Page 399, last line, $-0{\cdot}07$ cm^{-1} should read $-0{\cdot}07$ m dyn/A.

2. Page 400, paragraph 5, sentence 4, should read "also $\rho_{UF}^2 F_z$ is $\approx 0{\cdot}14$ m dyn/A so we might expect $\rho_{UF} F_{UF,z}$ to be $<0{\cdot}1$ m dyn/A.

3. Page 400, paragraph 5, end of last sentence, 0·1 cm^{-1} should read "0·1 m dyn/A".

4. Page 401 (centre), in brackets of the equation, v_1 should read v_i.